Ovarian cancer targeted medication: PARP inhibitors, anti-angiogenic drugs, immunotherapy, and more

Edited by
Zhaoqian Liu, Dan Liu, Jing Wang, Guang Lei and Nayiyuan Wu

About Frontiers

Frontiers is more than just an open access publisher of scholarly articles: it is a pioneering approach to the world of academia, radically improving the way scholarly research is managed. The grand vision of Frontiers is a world where all people have an equal opportunity to seek, share and generate knowledge. Frontiers provides immediate and permanent online open access to all its publications, but this alone is not enough to realize our grand goals.

Frontiers journal series

The Frontiers journal series is a multi-tier and interdisciplinary set of open-access, online journals, promising a paradigm shift from the current review, selection and dissemination processes in academic publishing. All Frontiers journals are driven by researchers for researchers; therefore, they constitute a service to the scholarly community. At the same time, the *Frontiers journal series* operates on a revolutionary invention, the tiered publishing system, initially addressing specific communities of scholars, and gradually climbing up to broader public understanding, thus serving the interests of the lay society, too.

Dedication to quality

Each Frontiers article is a landmark of the highest quality, thanks to genuinely collaborative interactions between authors and review editors, who include some of the world's best academicians. Research must be certified by peers before entering a stream of knowledge that may eventually reach the public - and shape society; therefore, Frontiers only applies the most rigorous and unbiased reviews. Frontiers revolutionizes research publishing by freely delivering the most outstanding research, evaluated with no bias from both the academic and social point of view. By applying the most advanced information technologies, Frontiers is catapulting scholarly publishing into a new generation.

What are Frontiers Research Topics?

Frontiers Research Topics are very popular trademarks of the *Frontiers journals series*: they are collections of at least ten articles, all centered on a particular subject. With their unique mix of varied contributions from Original Research to Review Articles, Frontiers Research Topics unify the most influential researchers, the latest key findings and historical advances in a hot research area.

Find out more on how to host your own Frontiers Research Topic or contribute to one as an author by contacting the Frontiers editorial office: frontiersin.org/about/contact

Ovarian cancer targeted medication: PARP inhibitors, anti-angiogenic drugs, immunotherapy, and more

Topic editors

Zhaoqian Liu — Central South University, China

Dan Liu — Huazhong University of Science and Technology, China

Jing Wang — Central South University, China

Guang Lei — University of Texas MD Anderson Cancer Center, United States

Nayiyuan Wu — Central South University, China

Topic Coordinator

Zhi-Bin Wang — Central South University, China

Table of
contents

Editorial: Ovarian cancer-targeted medication: PARP inhibitors, anti-angiogenic drugs, immunotherapy, and more

Zhi-Bin Wang[1,2†], Dan Liu[3†], Guang Lei[4†], Zhao-Qian Liu[5,6]*, Nayiyuan Wu[1,2]* and Jing Wang[1,2]*

[1]Hunan Key Laboratory of Cancer Metabolism, Hunan Cancer Hospital, The Affiliated Cancer Hospital of Xiangya School of Medicine, Central South University, Changsha, Hunan, China, [2]Public Service Platform of Tumor Organoids Technology, Hunan Gynecological Tumor Clinical Research Center, Changsha, Hunan, China, [3]Department of Gynecological Oncology, Tongji Hospital, Tongji Medical College, Huazhong University of Science and Technology, Wuhan, China, [4]Department of Experimental Radiation Oncology, The University of Texas MD Anderson Cancer Center, Houston, TX, United States, [5]Department of Clinical Pharmacology, Hunan Key Laboratory of Pharmacogenetics, National Clinical Research Center for Geriatric Disorders, Xiangya Hospital, Central South University, Changsha, Hunan, China, [6]Institute of Clinical Pharmacology, Engineering Research Center for applied Technology of Pharmacogenomics of Ministry of Education, Central South University, Changsha, Hunan, China

Editorial on the Research Topic
Ovarian cancer-targeted medication: PARP inhibitors, anti-angiogenic drugs, immunotherapy, and more

Ovarian cancer (OC) is a highly fatal malignancy, with tumor reduction and platinum-based chemotherapy being its primary treatments. However, acquired platinum resistance poses a challenge to patient management. Targeted therapies, such as PARP inhibitors (PARPi) and anti-angiogenic agents, are replacing conventional chemotherapy. Next-generation sequencing offers promise in identifying specific molecular targets for personalized treatment. Immunotherapy and modulation of the ferroptosis pathways also present new avenues for targeted therapy. Improving the efficacy and reducing side effects of existing therapies and exploring new options are pressing challenges. This Research Topic covers Research Topic in pharmacology, including immune-targeted therapy, prognostic biomarkers, and single-cell sequencing analysis of the immune microenvironment in OC (Figure 1). The following section provides a concise summary of the major highlights from the twelve articles included in this Research Topic.

1. Olaparib, a PARPi, has reshaped the treatment scenario of metastatic OC as a maintenance therapy post-platinum-based chemotherapy. Maiorano et al. review summarizes the efficacy and safety of several clinical trials, including Study 42, Study 19, SOLO2, OPINION, SOLO1, and PAOLA-1, which led to the FDA and EMA approval of olaparib for maintenance treatment in women with high-grade epithelial ovarian, fallopian tube, or primary peritoneal cancer without platinum progression, in the platinum-sensitive recurrent OC, and in newly diagnosed cases with BRCA mutations. Additionally, the review discusses the future developments and potential applications of olaparib in OC treatment.
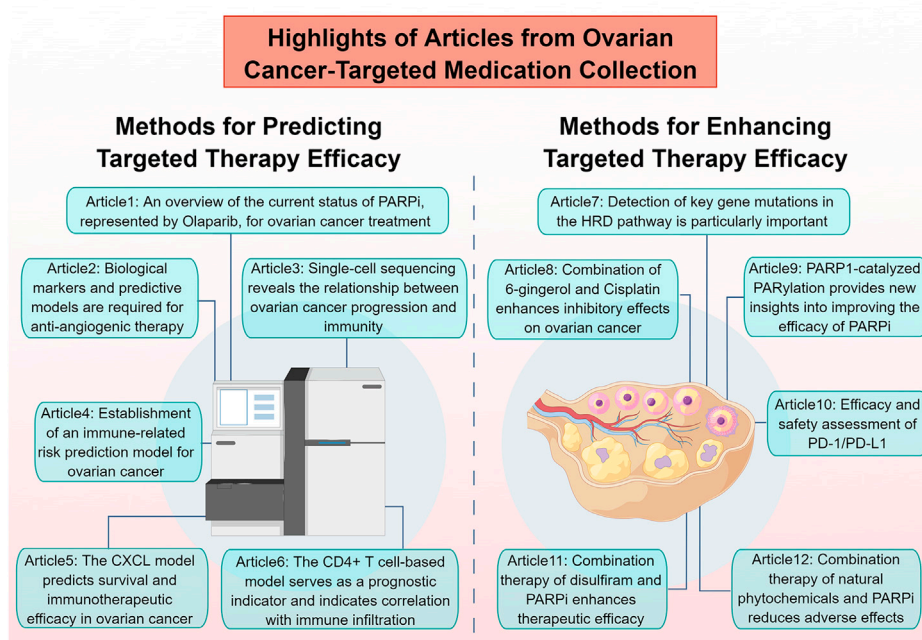
FIGURE 1
Highlights of articles from ovarian cancer-targeted medication collection (By FigDraw).

2. Although anti-angiogenic agents have been developed to target tumor angiogenesis in OC, Mei et al. review emphasizes the need for biomarkers and predictive models to guide precision therapy. The review aims to provide an updated understanding of the mechanisms of tumor angiogenesis and the latest reports on the clinical trial outcomes and resistance mechanisms of anti-angiogenic agents in OC.

3. Zhang et al. study provides key insights into the differences between healthy ovarian and ovarian cancer cells and demonstrates the potential of ScRNA-seq analysis in guiding personalized treatments. Furthermore, the study finds variations in immune-related and apoptosis-related gene expression between healthy ovarian and ovarian cancer cells. These findings provide key insights for further research into the treatment of OC. Overall, ScRNA-seq analysis has the potential to improve our understanding of OC at the cellular level and guide personalized treatments for patients.

4. Wu et al. study highlights the potential of a machine learning-based immune-related risk model to improve prognostic prediction and guide personalized treatment for HGSOC. The developed TMErisk scoring system demonstrated superior performance in predicting HGSOC prognosis across cohorts and was associated with BRCA1 mutation, C-X-C motif chemokine ligands deletion, and carcinogenic activation pathways. The low TMErisk group exhibited favorable prognosis and better immune response. Overall, this study offers valuable insights into the diversity of cell components in the TME of HGSOC and guides the development of potential therapeutic techniques for addressing tumor immunosuppression and enhancing the response to cancer therapy.

5. The main conclusion of Li et al. study is that the CXCL score has the potential to be a reliable biomarker for predicting clinical outcomes and immunotherapy responses in individual OC patients. The CXCL scoring model showed effectiveness in predicting immunotherapy response by assessing tumor microenvironment cell infiltration, tumor mutational burden estimation, PD-L1/CTLA4 expression, and immunophenoscore analysis. These findings suggest that the CXCL score has the potential to guide personalized immunotherapy in OC patients and improve treatment outcomes.

6. Hua et al. study offers valuable insights into the molecular mechanisms and clinical management of OC and may guide personalized treatments for patients. A risk signature consisting of 11 CD4+ conventional T-cells-related genes (CD4TGs) has prognostic value in OC and can guide clinical management. The study finds that a high risk score is significantly associated with poorer prognosis and could be used as an independent prognostic biomarker. The low-risk group patients tended to exhibit higher immune infiltration, immune-related gene expression, and greater sensitivity to immunotherapy and chemotherapy. These findings provide valuable insights into the molecular mechanisms and clinical management of OC and may guide personalized treatments for patients.

7. Huang et al. review highlights the potential of molecular targeted therapies to improve treatment outcomes for OC patients by overcoming the limitations of traditional

chemotherapy. Specifically, the review highlights the importance of detecting genetic mutations such as BRCA mutations and mutations of other homologous recombination repair defect (HRD) genes, which can guide the targeted drug treatment of patients.

8. The study conducted by Salari et al. compares the effects of cisplatin, 6-gingerol, and their combination on OC cells *in vitro* and *in vivo*. The results show that the combination therapy significantly promoted apoptosis and induced a higher S sequence extent in the cell cycle. Moreover, the expression of genes associated with apoptosis was amplified by the combination therapy, while the expression of genes linked to angiogenesis decreased. Therefore, this study highlights the potential benefits of using complementary treatments and herbal medicines to improve the performance of conventional medicine in treating OC.

9. According to Zhu et al. review, while PARPi are commonly used to treat BRCA1/2-deficient breast and ovarian cancers, resistance to PARPi frequently occurs. Therefore, the review focuses on identifying novel substrates and regulators of poly (ADP-ribosyl)ation (PARylation), which is catalyzed by PARP1, as potential targets for therapeutic intervention to overcome PARPi resistance. This study highlights the importance of understanding the underlying mechanisms of PARP1-catalyzed PARylation and provides new insights into potential strategies for improving the efficacy of PARP inhibitors in treating breast and ovarian cancers.

10. From the perspective of Zeng et al. study, while PD-1/PD-L1 inhibitors hold potential as a targeted therapy for recurrent/refractory OC, they offer modest efficacy when used alone. Their meta-analysis of 11 studies with 990 patients demonstrates an ORR of 6.7%, DCR of 37.9%, median OS of 10.70 months, and median PFS of 2.24 months, as well as TRAEs of 70.9% and iAEs of 29%. Therefore, the study suggests caution in using PD-1/PD-L1 inhibitors and the need for further research to optimize their use in treating OC.

11. Based on their research, Tang et al. and others conclude that disulfiram, in combination with PARPi, has potential as a therapeutic candidate for OC treatment. The combination significantly decreased the viability of OC cells and increased the expression of DNA damage index gH2AX and PARP cleavage. Based on these findings, the study offers a novel treatment strategy for patients with OC.

12. The principal outcome of Wang et al. study indicates that natural phytochemicals, including sulforaphane, lycopene, catechin, and curcumin, exhibit potential efficacy in mitigating and treating the negative effects correlated with BRCA mutations and PARPi exposure among OC

patients. These bioactive substances demonstrate significant therapeutic efficacy against atherosclerosis, nausea, and vomiting, which are prevalent chemotherapy-related side effects. The author anticipates that these findings may offer novel perspectives for exploring innovative and effective therapeutic approaches for treating BRCA-mutated OC patients.

In summary, this Research Topic provides insights into the development of targeted therapies for OC and offers solid evidence to improve their efficacy and reduce toxicity. However, due to the histological characteristics of the ovarian tissue microenvironment and its nature as a "cold tumor," research on targeted therapies for OC, represented by immunotherapy, still faces challenges. However, although the path may be long, progress will ultimately be made.

Author contributions

All authors listed have made a substantial, direct, and intellectual contribution to the work and approved it for publication.

Acknowledgments

Conflict of interest

The authors declare that the research was conducted in the absence of any commercial or financial relationships that could be construed as a potential conflict of interest.

Publisher's note

Natural phytochemicals prevent side effects in *BRCA*-mutated ovarian cancer and PARP inhibitor treatment

Chuanlin Wang[1,2], Pengning Gao[1,2], Jiali Xu[1,2], Shanling Liu[1,2], Wenda Tian[2,3], Jiayu Liu[4] and Lan Zhou[1,2]*

[1]Department of Clinical Nutrition, Yunnan Cancer Hospital, The Third Affiliated Hospital of Kunming Medical University, Kunming, Yunnan, China, [2]Yunnan Cancer Center, Kunming, Yunnan, China, [3]Department of Gynecology, Yunnan Cancer Hospital, The Third Affiliated Hospital of Kunming Medical University, Kunming, Yunnan, China, [4]Key Laboratory of Environmental Toxicology of Anhui Higher Education Institutes, Department of Toxicology, School of Public Health, Anhui Medical University, Hefei, Anhui, China

Ovarian cancer is among the most common malignant tumors in gynecology and is characterized by insidious onset, poor differentiation, high malignancy, and a high recurrence rate. Numerous studies have shown that poly ADP-ribose polymerase (PARP) inhibitors can improve progression-free survival (PFS) in patients with *BRCA*-mutated ovarian cancer. With the widespread use of *BRCA* mutation and PARP inhibitor (PARPi) combination therapy, the side effects associated with *BRCA* mutation and PARPi have garnered attention worldwide. Mutations in the *BRCA* gene increase KEAP1-NRF2 ubiquitination and reduce Nrf2 content and cellular antioxidant capacity, which subsequently produces side effects such as cardiovascular endothelial damage and atherosclerosis. PARPi has hematologic toxicity, producing thrombocytopenia, fatigue, nausea, and vomiting. These side effects not only reduce patients' quality of life, but also affect their survival. Studies have shown that natural phytochemicals, a class of compounds with antitumor potential, can effectively prevent and treat the side effects of chemotherapy. Herein, we reviewed the role of natural phytochemicals in disease prevention and treatment in recent years, including sulforaphane, lycopene, catechin, and curcumin, and found that these phytochemicals have significant alleviating effects on atherosclerosis, nausea, and vomiting. Moreover, these mechanisms of action significantly correlated with the side-effect-producing mechanisms of *BRCA* mutations and PARPi. In conclusion, natural phytochemicals may be effective in alleviating the side effects of *BRCA* mutant ovarian cancer cells and PARP inhibitors.

1 Introduction

Ovarian cancer is among most common malignancies in gynecology (Bookman et al., 2009). Two hundred thousand women worldwide are diagnosed with ovarian cancer each year, 70% of whom are intermediate to advanced cases, with a mortality rate of 62.5%. High-grade plasmacytoma is a common type of ovarian cancer that arises from ovarian epithelial cells. It is poorly differentiated, highly malignant, and has a high recurrence rate (Colombo et al., 2019). According to treatment guidelines, ovarian cancer is treated chiefly with platinum drugs in combination with paclitaxel or with the anti-angiogenic drug bevacizumab alone (Perren et al., 2011). Platinum drugs are key to treating platinum-sensitive recurrent ovarian cancer; however, as the number of recurrences increases, this type of ovarian cancer becomes resistant to platinum drugs (Foley et al., 2013). The median progression-free survival (PFS) for bevacizumab was 19.0 months, slightly higher than the median PFS in the standard treatment group (17.3 months), as noted by the European Society of Medical Oncology and the International Society for Gynecologic Cancer meetings (Perren et al., 2011). Although rational treatment significantly prolongs patient survival, 70–80% of patients experience relapse or further disease progression after first-line treatment (Lorusso et al., 2020). PARPi, an inhibitor of polyadenosine diphosphate ribose polymerase, extends PFS to approximately 5–6 months in patients with platinum-resistant, BRCA-deficient, or refractory ovarian cancer by affecting the self-replication of ovarian cancer cells, providing a new approach for the maintenance treatment of ovarian cancer patients (Mirza et al., 2019; Vanacker et al., 2021).

Numerous studies have demonstrated that phytochemicals extracted from foods have antitumor potential. Audesh et al. found that some phytochemicals extracted from fruits have significant inhibitory effects on human ovarian teratoma cells (PA-1) at their respective IC50 concentrations (Li et al., 2021). Phytochemicals have been extensively studied to inhibit the development of ovarian cancer, and interfere with cancer cells along with antioxidant and anti-inflammatory effects (Pundir et al., 2021). Islam et al. demonstrated that the antioxidant and anti-inflammatory effects of phytochemicals were effective in preventing some side effects of chemotherapy (Islam et al., 2021). Chemotherapy plays a very important role in ovarian cancer treatment, but its side effects also seriously affect patients' quality of life, and symptomatic supportive treatment to alleviate these side effects will further increase the burden on the patient's body. In contrast to drugs, various types of phytochemicals, such as phenols, terpenoids, and sulfur-containing compounds, are distributed in numerous fruits and vegetables consumed daily (Roy and Datta, 2019). The use of phytochemicals as an alternative to drugs would reduce the patient's fear and organismal burden of oncologic chemotherapy and improve patient compliance.

This study reviewed the mitigating effects of phytochemicals on PARPi side effects and the prevention of pathological changes caused by BRCA mutations. We further clarified the mechanisms by which phytochemicals alleviate the side effects of synergistic lethal treatment regimens.

2 PARP, PARPi, and ovarian cancer

2.1 PARP and ovarian cancer

Poly (adenosine diphosphate ribose) polymerase (PARP) is a cleavage substrate for the core members of apoptosis, caspases. PARP is also involved in damage repair after DNA breaks (Wei and Yu, 2016). PARP1 plays more than 90% of the total role of the PARP family, and PARP1 is active in base excision repair (BER) (Durkacz et al., 1980), DNA single-strand breaks (SSB) (Haince et al., 2008), DNA double-strand breaks (DSBs), and replication fork damage (Haince et al., 2008). After DNA damage, PARP1 recognizes the damage through the zinc finger structural domain and orientates to the nick for ADP ribosylation based on nicotinamide adenine dinucleotide (NAD+), forming PARP-1-ADP ribose branched chain, which reduces the binding of PARP1 to DNA and dissociates from DNA to participate in DNA repair (Bürkle, 2001; Lord and Ashworth, 2017), PARP2 is similar to PARP1 in function, but it acts on different substrates (Kutuzov et al., 2020), and PARP2 is crucial in the repair of SSBs. It is by damaging DNA and thus affecting mitosis that cisplatin treats ovarian cancer. Thus, PARP plays a key role in apoptosis and repair of platinum-induced DNA damage in ovarian cancer cells (Hoeijmakers, 2001; Damia and Broggini, 2019).

2.1 PARPi and ovarian cancer

PARPi competes with NAD+ for the PARP active site, thereby inhibiting the formation of poly (ADP-ribose) polymers; when single-strand damage occurs in DNA molecules, the repair is mainly accomplished by PARP and DNA ligase IIIa (Murai et al., 2012; Murai et al., 2014). PARPi can bind specifically to the NAD+ binding site of PARP1 (and/or PARP2), resulting in a significant reduction in DNA-PARP dissociation, maintaining PARP binding to DNA, thus perpetuating the DNA-PARP complex and inhibiting subsequent repair. This process is known as "trapping" of the DNA-PARP complex (Murai et al., 2012). The persistence of the complex on a single strand of DNA allows for the accumulation of large amounts of single-stranded broken DNA and thus DSBs, causing cell death. To resolve these barriers and restore the cell cycle, functional homologous recombination (HR) must be utilized (Bunting et al., 2010).
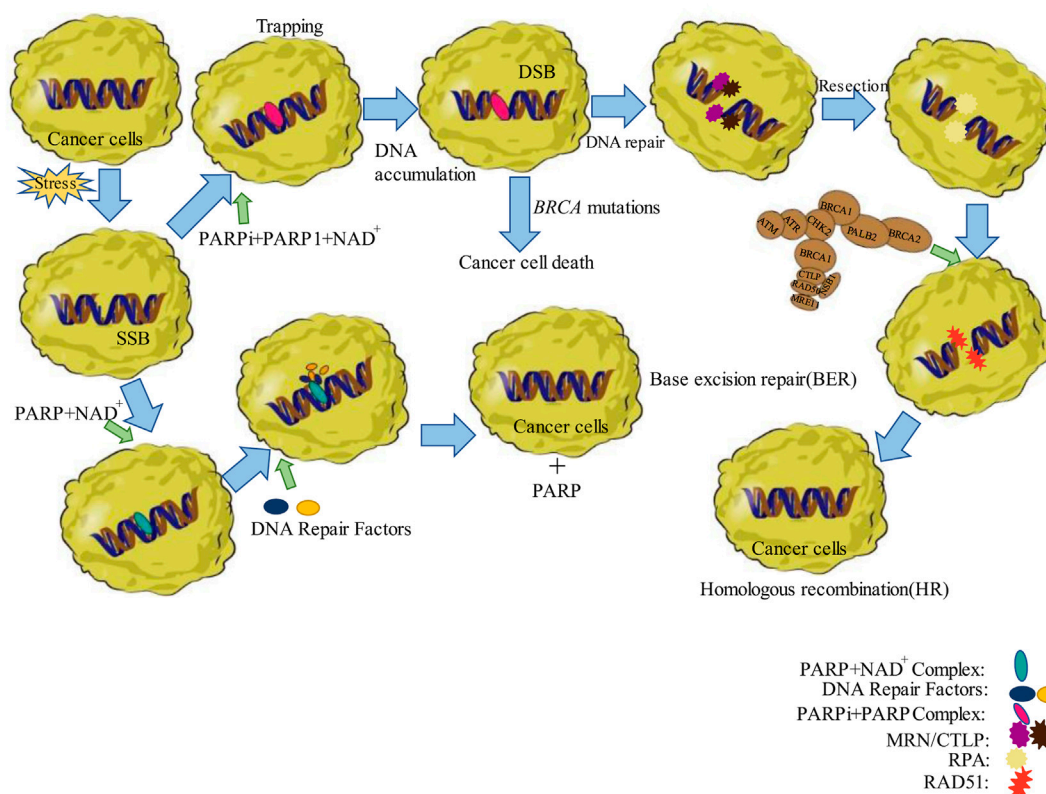
FIGURE 1
Schematic representation of the functions of PARP and *BRCA* in DNA repair. The left side shows base excision repair. Right side shows the "trapping" of the DNA-PARP complex and DNA homologous recombination repair. Abbreviations: DSB, double-strand break; MRN/CTLP, DNA damage sensor; NAD+, nicotinamide adenine dinucleotide; RAD51, restriction-associated site DNA51; RPA, replication proteinase A; SSB, single-strand break.

3 *BRCA* gene mutation, PARPi, and ovarian cancer

3.1 *BRCA* gene mutations and ovarian cancer

Breast cancer susceptibility gene (*BRCA*) participates in DNA repair and is present in the human body as a tumor suppressor gene (Prakash et al., 2015). Carriers of *BRCA1* and *BRCA2* germline mutations have a 54% and 23% risk, respectively, of developing ovarian cancer (Ramus and Gaylher, 2009; Milne and Antoniou, 2011). First, *BRCA* proteins act through the HR process to protect humans (Bryant et al., 2005). HR ensures that the cellular repair of DSBs in the S-phase is precise and error-free (Farmer et al., 2005). The function of *BRCA1* in HR is to cleave DSB $5'$–$3'$, leaving an overhanging $3'$. HR is an essential method of DNA double-strand break repair. The HR repair pathway is purportedly blocked by *BRCA* (*BRCA1/2*) mutations. In

this case, the DSB repair mechanism is no longer stable and the DNA damage repair function of the cell is greatly reduced. Therefore, cancer cells damaged by platinum cannot be repaired (Bryant et al., 2005; D'Andrea, 2018; Li et al., 2020). This suggests that BRCA plays a role in the repair of DSBs (Gudmundsdottir and Ashworth, 2006). The application of platinum-based drugs after *BRCA* mutations can inhibit DNA replication in ovarian cancer cells (Birkbak et al., 2012).

3.2 Synergistic lethal effects of *BRCA* mutations and PARPi in ovarian cancer

If PARPi is used in the presence of *BRCA* mutations in ovarian or breast cancer cells, then, it will further inhibit DNA break repair due to HR defects, and the cells will be unable to repair DSBs leading to cell death, a synergistic lethal phenomenon (Rottenberg et al., 2008; Srinivasan et al., 2017).

TABLE 1 The side effect loci of phytochemistry in the prevention of *BRCA* mutations and PARPi.

Category	Name	Mode of action	Site of action
Sulfur-containing compounds			
	Sulforaphane	Interferents	Keap1, Nrf2
	Allicin	Supplements	GSH, GPX
Terpenoids			
	Lycopene	Regulatory proteins	P62, Keap1, Nrf2
	Lutein	Regulatory proteins	ERK, Nrf2
Polyphenols			
	Catechins	Agonists	CAT, GSH
	Proanthocyanidins	Ca^+ regulation	NO, SOD2, GPX, NOX4
	Quercetin	o-Diphenol hydroxyl	-OH, O2-
Polyphenols			
	Anthocyanin	For electronics	Free radicals
	Soy isoflavones	For hydrogen atoms	Free radicals
	Curcumin	Regulatory proteins	miR-125b, HAT
	Ginger	Interferents	5-HT
	Cyclic adenosine monophosphate	Agonist	Erythropoietin
	Crocin	Interferon	Platelets

This phenomenon destabilizes the tumor genome, which can counteract the tumor cell proliferation and effectively increase the patients' survival time. Therefore, PARPi induces cell death in HR-deficient cells as a primary approach for the treatment of ovarian cancer (Noordermeer and van Attikum, 2019; Curtin and Szabo, 2020) as shown in Figure 1.

4 Mitigation of adverse drug reactions to PARPi by phytochemicals

4.1 Side effects of PARPi

The use of PARPi in patients with *BRCA*-deficient ovarian cancer has had notable success, but the use of PARPi induces discomfort in ovarian cancer patients. For example, the hematologic toxicity produced by niraparib (ZEJULA), a highly absorbed, highly permeable drug, should not be underestimated. Berek observed in 553 patients who added niraparib, that about 33% developed thrombocytopenia and 13% developed anemia (Berek et al., 2018). Meanwhile, data published by LaFargue et al. (2019) showed that the probability of fatigue in the first month after niraparib was approximately 32.4%, vomiting was about 19.6%, and nausea was up to 61.9%. Most of the fatigue was due to ischemia and decreased platelet count. Olaparib (Lynparza), a low permeability, low absorption drug, is highly susceptible to hypertension, with a 48% chance of nausea and vomiting. The side effects of PARPi seriously affect patients' quality of life (Munroe and Kolesar, 2016; Paik, 2021).

4.2 Mitigation of PARPi side effects by phytochemicals

Phytochemicals have strong antioxidant properties and are commonly used for skin care. However, numerous studies have shown that saffron, cyclic adenosine phosphate, and curcumin from ginger can reduce the incidence of some chemotherapy side effects, such as nausea, vomiting, and anemia, at the sites shown in Table 1.

4.2.1 Crocin

Crocin, a carotenoid present in the stigma of saffron, improves collagen-induced platelet aggregation and adhesion and A23187-mediated endogenous production of ROS and H_2O_2 in platelet mitochondria (Thushara et al., 2013; Yaribeygi et al., 2018). Pourmasoumi et al. (2019) reported significant decreases in diastolic blood pressure, body weight, and other factors associated with cardiovascular disease (CVD) in 622 individuals taking Crocin. Javandoost et al. (2017) found that adding Crocin was associated with a significant increase in high-density lipoprotein (HDL) levels during an 8-week Crocin intervention. The addition of Crocin to PARPi not only reduces oxidative stress but also prevents the reduction of platelets and increases blood pressure. Crocin also reduces HDL production, which can reduce the prevalence of CVD in several ways.

4.2.2 Adenosine cyclic phosphate

The high content of cyclic adenosine phosphate in jujube can dilate blood vessels, provide nutrients to the heart muscle and
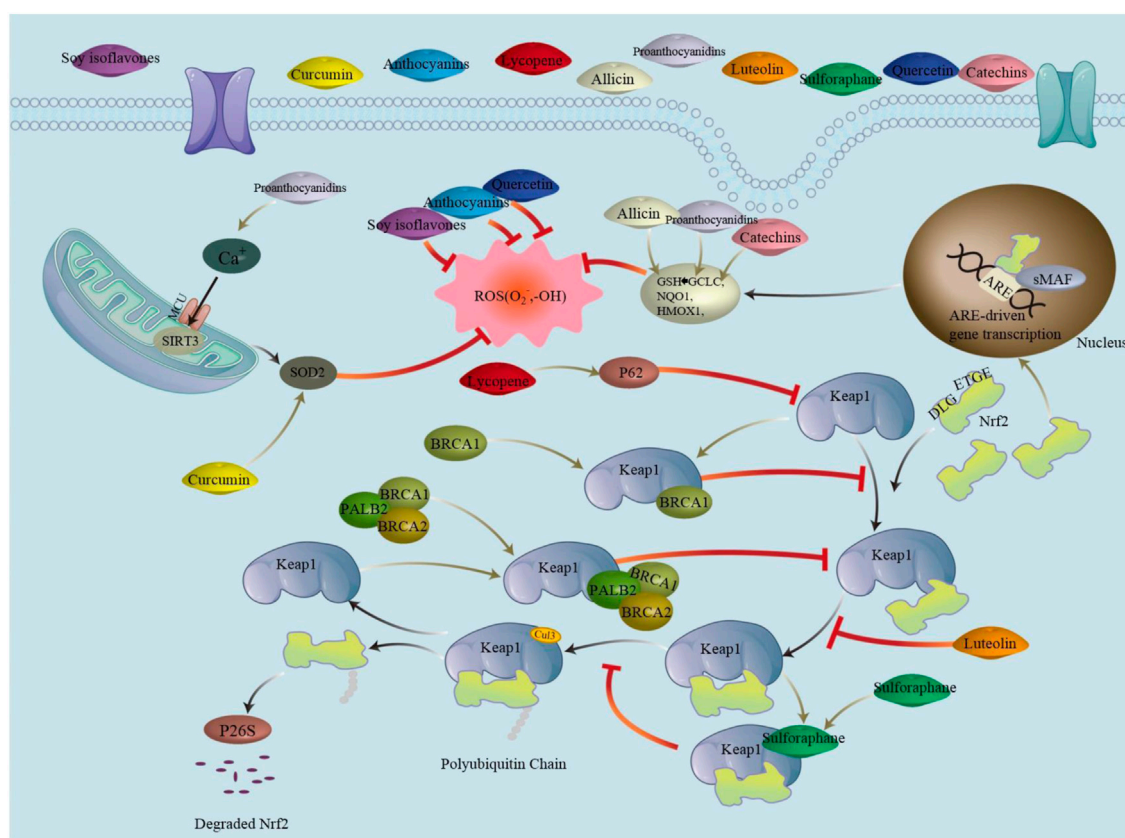
FIGURE 2
Nrf2/Keap1 is a signaling pathway in which Nrf2 binds to Keap1 *via* ETGE and DLG, ubiquitinating it, which is then degraded by the proteasome. Phytochemicals can promote nuclear translocation of Nrf2 by mediating the Keap1-Nrf2 complex. Binding ARE after forming a heterodimer with sMAF activates transcriptional production of downstream antioxidant enzymes. Phytochemicals can also affect ROS production by acting directly on ROS. Abbreviations: ARE, antioxidant response element; *BRCA* (1/2), breast cancer 1/2; CUL3, cullin3; DLG/ETGE, nrf2 structural domain; Keap1, recombinant kelch like ech associated protein1; MCU, mitochondrial calcium uniporter; Nrf2, nuclear factor erythroid 2-related factor 2; PALB2, partner and localizer of brca2; ROS, reactive oxygen species; SIRT3, silence regulatory protein3; sMAF, specific macrophage arming factor; SOD2, superoxide dismutase.

increase its contractility, induce the expression of erythropoietin, and stimulate hematopoiesis in the body (Chen and Tsim, 2020). The increase in hematopoietic parameters after cancer treatment in mice with jujube further suggests that jujube can ameliorate anemia in cancer patients (Periasamy et al., 2020). Improvement in anemia results in patients feeling less fatigued. The cyclic adenosine phosphate in dates may reduce the discomfort experienced by patients after niraparib administration.

4.2.3 Ginger active substance

The use of ginger as an antiemetic is well-known in China and is used in traditional Chinese medicine, where ginger is rich in curcumin, curcumin, gingerols, and curcuminoids (Ahmed et al., 2021). These active substances influence gastrointestinal motility and promote gastric emptying, while they affect the central nervous system by mediating the 5-hydroxytryptamine-3 of 5-hydroxytryptamine (5-HT), reducing nausea and vomiting

(Nocerino et al., 2021). Marx et al. (2017) conducted a double-blind randomized intervention with ginger in 51 patients, identifying less fatigue in the intervention group ($p = 0.006$) from the three chemotherapy cycles, especially in the third cycle. Subsequently, Crichton et al. (2019) found through a meta-analysis that ginger supplementation not only had a significant effect in suppressing nausea and vomiting but also reduced the likelihood of fatigue by approximately 80%. Therefore, the administration of ginger in the treatment of ovarian cancer with PARPi can reduce PARPi side effects in patients.

Saffron, cyclic adenosine phosphate, and curcumin have a significant inhibitory effect on the side effects caused by niraparib and olaparib, as shown in Figure 2. In the future, a rational combination could reduce the pain associated with treatment of ovarian cancer patients and increase their quality of life.

5 Phytochemicals attenuate adverse effects in *BRCA* mutations synergistically lethal with PARPi

5.1 *BRCA* mutations cause cardiovascular disease

Mutations or deletions of *BRCA* in normal individuals significantly increase the risk of developing cancers, such as ovarian cancer (Sekine et al., 2021). However, diseases beyond ovarian or breast cancer are associated with *BRCA*, and analysis excluding causes of cancer death found that survival was also significantly lower in individuals with mutations or deletions in *BRCA* (Mai et al., 2009).

Many survival studies on *BRCA* gene deletions have sufficiently demonstrated that cardiovascular-related diseases are another critical cause of death in individuals with *BRCA* mutations or deletions (Arts-de Jong et al., 2014; Lammert et al., 2022). Sajjad et al. (2017) studied 401 cancer-free female *BRCA1/2* mutation carriers and found that *BRCA* mutation carriers were at increased risk of cardiovascular disease compared to the general population. Zhou et al. noted that *BRCA* gene deletion causes cardiac diseases including ischemic heart disease, atherosclerosis, and other myocardial diseases (Arts-de Jong et al., 2014). Atherosclerosis is a major cause of aortic disease, peripheral vascular-related diseases, coronary heart disease, and cerebral infarction (Alexander et al., 2021; Shea et al., 2021). Therefore, addressing atherosclerosis is key to preventing cardiovascular diseases caused by *BRCA* defects.

Atherosclerosis has been extensively studied, and through the analysis of causative factor ranking, endothelial dysfunction has been established as the factor of atherosclerosis (Gimbrone and García-Cardeña, 2016), and apoptosis of endothelial cells plays a crucial role in the occurrence of endothelial dysfunction (Xu et al., 2021), thus, can be suggested that endothelial cell injury plays a driving role in atherosclerosis (Zheng et al., 2017). Therefore, inhibiting endothelial cell apoptosis in atherosclerosis can help prevent atherosclerosis development (Gimbrone and García-Cardeña, 2016).

Low-density lipoprotein (LDL) represents the beginning of the atherosclerotic response when it enters the subendothelial space from the endothelium by cellular action and is deposited in the subintima of the vessel where it is oxidized by ROS (Porter et al., 2013). Oxidation of LDL by ROS results in the formation of oxidized low-density lipoprotein (Ox-LDL), which is accompanied by endothelial destruction, binding of Ox-LDL to the scavenger receptors of macrophages, and intracellular accumulation of Ox-LDL after phagocytosis by vascular smooth muscle cells, resulting in the formation of foam cells (Porter et al., 2013). ROS cause endothelial cell apoptosis and atherosclerosis. Therefore, ROS can be used as both a marker of early atherosclerosis and as an entry point to control atherosclerosis (Panieri and Santoro, 2015). In Korea, Lee et al. (2021) used zearalenone (ZEN) to treat endothelial cells, and the rise of ROS after the activation of cytoplasmic calcium by ZEN further accelerated the apoptosis of endothelial cells, verifying that the difficulty in solving atherosclerosis lies in the treatment of LDL and ROS.

5.2 *BRCA* mutations affect atherosclerosis through Nrf2-mediated reactive oxygen species

BRCA1 regulates ROS as a newly identified Nrf2 (antioxidant transcription factor) binding protein (Vurusaner et al., 2012). In 2006, PALB2 was identified as a protein that interacts with *BRCA2* (Xia et al., 2006). *BRCA1*, *BRCA2*, and *PALB2* are involved in regulating the activity of Keap1 (KELCH-like ECH-associated protein 1)-mediated ubiquitination of Nrf2, thereby regulating the amount of Nrf2, and E3 ubiquitin ligase (cullin3) is a critical enzyme in the ubiquitination reaction, with Keap1 as its recognition subunit (Song et al., 2021). Japanese researchers have found that the ETGE and DLG motifs in the Neh2 structural domain of Nrf2 can bind to the Kelch structural domain of Keap1. ETGE of Nrf2 is bound to the Keap1 dimer using what is known as a hinge, while the Cul3-Rbx1 complex is stably bound to Keap1 using a DLG latching motif (Tong et al., 2006), forming KEAP1-NRF2, which lays the foundation for ubiquitination. Ubiquitinated Nrf2 is then transported to the 26S proteasome to be degraded and destroyed (Zhang et al., 2004). Laboratory analysis of the transfected gene revealed that cells with deletion of the *BRCA1/2* gene are more sensitive to oxidative stress (Fridlich et al., 2015). BRCA1 has an ETGE-like structure, competitively inhibits KEAP1-NRF2 ubiquitination, and increases Nrf2 content by binding to the ETGE-binding site of Keap1 (Zhou et al., 2021). Amino acids 9-44 of *PALB2* determine its linkage to *BRCA1* (Gardini et al., 2014). It was also found that PALB2 is linked to *BRCA2* in the N-terminal domain, and it is worth noting that PALB2 has a highly conserved ETGE-type Keap1 binding motif, which shares the same site of action as Keap1 and Nrf2 (Xia et al., 2007). Thus, *PALB2* can participate in the binding process between Nrf2 and Keap1, compete with Nrf2 for Keap1, inhibit KEAP1-NRF2, and stabilize Nrf2. As Nrf2 mediates the antioxidant response, PALB2 causes Nrf2 to remain in the nucleus to reduce the level of ROS in the cell and the rate of exit from the nucleus (Ma et al., 2012; Gorrini et al., 2013). In the absence of *BRCA1/2* or *PALB2*, KEAP1-NRF2 is not inhibited, ubiquitination of Nrf2 results in high ROS production, and regulating the Keap1 pathway to inhibit endothelial apoptosis and is an essential means of alleviating atherosclerosis from the root (Kobayashi et al., 2004; Singh et al., 2013).

5.3 Modulation of *BRCA* mutation-induced cardiovascular lesions by phytochemicals

The prevention of cardiovascular-related diseases through phytochemicals has garnered substantial public interest. Several phytochemicals have been shown to act as cardiovascular disease preventers in cells, animals, and human populations. Examples include sulfur-containing compounds, terpenoids, and polyphenols, the action points of which are listed in Table 1.

5.3.1 Sulfur-containing compounds
5.3.1.1 Sulforaphane

Sulforaphane (SFN), a natural isothiocyanate compound with excellent antioxidant properties, is abundant in cruciferous vegetables and is produced by the breakdown of glucose by endogenous mustard enzymes (Kaiser et al., 2021). Considering the antioxidant properties of SFN, Asif et al. (2022) found that SFN preferentially acts on c151 in Keap1 cysteine residues. In the cytoplasm, Nrf2 binds to Keap1 first due to high ETGE binding, followed by partial binding of DLG, and cullin3 recognizes Keap1 binding immediately, followed by ubiquitination and degradation of Nrf2. If Nrf2 binds to Keap1 and then SFN is added, SFN acts on c151 on Keap1, disrupting the binding of Keap1 to cullin3. Immobilization is prevented and Keap1 cannot continue to participate in the cycle to bind newly generated Nrf2 (Kobayashi et al., 2009). The reduction in Keap1 allows newly generated Nrf2 to enter the nucleus, where it binds to antioxidant response elements (ARE) to activate antioxidant responses, causing a reduction in ROS (Dinkova-Kostova et al., 2017). The regulation of Nrf2 by SFN effectively reduces endothelial cell injury, thus explaining its reduction in atherosclerosis and its role in combating cardiovascular disease (Dana and Alejandro, 2022).

5.3.1.2 Allicin

Glutathione is among the most studied cellular antioxidants. However, orally supplemented glutathione is hydrolyzed and oxidized by intestinal enzymes. Acetylcysteine (NAC) is a precursor of glutathione, and oral supplementation with NAC increases glutathione levels in the body after conversion in the liver (Schmitt et al., 2015). After NAC supplementation, glutathione peroxidase (GPX) activity is enhanced to convert reduced glutathione (GSH) to oxidized glutathione (GSSG), thereby protecting cells from ROS damage (Kwon, 2021). Allicin, also known as diallyl thiosulfate, is a sulfur-containing compound. When allicin was substituted for NAC in intervention studies, researchers also found enhanced GPX activity, which may indicate that allicin, a natural phytochemical, has specific antioxidant effects that counteract ROS production, and thus could be considered for the prevention of atherosclerosis caused by *BRCA* deficiency (Hasan et al., 2006; Catanzaro et al., 2022).

5.3.2 Terpenoids
5.3.2.1 Lycopene

Lycopene (LYC), a terpene fat-soluble natural pigment widely found in tomatoes, watermelon, carrots, and other red fruits and vegetables, can be an effective antioxidant because of its powerful ability to scavenge free radicals LYC induces autophagic degradation of Keap1 by increasing the expression of autophagic protein p62 (Ulasov et al., 2021). When Nrf2 dissociates from Keap1, then nuclear ectopic and binds to ARE in the nucleus to induce the expression of antioxidants downstream of the pathway to avoid oxidative cell death (Baird and Yamamoto, 2020; Wang et al., 2020). Since LYC intervention in rats results in a decrease in LDL and triglycerides and an increase in HDL, it was demonstrated that LYC is an anti-atherogenic phytochemical (Bentzon et al., 2014; Wong, 2014). ROS production was significantly decreased by LYC supplementation, which inhibited endothelial cell injury caused by *BRCA* deletion or mutation (Roy and Datta, 2021). This further demonstrated that LYC is essential for preventing atherosclerosis caused by *BRCA* deficiency.

5.3.2.2 Luteolin

Luteolin, also known as phytoalexin, is among the more common terpene antioxidants in nature that reduces free radical activity, prevents ROS damage to cells, and has a surprising effect on *BRCA*-deficient cancers (Gong et al., 2018). Lutein is an essential nutrient and one of the most common antioxidants found in egg yolks. Furthermore, Mitra et al. (2021) recently noted that dark-colored greens are usually high in luteins, such as kale, spinach, and lettuce. A recent study reconfirmed that the two parts of the carbon chain of lutein are hydrophilic (HO-) and hydrophobic (CH_2-), respectively (Nakamura and Sugiura, 2022). Moreover, the hydrophilic part of lutein remains on both sides of the cell membrane, whereas the hydrophobic part is in the phospholipid molecule layer, which allows lutein to bind tightly to the cell membrane lipids and increase the stability of the cell membrane (Algan et al., 2022). Conversely, luteolin activates extracellular regulated protein kinase (ERK), allowing Nrf2 phosphorylation and cleavage of the Nfr2/Keap1 complex. This causes nuclear translocation of Nrf2 to bind to the DNA regulatory region of ARE. It induces the expression of antioxidant genes and reduces intracellular ROS levels (Ahn and Kim, 2021). Luteolin can be expressed as an antioxidant that reduces the oxidative response of LDL and inhibits the development of atherosclerosis (Hajizadeh-Sharafabad et al., 2021; Ramanna and Somu, 2021). This suggests that luteolin can inhibit atherosclerosis, thereby preventing the development of CVD.

5.3.3 Polyphenols

Polyphenols significantly impact human health and are known as the "seventh nutrient." Their role in lowering antioxidant LDL and blood cholesterol has been extensively

studied (Abdal Dayem et al., 2016). Vegetables such as spinach, broccoli, and cabbage have high polyphenol contents (Zeb, 2021). Cherries, blueberries, and other dark fruits also have relatively high polyphenol contents. Polyphenols are a natural component of cocoa beans, and the high polyphenol content in black beans contributes to their unique flavor (Yang et al., 2018). Interestingly, Khan et al. (2021) reported that polyphenols not only prevent CVD, but also mediate *BRCA1/2* expression. Polyphenols can be divided into flavonoids and phenolic compounds, the most common of which are catechins, proanthocyanidins, quercetin, soy isoflavones, anthocyanins, and curcumin.

5.3.3.1 Catechins

The antioxidant capacity of catechins is even higher than that of vitamin E. Numerous studies have demonstrated that catechins can increase the activity of antioxidant enzymes (SOD2 and GPX), thus inhibiting the oxidation of LDL to Ox-LDL (Chen et al., 2020; Ahmadi et al., 2022; Dal and Yilmaz, 2022). Japanese researchers observed that LDL oxidation was prolonged in the catechin group by administering 1 g of catechin in capsule form to 19 healthy men in a double-blind crossover trial (Suzuki-Sugihara et al., 2016). The reduction in Ox-LDL levels led to a significant decrease in the probability of atherosclerosis and effectively prevented CVD caused by *BRCA* mutations.

5.3.3.2 Proanthocyanidins

Proanthocyanidins comprise varying amounts of catechins, epicatechin, and gallic acid, which are abundant in grapes and are converted into anthocyanins in plants. Proanthocyanidins play a role in CVD by preventing lipid peroxidation through calcium-dependent NO release, vasorelaxation, and the inhibition of Ox-LDL production (de la Iglesia et al., 2010). Proanthocyanidins reduce intracellular ROS production by increasing the NRF2/Keap1 ratio, increasing SOD2 expression, and inhibiting oxidase expression (NOX4 and iNOS) (Kowalska et al., 2021). In addition, proanthocyanidin supplementation can prevent ROS production from *BRCA* defects (Xian et al., 2019). This reduces the risk of atherosclerosis due to *BRCA* defects.

5.3.3.3 Quercetin

Quercetin is found at high levels in daily life in sea buckthorn, hawthorn, and buckwheat sticks. Its antioxidant capacity is 20 times that of vitamin C and 50 times that of vitamin E. This is due to the good scavenging ability of the o-diphenol hydroxyl group for superoxide anion (O_2-) and hydroxyl radical (-OH), reducing the production of oxidative stress ROS because the action of the o-diphenol hydroxyl group maintains biofilm integrity (Chu, 2022), and reduces necrosis of vascular endothelial cells. The reduction in ROS leads to the inhibition of LDL oxidation, reducing the risk of atherosclerosis and other cardiovascular diseases (Deng et al., 2020). Concurrently,

quercetin inhibits the production of platelet lipoxygenase and cyclooxygenase, which leads to the release of thrombolytic and vascular membrane-protective mediators from the endothelium to counteract thrombosis.

5.3.3.4 Anthocyanins

Anthocyanins are glycosylated anthocyanins that are widely distributed in black, red, and purple plant foods, such as black rice, mulberry, and eggplant, which have powerful antioxidant capacity (Bagchi et al., 2004). Anthocyanins are more substantial than common antioxidants, such as vitamin E, catechins, and quercetin, in scavenging free radicals. They have many phenolic hydroxyl groups, which can directly scavenge many free radicals by oxidizing and releasing electrons to maintain redox balance (Dangles and Fenger, 2018). At the same time, anthocyanins reduce the production of ROS by further activating the activity of SOD2 and GPX to reduce oxidative stress damage (Tian et al., 2019). In addition, it prevents the death of vascular endothelial cells and improves arterial blood-vessel stiffness. In patients with cardiovascular diseases deficient in *BRCA*, supplementation with anthocyanins may improve the risk of related diseases (Speciale et al., 2020).

5.3.3.5 Soy isoflavones

Estrogen secretion increases in ovarian cancer patients (Langdon et al., 2020). When estrogen levels are elevated, the structure of soy isoflavones becomes similar to that of estrogen. Therefore, soy isoflavones prevent estrogen from binding to the receptor, thus acting as estrogen antagonists (Kim, 2021). Moreover, soy isoflavones, similar to quercetin, can contribute to the antioxidant response by providing hydrogen atoms to inhibit the production of reactive oxygen radicals and reduce the level of ROS (Syamala et al., 2021). Su et al. conducted a logistic regression analysis of 500 patients with ovarian cancer and 500 normal subjects (mean age, 59 years) in southern China. They found that moderate intake of soy foods activated cellular autophagy, reduced the risk of ovarian cancer, and increased the sensitivity to carboplatin (Runlin et al., 2022). A Korean study investigated 5509 people at high risk of ovarian cancer and found a relationship between metabolism and soy isoflavone intake, with soy isoflavones being inversely associated with LDL in men and women and negatively associated with the incidence of metabolic syndrome in women. From these data, it can be concluded that soy isoflavone supplementation can inhibit metabolism-induced ROS and LDL production (Woo et al., 2019). Therefore, it is necessary to provide soy isoflavone supplementation to people with *BRCA* mutations, especially to patients with *BRCA* ovarian cancer.

5.3.3.6 Curcumin

Curcumin is a representative phenolic compound and, as a natural compound that can be extracted from the ginger family, deserves our attention as it mediates histone acetyltransferase

activity to regulate acetylation of DSB sites, thus reducing the aggregation of critical non-homologous end-joining factors to DSB sites and achieving PARPi sensitization (Ogiwara et al., 2013). Surprisingly, curcumin promotes the increase of ROS in tumor cells, causing tumor cell death (Mortezaee et al., 2019); however, in normal cells, curcumin downregulates the antioxidant response of miR-125b to reduce cell death (Schwertheim et al., 2017). When treating ovarian cancer patients with *BRCA* mutations, adjuvant treatment with curcumin can be considered, not only to increase synergistic lethality, but also to prevent the side effects of PARPi and CVD caused by *BRCA* mutations.

Phytochemicals, such as sulfur-containing compounds, terpenoids, and polyphenols, which regulate the production of ROS and the levels of HDL and LDL in different ways to prevent atherosclerosis caused by *BRCA* mutations and thus prevent CVD, are shown in Figure 2.

6 Conclusion and outlook

PARPi and *BRCA* mutations play a significant role in the treatment of ovarian cancer. Clinicians are increasingly concerned about the side effects associated with PARPi and *BRCA* mutations. Phytochemicals, mostly derived from fruits and vegetables, have a high safety profile and are easily accessible, and therefore, patients have high compliance. In this study, we sorted out the principles of phytochemicals in antioxidants and maintenance of metabolic substance balance. We found that phytochemicals such as sulfur-containing compounds, polyphenols, and terpenoids can modulate the development of atherosclerosis, a key pathological change in the process of CVD caused by *BRCA* mutations, by mediating Keap1-Nrf2, free radicals, and LDL. In addition, phytochemicals can reduce the common clinical side effects of phytochemicals in reducing nausea and vomiting, relieving fatigue, and reducing hematotoxicity by modulating 5-HT, stimulating erythropoietin secretion, and antioxidant substances. We conclude that phytochemicals can inhibit the pathological changes caused by *BRCA* mutations and alleviate the side

effects caused by PARPi by summarizing the relevant mechanisms. However, studies on phytochemicals that reduce the side effects of ovarian cancer treatment in animals are lacking, and natural phytochemicals are expected to gain wide usage in the clinical treatment of ovarian cancer.

Author contributions

CW writes the manuscript, PG and SL searches for articles, JX creates the images, WT provides valuable professional advice and guidance, JL gives language guidance, and LZ helps revise the manuscript.

Funding

Conflict of interest

The authors declare that the research was conducted in the absence of any commercial or financial relationships that could be construed as a potential conflict of interest.

Publisher's note

All claims expressed in this article are solely those of the authors and do not necessarily represent those of their affiliated organizations, or those of the publisher, the editors and the reviewers. Any product that may be evaluated in this article, or claim that may be made by its manufacturer, is not guaranteed or endorsed by the publisher.

References

Abdal Dayem, A., Choi, H. Y., Yang, G. M., Kim, K., Saha, S. K., and Cho, S. G. (2016). The anti-cancer effect of polyphenols against breast cancer and cancer stem cells: Molecular mechanisms. *Nutrients* 8 (9), 581. doi:10.3390/nu8090581

Ahmadi, A., Jamialahmadi, T., and Sahebkar, A. (2022). Polyphenols and atherosclerosis: A critical review of clinical effects on LDL oxidation. *Pharmacol. Res.* 184, 106414. doi:10.1016/j.phrs.2022.106414

Ahmed, S. H. H., Gonda, T., and Hunyadi, A. (2021). Medicinal chemistry inspired by ginger: Exploring the chemical space around 6-gingerol. *RSC Adv.* 11 (43), 26687–26699. doi:10.1039/d1ra04227k

Ahn, Y. J., and Kim, H. (2021). Lutein as a modulator of oxidative stress-mediated inflammatory diseases. *Antioxidants* 10 (9), 1448. doi:10.3390/antiox10091448

Alexander, Y., Osto, E., Schmidt-Trucksäss, A., Shechter, M., Trifunovic, D., Duncker, D. J., et al. (2021). Endothelial function in cardiovascular medicine: A consensus paper of the European society of cardiology working groups on atherosclerosis and vascular biology, aorta and peripheral vascular diseases, coronary pathophysiology and microcirculation, and thrombosis. *Cardiovasc. Res.* 117 (1), 29–42. doi:10.1093/cvr/cvaa085

Algan, A. H., Gungor-Ak, A., and Karatas, A. (2022). Nanoscale delivery systems of lutein: An updated review from a pharmaceutical perspective. *Pharmaceutics* 14 (9), 1852. doi:10.3390/pharmaceutics14091852

Arts-de Jong, M., Maas, A. H., Massuger, L. F., Hoogerbrugge, N., and de Hullu, J. A. (2014). BRCA1/2 mutation carriers are potentially at higher cardiovascular risk. *Crit. Rev. Oncol. Hematol.* 91 (2), 159–171. doi:10.1016/j.critrevonc.2014.01.008

Asif, M., Kala, C., Gilani, S. J., Imam, S. S., Mohamad, T., Naaz, F., et al. (2022). Protective effects of isothiocyanates against alzheimer's disease. *Curr. Tradit. Med.* 8 (3), 1–10. doi:10.2174/2215083807666211109121345

Bagchi, D., Sen, C., Bagchi, M., and Atalay, M. (2004). Anti-angiogenic, antioxidant, and anti-carcinogenic properties of a novel anthocyanin-rich berry extract formula. *Biochemistry*. 69 (1), 75–80. doi:10.1023/b:biry.0000016355.19999.93

Baird, L., and Yamamoto, M. (2020). The molecular mechanisms regulating the KEAP1-NRF2 pathway. *Mol. Cell. Biol.* 40 (13), 000999-20. doi:10.1128/mcb.00099-20

Bentzon, J. F., Otsuka, F., Virmani, R., and Falk, E. (2014). Mechanisms of plaque formation and rupture. *Circ. Res.* 114 (12), 1852–1866. doi:10.1161/circresaha.114.302721

Berek, J. S., Matulonis, U. A., Peen, U., Ghatage, P., Mahner, S., Redondo, A., et al. (2018). Safety and dose modification for patients receiving Niraparib. *Ann. Oncol.* 29 (8), 1784–1792. doi:10.1093/annonc/mdy181

Birkbak, N. J., Wang, Z. C., Kim, J. Y., Eklund, A. C., Li, Q., Tian, R., et al. (2012). Telomeric allelic imbalance indicates defective DNA repair and sensitivity to DNA-damaging agents. *Cancer Discov.* 2 (4), 366–375. doi:10.1158/2159-8290.Cd-11-0206

Bookman, M. A., Brady, M. F., McGuire, W. P., Harper, P. G., Alberts, D. S., Friedlander, M., et al. (2009). Evaluation of new platinum-based treatment regimens in advanced-stage ovarian cancer: A phase III trial of the gynecologic cancer intergroup. *J. Clin. Oncol.* 27 (9), 1419–1425. doi:10.1200/jco.2008.19.1684

Bryant, H. E., Schultz, N., Thomas, H. D., Parker, K. M., Flower, D., Lopez, E., et al. (2005). Specific killing of BRCA2-deficient tumours with inhibitors of poly(ADP-ribose) polymerase. *Nature* 434 (7035), 913–917. doi:10.1038/nature03443

Bunting, S. F., Callén, E., Wong, N., Chen, H. T., Polato, F., Gunn, A., et al. (2010). 53BP1 inhibits homologous recombination in Brca1-deficient cells by blocking resection of DNA breaks. *Cell* 141 (2), 243–254. doi:10.1016/j.cell.2010.03.012

Bürkle, A., and Burkle, A. (2001). Physiology and pathophysiology of poly(ADP-ribosyl)ation. *Bioessays* 23 (9), 795–806. doi:10.1002/bies.1115

Catanzaro, E., Canistro, D., Pellicioni, V., Vivarelli, F., and Fimognari, C. (2022). Anticancer potential of allicin: A review. *Pharmacol. Res.* 177, 106118. doi:10.1016/j.phrs.2022.106118

Chen, J., and Tsim, K. W. K. (2020). A review of edible jujube, the ziziphus jujuba fruit: A heath food supplement for anemia prevalence. *Front. Pharmacol.* 11, 593655. doi:10.3389/fphar.2020.593655

Chen, Y., She, Y., Shi, X., Zhang, X., Wang, R., and Men, K. (2020). Green tea catechin: Does it lower blood cholesterol? *IOP Conf. Ser. Earth Environ. Sci.* 559, 012027. doi:10.1088/1755-1315/559/1/012027

Chu, A. J. (2022). Quarter-century explorations of bioactive polyphenols: Diverse health benefits. *Front. Biosci.* 27 (4), 134. doi:10.31083/j.fbl2704134

Colombo, N., Sessa, C., du Bois, A., Ledermann, J., McCluggage, W. G., McNeish, I., et al. (2019). ESMO-ESGO consensus conference recommendations on ovarian cancer: Pathology and molecular biology, early and advanced stages, borderline tumours and recurrent disease. *Ann. Oncol.* 30 (5), 672–705. doi:10.1093/annonc/mdz062

Crichton, M., Marshall, S., Marx, W., McCarthy, A. L., and Isenring, E. (2019). Efficacy of ginger (zingiber officinale) in ameliorating chemotherapy-induced nausea and vomiting and chemotherapy-related outcomes: A systematic review update and meta-analysis. *J. Acad. Nutr. Diet.* 119 (12), 2055–2068. doi:10.1016/j.jand.2019.06.009

Curtin, N. J., and Szabo, C. (2020). Poly(ADP-ribose) polymerase inhibition: Past, present and future. *Nat. Rev. Drug Discov.* 19 (10), 711–736. doi:10.1038/s41573-020-0076-6

D'Andrea, A. D. (2018). Mechanisms of PARP inhibitor sensitivity and resistance. *DNA Repair (Amst)* 71, 172–176. doi:10.1016/j.dnarep.2018.08.021

Dal, H. Ö. G., and Yilmaz, Y. (2022). "Use of tea catechins in foods as a functional ingredient," in *Tea as a food ingredient* (Boca Raton, Florida, United States: CRC Press), 241–257.

Damia, G., and Broggini, M. (2019). Platinum resistance in ovarian cancer: Role of DNA repair. *Cancers (Basel)* 11 (1), 119. doi:10.3390/cancers11010119

Dana, A.-H., and Alejandro, S.-P. (2022). Role of sulforaphane in endoplasmic reticulum homeostasis through regulation of the antioxidant response. *Life Sci.* 299, 120554. doi:10.1016/j.lfs.2022.120554

Dangles, O., and Fenger, J.-A. (2018). The chemical reactivity of anthocyanins and its consequences in food science and nutrition. *Molecules* 23 (8), 1970. doi:10.3390/molecules23081970

de la Iglesia, R., Milagro, F. I., Campión, J., Boqué, N., and Martínez, J. A. (2010). Healthy properties of proanthocyanidins. *Biofactors* 36 (3), 159–168. doi:10.1002/biof.79

Deng, Q., Li, X. X., Fang, Y., Chen, X., and Xue, J. (2020). Therapeutic potential of quercetin as an antiatherosclerotic agent in atherosclerotic cardiovascular disease: A review. *Evid. Based. Complement. Altern. Med.* 2020, 5926381. doi:10.1155/2020/5926381

Dinkova-Kostova, A. T., Fahey, J. W., Kostov, R. V., and Kensler, T. W. (2017). KEAP1 and done? Targeting the NRF2 pathway with sulforaphane. *Trends Food Sci. Technol.* 69, 257–269. doi:10.1016/j.tifs.2017.02.002

Durkacz, B. W., Omidiji, O., Gray, D. A., and Shall, S. (1980). (ADP-ribose)n participates in DNA excision repair. *Nature* 283 (5747), 593–596. doi:10.1038/283593a0

Farmer, H., McCabe, N., Lord, C. J., Tutt, A. N., Johnson, D. A., Richardson, T. B., et al. (2005). Targeting the DNA repair defect in BRCA mutant cells as a therapeutic strategy. *Nature* 434 (7035), 917–921. doi:10.1038/nature03445

Foley, O. W., Rauh-Hain, J. A., and del Carmen, M. G. (2013). Recurrent epithelial ovarian cancer: An update on treatment. *Oncol. Willist. Park* 27 (4), 288–298.

Fridlich, R., Annamalai, D., Roy, R., Bernheim, G., and Powell, S. N. (2015). BRCA1 and BRCA2 protect against oxidative DNA damage converted into double-strand breaks during DNA replication. *DNA Repair (Amst)* 30, 11–20. doi:10.1016/j.dnarep.2015.03.002

Gardini, A., Baillat, D., Cesaroni, M., and Shiekhattar, R. (2014). Genome-wide analysis reveals a role for BRCA1 and PALB2 in transcriptional co-activation. *Embo J.* 33 (8), 890–905. doi:10.1002/embj.201385567

Gimbrone, M. A., Jr., and García-Cardeña, G. (2016). Endothelial cell dysfunction and the pathobiology of atherosclerosis. *Circ. Res.* 118 (4), 620–636. doi:10.1161/circresaha.115.306301

Gong, X., Smith, J. R., Swanson, H. M., and Rubin, L. P. (2018). Carotenoid lutein selectively inhibits breast cancer cell growth and potentiates the effect of chemotherapeutic agents through ROS-mediated mechanisms. *Molecules* 23 (4), 905. doi:10.3390/molecules23040905

Gorrini, C., Baniasadi, P. S., Harris, I. S., Silvester, J., Inoue, S., Snow, B., et al. (2013). BRCA1 interacts with Nrf2 to regulate antioxidant signaling and cell survival. *J. Exp. Med.* 210 (8), 1529–1544. doi:10.1084/jem.20121337

Gudmundsdottir, K., and Ashworth, A. (2006). The roles of BRCA1 and BRCA2 and associated proteins in the maintenance of genomic stability. *Oncogene* 25 (43), 5864–5874. doi:10.1038/sj.onc.1209874

Haince, J. F., McDonald, D., Rodrigue, A., Déry, U., Masson, J. Y., Hendzel, M. J., et al. (2008). PARP1-dependent kinetics of recruitment of MRE11 and NBS1 proteins to multiple DNA damage sites. *J. Biol. Chem.* 283 (2), 1197–1208. doi:10.1074/jbc.M706734200

Hajizadeh-Sharafabad, F., Tarighat-Esfanjani, A., Ghoreishi, Z., and Sarreshtedari, M. (2021). Lutein supplementation combined with a low-calorie diet in middle-aged obese individuals: Effects on anthropometric indices, body composition and metabolic parameters. *Br. J. Nutr.* 126 (7), 1028–1039. doi:10.1017/S0007114520004997

Hasan, N., Yusuf, N., Toossi, Z., and Islam, N. (2006). Suppression of *Mycobacterium tuberculosis* induced reactive oxygen species (ROS) and TNF-alpha mRNA expression in human monocytes by allicin. *FEBS Lett.* 580 (10), 2517–2522. doi:10.1016/j.febslet.2006.03.071

Hoeijmakers, J. H. (2001). Genome maintenance mechanisms for preventing cancer. *Nature* 411 (6835), 366–374. doi:10.1038/35077232

Islam, S. U., Ahmed, M. B., Ahsan, H., Lee, Y.-S., Shehzad, A., Sonn, J. K., et al. (2021). An update on the role of dietary phytochemicals in human skin cancer: New insights into molecular mechanisms. *Antioxidants* 10 (5), 916. doi:10.3390/antiox9100916

Javandoost, A., Afshari, A., Nikbakht-Jam, I., Khademi, M., Eslami, S., Nosrati, M., et al. (2017). Effect of crocin, a carotenoid from saffron, on plasma cholesteryl ester transfer protein and lipid profile in subjects with metabolic syndrome: A double blind randomized clinical trial. *ARYA Atheroscler.* 13 (5), 245–252.

Kaiser, A. E., Baniasadi, M., Giansiracusa, D., Giansiracusa, M., Garcia, M., Fryda, Z., et al. (2021). Sulforaphane: A broccoli bioactive phytocompound with cancer preventive potential. *Cancers* 13 (19), 4796. doi:10.3390/cancers13194796

Khan, H., Labanca, F., Ullah, H., Hussain, Y., Tzvetkov, N. T., Akkol, E. K., et al. (2021). Advances and challenges in cancer treatment and nutraceutical prevention: The possible role of dietary phenols in BRCA regulation. *Phytochem. Rev.* 21, 385–400. doi:10.1007/s11101-021-09771-3

Kim, I.-S. (2021). Current perspectives on the beneficial effects of soybean isoflavones and their metabolites for humans. *Antioxidants* 10 (7), 1064. doi:10.3390/antiox10071064

Kobayashi, A., Kang, M. I., Okawa, H., Ohtsuji, M., Zenke, Y., Chiba, T., et al. (2004). Oxidative stress sensor Keap1 functions as an adaptor for Cul3-based E3 ligase to regulate proteasomal degradation of Nrf2. *Mol. Cell. Biol.* 24 (16), 7130–7139. doi:10.1128/mcb.24.16.7130-7139.2004

Kobayashi, M., Li, L., Iwamoto, N., Nakajima-Takagi, Y., Kaneko, H., Nakayama, Y., et al. (2009). The antioxidant defense system Keap1-Nrf2 comprises a multiple sensing mechanism for responding to a wide range of chemical compounds. *Mol. Cell. Biol.* 29 (2), 493–502. doi:10.1128/mcb.01080-08

Kowalska, K., Dembczyński, R., Gołąbek, A., Olkowicz, M., and Olejnik, A. (2021). ROS modulating effects of lingonberry (vaccinium vitis-idaea L.) polyphenols on obese adipocyte hypertrophy and vascular endothelial dysfunction. *Nutrients* 13 (3), 885. doi:10.3390/nu13030885

Kutuzov, M. M., Belousova, E. A., Ilina, E. S., and Lavrik, O. I. (2020). Impact of PARP1, PARP2 & PARP3 on the base excision repair of nucleosomal DNA. *Adv. Exp. Med. Biol.* 1241, 47–57. doi:10.1007/978-3-030-41283-8_4

Kwon, Y. (2021). Possible beneficial effects of n-acetylcysteine for treatment of triple-negative breast cancer. *Antioxidants* 10 (2), 169. doi:10.3390/antiox10020169

LaFargue, C. J., Dal Molin, G. Z., Sood, A. K., and Coleman, R. L. (2019). Exploring and comparing adverse events between PARP inhibitors. *Lancet. Oncol.* 20 (1), e15–e28. doi:10.1016/s1470-2045(18)30786-1

Lammert, J., Basrai, M., Struck, J., Hartmann, O., Engel, C., Bischoff, S. C., et al. (2022). Associations of plasma bioactive adrenomedullin levels with cardiovascular risk factors in BRCA1/2 mutation carriers. *Geburtshilfe Frauenheilkd.* 82 (6), 601–609. doi:10.1055/a-1811-2164

Langdon, S. P., Herrington, C. S., Hollis, R. L., and Gourley, C. (2020). Estrogen signaling and its potential as a target for therapy in ovarian cancer. *Cancers* 12 (6), 1647. doi:10.3390/cancers12061647

Lee, H.-J., Oh, S.-Y., and Jo, I. (2021). Zearalenone induces endothelial cell apoptosis through activation of a cytosolic Ca2+/ERK1/2/p53/Caspase 3 signaling pathway. *Toxins* 13 (3), 187. doi:10.3390/toxins13030187

Li, H., Liu, Z. Y., Wu, N., Chen, Y. C., Cheng, Q., and Wang, J. (2020). PARP inhibitor resistance: The underlying mechanisms and clinical implications. *Mol. Cancer* 19 (1), 107. doi:10.1186/s12943-020-01227-0

Li, L., Mangali, S., Kour, N., Dasari, D., Ghatage, T., Sharma, V., et al. (2021). Syzygium cumini (jamun) fruit-extracted phytochemicals exert anti-proliferative effect on ovarian cancer cells. *J. Cancer Res. Ther.* 17 (6), 1547–1551. doi:10.4103/jcrt.JCRT_210_20

Lord, C. J., and Ashworth, A. (2017). PARP inhibitors: Synthetic lethality in the clinic. *Science* 355 (6330), 1152–1158. doi:10.1126/science.aam7344

Lorusso, D., Ceni, V., Daniele, G., Salutari, V., Pietragalla, A., Muratore, M., et al. (2020). Newly diagnosed ovarian cancer: Which first-line treatment? *Cancer Treat. Rev.* 91, 102111. doi:10.1016/j.ctrv.2020.102111

Ma, J., Cai, H., Wu, T., Sobhian, B., Huo, Y., Alcivar, A., et al. (2012). PALB2 interacts with KEAP1 to promote NRF2 nuclear accumulation and function. *Mol. Cell. Biol.* 32 (8), 1506–1517. doi:10.1128/mcb.06271-11

Mai, P. L., Chatterjee, N., Hartge, P., Tucker, M., Brody, L., Struewing, J. P., et al. (2009). Potential excess mortality in BRCA1/2 mutation carriers beyond breast, ovarian, prostate, and pancreatic cancers, and melanoma. *PLoS One* 4 (3), e4812. doi:10.1371/journal.pone.0004812

Marx, W., McCarthy, A. L., Ried, K., McKavanagh, D., Vitetta, L., Sali, A., et al. (2017). The effect of a standardized ginger extract on chemotherapy-induced nausea-related quality of life in patients undergoing moderately or highly emetogenic chemotherapy: A double blind, randomized, placebo controlled trial. *Nutrients* 9 (8), 867. doi:10.3390/nu9080867

Milne, R. L., and Antoniou, A. C. (2011). Genetic modifiers of cancer risk for BRCA1 and BRCA2 mutation carriers. *Ann. Oncol.* 22 (1), i11–i17. doi:10.1093/annonc/mdq660

Mirza, M. R., Åvall Lundqvist, E., Birrer, M. J., dePont Christensen, R., Nyvang, G. B., Malander, S., et al. (2019). Niraparib plus bevacizumab versus niraparib alone for platinum-sensitive recurrent ovarian cancer (NSGO-AVANOVA2/ENGOT-ov24): A randomised, phase 2, superiority trial. *Lancet. Oncol.* 20 (10), 1409–1419. doi:10.1016/s1470-2045(19)30515-7

Mitra, S., Rauf, A., Tareq, A. M., Jahan, S., Emran, T. B., Shahriar, T. G., et al. (2021). Potential health benefits of carotenoid lutein: An updated review. *Food Chem. Toxicol.* 154, 112328. doi:10.1016/j.fct.2021.112328

Mortezaee, K., Salehi, E., Mirtavoos-mahyari, H., Motevaseli, E., Najafi, M., Farhood, B., et al. (2019). Mechanisms of apoptosis modulation by curcumin: Implications for cancer therapy. *J. Cell. Physiol.* 234 (8), 12537–12550. doi:10.1002/jcp.28122

Munroe, M., and Kolesar, J. (2016). Olaparib for the treatment of BRCA-mutated advanced ovarian cancer. *Am. J. Health. Syst. Pharm.* 73 (14), 1037–1041. doi:10.2146/ajhp150550

Murai, J., Huang, S. Y., Das, B. B., Renaud, A., Zhang, Y., Doroshow, J. H., et al. (2012). Trapping of PARP1 and PARP2 by clinical PARP inhibitors. *Cancer Res.* 72 (21), 5588–5599. doi:10.1158/0008-5472.Can-12-2753

Murai, J., Huang, S. Y., Renaud, A., Zhang, Y., Ji, J., Takeda, S., et al. (2014). Stereospecific PARP trapping by BMN 673 and comparison with olaparib and rucaparib. *Mol. Cancer Ther.* 13 (2), 433–443. doi:10.1158/1535-7163.Mct-13-0803

Nakamura, M., and Sugiura, M. (2022). Serum lutein and zeaxanthin are inversely associated with high-sensitivity C-reactive protein in non-smokers: The mikkabi study. *Antioxidants* 11 (2), 259. doi:10.3390/antiox11020259

Nocerino, R., Cecere, G., Micillo, M., De Marco, G., Ferri, P., Russo, M., et al. (2021). Efficacy of ginger as antiemetic in children with acute gastroenteritis: A randomised controlled trial. *Aliment. Pharmacol. Ther.* 54 (1), 24–31. doi:10.1111/apt.16404

Noordermeer, S. M., and van Attikum, H. (2019). PARP inhibitor resistance: A tug-of-war in BRCA-mutated cells. *Trends Cell Biol.* 29 (10), 820–834. doi:10.1016/j.tcb.2019.07.008

Ogiwara, H., Ui, A., Shiotani, B., Zou, L., Yasui, A., and Kohno, T. (2013). Curcumin suppresses multiple DNA damage response pathways and has potency as a sensitizer to PARP inhibitor. *Carcinogenesis* 34 (11), 2486–2497. doi:10.1093/carcin/bgt240

Paik, J. (2021). Olaparib: A review as first-line maintenance therapy in advanced ovarian cancer. *Target. Oncol.* 16 (6), 847–856. doi:10.1007/s11523-021-00842-1

Panieri, E., and Santoro, M. M. (2015). ROS signaling and redox biology in endothelial cells. *Cell. Mol. Life Sci.* 72 (17), 3281–3303. doi:10.1007/s00018-015-1928-9

Periasamy, S., Wu, W. H., Chien, S. P., Liu, C. T., and Liu, M. Y. (2020). Dietary ziziphus jujuba fruit attenuates colitis-associated tumorigenesis: A pivotal role of the NF-κB/IL-6/JAK1/STAT3 pathway. *Nutr. Cancer* 72 (1), 120–132. doi:10.1080/01635581.2019.1615515

Perren, T. J., Swart, A. M., Pfisterer, J., Ledermann, J. A., Pujade-Lauraine, E., Kristensen, G., et al. (2011). A phase 3 trial of bevacizumab in ovarian cancer. *N. Engl. J. Med.* 365 (26), 2484–2496. doi:10.1056/NEJMoa1103799

Porter, S. A., Pedley, A., Massaro, J. M., Vasan, R. S., Hoffmann, U., and Fox, C. S. (2013). Aminotransferase levels are associated with cardiometabolic risk above and beyond visceral fat and insulin resistance: The framingham heart study. *Arterioscler. Thromb. Vasc. Biol.* 33 (1), 139–146. doi:10.1161/atvbaha.112.300075

Pourmasoumi, M., Hadi, A., Najafgholizadeh, A., Kafeshani, M., and Sahebkar, A. (2019). Clinical evidence on the effects of saffron (crocus sativus L.) on cardiovascular risk factors: A systematic review meta-analysis. *Pharmacol. Res.* 139, 348–359. doi:10.1016/j.phrs.2018.11.038

Prakash, R., Zhang, Y., Feng, W., and Jasin, M. (2015). Homologous recombination and human health: The roles of BRCA1, BRCA2, and associated proteins. *Cold Spring Harb. Perspect. Biol.* 7 (4), a016600. doi:10.1101/cshperspect.a016600

Pundir, M., Sharma, A., and Kumar, J. (2021). Phytochemicals used as inhibitors in the treatment of ovarian cancer: A mini-review. *Mater. Today Proc.* 48, 1620–1625. doi:10.1016/j.matpr.2021.09.505

Ramanna, M. K., Somu, L., L, S., and Prasad T, K. (2021). A comparative study on efficacy of lutein and atorvastatin on lipid profile and lipoprotein (A) in hypercholesterolemic male wistar rats. *Biomed. Pharmacol. J.* 14 (1), 503–511. doi:10.13005/bpj/2151

Ramus, S. J., and Gayther, S. A. (2009). The contribution of BRCA1 and BRCA2 to ovarian cancer. *Mol. Oncol.* 3 (2), 138–150. doi:10.1016/j.molonc.2009.02.001

Rottenberg, S., Jaspers, J. E., Kersbergen, A., van der Burg, E., Nygren, A. O., Zander, S. A., et al. (2008). High sensitivity of BRCA1-deficient mammary tumors to the PARP inhibitor AZD2281 alone and in combination with platinum drugs. *Proc. Natl. Acad. Sci. U. S. A.* 105 (44), 17079–17084. doi:10.1073/pnas.0806092105

Roy, M., and Datta, A. (2019). "Fundamentals of phytochemicals," in *Cancer genetics and therapeutics* (New York, United States: Springer), 49–81.

Roy, M., and Datta, A. (2021). "Phytochemicals in ROS mediated epigenetic modulation of cancer," in *Handbook of oxidative stress in cancer: Mechanistic aspects* (New York, United States: Springer), 1–18.

Runlin, W., Xiang, P., Juan, L., and Shu, Y. (2022). Soybean isoflavones activating autophagy and improving the chemosensitivity of carboplatin to ovarian cancer cells. *J. Biomater. tissue Eng.* 12 (9), 1805–1812. doi:10.1166/jbt.2022.3108

Sajjad, M., Fradley, M., Sun, W., Kim, J., Zhao, X., Pal, T., et al. (2017). An exploratory study to determine whether BRCA1 and BRCA2 mutation carriers have higher risk of cardiac toxicity. *Genes (Basel)* 8 (2), 59. doi:10.3390/genes8020059

Schmitt, B., Vicenzi, M., Garrel, C., and Denis, F. M. (2015). Effects of N-acetylcysteine, oral glutathione (GSH) and a novel sublingual form of GSH

on oxidative stress markers: A comparative crossover study. *Redox Biol.* 6, 198–205. doi:10.1016/j.redox.2015.07.012

Schwertheim, S., Wein, F., Lennartz, K., Worm, K., Schmid, K. W., and Sheu-Grabellus, S.-Y. (2017). Curcumin induces G2/M arrest, apoptosis, NF-κB inhibition, and expression of differentiation genes in thyroid carcinoma cells. *J. Cancer Res. Clin. Oncol.* 143 (7), 1143–1154. doi:10.1007/s00432-017-2380-z

Sekine, M., Nishino, K., and Enomoto, T. (2021). Differences in ovarian and other cancers risks by population and BRCA mutation location. *Genes (Basel)* 12 (7), 1050. doi:10.3390/genes12071050

Shea, S., Navas-Acien, A., Shimbo, D., Brown, E. R., Budoff, M., Bancks, M. P., et al. (2021). Spatially weighted coronary artery calcium score and coronary heart disease events in the multi-ethnic study of atherosclerosis. *Circ. Cardiovasc. Imaging* 14 (1), e011981. doi:10.1161/circimaging.120.011981

Singh, K. K., Shukla, P. C., Quan, A., Al-Omran, M., Lovren, F., Pan, Y., et al. (2013). BRCA1 is a novel target to improve endothelial dysfunction and retard atherosclerosis. *J. Thorac. Cardiovasc. Surg.* 146 (4), 949–960. doi:10.1016/j.jtcvs.2012.12.064

Song, M.-Y., Lee, D.-Y., Chun, K.-S., and Kim, E.-H. (2021). The role of NRF2/KEAP1 signaling pathway in cancer metabolism. *Int. J. Mol. Sci.* 22 (9), 4376. doi:10.3390/ijms22094376

Speciale, A., Saija, A., Bashllari, R., Molonia, M. S., Muscarà, C., Occhiuto, C., et al. (2020). Anthocyanins as modulators of cell redox-dependent pathways in non-communicable diseases. *Curr. Med. Chem.* 27 (12), 1955–1996. doi:10.2174/0929867325666181112093336

Srinivasan, G., Sidhu, G. S., Williamson, E. A., Jaiswal, A. S., Najmunnisa, N., Wilcoxen, K., et al. (2017). Synthetic lethality in malignant pleural mesothelioma with PARP1 inhibition. *Cancer Chemother. Pharmacol.* 80 (4), 861–867. doi:10.1007/s00280-017-3401-y

Suzuki-Sugihara, N., Kishimoto, Y., Saita, E., Taguchi, C., Kobayashi, M., Ichitani, M., et al. (2016). Green tea catechins prevent low-density lipoprotein oxidation via their accumulation in low-density lipoprotein particles in humans. *Nutr. Res.* 36 (1), 16–23. doi:10.1016/j.nutres.2015.10.012

Syamala, S., Sreepriya, M., and Sudhandiran, G. (2021). "Soy isoflavones, mitochondria and cell fate," in *Mitochondrial physiology and vegetal molecules* (Cambridge, Massachusetts, United States: Academic Press), 625–643. doi:10.1016/b978-0-12-821562-3.00046-0

Thushara, R. M., Hemshekhar, M., Santhosh, M. S., Jnaneshwari, S., Nayaka, S. C., Naveen, S., et al. (2013). Crocin, a dietary additive protects platelets from oxidative stress-induced apoptosis and inhibits platelet aggregation. *Mol. Cell. Biochem.* 373 (1-2), 73–83. doi:10.1007/s11010-012-1476-7

Tian, X., Xin, H., Paengkoum, P., Paengkoum, S., Ban, C., and Sorasak, T. (2019). Effects of anthocyanin-rich purple corn (Zea mays L.) stover silage on nutrient utilization, rumen fermentation, plasma antioxidant capacity, and mammary gland gene expression in dairy goats. *J. Anim. Sci.* 97 (3), 1384–1397. doi:10.1093/jas/sky477

Tong, K. I., Katoh, Y., Kusunoki, H., Itoh, K., Tanaka, T., and Yamamoto, M. (2006). Keap1 recruits Neh2 through binding to ETGE and DLG motifs: Characterization of the two-site molecular recognition model. *Mol. Cell. Biol.* 26 (8), 2887–2900. doi:10.1128/mcb.26.8.2887-2900.2006

Ulasov, A. V., Rosenkranz, A. A., Georgiev, G. P., and Sobolev, A. S. (2021). Nrf2/Keap1/ARE signaling: Towards specific regulation. *Life Sci.* 291, 120111. doi:10.1016/j.lfs.2021.120111

Vanacker, H., Harter, P., Labidi-Galy, S. I., Banerjee, S., Oaknin, A., Lorusso, D., et al. (2021). PARP-inhibitors in epithelial ovarian cancer: Actual positioning and future expectations. *Cancer Treat. Rev.* 99, 102255. doi:10.1016/j.ctrv.2021.102255

Vurusaner, B., Poli, G., and Basaga, H. (2012). Tumor suppressor genes and ROS: Complex networks of interactions. *Free Radic. Biol. Med.* 52 (1), 7–18. doi:10.1016/j.freeradbiomed.2011.09.035

Wang, S., Wu, Y. Y., Wang, X., Shen, P., Jia, Q., Yu, S., et al. (2020). Lycopene prevents carcinogen-induced cutaneous tumor by enhancing activation of the Nrf2 pathway through p62-triggered autophagic Keap1 degradation. *Aging (Albany NY)* 12 (9), 8167–8190. doi:10.18632/aging.103132

Wei, H., and Yu, X. (2016). Functions of PARylation in DNA damage repair pathways. *Genomics Proteomics Bioinforma.* 14 (3), 131–139. doi:10.1016/j.gpb.2016.05.001

Wong, N. D. (2014). Epidemiological studies of CHD and the evolution of preventive cardiology. *Nat. Rev. Cardiol.* 11 (5), 276–289. doi:10.1038/nrcardio.2014.26

Woo, H. W., Kim, M. K., Lee, Y. H., Shin, D. H., Shin, M. H., and Choi, B. Y. (2019). Habitual consumption of soy protein and isoflavones and risk of metabolic syndrome in adults ≥ 40 years old: A prospective analysis of the Korean multi-rural communities cohort study (MRCohort). *Eur. J. Nutr.* 58 (7), 2835–2850. doi:10.1007/s00394-018-1833-8

Xia, B., Dorsman, J. C., Ameziane, N., de Vries, Y., Rooimans, M. A., Sheng, Q., et al. (2007). Fanconi anemia is associated with a defect in the BRCA2 partner PALB2. *Nat. Genet.* 39 (2), 159–161. doi:10.1038/ng1942

Xia, B., Sheng, Q., Nakanishi, K., Ohashi, A., Wu, J., Christ, N., et al. (2006). Control of BRCA2 cellular and clinical functions by a nuclear partner, PALB2. *Mol. Cell* 22 (6), 719–729. doi:10.1016/j.molcel.2006.05.022

Xian, D., Lai, R., Song, J., Xiong, X., and Zhong, J. (2019). Emerging perspective: Role of increased ROS and redox imbalance in skin carcinogenesis. *Oxid. Med. Cell. Longev.* 2019, 8127362. doi:10.1155/2019/8127362

Xu, S., Ilyas, I., Little, P. J., Li, H., Kamato, D., Zheng, X., et al. (2021). Endothelial dysfunction in atherosclerotic cardiovascular diseases and beyond: From mechanism to pharmacotherapies. *Pharmacol. Rev.* 73 (3), 924–967. doi:10.1124/pharmrev.120.000096

Yang, Q. Q., Gan, R. Y., Ge, Y. Y., Zhang, D., and Corke, H. (2018). Polyphenols in common beans (Phaseolus vulgaris L.): Chemistry, analysis, and factors affecting composition. *Compr. Rev. Food Sci. Food Saf.* 17 (6), 1518–1539. doi:10.1111/1541-4337.12391

Yaribeygi, H., Mohammadi, M. T., and Sahebkar, A. (2018). Crocin potentiates antioxidant defense system and improves oxidative damage in liver tissue in diabetic rats. *Biomed. Pharmacother.* 98, 333–337. doi:10.1016/j.biopha.2017.12.077

Zeb, A. (2021). "Phenolic AntioxidantsAntioxidants in vegetables," in *Phenolic antioxidants in foods: Chemistry, biochemistry and analysis* (Cham: Springer International Publishing), 131–148.

Zhang, D. D., Lo, S. C., Cross, J. V., Templeton, D. J., and Hannink, M. (2004). Keap1 is a redox-regulated substrate adaptor protein for a Cul3-dependent ubiquitin ligase complex. *Mol. Cell. Biol.* 24 (24), 10941–10953. doi:10.1128/mcb.24.24.10941-10953.2004

Zheng, B., Yin, W. N., Suzuki, T., Zhang, X. H., Zhang, Y., Song, L. L., et al. (2017). Exosome-mediated miR-155 transfer from smooth muscle cells to endothelial cells induces endothelial injury and promotes atherosclerosis. *Mol. Ther.* 25 (6), 1279–1294. doi:10.1016/j.ymthe.2017.03.031

Zhou, S., Jin, J., Wang, J., Zhang, Z., Huang, S., Zheng, Y., et al. (2021). Effects of breast cancer genes 1 and 2 on cardiovascular diseases. *Curr. Probl. Cardiol.* 46 (3), 100421. doi:10.1016/j.cpcardiol.2019.04.001

Human PARP1 substrates and regulators of its catalytic activity: An updated overview

Tao Zhu[1]*[†], Ju-Yan Zheng[2†], Ling-Ling Huang[1], Yan-Hong Wang[1], Di-Fei Yao[1] and Hai-Bin Dai[1]*

[1]Department of Pharmacy, The Second Affiliated Hospital, Zhejiang University School of Medicine, Hangzhou, China, [2]Institute of Clinical Pharmacology, Xiangya Hospital, Central South University, Changsha, China

Poly (ADP-ribose) polymerase 1 (PARP1) is a key DNA damage sensor that is recruited to damaged sites after DNA strand breaks to initiate DNA repair. This is achieved by catalyzing attachment of ADP-ribose moieties, which are donated from NAD^+, on the amino acid residues of itself or other acceptor proteins. PARP inhibitors (PARPi) that inhibit PARP catalytic activity and induce PARP trapping are commonly used for treating *BRCA1/2*-deficient breast and ovarian cancers through synergistic lethality. Unfortunately, resistance to PARPi frequently occurs. In this review, we present the novel substrates and regulators of the PARP1-catalyzed poly (ADP-ribosyl)ation (PARylatison) that have been identified in the last 3 years. The overall aim is the presentation of protein interactions of potential therapeutic intervention for overcoming the resistance to PARPi.

KEYWORDS

PARP inhibitors, poly-ADP ribosylation, substrate, DNA damage repair, synthetic lethality

1 Introduction

Poly (ADP-ribose) polymerases (PARPs) are a group of enzymes that may regulate cellular processes such as DNA damage response, chromatin remodeling, cell metabolism and transcriptional regulation (Bai and Canto, 2012; Schiewer et al., 2012). Poly (ADP-ribosyl)ation (PARylation) is central to the key functions of PARPs, about 90% of PARylation produced in a cell is catalyzed by PARP1, the founding member of PARP family. PARP1 catalyzes PARylation by covalently attaching the ADP-ribose moieties to the acceptor amino acid residues on target proteins. Although PARP1 was initially identified as being involved in the sensing and repairing of single strand DNA breaks, PARP1-mediated PARylation may lead to the recruitment of different DNA repair proteins to damaged sites. The overall effect is that PARP1 affects multiple DNA repair pathways, including base excision repair (BER), non-homologous end joining (NHEJ), and homologous recombination (HR) (Masson et al., 1998; Schultz et al., 2003; Wang et al., 2006). As a result, PARP1 has been recognized as a desirable target to achieve DNA damage-induced cell death for anticancer therapy, with several generations of PARP1 inhibitors having been developed and approved in clinical use.

PARP1 inhibitors are characterized by their remarkable efficacy in *BRCA1/2*-mutated breast, ovarian, and prostate cancers. Cancer cells with HR deficiency due to *BRCA1/2* gene mutations are viable by virtue of complementary functions of non-HR DNA repair pathways. However, since PARP1 is involved in non-HR repair, HR deficient cancer cells are extremely vulnerable to PARP1 inhibitors. Currently, there are six FDA-approved PARP inhibitors (olaparib, rucaparib, niraparib, talazoparib, fluzoparib, and
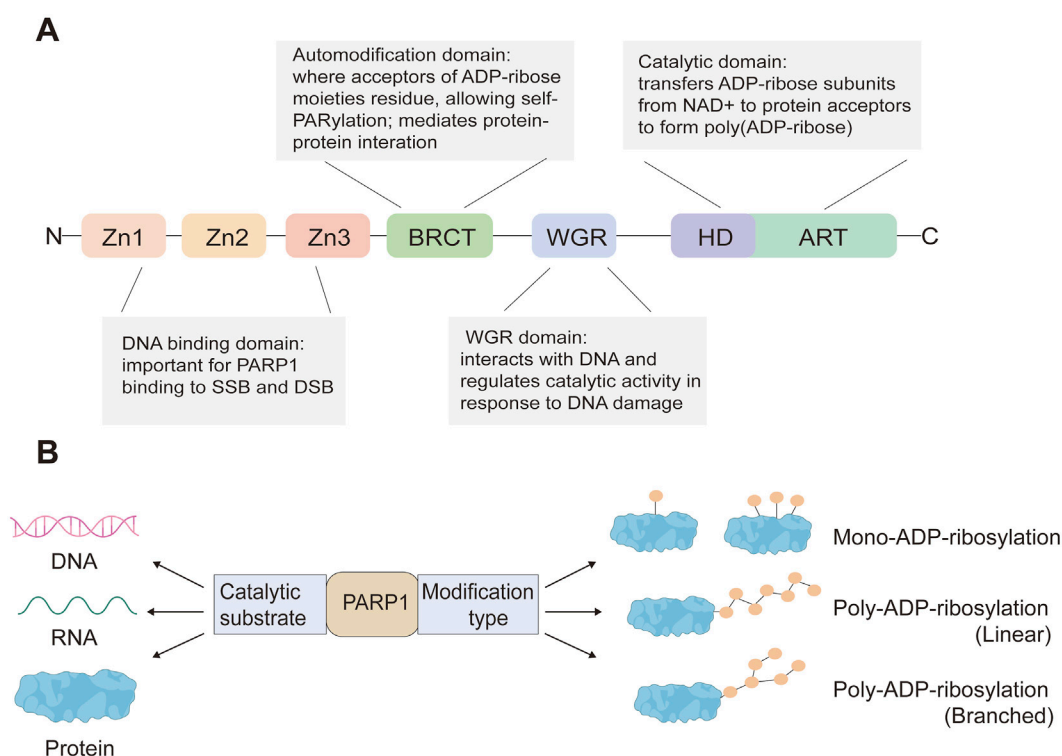
FIGURE 1
PARP1 protein domains **(A)** and PARP1-mediated ADP-ribosylation modification types of its substrates **(B)**.

pamiparib) for anticancer treatment (Dias et al., 2021; Lee, 2021; Markham, 2021), and several other compounds are being tested in clinical trials such as veliparib (NCT01434316). Unfortunately, despite a dramatic initial response to PARP inhibitors, most patients often develop drug resistance, leading to tumor recurrence. Mechanisms of resistance to PARP inhibitors include restoration of HR capacity, stabilization of replication forks, reduced trapping of PARP1, and P-glycoprotein-mediated drug efflux (Kim et al., 2021). Combination therapies have been recognized as an efficient approach to tackle PARP inhibitors resistance. Accumulating evidence shows superior antitumor efficacy of combinational strategies comprising PARP inhibitors and other kinase or immune checkpoint blockers, such as ATR inhibitors that block BRCA1-independent RAD51 recruitment to DSBs and disrupt fork progression (Yazinski et al., 2017; Kim et al., 2020), and anti-PD-(L)1 antibodies which show a synergistic effect with PARPi (Konstantinopoulos et al., 2019; Domchek et al., 2020; Peyraud and Italiano, 2020).

An increasing number of target proteins that can be PARylated by PARP1 have been identified, further complementing our understanding of the biological function of PARP1. Besides proteins, nucleic acids are also found as substrates of PARylation, which have been comprehensively summarized by Groslambert and colleagues (Groslambert et al., 2021) and are not the focus of this review. Moreover, molecules that regulate PARP1 catalytic activity to influence ADP-ribosylation and PARP1 inhibitor efficacy are being discovered. Herein, we review protein substrates of PARylation catalyzed by PARP1 and regulators of

PARP1 catalytic activity identified in the last 3 years, aiming to summarize candidate targets that can be exploited in novel combinational therapies to improve the antitumor efficacy of PARP inhibitors.

2 Mechanisms of action of PARP inhibitors

The PARP family consists of 17 enzymes, with a conserved catalytic motif (Schreiber et al., 2006; van Beek et al., 2021) that catalyzes transfer of the ADP-ribose unit from nicotinamide adenine dinucleotide (NAD^+) onto target proteins. As the first family member, PARP1 is crucial for maintaining genome stability by synthesizing PAR which serves as a docking site for the recruitment of DNA repair effectors to DNA strand breaks. PARP1 has a modular structure with six domains (Figure 1). Three zinc-finger DNA-binding domains (Zn1, Zn2, and Zn3) in the N-terminus are responsible for recognizing particular DNA structures and mediating interdomain contacts (Langelier et al., 2008; Langelier et al., 2011). An adjacent BRCA1 C-terminus (BRCT) domain mediates protein-protein interactions and is the region where PARP1 auto-modification occurs. The Trp-Gly-Arg (WGR) domain also interacts with DNA and regulates the catalytic activity of PARP1 in response to DNA damage (Langelier et al., 2012; Langelier et al., 2018). The C-terminal catalytic domain comprises two subdomains, the auto-inhibitory helical subdomain (HD) and the ADP-ribosyl transferase (ART)
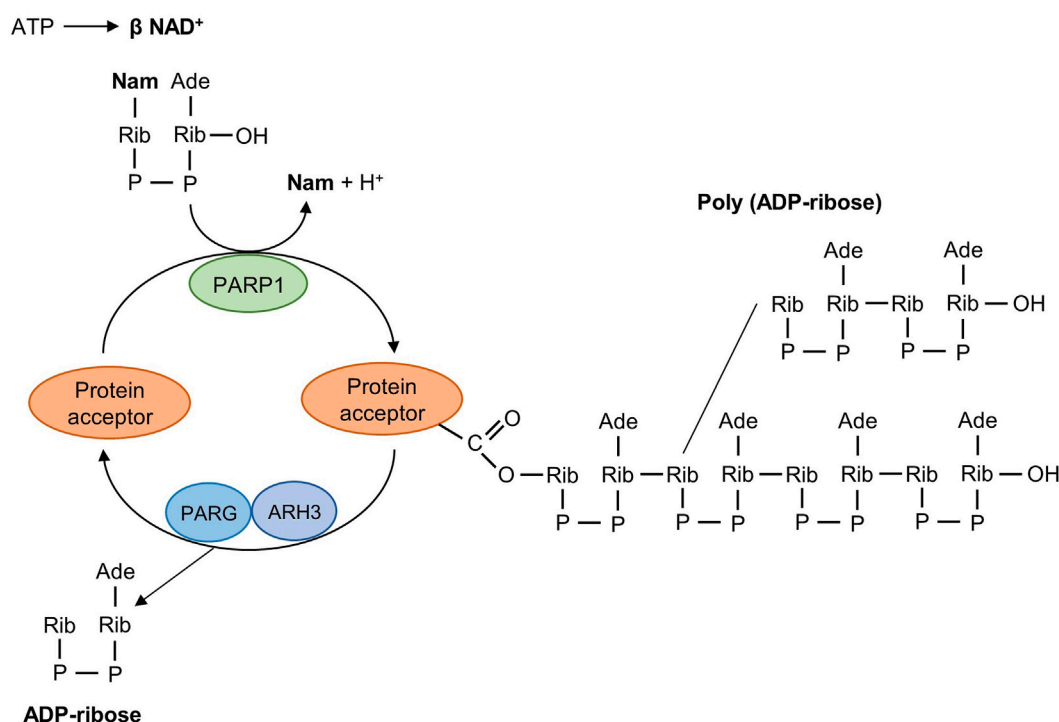
FIGURE 2
Mechanism of poly (ADP-ribosyl)ation reaction catalyzed by PARP1. PARP1 detects DNA strand breaks, hydrolyses NAD⁺, and catalyzes the transfer of ADP-ribose units on amino acid residues of protein acceptors. The poly (ADP-ribosyl)ation reaction is reversible and the degradative nuclear enzymes PARG and ARH3 cleave poly (ADP-ribose) into ADP-ribose units. PARG, poly (ADP-ribose) glycohydroiase; ARH3, poly (ADP-ribose) hydrolase-3; Nam, nicotinamide; Ade, adenine; Rib, ribose; P, phosphate.

subdomain. The conserved ART subdomain bears amino acids that form the catalytic pocket, which interacts with NAD⁺ and catalyzes ADP-ribosylation. HD inhibits the binding of PARP1 with NAD⁺ when PARP1 is in the non-DNA bound state (Ruf et al., 1998; Langelier et al., 2012; Eustermann et al., 2015). In response to DNA strand breaks, PARP1 hydrolyses NAD⁺ and catalyzes covalent attachment of ADP-ribose units on amino acid residues of protein acceptors. This is a dynamic process, the ADP-ribose polymer has a short half-life and is degraded by the poly (ADP-ribose) glycohydrolase (PARG) and the poly (ADP-ribose) hydrolase 3 (ARH3) (Meyer-Ficca et al., 2004; Oka et al., 2006) (Figure 2).
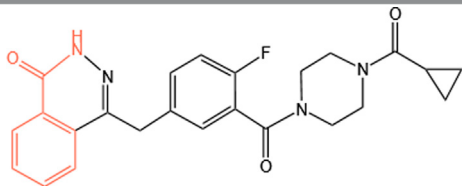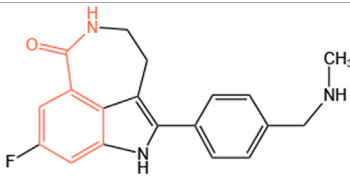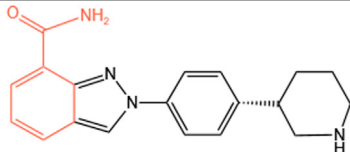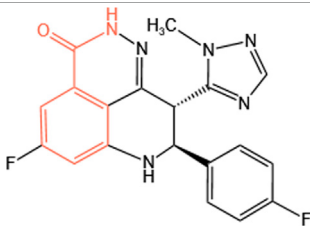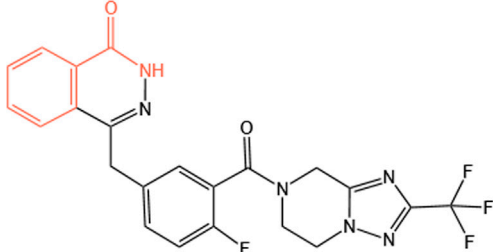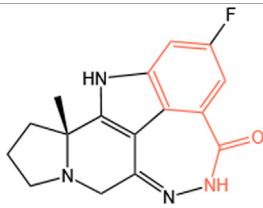
Clinical PARP inhibitors are basically NAD⁺ analogs, all of which contain the nicotinamide moiety (Lord and Ashworth, 2017) (Table 1). PARP inhibitors block the catalytic activity of PARP1 and PARP2 by competitively binding to the NAD⁺-binding catalytic pocket of PARP enzymes, resulting in no formation of PAR polymers and thus no recruitment of DNA damage repair proteins (Min and Im, 2020). PARP inhibitors are lethal to *BRCA*-mutant cancer cells, since they induce single strand DNA lesions, and persistent single strand DNA breaks lead to DSBs that cannot be repaired by impaired homologous recombination. This is so-called synthetic lethality (Farmer et al., 2005). However, later evidence demonstrated that PARP inhibition impeded DNA damage repair and induced cell death to a greater extent than PARP depletion alone (Strom et al., 2011). These data suggest that PARP may exert more activities than its mere enzymatic action.

PARP1-DNA complexes were detected in PARP inhibitors-treated cells and a PARP1-trapping model was hence presented to further explain the synthetic lethality (Helleday, 2011; Murai et al., 2012) (Figure 3). Normally, PARP1 binds damaged DNA and undergoes allosteric switch to activate its catalytic domain, thereby to PARylate and recruit DNA repair proteins such as XRCC1. Subsequent PARP1 autoPARylation leads to its release from DNA due to the repulsion force between highly negatively charged PAR chains, allowing DNA repair and replication to proceed (Eustermann et al., 2015; Lord and Ashworth, 2017). PARP inhibitors trap PARP1 onto DNA, preventing its autoPARylation and release. Although all current PARP inhibitors used in clinical practice are catalytic inhibitors, their ability to trap PARP1 onto DNA varies and is parallel to their cytotoxic potency (Murai et al., 2012). However, it should be noted that PARP1 trapping is linked to catalytic inhibition and is determined by the ability of PARP1 inhibitors to outcompete NAD⁺ binding (Pommier et al., 2016; Xue et al., 2022). Hence, it is rational to reason that molecules regulating PARP1 affinity to NAD⁺ substrate may also affect the PARP1-trapping potency of PARPi, and therefore PARPi cytotoxicity.

3 Downstream substrates of PARP1

The protein-targeting domains of PARP1 may constitute the major mechanism by which PARP1 selects specific proteins to

TABLE 1 Chemical structure of the clinical PARP inhibitors.

PARP inhibitor	Structure	References
Olaparib		Deeks (2015)
Rucaparib		Anscher et al. (2021)
Niraparib		Zhi et al. (2022)
Talazoparib		Hoy (2018)
Fluzoparib		Lee (2021)
Pamiparib		Markham (2021)

The nicotinamide moiety shown in red is common to PARP inhibitors and NAD.

modify. PARP1 is targeted to its substrates by the non-catalytic domains, and the regions adjacent to the catalytic domain determine to ADP-ribosylate which amino acids (Cohen and Chang, 2018). Growing evidence has shown the diversity of protein substrates of PARP1, which helps to get insights into the multiple functions of PARP1.

3.1 Histones and chromatin remodeling-related proteins

Chromatin is a dynamic DNA scaffold that can modulate the multiple uses of DNA in response to different cellular contexts. Nucleosome is the basic building block of chromatin, which is
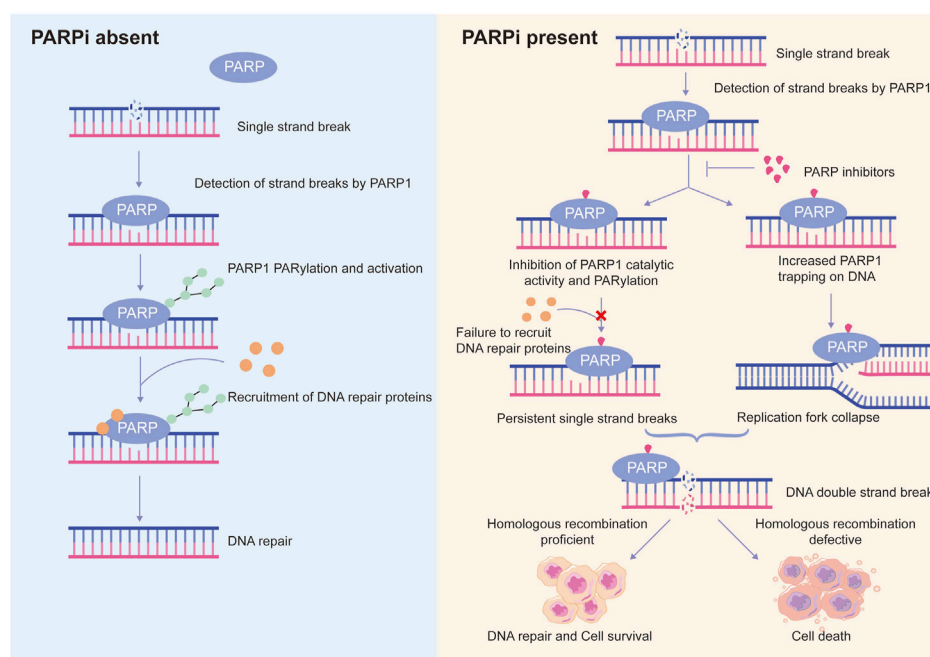
FIGURE 3
Schematic representation of the proposed mechanisms of action of PARP inhibitors. Normally, PARP1 detects DNA single strand breaks and is activated by them, leading to PARP1 auto-PARylation and recruitment of DNA repair proteins to trigger DNA repair. However, in the presence of PARP inhibitors (PARPi), on the one hand, PARPi suppresses PARP1 activity, recruitment of DNA repair proteins to damaged sites is inhibited, resulting in persistent single strand breaks; on the other hand, PARPi traps PARP1 at DNA lesions, the trapped PARP1-DNA complexes are cytotoxic and cause collapse of replication fork. Persistent single strand breaks and replication fork collapse will ultimately lead to DNA double strand breaks. In homologous recombination-proficient cells, double strand breaks can be efficiently repaired. In contrast, homologous recombination-defective cells are not able to repair double strand breaks efficiently and accurately, leading to cell death. This is a phenomenon known as synthetic lethality.

formed by an octamer of core histones (H3, H4, H2A, and H2B) and 147 bp of DNA that wraps nearly twice around the octamer (Peterson and Laniel, 2004). Posttranslational modification of histones mediates a variety of critical biological processes that are implicated in modifying DNA and regulating gene expression, many of which is dysregulated during cancer progression. For example, a significant correlation of histone modification status with malignant phenotype and clinical outcome was found in breast cancer, with relatively high global histone acetylation and methylation levels associated with a favorable prognosis (Elsheikh et al., 2009). ADP-ribosylation is a less prevalent histone modification, yet all core histones and the linker histone H1 can be ADP-ribosylated (Messner et al., 2010; Li et al., 2018). Histone ADP-ribosylation catalyzed by PARP1 is thought as a way for PARP1 to induce chromatin relaxation and fulfill DNA repair function. H2AX is a histone H2A variant on which posttranslational modifications frequently occur upon DNA damage (Mattiroli et al., 2012; Sone et al., 2014; Ikura et al., 2015). Compared with the H2A nucleosome, PARP1 shows a higher affinity for nucleosomes containing γH2AX, the serine 139 phosphorylation form of H2AX and a sensitive marker of DNA double-strand breaks (DSBs). This preference renders PARP1 a greater catalytic efficiency (Sharma et al., 2019). Using unbiased high-resolution mass spectrometry, the glutamate residue 141 (E141) of H2AX has been identified as a novel ADP-ribosylation site. E141 ADP-ribosylation facilitates the recruitment of Neil3 glycosylase to the DNA damage sites for removal of

damaged base during base excision repair after oxidative DNA damage (Chen et al., 2021). Noteworthily, E141 ADP-ribosylation and serine 139 phosphorylation of H2AX are mutually exclusive, suggesting that this ADP-ribosylation also suppresses γH2AX-involved DSB response (Chen et al., 2021). Histones H3 and H2B are also primary targets that undergo ADP-ribosylation modification on their serine residues in the context of DNA damage. Hananya and colleagues have recently shown that ADP-ribosylation of H2B serine 6 and H3 serine 10 collaboratively restrains chromatin folding and its higher-order organization (Hananya et al., 2021). Their study established that histone mono-ADP-ribosylation is sufficient to inhibit chromatin compaction, and further complemented the previous perspective that PARP1-catalyzed poly-ADP-ribosylation causes chromatin relaxation, which increases the accessibility of repair factors to DNA damage sites (Poirier et al., 1982; Hananya et al., 2021).

PARP1 also mediates ADR-ribosylation of other targets involved in chromatin remodeling. NSD2 is a histone methyltransferase that specifically catalyzes dimethylation of histone H3 lysine 36 (H3K36me2). Its expression plays a role in chromatin accessibility by regulating the balance of H3K36me2 and H3K27me3 modifications (Xie et al., 2022). PARP1 interacts with NSD2 and catalyzes PARylation of NSD2 upon oxidative stress, leading to decreased histone methyltransferase activity of NSD2 and impaired NSD2 recruitment to target genes in multiple myeloma (Huang et al., 2019). This shows an indirect involvement of

PARP1 in regulating histone methylation in response to DNA damage.

MORC2 is chromatin remodeling enzyme, with critical roles in gene transcription and DNA damage response through its N-terminal ATPase module (Li et al., 2012; Moissiard et al., 2012). After DNA damage, PARP1 interacts with and recruits MORC2 to DNA damage sites, and PARylates MORC2 at E516 and K517 (Zhang and Li, 2019). PARylation modification stimulates MORC2 ATPase activity to facilitate chromatin remodeling and DNA repair (Zhang and Li, 2019).

In addition, Hu et al. has found that BRD7, a component of the SWI/SNF chromatin remodelling complex, is a substrate of PARylation. PARP1 catalyzes PARylation of BRD7 and enhances its degradation *via* the ubiquitin-proteasome pathway, resulting in resistance to chemotherapy in breast cancer cells (Hu et al., 2019).

ALC1 is a chromatin remodeler recruited to DNA damage sites in a PARylation-dependent manner. PARP1 can PARylate ALC1 to cause the E3 ligase CHFR-mediated ALC1 ubiquitination and degradation (Wang et al., 2019a). In HR-deficient cells, ALC1 is a critical determinant of PARPi cytotoxicity, loss of which reduces cell viability and increases sensitivity to PARPi (Verma et al., 2021).

3.2 Transcription factors

Emerging evidence has shown that many transcription factors are substrates of PARP1-mediated PARylation. Signal transducer and activator of transcription (STAT) family of transcription factors is constitutively active in tumorigenesis and promote tumor progression (Heppler and Frank, 2017). In acute myeloid leukemia (AML) with internal tandem duplications of fms-like tyrosine kinase 3 (FLT3-ITD), PARP1 is indispensable for STAT5 activity through interacting and PARylating STAT5 to prevent its proteasomal degradation. Moreover, since PARP1 inhibition constrains STAT5 signaling cascade that contributes to resistance to tyrosine kinase inhibitors (TKIs), it shows a synergistic effect with TKIs for treating AML (Dellomo et al., 2022).

The tumor suppressor p53 guards the genome *via* orchestrating multiple DNA damage repair machineries. It halts cell cycle to allow time for DNA repair and genome stability restoration. P53 can be PARylated by PARP1 in the C-terminal domain, which influences its transcriptional activity (Fischbach et al., 2018). PARylated p53 becomes inactive and induces tumor development in a glioma cell model (Liu et al., 2021).

NFAT5, a transcriptional factor involved in macrophage activation and T-cell development, has been identified as a novel PARylation substrate that mediates PARP1-related DNA damage response. PARP1 PARylates NFAT5 and promotes its recruitment to DNA damage sites where NFAT5 prevents R-loop-associated DNA damage in hepatoma cells (Ye et al., 2021).

In addition, KLF4 is a PARP1-interatcting transcription factor that mediates PARP1 function in controlling telomerase expression (Hsieh et al., 2017). Zhou et al. recently revealed that KLF4 can be PARylated by PARP1 at Y430, Y451, and R452, and KLF4 PARylation is critical for its subcellular location, transcriptional activity, and its function in DNA damage response (Zhou et al., 2020).

HIF-1α is a subunit of the hypoxia-inducible factors (HIF), orchestrating the cell to adapt to hypoxic conditions. It has been shown that PARP1 is a novel regulator in hypoxic adaptation by PARylating HIF-1α at specific K/R residues in the C-terminus domain. This contributes to maintain HIF-1α stability and to enhance its recruitment to target promoters in hypoxia, allowing tumor cells to survive in hypoxic challenges (Marti et al., 2021).

RUNX3 contributes to genome maintenance by regulating the Fanconi anemia (FA) pathway independent of its transcription activity. Multiple PARylable sites have been recognized in RUNX3, and RUNX3 PARylation by PARP1 after DNA damage is crucial for its binding to DNA repair structures and activation of FA pathway-related DNA repair (Zhang et al., 2013; Tay et al., 2018).

ELF4 is a member of the E74-like factor (ELF) transcription factor family that modulates immune cell development and immune responses (Suico et al., 2017). Du et al. found that PARP1 interacts and PARylates ELF4. PARylated ELF4, by transcriptionally regulating elements of DNA damage repair machinery, is pivotal in safeguarding the genome of colon epithelial cells and preventing colitis-associated cancer (Du et al., 2021).

OVOL2 is a negative regulator of mitosis by inhibiting the RHO GTPase signaling (Gugnoni et al., 2022). Multiple PARylable sites within its C2H2 zinc finger domain have been found. PARylated OVOL2 suppresses transcription of SKP2, an E3 ligase of Cyclin E, resulting in centrosome over-duplication and cell death (Zhang et al., 2019).

ER-alpha is an intracellular receptor for hormone estrogen, which promotes cell division and tumor growth through transcriptionally activating its target genes. Recent studies have shown that ER-alpha can be mono- and poly-ADP-ribosylated by PARP1, and its PARylation correlates with tamoxifen resistance (Pulliam et al., 2019; Rasmussen et al., 2021).

3.3 Enzymes involved in nucleic acid processing

In addition to nucleic acids such as phosphorylated DNA and RNA ends that serve as substrates of ADP-ribosylation (Groslambert et al., 2021), emerging evidence has shown that ADP-ribosylation can also occur on nucleic acid processing-related enzymes. The DNA polymerase theta (Polθ)-mediated end joining (TMEJ) pathway is essential for DSB repair when the homologous recombination pathway is defective. PARP1 catalytic activity has been shown to facilitate chromosomal TMEJ (Luedeman et al., 2022). However, the helicase domain of Polθ can be PARylated by PARP1, which leads to reduced affinity for single-stranded DNA and impaired ability to bridge DNA overhangs (Schaub et al., 2022). This indicates that PARP1 also negatively regulates TMEJ through Polθ PARylation to maintain appropriate activity of the TMEJ pathway. RNA polymerase III is a binding partner of truncated PARP1, and three subunits (POLR3B, POLR3F, and POLR3G) can be ADP-ribosylated during cytosolic DNA-induced apoptosis (Chen et al., 2022). In addition, PARP1 inhibits elongation of RNA polymerase II *via* suppressing the transcription elongation factor P-TEFb. Upon DNA damage, PARP1 interacts and PARylates the histidine-rich domain of CycT1, a subunit of P-TEFb, disrupting

CycT1 phase separation that is required for RNA polymerase II hyperphosphorylation and elongation stimulation (Fu et al., 2022). Interestingly, PARP1 also regulates RNA polymerase elongation independent of its PARylation activity (Matveeva et al., 2022).

DDX21 is a DEAD box-containing RNA helicase that modulates gene transcription and ribosomal RNA processing. PARP1 PARylates DDX21 at its N-terminus, leading to increased PARP1-DDX21 interaction and breast cancer cell proliferation (Kim et al., 2019).

A study by Liu et al. proved that NAT10, an RNA cytidine acetyltransferase, can undergo PARP1-mediated PARylation on K1016, K1017, and K1020 within its C-terminus after DNA damage. NAT10 PARylation enables its nucleoplasmic translocation and increases co-localization and interaction of NAT10 with its substrate MORC2, increasing cell survival in response to irradiation-induced DNA damage (Liu et al., 2022).

3.4 Ubiquitination and deubiquitination related enzymes

The ubiquitin (Ub) system regulates protein degradation and signaling pathways to coordinate cellular physiology, which is achieved by a sequential cascade involving Ub-activating enzymes (E1), Ub-conjugating enzymes (E2), Ub ligases (E3), and deubiquitylases (DUBs) (Clague et al., 2015). Accumulating studies indicate a critical role of PARP1 in regulating protein homeostasis through PARylation activity, and increasing enzymes have been identified as substrates of PARylation. E3 ligases NEDD4 and CHFR are such substrates (Correani et al., 2019; Kannan et al., 2019). PARylation of CHFR by PARP1 is important for its activation and mediation of target proteins degradation (Kannan et al., 2019). There is negative feedback between PARP1 and CHFR, as CHFR also mediates PARP1 ubiquitination and degradation (Chung et al., 2021). This is probably because that the PAR-binding pocket of CHFR gives an affinity of CHFR for auto-PARylated PARP1. In other cases, PARP1-mediated PARylation of E3 ligases will prevent their ubiquitylation of target proteins. For example, PARP1 catalyzes PARylation of RNF126 and promotes its proteasome-mediated degradation by recruiting a PAR-binding E3 ligase, resulting in stabilization of targets of RNF126 (Wu et al., 2021). Hence, besides directly PARylating enzymes of the Ub system to participate in the regulation of protein degradation, PARP1-mediated substrate PARylation also serves as bait for recruitment of PAR-binding E3 ligases, such as DTX2 and RNF146 (Hu et al., 2019; Ahmed et al., 2020), to regulate protein turnover.

USP10, a deubiquitylase that can deubiquitinate the tumor suppressor p53, is a PARylation substrate and its stabilization of p53 requires the activity of PARP1 (Correani et al., 2019). BAP1 is a deubiquitylase implicated in DNA repair, in which multiple PARylable sites have been identified. PARP1-mediated PARylation of BAP1 is critical for its deubiquitination activity, protein stability, and recruitment to UV-induced DNA damage sites (Lee et al., 2022). ATXN3 is another DNA repair-related deubiquitylase which dissembles ubiquitin chains on DNA repair substrates. Although no evidence shows that ATXN3 can be

PARylated by PARP1, their direct interaction was observed and ATXN3 recruitment to DNA damage sites to mediate retention of DNA repair proteins relies on DNA damage-induced PARylation (Pfeiffer et al., 2021). These above findings suggest a sophisticated role of PARP1 in governing protein degradation either by modulating enzymatic activity in the Ub system or by mediating crosstalk between PARylation and ubiquitination modifications of substrates.

3.5 Other substrates

In addition to the substrates mentioned above, several other proteins involved in different cellular processes have been identified as substrates of PARP1-mediated PARylation. These includes players in DNA damage response, such as the DNA-dependent protein kinase DNA-PKcs (Munnur et al., 2019) and the Rho GTPase RAC1 (Marcar et al., 2019). Besides, DNA demethylation enzymes TET1 and TET2 (Tolic et al., 2022), the cytosolic dsDNA sensor cGAS that mediates antiviral immunity (Wang et al., 2022a), and the inflammatory response-involving factor HMGB1 (Kong et al., 2020; Pal Singh et al., 2020) can also be PARylated by PARP1.

With the continuing identification of novel PARylation substrates mediated by PARP1 (Figure 4), a deeper understanding of the roles of PARP1 in DNA damage repair and other biological processes has been achieved, which provides opportunities to develop combination strategies with PARP inhibitors for more effective cancer treatment. However, it should be bear in mind that there is crosstalk between PARP1-mediated PARylation and other posttranslational modifications, which can affect combination therapy efficacy. For instance, PARP1 inhibition suppresses BRD7 PARylation and its ubiquitination degradation, sensitizing BRD7-positive, rather than BRD7-negative cancer cells to chemotherapeutic drugs (Hu et al., 2019). This is a case reminding us that cellular contexts should be taken into consideration when exploiting combination strategies.

4 Upstream regulators of PARP1 catalytic activity

DNA binding induces conformational changes in the catalytic domain of PARP1 that initiate PARylation of acceptor proteins. Hence, PARP1 catalytic activity is dependent on DNA-binding domains that identify and binds DNA strand breaks. In addition, factors affect the catalytic domain itself and the allosteric signals are also determinants of PARP1 catalytic activity. In this section, we will summarize recently identified upstream regulators of PARP1 activity.

4.1 Positive regulators of PARP1 catalytic activity

Increasing studies have revealed the upstream molecules that can enhance the enzymatic activity of PARP1. The tumor susceptibility gene TSG101 interacts with PARP1 and is essential for PARP1 activation. Its loss markedly abolishes cellular

FIGURE 4
Schematic summary of PARP1 catalytic substrates and regulators of PARP1 enzymatic activity identified in the last 3 years.
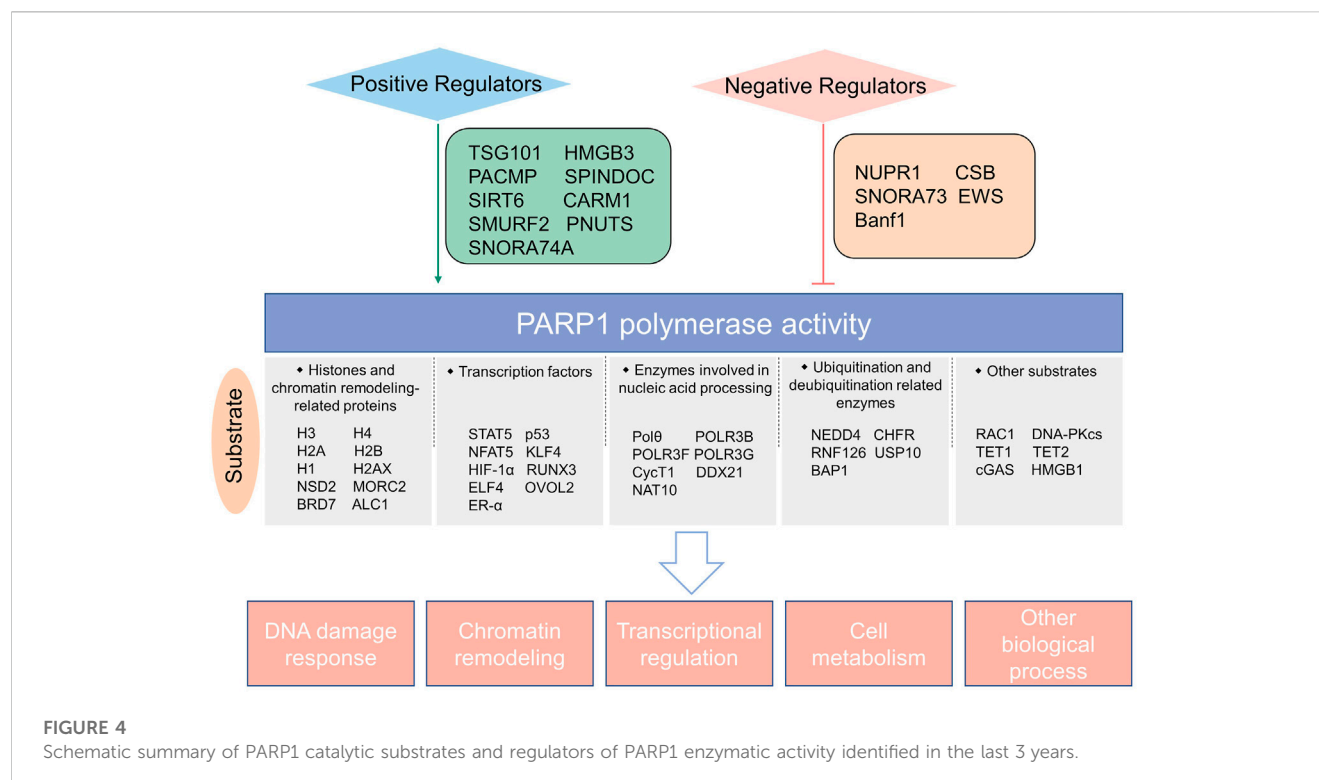
PARylation and induces PARP1 trapping in DNA lesions, leading to DNA repair impairment and cell apoptosis (Tufan et al., 2022). HMGB3 is a novel interactor of PARP1 that can stimulate the PARylation activity of PARP1 and inhibit PARP trapping, resulting in olaparib resistance in ovarian cancer (Ma et al., 2022). A recent study by Zhang and colleagues found that PACMP, a lncRNA-derived micropeptide, is an activator that promotes PARP1-meidiated PARylation, and PACMP inhibition renders sensitivity of cancer cells to diverse chemo- and targeted therapies (Zhang et al., 2022). SPINDOC is a component of the histone-code effector protein complex SPIN1. Yang et al. found a SPIN1-independent role for SPINDOC in DNA damage response, which is achieved by directly interacting with PARP1 and facilitating PARP1-mediated PARylation (Yang et al., 2021). Furthermore, the E3 ligase SMURF2, although responsible for ubiquitination and degradation of PARP1 (Qian et al., 2020), can stimulate the enzymatic activity of PARP1 by reducing its monoubiquitination (Ilic et al., 2021). CARM1 is an arginine methyltransferase and functions in regulating DNA replication fork speed through enhancing PARP1 activity, by both enhancing DNA binding of PARP1 and acting corporately with HPF1, a regulator of PARP-1-dependent ADP-ribosylation (Genois et al., 2021). Kong et al. found that the chromatin-associated protein SIRT6 is an upstream signal for PARP1 activation through monoADP-ribosylation (Kong et al., 2020). However, this is challenged by a later study which showed that SIRT6 does not regulate PARP1 activation (Koczor et al., 2021). Hence, further more comprehensive research is needed. Small nucleolar RNAs, such as SNORA74A, were reported to interact with PARP1, serve as activators of PARP-1 catalytic activity, and regulate ribosome biogenesis and cell growth (Kim et al., 2019). In addition, the DNA damage response-involving protein PNUTS is found as a

PARP1-binding partner. It is recruited to DNA lesions in a PARP1-dependent fashion and is essential for PARylation modification in response to DNA damage (Wang et al., 2019b), suggesting a possible role of PNUTS in stimulating PARP1 activity. Further endeavors are needed to evaluate if these positive regulators of PARP1 enzymatic activity mentioned above may serve as potential targets to increase anticancer efficacy of PARP inhibitors.

4.2 Negative regulators of PARP1 catalytic activity

To avoid hyper-PARylation, cells developed mechanisms to repress PARP1 activity. NUPR1 is a nuclear stress protein which is able to bind to PARP1 and inhibit its enzymatic activity. Pharmacological inhibition of NUPR1 causes deleterious PARylation, mitochondrial dysfunction and cell death (Santofimia-Castano et al., 2022). Han et al. found that SNORA73, a chromatin-associated small nucleolar RNAs, restrains PARP1 auto-PARylation and contributes to genome instability in hematopoietic malignancy (Han et al., 2022). Moreover, the chromatin remodeler CSB was demonstrated as a PARP1-interacting partner. CSB prevents PARP1 overactivation in initial response to oxidative stress, but later CSB helps to maintain chromatin PAR levels (Lake et al., 2022). A study in $Ews^{-/-}$ embryonic tissues by Lee et al. found that EWS suppresses PARP1 activity and reduces DNA damage level by preventing excessive PARP1 accumulation on DNA. Loss of EWS leads to PARP1 hyperactivation and excessive PARylation (Lee et al., 2020). Bolderson et al. reported that Banf1, a DNA-binding protein, interacts directly with the NAD^+-binding domain of PARP1 and

inhibits PARP1 activity, causing defective repair of oxidative DNA lesions (Bolderson et al., 2019).

As described above, PARP1 has multiple interacting partners which can either promote or suppress the activity of PARP1, suggesting that the innate PARP1 catalytic activity is under cunning orchestration (Figure 4). In-depth understanding of this can offer insights to develop strategies to manipulate PARP1 activity more precisely.

5 Conclusion and perspectives

PARP inhibitors have shown superior efficacy in patients with breast, ovarian, and prostate cancer, especially those with *BRCA1/2* mutations. However, resistance to PARPi is common, and several mechanisms to explain this phenomenon have been proposed, such as increased drug efflux, loss of PARP1 function, HR reactivation, stabilization of the replication fork, and inactivation of PARG (Chiappa et al., 2021). To overcome PARPi resistance and improve therapeutic efficacy, multiple strategies combining PARPi and other inhibitors have been designed and evaluated under clinical trials (Wang et al., 2022b). In this review, we summarized PARylable substrates of PARP1 and regulators of PARP1 catalytic activity identified in the last 3 years, which we believe will advance the comprehensive understanding of function of PARP1 and offer clues to guide design of pre-clinical and clinical trials to reverse PARPi resistance.

The function of PARP1 other than its DNA repair ability is being revealed with the continuous identification of its enzymatic substrates. We propose that a systematic knowledge of PARP1 function is a prerequisite for us to thoroughly comprehend how PARPi works. According to the PRIMA trial, among newly diagnosed advanced ovarian cancer patients that are responsive to platinum-based chemotherapy, PARPi (niraparib) treatment significantly prolong progression-free survival of patients with or without HR deficiency (Gonzalez-Martin et al., 2019). This suggests a possible cytotoxic effect of PARPi independent of its DNA repair inhibition (Li et al., 2020). Moreover, adverse events caused by PARPi due to on-target effect are a concern that needs attention. We believe that a broad spectrum of substrate proteins of PARP1-catalzyed PARylation may explain the incidence of adverse drug reactions. In future studies, it is necessary to determine whether there are critical substrates with strikingly high contribution weight in mediating PARP1's DNA repair and other functions that are exploited by PARPi. Compared to PARPi, targeting these substrates may offer an alternative avenue to avoid adverse events without compromising the anti-tumor efficacy.

Regulators of PARP1 catalytic activity are important factors that affect PARPi efficacy, as PARPi cytotoxicity is dependent on cellular PARP1 polymerase activity (Chen et al., 2019). Accumulating positive and negative modulators of PARP1 enzymatic activity have been identified, although most of which are based on *in vitro* cell model or *in vivo* mouse model. If these regulators can be further validated in models more resembling human conditions, it should be better to take them into consideration to achieve the maximal efficacy of PARPi.

In conclusion, we still have a long way to go to cure HR defective cancers with PARPi. However, a deep insight into the downstream PARylable substrates of PARP1 and the critical upstream molecules influencing PARP1 polymerase activity will aid in design of more effective PARPi-based anti-tumor strategies and accelerate our journey to that end.

Author contributions

TZ and HD conceived the idea. JZ and TZ drafted the manuscript and drew the illustrations. All authors revised the manuscript and approved the final version.

Funding

Conflict of interest

The authors declare that the research was conducted in the absence of any commercial or financial relationships that could be construed as a potential conflict of interest.

Publisher's note

All claims expressed in this article are solely those of the authors and do not necessarily represent those of their affiliated organizations, or those of the publisher, the editors and the reviewers. Any product that may be evaluated in this article, or claim that may be made by its manufacturer, is not guaranteed or endorsed by the publisher.

References

Ahmed, S. F., Buetow, L., Gabrielsen, M., Lilla, S., Chatrin, C., Sibbet, G. J., et al. (2020). DELTEX2 C-terminal domain recognizes and recruits ADP-ribosylated proteins for ubiquitination. *Sci. Adv.* 6 (34), eabc0629. PubMed PMID: 32937373. PMCID: PMC7442474. Epub 2020/09/17. doi:10.1126/sciadv.abc0629

Anscher, M. S., Chang, E., Gao, X., Gong, Y., Weinstock, C., Bloomquist, E., et al. (2021). FDA approval summary: Rucaparib for the treatment of patients with deleterious BRCA-mutated metastatic castrate-resistant prostate cancer. *Oncologist* 26 (2), 139–146. PubMed PMID: 33145877. PMCID: PMC7873319. Epub 2020/11/05. doi:10.1002/onco.13585

Bai, P., and Canto, C. (2012). The role of PARP-1 and PARP-2 enzymes in metabolic regulation and disease. *Cell Metab.* 16 (3), 290–295. PubMed PMID: 22921416. Epub 2012/08/28. doi:10.1016/j.cmet.2012.06.016

Bolderson, E., Burgess, J. T., Li, J., Gandhi, N. S., Boucher, D., Croft, L. V., et al. (2019). Barrier-to-autointegration factor 1 (Banf1) regulates poly [ADP-ribose] polymerase 1 (PARP1) activity following oxidative DNA damage. *Nat. Commun.* 10 (1), 5501. PubMed PMID: 31796734. PMCID: PMC6890647 founders of Carpe Vitae Pharmaceuticals. E.B., J.T.B, K.J.O. and D.J.R. are inventors on provisional patent applications filed by Queensland University of Technology. D.A.S is a founder, equity owner, advisor, director, consultant, investor and/or inventor on patents licensed to

Vium, Jupiter Orphan Therapeutics, Cohbar, Galilei Biosciences, Wellomics, EdenRoc Sciences (affiliates Arc-Bio, Dovetail Genomics, Claret, Revere, UpRNA, MetroBiotech, Liberty) and Life Biosciences (affiliates Selphagy, Senolytic Therapeutics, Spotlight Therapeutics, Immetas, Animal Biosciences, Iduna, Continuum, Jumpstart). He is an inventor on a patent application filed by Harvard Medical School licensed to Elysium Health. See. Epub 2019/12/05. doi:10.1038/s41467-019-13167-5

Chen, H. D., Chen, C. H., Wang, Y. T., Guo, N., Tian, Y. N., Huan, X. J., et al. (2019). Increased PARP1-DNA binding due to autoPARylation inhibition of PARP1 on DNA rather than PARP1-DNA trapping is correlated with PARP1 inhibitor's cytotoxicity. *Int. J. Cancer* 145 (3), 714–727. PubMed PMID: 30675909. Epub 2019/01/25. doi:10.1002/ijc.32131

Chen, Q., Bian, C., Wang, X., Liu, X., Ahmad Kassab, M., Yu, Y., et al. (2021). ADP-ribosylation of histone variant H2AX promotes base excision repair. *EMBO J.* 40 (2), e104542. PubMed PMID: 33264433. PMCID: PMC7809701. Epub 2020/12/03. doi:10.15252/embj.2020104542

Chen, Q., Ma, K., Liu, X., Chen, S. H., Li, P., Yu, Y., et al. (2022). Truncated PARP1 mediates ADP-ribosylation of RNA polymerase III for apoptosis. *Cell Discov.* 8 (1), 3. PubMed PMID: 35039483. PMCID: PMC8764063. Epub 2022/01/19. doi:10.1038/s41421-021-00355-1

Chiappa, M., Guffanti, F., Bertoni, F., Colombo, I., and Damia, G. (2021). Overcoming PARPi resistance: Preclinical and clinical evidence in ovarian cancer. *Drug Resist Updat* 55, 100744. PubMed PMID: 33551306. Epub 2021/02/09. doi:10.1016/j.drup.2021.100744

Chung, W. C., Lee, S., Kim, Y., Seo, J. B., and Song, M. J. (2021). Kaposi's sarcoma-associated herpesvirus processivity factor (PF-8) recruits cellular E3 ubiquitin ligase CHFR to promote PARP1 degradation and lytic replication. *PLoS Pathog.* 17 (1), e1009261. PubMed PMID: 33508027. PMCID: PMC7872283. Epub 2021/01/29. doi:10.1371/journal.ppat.1009261

Clague, M. J., Heride, C., and Urbe, S. (2015). The demographics of the ubiquitin system. *Trends Cell Biol.* 25 (7), 417–426. PubMed PMID: 25906909. Epub 2015/04/25. doi:10.1016/j.tcb.2015.03.002

Cohen, M. S., and Chang, P. (2018). Insights into the biogenesis, function, and regulation of ADP-ribosylation. *Nat. Chem. Biol.* 14 (3), 236–243. PubMed PMID: 29443986. PMCID: PMC5922452. Epub 2018/02/15. doi:10.1038/nchembio.2568

Correani, V., Martire, S., Mignogna, G., Caruso, L. B., Tempera, I., Giorgi, A., et al. (2019). Poly(ADP-ribosylated) proteins in beta-amyloid peptide-stimulated microglial cells. *Biochem. Pharmacol.* 167, 50–57. PubMed PMID: 30414941. Epub 2018/11/12. doi:10.1016/j.bcp.2018.10.026

Deeks, E. D. (2015). Olaparib: First global approval. *Drugs* 75 (2), 231–240. PubMed PMID: 25616434. Epub 2015/01/27. doi:10.1007/s40265-015-0345-6

Dellomo, A. J., Abbotts, R., Eberly, C. L., Karbowski, M., Baer, M. R., Kingsbury, T. J., et al. (2022). PARP1 PARylates and stabilizes STAT5 in FLT3-ITD acute myeloid leukemia and other STAT5-activated cancers. *Transl. Oncol.* 15 (1), 101283. PubMed PMID: 34808460. PMCID: PMC8609071. Epub 2021/11/23. doi:10.1016/j.tranon.2021.101283

Dias, M. P., Moser, S. C., Ganesan, S., and Jonkers, J. (2021). Understanding and overcoming resistance to PARP inhibitors in cancer therapy. *Nat. Rev. Clin. Oncol.* 18 (12), 773–791. PubMed PMID: 34285417. Epub 2021/07/22. doi:10.1038/s41571-021-00532-x

Domchek, S. M., Postel-Vinay, S., Im, S. A., Park, Y. H., Delord, J. P., Italiano, A., et al. (2020). Olaparib and durvalumab in patients with germline BRCA-mutated metastatic breast cancer (MEDIOLA): An open-label, multicentre, phase 1/2, basket study. *Lancet Oncol.* 21 (9), 1155–1164. PubMed PMID: 32771088. Epub 2020/08/11. doi:10.1016/S1470-2045(20)30324-7

Du, H., Xia, H., Liu, T., Li, Y., Liu, J., Xie, B., et al. (2021). Suppression of ELF4 in ulcerative colitis predisposes host to colorectal cancer. *iScience* 24 (3), 102169. PubMed PMID: 33665583. PMCID: PMC7907480. Epub 2021/03/06. doi:10.1016/j.isci.2021.102169

Elsheikh, S. E., Green, A. R., Rakha, E. A., Powe, D. G., Ahmed, R. A., Collins, H. M., et al. (2009). Global histone modifications in breast cancer correlate with tumor phenotypes, prognostic factors, and patient outcome. *Cancer Res.* 69 (9), 3802–3809. PubMed PMID: 19366799. Epub 2009/04/16. doi:10.1158/0008-5472.CAN-08-3907

Eustermann, S., Wu, W. F., Langelier, M. F., Yang, J. C., Easton, L. E., Riccio, A. A., et al. (2015). Structural basis of detection and signaling of DNA single-strand breaks by human PARP-1. *Mol. Cell* 60 (5), 742–754. PubMed PMID: 26626479. PMCID: PMC4678113. Epub 2015/12/03. doi:10.1016/j.molcel.2015.10.032

Farmer, H., McCabe, N., Lord, C. J., Tutt, A. N., Johnson, D. A., Richardson, T. B., et al. (2005). Targeting the DNA repair defect in BRCA mutant cells as a therapeutic strategy. *Nature* 434 (7035), 917–921. PubMed PMID: 15829967. Epub 2005/04/15. doi:10.1038/nature03445

Fischbach, A., Kruger, A., Hampp, S., Assmann, G., Rank, L., Hufnagel, M., et al. (2018). The C-terminal domain of p53 orchestrates the interplay between non-covalent and covalent poly(ADP-ribosyl)ation of p53 by PARP1. *Nucleic Acids Res.* 46 (2), 804–822. PubMed PMID: 29216372. PMCID: PMC5778597. Epub 2017/12/08. doi:10.1093/nar/gkx1205

Fu, H., Liu, R., Jia, Z., Li, R., Zhu, F., Zhu, W., et al. (2022). Poly(ADP-ribosylation) of P-TEFb by PARP1 disrupts phase separation to inhibit global transcription after DNA damage. *Nat. Cell Biol.* 24 (4), 513–525. PubMed PMID: 35393539. PMCID: PMC9035116. Epub 2022/04/09. doi:10.1038/s41556-022-00872-5

Genois, M. M., Gagne, J. P., Yasuhara, T., Jackson, J., Saxena, S., Langelier, M. F., et al. (2021). CARM1 regulates replication fork speed and stress response by stimulating PARP1. *Mol. Cell* 81 (4), 784–800.e8. e8. PubMed PMID: 33412112. PMCID: PMC7897296. Epub 2021/01/08. doi:10.1016/j.molcel.2020.12.010

Gonzalez-Martin, A., Pothuri, B., Vergote, I., DePont Christensen, R., Graybill, W., Mirza, M. R., et al. (2019). Niraparib in patients with newly diagnosed advanced ovarian cancer. *N. Engl. J. Med.* 381 (25), 2391–2402. PubMed PMID: 31562799. Epub 2019/09/29. doi:10.1056/nejmoa1910962

Groslambert, J., Prokhorova, E., and Ahel, I. (2021). ADP-ribosylation of DNA and RNA. *DNA Repair* 105, 103144. PubMed PMID: 34116477. PMCID: PMC8385414. Epub 2021/06/12. doi:10.1016/j.dnarep.2021.103144

Gugnoni, M., Manzotti, G., Vitale, E., Sauta, E., Torricelli, F., Reggiani, F., et al. (2022). OVOL2 impairs RHO GTPase signaling to restrain mitosis and aggressiveness of Anaplastic Thyroid Cancer. *J. Exp. Clin. Cancer Res.* 41 (1), 41108. PubMed PMID: 35337349. PMCID: PMC8957195. Epub 2022/03/27. doi:10.1186/s13046-022-02316-2

Han, C., Sun, L. Y., Luo, X. Q., Pan, Q., Sun, Y. M., Zeng, Z. C., et al. (2022). Chromatin-associated orphan snoRNA regulates DNA damage-mediated differentiation via a non-canonical complex. *Cell Rep.* 38 (13), 110421. PubMed PMID: 35354054. Epub 2022/03/31. doi:10.1016/j.celrep.2022.110421

Hananya, N., Daley, S. K., Bagert, J. D., and Muir, T. W. (2021). Synthesis of ADP-ribosylated histones reveals site-specific impacts on chromatin structure and function. *J. Am. Chem. Soc.* 143 (29), 10847–10852. PubMed PMID: 34264659. Epub 2021/07/16. doi:10.1021/jacs.1c05429

Helleday, T. (2011). The underlying mechanism for the PARP and BRCA synthetic lethality: Clearing up the misunderstandings. *Mol. Oncol.* 5 (4), 387–393. PubMed PMID: 21821475. PMCID: PMC5528309. Epub 2011/08/09. doi:10.1016/j.molonc.2011.07.001

Heppler, L. N., and Frank, D. A. (2017). Targeting oncogenic transcription factors: Therapeutic implications of endogenous STAT inhibitors. *Trends Cancer* 3 (12), 816–827. PubMed PMID: 29198438. PMCID: PMC5727919. Epub 2017/12/05. doi:10.1016/j.trecan.2017.10.004

Hoy, S. M. (2018). Talazoparib: First global approval. *Drugs* 78 (18), 1939–1946. PubMed PMID: 30506138. Epub 2018/12/07. doi:10.1007/s40265-018-1026-z

Hsieh, M. H., Chen, Y. T., Chen, Y. T., Lee, Y. H., Lu, J., Chien, C. L., et al. (2017). PARP1 controls KLF4-mediated telomerase expression in stem cells and cancer cells. *Nucleic Acids Res.* 45 (18), 10492–10503. PubMed PMID: 28985359. PMCID: PMC5737510. Epub 2017/10/07. doi:10.1093/nar/gkx683

Hu, K., Wu, W., Li, Y., Lin, L., Chen, D., Yan, H., et al. (2019). Poly(ADP-ribosyl)ation of BRD7 by PARP1 confers resistance to DNA-damaging chemotherapeutic agents. *EMBO Rep.* 20 (5), e46166. PubMed PMID: 30940648. PMCID: PMC6500972. Epub 2019/04/04. doi:10.15252/embr.201846166

Huang, X., LeDuc, R. D., Fornelli, L., Schunter, A. J., Bennett, R. L., Kelleher, N. L., et al. (2019). Defining the NSD2 interactome: PARP1 PARylation reduces NSD2 histone methyltransferase activity and impedes chromatin binding. *J. Biol. Chem.* 294 (33), 12459–12471. PubMed PMID: 31248990. PMCID: PMC6699848. Epub 2019/06/30. doi:10.1074/jbc.RA118.006159

Ikura, M., Furuya, K., Matsuda, S., Matsuda, R., Shima, H., Adachi, J., et al. (2015). Acetylation of histone H2AX at lys 5 by the TIP60 histone acetyltransferase complex is essential for the dynamic binding of NBS1 to damaged chromatin. *Mol. Cell Biol.* 35 (24), 4147–4157. PubMed PMID: 26438602. PMCID: PMC4648820. Epub 2015/10/07. doi:10.1128/MCB.00757-15

Ilic, N., Tao, Y., Boutros-Suleiman, S., Kadali, V. N., Emanuelli, A., Levy-Cohen, G., et al. (2021). SMURF2-mediated ubiquitin signaling plays an essential role in the regulation of PARP1 PARylating activity, molecular interactions, and functions in mammalian cells. *FASEB J.* 35 (4), e21436. PubMed PMID: 33734501. Epub 2021/03/19. doi:10.1096/fj.202001759R

Kannan, S., Aitken, M. J. L., Herbrich, S. M., Golfman, L. S., Hall, M. G., Mak, D. H., et al. (2019). Antileukemia effects of notch-mediated inhibition of oncogenic PLK1 in B-cell acute lymphoblastic leukemia. *Mol. Cancer Ther.* 18 (9), 1615–1627. PubMed PMID: 31227645. PMCID: PMC6726528. Epub 2019/06/23. doi:10.1158/1535-7163.MCT-18-0706

Kim, D. S., Camacho, C. V., and Kraus, W. L. (2021). Alternate therapeutic pathways for PARP inhibitors and potential mechanisms of resistance. *Exp. Mol. Med.* 53 (1), 42–51. PubMed PMID: 33487630. PMCID: PMC8080675 coholder of U.S. Patent 9,599,606 covering a set of ADP-ribose detection reagents, which have been licensed to and are sold by EMD Millipore. Epub 2021/01/26. doi:10.1038/s12276-021-00557-3

Kim, D. S., Camacho, C. V., Nagari, A., Malladi, V. S., Challa, S., and Kraus, W. L. (2019). Activation of PARP-1 by snoRNAs controls ribosome biogenesis and cell growth via the RNA helicase DDX21. *Mol. Cell* 75 (6), 1270–1285.e14. PubMed PMID: 31351877. PMCID: PMC6754283. Epub 2019/07/29. doi:10.1016/j.molcel.2019.06.020

Kim, H., Xu, H., George, E., Hallberg, D., Kumar, S., Jagannathan, V., et al. (2020). Combining PARP with ATR inhibition overcomes PARP inhibitor and platinum resistance in ovarian cancer models. *Nat. Commun.* 11 (1), 3726. PubMed PMID: 32709856. PMCID: PMC7381609 advisory board for AstraZeneca (unpaid). E.J.B. serves on the scientific advisory board of Atrin Pharmaceuticals and has been an

advisor for Sierra Oncology. RAG has consulted for Agios Pharmaceuticals and MoMa Therapeutics.V.E.V. is a founder of Personal Genome Diagnostics, a member of its Scientific Advisory Board and Board of Directors, and owns Personal Genome Diagnostics stock, which are subject to certain restrictions under university policy. V.E.V. is an advisor to Takeda Pharmaceuticals. Within the last 5 years, V.E.V. has been an advisor to Daiichi Sankyo, Janssen Diagnostics, and Ignyta. R.B.S. is a founder of and holds equity in Delfi Diagnostics. He also serves as the Head of Data Sciences at Delfi Diagnostics. The terms for these arrangements for V.E.V. and R.B.S. has been reviewed and approved by the Johns Hopkins University in accordance with its conflict of interest policies. G.B.M. receives support or acts as a consultant for AstraZeneca, ImmunoMET, Ionis, Nanostring, PDX Pharmaceuticals, Signalchem Lifesciences, Symphogen, and Tarveda and has transferred technology to Myriad and Nanostring. The remaining authors declare no competing interestsEpub 2020/07/28. doi:10.1038/s41467-020-17127-2

Koczor, C. A., Saville, K. M., Andrews, J. F., Clark, J., Fang, Q., Li, J., et al. (2021). Temporal dynamics of base excision/single-strand break repair protein complex assembly/disassembly are modulated by the PARP/NAD(+)/SIRT6 axis. *Cell Rep.* 37 (5), 109917. PubMed PMID: 34731617. PMCID: PMC8607749. Epub 2021/11/04. doi:10.1016/j.celrep.2021.109917

Kong, Q., Li, Y., Liang, Q., Xie, J., Li, X., and Fang, J. (2020). SIRT6-PARP1 is involved in HMGB1 polyADP-ribosylation and acetylation and promotes chemotherapy-induced autophagy in leukemia. *Cancer Biol. Ther.* 21 (4), 320–331. PubMed PMID: 31928132. PMCID: PMC7515491. Epub 2020/01/14. doi:10.1080/15384047.2019.1702397

Konstantinopoulos, P. A., Waggoner, S., Vidal, G. A., Mita, M., Moroney, J. W., Holloway, R., et al. (2019). Single-arm phases 1 and 2 trial of niraparib in combination with pembrolizumab in patients with recurrent platinum-resistant ovarian carcinoma. *JAMA Oncol.* 5 (8), 1141–1149. PubMed PMID: 31194228. PMCID: PMC6567832 advisory boards for AstraZeneca, Pfizer, and Merck and Co. Dr Vidal reported consulting for Pfizer and Eli Lilly and Company and received research funding from Eli Lilly and Company, Genentech, AstraZeneca, Merck Serono, TESARO, Puma Biotechnology, and Bristol-Myers Squibb. Dr Holloway reported serving on a speaker bureau for TESARO. Dr Sachdev reported receiving research funding from Celgene and Pfizer; advisory board honoraria from Celgene and TapImmune, Inc; drug-only support for an investigator-sponsored trial from Genentech; and travel support from Celgene. Dr Colon-Otero reported receiving research funding from Novartis. Dr Penson reported serving on scientific advisory boards for Merck and Co and TESARO. Dr Matulonis reported serving in consulting/advisory roles for Merck KGaA, Clovis Oncology, Geneos Therapeutics, Eli Lilly and Company, and 2X Oncology. Dr Moore reported receiving fees from AstraZeneca, Clovis Oncology, TESARO, Genentech/Roche, ImmunoGen, Inc, Merck and Co, VBL Therapeutics, Janssen Pharmaceuticals, and OncoMed Pharmaceuticals, Inc. Dr Swisher reported receiving fees from IDEAYA Biosciences, SAB-Pharma, Inc, and Johnson and Johnson. Dr D'Andrea reported receiving funding from Stand Up to Cancer. Dr Stringer-Reasor reported serving as an investigator on an investigator-sponsored trial using niraparib and trastuzumab (Herceptin) in the treatment of metastatic HER2-positive breast cancer sponsored by TESARO. Drs Wang, Graham, Bobilev, and Dezube, Mr Buerstatte, and Ms Arora are employees of TESARO. Dr Munster reported receiving fees from Merck and Co, Pfizer, Novartis, GlaxoSmithKline, OncoMed Pharmaceuticals, Inc, Celgene, Intellikine, OncoNova Therapeutics, Nektar, Sanofi, Merrimack Pharmaceuticals, Genentech/Roche, OncoSec Medical Incorporated, Bristol-Myers Squibb, Plexxikon, Piramal Life Science, Andes Biotechnologies, Immune Design, BioMarin Pharmaceuticals, HUYA Bioscience International, and Threshold Pharmaceuticals outside the submitted work. No other disclosures were reported. Epub 2019/06/14. doi:10.1001/jamaoncol.2019.1048

Lake, R. J., Bilkis, R., and Fan, H. Y. (2022). Dynamic interplay between cockayne syndrome protein B and poly(ADP-ribose) polymerase 1 during oxidative DNA damage repair. *Biomedicines* 10 (2), 361. PubMed PMID: 35203571. PMCID: PMC8962439. Epub 2022/02/26. doi:10.3390/biomedicines10020361

Langelier, M. F., Eisemann, T., Riccio, A. A., and Pascal, J. M. (2018). PARP family enzymes: Regulation and catalysis of the poly(ADP-ribose) posttranslational modification. *Curr. Opin. Struct. Biol.* 53, 187–198. PubMed PMID: 30481609. PMCID: PMC6687463. Epub 2018/11/28. doi:10.1016/j.sbi.2018.11.002

Langelier, M. F., Planck, J. L., Roy, S., and Pascal, J. M. (2011). Crystal structures of poly(ADP-ribose) polymerase-1 (PARP-1) zinc fingers bound to DNA: Structural and functional insights into DNA-dependent PARP-1 activity. *J. Biol. Chem.* 286 (12), 10690–10701. PubMed PMID: 21233213. PMCID: PMC3060520. Epub 2011/01/15. doi:10.1074/jbc.m110.202507

Langelier, M. F., Planck, J. L., Roy, S., and Pascal, J. M. (2012). Structural basis for DNA damage-dependent poly(ADP-ribosyl)ation by human PARP-1. *Science* 336 (6082), 728–732. PubMed PMID: 22582261. PMCID: PMC3532513. Epub 2012/05/15. doi:10.1126/science.1216338

Langelier, M. F., Servent, K. M., Rogers, E. E., and Pascal, J. M. (2008). A third zinc-binding domain of human poly(ADP-ribose) polymerase-1 coordinates DNA-dependent enzyme activation. *J. Biol. Chem.* 283 (7), 4105–4114. PubMed PMID: 18055453. Epub 2007/12/07. doi:10.1074/jbc.m708558200

Lee, A. (2021). Fuzuloparib: First approval. *Drugs* 81 (10), 1221–1226. PubMed PMID: 34118019. PMCID: PMC8380563 offered an opportunity to comment on the article. Changes resulting from any comments received were made by the authors on the basis of scientific completeness and accuracy. Arnold Lee is a salaried employee of Adis International Ltd/Springer Nature, and declares no relevant conflicts of interest. All authors contributed to the review and are responsible for the article contentEpub 2021/06/13. doi:10.1007/s40265-021-01541-x

Lee, S. A., Lee, D., Kang, M., Kim, S., Kwon, S. J., Lee, H. S., et al. (2022). BAP1 promotes the repair of UV-induced DNA damage via PARP1-mediated recruitment to damage sites and control of activity and stability. *Cell Death Differ.* 29, 2381–2398. PubMed PMID: 35637285. Epub 2022/06/01. doi:10.1038/s41418-022-01024-w

Lee, S. G., Kim, N., Kim, S. M., Park, I. B., Kim, H., Kim, S., et al. (2020). Ewing sarcoma protein promotes dissociation of poly(ADP-ribose) polymerase 1 from chromatin. *EMBO Rep.* 21 (11), e48676. PubMed PMID: 33006225. PMCID: PMC7645264. Epub 2020/10/03. doi:10.15252/embr.201948676

Li, D. Q., Nair, S. S., Ohshiro, K., Kumar, A., Nair, V. S., Pakala, S. B., et al. (2012). MORC2 signaling integrates phosphorylation-dependent, ATPase-coupled chromatin remodeling during the DNA damage response. *Cell Rep.* 2 (6), 1657–1669. PubMed PMID: 23260667. PMCID: PMC3554793. Epub 2012/12/25. doi:10.1016/j.celrep.2012.11.018

Li, H., Liu, Z. Y., Wu, N., Chen, Y. C., Cheng, Q., and Wang, J. (2020). PARP inhibitor resistance: The underlying mechanisms and clinical implications. *Mol. Cancer* 19 (1), 107. PubMed PMID: 32563252. PMCID: PMC7305609. Epub 2020/06/22. doi:10.1186/s12943-020-01227-0

Li, Z., Li, Y., Tang, M., Peng, B., Lu, X., Yang, Q., et al. (2018). Destabilization of linker histone H1.2 is essential for ATM activation and DNA damage repair. *Cell Res.* 28 (7), 756–770. PubMed PMID: 29844578. PMCID: PMC6028381. Epub 2018/05/31. doi:10.1038/s41422-018-0048-0

Liu, H. Y., Liu, Y. Y., Zhang, Y. L., Ning, Y., Zhang, F. L., and Li, D. Q. (2022). Poly(ADP-ribosyl)ation of acetyltransferase NAT10 by PARP1 is required for its nucleoplasmic translocation and function in response to DNA damage. *Cell Commun. Signal* 20 (1), 127. PubMed PMID: 35986334. PMCID: PMC9389688. Epub 2022/08/20. doi:10.1186/s12964-022-00932-1

Liu, J., Tao, X., Zhu, Y., Li, C., Ruan, K., Diaz-Perez, Z., et al. (2021). NMNAT promotes glioma growth through regulating post-translational modifications of P53 to inhibit apoptosis. *Elife* 10, e70046. PubMed PMID: 34190052. PMCID: PMC8683086. Epub 2021/12/18. doi:10.7554/eLife.70046

Lord, C. J., and Ashworth, A. (2017). PARP inhibitors: Synthetic lethality in the clinic. *Science* 355 (6330), 1152–1158. PubMed PMID: 28302823. PMCID: PMC6175050. Epub 2017/03/18. doi:10.1126/science.aam7344

Luedeman, M. E., Stroik, S., Feng, W., Luthman, A. J., Gupta, G. P., and Ramsden, D. A. (2022). Poly(ADP) ribose polymerase promotes DNA polymerase theta-mediated end joining by activation of end resection. *Nat. Commun.* 13 (1), 4547. PubMed PMID: 35927262. PMCID: PMC9352658 developing inhibitors of Poltheta. D.A.R. has a materials transfer agreement with Artios Pharma and is using an Artios Pharma compound that inhibits Poltheta for research purposes with no financial compensation. M.L. accepted employment at Promega Corporation, manufacturer of the Halo-tag and ligand. The remaining authors declare no competing interests. Epub 2022/08/05. doi:10.1038/s41467-022-32166-7

Ma, H., Qi, G., Han, F., Lu, W., Peng, J., Li, R., et al. (2022). HMGB3 promotes PARP inhibitor resistance through interacting with PARP1 in ovarian cancer. *Cell Death Dis.* 13 (3), 263. PubMed PMID: 35332131. PMCID: PMC8948190. Epub 2022/03/26. doi:10.1038/s41419-022-04670-7

Marcar, L., Bardhan, K., Gheorghiu, L., Dinkelborg, P., Pfaffle, H., Liu, Q., et al. (2019). Acquired resistance of EGFR-mutated lung cancer to tyrosine kinase inhibitor treatment promotes PARP inhibitor sensitivity. *Cell Rep.* 27 (12), 3422–3432.e4. e4. PubMed PMID: 31216465. PMCID: PMC6624074. Epub 2019/06/20. doi:10.1016/j.celrep.2019.05.058

Markham, A. (2021). Pamiparib: First approval. *Drugs* 81 (11), 1343–1348. PubMed PMID: 34287805. Epub 2021/07/22. doi:10.1007/s40265-021-01552-8

Marti, J. M., Garcia-Diaz, A., Delgado-Bellido, D., O'Valle, F., Gonzalez-Flores, A., Carlevaris, O., et al. (2021). Selective modulation by PARP-1 of HIF-1α-recruitment to chromatin during hypoxia is required for tumor adaptation to hypoxic conditions. *Redox Biol.* 41, 101885. PubMed PMID: 33581682. PMCID: PMC7878192. Epub 2021/02/14. doi:10.1016/j.redox.2021.101885

Masson, M., Niedergang, C., Schreiber, V., Muller, S., Menissier-de Murcia, J., and de Murcia, G. (1998). XRCC1 is specifically associated with poly(ADP-ribose) polymerase and negatively regulates its activity following DNA damage. *Mol. Cell Biol.* 18 (6), 3563–3571. PubMed PMID: 9584196. PMCID: PMC108937. Epub 1998/06/20. doi:10.1128/MCB.18.6.3563

Mattiroli, F., Vissers, J. H., van Dijk, W. J., Ikpa, P., Citterio, E., Vermeulen, W., et al. (2012). RNF168 ubiquitinates K13-15 on H2A/H2AX to drive DNA damage signaling. *Cell* 150 (6), 1182–1195. PubMed PMID: 22980979. Epub 2012/09/18. doi:10.1016/j.cell.2012.08.005

Matveeva, E. A., Dhahri, H., and Fondufe-Mittendorf, Y. (2022). PARP1's involvement in RNA polymerase II elongation: Pausing and releasing regulation through the integrator and super elongation complex. *Cells* 11 (20), 3202. PubMed PMID: 36291070. PMCID: PMC9600911. Epub 2022/10/28. doi:10.3390/cells11203202

Messner, S., Altmeyer, M., Zhao, H., Pozivil, A., Roschitzki, B., Gehrig, P., et al. (2010). PARP1 ADP-ribosylates lysine residues of the core histone tails. *Nucleic Acids Res.* 38 (19), 6350–6362. PubMed PMID: 20525793. PMCID: PMC2965223. Epub 2010/06/08. doi:10.1093/nar/gkq463

Meyer-Ficca, M. L., Meyer, R. G., Coyle, D. L., Jacobson, E. L., and Jacobson, M. K. (2004). Human poly(ADP-ribose) glycohydrolase is expressed in alternative splice

variants yielding isoforms that localize to different cell compartments. *Exp. Cell Res.* 297 (2), 521–532. PubMed PMID: 15212953. Epub 2004/06/24. doi:10.1016/j.yexcr.2004.03.050

Min, A., and Im, S. A. (2020). PARP inhibitors as therapeutics: Beyond modulation of PARRylation. *Cancers (Basel)* 12 (2), 394. PubMed PMID: 32046300. PMCID: PMC7072193. Epub 2020/02/13. doi:10.3390/cancers12020394

Moissiard, G., Cokus, S. J., Cary, J., Feng, S., Billi, A. C., Stroud, H., et al. (2012). MORC family ATPases required for heterochromatin condensation and gene silencing. *Science* 336 (6087), 1448–1451. PubMed PMID: 22555433. PMCID: PMC3376212. Epub 2012/05/05. doi:10.1126/science.1221472

Munnur, D., Somers, J., Skalka, G., Weston, R., Jukes-Jones, R., Bhogadia, M., et al. (2019). NR4A nuclear receptors target poly-ADP-ribosylated DNA-PKcs protein to promote DNA repair. *Cell Rep.* 26 (8), 2028–2036.e6. e6. PubMed PMID: 30784586. PMCID: PMC6381605. Epub 2019/02/21. doi:10.1016/j.celrep.2019.01.083

Murai, J., Huang, S. Y., Das, B. B., Renaud, A., Zhang, Y., Doroshow, J. H., et al. (2012). Trapping of PARP1 and PARP2 by clinical PARP inhibitors. *Cancer Res.* 72 (21), 5588–5599. PubMed PMID: 23118055. PMCID: PMC3528345. Epub 2012/11/03. doi:10.1158/0008-5472.CAN-12-2753

Oka, S., Kato, J., and Moss, J. (2006). Identification and characterization of a mammalian 39-kDa poly(ADP-ribose) glycohydrolase. *J. Biol. Chem.* 281 (2), 705–713. PubMed PMID: 16278211. Epub 2005/11/10. doi:10.1074/jbc.m510290200

Pal Singh, M., Pal Khaket, T., Bajpai, V. K., Alfarraj, S., Kim, S. G., Chen, L., et al. (2020). Morin hydrate sensitizes hepatoma cells and xenograft tumor towards cisplatin by downregulating PARP-1-HMGB1 mediated autophagy. *Int. J. Mol. Sci.* 21 (21), 8253. PubMed PMID: 33158052. PMCID: PMC7885522. Epub 2020/11/08. doi:10.3390/ijms21218253

Peterson, C. L., and Laniel, M. A. (2004). Histones and histone modifications. *Curr. Biol.* 14 (14), R546–R551. PubMed PMID: 15268870. Epub 2004/07/23. doi:10.1016/j.cub.2004.07.007

Peyraud, F., and Italiano, A. (2020). Combined PARP inhibition and immune checkpoint therapy in solid tumors. *Cancers (Basel)* 12 (6), 1502. PubMed PMID: 32526888. PMCID: PMC7352466. Epub 2020/06/13. doi:10.3390/cancers12061502

Pfeiffer, A., Herzog, L. K., Luijsterburg, M. S., Shah, R. G., Rother, M. B., Stoy, H., et al. (2021). Poly(ADP-ribosyl)ation temporally confines SUMO-dependent ataxin-3 recruitment to control DNA double-strand break repair. *J. Cell Sci.* 134 (3). PubMed PMID: 33408245. Epub 2021/01/08. doi:10.1242/jcs.247809

Poirier, G. G., de Murcia, G., Jongstra-Bilen, J., Niedergang, C., and Mandel, P. (1982). Poly(ADP-ribosyl)ation of polynucleosomes causes relaxation of chromatin structure. *Proc. Natl. Acad. Sci. U. S. A.* 79 (11), 3423–3427. PubMed PMID: 6808510. PMCID: PMC346432. Epub 1982/06/01. doi:10.1073/pnas.79.11.3423

Pommier, Y., O'Connor, M. J., and de Bono, J. (2016). Laying a trap to kill cancer cells: PARP inhibitors and their mechanisms of action. *Sci. Transl. Med.* 8 (362), 362ps17. PubMed PMID: 27797957. Epub 2016/11/01. doi:10.1126/scitranslmed.aaf9246

Pulliam, N., Tang, J., Wang, W., Fang, F., Sood, R., O'Hagan, H. M., et al. (2019). Poly-ADP-ribosylation of estrogen receptor-alpha by PARP1 mediates antiestrogen resistance in human breast cancer cells. *Cancers (Basel)* 11 (1), 43. PubMed PMID: 30621214. PMCID: PMC6357000. Epub 2019/01/10. doi:10.3390/cancers11010043

Qian, H., Zhang, N., Wu, B., Wu, S., You, S., Zhang, Y., et al. (2020). The E3 ubiquitin ligase Smurf2 regulates PARP1 stability to alleviate oxidative stress-induced injury in human umbilical vein endothelial cells. *J. Cell Mol. Med.* 24 (8), 4600–4611. PubMed PMID: 32167680. PMCID: PMC7176845. Epub 2020/03/14. doi:10.1111/jcmm.15121

Rasmussen, M., Tan, S., Somisetty, V. S., Hutin, D., Olafsen, N. E., Moen, A., et al. (2021). PARP7 and mono-ADP-ribosylation negatively regulate estrogen receptor alpha signaling in human breast cancer cells. *Cells* 10 (3), 623. PubMed PMID: 33799807. PMCID: PMC8001409. Epub 2021/04/04. doi:10.3390/cells10030623

Ruf, A., de Murcia, G., and Schulz, G. E. (1998). Inhibitor and NAD+ binding to poly(ADP-ribose) polymerase as derived from crystal structures and homology modeling. *Biochemistry* 37 (11), 3893–3900. PubMed PMID: 9521710. Epub 1998/04/02. doi:10.1021/bi972383s

Santofimia-Castano, P., Huang, C., Liu, X., Xia, Y., Audebert, S., Camoin, L., et al. (2022). NUPR1 protects against hyperPARRylation-dependent cell death. *Commun. Biol.* 5 (1), 732. PubMed PMID: 35869257. PMCID: PMC9307593 J.L.N., and J.I. are inventors of the Patent "NUPR1 INHIBITION FOR TREATING CANCER", Application number WO-2019229236-A1. The other authors declare no competing interests. This work was supported by La Ligue Contre le CancerEpub 2022/07/23, INCa, Canceropole PACA, and INSERM. C.H. and X.L. are recipient of the predoctoral fellowship from China Scholarship Council (CSC). doi:10.1038/s42003-022-03705-1

Schaub, J. M., Soniat, M. M., and Finkelstein, I. J. (2022). Polymerase theta-helicase promotes end joining by stripping single-stranded DNA-binding proteins and bridging DNA ends. *Nucleic Acids Res.* 50 (7), 3911–3921. PubMed PMID: 35357490. PMCID: PMC9023281. Epub 2022/04/01. doi:10.1093/nar/gkac119

Schiewer, M. J., Goodwin, J. F., Han, S., Brenner, J. C., Augello, M. A., Dean, J. L., et al. (2012). Dual roles of PARP-1 promote cancer growth and progression. *Cancer Discov.* 2 (12), 1134–1149. PubMed PMID: 22993403. PMCID: PMC3519969. Epub 2012/09/21. doi:10.1158/2159-8290.CD-12-0120

Schreiber, V., Dantzer, F., Ame, J. C., and de Murcia, G. (2006). Poly(ADP-ribose): Novel functions for an old molecule. *Nat. Rev. Mol. Cell Biol.* 7 (7), 517–528. PubMed PMID: 16829982. Epub 2006/07/11. doi:10.1038/nrm1963

Schultz, N., Lopez, E., Saleh-Gohari, N., and Helleday, T. (2003). Poly(ADP-ribose) polymerase (PARP-1) has a controlling role in homologous recombination. *Nucleic Acids Res.* 31 (17), 4959–4964. PubMed PMID: 12930944. PMCID: PMC212803. Epub 2003/08/22. doi:10.1093/nar/gkg703

Sharma, D., De Falco, L., Padavattan, S., Rao, C., Geifman-Shochat, S., Liu, C. F., et al. (2019). PARP1 exhibits enhanced association and catalytic efficiency with γH2A.X-nucleosome. *Nat. Commun.* 10 (1), 5751. PubMed PMID: 31848352. PMCID: PMC6917767. Epub 2019/12/19. doi:10.1038/s41467-019-13641-0

Sone, K., Piao, L., Nakakido, M., Ueda, K., Jenuwein, T., Nakamura, Y., et al. (2014). Critical role of lysine 134 methylation on histone H2AX for gamma-H2AX production and DNA repair. *Nat. Commun.* 5, 5691. PubMed PMID: 25487737. PMCID: PMC4268694 and also has research grants from Oncotherapy Science. All other authors declare no competing financial interests. Epub 2014/12/10. doi:10.1038/ncomms6691

Strom, C. E., Johansson, F., Uhlen, M., Szigyarto, C. A., Erixon, K., and Helleday, T. (2011). Poly (ADP-ribose) polymerase (PARP) is not involved in base excision repair but PARP inhibition traps a single-strand intermediate. *Nucleic Acids Res.* 39 (8), 3166–3175. PubMed PMID: 21183466. PMCID: PMC3082910. Epub 2010/12/25. doi:10.1093/nar/gkq1241

Suico, M. A., Shuto, T., and Kai, H. (2017). Roles and regulations of the ETS transcription factor ELF4/MEF. *J. Mol. Cell Biol.* 9 (3), 168–177. PubMed PMID: 27932483. PMCID: PMC5907832. Epub 2016/12/10. doi:10.1093/jmcb/mjw051

Tay, L. S., Krishnan, V., Sankar, H., Chong, Y. L., Chuang, L. S. H., Tan, T. Z., et al. (2018). RUNX poly(ADP-ribosyl)ation and BLM interaction facilitate the Fanconi anemia pathway of DNA repair. *Cell Rep.* 24 (7), 1747–1755. Epub 2018/08/16. doi:10.1016/j.celrep.2018.07.038

Tolic, A., Ravichandran, M., Rajic, J., Dordevic, M., Dordevic, M., Dinic, S., et al. (2022). TET-mediated DNA hydroxymethylation is negatively influenced by the PARP-dependent PARRylation. *Epigenetics Chromatin* 15 (1), 11. PubMed PMID: 35382873. PMCID: PMC8985375. Epub 2022/04/07. doi:10.1186/s13072-022-00445-8

Tufan, A. B., Lazarow, K., Kolesnichenko, M., Sporbert, A., von Kries, J. P., and Scheidereit, C. (2022). TSG101 associates with PARP1 and is essential for PARRylation and DNA damage-induced NF-κB activation. *EMBO J.* 41 (21), e110372. PubMed PMID: 36124865. PMCID: PMC9627669. Epub 2022/09/21. doi:10.15252/embj.2021110372

van Beek, L., McClay, E., Patel, S., Schimpl, M., Spagnolo, L., and Maia de Oliveira, T. (2021). PARP power: A structural perspective on PARP1, PARP2, and PARP3 in DNA damage repair and nucleosome remodelling. *Int. J. Mol. Sci.* 22 (10), 5112. PubMed PMID: 34066057. PMCID: PMC8150716. Epub 2021/06/03. doi:10.3390/ijms22105112

Verma, P., Zhou, Y., Cao, Z., Deraska, P. V., Deb, M., Arai, E., et al. (2021). ALC1 links chromatin accessibility to PARP inhibitor response in homologous recombination-deficient cells. *Nat. Cell Biol.* 23 (2), 160–171. PubMed PMID: 33462394. PMCID: PMC7880902. Epub 2021/01/20. doi:10.1038/s41556-020-00624-3

Wang, F., Zhao, M., Chang, B., Zhou, Y., Wu, X., Ma, M., et al. (2022). Cytoplasmic PARP1 links the genome instability to the inhibition of antiviral immunity through PARRylating cGAS. *Mol. Cell* 82 (11), 2032–2049.e7. e7. PubMed PMID: 35460603. Epub 2022/04/24. doi:10.1016/j.molcel.2022.03.034

Wang, F., Zhu, S., Fisher, L. A., Wang, L., Eurek, N. J., Wahl, J. K., 3rd, et al. (2019). Phosphatase 1 nuclear targeting subunit mediates recruitment and function of poly (ADP-Ribose) polymerase 1 in DNA repair. *Cancer Res.* 79 (10), 2526–2535. PubMed PMID: 30733193. PMCID: PMC6522276. Epub 2019/02/09. doi:10.1158/0008-5472.CAN-18-1673

Wang, M., Wu, W., Wu, W., Rosidi, B., Zhang, L., Wang, H., et al. (2006). PARP-1 and Ku compete for repair of DNA double strand breaks by distinct NHEJ pathways. *Nucleic Acids Res.* 34 (21), 6170–6182. PubMed PMID: 17088286. PMCID: PMC1693894. Epub 2006/11/08. doi:10.1093/nar/gkl840

Wang, N., Yang, Y., Jin, D., Zhang, Z., Shen, K., Yang, J., et al. (2022). PARP inhibitor resistance in breast and gynecological cancer: Resistance mechanisms and combination therapy strategies. *Front. Pharmacol.* 13, 967633. PubMed PMID: 36091750. PMCID: PMC9455597. Epub 2022/09/13. doi:10.3389/fphar.2022.967633

Wang, Y., Wang, Y., Wang, N., You, L., Long, F., Shao, C., et al. (2019). Poly(ADP-ribose) polymerase 1/2 inhibitors decrease the ubiquitination of ALC1 mediated by CHFR in breast cancer. *Oncol. Rep.* 42 (4), 1467–1474. PubMed PMID: 31322269. Epub 2019/07/20. doi:10.3892/or.2019.7242

Wu, W., Zhao, J., Xiao, J., Wu, W., Xie, L., Xie, X., et al. (2021). CHFR-mediated degradation of RNF126 confers sensitivity to PARP inhibitors in triple-negative breast cancer cells. *Biochem. Biophys. Res. Commun.* 573, 62–68. PubMed PMID: 34388456. Epub 2021/08/14. doi:10.1016/j.bbrc.2021.08.011

Xie, Y., Han, N., Li, F., Wang, L., Liu, G., Hu, M., et al. (2022). Melatonin enhances osteoblastogenesis of senescent bone marrow stromal cells through NSD2-mediated chromatin remodelling. *Clin. Transl. Med.* 12 (2), e746. PubMed PMID: 35220680. PMCID: PMC8882236. Epub 2022/02/28. doi:10.1002/ctm2.746

Xue, H., Bhardwaj, A., Yin, Y., Fijen, C., Ephstein, A., Zhang, L., et al. (2022). A two-step mechanism governing PARP1-DNA retention by PARP inhibitors. *Sci. Adv.* 8 (36), eabq0414. PubMed PMID: 36070389. PMCID: PMC9451145. Epub 2022/09/08. doi:10.1126/sciadv.abq0414

Yang, F., Chen, J., Liu, B., Gao, G., Sebastian, M., Jeter, C., et al. (2021). SPINDOC binds PARP1 to facilitate PARylation. *Nat. Commun.* 12 (1), 6362. PubMed PMID: 34737271. PMCID: PMC8568969 interests. Epub 2021/11/06. doi:10.1038/s41467-021-26588-y

Yazinski, S. A., Comaills, V., Buisson, R., Genois, M. M., Nguyen, H. D., Ho, C. K., et al. (2017). ATR inhibition disrupts rewired homologous recombination and fork protection pathways in PARP inhibitor-resistant BRCA-deficient cancer cells. *Genes Dev.* 31 (3), 318–332. PubMed PMID: 28242626. PMCID: PMC5358727. Epub 2017/03/01. doi:10.1101/gad.290957.116

Ye, B. J., Kang, H. J., Lee-Kwon, W., Kwon, H. M., and Choi, S. Y. (2021). PARP1-mediated PARylation of TonEBP prevents R-loop-associated DNA damage. *DNA Repair (Amst)* 104, 103132. PubMed PMID: 34049076. Epub 2021/05/29. doi:10.1016/j.dnarep.2021.103132

Zhang, C., Zhou, B., Gu, F., Liu, H., Wu, H., Yao, F., et al. (2022). Micropeptide PACMP inhibition elicits synthetic lethal effects by decreasing CtIP and poly(ADP-ribosyl)ation. *Mol. Cell* 82 (7), 1297–1312.e8. e8. PubMed PMID: 35219381. Epub 2022/02/28. doi:10.1016/j.molcel.2022.01.020

Zhang, L., and Li, D. Q. (2019). MORC2 regulates DNA damage response through a PARP1-dependent pathway. *Nucleic Acids Res.* 47 (16), 8502–8520.

PubMed PMID: 31616951. PMCID: PMC6895267. Epub 2019/10/17. doi:10.1093/nar/gkz545

Zhang, R., Hong, J. J., Yang, Q., Ong, C. T., Li, B. A., and Liou, Y. C. (2019). Poly(ADP-ribosyl)ation of OVOL2 regulates aneuploidy and cell death in cancer cells. *Oncogene* 38 (15), 2750–2766. PubMed PMID: 30542118. Epub 2018/12/14. doi:10.1038/s41388-018-0615-3

Zhang, Y., Wang, J., Ding, M., and Yu, Y. (2013). Site-specific characterization of the asp- and glu-ADP-ribosylated proteome. *Nat. Methods* 10 (10), 981–984. PubMed PMID: 23955771. Epub 2013/08/21. doi:10.1038/nmeth.2603

Zhi, W., Li, S., Wan, Y., Wu, F., and Hong, L. (2022). Short-term starvation synergistically enhances cytotoxicity of Niraparib via Akt/mTOR signaling pathway in ovarian cancer therapy. *Cancer Cell Int.* 22 (1), 18. PubMed PMID: 35016681. PMCID: PMC8753877. Epub 2022/01/13. doi:10.1186/s12935-022-02447-8

Zhou, Z., Huang, F., Shrivastava, I., Zhu, R., Luo, A., Hottiger, M., et al. (2020). New insight into the significance of KLF4 PARylation in genome stability, carcinogenesis, and therapy. *EMBO Mol. Med.* 12 (12), e12391. PubMed PMID: 33231937. PMCID: PMC7721363. Epub 2020/11/25. doi:10.15252/emmm.202012391

The inhibitory effect of 6-gingerol and cisplatin on ovarian cancer and antitumor activity: *In silico*, *in vitro*, and *in vivo*

Zohreh Salari[1], Ahmad Khosravi[2*], Elham Pourkhandani[1*], Elaheh Molaakbari[3], Ehsan Salarkia[2], Alireza Keyhani[2], Iraj Sharifi[2], Hadi Tavakkoli[4], Samira Sohbati[1], Shahriar Dabiri[5], Guogang Ren[6] and Mohammad Shafie'ei[7]

[1]Obstetrics and Gynecology Center, Afzalipour School of Medicine, Kerman University of Medical Sciences, Kerman, Iran, [2]Leishmaniasis Research Center, Kerman University of Medical Sciences, Kerman, Iran, [3]Department of Chemistry, Shahid Bahonar University of Kerman, Kerman, Iran, [4]Department of Clinical Science, School of Veterinary Medicine, Shahid Bahonar University of Kerman, Kerman, Iran, [5]Afzalipour School of Medicine and Pathology and Stem Cells Research Center, Kerman University of Medical Sciences, Kerman, Iran, [6]School of Engineering and Computer Science, University of Hertfordshire, Hatfield, United Kingdom, [7]Faculty of Medicine, Kerman University of Medical Sciences, Kerman, Iran

Background: Epithelial ovarian cancer is very common in women and causes hundreds of deaths per year worldwide. Chemotherapy drugs including cisplatin have adverse effects on patients' health. Complementary treatments and the use of herbal medicines can help improve the performance of medicine. 6-Gingerol is the major pharmacologically active component of ginger. In this study, we compared the effects of 6-gingerol, cisplatin, and their combination in apoptotic and angiogenetic activities *in silico*, in test tubes, and in *in vivo* assays against two ovarian cancer cell lines: OVCAR-3 and human umbilical vein endothelial cells (HUVECs).

Methods: The drug-treated cell lines were evaluated for their cytotoxicity, cell cycle, and apoptotic and angiogenetic gene expression changes.

Results: The proportion of apoptosis treated by 6-gingerol coupled with cisplatin was significantly high. In the evaluation of the cell cycle, the combination therapy also showed a significant promotion of a higher extent of the S sequence. The expression of p53 level, Caspase-8, Bax, and Apaf1 genes was amplified again with combination therapy. Conversely, in both cell lines, the cumulative drug concentrations reduced the expression of VEGF, FLT1, KDR, and Bcl-2 genes. Similarly, in the control group, combination treatment significantly decreased the expression of VEGF, FLT1, KDR, and Bcl-2 genes in comparison to cisplatin alone.

Conclusions: The findings of the present study demonstrated that the cisplatin and 6-gingerol combination is more effective in inducing apoptosis and suppressing the angiogenesis of ovarian cancer cells than using each drug alone.

KEYWORDS

ovarian neoplasm, gingerol, cisplatin, apoptosis, angiogenesis, molecular dynamics simulation, chick embryo

1 Introduction

Cancer is the most prevalent cause of death worldwide. Ovarian malignancy is the third most common gynecological cancer in women after cervical cancer (1). This cancer has the worst prognosis and the highest mortality rate (2, 3). Although it is less common than breast cancer, it is three times more deadly and is projected to increase dramatically by 2040 (1). The high mortality of this cancer is because its growth is secretive and asymptomatic until the end stages of the disease (4). That is why it is called the silent killer (2).

More than half of ovarian cancers have local recurrences and eventually extrapulmonary metastases that are non-surgical and require systemic and palliative care at this stage. Chemotherapy is a systemic treatment for advanced cancer that lowers the size of the tumor and minimizes the symptoms of the disease. Numerous studies have shown that the use of chemoradiotherapy before surgery increases the complete pathological response of the tumor, which is one of the critical factors in the prognosis of the disease (5–7).

Cisplatin is among the most widely applied drugs that can be used alone or combined with other chemotherapy drugs such as paclitaxel, carboplatin, topotecan, etoposide, and doxorubicin in the treatment of most solid tumors, including ovarian cancer. It reacts with the nitrogen atoms of adenine and guanine in the DNA molecule of the cancer cells, causing DNA damage and blocking cell division, and eventually apoptosis or cell death. However, despite the initial efficacy of this drug, its long-term administration not only causes drug resistance (8) but also results in side effects such as neutropenia, anemia, and thrombocytopenia (5, 9).

Angiogenesis, which involves the production of new blood vessels in the growth areas of new tissues, is a normal physiological phenomenon that occurs in conditions such as wound healing or fetal growth. This phenomenon also occurs in cases of mass tumor expansion. There are many genes involved in angiogenesis, of which one of the most important is VEGF-A. Increased mRNA of this factor has been observed in malignant ovarian cancer cells (10, 11).

In recent decades, researchers have sought to find herbal compounds that, in addition to having no side effects, can be used as adjunctive drugs in addition to chemotherapy to treat cancer. Studies show that vegetable oils have an anticancer role and can effectively treat cancer with an anti-inflammatory effect (12).

Ginger is one of the plants containing phenolic compounds that have been used in various cultures, especially in Iran, for various uses, including cooking as a spice and in traditional medicine. This plant has different components, including 3-gingerol, 6-gingerol, 3-shogaols, 6-shogaols, and paradole, among which 6-gingerol is the most active metabolite of ginger, which has a broad range of pharmacological properties such as anti-nausea, anticoagulant, antimicrobial, antioxidant, anti-inflammatory, and anticancer properties. Among 6-gingerols, 6-gingerol-6 is the most pharmacologically active metabolite (13, 14).

Studies showed that 6-gingerol had a greater anti-angiogenic and apoptotic effect than those of other components of ginger. It has an inhibitory effect on the growth of cancerous breast, ovary, pancreas, prostate, and intestine tumors (15, 16) while 6-gingerol slowed the progression of skin cancer cells in mice by preventing the induction of p53 proto-oncogene (17). 6-Gingerol can also prevent the proliferation of different types of cancers including HPV-infected cells in the cervix, reactivates the apoptotic factor p53, and accelerates DNA destruction by cancer cells. Interestingly, 6-gingerol also induces the expression of apoptotic-associated genes including Caspase-3 and PARP, and reduces tumor volume (18–21)

The foundation for docking conformations was the binding affinity of 6-gingerol and cisplatin with apoptotic (Bax, Bcl-2, and Caspase-8) and angiogenetic (VEGF-A and KDR1) mediator genes (22). Considering the anti-inflammatory effect of 6-gingerol and its positive effects on cancer cell lines, we decided to investigate a wide range of experimentation to assess the effect of the substances on their apoptosis and angiogenesis against ovarian cancer *in silico*, *in vitro*, and *in vivo* models using a chick model in compositions of cisplatin alone and their combination.

2 Materials and methods

2.1 *In silico* modeling

2.1.1 Ligand and target/receptor preparation

The conformers of 6-gingerol and cisplatin in three dimensions and sdf format (Figures 1 IA, B) were retrieved from the PubChem compounds database at the National Center for Biotechnology Information (NCBI) website (www.pubchem.ncbi.nlm.nih.gov). KDR 1 and VEGF-A as the consistent angiogenic-regulating genes and Bax and Caspase-8 as apoptotic-regulator proteins were chosen as our receptors in this investigation. At first, the target protein structures of Bax, Caspase-8, KDR1, and VEGF-A targets (PDB ID: 5W5X, 5JSN, 1I4E, 2QU5, and 5T89, respectively) were obtained from the RCSB Protein Data Bank (https://www.rcsb.org/) (Figures 1 IIA-E). Subsequently, to prepare a structure for molecular docking, supplementary factors in the PDB file were removed using MVD software.

2.1.2 Molecular docking (MVD) process

The precision of the AutoDock Vina package is approximately 80%, more advanced than that of AutoDock 4.2 (23), while this is close to 87% for the MVD software (24). The structure of protein and compounds was organized, employing the "preparation molecule for docking" unit of MVD; then, cavities of protein were detected as appropriate poses on the receptor for ligand binding. A maximum iteration of 1,500, a grid resolution of 0.30Å, and a maximum population size of 50 were established as docking boundaries. The internal electrostatic interaction (internal ES), sp2–sp2 rotations, and the internal H-bond interactions were recorded to assess the chemical affinity and connections of the mixes with the Bax, Bcl-2, Caspase-8, KDR1, and VEGF-A. Simplex development was established at maximum stages of 300 with a
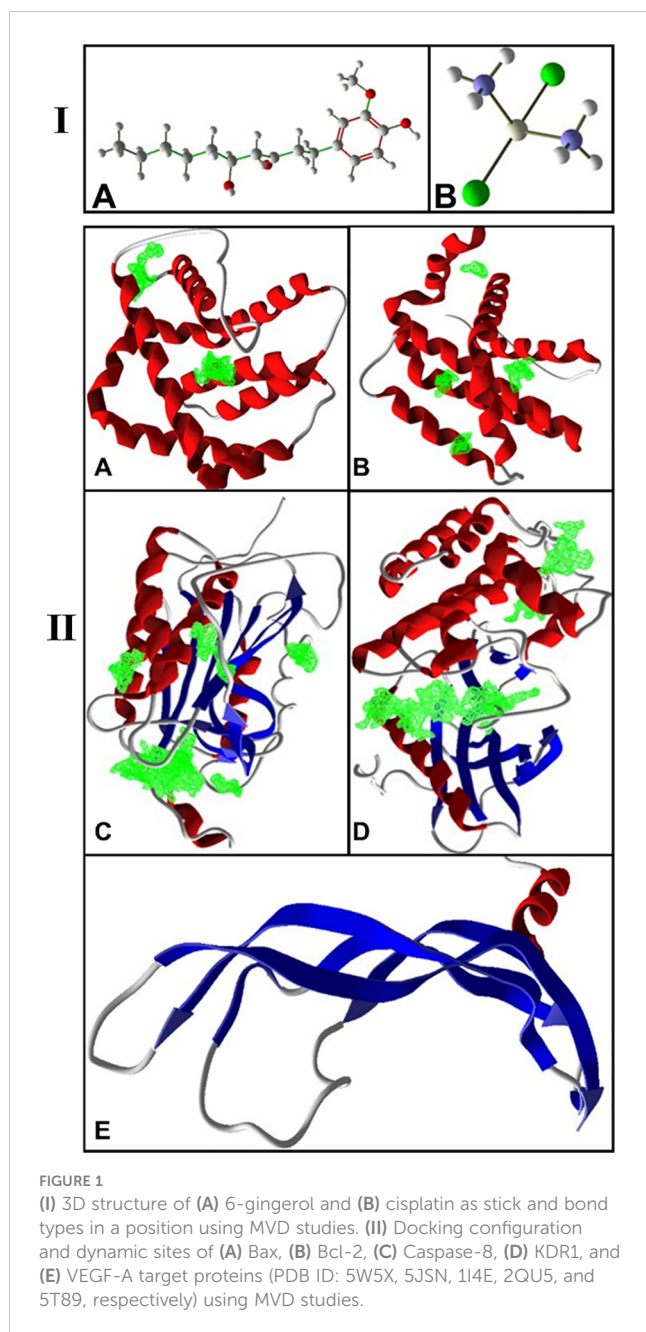
neighborhood distance feature of 1. Ten circles of docking were run, tested by post dock energy minimization applying the Nelder-Mead Simplex Minimization. The results were examined through Molegro Molecular Viewer and Discovery Studio, and the finest interrelating complex was designated from each database (25–27). Figure 1B shows the cavities of the targets (5W5X, 5JSN, 1I4E, 2QU5, and 5T89), which have the greatest potential for binding to ligands.

2.1.3 ADME and toxicity forecasts

A successful medication candidate is defined by its good potential and, likewise, by sufficient ADME prediction. It is proposed that computational ADME utilization in a variety of *in vivo* and *in vitro* predictions leads to a decrease in the number of safety issues in the drug discovery procedure (28). In the medicine

detection server (AdmetSAR), computational programs were utilized to evaluate the ADME and toxicity properties. AdmetSAR is a free and useful source in the ADMET prediction, and the properties of original chemical constituents are presented such as Absorption, Delivery, Digestion, and Elimination studies (http://lmmd.ecust.edu.cn/admetsar2/) (29–31).

2.2 *In vitro* examination

This study is an experimental study that has been performed in several stages on two human umbilical vein endothelial cell (HUVEC) cell lines as a control group and OVCAR-3 cells (ovarian cancer cells).

2.2.1 Drug preparation

6-Gingerol (Catalog No. 23513-14-6) and cisplatin (CAS 15663-27) were purchased from Sigma-Aldrich Co. USA. Different concentrations of 6-gingerol as experimental groups and of cisplatin as positive control groups were prepared in sterile distilled water (25, 50, 100, and 200 μM).

2.2.2 Cell culturing

HUVECs and OVCAR-3 cell lines were purchased from the Pasteur Institute of Iran (Tehran, Iran) and harvested in DMEM (Biosera, France) enriched with 10% fetal bovine serum (FBS) (Biosera, France) and 10,000 U/ml Pen/Strep (Thermo Fisher Scientific, USA) and incubated at 37°C in 5% of CO_2.

2.2.3 Cytotoxicity tests

HUVEC cell lines (5×10^4) were counted and harvested in a 96-well plate and kept for 24 h. The plate's medium was replaced by fresh medium and 10 μl of different concentrations (25, 50, 100, and 200 μM) of 6-gingerol, cisplatin, and a mixture of them was added to each well. Treated cells were incubated at different time responses of 24, 48, and 72 h, and then 10 μl of MTT solution (Sigma-Aldrich, USA) and 5 mg/ml of MTT solution were added to each well and maintained for 3 h. This was followed by adding 100 μl of DMSO (Merk, Germany) to each well, which was kept in the dark for 1 h. The OD of absorbance was read at 490 nm by an ELISA reader (Bio Tek-ELX 800 Winooski, Vermont, USA). Fifty percent chemical concentrations (CC_{50}) of the drug were considered using the probit test in the SPSS package.

2.2.4 Selectivity index

The selectivity index (SI) as a measure of safety was calculated using the following equation: [SI = IC_{50} OVCAR-3/IC_{50} HUVECs] ≥10 to prove it is non-toxic. We also evaluated the combination index (CI) by the following formula: [CI = (D)/(D_x)1 + (D)/(D_x)2], where (D_x)1 and (D_x)2 are the concentration of the 6-gingerol and the cisplatin, respectively, used in the single treatment that was required to decrease the cell number by x% and (D) is the concentration of 6-gingerol in combination with the concentration of cisplatin that together decreased the cell number by x%. The CI value quantitatively defines synergism (CI < 1),

additive effect (CI = 1), and antagonism (CI > 1). To determine the synergism activity of combination therapy, we determined the theoretic IC$_{50}$ by the following method: [theoretic IC$_{50}$ = (IC$_{50}$ cisplatin/2) + (IC$_{50}$ gingerol/2)].

2.2.5 Cell cycle

The cells were counted, and 1×10^6 cells were cultured in each well of a six-well plate. These steps were performed separately for both HUVECs and OVCAR-3 cell lines. After 72 h, viable cells were collected by trypsinization, and cell cycle analysis was performed after PI staining. Finally, the outcomes of cell nuclei stained with propidium iodide in its suspensions were analyzed by using a flow cytometer (Becton Dickinson, USA).

2.2.6 Measurement of gene expression

The relative expression of apoptotic (Bax, Bcl-2, Caspase, and Apaf1) and angiogenetic (KDR, FLT1, and VEGF-A) mediator genes was determined by qPCR. Ovarian cancer cell lines were treated with 25, 50, and 100 μM of 6-gingerol, cisplatin, and a mixture of them and incubated for 48 h. Then, the cells' total RNA was isolated with Trizol Reagenzien (Thermo Fisher Scientific, USA).

With the help of the High-Capacity cDNA Reverse Transcription Kit, corresponding DNA (cDNA) was created. The qPCR reaction was carried out using SYBR Green (Thermo Fisher

Scientific, USA) and the Rotorgene Cycler system (Rotorgene 3000 cycler system). Table 1A demonstrates the template and control gene sequences. Gene expression was evaluated using the $2^{-\Delta\Delta CT}$ method. The ΔCT was calculated by the following formulation: [ΔCT = CT (target) − CT].

2.3 In vivo examination

2.3.1 YSM assay

Ross 308 fertile eggs with a weight of 55 ± 0.5 g were purchased from Simorgh Co. (Kerman, Iran) and kept under standard conditions (37°C ± 1°C in 75% humidity). To evaluate the anti-angiogenic activity of 6-gingerol and cisplatin, the yolk sac membrane (YSM) assay was conducted using a mixture of them in a chick embryo model. At first, fertile eggshells were cleaned and a little spot was created on the shell; then, 50 μl of 6-gingerol, cisplatin, and their combination (as the experimental group) and PBS (as control) were injected into the embryo. In the next 24 and 48 h, the drugs were re-injected into the eggs repeatedly. After each injection, the eggshells were cleaned and closed with molten paraffin and incubated under the same standard conditions. On day 4 (22–24 stages of the Hamburger–Hamilton growth stage), the eggshell membranes broke and were studied under a stereomicroscope (Luxeo 4D Stereozoom Microscope, Labomed, CA, USA), and

TABLE 1 The specific primers and reference gene sequences for RT-qPCR in (A) in vivo and (B) in vitro examination.

	Gene	Forward sequence (5′–3′)	Reverse sequence (5′–3′)	Product size (bp)
	Bax	CCCGAGAGGTCTTTTTCCGAG	CCAGCCCATGATGGTTCTGAT	155
	Bcl-2	GGTGGGGTCATGTGTGTGG	CGGTTCAGGTACTCAGTCATCC	89
	Caspase-8	AGAGTCTGTGCCCAAATCAAC	GCTGCTTCTCTCTTTGCTGAA	78
	p53	CAGCACATGACGGAGGTTGT	TCATCCAAATACTCCACACGC	125
	FLT	CAGGCCCAGTTTCTGCCATT	TTCCAGCTCAGCGTGGTCGTA	82
A. In vitro	APAF1	AAG GTG GAG TAC CAC AGA GC	TCC ATG TAT GGT GAC CCA TCC	116
	KDR	CCA GCA AA CA GG GTCTGT	TGTCTGTGTCATCGGAGTGATATCC	87
	VEGF	CTACCTCCACCATGCCAAGT	GCA GTAGCTGCGCTGATAGA	109
	HPRT	CCTGGCGTCGTGATTAGTGAT	AGACGTTCAGTCCTGTCCATAA	131
	B2A	CATGTACGTTGCTATCCAGGC	CTCCTTAATGTCACGCACGAT	250
	GAPDH	ACAACTTTGGTATCGTGGAAGG	GCCATCACGCCACAGTTTC	101
	Bax	CCCGAGAGGTCTTTTTCCGAG	CCAGCCCATGATGGTTCTGAT	180
	Bcl-2	GGTGGGGTCATGTGTGTGG	CGGTTCAGGTACTCAGTCATCC	136
	APAF1	TTGCCAACCAGAGACATCAGAGG	TGCGGACGAACAACAACCAGACG	128
	TP53	ACCTGCACTTACTCCCCGGT	TCTTATAGACGGCCACGGCG	127
B. In vivo	KDR	GCCAACTCTATGGCAGAAGC	CTGAACACCATGCCACTGTC	86
	VEGF	CAATTGAGACCCTGGTGGAC	TCTCATCAGAGGCACACAGG	86
	B2M	GTGCTGGTGACCCTGGTG	CAGTTGAGGACGTTCTTGGTG	113
	HPRT	GATGAACAAGGTTACGACCTGGA	TATAGCCACCCTTGAGTACACAGAG	103
	GAPDH	CCTCTCTGGCAAAGTCCAAG	GGTCACGCTCCTGGAAGATA	176

high-quality images (4,000 × 3,000 pixels) were taken for YSM analysis by using ImageJ[®] 1.48 (National Institutes of Health, Bethesda, Maryland, USA) and MATLAB[®] (Mathworks Matlab R2015a) software. Vascular density was computed with these data.

2.3.2 Molecular assay

Relative angiogenetic (KDR and VEGF) and apoptotic (Bax, Bcl-2, TP53, and Apaf1) mediator gene expression changes in chick embryos that were treated with 6-gingerol, cisplatin, and their mixture were evaluated by real-time qPCR. The entire RNA isolated from the extraembryonic membrane was extracted with Trizol Reagenzien (Thermo Fisher Scientific, USA) and the concentration of RNA was read by a Nanodrop device (Thermo Scientific, Wilmington, DE). After the synthesis of cDNA by using the High-Capacity cDNA Reverse Transcription Kit (Thermo Fisher Scientific, USA), the qPCR assay was carried out using a SYBR Green assay (SYBR Premix Ex Taq TM II, Takara Bio, Inc., Shiga, Japan).

Table 1B lists the specific primers and common gene combinations. Forty cycles of magnification were carried out after the initial step of 95°C for 1 min. Each cycle lasted for 10 s at 9°C for DNA denaturation, 30 s at 60°C for annealing, and 30 s at 72°C as an extension. The expression profile was examined using the predefined standard genes.

2.3.3 Histopathological assessment

The chicken embryo specimens were fixed in a 10% formalin solution first. The formalin-fixed paraffin-embedded samples were processed using the microtome (Slee-Germany) in 4-μm sections and thereby stained with routine hematoxylin and eosin (H&E) for assessment of histopathological changes. After that, selected samples were stained by immunohistochemical (IHC) apoptosis and angiogenesis markers including Bax (Zytomed Germany, code number: 502-17990), Bcl-2 (mouse monoclonal antibody; code number: PDMO16- lot No. H147 from the US), and CD34. Positively stained cells were counted in 10 fields, and their means show the Bcl-2, Bax, and CD34 expression levels.

2.4 Statistical analysis

Statistical analyses were performed using IBM[®] SPSS[®] (V.20) and GraphPad Prism (V.8.0) software. All data were analyzed by one-way ANOVA and paired *t*-test analysis. Statistical significance

was set at $p < 0.05$. All experiments were replicated at least three times.

3 Results

3.1 *In silico* modeling

3.1.1 MVD molecular docking

In this research work, the focus is on the interactions of 6-gingerol, cisplatin, and the combination of these drugs. MVD molecular docking conformation and analysis showed the 6-gingerol, cisplatin, and combination forms of the three drug reagents that interacted with Bax, Bcl-2, Caspase-8, VEGF-A, and KDR1. Free total energy or MolDock Score values were subject to negative energy values, indicating that the binding events of the complexes were spontaneous. Table 2 displays the docked configuration of the complexes with the related parameters. Schematic molecular docking results and ligand maps of structures and the 5W5X, 5JSN, 1I4E, 2QU5, and 5T89 targets are shown in Figures 2–4.

The MolDock Score values for 6-gingerol were −103.917, −103.36, −106.16, −121.37, and −83.42 where they were docked to Bax, Bcl-2, Caspase-8, KDR1, and VEGF-A receptors, respectively.

The resulting data from molecular docking is presented in Figure 2A where 6-gingerol forms van der Waals, conventional hydrogen bonds, carbon hydrogen bonds, pi-donor hydrogen bonds, alkyl, and pi-alkyl with amino acids of the Bax using Asp 53, Thr 56, Gly 156, Asp 159, Leu 59, and Trp 158. Furthermore, 6-gingerol forms van der Waals forces, carbon hydrogen bonds, pi-lone pair, alkyl, and unfavorable bumps with amino acid residues (Arg 109, Asp 102, Glu 152, Arg 26, Val 159, and Lys 22) of the Bax (Figure 2B). In Figure 2C, the 6-gingerol molecule forms van der Waals, carbon hydrogen bonds, pi-alkyl, and unfavorable bumps with amino acid residues of Caspase-8 receptor including Gly 2331, Ser 2338, Ile 2333, Leu 2401, Thr 2337, and Thr 2467. Moreover, 6-gingerol was stabilized by KDR1 using van der Waals, conventional hydrogen bond, carbon hydrogen bonds, alkyl, pi-alkyl, pi–pi T-shaped, unfavorable donor–donor, and unfavorable bumps with the following amino acid residues: Ile 2025, His 1026, Cys 1045, Leu 840, Ala 866, Phe 918, Phe 1047, Val 899, and Asp 1046 (Figure 2D). Subsequently, the residues Glu 38, Ser 95, Leu 97, His 99, and Tyr 39 of VEGF-A interact with 6-gingerol as seen in Figure 2E by van der Waals, conventional hydrogen bond, carbon hydrogen bonds, alkyl, pi-alkyl, pi-sigma, and unfavorable bumps.

TABLE 2 Parameters from the interaction between 6-gingerol, cisplatin, and their mixture with angiogenetic and apoptotic mediators.

Compound	Docking score for 6-gingerol	Docking score for cisplatin	Docking Score for the mixture of the drugs
Bax	−103.917	−44.78	−146.78
Bcl-2	−103.36	−41.01	−119.152
Caspase-8	−106.16	−48.31	−156.54
KDR1	−121.37	−39.86	−153.52
VEGF-A	−83.42	−41.36	−142.16
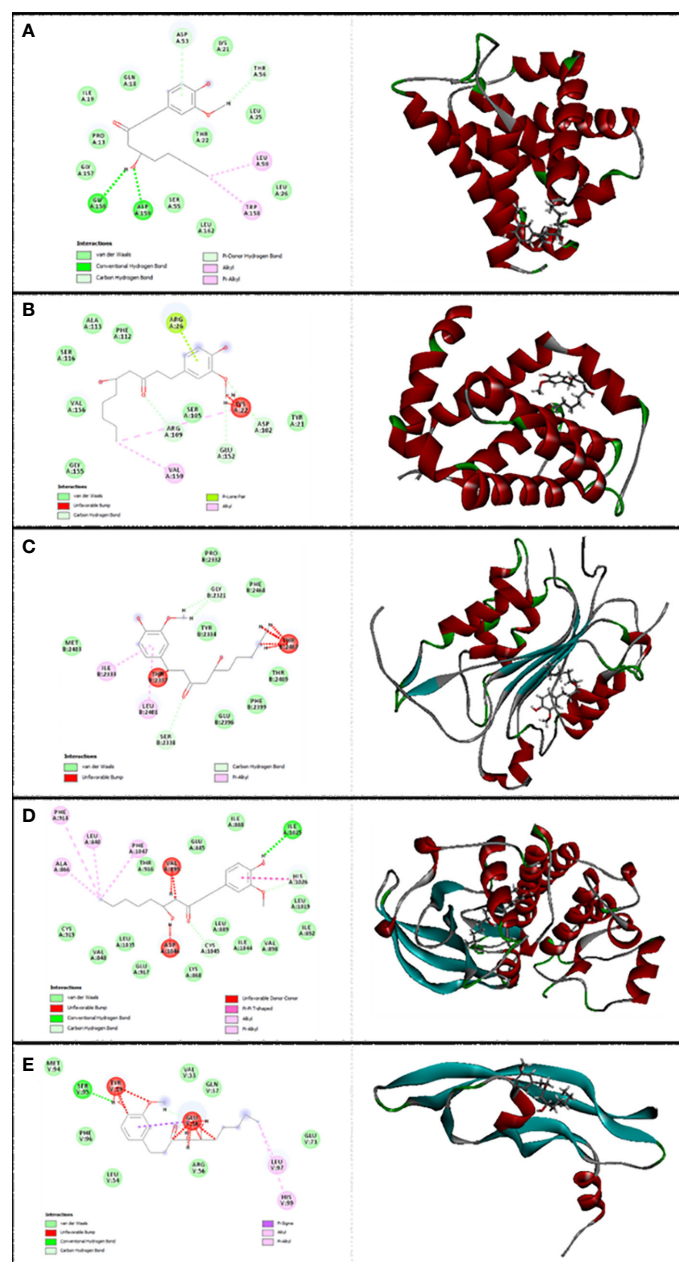
FIGURE 2
Illustration of the finest score docking solution of the 6-gingerol ligands and **(A)** Bax, **(B)** Bcl-2, **(C)** Caspase-8, **(D)** KDR1, and **(E)** VEGF-A receptor with the designated crystal construction of 5W5X, 5JSN, 1I4E, 2QU5, and 5T89, respectively, and a ligand map with various chemical bonds courtesy of Discovery Studio.

Values of the MolDock Score for cisplatin were −44.78, −41.01, −48.31, −39.86, and −41.36, which were docked to Bax, Bcl-2, Caspase-8, KDR1, and VEGF-A receptors, respectively. Also, cisplatin forms van der Waals and conventional hydrogen bonds with the amino acid residue (Asp 159) of the Bax (Figure 3A). Figure 3B shows that cisplatin forms van der Waals and conventional hydrogen bonds with amino acids of the Bcl-2 using Lys 22, Arg 26, and Glu 152. Additionally, cisplatin binds to the Caspase-8 receptor with a binding site consisting of amino acid residues Gly 2318, Asp 2319, Gly 2362, and Asp 2363 with van der Waals and conventional hydrogen bond (Figure 3C). Cisplatin forms van der Waals,

conventional hydrogen bond, and unfavorable bumps with amino acids of the KDR1 using Glu 885, His 1026, Asp 1046, and Ala 1050 (Figure 3D). Cisplatin binds into the dynamic spot of VEGF-A with a binding site consisting of amino acid residues like Ser 50, Asp 34, and Phe 36 with van der Waals, conventional hydrogen bond, and unfavorable bumps (Figure 3E).

Furthermore, the MolDock Score values of Bax Bcl-2, Caspase-8, KDR1 and VEGF-A for the mixture of these two compounds were −146.78, −119.152, −156.54, −153.52, and −142.16, respectively.

Subsequently, Figure 4A shows that the mixture of these two compounds forms van der Waals, conventional hydrogen bond,
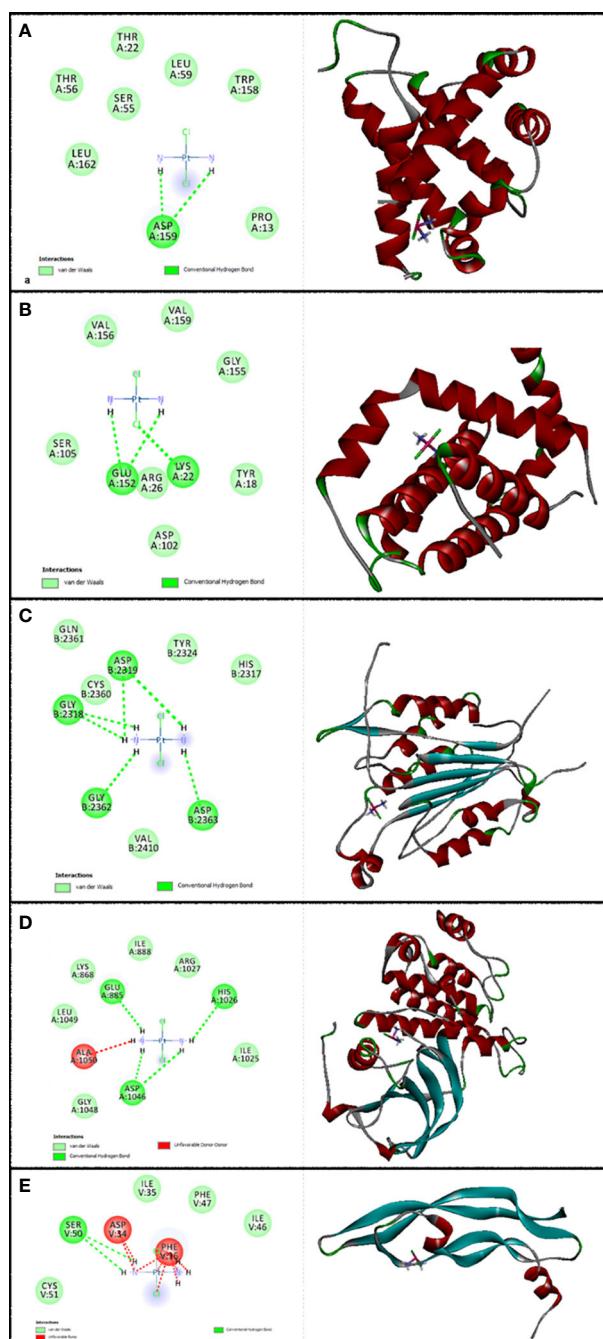
FIGURE 3
Illustration of the finest score docking solution of the cisplatin ligands and **(A)** Bax, **(B)** Bcl-2, **(C)** Caspase-8, **(D)** KDR1, and **(E)** VEGF-A receptor with the designated crystal construction of 5W5X, 5JSN, 1I4E, 2QU5, and 5T89, respectively, and a ligand map with various chemical bonds courtesy of Discovery Studio.

carbon hydrogen bonds, alkyl, pi-alkyl, pi-donor hydrogen bonds, unfavorable acceptor–acceptor, and unfavorable bumps with amino acids of the Bax when targeting Thr 56, Asp 53, Asp 159, Ile 19, Trp 158, Leu 59, and Thr 22. From the docking analysis, its outcome data expressed clearly in Figure 4B that the mixture of these two compounds formed van der Waals, conventional hydrogen bonds, carbon hydrogen bonds, amide-pi stacked hydrogen bonds, alkyl, pi-alkyl, and unfavorable bumps with amino acids of the Bcl-2

against Met 115, Arg129, Asp 111, Phe 112, Phe 153, Val 159, Glu 114, and Leu 119. Also, residues Ser 2316, Gly 2318, Asp 2319, Gly 2362, Asp 2363, Cys 2360, Ser 2411, Tyr 2412, and Arg 2413 of Caspase-8 interacted with the two compounds' mixture as displayed in Figure 4C by van der Waals, conventional hydrogen bond, pi-sigma, alkyl, pi-alkyl, pi–pi T-shaped, and unfavorable bumps. At the same time, we need to point out that cisplatin formed van der Waals, conventional hydrogen bonds, carbon hydrogen bonds, pi-
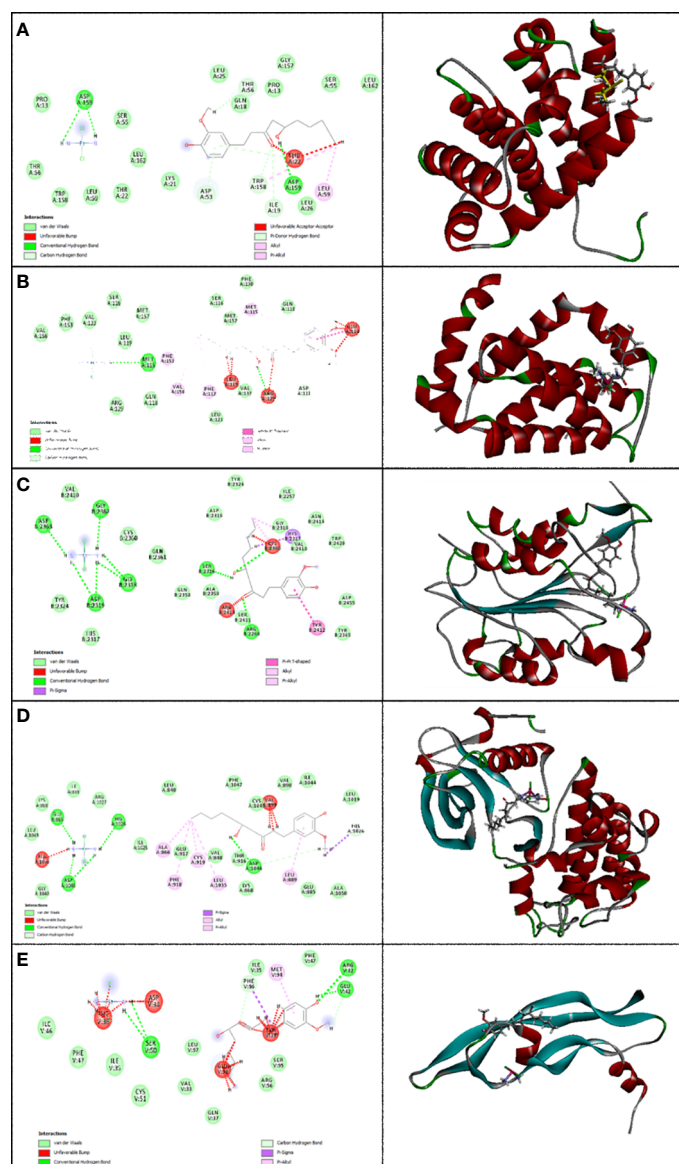
FIGURE 4
Representation of the finest score docking solution of the mixture of the two drugs and best ligands and **(A)** Bax, **(B)** Bcl-2, **(C)** Caspase-8, **(D)** KDR1, and **(E)** VEGF-A receptor with the designated crystal structure of 5W5X, 5JSN, 1I4E, 2QU5, and 5T89, respectively, and a ligand map with various chemical bonds courtesy of Discovery Studio.

sigma, alkyl, pi-alkyl, and unfavorable bumps of the KDR1 against Glu 885, His 1026, Asp 1046, Ala 866, Phe 819, Cys 919, Leu 1035, and Ala 1050 (Figure 4D). In addition, the mixture was stabilized by VEGF-A using van der Waals, conventional hydrogen bond, carbon hydrogen bonds, pi-sigma, pi-alkyl, and unfavorable bumps with amino acid residues Phe 96, Ser 50, Glu 42, Arg 82, Met 94, Asp 34, Phe 36, Glu 38, and Tyr 39 (shown in Figure 4E).

This study indicates that 6-gingerol and cisplatin interacted with apoptotic and antiapoptotic proteins of Bax, Bcl-2, Caspase-8, KDR1, and VEGF-A. Consequently, 6-gingerol was more effective than cisplatin. Subsequently, there is the ultimate confirmation that the binding affinity of 6-gingerol is better than that of cisplatin, while that of the mixture of the two drugs is the best with Bax, Bcl-2, Caspase-8, KDR1, and VEGF-A.

3.1.2 ADMET prediction

Before experimental approaches, ADMET prediction (Chemical Absorption, Distribution, Metabolism, Excretion, and Toxicity analysis) is employed to indicate the pharmacokinetics of molecules (31).

ADMET properties showed that cisplatin had a less human intestinal absorption (HIA) score than 6-gingerol, which implies that the compound could have less intestinal absorption against oral administration. The greatest penetration within the blood–brain barrier (BBB) is seen for cisplatin. While it appears to indicate the efflux by P-glycoprotein (P-GP), both compounds' measurement results show them as a substrate and inhibitor of P-GP. Likewise, in terms of metabolism, 6-gingerol and cisplatin were substrates (but non-inhibitors) of the CYP450 microsomal enzyme. A non-

inhibitor of CYP450 demonstrates that the compounds will not prohibit the biotransformation of the drug metabolized by the CYP450 enzyme. The test of AMES toxicity is used to determine the mutagenic molecule. 6-Gingerol and cisplatin indicated a negative AMES toxicity test, which implies that these are not mutagenic. Furthermore, the carcinogenic terms showed that the molecules were not carcinogenic. Subsequently, 6-gingerol included lower oral toxicity than cisplatin. Likewise, considerable data were estimated by ADMET prediction, such as the LD_{50} dose in a rat model. In comparison, a compound with a greater LD_{50} dose is less deadly than that having a lower LD_{50} dose. It has been defined from ADMET results that 6-gingerol had less LD_{50} and was more toxic compared to cisplatin (2.4106 versus 2.7419, respectively). Likewise, the greater value of the log S, the lower the solubility, which would reduce the absorption (32). Consequently, cisplatin with a lower log S has better absorption than 6-gingerol, indicating its low bioavailability, which makes it more resistant to oxidation and hydrolysis, and thus, with improved stability, improved protection toward degradation of the cisplatin molecules, and increased bioavailability compared to 6-gingerol (33). Supplementary 1 represents the different ADMET parameters gained from the admetSAR tool.

3.2 *In vitro*

3.2.1 Cytotoxicity

To evaluate the cytotoxicity and effect of 6-gingerol alone, cisplatin alone, and their combination on HUVECs and OVCAR-3, the colorimetric method was used. The results showed that combining these two has a far more significant effect than each drug alone: in HUVECs, 118.6 ± 18.52 in mixed compared to 136.52 ± 21.36 and 154.2 ± 38.43 for cisplatin and 6-gingerol, respectively; in OVCAR-3, 46.33 ± 3.68 in mixed compared to 61.23 ± 4.22 and 154.2 ± 38.43 for cisplatin and 6-gingerol, respectively (Table 3). The isobologram analysis results are demonstrated in Figure 5.

3.2.2 6-Gingerol, cisplatin, and their combination-induced apoptosis

Treatment of HUVECs and OVCAR-3 with 6-gingerol alone, cisplatin alone, and their combination led to apoptosis. All concentrations of the three treated sets presented significant differences relative to the negative control group ($p < 0.001$). Cisplatin significantly increased the apoptotic level compared to 6-gingerol. Also, all 6-gingerol plus cisplatin combined concentrations showed significantly higher apoptosis and decreased necrosis (Figure 6).

3.2.3 Cell cycle

Cell cycle analysis showed that in the treatment of HUVECs and OVCAR-3 cell lines by different concentrations of cisplatin, 6-gingerol, and the combination therapy, the duration of the S cycle increases with increasing concentrations of drugs, indicating a prolongation of cell division time, which, in turn, slows down cell division. The results showed that this rate was significantly higher at a dose of 100 µg/ml combination therapy than in the cisplatin treatment group alone (Figure 7).

3.2.4 Gene expression

The study of apoptotic (Bax, Bcl-2, Caspase-8, p53, and Apaf1) and angiogenetic (KDR, FLT1, and VEGF-A) gene expression showed that in terms of the cumulative concentrations of drugs in cell lines, the expression levels were significantly elevated compared to the control group ($p < 0.001$). This significant increase in combination treatment was also detected when compared to cisplatin therapy ($p < 0.05$) (Figure 8).

3.3 *In vivo*

3.3.1 Vascular density

The effect of the 6-gingerol, cisplatin, and the combination therapy on the chick's YSM at 24, 48, and 72 h of primary growth is given. The vascular density of the treated embryos' vasculature significantly decreased in both 6-gingerol- and cisplatin-treated groups. According to statistical analysis, 6-gingerol-treated embryos had less vascular density than cisplatin embryos (Figures 9 IA–E).

3.3.2 Gene expression

The results revealed that the expression profile of apoptotic gene markers (Bax, Apaf1, and TP53) was significantly increased in cisplatin, 6-gingerol, and combination therapy compared to the untreated control group ($p < 0.05$). The Bcl-2 gene expression as an apoptotic mediator in all treated groups decreased compared to the untreated control groups ($p < 0.05$). Angiogenesis mediator genes including VEGF and KDR in all treated groups significantly decreased in comparison to the untreated control group ($p < 0.05$) (Figure 9 II).

3.3.3 Immunohistochemistry assay

From a histopathological point of view and by comparing different patterns with each other and the control group, we concluded that cisplatin had teratogenic effects by decreasing the growth and development of most of the three germ layer cells and induced tissue atrophy in their absence. 6-Gingerol had no major effects on

TABLE 3 Evaluating the IC$_{50}$ values and selective index (SI) of cisplatin, gingerol, and combination therapy.

Drugs	IC$_{50}$ HUVECs	IC$_{50}$ OVCAR-3	SI (OVCAR-3/HUVECs)
Cisplatin	136.52 ± 21.36	61.23 ± 4.22	2.22
6-gingerol	154.2 ± 38.43	79.66 ± 8.63	1.93
Mix	118.6 ± 18.52	46.33 ± 3.68	2.55
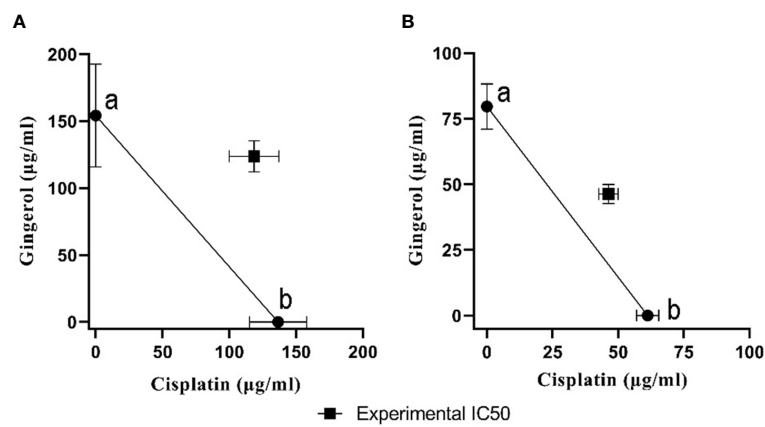
FIGURE 5

The isobologram analysis of the effects of the drug combination of cisplatin and 6-gingerol. **(A)** In HUVECs, foci a and b displayed the IC_{50} value of cisplatin (136.52 ± 21.36 µM) and 6-gingerol (154.2 ± 38.43 µM), respectively. Theoretical IC_{50} was 145.36 µM and our experimental IC_{50} was 118.6 ± 18.52 µM. **(B)** In OVCAR-3 cells, foci a and b displayed the IC_{50} value of cisplatin (61.23 ± 4.22 µM) and 6-gingerol (79.66 ± 8.63 µM), respectively. Theoretical IC_{50} was 70.46 µM and our experimental IC_{50} was 46.33 ± 3.68 µM. Statistical analysis revealed that there was a significant difference between experimental IC_{50} and theoretical IC_{50} ($p < 0.001$).
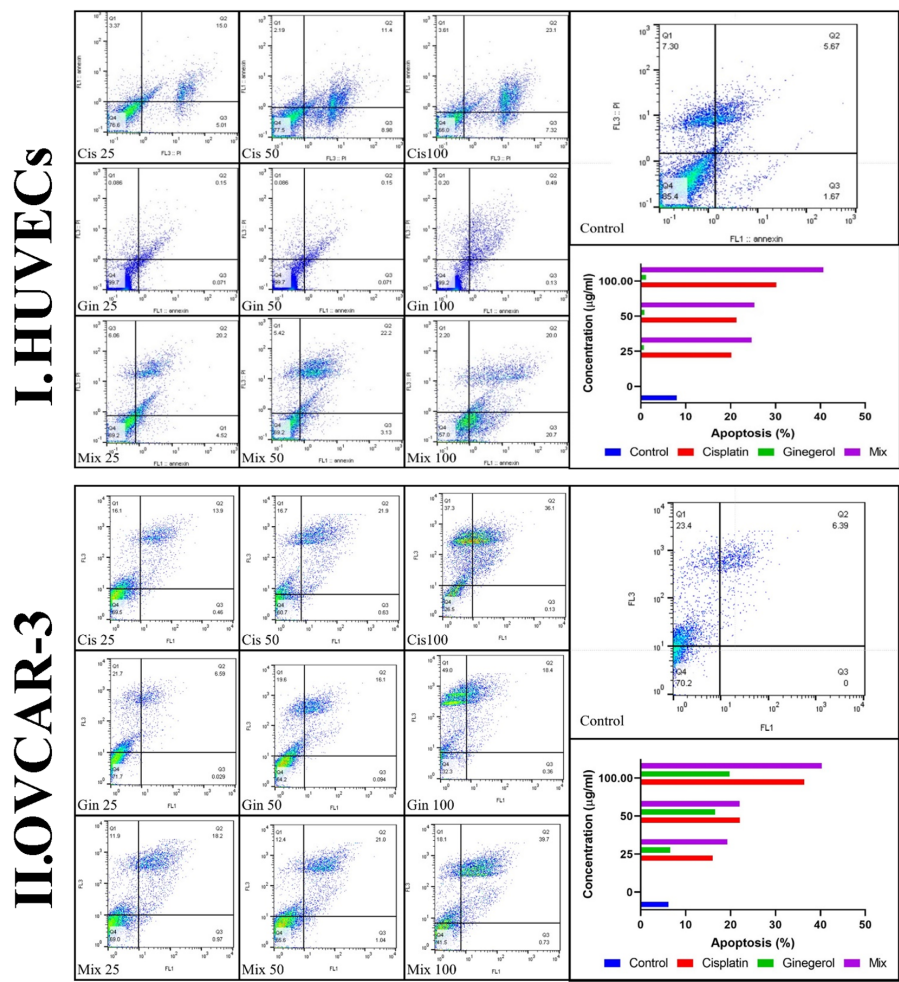
FIGURE 6

Characteristics of apoptosis and necrosis of **(I)** HUVECs and **(II)** the OVCAR-3 cell line treated with different concentrations of cisplatin, 6-gingerol, and the combination therapy.
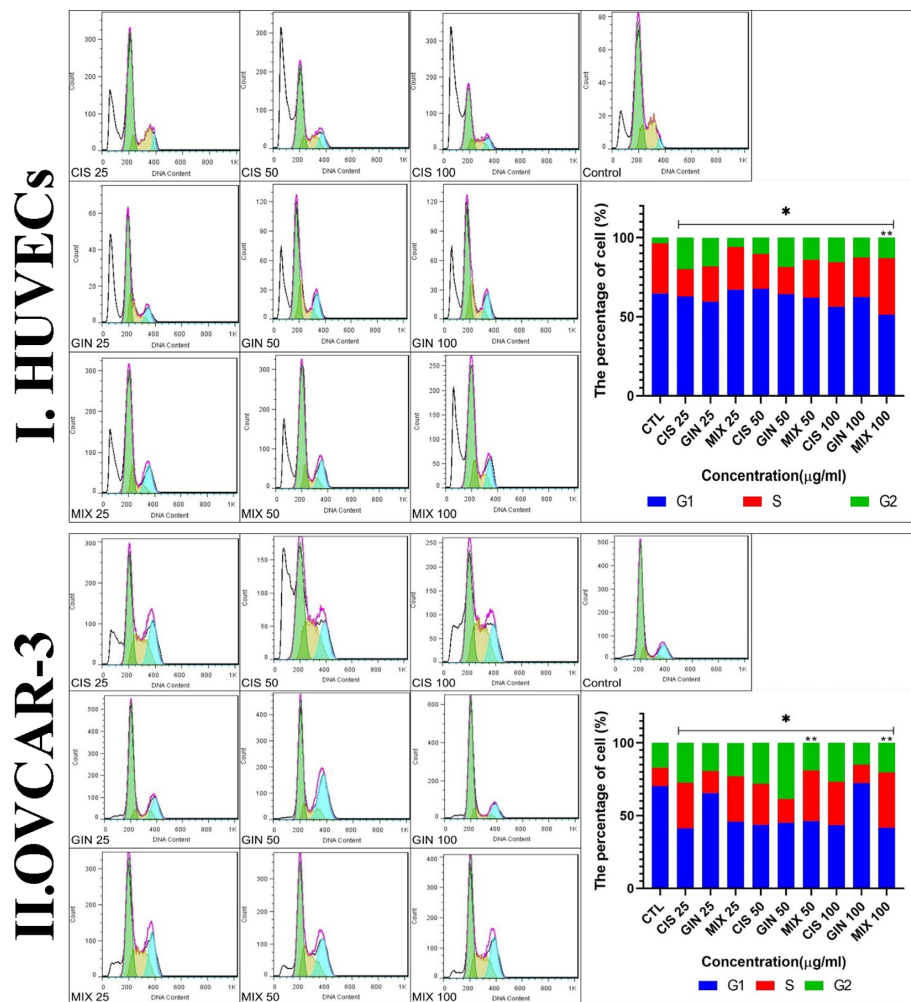
FIGURE 7
Cell cycle characteristics of **(I)** HUVECs and **(II)** the cell line treated with different concentrations of cisplatin, 6-gingerol, and the combination therapy [*significant difference with the control group ($p < 0.001$), **significant difference between drug combination therapy and cisplatin ($p < 0.001$)].

embryogenesis, which was mostly similar to normal control. However, in the combination of 6-gingerol and cisplatin, it seemed that the teratogenic effects of cisplatin decreased markedly, but still observed a dispersed disruption of the embryogenesis. These changes were evaluated by H&E staining and also immunohistochemical staining for Bax, which were more prominent in cisplatin. Bcl-2 and CD34 had fewer changes in 6-gingerol and combination therapy, in order of frequency (Figure 10).

In the H&E assay, results show that cisplatin has degenerative to necrotic changes in embryonic tissue as a result of disruption of the integrity of structural cells. For 6-gingerol, both mesenchymal and epithelial cells and even neural tube components seemed to react normally with non-damaged embryonic growth and development, and the heart and its chambers that were subjected to mixed therapy seem to have a well-preserved architecture with less likely degenerative changes compared with the cisplatin group.

The Bax marker, an apoptotic mediator, showed that cisplatin induced multifocal strong positive staining of both embryonic mesenchymal and epithelial cells. 6-Gingerol showed weak positive staining in embryonic tissues, and the combination

therapy showed moderate positive cytoplasmic staining in different embryonic tissues. The Bcl-2 marker, another apoptotic mediator, showed that cisplatin influences damaged embryonic tissues with negative cytoplasmic staining in embryonic mesenchymal and epithelial tissues. In 6-gingerol, focally positive staining of mesenchymal cells was noted. In the combination therapy, dispersed cytoplasmic staining of embryonic tissue was noted. The CD34 marker, an angiogenetic mediator, showed that cisplatin and vascular channels seemed to have opened, but atrophic lumen and sloughing of endothelial cells were noted. In 6-gingerol, vessels seemed to open without damage to the components of the vessel wall. In combination therapy, the lumen of the vessel was opened but focal sloughing of endothelial cells and degeneration of the vessel wall components were noted.

4 Discussion

Herbal products are traditionally used to treat disease, and in current clinical trials, more than 50% of medicines are from natural
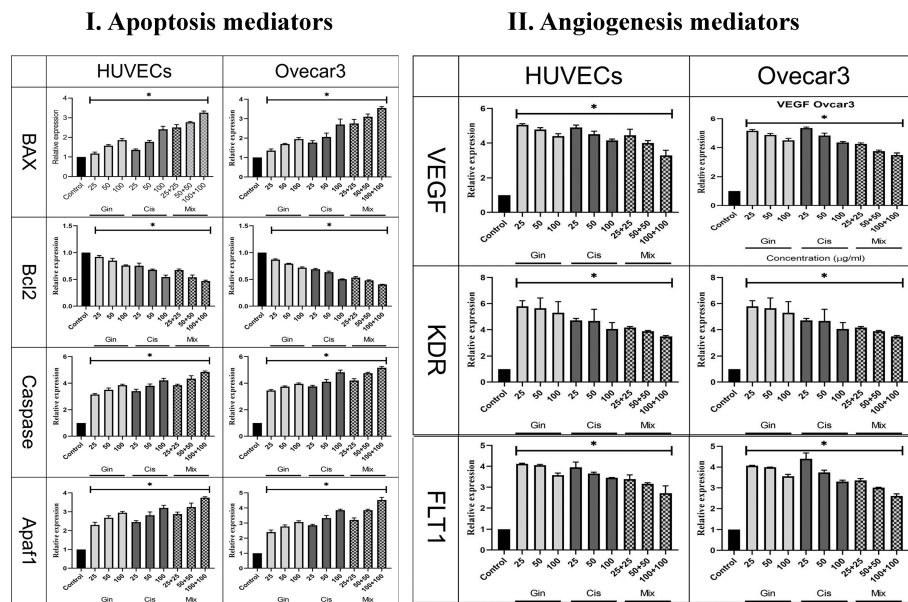
FIGURE 8
Evaluation of **(I)** apoptotic (Bax, Bcl-2, Caspase, p53, and Apaf1) and **(II)** angiogenetic (KDR, FLT1, and VEGF) gene expression in HUVECs and OVCAR-3 cell lines treated with different concentrations of cisplatin, 6-gingerol, and the combination therapy [*significant difference with the control group ($p < 0.001$)].

resources (34). 6-Gingerol is the most active metabolite derived from ginger, which is an anti-angiogenic and apoptotic drug (35). Due to the anticancer properties of 6-gingerol, and the risks of cisplatin, in this study, we compared the outcome of 6-gingerol, cisplatin, and their combination therapy on the process of angiogenesis and apoptosis of ovarian cancer cells and HUVEC.

Cytotoxicity analysis of this study shows that combination therapy was increased compared to cisplatin or 6-gingerol in both cell lines. CI and isobologram analysis show the combination therapy in both cell lines had an antagonistic activity. Nevertheless, various combinations of treatment besides cisplatin displayed degrees of antagonism based on the CI values or isobologram analysis (36). Although the combination treatment of 6-gingerol and cisplatin has shown the antagonistic effects of the drugs, other methods used in this study confirm the reduction of the adverse effects of the combined treatment compared to the treatment with cisplatin.

A similar study by Kapoor et al. (19) in 2016 evaluated the antitumor activity of 6-gingerol on human oral cell lines (SCC4 and KB) and cervical malignancy (HeLa) with or without cortmanine, rapamycin, and cisplatin. Moreover, in the MTT assay evaluation, the percentage of viable cells in the mixture of 6-gingerol with cortmanine and cisplatin was lower than in the treatment with 6-gingerol or cisplatin and cortmanine alone. Although the toxicity of 6-gingerol and cisplatin has not been studied in any other study, the results of similar studies (33, 37) in this field show that the cytotoxicity of 6-gingerol increases with increasing dose. The study by Kim et al. (38) had no toxicity of 6-gingerol at doses below 20 μg. As shown in the results of the colorimetric analysis of our study, cytotoxicity at doses below 25 μg was lower in 6-gingerol than in the mixed group, and cisplatin was more toxic. According to

these results, it can be said that, in addition to enhancing the performance of cisplatin, combined treatment also reduces its side effects to a great extent.

Flow cytometry findings demonstrated that the apoptotic value of the two combined drugs was higher while the necrosis was lower than cisplatin in both OVCAR-3 cells and HUVECs alone, and increased with enhanced concentrations. In the case of 6-gingerol in HUVECs, the apoptosis rate was low due to the antioxidant nature of the drug and the resistance of these cells. The apoptotic effect of 6-gingerol was more significant in OVCAR-3 cells than in HUVECs. In support of the above results, we can point out several similar studies are in line with the present study results. For example, the results of the study from Kapoor et al. (19) showed that the combination therapy of 6-gingerol with cortmanine, rapamycin, and cisplatin significantly increased the rate of apoptosis in human oral cancer cells (SCC4 and KB) and cervical cancer (HeLa). Numerous studies (39–41) have shown that combination therapy with expected agents sensitizes HeLa cells to lower concentrations of cisplatin. Rastogi et al. (18) conducted a study to evaluate this effect. Their study showed that a concentration of 50 μM 6-gingerol sensitizes cervical malignant cells to 2.5 μM cisplatin. This combination promoted the apoptotic cells following 24 h of treatment. Similarly, in a study by Nipin et al., 6-gingerol increased early apoptosis (42).

The activity of the 6-gingerol and cisplatin combination on the cell cycle showed that the S phase at a concentration of 100 μg/L in both OVCAR-3 cells and HUVECs had the shortest time. There are several studies on the apoptosis of various cancer cells in the vicinity of 6-gingerol, although a small number, such as the present study, have examined the effect of 6-gingerol and cisplatin alone or their combination therapy. In 2021, Nipin et al. (42) examined the action
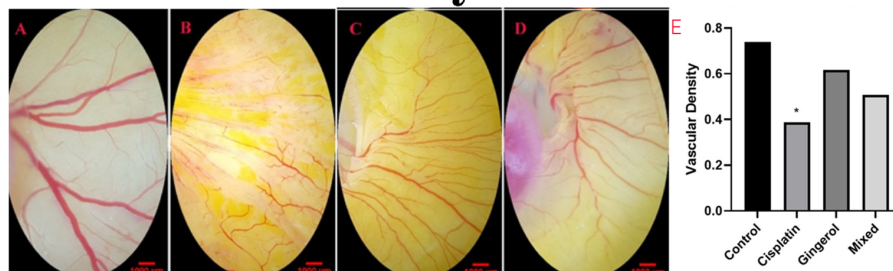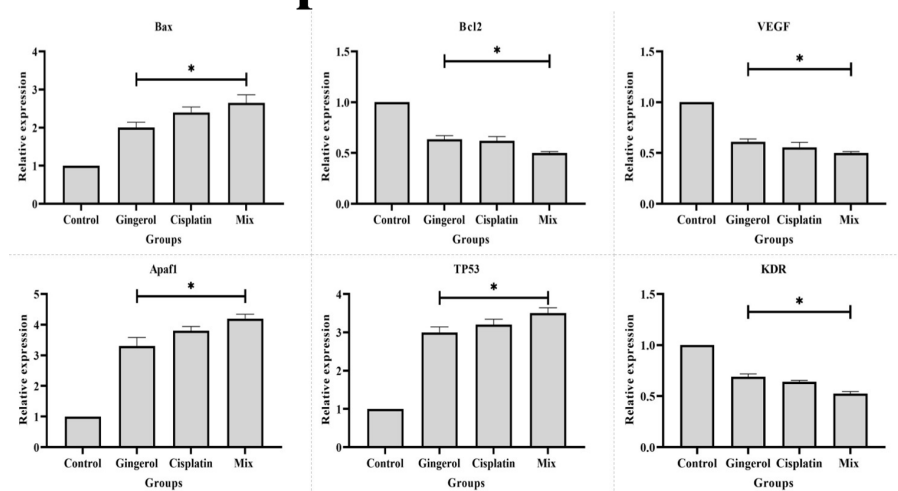
FIGURE 9

(I) Effect of cisplatin, 6-gingerol, and the combination therapy on the chick embryo's blood vessels. **(A)** Control group, **(B)** cisplatin, **(C)** 6-gingerol, **(D)** mixture, and **(E)** vascular density (error bars show mean $\pm$ standard error; *$p < 0.05$ compared to the control group). **(II)** Effect of cisplatin, 6-gingerol, and the combination therapy on the apoptotic (Bax, Bcl-2, Apaf1, and TP53) and angiogenetic (VEGF and KDR) mediator gene expression changes treated embryos compared to controls. The expression levels were normalized to GAPDH and HPRT and calibrated to controls (error bars show mean $\pm$ standard error; *$p < 0.05$).

of 6-gingerol on the apoptosis of breast cancer cells. According to their study, 6-gingerol stopped the cell cycle in the G0/G1 phase. This study showed that 6-gingerol could induce early and late apoptosis by failing to induce DNA repair and long-term cessation of the cell cycle.

Another study (33) showed that treatment with 6-gingerol inhibited HPV-positive cervical cancer cell proliferation by reactivating p53, increasing oxidative stress, and inducing DNA impairment related to G2/M cell cycle arrest and apoptosis.

The findings showed a concentration of 50 µM 6-gingerol sensitized cervical cancer cells to 2.5 µM cisplatin. This mixture augmented the apoptotic level in cells treated for 24 h. The cell cycle analysis showed that when the combination of 6-gingerol and cisplatin was used, a significant accumulation of cells in the G2/M cell cycle phase occurred. In addition, it exhibited an increase in apoptotic cells treated with 6-gingerol and cisplatin compared to each drug treatment alone. Overall, these results confirmed that 6-gingerol enhances the antiproliferative effects of cisplatin by inducing DNA damage due to oxidative stress and cell death in cervical cancer cells and a potent stimulus for p53 reactivation in cervical HPV cancer cells. It is positive and the results can be used as

a chemical sensitizer for conventional chemotherapy drugs such as cisplatin.

The study carried out by Kapoor et al. (19) examined the apoptotic and anticancer properties of 6-gingerol with and without cisplatin in the treatment of oral cancer cell lines (Scc4 and KB) and a cervical cancer cell line (HeLa). This study showed that when 6-gingerol and cisplatin were coupled, their effect was significantly increased by 50% against the apoptosis of the above cancer cells, compared to individual drugs alone. Furthermore, treatment with 6-gingerol or with cisplatin alone had better therapeutic results in all three cancer cell lines.

The possibility of 6-gingerol combined with cisplatin as a novel treatment for gastric cancer was examined by Luo et al. (43). The mixture of 6-gingerol and cisplatin repressed cell viability and enhanced cell cycle arrest in the G1 phase compared with cisplatin alone. Combination treatment lowered cyclin D1, cyclin A2, matrix metalloproteinase-9, p-PI3K, AKT, and p-AKT protein expression; raised P21 P27 mRNA levels; and hindered the capacity of cells to relocate and migrate. This study demonstrated that 6-gingerol improves gastric cancer cells' susceptibility to the chemotherapy drug cisplatin, and the processes involved in
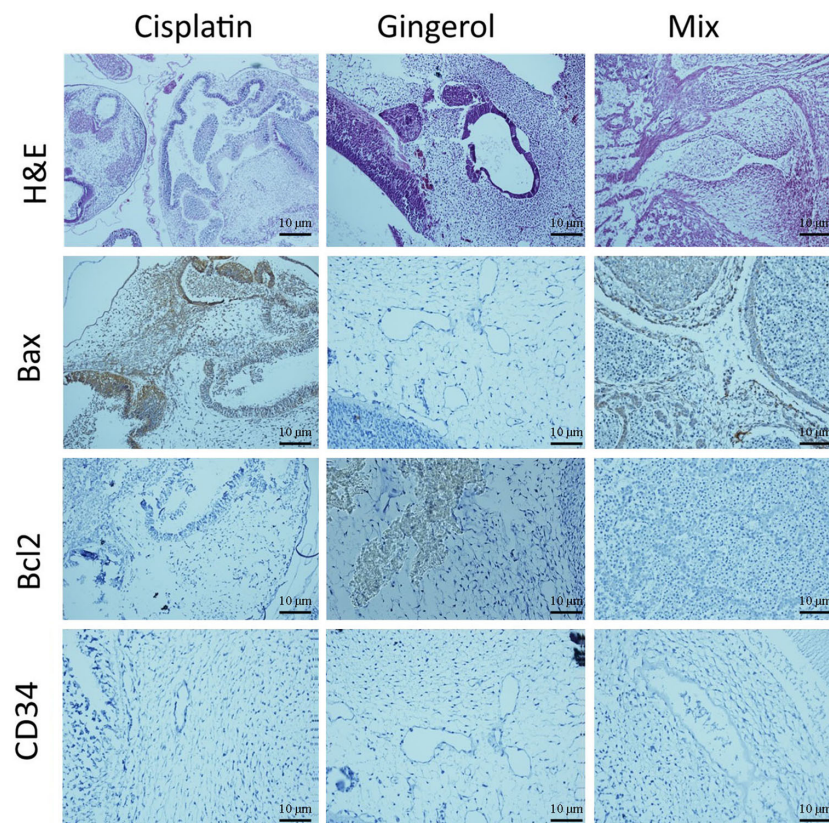
FIGURE 10
Histopathological changes in H&E and IHC study [apoptotic (Bax and Bcl-2) and angiogenetic (CD34) markers] of the chick embryo treated with cisplatin, 6-gingerol, and the combination therapy.

migratory inhibition, suppression of invasion, and G1 phase arrest *via* the PI3K/AKT signaling pathway.

Another investigation by Park et al. (44) found that 6-gingerol inhibited cell growth by stopping the cell cycle in the G1 phase in each cell line of pancreatic cancer and by preventing cells from entering phase S. This stops the growth and proliferation of cancer cells.

Regarding the effect of 6-gingerol, cisplatin, and their combination on the expression of oncogenes and genes for the induction of apoptosis and cellular angiogenesis, the findings of our study revealed that the combination of these two drugs, as against each alone, in both OVCAR-3 and HUVEC cell lines increased the expression of cells that induce cell apoptosis such as Apaf1, Bax, Caspase-8, and p53 and decreased the expression of Bcl-2 (as oncogenes) and VEGF, KDR, and FLT1 (as cells that induce angiogenesis). The analysis of gene expression results in our study is consistent with several similar studies in this field, each of which is discussed separately.

Protease 1-activating apoptosis factor (Apaf1) is a gene that encodes a cytoplasmic protein that is one of the major gateways to the cell death regulatory network. In the present study, the expression of the Apaf1 gene showed that by promoting the concentration of drugs in both cell lines, the expression of the Apaf1 gene also increased, which showed a significant difference

from the control group. This significant increase was also observed in combination therapy compared to cisplatin therapy. The above results are consistent with the results of several similar studies, which are given below.

In the study of Nigam et al. (17), 6-gingerol was evaluated for its anti-apoptotic potential in human epidermoid carcinoma (A431). Treatment with 6-gingerol showed significant cytotoxicity, as it inhibited the proliferation of A431 cells. Mediated production of ROS was identified. Increased ROS decreased mitochondrial membrane potential (MMP) and triggered subsequent apoptosis. Treatment with 6-gingerol also resulted in high regulation of cytochrome c and Apaf1, followed by caspase cascade and apoptosis.

The tumor suppressor gene p53 enhances Bax gene expression, and this protein plays an essential role in p53-dependent apoptosis. Bcl-2 is an oncogene that inhibits apoptosis and cancer progression. A drug that can increase Bax expression and decrease Bcl-2 expression can prevent cancer growth. Examination of Bax gene expression in our study showed that with rising drug concentrations in both cell lines, the expression of the Bax gene also rose, demonstrating a considerable departure from the control group. This difference between combination therapy and cisplatin treatment was also detected. Regarding the expression of the Bcl-2 gene, the results of our study showed that, in both cell lines, by

increasing the concentration of drugs, the expression of the Bcl-2 gene decreased, which shows a significant difference from the control group; this significant decrease in combination therapy was also observed in comparison to cisplatin treatment alone.

The results of similar studies in this field support the above finding. In the study of Nipin et al. (42), 6-gingerol increased Bax expression and decreased Bcl-2 expression, followed by loss of membrane potential and subsequent formation of pores in the mitochondrial membrane of breast cancer cells, which indicates that a positive effect of 6-gingerol is involved in inducing apoptosis in cancer cells. Luo et al. (43) investigated the anti-apoptotic effects of 6-gingerol on gastric adenocarcinoma (AGS) cells. The results showed that abnormalities in MMP were associated with the deregulation of the Bax/Bcl-2 ratio at the protein level, which resulted in positive regulation of cytochrome-c, resulting in a caspase cascade and subsequent induction of apoptosis. Chakraborty et al. (45) looked at how 6-gingerol affected the apoptosis of HeLa cells. The results showed that 6-gingerol therapy decreased the overexpression of NFk, AKT, and Bcl-2 genes in cancer cells. On the other hand, 6-gingerol-treated cells showed an increase in the expression of TNF, Bax, and cytochrome c. They concluded that 6-gingerol might bind to DNA and cause cell death *via* apoptosis and autophagy mediated by caspase.

The p53 gene is the most well-known tumor-blocking gene, mutating in more than 50% of human cancers. This vital role in genomic stability and tumor suppression is mainly involved in inducing cell cycle arrest, aging, programmed cell death, and inhibition of angiogenesis. The study of p53 gene expression showed that, in both cell lines, by elevating the concentration of drugs, the expression of the p53 gene was also augmented, which shows a significant difference from the control group. This significant increase in combination therapy compared to treatment with cisplatin was also detected. A review of similar studies showed that 6-gingerol induced apoptosis in various cancers by increasing p53 expression. In the study by Liu et al. (46), 6-gingerol increased p53 levels and decreased the Bcl-2/Bax ratio, and, of course, endometrial cancer cell death and mitochondrial membrane potential were significantly increased in endometrial cancer cell lines after exposure. Exposure was reduced and induced. Also, in a study by Park et al. (44), 6-gingerol increased p53 expression and induced apoptosis of pancreatic cancer cells. In a study by Rastogi et al. (18), it was found that 6-gingerol inhibited proteasome and oxidative stress by increasing p53, which stopped apoptosis and cell division in breast cancer cell lines. A tumor suppressor gene induces cell apoptosis by increasing its expression and preventing cancer cell proliferation. With rising medication concentrations in both cell lines in the current study, the expression of the Caspase-8 gene also rose, demonstrating a substantial difference from the control group. This large increase in combination treatment is also related to the factor to be seen after receiving cisplatin therapy.

In the present investigation, the apoptotic effect of 6-gingerol, cisplatin, and their combination demonstrated in embryonic vessels was assessed through *in silico* and *in vivo* studies. In this regard, we discuss various highlights of the findings regarding vascular changes

and the interactions of 6-gingerol, cisplatin, and their combination with proteins, which are associated with apoptosis.

In the current paper, we applied a docking assay to clarify some details about the apoptotic effect of 6-gingerol, cisplatin, and their combination demonstrated in vessels. Currently, docking is considered a useful technique to study the interactions between receptors and ligands; thus, it is applied in various molecular investigations (47, 48). It is well known that the Bcl-2 family members are important targets for apoptotic and anti-apoptotic factors (49, 50).

Combination treatment demonstrated promising *in silico* results, which are revealed by their substantial scoring roles and increased protein–ligand interface binding energy. The *in silico* ADMET results indicated that combination treatment is promising for the improvement of a particular, safe, and efficient anticancer process. The conclusion of the analysis provided a significant development for combination therapy as a great anticancer agent in general.

To confirm our prediction; the toxicity of 6-gingerol, cisplatin, and the combination treatment was also accessed *via in vivo* (YSM) assay. Due to the considerable decreases in vessel area and diameter seen in the YSM vessels, it can be concluded that 6-gingerol and cisplatin demonstrated a negative effect on the embryonic vasculature. Based on these results, we suggest the use of the combination treatment (compared to cisplatin alone) on the fetus.

To the best of our knowledge, this is the first study that targets the different aspects of 6-gingerol, cisplatin, and combination treatment toxicity with a chick embryo model.

In our study, vascular analysis of YSM shows that 6-gingerol, cisplatin, and the combination treatment damaged the embryonic vessels. The method used to assess the apoptotic effect of 6-gingerol, cisplatin, and the combination treatment was to calculate the MCA in the obtained images. Until now, this technique has been used in various research (51, 52). Another highlight to be explained is the significant change in the expression of Bax and Bcl-2 proteins following 6-gingerol, cisplatin, and the combination treatment. These altered expressions in apoptotic–regulator components can make a link between 6-gingerol, cisplatin, and the combination treatment and vascular defect that was seen in the current study. The pathways or mechanisms by which 6-gingerol, cisplatin, and the combination treatment cause toxic effects on blood vessels are not fully understood, but according to our results, it can be suggested that the vascular toxicity of 6-gingerol, cisplatin, and the combination treatment is associated with the induction of apoptotic-signaling pathways. The IHC results also confirmed the changes in the expressions of Bax and Bcl-2 in the 6-gingerol-, cisplatin-, and the combination treatment-exposed embryos.

5 Conclusion

The results of this study showed that cisplatin as the first line of ovarian cancer treatment can prevent the progression and proliferation of cancer cells, but it also causes some complications for the cells. 6-gingerol can reduce the side effects of this drug and

increases its effectiveness when combined with cisplatin. On the other hand, because of the anti-nausea properties of ginger, it is possible to use this herbal substance widely and in combination with cisplatin drugs by presenting specific drug protocols.

Finally, other studies in this field could be performed *in vivo* and in later stages of human trials to provide the basis for progression in the administration of this drug combination to improve the quality of life for patients with ovarian cancer.

Data availability statement

The original contributions presented in the study are included in the article/Supplementary Material. Further inquiries can be directed to the corresponding authors.

Ethics statement

The animal study was reviewed and approved by the present study and was performed based on the suggested European Ethical Guidelines by the care of animals in experimental investigations. It was approved by ethical committee of Kerman University of Medical Sciences (Project No. 97000719) and ethic code IR.KMU.REC.1397.154.

Author contributions

ZS: original draft preparation, data validation, review, and editing. AK: original draft preparation and supervision. EP: original draft preparation and supervision. EM: software and molecular docking analysis. ES, ARK, HT, and SS: methodology. SD: visitation. GR: review and editing. All authors contributed to the article and approved the submitted version.

Conflict of interest

The authors declare that the research was conducted in the absence of any commercial or financial relationships that could be construed as a potential conflict of interest.

Publisher's note

All claims expressed in this article are solely those of the authors and do not necessarily represent those of their affiliated organizations, or those of the publisher, the editors and the reviewers. Any product that may be evaluated in this article, or claim that may be made by its manufacturer, is not guaranteed or endorsed by the publisher.

Supplementary material

The Supplementary Material for this article can be found online at: https://www.frontiersin.org/articles/10.3389/fonc.2023.1098429/full#supplementary-material

References

1. Cabasag CJ, Fagan PJ, Ferlay J, Vignat J, Laversanne M, Liu L, et al. Ovarian cancer today and tomorrow: A global assessment by world region and human development index using GLOBOCAN 2020. *Int J Cancer* (2022). doi: 10.1002/ijc.34002

2. Momenimovahed Z, Tiznobaik A, Taheri S, Salehiniya H. Ovarian cancer in the world: epidemiology and risk factors. *Int J Womens Health* (2019) 11:287. doi: 10.2147/IJWH.S197604

3. Bray F, Ferlay J, Soerjomataram I, Siegel RL, Torre LA, Jemal A. Global cancer statistics 2018: GLOBOCAN estimates of incidence and mortality worldwide for 36 cancers in 185 countries. *CA Cancer J Clin* (2018) 68:394–424. doi: 10.3322/caac.21492

4. Akter S, Rahman MA, Hasan MN, Akhter H, Noor P, Islam R, et al. Recent advances in ovarian cancer: Therapeutic strategies, potential biomarkers, and technological improvements. *Cells* (2022) 11:650. doi: 10.3390/cells11040650

5. Kurnit KC, Fleming GF, Lengyel E. Updates and new options in advanced epithelial ovarian cancer treatment. *Obstet Gynecol* (2021) 137:108. doi: 10.1097/AOG.0000000000004173

6. Orr B, Edwards RP. Diagnosis and treatment of ovarian cancer. *Hematol Clin* (2018) 32:943–64. doi: 10.1016/j.hoc.2018.07.010

7. Kefayat A, Ghahremani F, Safavi A, Hajiaghababa A, Moshtaghian J. C-phycocyanin: a natural product with radiosensitizing property for enhancement of colon cancer radiation therapy efficacy through inhibition of COX-2 expression. *Sci Rep* (2019) 9:19161. doi: 10.1038/s41598-019-55605-w

8. Mirza-Aghazadeh-Attari M, Ostadian C, Saei AA, Mihanfar A, Darband SG, Sadighparvar S, et al. DNA Damage response and repair in ovarian cancer: Potential targets for therapeutic strategies. *DNA Repair (Amst)* (2019) 80:59–84. doi: 10.1016/j.dnarep.2019.06.005

9. Grabosch S, Bulatovic M, Zeng F, Ma T, Zhang L, Ross M, et al. Cisplatin-induced immune modulation in ovarian cancer mouse models with distinct inflammation profiles. *Oncogene* (2019) 38:2380–93. doi: 10.1038/s41388-018-0581-9

10. Chen X, Mangala LS, Mooberry L, Bayraktar E, Dasari SK, Ma S, et al. Identifying and targeting angiogenesis-related microRNAs in ovarian cancer. *Oncogene* (2019) 38:6095–108. doi: 10.1038/s41388-019-0862-y

11. Wang H, Xu T, Zheng L, Li G. Angiogenesis inhibitors for the treatment of ovarian cancer: an updated systematic review and meta-analysis of randomized controlled trials. *Int J Gynecol Cancer* (2018) 28:903–14. doi: 10.1097/IGC.0000000000001258

12. Wang S, Long S, Deng Z, Wu W. Positive role of Chinese herbal medicine in cancer immune regulation. *Am J Chin Med* (2020) 48:1577–92. doi: 10.1142/S0192415X20500780

13. Nafees S, Zafaryab M, Mehdi SH, Zia B, Rizvi MA, Khan MA. Anti-cancer effect of gingerol in cancer prevention and treatment. *Anti-Cancer Agents Med Chem (Formerly Curr Med Chem Agents)* (2021) 21:428–32. doi: 10.2174/1871520620666200918100833

14. Keyhani A, Sharifi I, Salarkia E, Khosravi A, Oliaee RT, Babaei Z, et al. *In vitro* and *in vivo* therapeutic potentials of 6-gingerol in combination with amphotericin b for

treatment of leishmania major infection: Powerful synergistic and multifunctional effects. *Int Immunopharmacol* (2021) 101:108274. doi: 10.1016/j.intimp.2021.108274

15. Wang S, Zhang C, Yang G, Yang Y. Biological properties of 6-gingerol: a brief review. *Nat Prod Commun* (2014) 9:1934578X1400900736. doi: 10.1177/1934578X1400900736

16. Kumara M, Shylajab MR, Nazeemc PA, Babu T. 6-gingerol is the most potent anticancerous compound in ginger (Zingiber officinale rosc.). *J Dev Drugs* (2017) 6:1–6. doi: 10.4172/2329-6631.1000167

17. Nigam N, George J, Srivastava S, Roy P, Bhui K, Singh M, et al. Induction of apoptosis by [6]-gingerol associated with the modulation of p53 and involvement of mitochondrial signaling pathway in b [a] p-induced mouse skin tumorigenesis. *Cancer Chemother Pharmacol* (2010) 65:687–96. doi: 10.1007/s00280-009-1074-x

18. Rastogi N, Duggal S, Singh SK, Porwal K, Srivastava VK, Maurya R, et al. Proteasome inhibition mediates p53 reactivation and anti-cancer activity of 6-gingerol in cervical cancer cells. *Oncotarget* (2015) 6:43310. doi: 10.18632/oncotarget.6383

19. Kapoor V, Aggarwal S, Das SN. 6-gingerol mediates its anti tumor activities in human oral and cervical cancer cell lines through apoptosis and cell cycle arrest. *Phyther Res* (2016) 30:588–95. doi: 10.1002/ptr.5561

20. Luna-Dulcey L, Tomasin R, Naves MA, da Silva JA, Cominetti MR. Autophagy-dependent apoptosis is triggered by a semi-synthetic [6]-gingerol analogue in triple negative breast cancer cells. *Oncotarget* (2018) 9:30787. doi: 10.18632/oncotarget.25704

21. Rasmussen A, Murphy K, Hoskin DW. 10-gingerol inhibits ovarian cancer cell growth by inducing G2 arrest. *Adv Pharm Bull* (2019) 9:685. doi: 10.15171/apb.2019.080

22. Swaan PW, Ekins S. Reengineering the pharmaceutical industry by crash-testing molecules. *Drug Discovery Today* (2005) 10:1191–200. doi: 10.1016/S1359-6446(05)03557-9

23. Trott O, Olson AJ. AutoDock vina: improving the speed and accuracy of docking with a new scoring function, efficient optimization, and multithreading. *J Comput Chem* (2010) 31:455–61. doi: 10.1002/jcc.21334

24. Kusumaningrum S, Budianto E, Kosela S, Sumaryono W, Juniarti F. The molecular docking of 1, 4-naphthoquinone derivatives as inhibitors of polo-like kinase 1 using molegro virtual docker. *J Appl Pharm Sci* (2014) 4:47–53. doi: 10.7324/JAPS.2014.4119

25. Byrnes JEK, Baskerville EB, Caron B, Neylon C, Tenopir C, Schildhauer M, et al. The four pillars of scholarly publishing: The future and a foundation. *Ideas Ecol Evol* (2014). doi: 10.7287/peerj.preprints.11v1

26. Vieira TF, Sousa SF. Comparing AutoDock and vina in ligand/decoy discrimination for virtual screening. *Appl Sci* (2019) 9:4538. doi: 10.3390/app9214538

27. Pagadala NS, Syed K, Tuszynski J. Software for molecular docking: a review. *Biophys Rev* (2017) 9:91–102. doi: 10.1007/s12551-016-0247-1

28. Lipinski CA, Lombardo F, Dominy BW, Feeney PJ. Experimental and computational approaches to estimate solubility and permeability in drug discovery and development settings. *Adv Drug Delivery Rev* (2012) 64:4–17. doi: 10.1016/j.addr.2012.09.019

29. Yang Q, Zhang H, Li Z. Leptin induces muscle wasting kras-driven hepatocell carcinoma model zebrafish dis mod mech. *Disease models & mechanisms* (2019) 12:1–12. doi: 10.1242/dmm.038240

30. Yang H, Lou C, Sun L, Li J, Cai Y, Wang Z, et al. admetSAR 2.0: web-service for prediction and optimization of chemical ADMET properties. *Bioinformatics* (2019) 35:1067–9. doi: 10.1093/bioinformatics/bty707

31. Rostkowski M, Spjuth O, Rydberg P. WhichCyp: prediction of cytochromes P450 inhibition. *Bioinformatics* (2013) 29:2051–2. doi: 10.1093/bioinformatics/btt325

32. Kotowski U, Kadletz L, Schneider S, Foki E, Schmid R, Seemann R, et al. 6-shogaol induces apoptosis and enhances radiosensitivity in head and neck squamous cell carcinoma cell lines. *Phyther Res* (2018) 32:340–7. doi: 10.1002/ptr.5982

33. Al-Abbasi FA, Alghamdi EA, Baghdadi MA, Alamoudi AJ, El-Halawany AM, El-Bassossy HM, et al. Gingerol synergizes the cytotoxic effects of doxorubicin against liver cancer cells and protects from its vascular toxicity. *Molecules* (2016) 21:886. doi: 10.3390/molecules21070886

34. Luo H, Vong CT, Chen H, Gao Y, Lyu P, Qiu L, et al. Naturally occurring anti-cancer compounds: shining from Chinese herbal medicine. *Chin Med* (2019) 14:1–58. doi: 10.1186/s13020-019-0270-9

35. Tsai Y, Xia C, Sun Z. The inhibitory effect of 6-gingerol on ubiquitin-specific peptidase 14 enhances autophagy-dependent ferroptosis and anti-tumor *in vivo* and *in vitro*. *Front Pharmacol* (2020) 11:598555. doi: 10.3389/fphar.2020.598555

36. Cesna V, Sukovas A, Jasukaitiene A, Naginiene R, Barauskas G, Dambrauskas Z, et al. Narrow line between benefit and harm: Additivity of hyperthermia to cisplatin cytotoxicity in different gastrointestinal cancer cells. *World J Gastroenterol* (2018) 24:1072. doi: 10.3748/wjg.v24.i10.1072

37. Yang G, Zhong L, Jiang L, Geng C, Cao J, Sun X, et al. Genotoxic effect of 6-gingerol on human hepatoma G2 cells. *Chem Biol Interact* (2010) 185:12–7. doi: 10.1016/j.cbi.2010.02.017

38. Kim SO, Kim MR. [6]-gingerol prevents disassembly of cell junctions and activities of MMPs in invasive human pancreas cancer cells through ERK/NF-κB/Snail signal transduction pathway. *Evidence-Based Complement Altern Med* (2013) 2013:1–9. doi: 10.1155/2013/761852

39. Zhang F, Zhang J-G, Qu J, Zhang Q, Prasad C, Wei Z-J. Assessment of anti-cancerous potential of 6-gingerol (Tongling white ginger) and its synergy with drugs on human cervical adenocarcinoma cells. *Food Chem Toxicol* (2017) 109:910–22. doi: 10.1016/j.fct.2017.02.038

40. Abdul AB, Abdelwahab SI, Bin JJ, Al-Zubairi AS, Taha MME. Combination of zerumbone and cisplatin to treat cervical intraepithelial neoplasia in female BALB/c mice. *Int J Gynecol Cancer* (2009) 19:1004–1010. doi: 10.1111/IGC.0b013e3181a83b51

41. Karaboz I. Antimicrobial and cytotoxic activities of zingiber officinalis extracts. *Fabad J Pharm Sci* (2010) 33:76–85. doi: 10.3390/ijms22094660

42. Sp N, Kang DY, Lee J-M, Bae SW, Jang K-J. Potential antitumor effects of 6-gingerol in p53-dependent mitochondrial apoptosis and inhibition of tumor sphere formation in breast cancer cells. *Int J Mol Sci* (2021) 22:4660. doi: 10.3390/ijms22094660

43. Luo Y, Zha L, Luo L, Chen X, Zhang Q, Gao C, et al. [6]-gingerol enhances the cisplatin sensitivity of gastric cancer cells through inhibition of proliferation and invasion *via* PI 3 K/AKT signaling pathway. *Phyther Res* (2019) 33:1353–62. doi: 10.1002/ptr.6325

44. Park YJ, Wen J, Bang S, Park SW, Song SY. [6]-gingerol induces cell cycle arrest and cell death of mutant p53-expressing pancreatic cancer cells. *Yonsei Med J* (2006) 47:688. doi: 10.3349/ymj.2006.47.5.688

45. Chakraborty D, Bishayee K, Ghosh S, Biswas R, Mandal SK, Khuda-Bukhsh AR. [6]-gingerol induces caspase 3 dependent apoptosis and autophagy in cancer cells: drug–DNA interaction and expression of certain signal genes in HeLa cells. *Eur J Pharmacol* (2012) 694:20–9. doi: 10.1016/j.ejphar.2012.08.001

46. Liu Y, Whelan RJ, Pattnaik BR, Ludwig K, Subudhi E, Rowland H, et al. Terpenoids from zingiber officinale (Ginger) induce apoptosis in endometrial cancer cells through the activation of p53. *PloS One* (2012) 7:e53178. doi: 10.1371/journal.pone.0053178

47. Jacob KS, Ganguly S, Kumar P, Poddar R, Kumar A. Homology model, molecular dynamics simulation and novel pyrazole analogs design of candida albicans CYP450 lanosterol 14 α-demethylase, a target enzyme for antifungal therapy. *J Biomol Struct Dyn* (2017) 35:1446–63. doi: 10.1080/07391102.2016.1185380

48. Tavakkoli H, Attaran R, Khosravi A, Salari Z, Salarkia E, Dabiri S, et al. Vascular alteration in relation to fosfomycine: *In silico* and *in vivo* investigations using a chick embryo model. *BioMed Pharmacother* (2019) 118:109240. doi: 10.1016/j.biopha.2019.109240

49. Warren CFA, Wong-Brown MW, Bowden NA. Bcl-2 family isoforms in apoptosis and cancer. *Cell Death Dis* (2019) 10:177. doi: 10.1038/s41419-019-1407-6

50. Trisciuoglio D, Del Bufalo D. New insights into the roles of antiapoptotic members of the Bcl-2 family in melanoma progression and therapy. *Drug Discovery Today* (2021) 26:1126–35. doi: 10.1016/j.drudis.2021.01.027

51. Seidlitz E, Korbie D, Marien L, Richardson M, Singh G. Quantification of anti-angiogenesis using the capillaries of the chick chorioallantoic membrane demonstrates that the effect of human angiostatin is age-dependent. *Microvasc Res* (2004) 67:105–16. doi: 10.1016/j.mvr.2003.12.005

52. Salari Z, Tavakkoli H, Khosravi A, Karamad E, Salarkia E, Ansari M, et al. Embryo-toxicity of docosahexaenoic and eicosapentaenoic acids: *In vivo* and *in silico* investigations using the chick embryo model. *BioMed Pharmacother* (2021) 136:111218. doi: 10.1016/j.biopha.2021.111218

Anti-angiogenic therapy in ovarian cancer: Current understandings and prospects of precision medicine

Chao Mei[1†], Weijing Gong[1,2†], Xu Wang[1], Yongning Lv[1], Yu Zhang[1], Sanlan Wu[1,2*†] and Chunqi Zhu[1*†]

[1]Department of Pharmacy, Union Hospital, Tongji Medical College, Huazhong University of Science and Technology, Wuhan, China, [2]Hubei Province Clinical Research Center for Precision Medicine for Critical Illness, Wuhan, China

Ovarian cancer (OC) remains the most fatal disease of gynecologic malignant tumors. Angiogenesis refers to the development of new vessels from pre-existing ones, which is responsible for supplying nutrients and removing metabolic waste. Although not yet completely understood, tumor vascularization is orchestrated by multiple secreted factors and signaling pathways. The most central proangiogenic signal, vascular endothelial growth factor (VEGF)/VEGFR signaling, is also the primary target of initial clinical anti-angiogenic effort. However, the efficiency of therapy has so far been modest due to the low response rate and rapidly emerging acquiring resistance. This review focused on the current understanding of the in-depth mechanisms of tumor angiogenesis, together with the newest reports of clinical trial outcomes and resistance mechanism of anti-angiogenic agents in OC. We also emphatically summarized and analyzed previously reported biomarkers and predictive models to describe the prospect of precision therapy of anti-angiogenic drugs in OC.

KEYWORDS

ovarian cancer, angiogenesis, biomarker, anti-angiogenic therapy, precision medicine

1 Introduction

Ovarian cancer (OC) possesses the highest death rate among gynecological malignant tumors (Bray et al., 2018). While treatments have been improving over the past few decades, the survival rate has barely improved (Liu et al., 2021). According to statistics, 60%–80% of patients achieved complete remission after first-line therapy, but 80% of them finally die of therapy resistance or relapse (Agarwal and Kaye, 2003; Lengyel, 2010). Approximately 70% of patients relapse within 3 years after initial therapy (Viallard and Larrivee, 2017). Recurrent OC is incurable and the progression-free survival (PFS) decreases at each subsequent relapse treatment (Papa et al., 2016). The 5-year survival rate of OC patients is lower than 30%, while the PFS is about 16–22 months (Bray et al., 2018).

Angiogenesis is indispensable for tumor growth and development. Under physiological conditions, angiogenesis is a complicated and dynamic process that grows new vessels from existing ones, supplying the requirement alterations in tissue. However, angiogenesis is abnormally stimulated in the majority of cancers. Blood vessels provide oxygen and nutrients for tumors to survive and growth, without which tumors cannot develop to larger than 1–2 mm (Viallard and Larrivee, 2017). Therapeutic strategies targeting angiogenesis has

been accepted for several types of solid tumors. The anti-angiogenic drug was the first targeted drug approved for OC. An increasing amount of innovative anti-angiogenesis agents are now being assessed in clinical trials of OC and mixed results are presented (Papa et al., 2016). However, individual differences and widespread resistance greatly limit the effectiveness of anti-angiogenic therapy. The above underscore the urgent need of discovering reliable molecular biomarkers to avoid resistance and improve the prognosis of OC patients.

2 Angiogenesis in tumor pathogenesis

In the pathological state of cancer, angiogenic signals will be exploited in a deregulated condition. Malignant cells release a series of growth factors, cytokines, and chemokines to stimulate quiescent cells to activate a cascade of signals. Except these, tumors may also trigger inflammatory reaction to recruit myeloid cells, releasing the stored soluble factors to facilitate the angiogenic response. These events quickly become deregulated and incline the balance toward secreting pro-angiogenic factors, thereby driving blood vessel growth (Ronca et al., 2015). These signals initiate formerly quiescent endothelial cell (EC) to sprout and proliferate on nearby vascular. Research indicated that tumor ECs lining blood vessels have a significant growth advantage, which probably divides 50 times quicker than in normal physiological conditions.

Normal vasculatures are arranged with a single-layer of tightly connected adherent ECs, which are polarized and aligned along the bloodstream for optimal perfusion. In comparison, tumor vasculature possesses the characteristics of abnormal structural dynamics, vascular immaturity, strikingly heterogeneous, tortuous, and high permeability (Dewhirst and Ashcraft, 2016; Dewhirst and Secomb, 2017; Zhang et al., 2019). Activated tumor ECs depolarize, slough off and piled up against each other, creating portals for malignant cells to entry the blood circulation. Tumor ECs are usually loosely connected and leaky, containing multiple fenestrations and trans-endothelial channels. In some tumors, these holes are more than 100 times larger than those in healthy blood vessels. Due to upregulated vessel resistance as well as disordered regulation, the bloodstream in the tumor is chaotic. The focal leaks and enhanced interstitial fluid pressure further create obstacles to the blood stream. The blood may flow rapidly in some vessels, but slowly in others, or even stagnant in some places (Carmeliet and Jain, 2011a). This pattern of blood flow leads to an abnormal microenvironment, seriously hindering the delivery of nutrients and drugs (Dewhirst et al., 1999). Fast-growing and metabolizing tumor cells constantly require abundant oxygen and nutrients. However, the non-productive blood vessel is far from the requirements of the tumor, which in turn stimulates tumor cells to produce an excess of pro-angiogenic factors. This leads to even more abnormal blood vessels, eventually creating an excess of the vicious cycle (Carmeliet and Jain, 2011a).

Tumor vessels often possess abnormal structure and function. This leads to a tumor microenvironment of hypoxia, inflammation, acidic pH and high interstitial hostile fluid pressure that interferes with the immune cellular function and the transport of chemotherapy drugs and oxygen. Therefore, abnormity of tumor vasculature leads to radiotherapy and chemotherapy resistance, and

the escape of tumor cells through leaky vessels. In addition, hypoxia stimulates tumor and stromal cells to secrete large amounts of angiogenic factors, further exacerbating vascular disorders and accelerating non-productive angiogenesis in an interminable self-enhanced circle.

To date, a large number of promoters of tumor angiogenesis have been discovered (Figure 1), such as the vascular endothelial growth factor (VEGF) family, angiopoietins (ANGPTs), fibroblast growth factors (FGFs), platelet-derived growth factor (PDGF), APLN (Apelin)/APLNR (G protein-coupled receptor APJ) pathway, hepatocyte growth factor (HGF)/hepatocyte growth factor receptor (c-MET), chemokines, Eph/Ephrin signaling, etc. Their targets, mechanisms, downstream signals and research status in OC are discussed below in detail.

3 Characteristics and functions of angiogenesis-related factors in OC

3.1 VEGF

VEGF, the most well-known pro-angiogenic factor, contains a group of ligands including VEGF-A to -D, as well as placental growth factor (PlGF) (Zhao and Adjei, 2015). VEGF can be secreted by malignant cells, fibroblasts, and inflammatory cells, usually in response to increased tissue hypoxia (Carmeliet and Jain, 2011b). VEGF binds to its receptor VEGFR tyrosine kinase and is activated to form homo- or heterodimers. VEGF-A tends to bind VEGFR-1 and 2. VEGF-B, PlGF-1, and PlGF-2 bind preferentially with VEGFR-1, while VEGF-C and -D mainly interact with VEGFR3 (Zhao and Adjei, 2015). The interaction between ligand and receptor triggers intracellular signaling cascades to promote the survival, proliferation, motility, permeability, and tube formation ability of ECs.

VEGF-A, VEGF-B, and PlGF play the uppermost functions in tumor angiogenesis, most of which are owing to the activation of VEGFR-2 by VEGF-A (Zhao and Adjei, 2015). PlGF binds to VEGFR-1 and its co-receptors neuropilin 1 (NRP1) and 2, which can directly facilitate vascular growth and maturation, or indirectly promote angiogenesis by recruiting monocyte-macrophage lineage cells and bone marrow-derived progenitors (De Falco, 2012). PlGF has been suggested as a potential participant in anti-VEGF resistance because of its upregulation in patients receiving anti-VEGF therapy (Willett et al., 2009; Bagley et al., 2011; Chiron et al., 2014). Aflibercept, which inhibits both VEGF-A and PlGF, has shown efficacy in cancer patient-derived xenograft models (Zhang and Lawler, 2007). VEGF-C and -D have the strongest binding affinity to VEGFR-3 and appear to be important in promoting lymph-angiogenesis.

The VEGF signaling is ubiquitous and upregulated in most cancer types. This overexpression is secondary to hypoxia and related transcription factors, like hypoxia-inducible factor -1α (HIF-1α) and HIF-2α. HIF-1α can stimulate several downstream proangiogenic growth factors, especially VEGF (Dewangan et al., 2019). Except this, insulin-like growth factor 1 (IGF-1), interleukin 6 (IL-6) (Salgado et al., 2002; Spiliotaki et al., 2011), and mutations in genes like p53, RAS, SRC, and VHL have also been shown to upregulate VEGF (White et al., 1997; Burger, 2011). Targeting
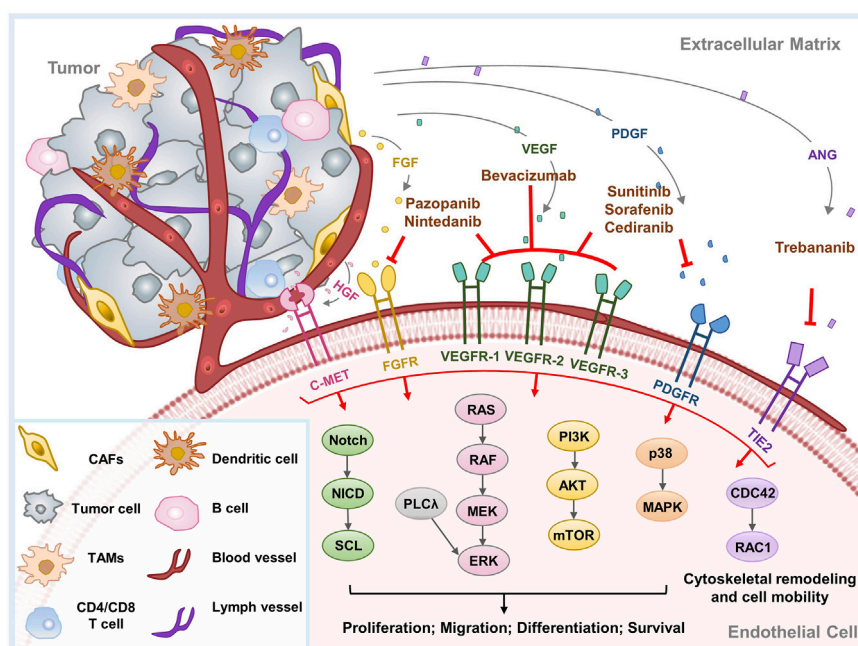
FIGURE 1
Major mechanisms of tumor angiogenesis and therapeutic agents implicated in OC. Tumor angiogenesis is induced by a series of proangiogenic factors. This diagram exhibits the principal angiogenic signaling pathways, as well as the molecular targets and therapeutic mechanisms of anti-angiogenic agents implicated in OC. CAFs, cancer associated fibroblasts; TAMs, tumor-associated macrophages.

VEGF can promote vascular normalization by recruiting pericytes, reducing the enlargement and tortuosity of vessels, and facilitating the normalization of the basement membrane (Carmeliet and Jain, 2011a). This results in a reduction in interstitial fluid pressure or edema, a transient increase in blood perfusion, oxygenation and improved efficiency of drug delivery.

In OC, VEGF signaling is highly activated and closely associated with metastatic potential, disease grade as well as poor prognosis (Wang et al., 2008). It is also a vital promotor of ascites production in the latter stage of OC cancer (Bamberger and Perrett, 2002; Numnum et al., 2006). VEGF activates its receptor VEGFR-2 on ECs to initiate multiple signaling pathways to mediate angiogenesis, for example, promoting EC proliferation and survival through extracellular signal-regulated kinase (ERK) and phosphatidylinositol 3-kinase (PI3K)/protein kinase B (AKT) pathways (Takahashi et al., 2001; Jiang and Liu, 2009); inducing cell invasion by activation of PI3K and Rho GTPases (Lamalice et al., 2007); mediating the basement membrane and extracellular matrix degradation as well as capillary sprout formation by mitochondrial membrane potential-2 (MMP-2), MMP-9, and urokinase plasminogen activator (uPA) (van Hinsbergh and Koolwijk, 2008; Jiang and Liu, 2009). VEGF–Akt–NF-κB signaling activation also induces an inflammatory response and promotes the recruitment of leukocytes, thereby contributing to the angiogenic process (Jiang and Liu, 2009). In addition, intracellular signaling including Janus kinase (JAK)-signal transducing activator of transcription (STAT), PI3K, and mitogen-activated protein kinase (MAPK) pathways have also been demonstrated to be related to VEGF signal (Banerjee and Kaye, 2011; Gavalas et al., 2013).

3.2 FGFs

The FGF family consists of 22 factors, 18 of which can bind and trigger the dimerization of their receptors FGFR1-4, initiating a series of intracellular signaling cascades (Turner and Grose, 2010). FGF is secreted by malignant cells, stromal cells, extracellular matrix and acts on ECs through paracrine signal. Among the FGF family, FGF1 and FGF2 exhibit uppermost proangiogenic abilities (Byron et al., 2010). In addition, the FGF/FGFR signal also contributed to tumor resistance to chemotherapy, radiotherapy, and targeted therapy (Katoh, 2016; Ghedini et al., 2018; Xie et al., 2020; Zhou et al., 2020). In OC, a spliced variant of FGFR and mutation events may confer binding sensitivity to the ligand and disrupt the downstream signaling cascade (Steele et al., 2001; Presta et al., 2005). The downstream signal pathways include the ERK/MAPK, JAK-STAT, phospsholipase-C (PLC)-inositol 1,4,5-triphosphate (IP3) cascade and PI3K-AKT pathway, which promotes angiogenesis, cell cycle progression as well as cell survival, proliferation and differentiation (Greenberg et al., 2008). FGFs also interferes with other signals like the Notch signal (Akai et al., 2005). In addition, FGF degrades the extracellular matrix *via* the promotion of plasminogen activators, MMPs, and collagenase (Turner and Grose, 2010). FGF also regulates cell metabolism through MYC-mediated glycolysis, which is essential for the proliferation, motility as well as sprouting of vascular ECs (Yu et al., 2017).

FGF signaling may be a compensatory angiogenesis mechanism that leads to VEGF-targeted therapy resistance. Increased FGF expression was found in patients with anti-VEGF therapy resistance. As FGF acts synergistically with VEGF to facilitate

angiogenesis in cancer, simultaneously inhibiting the FGF signal effectively decreased vascular density and reverted sensitivity to anti-VEGF agents (Burbridge et al., 2013; Lee et al., 2015; Norden et al., 2015).

3.3 PDGF

There are four isoforms, PDGF-A to -D, in PDGF family (Heldin and Westermark, 1999). These ligands appear to have potent angiogenic activity by interacting with PDGFR-α and -β (Franco et al., 2011). PDGF signaling is involved in the survival, proliferation and migration of multiple types of cells (Ghedini et al., 2018). Hyperactivated PDGF signal, alone or accompanied with FGF and VEGF, result in excessive tumor angiogenesis, comprising but not limited to OC (Cao, 2013; Cantanhede and de Oliveira, 2017). In various types of cancer, aberrant PDGF signaling mediates the secretion of pro-angiogenic factors; promotion of pericyte recruitment and vascular maturation; facilitation of proliferation, migration, sprouting of ECs; interference with stroma formation; stimulation of lymph-angiogenesis and subsequent lymphatic metastasis (Levitzki, 2004; Cao, 2013; Zhao and Adjei, 2015). PDGF is also cross-linked to VEGF, by either converging their signaling cascades or being activated following the resistance to anti-VEGF therapy (Erber et al., 2004; Lu et al., 2008; Pietras et al., 2008). PDGF receptors are highly expressed in the pericytes of solid tumors, together with the critical role of PDGF signaling in mediating the immune microenvironment, targeting PDGF/PDGFR signal is expected to be a prospective therapeutic strategy (Heldin, 2013; Ostman, 2017; Bartoschek and Pietras, 2018; Papadopoulos and Lennartsson, 2018). The downstream signaling activated by the PDGF pathway includes PI3K/Akt, MAPK, Phospholipase C-γ (PLC-γ), Src, Ras and STAT, etc. (Gavalas et al., 2013).

According to previous studies, PDGF expression level in OC cells is approximately five to six-fold higher than that in normal ovarian ECs (Matei et al., 2002). In human OC tissue samples, PDGF was highly expressed in tumor stroma instead of the corresponding epithelial components, while PDGFR was mainly expressed in tumor stroma but not in OC cells (Li et al., 2022). In addition, high serum PDGF-BB and FGF2 were of prognostic significance. PDGFR-α and serum PDGF-BB expression have been reported to correlate with the prognosis of OC patients (Lassus et al., 2004; Madsen et al., 2012). Studies further supported the potency of PDGF in the anti-vascular therapeutic approach, by demonstrating that PDGFR blocking effectively improves the antitumor effect of bevacizumab (Lu et al., 2010). Taken together, PDGF is a key regulatory molecule in angiogenesis and ovarian carcinogenesis. Further studies are needed in the hope of developing more effective anti-tumor approaches.

3.4 ANGPTs

The ANGPTs family of ligands, ANGPT1 and ANGPT2, play a crucial role in vascular maintenance, remodeling, and development by interacting with the receptor tyrosine kinase TIE2 receptor (Aghajanian et al., 2012; Pujade-Lauraine et al., 2014; Coleman

et al., 2017). ANGPT1 is an angiogenesis suppressor that mediates the neovascularization and maturation through Akt/surviving pathway, and is probably involved in the stabilization and protection of existing blood vessels (Thurston et al., 2000). As an endogenous antagonist of ANGPT1 function, ANGPT2 mainly mediates the remodeling process or vascular sprouting in response to VEGF (Scharpfenecker et al., 2005). Similar to cancer angiogenesis, ANGPT2 mostly promotes vascular instability and disruption that is characterized by unstable and leaky blood vessels (Tait and Jones, 2004; Reiss et al., 2009). ANGPT2 is involved in the predisposition of the endothelium towards the angiogenic statues required for angiogenic initiation and vascular destabilization (Scharpfenecker et al., 2005). It has also been suggested that ANGPT2 acts as an agonist in the absence of ANGPT1, while functioning as a dose-dependent antagonist when ANGPT1 exists (Yuan et al., 2009). The responders of ANGPT/Tie2 receptor include PI3K, MAPK/Erk, Ras signaling, etc. (Gavalas et al., 2013).

The serum levels of ANGPT1 and ANGPT2 were higher in ovarian tumor than normal ovaries, benign and/or borderline ovarian neoplasms (Sallinen et al., 2010; Sallinen et al., 2014). ANGPT1, ANGPT2 and ANGPT4 are upregulated in OC cells and tissues and indicate poor survival and a more aggressive phenotype, suggesting an attractive target in OC therapy (Brunckhorst et al., 2014). Upregulation of ANGPT2 is associated with decreased patient survival and resistance to anti-VEGF agents (Chae et al., 2010; Brunckhorst et al., 2014). Dual blocking of ANGPT2 and VEGFR2 effectively impaired glioma progression, promoted vascular normalization, blocked macrophage recruitment, and prolongered the prognosis of tumor-bearing mouse models (Kloepper et al., 2016; Peterson et al., 2016). This co-targeting effect has also been demonstrated in early colorectal, breast, and kidney cancer (Kloepper et al., 2016; Tuppurainen et al., 2017). However, ANG2/TIE2-induced tumor vessel instability may also make the established vasculature more resistant to anti-angiogenic agents (Gerald et al., 2013). Focusing on ANG/TIE2 signal to develop a targeted agent has proved to be challenging.

3.5 APLN/APLNR

APLN is a small, secreted peptide ligand of APLNR, which is predominantly expressed in ECs. APLN/APLNR signal is upregulated in several types of malignant T-cells and tumor ECs (Kalin et al., 2007; Seaman et al., 2007; Berta et al., 2010; Tolkach et al., 2019). APLN/APLNR signaling has been demonstrated to associate with neovascularization, tumor vessel density, microvascular proliferation, and tumor growth in other types of tumors (Sorli et al., 2006; Kalin et al., 2007; Sorli et al., 2007; Berta et al., 2010; Wu et al., 2017). APLN level is correlated with disease progress and worse clinical outcome, but its role in OC angiogenesis has seldom been identified (Berta et al., 2010; Heo et al., 2012; Lacquaniti et al., 2015; Feng et al., 2016). In OC, APLN functions as a mitogenic factor to promote cell proliferation (Hoffmann et al., 2017). APLN/APLNR signaling also drives OC metastasis in an angiogenesis-independent manner. Adipocyte-derived APLN promotes the uptake and utilization of lipids of OC cells, thus providing energy for the survival of OC cells in metastasis tissue (Dogra

et al., 2021). Targeting APLN/APLNR for OC therapy is of certain prospect, but extensive research is still needed.

3.6 HGF/c-MET

HGF/c-MET exerts pro-angiogenic effects by both directly activating epithelial cells as well as indirectly stimulating VEGF and other proangiogenic factors (Cloughesy et al., 2017; Lopes-Coelho et al., 2021). c-MET is upregulated in patients with bevacizumab resistance (Shojaei et al., 2010). Concurrent administration of sunitinib (VEGFR and PDGFR receptor tyrosine kinases inhibitor (RTKI)) and HGF/c-MET inhibitors effectively inhibited angiogenesis and tumor growth (Lu et al., 2012). However, the combination of obinutuzumab (anti-c-Met) and bevacizumab has not brought significant clinical benefit (Rini et al., 2008; Kim et al., 2021).

c-MET is a prognostic factor of OC patients, targeting c-MET inhibits peritoneal dissemination, tumor invasion, and metastasis *in vivo* (Sawada et al., 2007; Mitra et al., 2011). Cabozantinib is the only approved TKI targeting VEGFRs, MET, and AXL (Maroto et al., 2022). A phase II trial reported the clinical benifit (objective response rate, 21%) and improved PFS (5.9 vs. 1.4 months) of cabozantinib in OC patients compared with the placebo arm (Vergote et al., 2017).

3.7 Eph/Ephrin signaling

The large family of receptor tyrosine kinases (RTK), Ephs and their binding ligands Ephrins exhibit oncogenic transformation, angiogenesis, vascular remodeling, malignant T-cell survival, migration, and invasion (Lisle et al., 2013). Ephs and Ephrins are sorted into two groups, A and B: EphrinA1-5, EphrinB1-3 and EphA1-10, EphB1-6. EphA2 and EphrinA1 expression is critical for tumor neovascularization and progression (Ogawa et al., 2000; Brantley et al., 2002; Cheng et al., 2003; Dobrzanski et al., 2004). Ephrb4-Ephrinb2 signaling was correlated with angiogenesis, tumor progression and anti-angiogenic drug resistance (Noren et al., 2004; Krusche et al., 2016; Uhl et al., 2018). The relationship between Ephrin and VEGF signaling has also been demonstrated. Ephrin-B2 regulates VEGF signaling by inducing the internalization of VEGFR2 and VEGFR3, thus mediating angiogenesis and lymphangiogenesis in both physiological and tumor conditions (Sawamiphak et al., 2010; Wang et al., 2010).

The expression of EphA1-2, B1-2, B2-4, -A1, -A5 was increased in OC cells (Herath et al., 2006; Alam et al., 2008). Ephrin-A1, -A5, and -A2 were associated with poor prognosis (Han et al., 2005; Herath et al., 2006). Ephrin-B2 and -B4 were in proportion to the disease stage (Alam et al., 2008). Ephrin-A4 is upregulated in OC and recognized as a novel tumor-initiating marker. PF-06647263, a monoclonal antibody against Ephrin-A4 conjugated with the DNA damage agent calicheamicin, showing limited antitumor efficiency in OC (Garrido-Laguna et al., 2019). EphA8 mRNA levels are upregulated in OC tissues compared with normal ovarian and fallopian tube tissues (Liu et al., 2016). High EphA8 protein level was correlated with later-stage, metastatic disease, serum levels of tumor and positive ascetic fluid, and has been regarded as a prognostic biomarker in epithelial ovarian cancer (EOC) patients (Liu et al., 2016). The above studies suggested the significant role of Eph/Ephrin signaling in OC.

3.8 Galectins

Apart from the factors described above, there are still several pro-angiogenic factors contribute to angiogenesis in OC. Galectins are a class of endogenous lectins, whose family members have been reported to correlate with cancer stage and disease recurrence of OC patients, as well as the proliferation, migration, invasion of OC cells (Shimada et al., 2020; Mielczarek-Palacz et al., 2022). Among them, Galectin-1 was the first identified and the most intensively studied member, which is an important proangiogenic factor in several types of carcinomas. Research has shown the positive correlation between Galectin-1 expression and number of micro vessels (Pranjol et al., 2019). Galectin-1 mediates angiogenesis mainly by enhancing the VEGF signaling pathway. Galectin-1 interacts with NRP-1, the co-receptor for VEGF, thereby activating VEGFR2 and downstream SAPK/JNK signaling to induce endothelial cell migration and adhesion. It has been shown that Galectin-1 can directly bind and activate VEGFR2, leading to anti-VEGF therapeutic resistance in the absence of VEGF. In addition to VEGF-VEGFR pathway, Galectin-1 also regulates H-Ras and Raf/MEK/ERK signals to promote endothelial cell activation, proliferation, migration and angiogenesis process (Martinez-Bosch and Navarro, 2020). As for the other member, Galectin-3 promotes angiogenesis *via* VEGF, basic FGF (bFGF) and modifies N-glycans on integrin αvβ3. Galectin-8 is expressed on the vascular endothelial cells of both normal and tumor-associated vessels, and facilities angiogenesis by promoting endothelial cell migration (Delgado et al., 2011; Troncoso et al., 2014).

3.9 Anti-angiogenic factors

Except the pro-angiogenic factors described above, anti-angiogenic factors, such as Thrombospondin-1 (TSP-1), Angioarrestin and Endostatin also play indispensable roles in OC progression and clinical treatment. TSP-1, the first identified endogenous anti-angiogenic factor, possesses a well-established anti-angiogenic and anti-tumor activity. TSP-1 is highly expressed in ovarian tumors. It can be secreted by a series of cell types including ECs, fibroblasts and immune cells, etc., and is highly located in the tumor stroma instead of tumor cells (Zhao et al., 2018). Based on its anti-angiogenic properties, high TSP-1 expression has been demonstrated to correlate with higher survival rates in OC, colon cancer, lung cancer and cervical cancer, etc. However, this conclusion is inconsistent or even opposite in other types of tumors, such as hepatocellular carcinoma, breast cancer and melanoma, etc. (Grossfeld et al., 1997; Zhao et al., 2018). These inconsistent conclusions led to controversy over its use as a survival predictor in different types of cancer. Similarly, existing studies has not shown a clear correlation between VEGF and TSP-1 expression in different

TABLE 1 Summary of anti-angiogenic agents in OC.

Drug name	Targets	Approved indications	Adaptation in OC	Route of administration
Bevacizumab	VEGFR	OC; Colorectal cancer; Non-small cell lung cancer; Recurrent glioblastoma; Hepatocellular carcinoma; Cervical cancer; Renal carcinoma; Breast cancer	Combination with chemotherapy; Maintenance monotherapy	I.V.
Pazopanib	VEGFR, PDGFR, FGFR, c-Kit, c-Fms	Soft tissue sarcoma; Advanced renal carcinoma	Clinical study	Oral
Nintedanib	VEGFR, FGFR, PDGFR	Idiopathic pulmonary fibrosis	Clinical study	Oral
Cediranib	VEGFR	/	Clinical study	Oral
Sunitinib	PDGFR, VEGFR, Flt3, c-Kit	Kidney cancer; Gastrointestinal stromal tumor; Neuroendocrine tumor	Clinical study	Oral
Sorafenib	VEGFR, PDGFR, Raf, ERK	Renal cell carcinoma, Hepatocellular carcinoma, Thyroid carcinoma	Clinical study	Oral
Trebananib	Tie2	/	Clinical study	I.V.

I.V., intravenous injection; OC, ovarian cancer.

tumor types. A recent meta-analysis included 24 studies revealed high TSP-1 expression may be a promising biomarker of poor prognosis in cancer, especially in breast and gynecologic cancers (Sun et al., 2020). ABT-510, a TSP-1 mimetic peptide, is the first TSP-1 inhibitor. ABT-510 effectively reduced the abnormal vasculature increased mature blood vessels within tumor, but failed to pass the phase II clinical study (Campbell et al., 2010; Zhao et al., 2018). Besides, the interaction between TSP-1 with CD47 directly inhibits tumor adaptive immunity. TAX2 is a selective antagonist against the interaction between TSP-1 and CD47. It effectively suppresses CD47 activation by targeting TSP-1, and reprograms highly vascularized ovarian tumors into poorly angiogenic ones, while concurrently activating anti-tumor immunity (Jeanne et al., 2021). TSP-1 derived peptides and peptide mimetics showed satisfied efficiency in the treatment of tumors driven by excessive angiogenesis, and hold great promise to become innovative drugs in the future.

Angioarrestin is another angiogenesis-inhibiting protein that endogenously produced by the tumor. Angioarrestin is downregulated in many types of tumor tissues and exhibited strong anti-angiogenic ability both *in vitro* and *in vivo* (Dhanabal et al., 2005). Angioarrestin is involved in the migration, adhesion and tube formation abilities of endothelial cells. Mechanistically, it has been reported to inhibit VEGF/bFGF-induced endothelial cell proliferation in a dose-dependent manner (Dhanabal et al., 2005). Endostatin is also an anti-angiogenic factor and has a potent activity on the migration, survival, proliferation and apoptosis of endothelial cells (Poluzzi et al., 2016). A genome-wide expression profiling demonstrated that about 12% of human genes are regulated by Endostatin in human endothelial cells (Abdollahi et al., 2004). Research indicated that Endostatin participates in MMPs, FAK/Ras/p38-MAPK/ERK, HIF-1α/VEGFA and Wnt signal (Dhanabal et al., 2005). Elevated Endostatin serum level may be a prognostic indicator for EOC patients. Either RGD-P125A-Endostatin-Fc fusion proteins alone or in combination with bevacizumab can effectively inhibit angiogenesis and OC progression (Jing et al., 2011).

4 Molecular targets and agents against angiogenesis

Bevacizumab has been approved in stage III or IV EOC patients after primary surgical resection, for either combining with carboplatin and paclitaxel, or maintaining as monotherapy (Table 1). In addition to bevacizumab, several other anti-angiogenic agents have also been tested clinical studies in OC (Table 2).

4.1 Bevacizumab

Bevacizumab (Avastin®) is a humanized anti-VEGF monoclonal antibody. It was the first target medicine approved in 2014 and used for platinum-resistant OC in combination with chemotherapy (Monk et al., 2016a). It exerts therapeutic efficiency by blocking VEGF-A to bind VEGFR, destroying existing vessels, disturbing neovascularization, and releasing intratumor pressure, etc. (Reinthaller, 2016). Studies have shown that blocking VEGF signaling not only leads to the depletion of tumor vascularization, but also promotes the normalization of the remaining blood vessels in morphology and function. In addition, the pericyte coverage of remaining vessels increased to about 75% after bevacizumab treatment, compared with 7% in the placebo group (Arjaans et al., 2013).

The application of bevacizumab in OC was initially used as monotherapy in pretreated patients. The GOG-0170D trial evaluated the benefit of bevacizumab single agent in 62 recurrent OC patients that had been treated with up to two prior lines of chemotherapy. Bevacizumab was well tolerated. The ORR was 21%. PFS and overall survival (OS) was 4.7 and 17 months respectively (Burger et al., 2007). Other phase II studies evaluated the benefit of bevacizumab in OC patients that had experienced disease progression after multiple chemotherapeutic regimens (Monk et al., 2006; Cannistra et al., 2007). Single-agent bevacizumab showed modest benefits, but less than combination therapy (Fuh et al., 2015).

TABLE 2 Summary of phase III studies of antiangiogenic agents in OC.

Clinical trials	Disease condition	Patient number	Drug	Treatment arm	Clinical outcomes		References
					PFS	OS	
OVAR 12	Newly diagnosed advanced OC	1366	Nintedanib	CBP + PTX + PBO	16.6	/	du Bois et al. (2016)
				CBP + PTX + Nintedanib	17.2 (HR, 0.84; 95% CI, 0.72 to 0.98]; p = 0.024)	/	
OVAR 16	Advanced OC	940	Pazopanib	PBO	12.3	/	du Bois et al. (2014)
				Pazopanib	17.9 (HR, 0.77; 95% CI, 0.64 to 0.91; p = 0.0021)	/	
ICON6	PT-sensitive recurrent OC	456	Cediranib	PBO + CBP, PBO maintenance	8.7	19.9	Ledermann et al. (2016), Ledermann et al. (2021)
				Cediranib + CBP, PBO maintenance	10.1 (HR, 0.67; 95% CI, 0.53-0.87; p = 0.0022)	/	
				Cediranib + CBP, Cediranib maintenance	11.1 (HR 0.57, 0.44-0.72, p < 0.00001)	27.3(HR, 0.85; 95% CI, 0.66-1.10; p = 0.21)	
NRG-GY004	Recurrent Pt-sensitive OC	565	Cediranib	chemotherapy	10.3	/	Liu et al. (2022)
				Olaparib	8.2 (HR, 1.2; 95%CI, 0.93-1.5)	/	
				Olaparib + Cediranib	10.4 (HR, 0.856; 95% CI, 0.66-1.10; p = 0.077)	/	
TRINOVA-1	Recurrent OC	919	Trebananib	Weekly PTX + PBO	5.4	18.3	Monk et al. (2016b), Vergote et al. (2019a)
				Weekly PTX + Trebananib	7.2 (HR, 0.66; 95%CI, 0.57-0.77; p < 0.0001)	19.3 (HR, 0.95; 95% CI, 0.81-1.11; p = 0.52)	
TRINOVA-2	Recurrent OC	223	Trebananib	PLD + PBO	7.2	17	Monk et al. (2014)
				PLD + Trebananib	7.6 (HR, 0.92; 95%CI, 0.68-1.24; p = 0.57)	19.4(HR, 0.94; 95%CI, 0.64-1.39; p = 0.76)	
TRINOVA-3	Advanced OC	1015	Trebananib	PBO + PTX + CBP	15.0	43.6	Marth et al. (2017)
				Trebananib + PTX + CBP	15.9 (HR, 0.93; 95% CI, 0.79-1.09; p = 0.36)	46.6(HR, 0.99; 95%CI, 0.79-1.25; p = 0.94)	
AGO-OVAR16	Stage II-IV EOC	940	Pazopanib	PBO maintenance	17.9	18.3	du Bois et al. (2014), Vergote et al. (2019b)
				Pazopanib maintenance	12.3 (HR, 0.77; 95% CI, 0.64-0.91; p = 0.0021)	59.1 (HR, 0.960; 95% CI: 0.805-1.145; p = 0.6431)	

OC, ovarian cancer; CBP, carboplatin; PTX, paclitaxel; PBO, placebo; HR, hazard ratio; CI, confidence interval; PLD, pegylated liposomal doxorubicin.

In 2011, the outcomes of two prominent phase III trials, ICON7 and GOG-0218, were published simultaneously, which were the first attempt to add bevacizumab to standard adjuvant chemotherapy as a frontline maintenance of OC. In GOG-0218, incorporation of bevacizumab within 10 months after carboplatin (CBP) and paclitaxel (TAXOL) chemotherapy has been shown to prolong the PFS for approximately 4 months in 1873 newly diagnosed advanced EOC patients (medium PFS, 14.1 vs. 10.3 months; 95% CI, 0.625-0.824; p < 0.001) (Burger et al., 2011). As for the ICON7 trial, bevacizumab combination therapy improved the PFS to 24.1 months in 1528 OC patients compared with CBP and TAXOL chemotherapy alone (22.4 months). The benefit was more obvious in patients with high progression risk

(PFS, 18.1 vs. 14.5 months; OS, 36.6 vs. 28.2 months) (Perren et al., 2011).

Platinum (Pt) resistance is a serious problem that hinders the therapeutic benefit of OC. Factors leading to Pt resistance are various, including angiogenesis, hypoxia, immune infiltration, and abnormal regulation of breast cancer susceptibility gene (BRCA), ATP binding cassette subfamily B member 1 (ABCB1) and cyclin E1 (CCNE1), etc. (Pennington and Swisher, 2012; Patch et al., 2015). Anti-angiogenic drugs exert a satisfying therapeutic benefit in Pt-resistant OC (Haunschild and Tewari, 2020). An open-label, randomized, phase III trial, AURELIA, demonstrated that bevacizumab incorporated with standard-of-care chemotherapy (TAXOL or topotecan (TPT) or pegylated liposomal doxorubicin

(PLD)) improved the PFS of Pt-resistant OC patients compared to chemotherapy alone (medium PFS, 6.7 vs. 3.4 months; HR, 0.42; 95%CI, 0.32-0.53) (Pujade-Lauraine et al., 2012). The subsequent analysis indicated combining with TAXOL was the most effective regimen (Poveda et al., 2015). Based on the AURELIA trial, the Food and Drug Administration (FDA) had approved bevacizumab plus weekly TAXOL, PLD, or TPT for patients with Pt-resistant OC (Pujade-Lauraine et al., 2014).

Bevacizumab combination therapy has also been evaluated in Pt-sensitive OC patients. A phase III trial, OCEANS, was performed in 484 patients with Pt-sensitive recurrent OC. The medium PFS was 12.4 months in the bevacizumab/gemcitabine/ CBP and 8.4 months in chemotherapy only group (HR, 0.48; 95% CI, 0.39-0.61) (Aghajanian et al., 2012). GOG-0213 trail evaluated the efficiency of combining bevacizumab with CBP and TAXOL. The median OS (49.6 vs. 37.3 months; HR, 0.823; 95% CI, 0.680-0.996; p = 0.0447) was improved in the bevacizumab group compared with chemotherapy only group (Coleman et al., 2017). Both therapy regimens in the above two trials have been approved by FDA for this usage. The MITO16b phase III trial was performed in 406 Pt-sensitive recurrent OC patients and compared the PFS benefits of bevacizumab combination with standard chemotherapy. Continuing bevacizumab combination therapy significantly prolonged the PFS (medium PFS, 11.8 vs. 8.8 months; HR, 0.51; 95% CI, 0.41-0.65; p < 0.0001) (Pignata et al., 2021).

Taken together, the vast majority of clinical studies suggested that bevacizumab significantly extended PFS in OC patients by several months, while the improvement in OS was not obvious. Up to now, mechanism studies focused on bevacizumab resistance have achieved certain progress, and several multitargeted antiangiogenic agents have been tested in clinical studies. However, no effective clinical methods has been applied to overcome bevacizumab resistance. In addition, there is growing evidence that the combination of bevacizumab with immunotherapy or PARP inhibitors may improve the therapeutic outcome of OC patients. Further attempts of novel combination therapies hold promising prospects and are one of the major trends in antiangiogenic therapy.

4.2 Pazopanib

Pazopanib, an oral tyrosine kinase inhibitor (TKI) of multiple targets, inhibits VEGFR, PDGFR-α and -β, FGFR-1 and -3 and c-Kit. Pazopanib treatment significantly reduced the tumor microvessel density and pericyte coverage in the mouse orthotopic OC model (Merritt et al., 2010). Pazopanib has been approved by the FDA and European Medicines Agency (EMA) for soft tissue sarcoma as well as advanced renal carcinoma therapy. Although not yet approved in OC, many phase II and III clinical trials have evaluated the potential role of pazopanib in the therapy of OC (Plummer et al., 2013; du Bois et al., 2012; Davidson and Secord, 2014). The AGO-OVAR16 study assessed the potential role of pazopanib maintenance therapy in 940 OC patients without progressive disease after receiving the first-line chemotherapy. Pazopanib, when given as maintenance therapy, yielded a meaningful improvement in median PFS (17.9 v 12.3 months; HR, 0.77; 95% CI, 0.64-0.91; p = 0.0021), albeit with

added adverse event-induced therapy interruption (33.3% vs. 5.6%). However, no significant benefit of OS was identified (du Bois et al., 2014).

So far, there have been few phase III clinical trials of pazopanib in OC treatment, but it has already exhibited clear clinical benefit and future studies will gradually establish its value in OC. In addition, the curative effect of pazopanib in bevacizumab-resistant patients remains undefined and requires further investigation. Importantly, it is more necessary to discover valid predictive biomarkers to avoid potential toxicity and identify patients who are more likely to benefit from pazopanib treatment. A previous study showed that [^{18}F] Fluciclatide-PET uptake parameters may predict clinical outcomes of pazopanib treatment in patients with platinum-resistant/refractory OC, but studies in larger sample size are still needed for validation (Sharma et al., 2020). Besides, soluble VEGFR-2 and IL-8 have been revealed to be potential predict biomarkers in predict the therapeutic efficiency of pazopanib (Davidson and Secord, 2014). In summary, though the application of pazopanib in OC is still being explored and debated, the results of combination studies and further phase III studies will hopefully provide a rational foundation for the optimal role of pazopanib in OC treatment.

4.3 Nintedanib

Nintedanib (BIBF 1120) is an orally available, multitargeted antiangiogenic agents that approved for idiopathic pulmonary fibrosis treatment by FDA in 2014. Nintedanib competitively inhibits RTK (including VEGFR, FGFR, PDGFR-α and -β and FLT3 kinases) as well as non-RTK (including lymphocyte-specific protein tyrosine kinase (Lck), tyrosine-protein kinase Lyn (Lyn) and proto-oncogene tyrosine-protein kinase Src (Src)) (Cortez et al., 2018). Dynamic MRI assessments indicated that nintedanib treatment led to significant reduction of blood flow in about 55% OC patients. It also promotes the vascular normalization and regression of tumor in pre-clinical models (Khalique and Banerjee, 2017). A phase II trial investigated the efficacy of nintedanib maintenance therapy after chemotherapy for relapsed OC. 83 patients were included in this study. 36 weeks PFS rate was improved to some extent, but no statistical significance (16.3% and 5.0%; HR, 0.65; 95% CI, 0.42-1.02; p = 0.06) (Ledermann et al., 2011). A recent phase II study assessed the benefit and tolerance of combining nintedanib with oral cyclophosphamide in 117 relapsed OC. The median OS in nintedanib and placebo group were 6.8 and 6.4 months respectively (HR, 1.08; 95% CI, 0.72-1.62; p = 0.72), and the 6-month PFS rates were 29.6% and 22.8%, respectively (p = 0.57). No meaningful improvement was observed when nintedanib was added to oral cyclophosphamide (Hall et al., 2020). Another phase II trial investigated whether nintedanib is effective in bevacizumab-resistant recurrent EOC. According to research findings, nintedanib monotherapy was tolerable and showed minimal efficiency in bevacizumab-resistant EOC patients (Secord et al., 2019). In the AGO-OVAR 12 phase III clinical trial, nintedanib combined with CBP and TAXOL had a modest efficacy in patients with FIGO IIB-IV OC (PFS, 17.2 vs. 16.6 months; HR, 0.84; 95%CI, 0.72-0.98; p = 0.024), but was also accompanied by

more gastrointestinal adverse events (Secord et al., 2019). The follow-up study continually reported no significant different in OS (62.0 vs. 62.8 months; HR, 0.99; 95% CI, 0.83-1.17; $p = 0.86$). The updated PFS difference was in line with the primary report (17.6 vs. 16.6 months; HR, 0.86; 95% CI, 0.75-0.98; $p = 0.029$) favoring nintedanib (Ray-Coquard et al., 2020).

Based on the limited prognostic benefit and non-negligible toxic effects reported in clinical trials to date, it is not expected to approve nintedanib for OC therapy. Nevertheless, these studies were informative and suggested the demand of patient selection and tolerated therapy. Nintedanib may have a role in recurrent OC. The ongoing clinical trials and predictive biomarker identification will help to determine this (Khalique and Banerjee, 2017).

4.4 Cediranib

Cediranib (AZD2171) is an oral TKI that inhibits VEGFR-1, VEGFR-2, VEGFR-3 and c-kit. In preclinical models of OC, cediranib treatment led to significantly reduction of tumor vascular density and vessel regression (Ruscito et al., 2016). A phase II trial reported a significant activity of cediranib in Pt-sensitive instead of Pt-resistant patients with recurrent OC (Hirte et al., 2015). The ICON6 phase III study further evaluated whether orally given cediranib plus Pt-based chemotherapy and continued as maintenance therapy provided PFS benefits in 456 Pt-sensitive OC patients. A significantly prolonged PFS was found in the cediranib combination and maintenance group (11.0 vs. 8.7 months; HR, 0.56; 95%CI, 0.44-0.72; $p < 0.0001$), accompanied by added toxic effects (Ledermann et al., 2016). However, no significant difference was found in the extended follow-up of OS results (OS, 27.3 vs. 19.9 months; HR, 0.86; 95% CI, 0.67-1.11; $p = 0.24$). Even so, the result of OS was underpowered due to several limitations like drug supply restriction and the non-proportionality of the survival curves, and further research should be undertaken (Ledermann et al., 2021).

Olaparib is a poly (ADP-ribose) polymerase (PARP) inhibitor that applied for OC therapy, but widespread resistance greatly hindered its clinical benefit. Better strategies and potential combination administrations are in urgent need to overcome the resistance. A phase II study investigated whether combining cediranib with olaparib could improve the PFS of patients with Pt-sensitive recurrent OC. Median PFS were 9.0 and 17.7 months in the olaparib monotherapy and cediranib plus olaparib group, respectively (HR, 0.42; 95% CI, 0.23-0.76; $p = 0.005$) (Liu et al., 2014). The follow-up study characterized OS and updated PFS outcomes. The updated PFS result was consistant (16.5 vs. 8.2 months; HR, 0.50; $p = 0.007$). The OS showed no statistical difference (44.2 vs. 33.3 months, HR, 0.64; $p = 0.11$). Notably, for the subgroup of patients that did not carry deleterious germline BRCA1/2 mutation, both OS (37.8 vs. 23.0 months; $p = 0.047$) and PFS (23.7 vs. 5.7 months; $p = 0.002$) were significantly improved by adding cediranib to olaparib, suggesting that the further study should designed on the basis of BRCA status (Liu et al., 2019a). The EVOLVE trail evaluated the benefit of cediranib plus olaparib when confronted with PARPi treatment resistance. The cediranib–olaparib combination was tolerable and the efficiency was various in patients with different resistance mechanism.

Individuals with upregulated ABCB1 and/or abnormal homologous recombination repair activity should probably be considered for other treatment options (Lheureux et al., 2020).

Several clinical trials have compared the clinical benefit of olaparib and/or cediranib with that of chemotherapy. A phase II study reported no PFS improvement was identified in cediranib plus olaparib *versus* chemotherapy in unscreened, heavily pretreated Pt-resistant OC patients (Colombo et al., 2022). Consistent findings were reported in NRG-GY004 phase III trial which performed in 565 recurrent Pt-sensitive OC patients. The median PFS were 10.3, 8.2, and 10.4 months in the chemotherapy, olaparib, and olaparib + cediranib groups, respectively. Combining olaparib with cediranib showed no more PFS benefit than chemotherapy (HR, 0.86; 95%CI, 0.66-1.10; $p = 0.077$). However, for the subgroup with germline BRCA mutation, significant clinical activity was observed both in olaparib alone or in combination with cediranib (Liu et al., 2022). The above studies suggested the critical role of valid genetic biomarkers in screening susceptible individuals and predicting the efficacy of cediranib.

In addition to the clinical trials described above, numerous studies are ongoing. A phase II trial aims to compare the benefit and tolerability of olaparib plus cediranib *versus* olaparib monotherapy in Pt-resistant OC (Mansouri et al., 2021). The ICON 9 phase III randomized study assessed the maintenance treatment of olaparib plus cediranib in relapsed Pt-sensitive OC. The trail is ongoing and the primary results are expected in 2024 (Elyashiv et al., 2021).

Although not yet approved by FDA, the landscape of cediranib in OC therapy appears promising. Cediranib exhibited encouraging results when combined with chemotherapy or olaparib. Nevertheless, many key questions remain to be addressed in the future, such as which clinical regimen provides the best benefit; biomarkers to identify patients with higher probability to benefit are urgently needed; the unclear role of cediranib in bevacizumab resistant patients. In the near future, the outcomes of phase II/III clinical trials will help to better establish the role of cediranib in OC treatment.

4.5 Sunitinib

Sunitinib is a multiple-target TKI that inhibits PDGFR, VEGFR, Flt3, and c-Kit. The FDA granted sunitinib for the treatment of advanced kidney cancer and partial gastrointestinal stromal and neuroendocrine tumors, while its application in OC remains in clinical trials (Leone Roberti Maggiore et al., 2013). In a xenograft mouse model, sunitinib therapy significantly reduced the tumor microvascular density, and also inhibited tumor growth and peritoneal metastasis (Bauerschlag et al., 2010). The AGO-OVAR2.11 phase II trial showed that sunitinib exhibited feasibly and moderate activity in patients with recurrent Pt-resistant OC, and the non-continuous therapy schedule showed better superiority compared with continuous treatment (Baumann et al., 2012). Attached to this, the predictive value of VEGF, VEGFR-3 and Ang-2 was evaluated. Decreased serum Ang-2 levels were found to associate with longer PFS (8.4 vs. 2.7 months). However, the difference is not significant ($p = 0.0896$) and further research is needed (Bauerschlag et al., 2013). Another phase II trial also

reported a modest activity of 50 mg intermittent regimen of sunitinib monotherapy in recurrent Pt-sensitive OC (Biagi et al., 2011). The dosage regimen may be a vital consideration in further studies of sunitinib in OC (Biagi et al., 2011). Susana M Campos et al. demonstrated a modest response rate (8.3%) of sunitinib in recurrent OC in a phase II trial (Bodnar et al., 2011). Another phase II evaluation of sunitinib also reported limited effectiveness in persistent or recurrent clear cell OC (Campos et al., 2013).

Based on the above studies, sunitinib exhibited moderate antitumor activity together with acceptable toxicity in the OC treatment. However, given that serious adverse events have been reported (Abdollahi et al., 2004; Dhanabal et al., 2005; Poluzzi et al., 2016; Jeanne et al., 2021), more insight understanding of toxicity, elucidating the specific toxic mechanisms, and determination of optimal administration dosage are required in the future. It is also important to identify predictable biomarkers to guide individualized medication. In addition, current clinical studies have not attempted the combination therapy of sunitinib with cytotoxic agents, which may significantly improve therapeutic outcome and control toxicity.

4.6 Sorafenib

Sorafenib targets multiple kinases including VEGFR, PDGFR, Raf, MEK and ERK. It has been approved for renal cell carcinoma, hepatocellular carcinoma and differentiated thyroid carcinoma by FDA. A phase II trial indicated sorafenib provided no adequate objective response when given as a third-line therapy in EOC (Chan et al., 2018). In another phase II study, sorafenib was assessed as maintenance therapy in 246 EOC patients that had achieved a complete response in first-line therapy. Compared with placebo group, no obvious PFS improvement was achieved in sorafenib 400 mg BID treatment (median PFS, 12.7 vs. 15.7 months; HR, 1.09; 95% CI, 0.72-1.63). Adverse effects induced discontinuations were more frequently in the sorafenib group (37.4% vs. 6.5%) (Herzog et al., 2013).

A phase II study evaluated the efficiency and tolerability of sorafenib plus CBP/TAXOL in EOC. This study was terminated after patients occurred life-threatening toxicities (Erber et al., 2004), suggesting that sorafenib plus CBP/TAXOL cannot be recommend as neoadjuvant treatment in patients with primary advanced OC (Polcher et al., 2010). This result was consistent with another randomized phase II trial, which reported that the combination of sorafenib to standard TAXOL/CBP provided no benefit but more serious toxicity in patients with advanced EOC (Hainsworth et al., 2015). Another randomized phase II trial compared the benefit of sorafenib monotherapy, or combined with CBP/TAXOL in Pt-sensitive EOC. The median PFS of sorafenib monotherapy and combination group were 5.6 and 16.8 months, respectively ($p = 0.012$), while difference was not observed in OS (25.6 vs. 25.9 months, $p = 0.974$) (Schwandt et al., 2014).

The combination of sorafenib with TPT was evaluated in Pt-resistant or -refractory OC. Sorafenib combination significantly prolonged PFS *versus* placebo (6.7 vs. 4.4 months; HR, 0.60; 95% CI, 0.43-0.83; $p = 0.0018$) (Chekerov et al., 2018). However, another phase II trial reported conflicting results, pointing a significant toxicity but modest clinical efficacy in Pt-resistant OC patients

(Ramasubbaiah et al., 2011). The combination of sorafenib with TPT still required further investigation.

Continuous daily sorafenib combined with bevacizumab caused moderate toxicity in OC patients, whereas intermittent sorafenib plus bevacizumab had promising clinical efficacy with few side effects (Lee et al., 2010). A phase II trial reported potential clinical activity of bevacizumab plus sorafenib in bevacizumab-naive, Pt-resistant OC, whereas no activity was observed in the bevacizumab-prior group (Lee et al., 2020).

According to previous phase II studies, sorafenib showed limited clinical benefit in advanced relapsing OC when given as single agent or combination therapy. Sorafenib in combination with cytotoxic agents also provided less benefit, and severe adverse events were reported. Nonetheless, sorafenib combined with bevacizumab exhibited encouraging efficacy in advanced OC patients, but the cumulative toxicity also posed an ongoing therapeutic challenge. Future research should therefore focus on developing reliable predictive biomarkers to guide patient selection, optimal combination, order and dose of administration, so as to maximize clinical benefit and minimizing toxicity.

4.7 Trebananib

Trebananib (ANG386) targets and blocks the binding of ANGPT to their receptor Tie2. A study used photoacoustic tomography to detect changes in tumor vascularization in response to trebananib treatment. It showed that trebananib induced obvious vessel regression and reduced vessel density. It is worth noting that trebananib treatment did not completely block angiogenesis but promoted more stable and less permeable residual vascular structures (Bohndiek et al., 2015). The TRINOVA-1 trial assessed the benefit of trebananib plus TAXOL in 919 recurrent EOC patients. The median PFS was meaningfully improved in the trebananib plus TAXOL arm compared with placebo arm (7.2 vs. 5.4 months; HR, 0.66; 95% CI, 0.57-0.77; $p < 0.0001$). The adverse events were 125 (28%) and 159 (34%) in the placebo monotherapy group and trebananib combination group, respectively (Monk et al., 2014). The ENGOT-ov-6/TRINOVA-2 study investigated the potential benefit of combining trebananib with PLD in 223 recurrent EOC patients. The objective response rate (ORR, 46% vs. 21%) and duration of response (DOR, 7.4 vs. 3.9 months) were improved, while the median PFS had no obvious improvement (7.6 vs. 7.2 months; HR, 0.92; 95% CI, 0.68-1.24) (Marth et al., 2017). The TRINOVA-3 trail assessed the combination of trebananib with paclitaxel and carboplatin in 1015 advanced OC patients. However, no significant improvement was observed in PFS compared with placebo group (15.9 vs. 15.0 months; HR, 0.93; 95%CI, 0.79-1.09; $p = 0.36$). No new safety signals were produced, either Vergote et al. (2019a).

To summarize, the TRINOVA-1 trail showed that trebananib significantly improved PFS in recurrent OC compared with paclitaxel alone. The TRINOVA-2 trail compared paclitaxel plus placebo or paclitaxel plus trebananib in recurrent OC, and the PFS was modestly improved but no significant difference. The TRINOVA-3 trail indicated that trebananib + carboplatin + paclitaxel failed to improve PFS of advanced OC patients compared with placebo group. Based on the available studies and
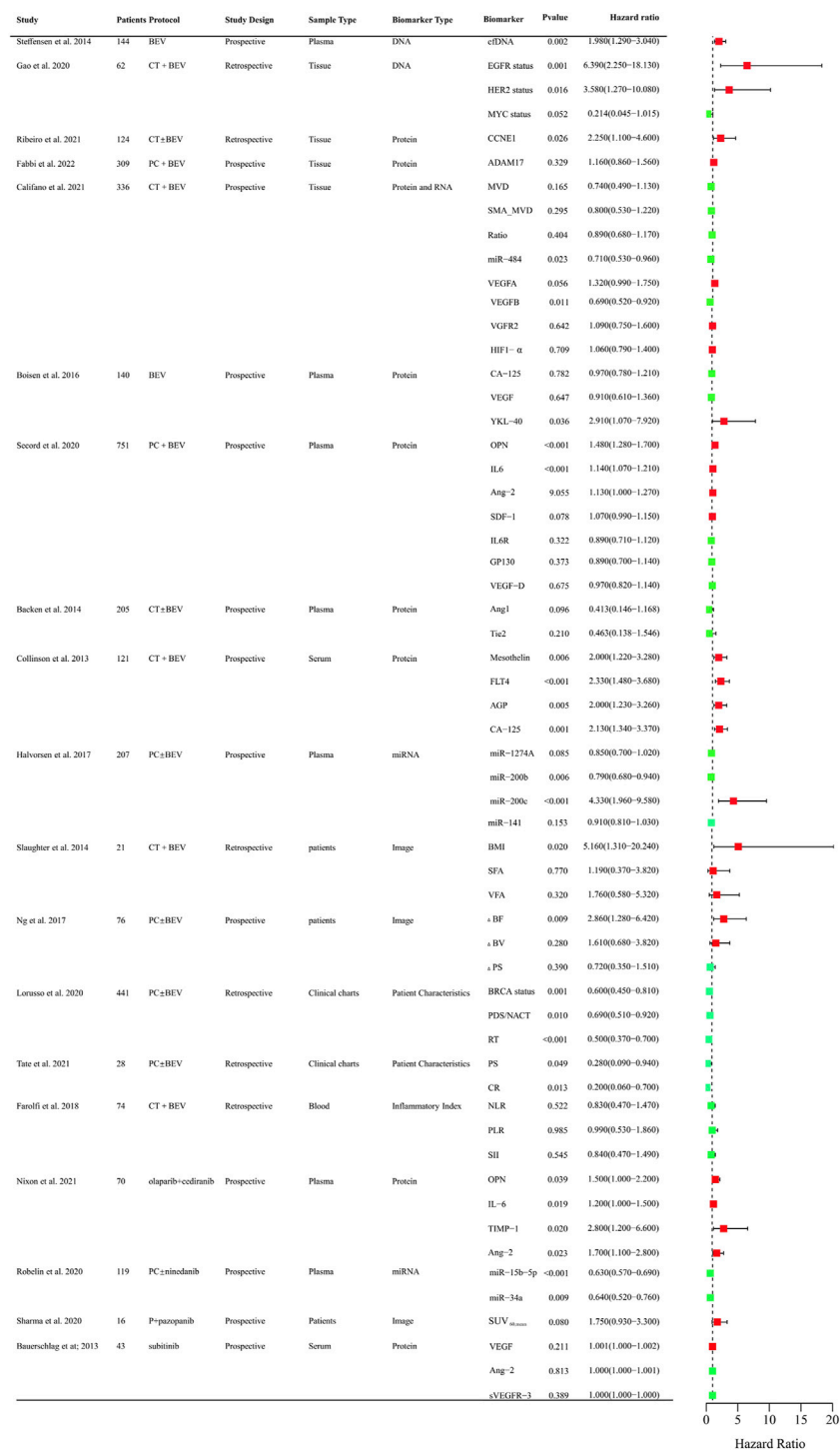
FIGURE 2
Clinical trials assessing biomarkers in relation to PFS of anti-angiogenic drugs in OC. BEV: Bevacizumab; CT: Chemotherapy; PC:TAXOL and CBP; DNA, Deoxyribonucleic Acid; RNA, Ribonucleic Acid; cfDNA, cell-free DNA; EGFR, Epidermal Growth Factor Receptor; HER2, Human Epidermal GrowthFactor Receptor 2; MYC, MYC Proto-Oncogene; CCNE1, Cyclin E1; ADAM17, a disintegrin and metalloprotease 17; MVD, microvessel density; SMA_MVD: Alfa-Smooth Muscle Actin + microvessel density; Ratio, α-SMA + MVD/MVD ratio; miRNA, microRNA; VEGFA, vascular endothelial growth factor A; VEGFB, vascular endothelial growth factor B; HIF-a, Hypoxia-Inducible Factor 1-alpha; OPN, osteopontin; SDF-1, stromal cell−derived factor-1; IL6R, IL6 receptor; FLT4, fms-like tyrosine kinase-4; AGP, a 1 -acid glycoprotein; BMI, body mass index; VFA, visceral fat area; SFA, subcutaneous fat area; ΔBF, change of Tumor Blood Flow; ΔBV, change of Tumor Blood Volume; ΔPS, change of Vessel Permeability Surface Product; PDS/NACT, Primary Debulking Surgery/Neoadjuvant chemotherapy; RT, Residual Tumor; PS, Performance Status; CR, Completeness of resection; NLR, neutrophil-to-lymphocyte ratio; PLR, platelet-to-lymphocyte ratio; SII, systemic immune inflammation index.

FIGURE 3
Clinical trials assessing biomarkers in relation to OS of anti-angiogenic drugs in OC. BEV: Bevacizumab; CT: Chemotherapy; PC:TAXOL and CBP; DNA, Deoxyribonucleic Acid; RNA, Ribonucleic Acid; cfDNA, cell-free DNA; ADAM17, a disintegrin and metalloprotease 17; MVD, microvessel density; SMA_MVD: Alfa-Smooth Muscle Actin + microvessel density; Ratio, α-SMA + MVD/MVD ratio; miRNA, microRNA; VEGFA, vascular endothelial growth factor A; VEGFB, vascular endothelial growth factor B; HIF-a, Hypoxia-Inducible Factor 1-alpha; OPN, osteopontin; SDF-1, stromal cell−derived factor-1; IL6R, IL6 receptor; FLT4, fms-like tyrosine kinase-4; AGP, a 1 -acid glycoprotein; BMI, body mass index; VFA, visceral fat area; SFA, subcutaneous fat area; ΔBF, change of Tumor Blood Flow; ΔBV, change of Tumor Blood Volume; ΔPS, change of Vessel Permeability Surface Product; PDS/NACT, Primary Debulking Surgery/Neoadjuvant chemotherapy; RT, Residual Tumor; PS, Performance Status; CR, Completeness of resection; NLR, neutrophil-to-lymphocyte ratio; PLR, platelet-to-lymphocyte ratio; SII, systemic immune inflammation index; SFD, subcutaneous fat density; VFD, visceral fat density.

in the absence of effective biomarkers, trebananib possessed an adequate safety profile, but its efficacy in the selected OC population was not significant.

5 Biomarkers of anti-angiogenic therapy in OC

Anti-angiogenic agents have demonstrated significant efficacy benefits in OC as single-agent or combination therapy. However, not all patients can benefit from these agents. It is crucial to identify clinical biomarkers to select sensitive population and monitor curative effect of anti-angiogenic drugs. So far, numerous studies focused on the research in OC and provided evidence indicating several predictive values for clinical, radiological, molecular, and gene profiling markers (Supplementary Table S1). The biomarkers related to PFS and OS that assessed in clinical trials were systematically summarized in Figures 2, 3, respectively.

Circulating cell-free DNA was shown to be an independent prognostic importance in multi-resistant epithelial OC patients

treated with bevacizumab (Steffensen et al., 2014). Epidermal growth factor receptor (EGFR), BRCA, and human epidermal growth factor receptor-2 (HER2) mutational status might be predictors for PFS of chemotherapy and bevacizumab combination therapy in retrospective studies (Lorusso et al., 2020; Gao et al., 2021). The protein expression of angiogenesis-related genes such as CCNE1, a disintegrin and metalloprotease 17 (ADAM17), mevalonate diphosphate decarboxylase (MVD), SMA_MVD, VEGFA, VEGFB, VGFR2, HIF-1α in tumor tissues was explored (Fabbi et al., 2022). Only CCNE1 and VEGFB were proved to be predictive markers for the efficacy of bevacizumab (Califano et al., 2021; Ribeiro et al., 2021). Circulating plasma or serum proteomic biomarkers are also assessed to their predictive value for PFS and OS. Chitinase three like 1 (YKL-40), osteopontin (OPN), IL-6, Ang-2, Mesothelin (MSLN), fms-like tyrosine kinase-4 (FLT4), Alpha-1 acid glycoprotein (AGP), and cancer antigen 125 (CA-125) might be predictive of therapeutic benefit from bevacizumab (Collinson et al., 2013; Backen et al., 2014; Boisen et al., 2016; Alvarez Secord et al., 2020). OPN, IL-6, TIMP-1, Ang-2 were also correlated with PFS in OC patients treated with olaparib + cediranib (Nixon et al., 2021). VEGR, Ang-2, VEGFR-3 were explored for the predictive value for PFS in Pt resistant or refractory OC patients with the treatment of sunitinib. However, there was no significance (Bauerschlag et al., 2013). Circulating microRNAs were also investigated to identify candidate predictive biomarkers for anti-angiogenic drugs in OC. The level of miR-200b, and miR-200c might be predictive of the effect of treatment with bevacizumab (Halvorsen et al., 2017). Low expression of miR-34a-5p and miR-93-5p were correlated with PFS and OS improvements in OC patients with the treatment of chemotherarpy ± nintedanib (Robelin et al., 2020). As obesity was associated with the level of VEGF, the main target of bevacizumab, adiposity was assessed. The measurements of adiposity such as subcutaneous fat area or density and visceral fat density are likely to be useful biomarkers for PFS or OS (Halvorsen et al., 2017; Buechel et al., 2021). CT perfusion biomarkers such as blood flow may offer early prognostic evidence for patients with newly diagnosed OC and received chemotherapy ± bevacizumab therapy (Ng et al., 2017). Baseline $SUV_{60,mean}$ (mean standardized uptake value at 60 min) was negatively correlated with PFS of patlinum-resistant/refractory OC patients received pazopanib and TAXOL combination therapy, which indicated [^{18}F] Fluciclatide-PET uptake parameters may be a predictor of clinical outcome in patients treated with pazopanib (Sharma et al., 2020). Inflammatory Indexes were prognostic markers for OC patients treated with chemotherapy, but not with chemotherapy and bevacizumab (Farolfi et al., 2018). These findings need to be validated in further different races and larger sample sizes. It is still urgent to identify predictive biomarkers in treating OC patients with anti-angiogenic agents.

6 Models of anti-angiogenic therapy in OC

Angiogenesis is an outcome of complex signaling involving a plethora of cells, their cellular signal transduction, activation, proliferation, differentiation, as well as their intercellular communication. Zhang et al. provided a comprehensive review of systems biology computational models of angiogenesis at the pathway-, cell-, tissue-, and whole body-levels, which advanced our understanding of signaling in angiogenesis and delivered new translational insights for human diseases (Zhang et al., 2022). An integrated model of VEGF-Ang-2 cooperation that accurately recapitulates molecular events constituting the angiogenic switch was proposed in ovarian cancer (Zhang et al., 2003). Adhikarla et al. established a computational model to simulate tumor-specific oxygenation changes based on the molecular image data, which incorporating therapeutic effects might serve as a powerful tool for analyzing tumor response to anti-angiogenic therapies (Adhikarla and Jeraj, 2016). Models combining biomarkers with other risk factors are also constructed to predict treatment outcomes of anti-angiogenic agents in OC. Previs et al. found that prior number of chemotherapy regimens, treatment-free interval (TFI), Pt sensitivity, and the presence of ascites were significant predictors of 5-year OS in 312 women with recurrent ovarian cancer treated with bevacizumab and chemotherapy. Based on the multivariate analysis, a nomogram for OS was constructed, which could provide insight to those women who will benefit the most while avoiding excessive costs and potentially catastrophic toxicities that would ultimately require discontinuation of therapy (Previs et al., 2014). Wang et al. reported three quantitative adiposity-related image feature-based models (multiple linear, logistic and Cox proportional hazards regressions), which provide a useful and Supplementary Information that could yield higher discriminatory power than BMI in predicting the association between adiposity and clinical outcome of EOC patients (including PFS and OS) treated with maintenance bevacizumab-based chemotherapy (Wang et al., 2016). Sostelly. et al. constructed an OS model combining tumor kinetics metrics describing the change in tumor size over time in Pt-resistant OC (PROC) patients treated with chemotherapy and bevacizumab, which could effectively help to simulate and optimize future trials in PROC population (Sostelly and Mercier, 2019).

7 Mechanisms of therapy resistance and adverse reaction

Despite the ever-growing number of anti-angiogenic drugs applied in clinical practice, the survival benefits to date have been quite limited, which only temporarily inhibiting tumor development before drug resistance occurs.

In OC, the vast majority of patients have innate or acquired resistance to anti-angiogenic therapy and eventually recurrence (Ellis and Hicklin, 2008). Even a small proportion of patients could benefit from bevacizumab, the effective duration is relatively short (only 3–8 months with monotherapy). There are several explanations for the modest efficacy, like the adoption of alternative patterns of angiogenesis by the tumor and the development of resistance mechanisms. In case of the high expense, adverse reactions and modest clinical benefit of anti-angiogenic drugs, an insight knowledge of resistance mechanisms and the exploration of reliable predictive biomarkers are in urgent needs to provide a basis for prolonging survival and overcoming resistance (Jin et al., 2022).

Both intrinsic and acquired resistance are considered the major leading to the therapeutic failure of anti-angiogenic agents. The

most frequently proposed mechanism is the increase in tumor hypoxia levels caused by anti-angiogenic therapy. Anti-angiogenic agents aggravate intra-tumoral hypoxia and the abnormal upregulation of HIF-1α, this further stimulates the production of angiogenic factors like FGF, ANGPT2, and IL-8, eventually leading to therapy resistance and higher risk of disease progression (Casanovas et al., 2005; Huang et al., 2010; Rigamonti et al., 2014). HIF-1 may be a promising target to improve chemoradiotherapy sensitivity and patient prognosis, upregulation of which greatly enhanced tumor angiogenesis, malignant progression as well as apoptosis resistance. However, there are no clinical studies focused on HIF-1 protein inhibitors yet (Bhattarai et al., 2018). Secondly, when the VEGF/VEGFR pathway is inhibited, other VEGF -independent angiogenic mechanisms such as ANG1, ANGPT-2, FGF-2, IL-8, Dll4/Notch and miRNA46 will be compensatively upregulated, ultimately causing resistance to anti-VEGF drugs (Liu et al., 2021). Thirdly, the heterogeneity of tumor cells is an important endogenous resistance mechanism of anti-angiogenic therapy. Heterogeneity in tumor vasculature itself leads to the differential requirement for VEGF. Among the different types of the blood vessel, the first-formed mother vessels and glomeruloid microvascular proliferations have a high response to anti-VEGF therapy, while the "late" formed capillaries, vascular malformations, feeder arteries, and draining veins are relatively insensitive (Nagy and Dvorak, 2012). Therefore, individual differences, the proportion of vascular subtypes varies in diverse tumor tissues, different ratios of VEGF-dependent and -independent angiogenesis all contribute to resistance to anti-angiogenic agents. Fourth, long-term anti-angiogenic therapy would result in widespread vascular morphological alterations *via* the regulation of pro-angiogenic factors, and the remodeled neovascularization structure results in resistance to existing anti-angiogenic drugs (Huang et al., 2004).

8 Combining with immunotherapy

Combination therapy holds great promise in overcoming resistance and enhancing the antitumor efficacy of anti-angiogenic drugs. Immune checkpoint inhibitors (ICIs) exert anticancer effects by reactivating exhausted or dysfunctional T-cells (Mellman et al., 2011; Topalian et al., 2016). Monoclonal antibodies targeting cytotoxic T lymphocyte-associated protein 4 (CTLA-4), programmed cell death protein (PD-1) and its ligand PD-L1 are the most wildly used ICIs. However, ICIs alone showed limited efficacy in advanced or recurrent OC, with an overall response rate (ORR) between 5.9% and 22.2% (Brahmer et al., 2012; Hamanishi et al., 2015; Liu et al., 2019b; Disis et al., 2019; Varga et al., 2019; Nishio et al., 2020; Hamanishi et al., 2021). A phase III study (JAVELIN Ovarian 200) showed that neither monotherapy nor combination of avelumab with chemotherapy improved PFS or OS in patients with platinum-resistant or platinum-refractory OC (Pujade-Lauraine et al., 2021).

The antitumor effect of immunotherapy relies on the accumulation of immune effector cells in tumor microenvironment (TME). The anti-angiogenic therapy-mediated tumor vascular normalization effectively increases the infiltration of immune effector cells in TME and promotes the reprogramming of intrinsically immunosuppressive TME into immune supportive one (Fukumura et al., 2018). Anti-angiogenic therapy also ameliorates antitumor immunity by inhibiting multiple immunosuppressive properties of angiogenesis (Huinen et al., 2021). On the contrary, ICIs-activated immunity improves anti-angiogenic efficiency by reducing the expression of angiogenic factors and alleviating hypoxia conditions (Song et al., 2020).

Mechanism studies have explained the immunosuppressive function of VEGF. For example, VEGF inhibits the maturation and differentiation of dendritic cells through NF-kB signaling pathway (Oyama et al., 1998; Curiel et al., 2003; Huang et al., 2007). It also upregulates the expression of PD-L1, thus inhibiting the antigen presentation function of dendritic cells, and further the activation and expansion of T-cells (Alfaro et al., 2009). Besides, VEGF inhibits the differentiation of monocytes into dendritic cells, which can be reversed by bevacizumab or sorafenib treatment (Motz and Coukos, 2011). VEGF-activated VEGFR-2 stimulates the expression of immune checkpoint molecules including PD-1, T-cell immunoglobulin mucin receptor 3 (TIM-3), and cytotoxic T lymphocyte antigen 4 (CTLA-4) on CD8^{+} cells, resulting in the exhaustion of CD8^{+}cytotoxic T-cells (Burger et al., 2011; Perren et al., 2011; Fuh et al., 2015). Moreover, VEGF facilitates the proliferation of Tregs, thereby inhibiting anti-tumor immunity and promoting the occurrence and tumor development (Pennington and Swisher, 2012; Patch et al., 2015). In addition, targeting VEGF/VEGFR can also enhance immunotherapy efficacy by upregulating adhesion molecules and chemokines that are critical for the capture and transendothelial migration of T-cells (Georganaki et al., 2018; Khan and Kerbel, 2018). In view of the demonstrated antitumor efficacy, the FDA has approved the combination of anti-angiogenic agents with ICIs for certain malignancies.

Improved antitumor efficacy and prolonged survival were observed in many clinical trials following the combination of ICIs with anti-angiogenic agents (Song et al., 2020). The combination of bevacizumab and ICIs has been evaluated in phase I and II clinical trials, and the ORR was between 15% and 32%, which was significantly higher than ICIs alone (Langenkamp et al., 2015; Liu et al., 2019c; González-Martín et al., 2020; Moroney et al., 2020). A phase Ib study in platinum-resistant OC showed that the ORR of atezolizumab plus bevacizumab was 15% (Moroney et al., 2020). Another phase II study in relapsed EOC demonstrated that the combination of nivolumab with bevacizumab had an ORR of 40.0% (19.1%-64.0%) and 16.7% (95% CI 3.6%-41.4%) in the platinum-sensitive and -resistant group, respectively (Liu et al., 2019c). In addition, LEAP-005 phase II study evaluated the efficacy and safety of lenvatinib and pembrolizumab (a PD-1 immune checkpoint inhibitor) in patients with OC. The combination reached an ORR of 32% with manageable adverse events (González-Martín et al., 2020).

In conclusion, co-applied ICIs with anti-angiogenic agents has shown satisfactory efficacy in several malignancies. However, several obstacles still exist, like low tumor penetrance and increased adverse reactions. New agents, such as engineered antibodies, may help provide safer and more effective therapies (Anderson et al., 2022).

9 Conclusion and prospect

The limitations in the use of anti-angiogenic therapy may be in part related to two main factors. First, the exact mechanisms of angiogenesis

and therapeutic resistance remain unclear. Secondly, the abrogation of blood supply also limits the effective transport of antineoplastic agents inside the tumor, thus weaken their anti-tumor effect. The vast majority of clinical studies focused on bevacizumab suggested a meaningful improvement in PFS of recurrent OC patients, regardless of the Pt sensitivity. Similarly, anti-anti-angiogenic drugs targeting TKIs, including sorafenib, pazopanib, cediranib, and nintedanib also exhibited satisfactory improvements in the PFS of OC. However, only a few studies reported significant improvements in the OS of OC patients. In addition, bevacizumab exerted its effectiveness in only a small proportion of patients, while no reliable predictive biomarkers have been identified and validated for more precise treatment with bevacizumab. Regarding the obvious toxicity and high cost, biomarkers are urgent and crucial for selecting patients with a higher possibility to benefit from anti-angiogenic therapy.

Author contributions

CM and WG wrote the draft. CZ and SW designed the organizational framework. XW, YL, and YZ made critical revisions.

Funding

Conflict of interest

The authors declare that the research was conducted in the absence of any commercial or financial relationships that could be construed as a potential conflict of interest.

Publisher's note

All claims expressed in this article are solely those of the authors and do not necessarily represent those of their affiliated organizations, or those of the publisher, the editors and the reviewers. Any product that may be evaluated in this article, or claim that may be made by its manufacturer, is not guaranteed or endorsed by the publisher.

Supplementary material

The Supplementary Material for this article can be found online at: https://www.frontiersin.org/articles/10.3389/fphar.2023.1147717/full#supplementary-material

References

Abdollahi, A., Hahnfeldt, P., Maercker, C., Grone, H. J., Debus, J., Ansorge, W., et al. (2004). Endostatin's antiangiogenic signaling network. *Mol. Cell* 13, 649–663. doi:10.1016/s1097-2765(04)00102-9

Adhikarla, V., and Jeraj, R. (2016). An imaging-based computational model for simulating angiogenesis and tumour oxygenation dynamics. *Phys. Med. Biol.* 61, 3885–3902. doi:10.1088/0031-9155/61/10/3885

Agarwal, R., and Kaye, S. B. (2003). Ovarian cancer: Strategies for overcoming resistance to chemotherapy. *Nat. Rev. Cancer* 3, 502–516. doi:10.1038/nrc1123

Aghajanian, C., Blank, S. V., Goff, B. A., Judson, P. L., Teneriello, M. G., Husain, A., et al. (2012). Oceans: A randomized, double-blind, placebo-controlled phase III trial of chemotherapy with or without bevacizumab in patients with platinum-sensitive recurrent epithelial ovarian, primary peritoneal, or fallopian tube cancer. *J. Clin. Oncol.* 30, 2039–2045. doi:10.1200/JCO.2012.42.0505

Akai, J., Halley, P. A., and Storey, K. G. (2005). FGF-dependent Notch signaling maintains the spinal cord stem zone. *Genes Dev.* 19, 2877–2887. doi:10.1101/gad.357705

Alam, S. M., Fujimoto, J., Jahan, I., Sato, E., and Tamaya, T. (2008). Coexpression of EphB4 and ephrinB2 in tumour advancement of ovarian cancers. *Br. J. Cancer* 98, 845–851. doi:10.1038/sj.bjc.6604216

Alfaro, C., Suarez, N., Gonzalez, A., Solano, S., Erro, L., Dubrot, J., et al. (2009). Influence of bevacizumab, sunitinib and sorafenib as single agents or in combination on the inhibitory effects of VEGF on human dendritic cell differentiation from monocytes. *Br. J. Cancer* 100, 1111–1119. doi:10.1038/sj.bjc.6604965

Alvarez Secord, A., Bell Burdett, K., Owzar, K., Tritchler, D., Sibley, A. B., Liu, Y., et al. (2020). Predictive blood-based biomarkers in patients with epithelial ovarian cancer treated with carboplatin and paclitaxel with or without bevacizumab: Results from GOG-0218. *Clin. Cancer Res.* 26, 1288–1296. doi:10.1158/1078-0432.CCR-19-0226

Anderson, T. S., Wooster, A. L., Piersall, S. L., Okpalanwaka, I. F., and Lowe, D. B. (2022). Disrupting cancer angiogenesis and immune checkpoint networks for improved tumor immunity. *Semin. Cancer Biol.* 86, 981–996. doi:10.1016/j.semcancer.2022.02.009

Arjaans, M., Oude Munnink, T. H., Oosting, S. F., Terwisscha van Scheltinga, A. G., Gietema, J. A., Garbacik, E. T., et al. (2013). Bevacizumab-induced normalization of blood vessels in tumors hampers antibody uptake. *Cancer Res.* 73, 3347–3355. doi:10.1158/0008-5472.CAN-12-3518

Backen, A., Renehan, A. G., Clamp, A. R., Berzuini, C., Zhou, C., Oza, A., et al. (2014). The combination of circulating Ang1 and Tie2 levels predicts progression-free survival advantage in bevacizumab-treated patients with ovarian cancer. *Clin. Cancer Res.* 20, 4549–4558. doi:10.1158/1078-0432.CCR-13-3248

Bagley, R. G., Ren, Y., Weber, W., Yao, M., Kurtzberg, L., Pinckney, J., et al. (2011). Placental growth factor upregulation is a host response to antiangiogenic therapy. *Clin. Cancer Res.* 17, 976–988. doi:10.1158/1078-0432.CCR-10-2687

Bamberger, E. S., and Perrett, C. W. (2002). Angiogenesis in epithelian ovarian cancer. *Mol. Pathol.* 55, 348–359. doi:10.1136/mp.55.6.348

Banerjee, S., and Kaye, S. (2011). The role of targeted therapy in ovarian cancer. *Eur. J. Cancer* 47 (3), S116–S130. doi:10.1016/S0959-8049(11)70155-1

Bartoschek, M., and Pietras, K. (2018). PDGF family function and prognostic value in tumor biology. *Biochem. Biophys. Res. Commun.* 503, 984–990. doi:10.1016/j.bbrc.2018.06.106

Bauerschlag, D. O., Hilpert, F., Meier, W., Rau, J., Meinhold-Heerlein, I., Maass, N., et al. (2013). Evaluation of potentially predictive markers for anti-angiogenic therapy with sunitinib in recurrent ovarian cancer patients. *Transl. Oncol.* 6, 305–310. doi:10.1593/tlo.13205

Bauerschlag, D. O., Schem, C., Tiwari, S., Egberts, J. H., Weigel, M. T., Kalthoff, H., et al. (2010). Sunitinib (SU11248) inhibits growth of human ovarian cancer in xenografted mice. *Anticancer Res.* 30, 3355–3360.

Baumann, K. H., du Bois, A., Meier, W., Rau, J., Wimberger, P., Sehouli, J., et al. (2012). A phase II trial (AGO 2.11) in platinum-resistant ovarian cancer: A randomized multicenter trial with sunitinib (SU11248) to evaluate dosage, schedule, tolerability, toxicity and effectiveness of a multitargeted receptor tyrosine kinase inhibitor monotherapy. *Ann. Oncol.* 23, 2265–2271. doi:10.1093/annonc/mds003

Berta, J., Kenessey, I., Dobos, J., Tovari, J., Klepetko, W., Jan Ankersmit, H., et al. (2010). Apelin expression in human non-small cell lung cancer: Role in angiogenesis and prognosis. *J. Thorac. Oncol.* 5, 1120–1129. doi:10.1097/JTO.0b013e3181e2c1ff

Bhattarai, D., Xu, X., and Lee, K. (2018). Hypoxia-inducible factor-1 (HIF-1) inhibitors from the last decade (2007 to 2016): A "structure-activity relationship" perspective. *Med. Res. Rev.* 38, 1404–1442. doi:10.1002/med.21477

Biagi, J. J., Oza, A. M., Chalchal, H. I., Grimshaw, R., Ellard, S. L., Lee, U., et al. (2011). A phase II study of sunitinib in patients with recurrent epithelial ovarian and primary peritoneal carcinoma: An NCIC clinical trials group study. *Ann. Oncol.* 22, 335–340. doi:10.1093/annonc/mdq357

Bodnar, L., Gornas, M., and Szczylik, C. (2011). Sorafenib as a third line therapy in patients with epithelial ovarian cancer or primary peritoneal cancer: A phase II study. *Oncol* 123, 33–36. doi:10.1016/j.ygyno.2011.06.019

Bohndiek, S. E., Sasportas, L. S., Machtaler, S., Jokerst, J. V., Hori, S., and Gambhir, S. S. (2015). Photoacoustic tomography detects early vessel regression and normalization during ovarian tumor response to the antiangiogenic therapy trebananib. *J. Nucl. Med.* 56, 1942–1947. doi:10.2967/jnumed.115.160002

Boisen, M. K., Madsen, C. V., Dehlendorff, C., Jakobsen, A., Johansen, J. S., and Steffensen, K. D. (2016). The prognostic value of plasma YKL-40 in patients with chemotherapy-resistant ovarian cancer treated with bevacizumab. *Int. J. Gynecol. Cancer* 26, 1390–1398. doi:10.1097/IGC.0000000000000798

Brahmer, J. R., Tykodi, S. S., Chow, L. Q., Hwu, W. J., Topalian, S. L., Hwu, P., et al. (2012). Safety and activity of anti-PD-L1 antibody in patients with advanced cancer. *N. Engl. J. Med.* 366, 2455–2465. doi:10.1056/NEJMoa1200694

Brantley, D. M., Cheng, N., Thompson, E. J., Lin, Q., Brekken, R. A., Thorpe, P. E., et al. (2002). Soluble Eph A receptors inhibit tumor angiogenesis and progression *in vivo*. *Oncogene* 21, 7011–7026. doi:10.1038/sj.onc.1205679

Bray, F., Ferlay, J., Soerjomataram, I., Siegel, R. L., Torre, L. A., and Jemal, A. (2018). Global cancer statistics 2018: GLOBOCAN estimates of incidence and mortality worldwide for 36 cancers in 185 countries. *CA Cancer J. Clin.* 68, 394–424. doi:10.3322/caac.21492

Brunckhorst, M. K., Xu, Y., Lu, R., and Yu, Q. (2014). Angiopoietins promote ovarian cancer progression by establishing a procancer microenvironment. *Am. J. Pathol.* 184, 2285–2296. doi:10.1016/j.ajpath.2014.05.006

Buechel, M. E., Enserro, D., Burger, R. A., Brady, M. F., Wade, K., Secord, A. A., et al. (2021). Correlation of imaging and plasma based biomarkers to predict response to bevacizumab in epithelial ovarian cancer (EOC). *Gynecol. Oncol.* 161, 382–388. doi:10.1016/j.ygyno.2021.02.032

Burbridge, M. F., Bossard, C. J., Saunier, C., Fejes, I., Bruno, A., Leonce, S., et al. (2013). S49076 is a novel kinase inhibitor of MET, AXL, and FGFR with strong preclinical activity alone and in association with bevacizumab. *Mol. Cancer Ther.* 12, 1749–1762. doi:10.1158/1535-7163.MCT-13-0075

Burger, R. A., Brady, M. F., Bookman, M. A., Fleming, G. F., Monk, B. J., Huang, H., et al. (2011). Incorporation of bevacizumab in the primary treatment of ovarian cancer. *N. Engl. J. Med.* 365, 2473–2483. doi:10.1056/nejmoa1104390

Burger, R. A. (2011). Overview of anti-angiogenic agents in development for ovarian cancer. *Gynecol. Oncol.* 121, 230–238. doi:10.1016/j.ygyno.2010.11.035

Burger, R. A., Sill, M. W., Monk, B. J., Greer, B. E., and Sorosky, J. I. (2007). Phase II trial of bevacizumab in persistent or recurrent epithelial ovarian cancer or primary peritoneal cancer: A gynecologic oncology group study. *J. Clin. Oncol.* 25, 5165–5171. doi:10.1200/JCO.2007.11.5345

Byron, S. A., Gartside, M. G., Wellens, C. L., Goodfellow, P. J., Birrer, M. J., Campbell, I. G., et al. (2010). FGFR2 mutations are rare across histologic subtypes of ovarian cancer. *Gynecol. Oncol.* 117, 125–129. doi:10.1016/j.ygyno.2009.12.002

Califano, D., Gallo, D., Rampioni Vinciguerra, G. L., De Cecio, R., Arenare, L., Signoriello, S., et al. (2021). Evaluation of angiogenesis-related genes as prognostic biomarkers of bevacizumab treated ovarian cancer patients: Results from the phase IV mito16a/ManGO OV-2 translational study. *Cancers (Basel)* 13, 5152. doi:10.3390/cancers13205152

Campbell, N. E., Greenaway, J., Henkin, J., Moorehead, R. A., and Petrik, J. (2010). The thrombospondin-1 mimetic ABT-510 increases the uptake and effectiveness of cisplatin and paclitaxel in a mouse model of epithelial ovarian cancer. *Neoplasia* 12, 275–283. doi:10.1593/neo.91880

Campos, S. M., Penson, R. T., Matulonis, U., Horowitz, N. S., Whalen, C., Pereira, L., et al. (2013). A phase II trial of Sunitinib malate in recurrent and refractory ovarian, fallopian tube and peritoneal carcinoma. *Gynecol. Oncol.* 128, 215–220. doi:10.1016/j.ygyno.2012.07.126

Cannistra, S. A., Matulonis, U. A., Penson, R. T., Hambleton, J., Dupont, J., Mackey, H., et al. (2007). Phase II study of bevacizumab in patients with platinum-resistant ovarian cancer or peritoneal serous cancer. *J. Clin. Oncol.* 25, 5180–5186. doi:10.1200/JCO.2007.12.0782

Cantanhede, I. G., and de Oliveira, J. R. M. (2017). PDGF family expression in glioblastoma multiforme: Data compilation from ivy glioblastoma atlas project database. *Sci. Rep.* 7, 15271. doi:10.1038/s41598-017-15045-w

Cao, Y. (2013). Multifarious functions of PDGFs and PDGFRs in tumor growth and metastasis. *Trends Mol. Med.* 19, 460–473. doi:10.1016/j.molmed.2013.05.002

Carmeliet, P., and Jain, R. K. (2011). Molecular mechanisms and clinical applications of angiogenesis. *Nature* 473, 298–307. doi:10.1038/nature10144

Carmeliet, P., and Jain, R. K. (2011). Principles and mechanisms of vessel normalization for cancer and other angiogenic diseases. *Nat. Rev. Drug Discov.* 10, 417–427. doi:10.1038/nrd3455

Casanovas, O., Hicklin, D. J., Bergers, G., and Hanahan, D. (2005). Drug resistance by evasion of antiangiogenic targeting of VEGF signaling in late-stage pancreatic islet tumors. *Cancer Cell* 8, 299–309. doi:10.1016/j.ccr.2005.09.005

Chae, S. S., Kamoun, W. S., Farrar, C. T., Kirkpatrick, N. D., Niemeyer, E., de Graaf, A. M., et al. (2010). Angiopoietin-2 interferes with anti-VEGFR2-induced vessel normalization and survival benefit in mice bearing gliomas. *Clin. Cancer Res.* 16, 3618–3627. doi:10.1158/1078-0432.CCR-09-3073

Chan, J. K., Brady, W., Monk, B. J., Brown, J., Shahin, M. S., Rose, P. G., et al. (2018). A phase II evaluation of sunitinib in the treatment of persistent or recurrent clear cell ovarian carcinoma: An NRG Oncology/Gynecologic Oncology Group Study (GOG-254). *Gynecol. Oncol.* 150, 247–252. doi:10.1016/j.ygyno.2018.05.029

Chekerov, R., Hilpert, F., Mahner, S., El-Balat, A., Harter, P., De Gregorio, N., et al. (2018). Sorafenib plus topotecan versus placebo plus topotecan for platinum-resistant ovarian cancer (TRIAS): A multicentre, randomised, double-blind, placebo-controlled, phase 2 trial. *Lancet Oncol.* 19, 1247–1258. doi:10.1016/s1470-2045(18)30372-3

Cheng, N., Brantley, D., Fang, W. B., Liu, H., Fanslow, W., Cerretti, D. P., et al. (2003). Inhibition of VEGF-dependent multistage carcinogenesis by soluble EphA receptors. *Neoplasia* 5, 445–456. doi:10.1016/s1476-5586(03)80047-7

Chiron, M., Bagley, R. G., Pollard, J., Mankoo, P. K., Henry, C., Vincent, L., et al. (2014). Differential antitumor activity of aflibercept and bevacizumab in patient-derived xenograft models of colorectal cancer. *Mol. Cancer Ther.* 13, 1636–1644. doi:10.1158/1535-7163.MCT-13-0753

Cloughesy, T., Finocchiaro, G., Belda-Iniesta, C., Recht, L., Brandes, A. A., Pineda, E., et al. (2017). Randomized, double-blind, placebo-controlled, multicenter phase II study of onartuzumab plus bevacizumab versus placebo plus bevacizumab in patients with recurrent glioblastoma: Efficacy, safety, and hepatocyte growth factor and O(6)-methylguanine-DNA methyltransferase biomarker analyses. *J. Clin. Oncol.* 35, 343–351. doi:10.1200/JCO.2015.64.7685

Coleman, R. L., Brady, M. F., Herzog, T. J., Sabbatini, P., Armstrong, D. K., Walker, J. L., et al. (2017). Bevacizumab and paclitaxel-carboplatin chemotherapy and secondary cytoreduction in recurrent, platinum-sensitive ovarian cancer (NRG oncology/gynecologic oncology group study GOG-0213): A multicentre, open-label, randomised, phase 3 trial. *Lancet Oncol.* 18, 779–791. doi:10.1016/S1470-2045(17)30279-6

Collinson, F., Hutchinson, M., Craven, R. A., Cairns, D. A., Zougman, A., Wind, T. C., et al. (2013). Predicting response to bevacizumab in ovarian cancer: A panel of potential biomarkers informing treatment selection. *Clin. Cancer Res.* 19, 5227–5239. doi:10.1158/1078-0432.CCR-13-0489

Colombo, N., Tomao, F., Benedetti Panici, P., Nicoletto, M. O., Tognon, G., Bologna, A., et al. (2022). Randomized phase II trial of weekly paclitaxel vs. cediranib-olaparib (continuous or intermittent schedule) in platinum-resistant high-grade epithelial ovarian cancer. *Gynecol. Oncol.* 164, 505–513. doi:10.1016/j.ygyno.2022.01.015

Cortez, A. J., Tudrej, P., Kujawa, K. A., and Lisowska, K. M. (2018). Advances in ovarian cancer therapy. *Cancer Chemother. Pharmacol.* 81, 17–38. doi:10.1007/s00280-017-3501-8

Curiel, T. J., Wei, S., Dong, H., Alvarez, X., Cheng, P., Mottram, P., et al. (2003). Blockade of B7-H1 improves myeloid dendritic cell-mediated antitumor immunity. *Nat. Med.* 9, 562–567. doi:10.1038/nm863

Davidson, B. A., and Secord, A. A. (2014). Profile of pazopanib and its potential in the treatment of epithelial ovarian cancer. *Int. J. Womens Health* 6, 289–300. doi:10.2147/IJWH.S49781

De Falco, S. (2012). The discovery of placenta growth factor and its biological activity. *Exp. Mol. Med.* 44, 1–9. doi:10.3858/emm.2012.44.1.025

Delgado, V. M., Nugnes, L. G., Colombo, L. L., Troncoso, M. F., Fernandez, M. M., Malchiodi, E. L., et al. (2011). Modulation of endothelial cell migration and angiogenesis: A novel function for the "tandem-repeat" lectin galectin-8. *FASEB J.* 25, 242–254. doi:10.1096/fj.09-144907

Dewangan, J., Srivastava, S., Mishra, S., Divakar, A., Kumar, S., and Rath, S. K. (2019). Salinomycin inhibits breast cancer progression via targeting HIF-1α/VEGF mediated tumor angiogenesis *in vitro* and *in vivo*. *Biochem. Pharmacol.* 164, 326–335. doi:10.1016/j.bcp.2019.04.026

Dewhirst, M. W., and Ashcraft, K. A. (2016). Implications of increase in vascular permeability in tumors by VEGF: A commentary on the pioneering work of harold Dvorak. *Cancer Res.* 76, 3118–3120. doi:10.1158/0008-5472.CAN-16-1292

Dewhirst, M. W., Ong, E. T., Braun, R. D., Smith, B., Klitzman, B., Evans, S. M., et al. (1999). Quantification of longitudinal tissue pO2 gradients in window chamber tumours: Impact on tumour hypoxia. *Br. J. Cancer* 79, 1717–1722. doi:10.1038/sj.bjc.6690273

Dewhirst, M. W., and Secomb, T. W. (2017). Transport of drugs from blood vessels to tumour tissue. *Nat. Rev. Cancer* 17, 738–750. doi:10.1038/nrc.2017.93

Dhanabal, M., Jeffers, M., LaRochelle, W. J., and Lichenstein, H. S. (2005). Angioarrestin: A unique angiopoietin-related protein with anti-angiogenic properties. *Biochem. Biophys. Res. Commun.* 333, 308–315. doi:10.1016/j.bbrc.2005.05.134

Disis, M. L., Taylor, M. H., Kelly, K., Beck, J. T., Gordon, M., Moore, K. M., et al. (2019). Efficacy and safety of avelumab for patients with recurrent or refractory ovarian cancer: Phase 1b results from the JAVELIN solid tumor trial. *JAMA Oncol.* 5, 393–401. doi:10.1001/jamaoncol.2018.6258

Dobrzanski, P., Hunter, K., Jones-Bolin, S., Chang, H., Robinson, C., Pritchard, S., et al. (2004). Antiangiogenic and antitumor efficacy of EphA2 receptor antagonist. *Cancer Res.* 64, 910–919. doi:10.1158/0008-5472.can-3430-2

Dogra, S., Neelakantan, D., Patel, M. M., Griesel, B., Olson, A., and Woo, S. (2021). Adipokine apelin/APJ pathway promotes peritoneal dissemination of ovarian cancer cells by regulating lipid metabolism. *Mol. Cancer Res.* 19, 1534–1545. doi:10.1158/1541-7786.MCR-20-0991

du Bois, A., Floquet, A., Kim, J. W., Rau, J., del Campo, J. M., Friedlander, M., et al. (2014). Incorporation of pazopanib in maintenance therapy of ovarian cancer. *J. Clin. Oncol.* 32, 3374–3382. doi:10.1200/JCO.2014.55.7348

du Bois, A., Kristensen, G., Ray-Coquard, I., Reuss, A., Pignata, S., Colombo, N., et al. (2016). Standard first-line chemotherapy with or without nintedanib for advanced ovarian cancer (AGO-OVAR 12): A randomised, double-blind, placebo-controlled phase 3 trial. *Lancet Oncol.* 17, 78–89. doi:10.1016/s1470-2045(15)00366-6

du Bois, A., Vergote, I., Wimberger, P., Ray-Coquard, I., Harter, P., Curtis, L. B., et al. (2012). Open-label feasibility study of pazopanib, carboplatin, and paclitaxel in women with newly diagnosed, untreated, gynaecologic tumours: A phase I/II trial of the AGO study group. *Br. J. Cancer* 106, 629–632. doi:10.1038/bjc.2011.608

Ellis, L. M., and Hicklin, D. J. (2008). Pathways mediating resistance to vascular endothelial growth factor-targeted therapy. *Clin. Cancer Res.* 14, 6371–6375. doi:10.1158/1078-0432.CCR-07-5287

Elyashiv, O., Ledermann, J., Parmar, G., Farrelly, L., Counsell, N., Feeney, A., et al. (2021). ICON 9-an international phase III randomized study to evaluate the efficacy of maintenance therapy with olaparib and cediranib or olaparib alone in patients with relapsed platinum-sensitive ovarian cancer following a response to platinum-based chemotherapy. *Int. J. Gynecol. Cancer* 31, 134–138. doi:10.1136/ijgc-2020-002073

Erber, R., Thurnher, A., Katsen, A. D., Groth, G., Kerger, H., Hammes, H. P., et al. (2004). Combined inhibition of VEGF and PDGF signaling enforces tumor vessel regression by interfering with pericyte-mediated endothelial cell survival mechanisms. *FASEB J.* 18, 338–340. doi:10.1096/fj.03-0271fje

Fabbi, M., Costa, D., Russo, D., Arenare, L., Gaggero, G., Signoriello, S., et al. (2022). Analysis of A Disintegrin and metalloprotease 17 (ADAM17) expression as a prognostic marker in ovarian cancer patients undergoing first-line treatment plus bevacizumab. *Diagn. (Basel)* 12, 2118. doi:10.3390/diagnostics12092118

Farolfi, A., Petrone, M., Scarpi, E., Galla, V., Greco, F., Casanova, C., et al. (2018). Inflammatory indexes as prognostic and predictive factors in ovarian cancer treated with chemotherapy alone or together with bevacizumab. A multicenter, retrospective analysis by the MITO group (MITO 24). *Oncol* 13, 469–479. doi:10.1007/s11523-018-0574-1

Feng, M., Yao, G., Yu, H., Qing, Y., and Wang, K. (2016). Tumor apelin, not serum apelin, is associated with the clinical features and prognosis of gastric cancer. *BMC Cancer* 16, 794. doi:10.1186/s12885-016-2815-y

Franco, M., Roswall, P., Cortez, E., Hanahan, D., and Pietras, K. (2011). Pericytes promote endothelial cell survival through induction of autocrine VEGF-A signaling and Bcl-w expression. *Blood* 118, 2906–2917. doi:10.1182/blood-2011-01-331694

Fuh, K. C., Secord, A. A., Bevis, K. S., Huh, W., ElNaggar, A., Blansit, K., et al. (2015). Comparison of bevacizumab alone or with chemotherapy in recurrent ovarian cancer patients. *Gynecol. Oncol.* 139, 413–418. doi:10.1016/j.ygyno.2015.06.041

Fukumura, D., Kloepper, J., Amoozgar, Z., Duda, D. G., and Jain, R. K. (2018). Enhancing cancer immunotherapy using antiangiogenics: Opportunities and challenges. *Nat. Rev. Clin. Oncol.* 15, 325–340. doi:10.1038/nrclinonc.2018.29

Gao, J., Li, F., Liu, Z., Huang, M., Chen, H., Liao, G., et al. (2021). Multiple genetic variants predict the progression-free survival of bevacizumab plus chemotherapy in advanced ovarian cancer: A retrospective study. *Med. Baltim.* 100, e27130. doi:10.1097/MD.0000000000027130

Garrido-Laguna, I., Krop, I., Burris, H. A., 3rd, Hamilton, E., Braiteh, F., Weise, A. M., et al. (2019). First-in-human, phase I study of PF-06647263, an anti-EFNA4 calicheamicin antibody-drug conjugate, in patients with advanced solid tumors. *Int. J. Cancer* 145, 1798–1808. doi:10.1002/ijc.32154

Gavalas, N. G., Liontos, M., Trachana, S. P., Bagratuni, T., Arapinis, C., Liacos, C., et al. (2013). Angiogenesis-related pathways in the pathogenesis of ovarian cancer. *Int. J. Mol. Sci.* 14, 15885–15909. doi:10.3390/ijms140815885

Georganaki, M., van Hooren, L., and Dimberg, A. (2018). Vascular targeting to increase the efficiency of immune checkpoint blockade in cancer. *Front. Immunol.* 9, 3081. doi:10.3389/fimmu.2018.03081

Gerald, D., Chintharlapalli, S., Augustin, H. G., and Benjamin, L. E. (2013). Angiopoietin-2: An attractive target for improved antiangiogenic tumor therapy. *Cancer Res.* 73, 1649–1657. doi:10.1158/0008-5472.CAN-12-4697

Ghedini, G. C., Ronca, R., Presta, M., and Giacomini, A. (2018). Future applications of FGF/FGFR inhibitors in cancer. *Expert Rev. Anticancer Ther.* 18, 861–872. doi:10.1080/14737140.2018.1491795

González-Martín, A., Chung, H., Saada-Bouzid, E., Yanez, E., Senellart, H., Cassier, P., et al. (2020) *Efficacy Saf. lenvatinib plus pembrolizumab patients previously Treat. ovarian cancer multicohort phase 2 LEAP-005 study* 30, 2. A1–A2.

Greenberg, J. I., Shields, D. J., Barillas, S. G., Acevedo, L. M., Murphy, E., Huang, J., et al. (2008). A role for VEGF as a negative regulator of pericyte function and vessel maturation. *Nature* 456, 809–813. doi:10.1038/nature07424

Grossfeld, G. D., Ginsberg, D. A., Stein, J. P., Bochner, B. H., Esrig, D., Groshen, S., et al. (1997). Thrombospondin-1 expression in bladder cancer: Association with p53 alterations, tumor angiogenesis, and tumor progression. *J. Natl. Cancer Inst.* 89, 219–227. doi:10.1093/jnci/89.3.219

Hainsworth, J. D., Thompson, D. S., Bismayer, J. A., Gian, V. G., Merritt, W. M., Whorf, R. C., et al. (2015). Paclitaxel/carboplatin with or without sorafenib in the first-line treatment of patients with stage III/IV epithelial ovarian cancer: A randomized phase II study of the sarah cannon research Institute. *Cancer Med.* 4, 673–681. doi:10.1002/cam4.376

Hall, M. R., Dehbi, H. M., Banerjee, S., Lord, R., Clamp, A., Ledermann, J. A., et al. (2020). A phase II randomised, placebo-controlled trial of low dose (metronomic) cyclophosphamide and nintedanib (BIBF1120) in advanced ovarian, fallopian tube or primary peritoneal cancer. *Gynecol. Oncol.* 159, 692–698. doi:10.1016/j.ygyno.2020.09.048

Halvorsen, A. R., Kristensen, G., Embleton, A., Adusei, C., Barretina-Ginesta, M. P., Beale, P., et al. (2017). Evaluation of prognostic and predictive significance of circulating MicroRNAs in ovarian cancer patients. *Dis. Markers* 2017, 3098542, doi:10.1155/2017/3098542

Hamanishi, J., Mandai, M., Ikeda, T., Minami, M., Kawaguchi, A., Murayama, T., et al. (2015). Safety and antitumor activity of anti-PD-1 antibody, nivolumab, in patients with platinum-resistant ovarian cancer. *J. Clin. Oncol.* 33, 4015–4022. doi:10.1200/JCO.2015.62.3397

Hamanishi, J., Takeshima, N., Katsumata, N., Ushijima, K., Kimura, T., Takeuchi, S., et al. (2021). Nivolumab versus gemcitabine or pegylated liposomal doxorubicin for patients with platinum-resistant ovarian cancer: Open-label, randomized trial in Japan (NINJA). *J. Clin. Oncol.* 39, 3671–3681. doi:10.1200/JCO.21.00334

Han, L., Dong, Z., Qiao, Y., Kristensen, G. B., Holm, R., Nesland, J. M., et al. (2005). The clinical significance of EphA2 and Ephrin A-1 in epithelial ovarian carcinomas. *Gynecol. Oncol.* 99, 278–286. doi:10.1016/j.ygyno.2005.06.036

Haunschild, C. E., and Tewari, K. S. (2020). Bevacizumab use in the frontline, maintenance and recurrent settings for ovarian cancer. *Future Oncol.* 16, 225–246. doi:10.2217/fon-2019-0042

Heldin, C. H. (2013). Targeting the PDGF signaling pathway in tumor treatment. *Cell Commun. Signal* 11, 97. doi:10.1186/1478-811X-11-97

Heldin, C. H., and Westermark, B. (1999). Mechanism of action and *in vivo* role of platelet-derived growth factor. *Physiol. Rev.* 79, 1283–1316. doi:10.1152/physrev.1999.79.4.1283

Heo, K., Kim, Y. H., Sung, H. J., Li, H. Y., Yoo, C. W., Kim, J. Y., et al. (2012). Hypoxia-induced up-regulation of apelin is associated with a poor prognosis in oral squamous cell carcinoma patients. *Oral Oncol.* 48, 500–506. doi:10.1016/j.oraloncology.2011.12.015

Herath, N. I., Spanevello, M. D., Sabesan, S., Newton, T., Cummings, M., Duffy, S., et al. (2006). Over-expression of Eph and ephrin genes in advanced ovarian cancer: Ephrin gene expression correlates with shortened survival. *BMC Cancer* 6, 144. doi:10.1186/1471-2407-6-144

Herzog, T. J., Scambia, G., Kim, B. G., Lhomme, C., Markowska, J., Ray-Coquard, I., et al. (2013). A randomized phase II trial of maintenance therapy with Sorafenib in front-line ovarian carcinoma. *Gynecol. Oncol.* 130, 25–30. doi:10.1016/j.ygyno.2013.04.011

Hirte, H., Lheureux, S., Fleming, G. F., Sugimoto, A., Morgan, R., Biagi, J., et al. (2015). A phase 2 study of cediranib in recurrent or persistent ovarian, peritoneal or fallopian tube cancer: A trial of the princess margaret, chicago and California phase II consortia. *Gynecol. Oncol.* 138, 55–61. doi:10.1016/j.ygyno.2015.04.009

Hoffmann, M., Fiedor, E., and Ptak, A. (2017). Bisphenol A and its derivatives tetrabromobisphenol A and tetrachlorobisphenol A induce apelin expression and secretion in ovarian cancer cells through a peroxisome proliferator-activated receptor gamma-dependent mechanism. *Toxicol. Lett.* 269, 15–22. doi:10.1016/j.toxlet.2017.01.006

Huang, D., Ding, Y., Zhou, M., Rini, B. I., Petillo, D., Qian, C. N., et al. (2010). Interleukin-8 mediates resistance to antiangiogenic agent sunitinib in renal cell carcinoma. *Cancer Res.* 70, 1063–1071. doi:10.1158/0008-5472.CAN-09-3965

Huang, J., Soffer, S. Z., Kim, E. S., McCrudden, K. W., Huang, J., New, T., et al. (2004). Vascular remodeling marks tumors that recur during chronic suppression of angiogenesis. *Mol. Cancer Res.* 2, 36–42. doi:10.1158/1541-7786.36.2.1

Huang, Y., Chen, X., Dikov, M. M., Novitskiy, S. V., Mosse, C. A., Yang, L., et al. (2007). Distinct roles of VEGFR-1 and VEGFR-2 in the aberrant hematopoiesis associated with elevated levels of VEGF. *Blood* 110, 624–631. doi:10.1182/blood-2007-01-065714

Huinen, Z. R., Huijbers, E. J. M., van Beijnum, J. R., Nowak-Sliwinska, P., and Griffioen, A. W. (2021). Anti-angiogenic agents - overcoming tumour endothelial cell anergy and improving immunotherapy outcomes. *Nat. Rev. Clin. Oncol.* 18, 527–540. doi:10.1038/s41571-021-00496-y

Jeanne, A., Sarazin, T., Charle, M., Moali, C., Fichel, C., Boulagnon-Rombi, C., et al. (2021). Targeting ovarian carcinoma with TSP-1:CD47 antagonist TAX2 activates anti-tumor immunity. *Cancers (Basel)* 13, 5019. doi:10.3390/cancers13195019

Jiang, B. H., and Liu, L. Z. (2009). PI3K/PTEN signaling in angiogenesis and tumorigenesis. *Adv. Cancer Res.* 102, 19–65. doi:10.1016/S0065-230X(09)02002-8

Jin, C., Yuan, M., Bu, H., and Jin, C. (2022). Antiangiogenic strategies in epithelial ovarian cancer: Mechanism, resistance, and combination therapy. *J. Oncol.* 2022, 4880355. doi:10.1155/2022/4880355

Jing, Y., Lu, H., Wu, K., Subramanian, I. V., and Ramakrishnan, S. (2011). Inhibition of ovarian cancer by RGD-P125A-endostatin-Fc fusion proteins. *Int. J. Cancer* 129, 751–761. doi:10.1002/ijc.25932

Kalin, R. E., Kretz, M. P., Meyer, A. M., Kispert, A., Heppner, F. L., and Brandli, A. W. (2007). Paracrine and autocrine mechanisms of apelin signaling govern embryonic and tumor angiogenesis. *Dev. Biol.* 305, 599–614. doi:10.1016/j.ydbio.2007.03.004

Katoh, M. (2016). Therapeutics targeting FGF signaling network in human diseases. *Trends Pharmacol. Sci.* 37, 1081–1096. doi:10.1016/j.tips.2016.10.003

Khalique, S., and Banerjee, S. (2017). Nintedanib in ovarian cancer. *Expert Opin. Investig. Drugs* 26, 1073–1081. doi:10.1080/13543784.2017.1353599

Khan, K. A., and Kerbel, R. S. (2018). Improving immunotherapy outcomes with anti-angiogenic treatments and vice versa. *Nat. Rev. Clin. Oncol.* 15, 310–324. doi:10.1038/nrclinonc.2018.9

Kim, B. J., Kim, D., Kim, J. H., Kim, H. S., and Jang, H. J. (2021). The efficacy and safety of onartuzumab in patients with solid cancers: A meta-analysis of randomized trials. *Indian J. Cancer* 58, 232–240. doi:10.4103/ijc.IJC_797_18

Kloepper, J., Riedemann, L., Amoozgar, Z., Seano, G., Susek, K., Yu, V., et al. (2016). Ang-2/VEGF bispecific antibody reprograms macrophages and resident microglia to anti-tumor phenotype and prolongs glioblastoma survival. *Proc. Natl. Acad. Sci. U. S. A.* 113, 4476–4481. doi:10.1073/pnas.1525360113

Krusche, B., Ottone, C., Clements, M. P., Johnstone, E. R., Goetsch, K., Lieven, H., et al. (2016). EphrinB2 drives perivascular invasion and proliferation of glioblastoma stem-like cells. *Elife* 5, e14845. doi:10.7554/eLife.14845

Lacquaniti, A., Altavilla, G., Picone, A., Donato, V., Chirico, V., Mondello, P., et al. (2015). Apelin beyond kidney failure and hyponatremia: A useful biomarker for cancer disease progression evaluation. *Clin. Exp. Med.* 15, 97–105. doi:10.1007/s10238-014-0272-y

Lamalice, L., Le Boeuf, F., and Huot, J. (2007). Endothelial cell migration during angiogenesis. *Circ. Res.* 100, 782–794. doi:10.1161/01.RES.0000259593.07661.1e

Langenkamp, E., Zhang, L., Lugano, R., Huang, H., Elhassan, T. E., Georganaki, M., et al. (2015). Elevated expression of the C-type lectin CD93 in the glioblastoma vasculature regulates cytoskeletal rearrangements that enhance vessel function and reduce host survival. *Cancer Res.* 75, 4504–4516. doi:10.1158/0008-5472.CAN-14-3636

Lassus, H., Sihto, H., Leminen, A., Nordling, S., Joensuu, H., Nupponen, N. N., et al. (2004). Genetic alterations and protein expression of KIT and PDGFRA in serous ovarian carcinoma. *Br. J. Cancer* 91, 2048–2055. doi:10.1038/sj.bjc.6602252

Ledermann, J. A., Embleton, A. C., Raja, F., Perren, T. J., Jayson, G. C., Rustin, G. J. S., et al. (2016). Cediranib in patients with relapsed platinum-sensitive ovarian cancer (ICON6): A randomised, double-blind, placebo-controlled phase 3 trial. *Lancet* 387, 1066–1074. doi:10.1016/S0140-6736(15)01167-8

Ledermann, J. A., Embleton-Thirsk, A. C., Perren, T. J., Jayson, G. C., Rustin, G. J. S., Kaye, S. B., et al. (2021). Cediranib in addition to chemotherapy for women with relapsed platinum-sensitive ovarian cancer (ICON6): Overall survival results of a phase III randomised trial. *ESMO Open* 6, 100043. doi:10.1016/j.esmoop.2020.100043

Ledermann, J. A., Hackshaw, A., Kaye, S., Jayson, G., Gabra, H., McNeish, I., et al. (2011). Randomized phase II placebo-controlled trial of maintenance therapy using the oral triple angiokinase inhibitor BIBF 1120 after chemotherapy for relapsed ovarian cancer. *J. Clin. Oncol.* 29, 3798–3804. doi:10.1200/JCO.2010.33.5208

Lee, C. K., Lee, M. E., Lee, W. S., Kim, J. M., Park, K. H., Kim, T. S., et al. (2015). Dovitinib (TKI258), a multi-target angiokinase inhibitor, is effective regardless of KRAS or BRAF mutation status in colorectal cancer. *Am. J. Cancer Res.* 5, 72–86.

Lee, J. M., Annunziata, C. M., Hays, J. L., Cao, L., Choyke, P., Yu, M., et al. (2020). Phase II trial of bevacizumab and sorafenib in recurrent ovarian cancer patients with or without prior-bevacizumab treatment. *Gynecol. Oncol.* 159, 88–94. doi:10.1016/j.ygyno.2020.07.031

Lee, J. M., Sarosy, G. A., Annunziata, C. M., Azad, N., Minasian, L., Kotz, H., et al. (2010). Combination therapy: Intermittent sorafenib with bevacizumab yields activity and decreased toxicity. *Br. J. Cancer* 102, 495–499. doi:10.1038/sj.bjc.6605514

Lengyel, E. (2010). Ovarian cancer development and metastasis. *Am. J. Pathol.* 177, 1053–1064. doi:10.2353/ajpath.2010.100105

Leone Roberti Maggiore, U., Valenzano Menada, M., Venturini, P. L., and Ferrero, S. (2013). The potential of sunitinib as a therapy in ovarian cancer. *Expert Opin. Investig. Drugs* 22, 1671–1686. doi:10.1517/13543784.2013.841138

Levitzki, A. (2004). PDGF receptor kinase inhibitors for the treatment of PDGF driven diseases. *Cytokine Growth Factor Rev.* 15, 229–235. doi:10.1016/j.cytogfr.2004.03.010

Lheureux, S., Oaknin, A., Garg, S., Bruce, J. P., Madariaga, A., Dhani, N. C., et al. (2020). Evolve: A multicenter open-label single-arm clinical and translational phase II trial of cediranib plus olaparib for ovarian cancer after PARP inhibition progression. *Clin. Cancer Res.* 26, 4206–4215. doi:10.1158/1078-0432.CCR-19-4121

Li, J., Zhi, X., Sun, Y., Chen, M., and Yao, L. (2022). The PDGF family is associated with activated tumor stroma and poor prognosis in ovarian cancer. *Dis. Markers* 2022, 5940049. doi:10.1155/2022/5940049

Lisle, J. E., Mertens-Walker, I., Rutkowski, R., Herington, A. C., and Stephenson, S. A. (2013). Eph receptors and their ligands: Promising molecular biomarkers and therapeutic targets in prostate cancer. *Biochim. Biophys. Acta* 1835, 243–257. doi:10.1016/j.bbcan.2013.01.003

Liu, J. F., Barry, W. T., Birrer, M., Lee, J. M., Buckanovich, R. J., Fleming, G. F., et al. (2014). Combination cediranib and olaparib versus olaparib alone for women with recurrent platinum-sensitive ovarian cancer: A randomised phase 2 study. *Lancet Oncol.* 15, 1207–1214. doi:10.1016/S1470-2045(14)70391-2

Liu, J. F., Barry, W. T., Birrer, M., Lee, J. M., Buckanovich, R. J., Fleming, G. F., et al. (2019). Overall survival and updated progression-free survival outcomes in a randomized phase II study of combination cediranib and olaparib versus olaparib in relapsed platinum-sensitive ovarian cancer. *Ann. Oncol.* 30, 551–557. doi:10.1093/annonc/mdz018

Liu, J. F., Brady, M. F., Matulonis, U. A., Miller, A., Kohn, E. C., Swisher, E. M., et al. (2022). Olaparib with or without cediranib versus platinum-based chemotherapy in recurrent platinum-sensitive ovarian cancer (NRG-GY004): A randomized, open-label, phase III trial. *J. Clin. Oncol.* 40, 2138–2147. doi:10.1200/jco.21.02011

Liu, J. F., Gordon, M., Veneris, J., Braiteh, F., Balmanoukian, A., Eder, J. P., et al. (2019). Safety, clinical activity and biomarker assessments of atezolizumab from a Phase I study in advanced/recurrent ovarian and uterine cancers. *Gynecol. Oncol.* 154, 314–322. doi:10.1016/j.ygyno.2019.05.021

Liu, J. F., Herold, C., Gray, K. P., Penson, R. T., Horowitz, N., Konstantinopoulos, P. A., et al. (2019). Assessment of combined nivolumab and bevacizumab in relapsed ovarian cancer: A phase 2 clinical trial. *JAMA Oncol.* 5, 1731–1738. doi:10.1001/jamaoncol.2019.3343

Liu, X., Xu, Y., Jin, Q., Wang, W., Zhang, S., Wang, X., et al. (2016). EphA8 is a prognostic marker for epithelial ovarian cancer. *Oncotarget* 7, 20801–20809. doi:10.18632/oncotarget.8018

Liu, Y., Luo, Y., Cai, M., Shen, P., Li, J., Chen, H., et al. (2021). Anti-angiogenic therapy in ovarian cancer: Current situation and prospects. *Indian J. Med. Res.* 154, 680–690. doi:10.4103/ijmr.IJMR_1160_19

Lopes-Coelho, F., Martins, F., Pereira, S. A., and Serpa, J. (2021). Anti-angiogenic therapy: Current challenges and future perspectives. *Int. J. Mol. Sci.* 22, 3765. doi:10.3390/ijms22073765

Lorusso, D., Marchetti, C., Conte, C., Giudice, E., Bolomini, G., Vertechy, L., et al. (2020). Bevacizumab as maintenance treatment in BRCA mutated patients with advanced ovarian cancer: A large, retrospective, multicenter case-control study. *Gynecol. Oncol.* 159, 95–100. doi:10.1016/j.ygyno.2020.07.022

Lu, C., Shahzad, M. M., Moreno-Smith, M., Lin, Y. G., Jennings, N. B., Allen, J. K., et al. (2010). Targeting pericytes with a PDGF-B aptamer in human ovarian carcinoma models. *Cancer Biol. Ther.* 9, 176–182. doi:10.4161/cbt.9.3.10635

Lu, C., Thaker, P. H., Lin, Y. G., Spannuth, W., Landen, C. N., Merritt, W. M., et al. (2008). Impact of vessel maturation on antiangiogenic therapy in ovarian cancer. *Am. J. Obstet. Gynecol.* 198, 477–e9. ; discussion 477 e479-410. doi:10.1016/j.ajog.2007.12.028

Lu, K. V., Chang, J. P., Parachoniak, C. A., Pandika, M. M., Aghi, M. K., Meyronet, D., et al. (2012). VEGF inhibits tumor cell invasion and mesenchymal transition through a MET/VEGFR2 complex. *Cancer Cell* 22, 21–35. doi:10.1016/j.ccr.2012.05.037

Madsen, C. V., Steffensen, K. D., Olsen, D. A., Waldstrom, M., Smerdel, M., Adimi, P., et al. (2012). Serial measurements of serum PDGF-AA, PDGF-BB, FGF2, and VEGF in multiresistant ovarian cancer patients treated with bevacizumab. *J. Ovarian Res.* 5, 23. doi:10.1186/1757-2215-5-23

Mansouri, A., McGregor, N., Dunn, R., Dobbie, S., Holmes, J., Collins, L., et al. (2021). Randomised phase II trial of olaparib, chemotherapy or olaparib and cediranib in patients with platinum-resistant ovarian cancer (OCTOVA): A study protocol. *BMJ Open* 11, e041463. doi:10.1136/bmjopen-2020-041463

Maroto, P., Porta, C., Capdevila, J., Apolo, A. B., Viteri, S., Rodriguez-Antona, C., et al. (2022). Cabozantinib for the treatment of solid tumors: A systematic review. *Ther. Adv. Med. Oncol.* 14, 17588359221107112. doi:10.1177/17588359221107112

Marth, C., Vergote, I., Scambia, G., Oberaigner, W., Clamp, A., Berger, R., et al. (2017). ENGOT-ov-6/TRINOVA-2: Randomised, double-blind, phase 3 study of pegylated liposomal doxorubicin plus trebananib or placebo in women with recurrent partially platinum-sensitive or resistant ovarian cancer. *Eur. J. Cancer* 70, 111–121. doi:10.1016/j.ejca.2016.09.004

Martinez-Bosch, N., and Navarro, P. (2020). Galectins in the tumor microenvironment: Focus on galectin-1. *Adv. Exp. Med. Biol.* 1259, 17–38. doi:10.1007/978-3-030-43093-1_2

Matei, D., Graeber, T. G., Baldwin, R. L., Karlan, B. Y., Rao, J., and Chang, D. D. (2002). Gene expression in epithelial ovarian carcinoma. *Oncogene* 21, 6289–6298. doi:10.1038/sj.onc.1205785

Mellman, I., Coukos, G., and Dranoff, G. (2011). Cancer immunotherapy comes of age. *Nature* 480, 480–489. doi:10.1038/nature10673

Merritt, W. M., Nick, A. M., Carroll, A. R., Lu, C., Matsuo, K., Dumble, M., et al. (2010). Bridging the gap between cytotoxic and biologic therapy with metronomic topotecan and pazopanib in ovarian cancer. *Mol. Cancer Ther.* 9, 985–995. doi:10.1158/1535-7163.MCT-09-0967

Mielczarek-Palacz, A., Kondera-Anasz, Z., Smycz-Kubanska, M., Englisz, A., Janusz, A., Krolewska-Daszczynska, P., et al. (2022). The role of galectins-1, 3, 7, 8 and 9 as potential diagnostic and therapeutic markers in ovarian cancer (Review). *Mol. Med. Rep.* 25, 166. doi:10.3892/mmr.2022.12682

Mitra, A. K., Sawada, K., Tiwari, P., Mui, K., Gwin, K., and Lengyel, E. (2011). Ligand-independent activation of c-Met by fibronectin and α(5)β(1)-integrin regulates ovarian cancer invasion and metastasis. *Oncogene* 30, 1566–1576. doi:10.1038/onc.2010.532

Monk, B. J., Han, E., Josephs-Cowan, C. A., Pugmire, G., and Burger, R. A. (2006). Salvage bevacizumab (rhuMAB VEGF)-based therapy after multiple prior cytotoxic regimens in advanced refractory epithelial ovarian cancer. *Gynecol. Oncol.* 102, 140–144. doi:10.1016/j.ygyno.2006.05.006

Monk, B. J., Minion, L. E., and Coleman, R. L. (2016). Anti-angiogenic agents in ovarian cancer: Past, present, and future. *Ann. Oncol.* 27 (1), i33–i39. doi:10.1093/annonc/mdw093

Monk, B. J., Poveda, A., Vergote, I., Raspagliesi, F., Fujiwara, K., Bae, D. S., et al. (2014). Anti-angiopoietin therapy with trebananib for recurrent ovarian cancer (TRINOVA-1): A randomised, multicentre, double-blind, placebo-controlled phase 3 trial. *Lancet Oncol.* 15, 799–808. doi:10.1016/S1470-2045(14)70244-X

Monk, B. J., Poveda, A., Vergote, I., Raspagliesi, F., Fujiwara, K., Bae, D. S., et al. (2016). Final results of a phase 3 study of trebananib plus weekly paclitaxel in recurrent ovarian cancer (TRINOVA-1): Long-term survival, impact of ascites, and progression-free survival-2. *Gynecol. Oncol.* 143, 27–34. doi:10.1016/j.ygyno.2016.07.112

Moroney, J. W., Powderly, J., Lieu, C. H., Bendell, J. C., Eckhardt, S. G., Chang, C. W., et al. (2020). Safety and clinical activity of atezolizumab plus bevacizumab in patients with ovarian cancer: A phase Ib study. *Clin. Cancer Res.* 26, 5631–5637. doi:10.1158/1078-0432.CCR-20-0477

Motz, G. T., and Coukos, G. (2011). The parallel lives of angiogenesis and immunosuppression: Cancer and other tales. *Nat. Rev. Immunol.* 11, 702–711. doi:10.1038/nri3064

Nagy, J. A., and Dvorak, H. F. (2012). Heterogeneity of the tumor vasculature: The need for new tumor blood vessel type-specific targets. *Clin. Exp. Metastasis* 29, 657–662. doi:10.1007/s10585-012-9500-6

Ng, C. S., Zhang, Z., Lee, S. I., Marques, H. S., Burgers, K., Su, F., et al. (2017). CT perfusion as an early biomarker of treatment efficacy in advanced ovarian cancer: An ACRIN and GOG study. *Clin. Cancer Res.* 23, 3684–3691. doi:10.1158/1078-0432.CCR-16-1859

Nishio, S., Matsumoto, K., Takehara, K., Kawamura, N., Hasegawa, K., Takeshima, N., et al. (2020). Pembrolizumab monotherapy in Japanese patients with advanced ovarian cancer: Subgroup analysis from the KEYNOTE-100. *Cancer Sci.* 111, 1324–1332. doi:10.1111/cas.14340

Nixon, A., Liu, J., Xiong, N., Hurwitz, H. I., Lyu, J., Liu, Y., et al. (2021). Blood-based biomarkers in patients with platinum-sensitive and resistant ovarian cancer treated with olaparib and cediranib: Results from the UM9825 trial. *Gynecol. Oncol.* 162, S99. doi:10.1016/s0090-8258(21)00831-3

Norden, A. D., Schiff, D., Ahluwalia, M. S., Lesser, G. J., Nayak, L., Lee, E. Q., et al. (2015). Phase II trial of triple tyrosine kinase receptor inhibitor nintedanib in recurrent high-grade gliomas. *J. Neurooncol.* 121, 297–302. doi:10.1007/s11060-014-1631-y

Noren, N. K., Lu, M., Freeman, A. L., Koolpe, M., and Pasquale, E. B. (2004). Interplay between EphB4 on tumor cells and vascular ephrin-B2 regulates tumor growth. *Proc. Natl. Acad. Sci. U. S. A.* 101, 5583–5588. doi:10.1073/pnas.0401381101

Numnum, T. M., Rocconi, R. P., Whitworth, J., and Barnes, M. N. (2006). The use of bevacizumab to palliate symptomatic ascites in patients with refractory ovarian carcinoma. *Gynecol. Oncol.* 102, 425–428. doi:10.1016/j.ygyno.2006.05.018

Ogawa, K., Pasqualini, R., Lindberg, R. A., Kain, R., Freeman, A. L., and Pasquale, E. B. (2000). The ephrin-A1 ligand and its receptor, EphA2, are expressed during tumor neovascularization. *Oncogene* 19, 6043–6052. doi:10.1038/sj.onc.1204004

Ostman, A. (2017). PDGF receptors in tumor stroma: Biological effects and associations with prognosis and response to treatment. *Adv. Drug Deliv. Rev.* 121, 117–123. doi:10.1016/j.addr.2017.09.022

Oyama, T., Ran, S., Ishida, T., Nadaf, S., Kerr, L., Carbone, D. P., et al. (1998). Vascular endothelial growth factor affects dendritic cell maturation through the inhibition of nuclear factor-kappa B activation in hemopoietic progenitor cells. *J. Immunol.* 160, 1224–1232. doi:10.4049/jimmunol.160.3.1224

Papa, A., Zaccarelli, E., Caruso, D., Vici, P., Benedetti Panici, P., and Tomao, F. (2016). Targeting angiogenesis in endometrial cancer - new agents for tailored treatments. *Expert Opin. Investig. Drugs* 25, 31–49. doi:10.1517/13543784.2016.1116517

Papadopoulos, N., and Lennartsson, J. (2018). The PDGF/PDGFR pathway as a drug target. *Mol. Asp. Med.* 62, 75–88. doi:10.1016/j.mam.2017.11.007

Patch, A. M., Christie, E. L., Etemadmoghadam, D., Garsed, D. W., George, J., Fereday, S., et al. (2015). Whole-genome characterization of chemoresistant ovarian cancer. *Nature* 521, 489–494. doi:10.1038/nature14410

Pennington, K. P., and Swisher, E. M. (2012). Hereditary ovarian cancer: Beyond the usual suspects. *Gynecol. Oncol.* 124, 347–353. doi:10.1016/j.ygyno.2011.12.415

Perren, T. J., Swart, A. M., Pfisterer, J., Ledermann, J. A., Pujade-Lauraine, E., Kristensen, G., et al. (2011). A phase 3 trial of bevacizumab in ovarian cancer. *N. Engl. J. Med.* 365, 2484–2496. doi:10.1056/nejmoa1103799

Peterson, T. E., Kirkpatrick, N. D., Huang, Y., Farrar, C. T., Marijt, K. A., Kloepper, J., et al. (2016). Dual inhibition of Ang-2 and VEGF receptors normalizes tumor vasculature and prolongs survival in glioblastoma by altering macrophages. *Proc. Natl. Acad. Sci. U. S. A.* 113, 4470–4475. doi:10.1073/pnas.1525349113

Pietras, K., Pahler, J., Bergers, G., and Hanahan, D. (2008). Functions of paracrine PDGF signaling in the proangiogenic tumor stroma revealed by pharmacological targeting. *PLoS Med.* 5, e19. doi:10.1371/journal.pmed.0050019

Pignata, S., Lorusso, D., Joly, F., Gallo, C., Colombo, N., Sessa, C., et al. (2021). Carboplatin-based doublet plus bevacizumab beyond progression versus carboplatin-based doublet alone in patients with platinum-sensitive ovarian cancer: A randomised, phase 3 trial. *Lancet Oncol.* 22, 267–276. doi:10.1016/S1470-2045(20)30637-9

Plummer, R., Madi, A., Jeffels, M., Richly, H., Nokay, B., Rubin, S., et al. (2013). A Phase I study of pazopanib in combination with gemcitabine in patients with advanced solid tumors. *Cancer Chemother. Pharmacol.* 71, 93–101. doi:10.1007/s00280-012-1982-z

Polcher, M., Eckhardt, M., Coch, C., Wolfgarten, M., Kubler, K., Hartmann, G., et al. (2010). Sorafenib in combination with carboplatin and paclitaxel as neoadjuvant chemotherapy in patients with advanced ovarian cancer. *Pharmacol* 66, 203–207. doi:10.1007/s00280-010-1276-2

Poluzzi, C., Iozzo, R. V., and Schaefer, L. (2016). Endostatin and endorepellin: A common route of action for similar angiostatic cancer avengers. *Adv. Drug Deliv. Rev.* 97, 156–173. doi:10.1016/j.addr.2015.10.012

Poveda, A. M., Selle, F., Hilpert, F., Reuss, A., Savarese, A., Vergote, I., et al. (2015). Bevacizumab combined with weekly paclitaxel, pegylated liposomal doxorubicin, or topotecan in platinum-resistant recurrent ovarian cancer: Analysis by chemotherapy cohort of the randomized phase III AURELIA trial. *J. Clin. Oncol.* 33, 3836–3838. doi:10.1200/JCO.2015.63.1408

Pranjol, M. Z. I., Zinovkin, D. A., Maskell, A. R. T., Stephens, L. J., Achinovich, S. L., Los, D. M., et al. (2019). Cathepsin L-induced galectin-1 may act as a proangiogenic factor in the metastasis of high-grade serous carcinoma. *J. Transl. Med.* 17, 216. doi:10.1186/s12967-019-1963-7

Presta, M., Dell'Era, P., Mitola, S., Moroni, E., Ronca, R., and Rusnati, M. (2005). Fibroblast growth factor/fibroblast growth factor receptor system in angiogenesis. *Cytokine Growth Factor Rev.* 16, 159–178. doi:10.1016/j.cytogfr.2005.01.004

Previs, R. A., Bevis, K. S., Huh, W., Tillmanns, T., Perry, L., Moore, K., et al. (2014). A prognostic nomogram to predict overall survival in women with recurrent ovarian cancer treated with bevacizumab and chemotherapy. *Gynecol. Oncol.* 132, 531–536. doi:10.1016/j.ygyno.2014.01.036

Pujade-Lauraine, E., Fujiwara, K., Ledermann, J. A., Oza, A. M., Kristeleit, R., Ray-Coquard, I. L., et al. (2021). Avelumab alone or in combination with chemotherapy versus chemotherapy alone in platinum-resistant or platinum-refractory ovarian cancer (JAVELIN ovarian 200): An open-label, three-arm, randomised, phase 3 study. *Lancet Oncol.* 22, 1034–1046. doi:10.1016/s1470-2045(21)00216-3

Pujade-Lauraine, E., Hilpert, F., Weber, B., Reuss, A., Poveda, A., Kristensen, G., et al. (2012). Aurelia: A randomized phase III trial evaluating bevacizumab (BEV) plus chemotherapy (CT) for platinum (PT)-resistant recurrent ovarian cancer. *OC)* 30, LBA5002.

Pujade-Lauraine, E., Hilpert, F., Weber, B., Reuss, A., Poveda, A., Kristensen, G., et al. (2014). Bevacizumab combined with chemotherapy for platinum-resistant recurrent ovarian cancer: The AURELIA open-label randomized phase III trial. *J. Clin. Oncol.* 32, 1302–1308. doi:10.1200/JCO.2013.51.4489

Ramasubbaiah, R., Perkins, S. M., Schilder, J., Whalen, C., Johnson, C. S., Callahan, M., et al. (2011). Sorafenib in combination with weekly topotecan in recurrent ovarian cancer, a phase I/II study of the Hoosier Oncology Group. *Gynecol. Oncol.* 123, 499–504. doi:10.1016/j.ygyno.2011.08.033

Ray-Coquard, I., Cibula, D., Mirza, M. R., Reuss, A., Ricci, C., Colombo, N., et al. (2020). Final results from GCIG/ENGOT/AGO-OVAR 12, a randomised placebo-controlled phase III trial of nintedanib combined with chemotherapy for newly diagnosed advanced ovarian cancer. *Int. J. Cancer* 146, 439–448. doi:10.1002/ijc.32606

Reinthaller, A. (2016). Antiangiogenic therapies in ovarian cancer. *Memo* 9, 139–143. doi:10.1007/s12254-016-0282-4

Reiss, Y., Knedla, A., Tal, A. O., Schmidt, M. H. H., Jugold, M., Kiessling, F., et al. (2009). Switching of vascular phenotypes within a murine breast cancer model induced by angiopoietin-2. *J. Pathol.* 217, 571–580. doi:10.1002/path.2484

Ribeiro, A. R. G., Salvadori, M. M., de Brot, L., Bovolin, G., Mantoan, H., Ilelis, F., et al. (2021). Retrospective analysis of the role of cyclin E1 overexpression as a predictive

marker for the efficacy of bevacizumab in platinum-sensitive recurrent ovarian cancer. *Ecancermedicalscience* 15, 1262. doi:10.3332/ecancer.2021.1262

Rigamonti, N., Kadioglu, E., Keklikoglou, I., Wyser Rmili, C., Leow, C. C., and De Palma, M. (2014). Role of angiopoietin-2 in adaptive tumor resistance to VEGF signaling blockade. *Cell Rep.* 8, 696–706. doi:10.1016/j.celrep.2014.06.059

Rini, B. I., Michaelson, M. D., Rosenberg, J. E., Bukowski, R. M., Sosman, J. A., Stadler, W. M., et al. (2008). Antitumor activity and biomarker analysis of sunitinib in patients with bevacizumab-refractory metastatic renal cell carcinoma. *J. Clin. Oncol.* 26, 3743–3748. doi:10.1200/JCO.2007.15.5416

Robelin, P., Tod, M., Colomban, O., Lachuer, J., Ray-Coquard, I., Rauglaudre, G., et al. (2020). Comparative analysis of predictive values of the kinetics of 11 circulating miRNAs and of CA125 in ovarian cancer during first line treatment (a GINECO study). *Gynecol. Oncol.* 159, 256–263. doi:10.1016/j.ygyno.2020.07.021

Ronca, R., Giacomini, A., Rusnati, M., and Presta, M. (2015). The potential of fibroblast growth factor/fibroblast growth factor receptor signaling as a therapeutic target in tumor angiogenesis. *Expert Opin. Ther. Targets* 19, 1361–1377. doi:10.1517/14728222.2015.1062475

Ruscito, I., Gasparri, M. L., Marchetti, C., De Medici, C., Bracchi, C., Palaia, I., et al. (2016). Cediranib in ovarian cancer: State of the art and future perspectives. *Tumour Biol.* 37, 2833–2839. doi:10.1007/s13277-015-4781-4

Salgado, R., Benoy, I., Weytjens, R., Van Bockstaele, D., Van Marck, E., Huget, P., et al. (2002). Arterio-venous gradients of IL-6, plasma and serum VEGF and D-dimers in human cancer. *Br. J. Cancer* 87, 1437–1444. doi:10.1038/sj.bjc.6600655

Sallinen, H., Heikura, T., Koponen, J., Kosma, V. M., Heinonen, S., Yla-Herttuala, S., et al. (2014). Serum angiopoietin-2 and soluble VEGFR-2 levels predict malignancy of ovarian neoplasm and poor prognosis in epithelial ovarian cancer. *BMC Cancer* 14, 696. doi:10.1186/1471-2407-14-696

Sallinen, H., Heikura, T., Laidinen, S., Kosma, V. M., Heinonen, S., Yla-Herttuala, S., et al. (2010). Preoperative angiopoietin-2 serum levels: A marker of malignant potential in ovarian neoplasms and poor prognosis in epithelial ovarian cancer. *Int. J. Gynecol. Cancer* 20, 1498–1505. doi:10.1111/IGC.0b013e3181f936e3

Sawada, K., Radjabi, A. R., Shinomiya, N., Kistner, E., Kenny, H., Becker, A. R., et al. (2007). c-Met overexpression is a prognostic factor in ovarian cancer and an effective target for inhibition of peritoneal dissemination and invasion. *Cancer Res.* 67, 1670–1679. doi:10.1158/0008-5472.CAN-06-1147

Sawamiphak, S., Seidel, S., Essmann, C. L., Wilkinson, G. A., Pitulescu, M. E., Acker, T., et al. (2010). Ephrin-B2 regulates VEGFR2 function in developmental and tumour angiogenesis. *Nature* 465, 487–491. doi:10.1038/nature08995

Scharpfenecker, M., Fiedler, U., Reiss, Y., and Augustin, H. G. (2005). The Tie-2 ligand angiopoietin-2 destabilizes quiescent endothelium through an internal autocrine loop mechanism. *J. Cell Sci.* 118, 771–780. doi:10.1242/jcs.01653

Schwandt, A., von Gruenigen, V. E., Wenham, R. M., Frasure, H., Eaton, S., Fusco, N., et al. (2014). Randomized phase II trial of sorafenib alone or in combination with carboplatin/paclitaxel in women with recurrent platinum sensitive epithelial ovarian, peritoneal, or fallopian tube cancer. *Invest. New Drugs* 32, 729–738. doi:10.1007/s10637-014-0078-5

Seaman, S., Stevens, J., Yang, M. Y., Logsdon, D., Graff-Cherry, C., and St Croix, B. (2007). Genes that distinguish physiological and pathological angiogenesis. *Cancer Cell* 11, 539–554. doi:10.1016/j.ccr.2007.04.017

Secord, A. A., McCollum, M., Davidson, B. A., Broadwater, G., Squatrito, R., Havrilesky, L. J., et al. (2019). Phase II trial of nintedanib in patients with bevacizumab-resistant recurrent epithelial ovarian, tubal, and peritoneal cancer. *Gynecol. Oncol.* 153, 555–561. doi:10.1016/j.ygyno.2019.03.246

Sharma, R., Valls, P. O., Inglese, M., Dubash, S., Chen, M., Gabra, H., et al. (2020). [(18)F]Fluciclatide PET as a biomarker of response to combination therapy of pazopanib and paclitaxel in platinum-resistant/refractory ovarian cancer. *Eur. J. Nucl. Med. Mol. Imaging* 47, 1239–1251. doi:10.1007/s00259-019-04532-z

Shimada, C., Xu, R., Al-Alem, L., Stasenko, M., Spriggs, D. R., and Rueda, B. R. (2020). Galectins and ovarian cancer. *Cancers (Basel)* 12 (6), 1421. doi:10.3390/cancers12061421a

Shojaei, F., Lee, J. H., Simmons, B. H., Wong, A., Esparza, C. O., Plumlee, P. A., et al. (2010). HGF/c-Met acts as an alternative angiogenic pathway in sunitinib-resistant tumors. *Cancer Res.* 70, 10090–10100. doi:10.1158/0008-5472.CAN-10-0489

Song, Y., Fu, Y., Xie, Q., Zhu, B., Wang, J., and Zhang, B. (2020). Anti-angiogenic agents in combination with immune checkpoint inhibitors: A promising strategy for cancer treatment. *Front. Immunol.* 11, 1956. doi:10.3389/fimmu.2020.01956

Sorli, S. C., Le Gonidec, S., Knibiehler, B., and Audigier, Y. (2007). Apelin is a potent activator of tumour neoangiogenesis. *Oncogene* 26, 7692–7699. doi:10.1038/sj.onc.1210573

Sorli, S. C., van den Berghe, L., Masri, B., Knibiehler, B., and Audigier, Y. (2006). Therapeutic potential of interfering with apelin signalling. *Drug Discov. Today* 11, 1100–1106. doi:10.1016/j.drudis.2006.10.011

Sostelly, A., and Mercier, F. (2019). Tumor size and overall survival in patients with platinum-resistant ovarian cancer treated with chemotherapy and bevacizumab. *Clin. Med. Insights Oncol.* 13, 1179554919852071. doi:10.1177/1179554919852071

Spiliotaki, M., Markomanolaki, H., Mela, M., Mavroudis, D., Georgoulias, V., and Agelaki, S. (2011). Targeting the insulin-like growth factor I receptor inhibits proliferation and VEGF production of non-small cell lung cancer cells and enhances paclitaxel-mediated anti-tumor effect. *Lung Cancer* 73, 158–165. doi:10.1016/j.lungcan.2010.11.010

Steele, I. A., Edmondson, R. J., Bulmer, J. N., Bolger, B. S., Leung, H. Y., and Davies, B. R. (2001). Induction of FGF receptor 2-IIIb expression and response to its ligands in epithelial ovarian cancer. *Oncogene* 20, 5878–5887. doi:10.1038/sj.onc.1204755

Steffensen, K. D., Madsen, C. V., Andersen, R. F., Waldstrom, M., Adimi, P., and Jakobsen, A. (2014). Prognostic importance of cell-free DNA in chemotherapy resistant ovarian cancer treated with bevacizumab. *Eur. J. Cancer* 50, 2611–2618. doi:10.1016/j.ejca.2014.06.022

Sun, S., Dong, H., Yan, T., Li, J., Liu, B., Shao, P., et al. (2020). Role of TSP-1 as prognostic marker in various cancers: A systematic review and meta-analysis. *BMC Med. Genet.* 21, 139. doi:10.1186/s12881-020-01073-3

Tait, C. R., and Jones, P. F. (2004). Angiopoietins in tumours: The angiogenic switch. *J. Pathol.* 204, 1–10. doi:10.1002/path.1618

Takahashi, T., Yamaguchi, S., Chida, K., and Shibuya, M. (2001). A single autophosphorylation site on KDR/Flk-1 is essential for VEGF-A-dependent activation of PLC-gamma and DNA synthesis in vascular endothelial cells. *EMBO J.* 20, 2768–2778. doi:10.1093/emboj/20.11.2768

Thurston, G., Rudge, J. S., Ioffe, E., Zhou, H., Ross, L., Croll, S. D., et al. (2000). Angiopoietin-1 protects the adult vasculature against plasma leakage. *Nat. Med.* 6, 460–463. doi:10.1038/74725

Tolkach, Y., Ellinger, J., Kremer, A., Esser, L., Muller, S. C., Stephan, C., et al. (2019). Apelin and apelin receptor expression in renal cell carcinoma. *Br. J. Cancer* 120, 633–639. doi:10.1038/s41416-019-0396-7

Topalian, S. L., Taube, J. M., Anders, R. A., and Pardoll, D. M. (2016). Mechanism-driven biomarkers to guide immune checkpoint blockade in cancer therapy. *Nat. Rev. Cancer* 16, 275–287. doi:10.1038/nrc.2016.36

Troncoso, M. F., Ferragut, F., Bacigalupo, M. L., Cardenas Delgado, V. M., Nugnes, L. G., Gentilini, L., et al. (2014). Galectin-8: A matricellular lectin with key roles in angiogenesis. *Glycobiology* 24, 907–914. doi:10.1093/glycob/cwu054

Tuppurainen, L., Sallinen, H., Karvonen, A., Valkonen, E., Laakso, H., Liimatainen, T., et al. (2017). Combined gene therapy using AdsVEGFR2 and AdsTie2 with chemotherapy reduces the growth of human ovarian cancer and formation of ascites in mice. *Int. J. Gynecol. Cancer* 27, 879–886. doi:10.1097/IGC.0000000000000973

Turner, N., and Grose, R. (2010). Fibroblast growth factor signalling: From development to cancer. *Nat. Rev. Cancer* 10, 116–129. doi:10.1038/nrc2780

Uhl, C., Markel, M., Broggini, T., Nieminen, M., Kremenetskaia, I., Vajkoczy, P., et al. (2018). EphB4 mediates resistance to antiangiogenic therapy in experimental glioma. *Angiogenesis* 21, 873–881. doi:10.1007/s10456-018-9633-6

van Hinsbergh, V. W., and Koolwijk, P. (2008). Endothelial sprouting and angiogenesis: Matrix metalloproteinases in the lead. *Cardiovasc. Res.* 78, 203–212. doi:10.1093/cvr/cvm102

Varga, A., Piha-Paul, S., Ott, P. A., Mehnert, J. M., Berton-Rigaud, D., Morosky, A., et al. (2019). Pembrolizumab in patients with programmed death ligand 1-positive advanced ovarian cancer: Analysis of KEYNOTE-028. *Gynecol. Oncol.* 152, 243–250. doi:10.1016/j.ygyno.2018.11.017

Vergote, I. B., Smith, D. C., Berger, R., Kurzrock, R., Vogelzang, N. J., Sella, A., et al. (2017). A phase 2 randomised discontinuation trial of cabozantinib in patients with ovarian carcinoma. *Eur. J. Cancer* 83, 229–236. doi:10.1016/j.ejca.2017.06.018

Vergote, I., du Bois, A., Floquet, A., Rau, J., Kim, J. W., Del Campo, J. M., et al. (2019). Overall survival results of AGO-OVAR16: A phase 3 study of maintenance pazopanib versus placebo in women who have not progressed after first-line chemotherapy for advanced ovarian cancer. *Gynecol. Oncol.* 155, 186–191. doi:10.1016/j.ygyno.2019.08.024

Vergote, I., Scambia, G., O'Malley, D. M., Van Calster, B., Park, S. Y., Del Campo, J. M., et al. (2019). Trebananib or placebo plus carboplatin and paclitaxel as first-line treatment for advanced ovarian cancer (TRINOVA-3/ENGOT-ov2/GOG-3001): A randomised, double-blind, phase 3 trial. *Lancet Oncol.* 20, 862–876. doi:10.1016/S1470-2045(19)30178-0

Viallard, C., and Larrivee, B. (2017). Tumor angiogenesis and vascular normalization: Alternative therapeutic targets. *Angiogenesis* 20, 409–426. doi:10.1007/s10456-017-9562-9

Wang, J. Y., Sun, T., Zhao, X. L., Zhang, S. W., Zhang, D. F., Gu, Q., et al. (2008). Functional significance of VEGF-a in human ovarian carcinoma: Role in vasculogenic mimicry. *Cancer Biol. Ther.* 7, 758–766. doi:10.4161/cbt.7.5.5765

Wang, Y., Nakayama, M., Pitulescu, M. E., Schmidt, T. S., Bochenek, M. L., Sakakibara, A., et al. (2010). Ephrin-B2 controls VEGF-induced angiogenesis and lymphangiogenesis. *Nature* 465, 483–486. doi:10.1038/nature09002

Wang, Y., Thai, T., Moore, K., Ding, K., McMeekin, S., Liu, H., et al. (2016). Quantitative measurement of adiposity using CT images to predict the benefit of bevacizumab-based chemotherapy in epithelial ovarian cancer patients. *Oncol. Lett.* 12, 680–686. doi:10.3892/ol.2016.4648

White, F. C., Benehacene, A., Scheele, J. S., and Kamps, M. (1997). VEGF mRNA is stabilized by ras and tyrosine kinase oncogenes, as well as by UV radiation--evidence for divergent stabilization pathways. *Growth factors.* 14, 199–212. doi:10.3109/08977199709021520

Willett, C. G., Duda, D. G., di Tomaso, E., Boucher, Y., Ancukiewicz, M., Sahani, D. V., et al. (2009). Efficacy, safety, and biomarkers of neoadjuvant bevacizumab, radiation therapy, and fluorouracil in rectal cancer: A multidisciplinary phase II study. *J. Clin. Oncol.* 27, 3020–3026. doi:10.1200/JCO.2008.21.1771

Wu, L., Chen, L., and Li, L. (2017). Apelin/APJ system: A novel promising therapy target for pathological angiogenesis. *Clin. Chim. Acta* 466, 78–84. doi:10.1016/j.cca.2016.12.023

Xie, Y., Su, N., Yang, J., Tan, Q., Huang, S., Jin, M., et al. (2020). FGF/FGFR signaling in health and disease. *Signal Transduct. Target Ther.* 5, 181. doi:10.1038/s41392-020-00222-7

Yu, P., Wilhelm, K., Dubrac, A., Tung, J. K., Alves, T. C., Fang, J. S., et al. (2017). FGF-dependent metabolic control of vascular development. *Nature* 545, 224–228. doi:10.1038/nature22322

Yuan, H. T., Khankin, E. V., Karumanchi, S. A., and Parikh, S. M. (2009). Angiopoietin 2 is a partial agonist/antagonist of Tie2 signaling in the endothelium. *Mol. Cell. Biol.* 29, 2011–2022. doi:10.1128/MCB.01472-08

Zhang, D., Huang, J., Sun, Y., and Guo, Q. (2019). Long-term progression-free survival of apatinib monotherapy for relapsed ovarian cancer: A case report and literature review. *Onco Targets Ther.* 12, 3635–3644. doi:10.2147/OTT.S198946

Zhang, L., Yang, N., Park, J. W., Katsaros, D., Fracchioli, S., Cao, G., et al. (2003). Tumor-derived vascular endothelial growth factor up-regulates angiopoietin-2 in host endothelium and destabilizes host vasculature, supporting angiogenesis in ovarian cancer. *Cancer Res.* 63, 3403–3412.

Zhang, X., and Lawler, J. (2007). Thrombospondin-based antiangiogenic therapy. *Microvasc. Res.* 74, 90–99. doi:10.1016/j.mvr.2007.04.007

Zhang, Y., Wang, H., Oliveira, R. H. M., Zhao, C., and Popel, A. S. (2022). Systems biology of angiogenesis signaling: Computational models and omics. *WIREs Mech. Dis.* 14, e1550. doi:10.1002/wsbm.1550

Zhao, C., Isenberg, J. S., and Popel, A. S. (2018). Human expression patterns: Qualitative and quantitative analysis of thrombospondin-1 under physiological and pathological conditions. *J. Cell. Mol. Med.* 22, 2086–2097. doi:10.1111/jcmm.13565

Zhao, Y., and Adjei, A. A. (2015). Targeting angiogenesis in cancer therapy: Moving beyond vascular endothelial growth factor. *Oncologist* 20, 660–673. doi:10.1634/theoncologist.2014-0465

Zhou, Y., Wu, C., Lu, G., Hu, Z., Chen, Q., and Du, X. (2020). FGF/FGFR signaling pathway involved resistance in various cancer types. *J. Cancer* 11, 2000–2007. doi:10.7150/jca.40531

Glossary

ABCB1 ATP binding cassette subfamily B member 1

ADAM17 a disintegrin and metalloprotease 17

AGP Alpha-1 acid glycoprotein

AKT protein kinase B

ANGPTs angiopoietins

APLN Apelin

APLNR G protein-coupled receptor APJ

BRCA breast cancer susceptibility gene

CA-125 cancer antigen 125

CAFs cancer associated fibroblasts

CBP carboplatin

CCNE1 cyclin E1

c-MET hepatocyte growth factor receptor

CTLA-4 cytotoxic T lymphocyte-associated protein 4

EC endothelial cell

EGFR epidermal growth factor receptor

EMA European Medicines Agency

EOC epithelial ovarian cancer

ERK extracellular signal-regulated kinase

FDA Food and Drug Administration

FGFs fibroblast growth factors

FLT4 fms-like tyrosine kinase-4

HER2 human epidermal growth factor receptor-2

HGF hepatocyte growth factor

HIF-1α hypoxia-inducible factor -1α

IGF-1 insulin-like growth factor 1

IL-6 interleukin 6

ICIs Immune checkpoint inhibitors

IP3 inositol 1,4,5-triphosphate

JAK Janus kinase

Lck lymphocyte-specific protein tyrosine kinase

Lyn tyrosine-protein kinase Lyn

MAPK mitogen-activated protein kinase

MMP-2 mitochondrial membrane potential-2

MSLN Mesothelin

MVD mevalonate diphosphate decarboxylase

NRP1 neuropilin 1; OC, ovarian cancer

OPN osteopontin

ORR overall response rate

OS overall survival

PARP poly (ADP-ribose) polymerase

PDGF platelet-derived growth factor

PD-1 programmed cell death protein

PFS progression-free survival

PI3K phosphatidylinositol 3-kinase

PLC phospsholipase-C

PLC-γ Phospholipase C-γ

PLD pegylated liposomal doxorubicin

PlGF placental growth factor

Pt platinum

RTK receptor tyrosine kinases

RTKi receptor tyrosine kinase inhibitor

Src proto-oncogene tyrosine-protein kinase Src

STAT signal transducing activator of transcription

SUV standardized uptake value

TAMs tumor-associated macrophages

TAXOL paclitaxel

TFI treatment-free interval

TKI tyrosine kinase inhibitor

TPT topotecan

uPA urokinase plasminogen activator

VEGF vascular endothelial growth factor

YKL-40 Chitinase three like 1

Comprehensive bioinformatic analysis constructs a CXCL model for predicting survival and immunotherapy effectiveness in ovarian cancer

Shuang Li[1,2], Dawei Zou[3]* and Zhaoqian Liu[1,2]*

[1]Hunan Key Laboratory of Pharmacogenetics, Department of Clinical Pharmacology, National Clinical Research Center for Geriatric Disorders, Xiangya Hospital, Central South University, Changsha, China, [2]Institute of Clinical Pharmacology, Central South University, Changsha, China, [3]Department of Surgery, Immunobiology and Transplant Science Center, Houston Methodist Research Institute and Institute for Academic Medicine, Houston Methodist Hospital, Houston, TX, United States

Background: Immunotherapy has limited effectiveness in ovarian cancer (OC) patients, highlighting the need for reliable biomarkers to predict the effectiveness of these treatments. The C-X-C motif chemokine ligands (CXCLs) have been shown to be associated with survival outcomes and immunotherapy efficacy in cancer patients. In this study, we aimed to evaluate the predictive value of 16 CXCLs in OC patients.

Methods: We analyzed RNA-seq data from The Cancer Genome Atlas, Gene Expression Omnibus, and UCSC Xena database and conducted survival analysis. Consensus cluster analysis was used to group patients into distinct clusters based on their expression patterns. Biological pathway alterations and immune infiltration patterns were examined across these clusters using gene set variation analysis and single-sample gene set enrichment analysis. We also developed a CXCL scoring model using principal component analysis and evaluated its effectiveness in predicting immunotherapy response by assessing tumor microenvironment cell infiltration, tumor mutational burden estimation, PD-L1/CTLA4 expression, and immunophenoscore analysis (IPS).

Results: Most CXCL family genes were overexpressed in OC tissues compared to normal ovarian tissues. Patients were grouped into three distinct CXCL clusters based on their CXCL expression pattern. Additionally, using differentially expressed genes among the CXCL clusters, patients could also be grouped into three gene clusters. The CXCL and gene subtypes effectively predicted survival and immune cell infiltration levels for OC patients. Furthermore, patients with high CXCL scores had significantly better survival outcomes, higher levels of immune cell infiltration, higher IPS, and higher expression of PD-L1/CTLA4 than those with low CXCL scores.

Conclusion: The CXCL score has the potential to be a promising biomarker to guide immunotherapy in individual OC patients and predict their clinical outcomes and immunotherapy responses.

KEYWORDS

immunotherapy, the C-X-C motif chemokine ligands (CXCLs), tumor microenvironment, ovarian cancer, prognosis

Introduction

Ovarian cancer (OC) is estimated to be the fifth leading cause of cancer-related deaths among women in the United States in 2023 (Siegel et al., 2023). The standard treatment for OC involves radical surgery and chemotherapy (Ledermann et al., 2013), but the 5-year survival rate for OC patients remains low despite these efforts (Oronsky et al., 2017). Immunotherapy has emerged as a promising new approach for treating various types of cancer (Kraehenbuehl et al., 2022). The FDA has approved six types of immune checkpoint inhibitors (ICIs) for cancer therapy since 2011, including targeting cytotoxic T lymphocyte-associated protein 4 (CTLA-4), programmed death-1 (PD-1), and programmed death-ligand 1 (PD-L1) (Hargadon et al., 2018). Although ICIs have shown success in treating several cancers, not all patients with ovarian cancer respond to immunotherapy (Hamanishi et al., 2021; Moore et al., 2021). Therefore, it is critical and urgent to identify new and effective strategies to guide immunotherapy in OC patients, in order to improve their outcomes.

Biomarkers are essential in directing the efficacy of immunotherapy in cancer and enhancing patient outcomes. The use of specific biomarkers can help predict which patients will likely respond positively to immunotherapy, allowing for a tailored treatment plan. One significant biomarker is the expression of specific proteins, such as PD-L1, on the surface of cancer cells. High PD-L1 expression has been linked to improved responses to immunotherapy drugs that target this protein (Patel and Kurzrock, 2015). Another biomarker is the presence of immune cells, known as tumor-infiltrating lymphocytes (TILs), within the tumor tissue. High levels of TILs have also been associated with improved responses to immunotherapy (Presti et al., 2022). Moreover, the genetic composition of the tumor can also impact the response to immunotherapy. For instance, mutations in genes like TP53 have been connected with improved responses to immunotherapy in cancer (Dong et al., 2017). However, the current biomarkers do not fully explain the responses to immunotherapy in OC, and there is a pressing need for more effective biomarkers to guide immunotherapy in this patient population.

C-X-C motif chemokine ligands (CXCLs) are a group of chemical molecules that guide cell migration and are widely associated with tumor progression and response to immunotherapy (Charo and Ransohoff, 2006; Markl et al., 2022). For instance, CXCL1 has been linked to the promotion of cancer cell migration and the progression of gastric cancer (Wang et al., 2017) and breast cancer metastasis (Wang et al., 2018). On the other hand, CXCL8 is a target for solid tumor immunotherapy (Dominguez et al., 2017), and CXCL9/10 has been demonstrated to enhance the accumulation of effector T cells at the tumor site and suppress tumor growth (Karin, 2020). In ovarian cancer, high levels of CXCL1 expression have been found to promote cancer progression by inducing cell proliferation (Bolitho et al., 2010), whereas CXCL9 has been shown to potentiate anti-tumor activity and drive a positive response to anti-PD-L1 therapy (Seitz et al., 2022). Despite these findings, the systematic predictive value of CXCLs in terms of overall survival and response to immunotherapy in individual OC patients remains unclear.

Our study aimed to systematically evaluate the role of CXCLs in OC prognosis and immunotherapy. We found that most of the CXCL family genes were overexpressed in OC compared to normal tissues, and were independent predictors of patient outcomes. Based on the expression levels of CXCLs, OC patients were grouped into three distinct CXCL patterns or gene clusters, each with a distinct relationship to patient outcome and immune cell infiltration. Additionally, we developed a CXCL scoring model using principal component analysis (PCA), which accurately predicted the prognosis and immunotherapy response of individual patients with OC. Patients with high CXCL scores had improved survival, increased immune cell infiltration, and a higher sensitivity to immunotherapy.

Materials and methods

Data download and processing

To assess the expression of CXCLs in normal and OC tissues, we collected 88 normal ovary samples and 427 ovarian cancer samples with normalized TPM (transcripts per kilobase million) from the UCSC Xena database (https://xena.ucsc.edu/). The gene transcription data and clinical information of OC were obtained from The Cancer Genome Atlas (TCGA) (https://portal.gdc.cancer.gov/) and Gene Expression Omnibus (GEO) (https://www.ncbi.nlm.nih.gov/geo/) databases, which were merged into a TCGA-GEO matrix (totaling 758 samples) after adjusting for batch effects using the "SVA" R package. We used the "limma" R package to compare the expression levels of CXCLs between normal and OC tissues. Information on copy number and somatic mutations was also obtained from the UCSC Xena database for generating Circos plots with the "RCircos" R package and calculating the tumor mutational burden (TMB) with the "maftools" R package. Survival analysis was conducted using Cox regression analysis and Kaplan–Meier (KM) methods, statistical significance was defined as a p-value less than 0.1 for Cox regression analysis and less than 0.05 for Kaplan-Meier methods.

Consensus cluster analysis to build clusters based on the expression of CXCLs

We used consensus cluster analysis to group the TCGA-GEO cohort based on the expression levels of the 16 CXCLs, with the help of the "ConsensusClusterPlus" R package (Wilkerson and Hayes, 2010). The analysis showed that grouping the samples into three clusters (k = 3) had the best association of intra-typical samples, a low coefficient of variation, and an adequate sample size for each cluster. The fitness of the classification was evaluated using Principal Component Analysis (PCA) (Ringner, 2008). A heatmap of the CXCL expression levels among the three CXCL clusters and their corresponding clinical features was generated using the "pheatmap" R package.

Gene set variation analysis (GSVA) of three CXCL clusters

To understand the distinct biological pathways associated with the three CXCL clusters, we conducted gene set variation analysis

(GSVA) using the "GSVA" R package (Hanzelmann et al., 2013). The "c2. cp.kegg.v2022.1. Hs.symbols" gene set was obtained from the GSEA website (https://www.gsea-msigdb.org) and used to analyze the enrichment of gene sets in each of the three CXCL clusters. This analysis aimed to provide insights into the biological processes that may contribute to the observed differences in CXCL expression between the three clusters. The top 20 enriched pathways were visualized in a heatmap, with adjusted p-values less than 0. 05 considered significant.

Infiltration levels of immune cells

The tumor microenvironment (TME) infiltration immune cell type was defined by Zhang et al. (2020). The relative infiltration levels of each type of immune cell in each sample were calculated using the single-sample gene set enrichment analysis (ssGSEA) (Subramanian et al., 2005). The enrichment score represented the enrichment of each type of immune cell in the sample. The correlation between the CXCL score and each type of infiltration immune cell was analyzed using the "corrplot" R package.

Differentially expressed genes analysis among CXCL patterns

To identify the differentially expressed genes (DEGs) among the three CXCL patterns, a differentially expressed genes analysis was performed using the "limma" R package on the normalized TPM data of 758 ovarian cancer patients from the three CXCL clusters (Smyth, 2004). A significance threshold of adjusted p-value <0.001 was applied to filter DEGs. As a result, 3811 DEGs were identified between CXCL clusters A and B, 552 DEGs between CXCL clusters A and C, 1941 DEGs between CXCL clusters B and C, and 244 shared DEGs. The results of differentially expressed genes analysis were visualized using Venn diagrams generated by the "VennDiagram" R package. The shared DEGs were further evaluated for their potential biological functions using Gene Ontology (GO) (Ashburner et al., 2000) and Kyoto Encyclopedia of Genes and Genomes (KEGG) pathway enrichment analysis (Kanehisa and Goto, 2000). A univariate Cox regression analysis was conducted to identify shared survival related DEGs, and a significance threshold of $p < 0.05$ was applied. Based on the expression levels of shared survival related DEGs, the TCGA-GEO cohort was grouped into three gene clusters using consensus cluster analysis. The expression of shared survival related DEGs in the three gene clusters was visualized using the "pheatmap" R package, and the "limma" R package was used to analyze the expression profiles of 16 CXCLs among the three gene subtypes.

Differences in survival among CXCL clusters, gene clusters, or CXCL score model

For survival analysis, patients with missing follow-up information were excluded. The probability of survival was compared across CXCL clusters, gene clusters, and CXCL score groups, respectively, using the "survival" and "survminer" R packages. The assessment of the survival curves was performed through the Kaplan-Meier method and log-rank tests.

Estimating tumor mutational burden (TMB)

The tumor mutational burden (TMB) is calculated as the number of mutated bases per million bases. The simple nucleotide variations of OC patients were obtained from the TCGA database and processed using Practical Extraction and Report Language (Perl) version 5.30.0. The patients were divided into two groups, high TMB and low TMB, based on the optimal cutoff value of TMB. Survival analysis was performed to compare the prognosis between the high and low TMB groups and to assess the impact of TMB on prognosis when combined with CXCL scores.

Immunophenoscore (IPS) analysis in the CXCL score model

Charoentong et al. introduced the Immune Prediction Score (IPS), which is used to predict a patient's response to checkpoint blockade in cancer (Charoentong et al., 2017). The clinical data and IPS for OC patients were obtained from The Cancer Immunome Atlas (https://tcia.at/). In this study, the IPS was analyzed to evaluate the effectiveness of immunotherapy in OC patients with high and low CXCL scores.

Construct a CXCL score model

To evaluate the predictive value of CXCLs in individual patients, we developed a CXCL score model based on the expression levels of the shared survival related DEGs among the three CXCL clusters. The CXCL score was calculated by summing the signature scores, which were extracted from the PCA as the first and second principal components (PC1 and PC2). The formula for defining the CXCL score is as follows (Ringner, 2008).

$$CXCL\ score = \sum (PC1_i + PC2_i)$$

Where "i" represents the expression levels of the shared survival related DEGs among the three CXCL clusters.

Statistical analysis

Statistical analyses were conducted using R software version 4.2.1. The Student's t-test or Wilcoxon rank-sum test was applied to evaluate the distribution of variables. The Log-rank test or Kruskal-Wallis test was used to compare data between two or more groups, respectively. Correlations between two variables were analyzed using Pearson or Spearman correlation analysis. The "survival" R package was used to subgroup samples. Kaplan-Meier survival analysis and univariate Cox regression analysis were performed using the "survminer" package.
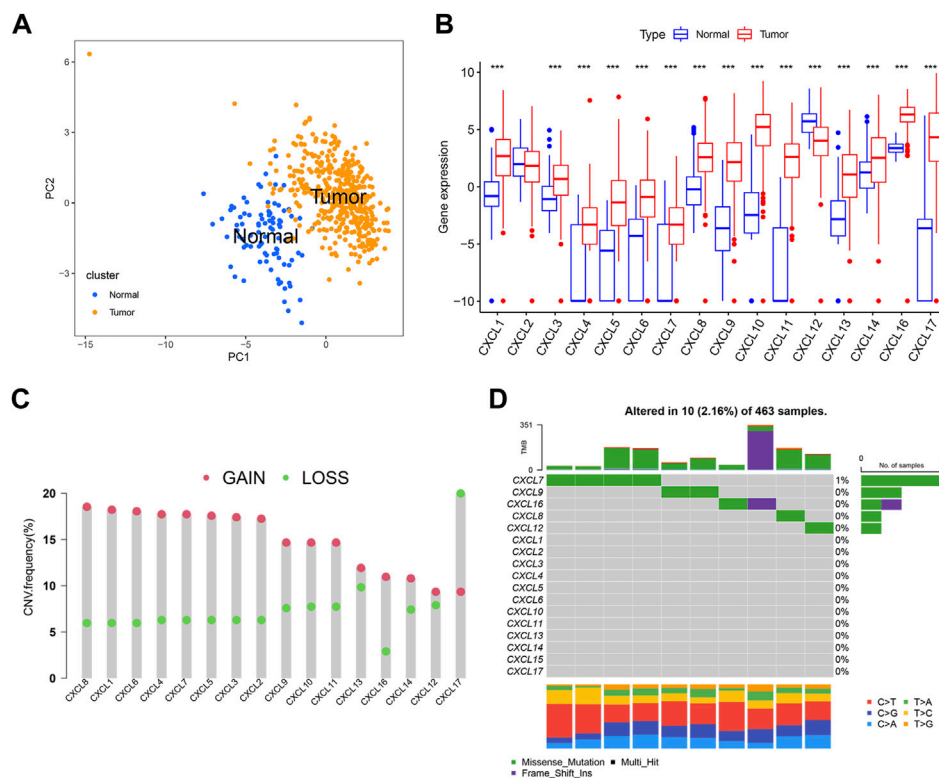
FIGURE 1
Characteristics of CXCLs in OC. **(A)** The PCA plots demonstrate a clear distinction between normal and OC tissue, with blue dots representing normal tissue and yellow dots representing tumor tissue. **(B)** The box plots depict the mRNA expression (log2 x + 1) profiles of 16 CXCLs in normal and OC tissue. ***p < 0.001. **(C)** The CNV frequency of CXCLs in TCGA-OC is illustrated by the height of the column, with red dots representing an increase in frequency and green dots representing a decrease in frequency. **(D)** The somatic mutation rate of CXCL family genes in TCGA-OC patients. The bottom bar graph represents mutation transformation.

Results

The characteristics of CXCLs in OC

To investigate the characteristics of CXCLs in OC, we compared the expression levels of 16 CXCL family genes between normal ovarian tissues and OC tissues using the UCSC Xena and TCGA databases. The PCA results showed that the gene expression profiles of normal and OC tissue were different (Figure 1A). Among the CXCLs, mRNA levels of CXCL1, CXCL3, CXCL4, CXCL5, CXCL6, CXCL7, CXCL8, CXCL9, CXCL10, CXCL11, CXCL13, CXCL14, and CXCL16 were upregulated in OC, while the expression of CXCL12 was significantly higher in normal ovarian tissue (Figure 1B). We also analyzed copy number variation (CNV) and somatic mutation frequency of the CXCL family genes using the TCGA-OC cohort. Figure 1C shows that, for most CXCLs (excluding CXCL17), the frequency of gain copy number was higher than that of lost copy number (Figure 1C). CXCL family genes (CXCL7, CXCL9, CXCL16, CXCL6, and CXCL12) showed somatic mutation events in 10 of 463 TCGA-OC samples, with CXCL7 exhibiting the highest mutation frequency (4/463) (Figure 1D).

The prognostic value of CXCLs in OC

To assess the prognostic value of individual CXCL family genes in OC patients, we performed Kaplan-Meier (K-M) survival analysis and univariate Cox regression analysis using the TCGA and GSE140082 databases. The K-M curve showed that the expression levels of CXCL4, CXCL6, CXCL7, CXCL12, and CXCL14 were associated with worse survival outcomes (Figures 2B, D, E, J, L), while the expression levels of CXCL2, CXCL5, CXCL8, CXCL9, CXCL10, CXCL11, and CXCL13 were correlated with better overall survival (OS) of patients (Figures 2A, C, F–I, K). Univariate Cox regression analysis also showed that 5 CXCL family genes (CXCL9, CXCL10, CXCL11, CXCL13, and CXCL14) were single risk factors for the OS of patients (Supplementary Table S1). These results suggest that CXCL9, CXCL10, CXCL11, CXCL13, and CXCL14 could be used as potential prognostic biomarkers for OC patients.

CXCLs expression-based subtypes in OC patients

To understand the role of CXCLs in OC, patients from the TCGA-OC and GSE140082 cohorts were combined and grouped
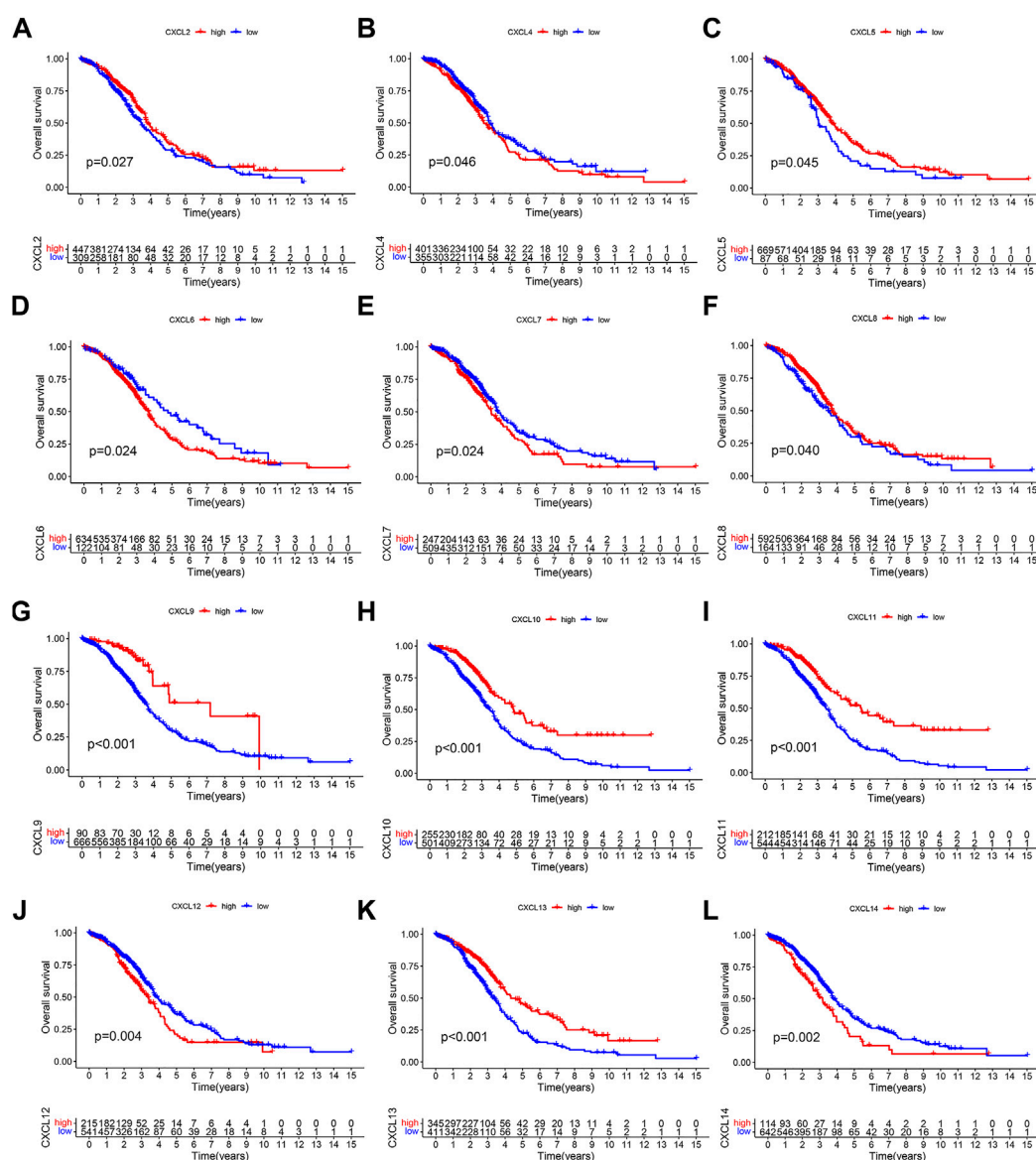
FIGURE 2
The prognostic significance of CXCLs in OC. Kaplan-Meier curve displays the difference in overall survival between patients with high and low expression levels of **(A)** CXCL2, **(B)** CXCL4, **(C)** CXCL5, **(D)** CXCL6, **(E)** CXCL7, **(F)** CXCL8, **(G)** CXCL9, **(H)** CXCL10, **(I)** CXCL11, **(J)** CXCL12, **(K)** CXCL13, and **(L)** CXCL14. All data are derived from TCGA-OC and GSE140082 datasets.

into multiple patterns based on the similarity of CXCL family member expressions using consensus cluster analysis. The analysis identified three subgroups based on the lack of significant increase in the area under the cumulative distribution function (CDF) curve and the clear boundaries observed between the subgroups (Figures 3A, B). The differences among the subclasses were further evaluated using PCA, which revealed that CXCL clusters A, B, and C were significantly distinct from each other (Figure 3C). The heatmap showed that CXCL family genes were upregulated in CXCL cluster A and downregulated in CXCL cluster B (Figure 3D). In cluster C, some CXCL genes were upregulated while others were downregulated (Figure 3D).

To gain further insights into the biological differences among the three CXCL clusters, Gene Set Variation Analysis (GSVA) was performed. Results indicated that CXCL cluster C was mainly associated with immune responses, such as regulating the T cell receptor and Toll-like receptor signaling pathways (Figure 3E,Supplementary Figures S1A, B). A survival analysis was also conducted on patients in each CXCL cluster. The results showed that patients in CXCL cluster C had a better overall survival rate compared to those in CXCL cluster A and B ($p < 0.001$) (Figure 3F). Single-sample gene set enrichment analysis (ssGSEA) revealed a significantly higher infiltration of immune cells in CXCL cluster C compared to CXCL clusters A and B, which may explain the better survival outcomes of patients in CXCL cluster C compared to CXCL clusters A and B (Figure 3G). Therefore, OC patients can be successfully divided into three subtypes based on the similarity of CXCLs expression.

FIGURE 3
CXCLs expression-based subtypes of OC patients. **(A,B)** Consensus clustering analysis was performed based on the expression of CXCLs. The consensus cumulative distribution function (CDF) from k = 2 to 9 is shown in **(A)**, and the heatmap of the consensus matrix (k = 3) is shown in **(B)**. **(C)** PCA plots of the three CXCL subtypes. Blue dots represent CXCL cluster A, yellow dots represent CXCL cluster B, and red dots represent CXCL cluster C. **(D)** The mRNA expression of 16 CXCLs in the three subtypes is shown in a heatmap. **(E)** A heatmap shows the results of KEGG pathway enrichment analysis between CXCL clusters B and C. **(F)** The Kaplan-Meier curve displays the outcome of patients in the three CXCL subtypes. **(G)** Box plots display the level of immune cell infiltration in the three CXCL subtypes. ***$p < 0.001$.

Identification of three gene clusters based on the expression patterns of DEGs among three CXCL clusters

To further examine the biological significance of the CXCLs, 244 shared DEGs were identified across the three CXCL subtypes (Figure 4A). These shared DEGs were found to be enriched in several immune cell-related pathways, such as T cell differentiation (Figures 4B, C; Supplementary Figures 2A, B), and 94 DEGs were significantly associated with the OS of patients (Supplementary Table S2). Patients were then divided into three gene clusters based on these 94 OS-related shared DEGs (Supplementary Figures 3A, B). The Kaplan-Meier curve showed that patients in gene cluster C had a better survival rate compared to patients in gene clusters A and B (Figure 4D). The expression profile of the 94 OS-related shared DEGs along with clinical characteristics among the three gene clusters is

displayed in a heatmap (Figure 4E). Additionally, we compared the expression levels of the CXCLs in the three gene clusters. As indicated by the box plot, patients in gene cluster A expressed the lowest mRNA levels of the CXCLs, while most patients in gene cluster B had higher expression levels of CXCLs than those in gene cluster C (Figure 4F). In conclusion, patients can be effectively separated into three gene clusters that can predict their overall survival.

Construct a CXCL score model

Due to the diversity of tumors, we utilized PCA methodology to accurately evaluate the CXCL pattern of individual OC patients, which was named the CXCL score. The attribute changes of individual patients were depicted in a Sankey diagram (Figure 5A). Next, OC patients were divided into high-score and low-score groups based on their CXCL
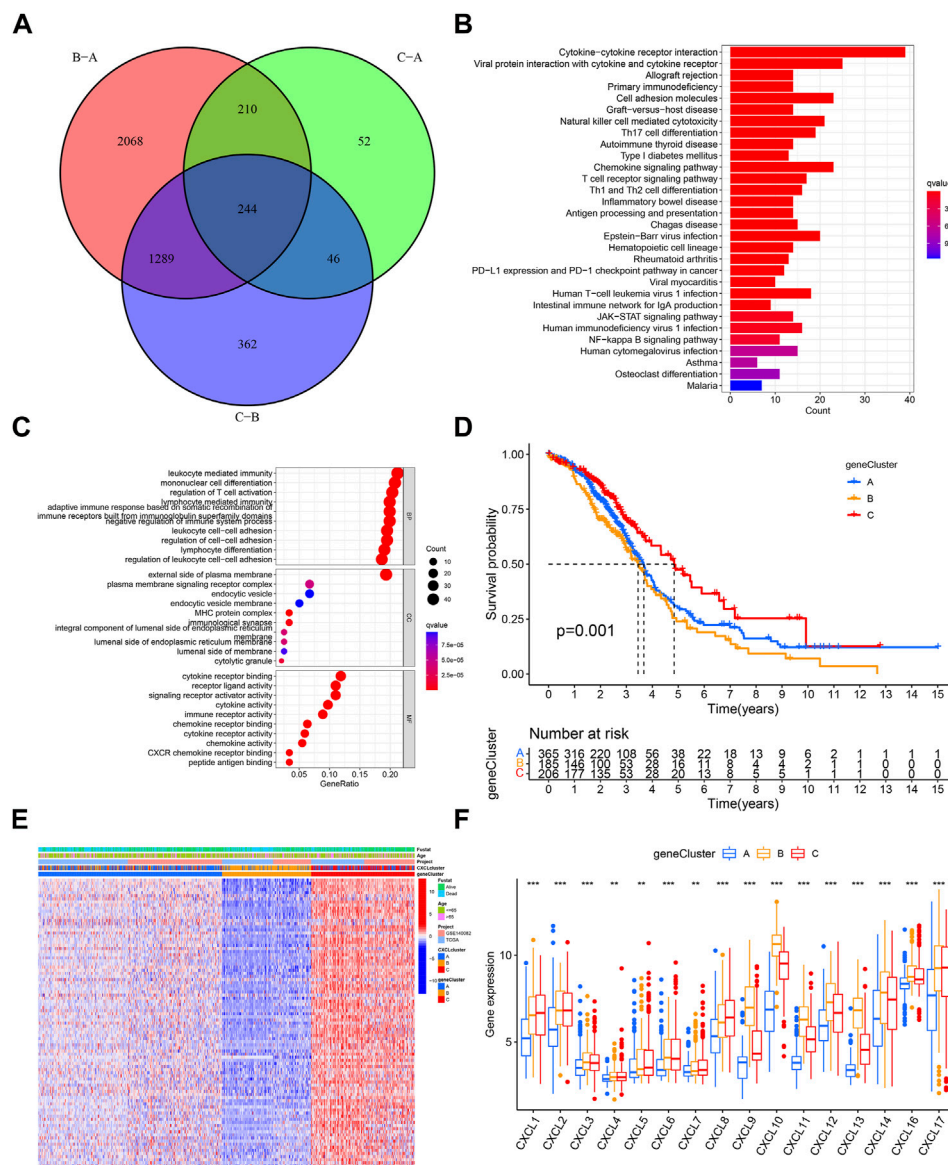
FIGURE 4
Three prognosis gene clusters in OC. **(A)** Venn diagram displays DEGs among three gene subtypes, with 244 genes identified as shared DEGs. **(B)** The top 30 enriched KEGG pathways based on the shared DEGs. **(C)** Dot plots show the top 10 GO terms in each biological process, based on the shared DEGs. **(D)** Kaplan-Meier curve displays the survival probability of patients in the three gene subtypes. **(E)** The heatmap displays the distribution of shared survival related DEGs, clinical characteristics, and the CXCL cluster in the three gene clusters. **(F)** Box plots display the expression of CXCLs in the three gene clusters. **p < 0.01, ***p < 0.001.

scores, and the survival outcomes of patients in these two groups were compared. The results showed that patients with high CXCL scores had a better survival rate compared to those with low CXCL scores (Figures 5B–D). We then analyzed the correlation between CXCL score and immune cell infiltration level using Spearman correlation analysis. Our results showed that a high CXCL score was positively correlated with higher immune cell infiltration (Figure 5E). Additionally, we calculated the CXCL scores of patients in different CXCL clusters and gene clusters. Among the three CXCL patterns, patients in CXCL cluster C had the highest CXCL score, while CXCL cluster B had the lowest CXCL score (Figure 5F). In the three gene clusters, the average CXCL score of patients in gene cluster C was higher than those in gene clusters

A and B (Figure 5G). Therefore, the CXCL score may serve as a potential positive biomarker for predicting the prognosis of OC patients.

The association between CXCL score and TMB/somatic mutation rates

High levels of tumor mutational burden (TMB) and the presence of cancer gene mutations have been positively linked to sensitivity to immunotherapy in some types of tumors (Bai et al., 2020). To assess the immunotherapeutic response of individual OC patients, we
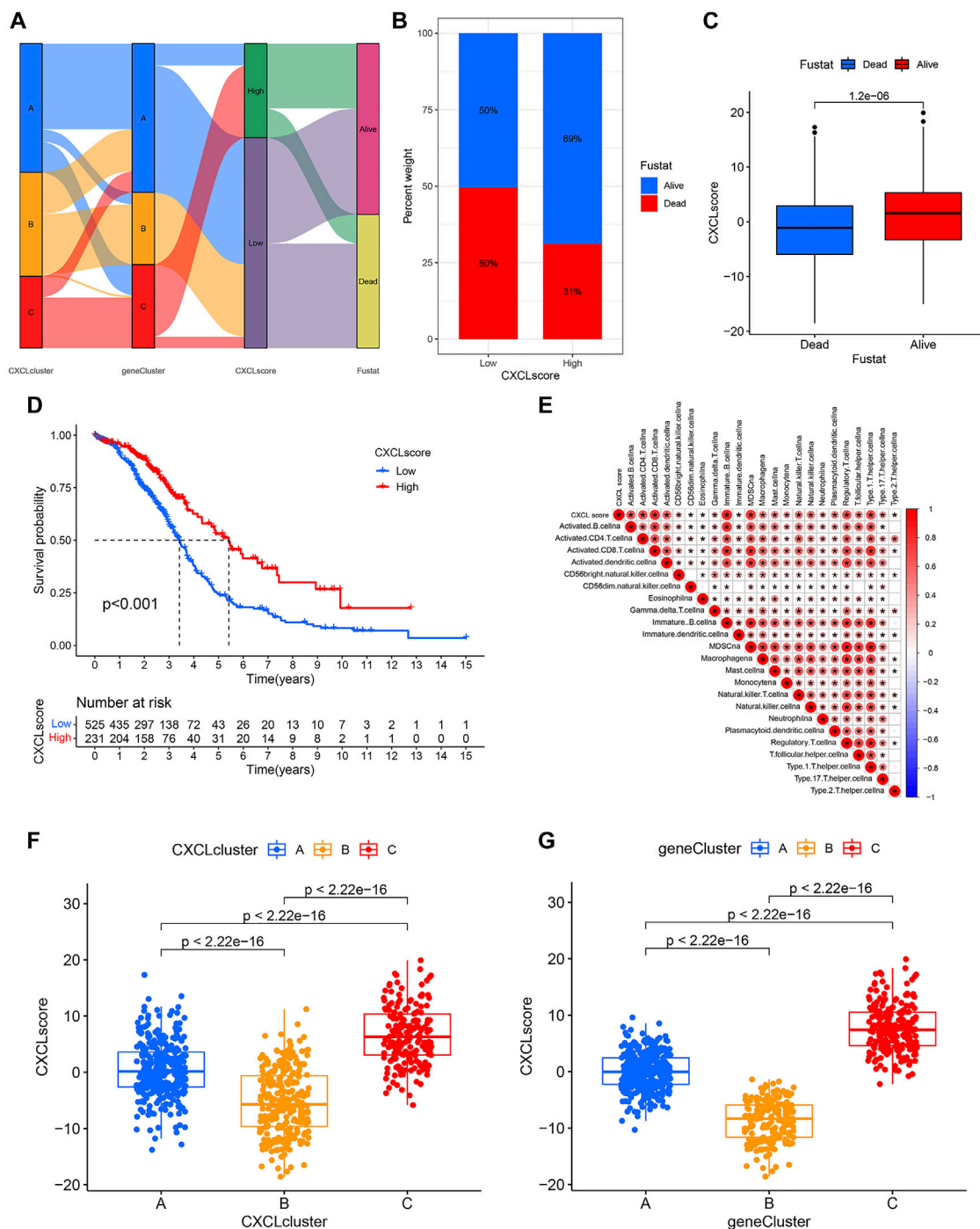
FIGURE 5
Construct a CXCL score model through PCA. **(A)**The Sankey diagram illustrates the connections between CXCL clusters, gene clusters, CXCL score patterns, and patient survival outcomes. **(B)** The distribution of patients with low or high CXCL scores who are alive or deceased. **(C)** Bar plots show the CXCL score distribution in patients with different prognoses. **(D)** Kaplan-Meier curve displays the survival probability of patients with varying CXCL scores. **(E)** The relationship between CXCL score and the level of immune cell infiltration is shown, with blue indicating negative correlations and red indicating positive correlations. **(F,G)** Bar plots illustrate the difference in CXCL score between the three CXCL clusters **(F)** and three gene clusters **(G)**, respectively, with *p* values indicated.

analyzed the relationship between the CXCL score and TMB. Although there was not a strong correlation between TMB and CXCL score, there was a trend towards patients with high CXCL scores having higher TMB values (Figures 6A, B). We then divided

patients into two classes based on their TMB value, with 108 patients in the high TMB (H-TMB) class and 145 patients in the low TMB value class (L-TMB). Survival analysis showed that patients in the H-TMB group had better survival outcomes than those in the
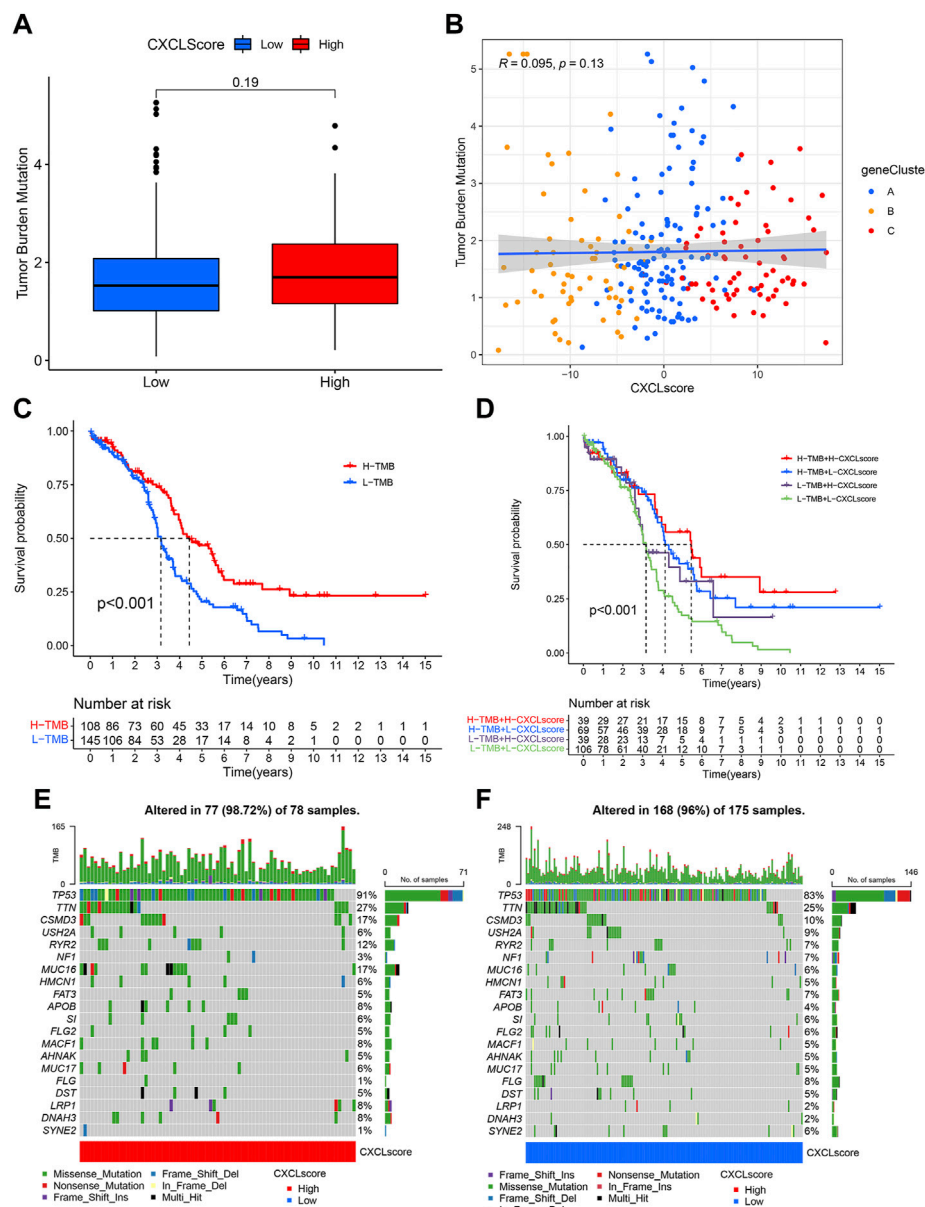
FIGURE 6
The association between CXCL score and TMB/somatic mutation rates. **(A)** Box plots show the TMB values in the high and low CXCL score groups. The *p*-value is indicated. **(B)** Scatter plots demonstrate the relationship between CXCL score, TMB, and the three gene clusters. Gene Cluster A is represented by blue dots, Gene Cluster B by yellow dots, and Gene Cluster C by red dots. **(C)** Kaplan-Meier curve presents the survival of patients with high and low TMB values, designated as H-TMB and L-TMB, respectively. **(D)** Survival analysis for patients grouped by both CXCL score and TMB values. **(E,F)** Waterfall plot displays the distribution of somatic mutations in patients with high **(E)** and low **(F)** CXCL scores. Each column represents an individual patient.

L-TMB group (*p* < 0.001) (Figure 6C). The results of the joint analysis of the CXCL score and TMB showed that patients in the H-TMB group with high CXCL scores had the best survival, while those in the L-TMB group with low CXCL scores had the worst outcome (Figure 6D). We also analyzed the somatic mutations of patients in the two CXCL score groups using the TCGA-OC cohort. Results showed that the somatic mutation rate of patients in the high CXCL score group (98.72%) was higher than in the low CXCL score group (96%). The mutation rate of the TP53 gene was 91% in the high CXCL score group and 83% in the low CXCL score group

(Figures 6E, F). Collectively, these results suggest that higher CXCL scores are associated with higher TMB values, indicating better responses to immunotherapy.

Predictive value of CXCL score for immunotherapy outcomes

Expression of PD-L1 is a clinically recognized indicator for anti-PD-1/PD-L1 therapy in cancer patients (Luchini et al., 2019;
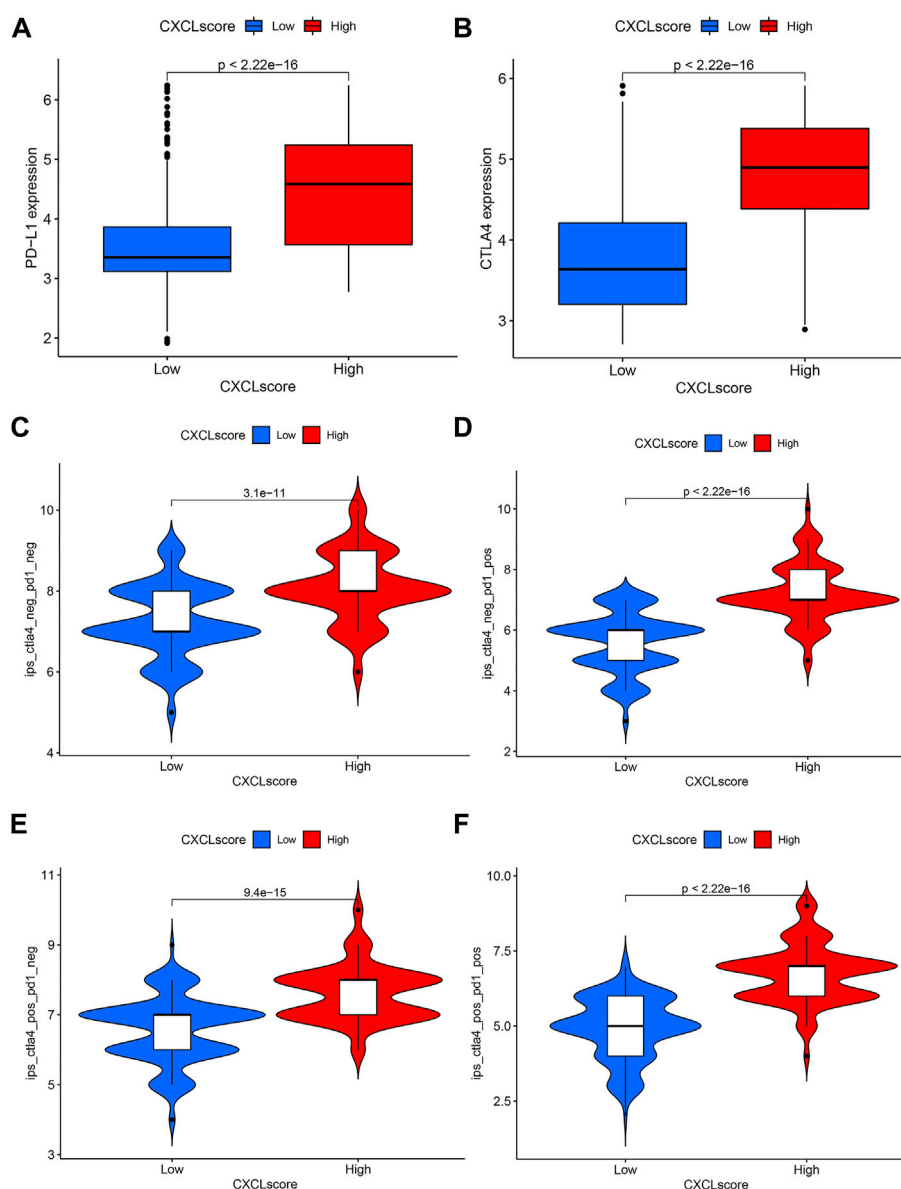
FIGURE 7
The predictive value of the CXCL score in immunotherapy. **(A,B)** Box plots present the expression levels of PD-L1 **(A)** and CTLA4 **(B)** in patients with high and low CXCL scores. **(C–F)** Violin plots display the IPS scores of patients with low and high CXCL scores who received non-ICI therapy **(C)**, PD-1 therapy alone **(D)**, CTLA4 therapy alone **(E)**, or a combination of PD-1 and CTLA4 therapy **(F)**.

Twomey and Zhang, 2021), while CTLA-4 is another potential target for immune checkpoint inhibitor (ICI) therapy (Rowshanravan et al., 2018). To determine the predictive value of the CXCL score in immunotherapy, we compared the expression levels of PD-L1 and CTLA-4 between patients with high and low CXCL scores. Results showed that patients with high CXCL scores expressed higher levels of PD-L1 (Figure 7A) and CTLA-4 (Figure 7B) compared to those with low CXCL scores, indicating that these patients may benefit more from ICI treatment.

Additionally, the immunophenoscore (IPS) has been found to predict the efficacy of anti-PD-1 and anti-CTLA-4 therapy

(Charoentong et al., 2017). To further validate the value of the CXCL score in predicting immunotherapy response, we evaluated the sensitivity of ICI therapy using IPS. Results indicated that patients with high CXCL scores had better survival outcomes compared to those with low CXCL scores with either anti-PD-1 or anti-CTLA-4 therapy (Figures 7C–E). Clinical trials have shown that combination therapy with anti-PD-1 and anti-CTLA-4 is effective in treating lung cancer and melanoma (Wolchok et al., 2013; Hellmann et al., 2019). The results as depicted in Figure 7F indicate that patients with high CXCL scores have higher IPS levels compared to those with low CXCL scores when treated with the combination therapy of anti-PD-

1 and anti-CTLA-4 (Figure 7F). This suggests that patients with high CXCL scores may experience a greater benefit from this combination therapy.

Taken together, the CXCL score may serve as a positive predictor for a patient's response to immunotherapy and could be used to select the appropriate patient population for the treatment in ovarian cancer.

Discussion

The CXCL family genes play a crucial role in the progression of tumors and in the microenvironment (Bikfalvi and Billottet, 2020). However, the full extent of their importance in OC remains unclear. Our study confirmed the expression of CXCLs in OC tissue compared to normal tissue and found that most CXCLs were overexpressed in OC tissue. Based on this expression profile, we were able to group OC patients into three CXCL clusters. Of these clusters, patients in cluster C had better survival rates and higher infiltration of immune cells. By using DEGs among CXCL clusters, we identified three gene clusters, and developed a CXCL score to predict prognosis and immunotherapy response in individual patients. The relationships of the CXCL score with clinical outcomes, cell infiltration levels, somatic mutations, and immunotherapy sensitivity were also studied to evaluate the value of CXCLs in OC.

The CXCLs are involved in tumor progression. For instance, CXCL1 and CXCL8 have been found to stimulate ovarian cancer cell growth *via* activation of the p38 and Wnt/β-catenin pathway (Duckworth et al., 2016; Wen et al., 2020; Park et al., 2021). CXCL5, secreted by ovarian cancer-associated mesothelial cells, has been demonstrated to have tumor-promoting properties (Peng et al., 2019). Furthermore, high levels of CXCL11 expressed in cancer-associated fibroblasts in ovarian cancer biopsies were found to facilitate cancer cell metastasis (Lau et al., 2014). Our results align with these findings and show that CXCL1, CXCL5, CXCL8, and CXCL11 are overexpressed in ovarian cancer. Additionally, previous studies have found that overexpressed CXCL9, CXCL10, and CXCL13 are positively associated with better overall survival, while elevated CXCL12 and CXCL14 levels are linked to poor outcomes (Popple et al., 2012; Bronger et al., 2016; Li et al., 2020; Ukita et al., 2022). Our study validated these findings and showed that CXCL9, CXCL10, CXCL12, CXCL13, and CXCL14 are independent risk factors for clinical outcomes. High levels of CXCL9, CXCL10, and CXCL13 were found to be associated with good prognosis, while high expression levels of CXCL12 and CXCL14 were correlated with poor survival. These findings suggest that CXCLs may play a crucial role in the progression of ovarian cancer.

The relationship between genomic profiling and survival outcome in cancer patients has gained significant attention in recent years. Research has shown that chemokine ligands CXCL10 and CXCL11 have anti-angiogenic properties and can effectively inhibit tumor progression (Romagnani et al., 2004; Billottet et al., 2013). Additionally, CXCL9, CXCL10, and CXCL13 are involved in attracting CD8 effector T cells, and a high infiltration of T lymphocytes has been linked to improved survival outcomes (Sato et al., 2005; Harlin et al., 2009; Ukita et al., 2022). Our study found three subfamilies of OC patients with distinct survival outcomes based on the expression of the CXCLs.

Patients in cluster C with the highest expression of CXCL9/10/11/13, who also showed activation of immune-related pathways and high infiltration of immune cells including T cells, had the best survival outcomes. Conversely, patients in cluster B, characterized by low expression of CXCL9/10/11/13 and low immune cell infiltration, had a poor prognosis. These findings highlight the potential use of CXCL expression as a biomarker for the treatment and prognosis of ovarian cancer.

Immunotherapy, including anti-PD-1/PD-L1 and CTLA-4, is commonly employed in various solid tumors, but its efficacy in OC is limited (Marabelle et al., 2020; Robert, 2020; Marcus et al., 2021; O'Malley et al., 2022). Identifying reliable biomarkers to direct immunotherapy may broaden the reach of immunotherapy to OC patients (Zamarin and Jazaeri, 2016). In our study, we utilized the CXCL score as a biomarker to predict individual patients' responses to immunotherapy in OC. High PD-L1/CTLA4 expression levels, high IPS scores, and a greater number of cancer gene mutations have been established as solid predictive biomarkers for patients who are more likely to benefit from immunotherapy (Egen et al., 2002; Garon et al., 2015; Herbst et al., 2016; Charoentong et al., 2017; Bai et al., 2020; Marabelle et al., 2020). We examined the prognostic significance of the CXCL score in immunotherapy response by evaluating these predictive biomarkers. Our findings indicate that patients with high CXCL scores had elevated levels of PD-L1/CTLA4, high IPS scores, and a high frequency of cancer gene mutations. Therefore, the CXCL score can be used as a predictor of immunotherapy response in OC patients.

Immune cells express chemokine receptors and can be attracted to tumors through chemokines, including CXCLs. Our study revealed a positive correlation between the CXCL score and the infiltration of immune cells. However, the underlying mechanism behind this connection is still unclear. It is plausible that the CXCL score serves as a measure of the concentration of immune cells in the tumor microenvironment. A high CXCL score, indicating a high expression of anti-tumor CXCL, may attract a larger number of immune cells to the tumor, resulting in a more inflamed microenvironment and enhanced response to immunotherapy. On the other hand, a low CXCL score may indicate a lack of immune cell infiltration and a less favorable tumor microenvironment, leading to a weaker response to immunotherapy. Further studies are needed to fully understand the mechanisms linking the CXCL score to clinical outcomes and immunotherapy responses in patients.

In conclusion, our comprehensive evaluation of CXCLs in ovarian cancer has uncovered a promising biomarker that could forecast the prognosis and response to immunotherapy for individual patients. This has the potential to enhance the implementation of precision-targeted, personalized immunotherapy in ovarian cancer patients.

Data availability statement

Publicly available datasets were analyzed in this study. This data can be found here: The Cancer Genome Atlas (TCGA) (https://portal.gdc.cancer.gov/) ,the UCSC Xena database (https://xena.ucsc.edu/),and Gene Expression Omnibus (GEO) (https://www.ncbi.nlm.nih.gov/geo/) databases.

Author contributions

SL, DZ, and ZL conceived and designed the study. SL and DZ collected and assembled data and wrote the manuscript. ZL provided administrative support. DZ and ZL revised the manuscript. All authors contributed to the article and approved the final version of the manuscript.

Funding

Acknowledgments

Conflict of interest

The authors declare that the research was conducted in the absence of any commercial or financial relationships that could be construed as a potential conflict of interest.

Publisher's note

All claims expressed in this article are solely those of the authors and do not necessarily represent those of their affiliated organizations, or those of the publisher, the editors and the reviewers. Any product that may be evaluated in this article, or claim that may be made by its manufacturer, is not guaranteed or endorsed by the publisher.

Supplementary material

The Supplementary Material for this article can be found online at: https://www.frontiersin.org/articles/10.3389/fphar.2023.1127557/full#supplementary-material

References

Ashburner, M., Ball, C. A., Blake, J. A., Botstein, D., Butler, H., Cherry, J. M., et al. (2000). Gene ontology: Tool for the unification of biology. The gene Ontology consortium. *Nat. Genet.* 25 (1), 25–29. doi:10.1038/75556

Bai, X., Wu, D. H., Ma, S. C., Wang, J., Tang, X. R., Kang, S., et al. (2020). Development and validation of a genomic mutation signature to predict response to PD-1 inhibitors in non-squamous NSCLC: A multicohort study. *J. Immunother. Cancer* 8 (1), e000381. doi:10.1136/jitc-2019-000381

Bikfalvi, A., and Billottet, C. (2020). The CC and CXC chemokines: Major regulators of tumor progression and the tumor microenvironment. *Am. J. Physiol. Cell Physiol.* 318 (3), C542–C554. doi:10.1152/ajpcell.00378.2019

Billottet, C., Quemener, C., and Bikfalvi, A. (2013). CXCR3, a double-edged sword in tumor progression and angiogenesis. *Biochim. Biophys. Acta* 1836 (2), 287–295. doi:10.1016/j.bbcan.2013.08.002

Bolitho, C., Hahn, M. A., Baxter, R. C., and Marsh, D. J. (2010). The chemokine CXCL1 induces proliferation in epithelial ovarian cancer cells by transactivation of the epidermal growth factor receptor. *Endocr. Relat. Cancer* 17 (4), 929–940. doi:10.1677/ERC-10-0107

Bronger, H., Singer, J., Windmuller, C., Reuning, U., Zech, D., Delbridge, C., et al. (2016). CXCL9 and CXCL10 predict survival and are regulated by cyclooxygenase inhibition in advanced serous ovarian cancer. *Br. J. Cancer* 115 (5), 553–563. doi:10.1038/bjc.2016.172

Charo, I. F., and Ransohoff, R. M. (2006). The many roles of chemokines and chemokine receptors in inflammation. *N. Engl. J. Med.* 354 (6), 610–621. doi:10.1056/NEJMra052723

Charoentong, P., Finotello, F., Angelova, M., Mayer, C., Efremova, M., Rieder, D., et al. (2017). Pan-cancer immunogenomic analyses reveal genotype-immunophenotype relationships and predictors of response to checkpoint blockade. *Cell Rep.* 18 (1), 248–262. doi:10.1016/j.celrep.2016.12.019

Dominguez, C., McCampbell, K. K., David, J. M., and Palena, C. (2017). Neutralization of IL-8 decreases tumor PMN-MDSCs and reduces mesenchymalization of claudin-low triple-negative breast cancer. *JCI Insight* 2 (21), e94296. doi:10.1172/jci.insight.94296

Dong, Z. Y., Zhong, W. Z., Zhang, X. C., Su, J., Xie, Z., Liu, S. Y., et al. (2017). Potential predictive value of TP53 and KRAS mutation status for response to PD-1 blockade immunotherapy in lung adenocarcinoma. *Clin. Cancer Res.* 23 (12), 3012–3024. doi:10.1158/1078-0432.CCR-16-2554

Duckworth, C., Zhang, L., Carroll, S. L., Ethier, S. P., and Cheung, H. W. (2016). Overexpression of GAB2 in ovarian cancer cells promotes tumor growth and angiogenesis by upregulating chemokine expression. *Oncogene* 35 (31), 4036–4047. doi:10.1038/onc.2015.472

Egen, J. G., Kuhns, M. S., and Allison, J. P. (2002). CTLA-4: New insights into its biological function and use in tumor immunotherapy. *Nat. Immunol.* 3 (7), 611–618. doi:10.1038/ni0702-611

Garon, E. B., Rizvi, N. A., Hui, R., Leighl, N., Balmanoukian, A. S., Eder, J. P., et al. (2015). Pembrolizumab for the treatment of non-small-cell lung cancer. *N. Engl. J. Med.* 372 (21), 2018–2028. doi:10.1056/NEJMoa1501824

Hamanishi, J., Takeshima, N., Katsumata, N., Ushijima, K., Kimura, T., Takeuchi, S., et al. (2021). Nivolumab versus gemcitabine or pegylated liposomal doxorubicin for patients with platinum-resistant ovarian cancer: Open-label, randomized trial in Japan (NINJA). *J. Clin. Oncol.* 39 (33), 3671–3681. doi:10.1200/JCO.21.00334

Hanzelmann, S., Castelo, R., and Guinney, J. (2013). Gsva: Gene set variation analysis for microarray and RNA-seq data. *BMC Bioinforma.* 14, 7. doi:10.1186/1471-2105-14-7

Hargadon, K. M., Johnson, C. E., and Williams, C. J. (2018). Immune checkpoint blockade therapy for cancer: An overview of FDA-approved immune checkpoint inhibitors. *Int. Immunopharmacol.* 62, 29–39. doi:10.1016/j.intimp.2018.06.001

Harlin, H., Meng, Y., Peterson, A. C., Zha, Y., Tretiakova, M., Slingluff, C., et al. (2009). Chemokine expression in melanoma metastases associated with CD8+ T-cell recruitment. *Cancer Res.* 69 (7), 3077–3085. doi:10.1158/0008-5472.CAN-08-2281

Hellmann, M. D., Paz-Ares, L., Bernabe Caro, R., Zurawski, B., Kim, S. W., Carcereny Costa, E., et al. (2019). Nivolumab plus ipilimumab in advanced non-small-cell lung cancer. *N. Engl. J. Med.* 381 (21), 2020–2031. doi:10.1056/NEJMoa1910231

Herbst, R. S., Baas, P., Kim, D. W., Felip, E., Perez-Gracia, J. L., Han, J. Y., et al. (2016). Pembrolizumab versus docetaxel for previously treated, PD-L1-positive, advanced non-small-cell lung cancer (KEYNOTE-010): A randomised controlled trial. *Lancet* 387 (10027), 1540–1550. doi:10.1016/S0140-6736(15)01281-7

Kanehisa, M., and Goto, S. (2000). Kegg: Kyoto encyclopedia of genes and genomes. *Nucleic Acids Res.* 28 (1), 27–30. doi:10.1093/nar/28.1.27

Karin, N. (2020). CXCR3 ligands in cancer and autoimmunity, chemoattraction of effector T cells, and beyond. *Front. Immunol.* 11, 976. doi:10.3389/fimmu.2020.00976

Kraehenbuehl, L., Weng, C. H., Eghbali, S., Wolchok, J. D., and Merghoub, T. (2022). Enhancing immunotherapy in cancer by targeting emerging immunomodulatory pathways. *Nat. Rev. Clin. Oncol.* 19 (1), 37–50. doi:10.1038/s41571-021-00552-7

Lau, T. S., Chung, T. K., Cheung, T. H., Chan, L. K., Cheung, L. W., Yim, S. F., et al. (2014). Cancer cell-derived lymphotoxin mediates reciprocal tumour-stromal interactions in human ovarian cancer by inducing CXCL11 in fibroblasts. *J. Pathol.* 232 (1), 43–56. doi:10.1002/path.4258

Ledermann, J. A., Raja, F. A., Fotopoulou, C., Gonzalez-Martin, A., Colombo, N., Sessa, C., et al. (2013). Newly diagnosed and relapsed epithelial ovarian carcinoma: ESMO clinical practice guidelines for diagnosis, treatment and follow-up. *Ann. Oncol.* 24 (6), vi24–32. doi:10.1093/annonc/mdt333

Li, X., Zhao, L., and Meng, T. (2020). Upregulated CXCL14 is associated with poor survival outcomes and promotes ovarian cancer cells proliferation. *Cell Biochem. Funct.* 38 (5), 613–620. doi:10.1002/cbf.3516

Luchini, C., Bibeau, F., Ligtenberg, M. J. L., Singh, N., Nottegar, A., Bosse, T., et al. (2019). ESMO recommendations on microsatellite instability testing for immunotherapy in cancer, and its relationship with PD-1/PD-L1 expression and tumour mutational burden: A systematic review-based approach. *Ann. Oncol.* 30 (8), 1232–1243. doi:10.1093/annonc/mdz116

Marabelle, A., Le, D. T., Ascierto, P. A., Di Giacomo, A. M., De Jesus-Acosta, A., Delord, J. P., et al. (2020). Efficacy of pembrolizumab in patients with noncolorectal high microsatellite instability/mismatch repair-deficient cancer: Results from the phase II KEYNOTE-158 study. *J. Clin. Oncol.* 38 (1), 1–10. doi:10.1200/JCO.19.02105

Marcus, L., Fashoyin-Aje, L. A., Donoghue, M., Yuan, M., Rodriguez, L., Gallagher, P. S., et al. (2021). FDA approval summary: Pembrolizumab for the treatment of tumor mutational burden-high solid tumors. *Clin. Cancer Res.* 27 (17), 4685–4689. doi:10.1158/1078-0432.CCR-21-0327

Markl, F., Huynh, D., Endres, S., and Kobold, S. (2022). Utilizing chemokines in cancer immunotherapy. *Trends Cancer* 8 (8), 670–682. doi:10.1016/j.trecan.2022.04.001

Moore, K. N., Bookman, M., Sehouli, J., Miller, A., Anderson, C., Scambia, G., et al. (2021). Atezolizumab, bevacizumab, and chemotherapy for newly diagnosed stage III or IV ovarian cancer: Placebo-controlled randomized phase III trial (IMagyn050/GOG 3015/ENGOT-OV39). *J. Clin. Oncol.* 39 (17), 1842–1855. doi:10.1200/JCO.21.00306

O'Malley, D. M., Bariani, G. M., Cassier, P. A., Marabelle, A., Hansen, A. R., De Jesus Acosta, A., et al. (2022). Pembrolizumab in patients with microsatellite instability-high advanced endometrial cancer: Results from the KEYNOTE-158 study. *J. Clin. Oncol.* 40 (7), 752–761. doi:10.1200/JCO.21.01874

Oronsky, B., Ray, C. M., Spira, A. I., Trepel, J. B., Carter, C. A., and Cottrill, H. M. (2017). A brief review of the management of platinum-resistant-platinum-refractory ovarian cancer. *Med. Oncol.* 34 (6), 103. doi:10.1007/s12032-017-0960-z

Park, G. Y., Pathak, H. B., Godwin, A. K., and Kwon, Y. (2021). Epithelial-stromal communication via CXCL1-CXCR2 interaction stimulates growth of ovarian cancer cells through p38 activation. *Cell Oncol. (Dordr)* 44 (1), 77–92. doi:10.1007/s13402-020-00554-0

Patel, S. P., and Kurzrock, R. (2015). PD-L1 expression as a predictive biomarker in cancer immunotherapy. *Mol. Cancer Ther.* 14 (4), 847–856. doi:10.1158/1535-7163.Mct-14-0983

Peng, Y., Kajiyama, H., Yuan, H., Nakamura, K., Yoshihara, M., Yokoi, A., et al. (2019). PAI-1 secreted from metastatic ovarian cancer cells triggers the tumor-promoting role of the mesothelium in a feedback loop to accelerate peritoneal dissemination. *Cancer Lett.* 442, 181–192. doi:10.1016/j.canlet.2018.10.027

Popple, A., Durrant, L. G., Spendlove, I., Rolland, P., Scott, I. V., Deen, S., et al. (2012). The chemokine, CXCL12, is an independent predictor of poor survival in ovarian cancer. *Br. J. Cancer* 106 (7), 1306–1313. doi:10.1038/bjc.2012.49

Presti, D., Dall'Olio, F. G., Besse, B., Ribeiro, J. M., Di Meglio, A., and Soldato, D. (2022). Tumor infiltrating lymphocytes (TILs) as a predictive biomarker of response to checkpoint blockers in solid tumors: A systematic review. *Crit. Rev. Oncol. Hematol.* 177, 103773. doi:10.1016/j.critrevonc.2022.103773

Ringner, M. (2008). What is principal component analysis? *Nat. Biotechnol.* 26 (3), 303–304. doi:10.1038/nbt0308-303

Robert, C. (2020). A decade of immune-checkpoint inhibitors in cancer therapy. *Nat. Commun.* 11 (1), 3801. doi:10.1038/s41467-020-17670-y

Romagnani, P., Lasagni, L., Annunziato, F., Serio, M., and Romagnani, S. (2004). CXC chemokines: The regulatory link between inflammation and angiogenesis. *Trends Immunol.* 25 (4), 201–209. doi:10.1016/j.it.2004.02.006

Rowshanravan, B., Halliday, N., and Sansom, D. M. (2018). CTLA-4: A moving target in immunotherapy. *Blood* 131 (1), 58–67. doi:10.1182/blood-2017-06-741033

Sato, E., Olson, S. H., Ahn, J., Bundy, B., Nishikawa, H., Qian, F., et al. (2005). Intraepithelial CD8+ tumor-infiltrating lymphocytes and a high CD8+/regulatory T cell ratio are associated with favorable prognosis in ovarian cancer. *Proc. Natl. Acad. Sci. U. S. A.* 102 (51), 18538–18543. doi:10.1073/pnas.0509182102

Seitz, S., Dreyer, T. F., Stange, C., Steiger, K., Brauer, R., Scheutz, L., et al. (2022). CXCL9 inhibits tumour growth and drives anti-PD-L1 therapy in ovarian cancer. *Br. J. Cancer* 126 (10), 1470–1480. doi:10.1038/s41416-022-01763-0

Siegel, R. L., Miller, K. D., Wagle, N. S., and Jemal, A. (2023). Cancer statistics, 2023. *CA Cancer J. Clin.* 73 (1), 17–48. doi:10.3322/caac.21763

Smyth, G. K. (2004). Linear models and empirical bayes methods for assessing differential expression in microarray experiments. *Stat. Appl. Genet. Mol. Biol.* 3. Article3. doi:10.2202/1544-6115.1027

Subramanian, A., Tamayo, P., Mootha, V. K., Mukherjee, S., Ebert, B. L., Gillette, M. A., et al. (2005). Gene set enrichment analysis: A knowledge-based approach for interpreting genome-wide expression profiles. *Proc. Natl. Acad. Sci. U. S. A.* 102 (43), 15545–15550. doi:10.1073/pnas.0506580102

Twomey, J. D., and Zhang, B. (2021). Cancer immunotherapy update: FDA-approved checkpoint inhibitors and companion diagnostics. *AAPS J.* 23 (2), 39. doi:10.1208/s12248-021-00574-0

Ukita, M., Hamanishi, J., Yoshitomi, H., Yamanoi, K., Takamatsu, S., Ueda, A., et al. (2022). CXCL13-producing CD4+ T cells accumulate in the early phase of tertiary lymphoid structures in ovarian cancer. *JCI Insight* 7 (12), e157215. doi:10.1172/jci.insight.157215

Wang, N., Liu, W., Zheng, Y., Wang, S., Yang, B., Li, M., et al. (2018). CXCL1 derived from tumor-associated macrophages promotes breast cancer metastasis via activating NF-κB/SOX4 signaling. *Cell Death Dis.* 9 (9), 880. doi:10.1038/s41419-018-0876-3

Wang, Z., Wang, Z., Li, G., Wu, H., Sun, K., Chen, J., et al. (2017). CXCL1 from tumor-associated lymphatic endothelial cells drives gastric cancer cell into lymphatic system via activating integrin β1/FAK/AKT signaling. *Cancer Lett.* 385, 28–38. doi:10.1016/j.canlet.2016.10.043

Wen, J., Zhao, Z., Huang, L., Wang, L., Miao, Y., and Wu, J. (2020). IL-8 promotes cell migration through regulating EMT by activating the Wnt/β-catenin pathway in ovarian cancer. *J. Cell Mol. Med.* 24 (2), 1588–1598. doi:10.1111/jcmm.14848

Wilkerson, M. D., and Hayes, D. N. (2010). ConsensusClusterPlus: A class discovery tool with confidence assessments and item tracking. *Bioinformatics* 26 (12), 1572–1573. doi:10.1093/bioinformatics/btq170

Wolchok, J. D., Kluger, H., Callahan, M. K., Postow, M. A., Rizvi, N. A., Lesokhin, A. M., et al. (2013). Nivolumab plus ipilimumab in advanced melanoma. *N. Engl. J. Med.* 369 (2), 122–133. doi:10.1056/NEJMoa1302369

Zamarin, D., and Jazaeri, A. A. (2016). Leveraging immunotherapy for the treatment of gynecologic cancers in the era of precision medicine. *Gynecol. Oncol.* 141 (1), 86–94. doi:10.1016/j.ygyno.2015.12.030

Zhang, B., Wu, Q., Li, B., Wang, D., Wang, L., and Zhou, Y. L. (2020). m(6)A regulator-mediated methylation modification patterns and tumor microenvironment infiltration characterization in gastric cancer. *Mol. Cancer* 19 (1), 53. doi:10.1186/s12943-020-01170-0

Efficacy and safety of PD-1/PD-L1 inhibitors in the treatment of recurrent and refractory ovarian cancer: A systematic review and a meta-analysis

Siyuan Zeng[1,2], Daju Liu[1], Yongai Yu[1], Lei Zou[1], Xianyu Jin[1], Bing Liu[1]* and Lifeng Liu[1,2]*

[1]Department of Obstetrics and Gynecology, Dalian Municipal Central Hospital, Dalian, China, [2]Dalian municipal Central Hospital, China Medical University, Shenyang, China

Objective: To explore the efficacy and safety of PD-1/PD-L1 inhibitors in treating recurrent/refractory ovarian cancer (OC).

Methods: The online databases, including PubMed, Embase and Cochrane Library, were searched for relevant literatures on exploring the efficacy and safety of PD-1/PD-L1 inhibitors in the treatment of recurrent/refractory OC. The keywords are as follows: Ovarian neoplasms, programmed death receptor, PD-1, PD-L1, immunotherapy, and immune checkpoint inhibitor. Furthermore, qualified studies were screened for further meta-analysis.

Results: In this study, 11 studies (990 patients) were analyzed to evaluate the efficacy of PD-1/PD-L1 inhibitors in the treatment of recurrent/refractory OC. The combined results proved that the objective response rate (ORR) was 6.7%, 95% CI (4.6%,9.2%), disease control rate (DCR) was 37.9%, 95% CI (33.0%, 42.8%), median overall survival (OS) was 10.70 months, 95% CI (9.23, 12.17), and median progression free survival (PFS) was 2.24 months, 95% CI (2.05, 2.43). In addition, in terms of the safety of patients suffering from recurrent/refractory OC and receiving PD-1/PD-L1 inhibitors, the combined treatment related adverse events (TRAEs) were 70.9% (61.7%−80.2%), and the combined immune related adverse events (iAEs) were 29%, 95% CI (14.7%, 43.3%).

Conclusion: In patients with recurrent/refractory OC, PD-1/PD-L1 inhibitors were used alone and there was no obvious evidence of improved efficacy and survival. As for safety, the incidences of TRAEs and iAEs are high, so PD1/PD-L1 inhibitors should be applied according to individual conditions.

Clinical Trial Registration: https://www.crd.york.ac.uk/PROSPERO/display_record.php?RecordID=367525, identifier CRD42022367525.

Introduction

Ovarian cancer (OC) is the second leading cause of female gynecological cancer death worldwide (Bray et al., 2020). It was estimated that 313,959 people were diagnosed with OC and 207,252 people died of OC in the world in 2020 (Global, 2020; Siegel et al., 2021). The early symptoms of OC were insidious, and most of the patients were advanced at the time of treatment. Traditional treatment for OC was mainly surgery plus adjuvant chemotherapy, while the emergence of chemotherapy resistance affects the prognosis of patients to a certain extent, so the median survival period of advanced/recurrent epithelial OC is only 14.6 months (Shimokawa et al., 2018). The latest concept pointed out that the treatment for OC can be evolved into the treatment for chronic diseases, and the future treatment mode of OC will gradually move towards the trend of combined treatment, including surgery, chemotherapy, endocrine therapy, immunotherapy, and other methods (Ovarian, 2022).

Tumor immunotherapy is the fourth anti-tumor therapy after surgery, chemotherapy, and radiotherapy. In the tumor microenvironment, tumor cells express corresponding ligands, thus leading to T cell dysfunction, which enables tumor cells to escape the surveillance and clearance of the immune system.

Targeted drugs against cytotoxic T-lymphocyte associated protein 4 (CTLA4) and programmed cell death receptor 1 (PDCD1, also known as PD-1)/programmed cell death receptor ligand 1 (PDCD1LG1, also known as PD-L1) play an anti-tumor effect by relieving tumor cells' inhibition of T cell function (O'Donnell et al., 2017). In recent years, immune checkpoint inhibitors (ICI), as the most common immunotherapy, have brought hope for treating malignant tumors (Boustani et al., 2021).

On 17 August 2021, Food and Drug Administration (FDA) approved Dostarlimab-gxly (JEMPERLI) for adult patients with dMMR, relapsed, or advanced solid tumors who have progressed on or after prior therapy and had no satisfactory alternative therapy. (Markham, 2021). In September 2021, the National Comprehensive Cancer Network (NCCN) guidelines were recommended for use in the guidelines for uterine tumors and ovarian cancer. In 2022, the NCCN guidelines recommended that the indications for using PD-1/PD-L1 inhibitors in advanced/recurrent OC mainly include: Tumor tissue is in deficient mismatch repair (dMMR) or microsatellite instability high (MSI-H) state, and tumor mutation burden-high (TMB-H ≥10 muts/MB) (Ovarian, 2022).

The effects of PD-1/PD-L1 inhibitors, such as Nivolumab, Pembrolizumab, Avelumab, and Atezolizumab, have been confirmed by clinical studies (Brahmer et al., 2012; Hamanishi

TABLE 1 Characteristics of studies included in this meta-analysis.

Study, year	Sample size	Age	Median follow-up (months)	Drugs	Interventions	Median OS with 95% CI (months)	Median PFS with 95% CI (months)
Brahmer 2012	17	NA	NA	BMS-936559 (Nivolumab)	3 or 10 mg/kg every 2 weeks	NA	NA
Hamanishi 2015	20	Median: 60.0	8	Nivolumab	Every 2 weeks at a dose of 1 or 3 mg/kg	20.0 (7.0-NR)	3.5 (1.7–3.9)
Varga 2018	26	Median: 57.5	15.4	Pembrolizumab	10 mg/kg every 2 weeks for ≤24 months	13.8 (6.7–18.8)	1.9 (1.8–3.5)
Disis 2019	125	Median: 62.0	26.6	Avelumab	Avelumab 10 mg/kg was administered by 1 h intravenous infusion every 2 weeks	11.2 (8.7–15.4)	2.6 (1.4–2.8)
Liu 2019	12	Median: 60.5	7.6	Atezolizumab	Atezolizumab was administered intravenously at 15 mg/kg or 1,200 mg every 3 weeks	11.3 (5.5–27.7)	2.9 (1.3–5.5)
Matulonis 2019 1	285	NA	16.7	Pembrolizumab	Pembrolizumab 200 mg was administered intravenously every 3 weeks	NR (16.8-NR)	2.1 (2.1–2.2)
Matulonis 2019 2	91	NA	17.3	Pembrolizumab	Pembrolizumab 200 mg was administered intravenously every 3 weeks	17.6 (13.3-NR)	2.1 (2.1–2.6)
Normann 2019	18	Median: 61.0	7.5	Nivolumab	Nivolumab 3 mg/kg bodyweight every second week	7.5 (3.75–11.25)	3.75 (3.25–4.25)
Desai 2020	51	Median: 61.0	13.6	Tislelizumab	2 mg/kg administered every 2 weeks	NA	NA
Eric 2021	188	Median: 61.0	18.2	Avelumab	Avelumab 10 mg/kg was administered by 1 h intravenous infusion every 2 weeks	11.8 (8.9–14.1)	1.9 (1.8–1.9)
Hamanishi 2021	157	Median: 58.0	NA	Nivolumab	Nivolumab 240 mg was administered intravenously every 2 weeks	10.1 (8.3–14.4)	2.0 (1.9–2.2)

NA: not acpuired; NR: not reached.

et al., 2015; Disis et al., 2019; Liu et al., 2019; Matulonis et al., 2019; Normann et al., 2019; Varga et al., 2019; Desai et al., 2020; Hamanishi et al., 2021; Pujade-Lauraine et al., 2021). Most of these tests are designed as single arm tests, and the form is irreparable. Therefore, we conducted a meta-analysis to investigate the efficacy of anti-PD-1/PD-L1 alone in OC.

Materials and methods

Searching strategy and selection criteria

This meta-analysis was conducted through the Preferred Reporting Items for Systematic Reviews and Meta-analysis (PRISMA) standard (Moher et al., 2009). The following keywords were searched in PubMed, Embase, Cochrane Library and other online databases: Ovarian neoplasms, programmed death receptor, PD-1, PD-L1, immunotherapy, and immune checkpoint inhibitor. The selection criteria are as follows: 1) The data of observation indicators were complete; 2) The studies were prospective clinical studies, including randomized controlled trials and single arm studies. For clinical controlled trials, only the study group receiving single drug treatment of PD-1/PD-L1 inhibitors was included; 3) Patients with recurrent/refractory OC received single drug treatment of PD-1/PD-L1 inhibitors (Nivolumab, Pembrolizumab, Avelumab, and Atezolizumab); 4) Literature published in English. Exclusion criteria are as follows: 1) Article type: Letters, editorials, expert opinions, case reports and comments; 2) Research without available data; 3) Repetitive publications.

Data extraction and quality assessment

Two researchers were independently responsible for data extraction, and any differences were resolved by third-party contributors. The following data were extracted using the previously developed data extraction table: 1) Literature related information: Author's name, research year, research type, total number of people in the study and the corresponding number of people in each group; 2) Study event indicators: Objective response rate (ORR) and disease control rate (DCR), median overall survival (OS) and median progression free survival (PFS), and treatment related adverse events (TRAEs)/immune related adverse events (iAEs).

Statistical analysis

The combined ORR/DCR/medium OS/median PFS/TRAEs/iAEs were statistically analyzed using Stata version 15.0. Cochran Q test and I^2 statistical evaluation were used for data heterogeneity assessment. For Q test, p-value less than 0.05 indicates significant heterogeneity; For I^2 statistics, I^2 values greater than 50% are considered significant heterogeneity. Subgroup analysis was conducted to explore potential sources of heterogeneity. By removing each study and calculating, the sensitivity analysis was used to determine the related effects of individual studies on the combined results. Begg's and Egger's test were depicted to assess publication bias. $p < 0.05$ was considered to be statistically significant.

Results

Eligible literatures

A total of 2,109 articles were initially searched, and 1,874 articles remained after eliminating duplication. By reviewing the title and abstract according to the inclusion and exclusion criteria, 1,858 articles were excluded. Finally, through full text review, 10 articles with 11 researches, involving 990 OC patients, were recruited. PD-1/PD-L1 inhibitors used included Nivolumab ($n = 4$), Pembrolizumab ($n = 3$), Avelumab ($n = 2$), Atezolizumab ($n = 1$), and Tislelizumab ($n = l$). All the PD-1/PD-L1 inhibitors have been approved by FDA. The basic information of eligible research in Table 1. All participants in the 11 studies were diagnosed with recurrent or refractory OC. See the following detailed flow chart (Figure 1). According to the indicators of the Methodological Index for Non-randomized Studies (MINORS) scale, the total score of the quality evaluation is 16 points; 0 point means that the literature was not reported; 1 point refers to that the literature has been reported but the data information was insufficient; 2 points represents that the literature has been reported and provided sufficient information. The results are shown in (Supplementary Table S1).

Efficacy evaluation

Eleven of the included studies made statistics on ORR. The total sample size was 949 cases, with 72 cases of objective response. Meta

TABLE 2 Summary of effectiveness and safety of different treatment combinations.

Subgroup	Effect value (95%CI)					
	ORR	DCR	OS	PFS	TRAEs	iAEs
Avelumab	5.8% (3.4%–8.7%)	40.0% (34.7%–45.4%)	11.57 months (9.52–13.63)	2.16 months (1.5–2.82)	70.9% (65.9%–75.9%)	16.8% (10.7%–24.5%)
Nivolumab	6.1% (1.9%–11.8%)	35.7% (28.7%–42.8%)	9.13 months (6.83–11.42)	3.05 months (1.66–4.43)	60.6% (27.7%–93.5%)	50.0% (41.9%–58.1%)
Pembrolizumab	7.7% (5.2%–10.7%)	37.3% (32.6%–42.0%)	13.8 months (7.75–19.85)	2.10 months (2.05–2.15)	73.1% (68.4%–77.6%)	22.9% (18.8%–27.0%)
Other	10.2% (3.0%–20.1%)	22.2% (2.8%–60.0%)	11.30 months (0.20–22.40)	2.90 months (0.80–5.00)	83.2% (71.6%–94.7%)	—

analysis results are as follows: $I^2 = 26.33\%$, $p = 0.193$ indicates that there is no heterogeneity among the 11 studies. The fixed effect model was selected, and the combined effect value ORR = 6.7%, 95% CI (4.6%,9.2%), (Figure 2). Ten of the included studies made statistics on DCR. The total sample size was 898 cases, with 342 cases of disease control. Meta analysis results are as follows: $I^2 = 45.078\%$, $p = 0.059$ refers to that there was moderate heterogeneity among the studies, the random effect model was used with the combined effect value of DCR = 37.9%, 95% CI (33.0%, 42.8%), (Figure 3). Six of the included studies made statistics on the median OS. Meta analysis results are that $I^2 = 0.0\%$, $p = 0.447$ suggests that there was no significant heterogeneity among the 6 studies, so the fixed effect model was used, with the combined effect value median OS = 10.70 months, 95% CI (9.23, 12.17), (Figure 4). Nine of the included studies made statistics on the median PFS. Meta analysis results are that $I^2 = 91.0\%$, $p < 0.001$ represents that there was significant heterogeneity among the studies, so a random effect model was used, with the combined effect value median PFS = 2.24 months, 95% CI (2.05, 2.43), (Figure 5).

Safety assessment

There were 8 articles that counted the incidence of TRAEs. Meta analysis results are as follows: $I^2 = 88.745\%$, $p < 0.001$ indicates that there is a certain heterogeneity among the studies, so a random effect model was used, with combined effect values of TRAEs = 70.9%, 95% CI (61.7%, 80.2%), (Figure 6). TRAEs can be divided into mild-moderate TRAEs (Grade 1 = mild, Grade 2 = moderate) and severe TRAEs (Grade 3 = severe, Grade 4 = life-threatening, and Grade 5 = death) according to severity. As shown in Supplementary Figure S1, the pooled mild-moderate TRAEs is 53.0%, 95% CI (44.0%, 62.0%) with huge heterogeneity ($I^2 = 83.817\%$, $p < 0.001$). The combined effect value of severe TRAEs was 13.3%, 95% CI (8.0%, 18.6%) with significant heterogeneity ($I^2 = 77.433\%$, $p < 0.001$). There were 4 articles that counted the incidence of iAEs. Meta analysis results are that $I^2 = 93.477\%$, $p < 0.001$ marks that there is some heterogeneity between the four studies, so a random effect model was used, with combined effect values of iAEs = 29.0%, 95% CI (14.7%, 43.3%), (Figure 7).

Subgroup analysis

In Table 2, according to Avelumab, Nivolumab, Pembrolizumab, and others, the ORR was divided into four subgroups. Meta analysis results are as follows: the ORR of Avelumab combination effect value is 5.8% (3.4%–8.7%), DCR is 40.0% (34.7%–45.4%), median OS is 11.57 months (9.52–13.63), median PFS is 2.16 months (1.5–2.82), TRAEs is 70.9% (65.9%–75.9%), and iAEs is 16.8% (10.7%–24.5%);

FIGURE 1
Flow chart of the meta-analysis.
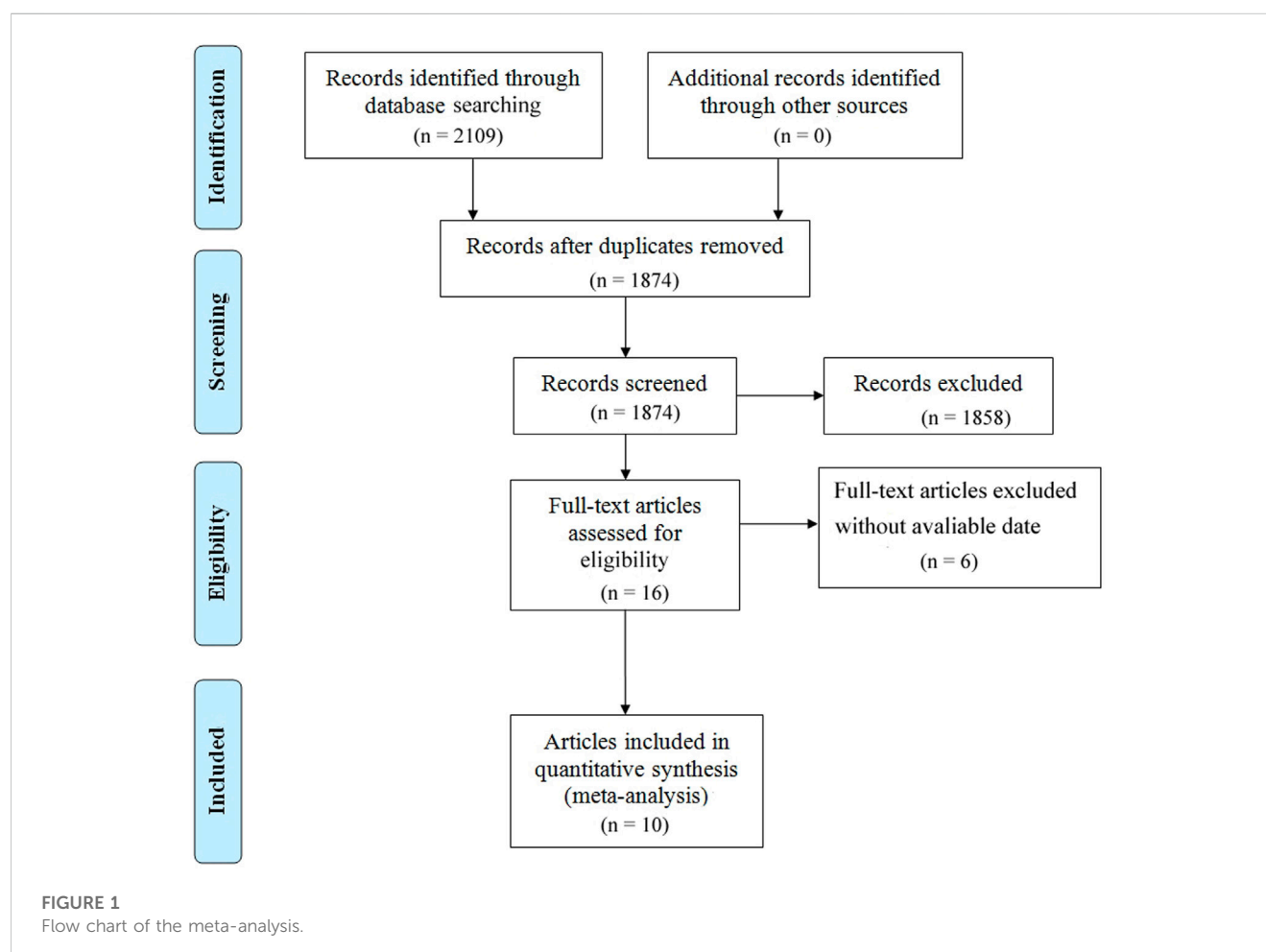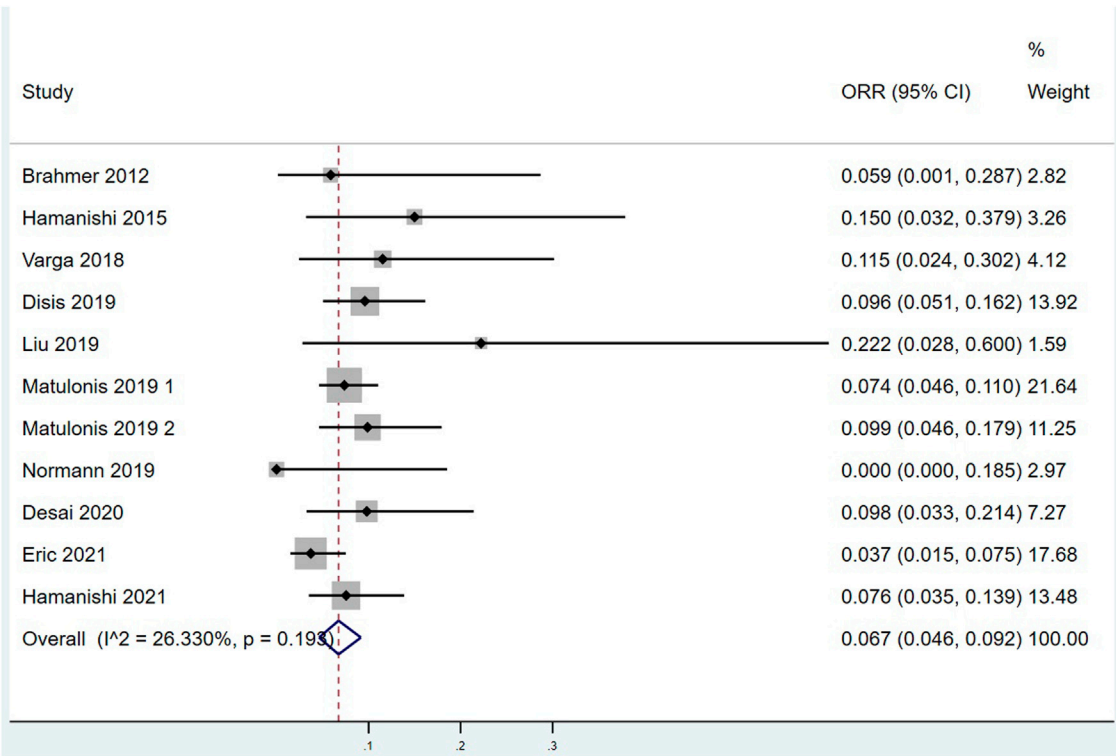
FIGURE 2
Forest plots of the pooled objective response rate (ORR).
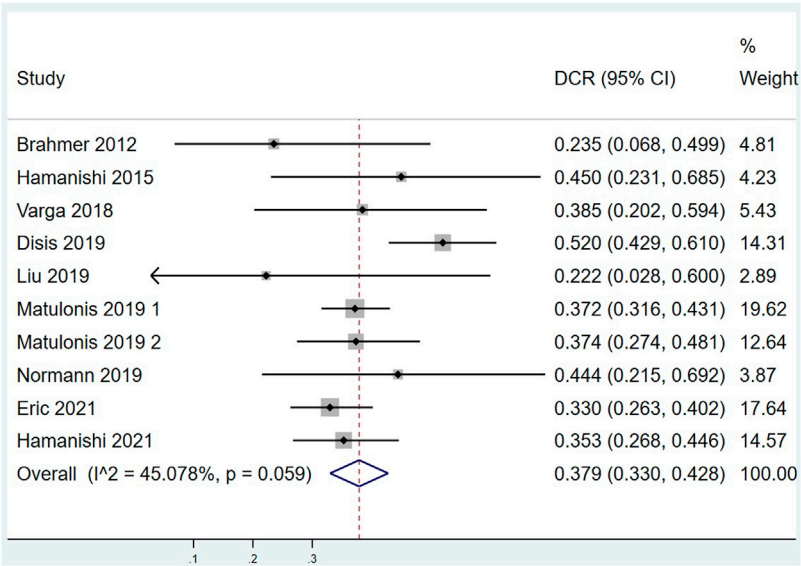
FIGURE 3
Forest plots of the pooled disease control rate (DCR).

Nivolumab combination effect value ORR is 6.1% (1.9%–11.8%), DCR is 35.7% (28.7%–42.8%), median OS is 9.13 months (6.83–11.42), median PFS is 3.05 months (1.66–4.43), TRAEs is 60.6% (27.7%–93.5%), and iAEs is 50.0% (41.9%–58.1%); Pembrolizumab combination ORR is 7.7% (5.2%–10.7%), DCR is 37.3% (32.6%–42.0%), median
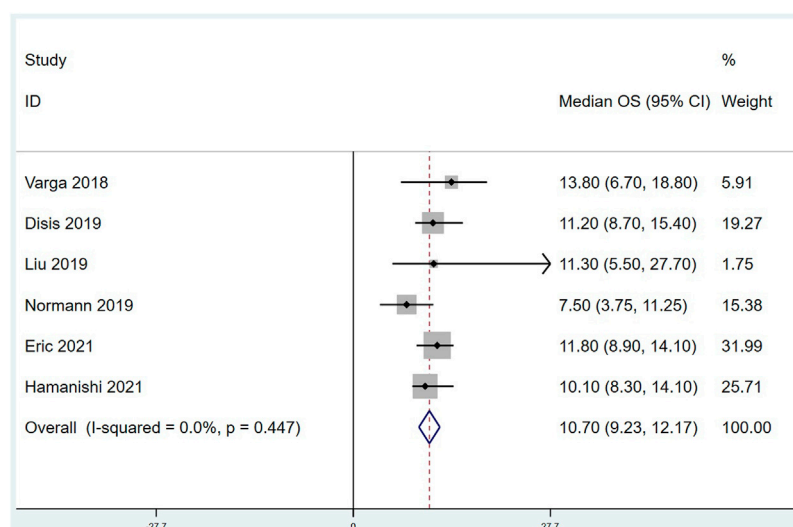
FIGURE 4
Forest plots of the Summarized median overall survival (OS).

OS is 13.8 months (7.75–19.85), median PFS is 2.10 months (2.05–2.15), TRAEs is 73.1% (68.4%–77.6%), and iAEs is 22.9% (18.8%–27.0%); Others combination effect value ORR is 10.2% (3.0%–20.1%), DCR is 22.2% (2.8%–60.0%), median OS is 11.30 months (0.20–22.40), median PFS is 2.90 months (0.80–5.00), and TRAEs is 83.2% (71.6%–94.7%).

Publication bias and sensitivity analyses

We performed Begg's and Egger's tests to assess the presence of publication bias in this study. As displayed in Supplementary Figure S2, publication bias was not significant in studies on ORR ($p = 0.107$), DCR ($p = 0.592$), OS ($p = 0.707$), PFS ($p = 0.466$), TRAEs ($p = 0.711$), and iRAEs ($p = 0.734$) based on Begg's tests. Similar results were observed based on Egger's tests (ORR: $p = 0.06$; DCR: $p = 0.919$; OS: $p = 0.724$; PFS: $p = 0.225$; TRAEs: $p = 0.775$; iRAEs: $p = 0.653$) (Supplementary Figure S3). Sensitivity analysis proved that our results were robust (Supplementary Figure S4).

Discussion

In this study, 11 studies, involving 990 patients, were analyzed to evaluate the efficacy of PD-1/PD-L1 inhibitors in the treatment of recurrent/refractory OC. Our results indicated that in patients with recurrent/refractory OC, PD-1/PD-L1 inhibitors were used alone and there was no obvious evidence for the improvement of efficacy and survival. As for safety, the incidences of TRAEs and iAEs are high, so PD-1/PD-L1 inhibitors should be applied based on individual conditions.

Currently, the 2022 NCCN guidelines show that PD-1/PD-L1 inhibitors are effective in some cases of recurrent epithelial OC (including rare pathological types) and recurrent malignant germ cell tumors, but PD1/PD-L1 inhibitors are not recommended for recurrent malignant sex cord stromal tumors. Therefore, in the case of unsatisfactory effects of surgery, chemotherapy and other treatment methods, immunotherapy can be considered for such patients (Ovarian, 2022). However, the guidelines only recommend that patients with MSI-H/dMMR may benefit from immunotherapy. Although PD-1/PD-L1 inhibitors have made breakthrough progress in the treatment of gynecological tumors, the current immunotherapy effect in OC is still not satisfactory or perfect. The reasons are closely related to the immune escape mechanism of OC and the changes of tumor immune microenvironment (TIME): 1) Recognizing related antigens is weakly developed: Among various cancers, including OC, NY-ESO-1 is considered as a promising and effective target for immunotherapy (Gordeeva, 2018). Some studies revealed that no NY-ESO-1 peptide antigen was found in major histocompatibility complex (MHC-1) or MHC-2 molecules in 42 epithelial OC samples (Schuster et al., 2017). In clinical trials of OC, many solid tumor targets rely on tumor related antigens that have been discovered, such as HER2, WT1, NY-ESO-1, and p53, while they do not all exist on MHC molecules. Meanwhile, these studies has not been proved that the tumor antigens in question do not get processed and presented on MHC-1 or MHC-2 molecules. Therefore, the induction of immune response against these antigens may mislead immune cells, and thus prevent them from attacking tumor cells. 2) Inhibition of antigen presenting cells: Antigen presenting cells include macrophages, dendritic cells, and B lymphocytes. Severe dysfunction of dendritic cells occurs in advanced OC. Cancer cells infiltrate dendritic cells in large quantities and secrete PGE2 and TGF-β. By inducing PD-L1 and arginase activity, normal dendritic cells with immune function can be transformed into immunosuppressive cells (Chae et al., 2017). 3) Inhibition of tumor killing immune cells and activation of immunosuppressive cells: Regulatory T cells (Tregs) can inhibit the anti-tumor response of T cells. Tregs negatively regulates anti-tumor
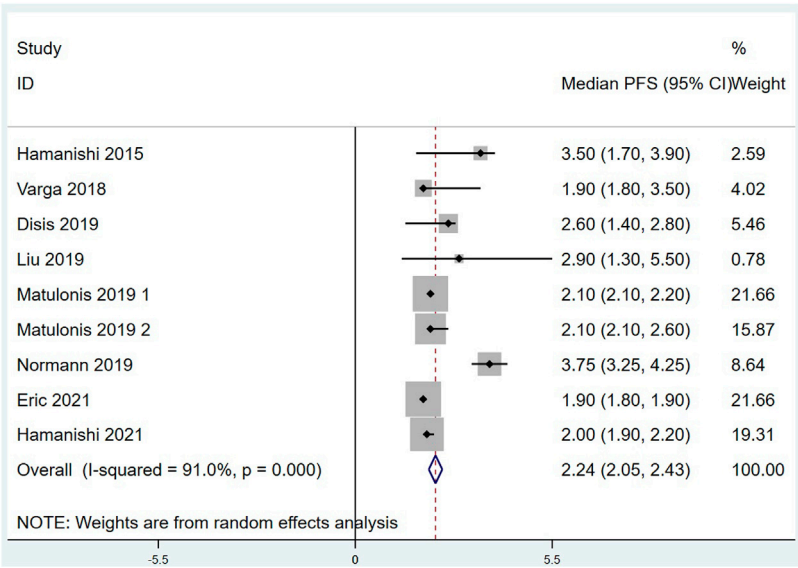
FIGURE 5
Forest plots of the Summarized median progression free survival (PFS).

response in a direct and indirect manner (Mishra et al., 2021; Puleo and Polyak, 2022). Curiel et al. confirmed that CD4⁺CD25+FOXP3+Tregs specifically inhibited anti-tumor T cells *in vivo* and promoted tumor growth (Curiel et al., 2004). Their existence is correlated with the poor prognosis of OC. Myeloid derived suppressor cells (MDSCs) have a significant ability to inhibit T cell response (Lim et al., 2020), and they increase in OC patients and play an important role in disease progression. 4) The mechanisms of the OC immunosuppressive network include the inhibition of CD8+effector T cells by Tregs, as described previously. Secondly, indoleamine-2, 3-dioxygenase (IDO), an immune regulatory enzyme, induces immune tolerance by locally consuming tryptophan and producing toxic tryptophan metabolites (such as kynurenine), thus resulting in the growth of effector T cells or NK cells in TME that is hindered and inhibits their killing function. IDO inhibitors can improve the anti-tumor efficacy of current chemotherapy or immunotherapy (Zhai et al., 2020); The most
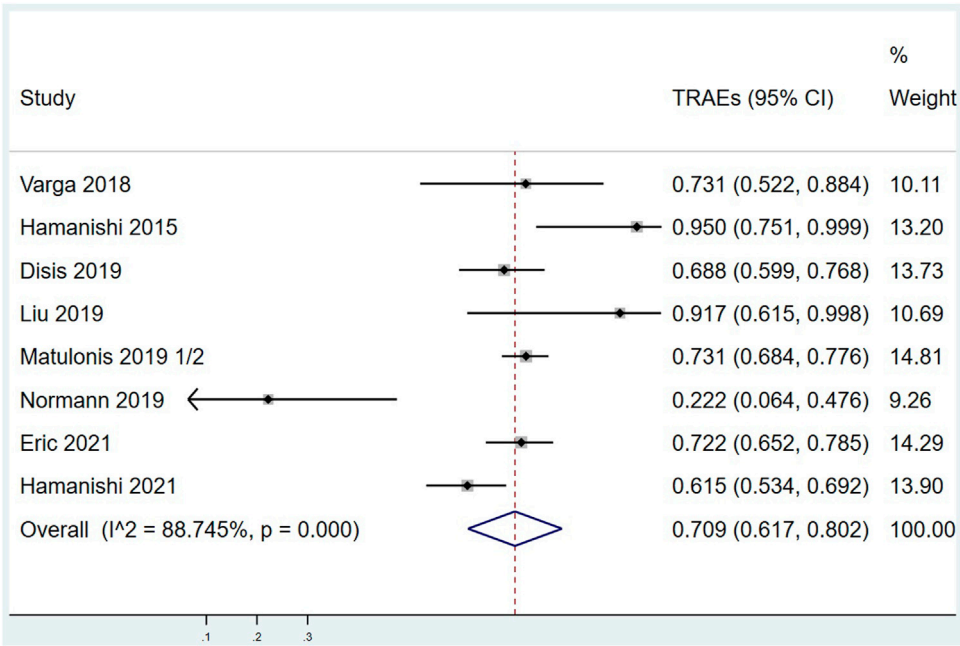
FIGURE 6
Forest plots of the overall treatment related adverse events rate (TRAEs).

classical inhibition pathway is the combination of inhibitory immune checkpoint CTLA4 and PD-1 with ligand PD-L1; in addition, MDSCs and inhibitors, such as TGF- β, also participate in regulating the immunosuppressive network of OC (Odunsi, 2017).

Future research directions of immunotherapy are displayed as follows. Most preclinical and clinical studies focus on recurrent/metastatic/persistent/late unresectable gynecologic tumors (Brahmer et al., 2012; Hamanishi et al., 2015; Disis et al., 2019; Liu et al., 2019; Matulonis et al., 2019; Normann et al., 2019; Varga et al., 2019; Desai et al., 2020; Hamanishi et al., 2021; Pujade-Lauraine et al., 2021). However, more and more evidence supports that it should be used as early as possible when the patients are in generally good condition and the tumor load is small. In recent years, studies have suggested that early application of PD-1/PD-L1 inhibitor in the treatment of triple negative breast cancer and non-small cell lung cancer could benefit patients (Topalian et al., 2020). Another highly concerned treatment direction is combination therapy. Research in OC illustrated that the ORR of the combination of PD-1/PD-L1 inhibitors and chemotherapy was the highest [36% (95% CI: 24%, 51%)], the ORR of the combination of PD-1/PD-L1 inhibitors and anti-angiogenesis therapy was 30% (95% CI: 19%, 44%), and the ORR of the combination of PD-1/PD-L1 inhibitors and poly adenosine diphosphate ribose polymerase (PARP) inhibitors was 17% (95% CI:11%, 26%) (Zhu et al., 2021). However, the combined use of multiple drugs is like a double-edged sword, which brings about a new problem: the toxic and side effects of drugs. Compared with the existing PD-1/PD-L1 inhibitor combined with chemotherapy, this study showed that the

single drug treatment of PD1/PD-L1 inhibitor could not significantly reduce the incidence of serious adverse reactions. Therefore, how to achieve the best treatment effect for patients with the least toxic and side effects is an urgent problem to be solved in the combined application of PD-1/PD-L1 inhibitors. It is also one of the research directions in the future to explore more effective predictors. At present, clinical efficacy predictors include dMMR/MSI-H, PD-L1, and TMB-H, but these predictors are not ideal. On the one hand, it is because the ORR of PD-1 inhibitor is poor, even in PD-L1 positive OC patients (Varga et al., 2019). On the other hand, KEYNOTE-100 shows a low MSI rate in OC (Matulonis et al., 2019), and the TMB of OC patients is also very low.

Moreover, before using immunotherapy, we should carefully consider the patient's sociological factors, lifestyle, metabolic disorders, and other variables, aiming to obtain the best treatment results. In this study, it showed that race, obesity, smoking, exercise, and drinking habits affect the effectiveness of immunotherapy, while diabetes and hypertension are the results of immunotherapy, rather than the causes. Hormone signaling also affects prostate cancer, endometrial cancer, OC, and colon cancer. It is imperative to determine the hormone response profile of individual tumor in the context of ICI therapy (Deshpande et al., 2020).

Zhu J et al. pointed out that PD-1/PD-L1 inhibitors alone have limited efficacy in OC. PD-1/PD-L1 inhibitor combined with chemotherapy can be recommended for further research. Compared with their research, this study further explored the safety of immunotherapy, the immune escape mechanism of OC and the efficacy of various types of PD-1/PD-L1 inhibitors on OC (Zhu et al., 2021).
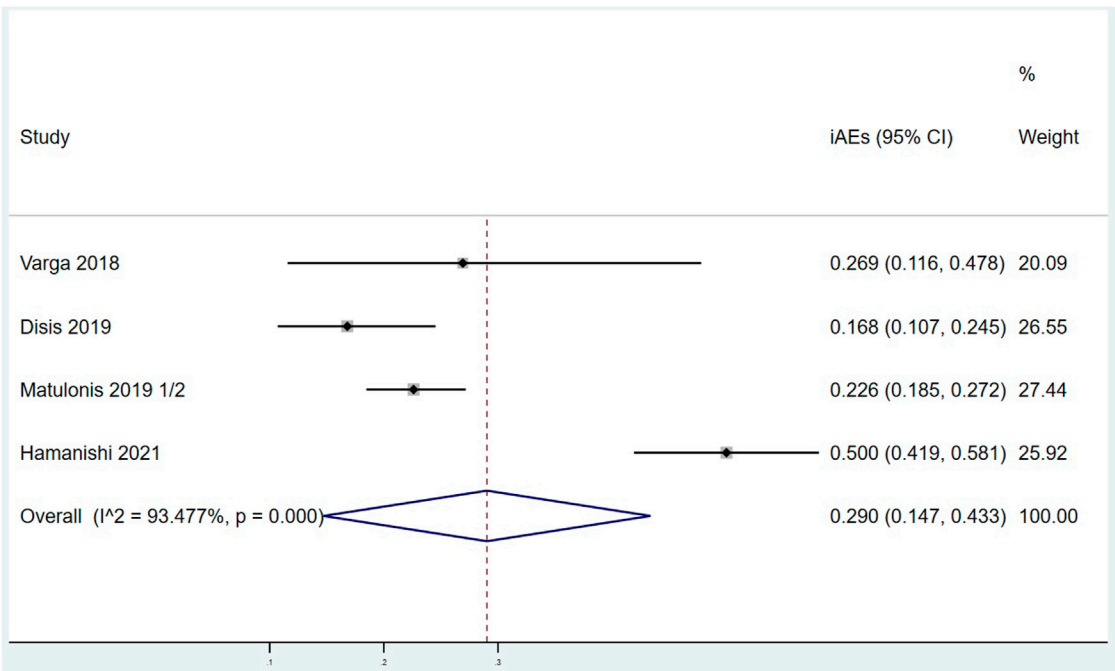

FIGURE 7
Forest plots of the overall immune related adverse events rate (iAEs).

This study has some limitations. First, most of the articles included were non-comparable, and include phase I–III clinical studies, which makes this study have certain heterogeneity. Second, PD-1/PD-L1 inhibitors are different in the study, which inevitably leads to deviation. Third, there is not enough data to evaluate the patient's Body Mass Index, allergy history, race, drinking history, smoking history, and other characteristics.

Conclusion

To our knowledge, this meta-analysis is the first to focus on the efficacy of PD-1/PD-L1 inhibitors alone in recurrent/refractory OC, which is timely and necessary. According to this study, the efficacy and safety of PD-1/PD-L1 inhibitors in patients with recurrent and refractory OC are not satisfactory, which is far from the role of PARP inhibitors and immunotherapy in the treatment of metastatic and recurrent cervical cancer. At present, we often put PD-1/PD-L1 inhibitors in the post-treatment of OC. When other drugs are not effective, PD-1/PD-L1 inhibitors can be used alone or in combination with other drugs according to the patient's genetic status.

Data availability statement

Publicly available datasets were analyzed in this study. This data can be found here: The datasets presented in this study can be found in online repositories. The names of the repository/repositories and accession number(s) can be found below: PubMed, Embase, and the Cochrane Library.

Author contributions

SZ, Conceptualization, Methodology, Data curation, Writing-Original draft preparation, Visualization, Software, investigation, writing - review and editing. DL, YY, LZ and XJ conceptualization, investigation, ,writing-review and editing. LL and BL, final approval

of the version, writing- review and editing. All authors contributed to the article and approved the submitted version.

Conflict of interest

The authors declare that the research was conducted in the absence of any commercial or financial relationships that could be construed as a potential conflict of interest.

Publisher's note

All claims expressed in this article are solely those of the authors and do not necessarily represent those of their affiliated organizations, or those of the publisher, the editors and the reviewers. Any product that may be evaluated in this article, or claim that may be made by its manufacturer, is not guaranteed or endorsed by the publisher.

Supplementary material

The Supplementary Material for this article can be found online at: https://www.frontiersin.org/articles/10.3389/fphar.2023.1111061/full#supplementary-material

SUPPLEMENTARY FIGURE S1
Forest plots of the pooled mild-moderate TRAEs rate **(A)**, and severe TRAEs rate **(B)**.

SUPPLEMENTARY FIGURE S2
Begg's publication bias funnel plots. **(A)** ORR; **(B)** DCR; **(C)** OS; **(D)** PFS; **(E)** TRARs; **(F)** iAEs.

SUPPLEMENTARY FIGURE S3
Egger's publication bias funnel plots. **(A)** ORR; **(B)** DCR; **(C)** OS; **(D)** PFS; **(E)** TRARs; **(F)** iAEs.

SUPPLEMENTARY FIGURE S4
Sensitivity analysis for the meta-analysis. **(A)** ORR; **(B)** DCR; **(C)** OS; **(D)** PFS; **(E)** TRARs; **(F)** iAEs.

References

Boustani, J., Lecoester, B., Baude, J., Latour, C., Adotevi, O., Mirjolet, C., et al. (2021). Anti-PD-1/Anti-PD-L1 drugs and radiation therapy: Combinations and optimization strategies. *Cancers (Basel)* 13 (19), 4893. doi:10.3390/cancers13194893

Brahmer, J. R., Tykodi, S. S., Chow, L. Q., Hwu, W. J., Topalian, S. L., Hwu, P., et al. (2012). Safety and activity of anti-PD-L1 antibody in patients with advanced cancer. *N. Engl. J. Med.* 366 (26), 2455–2465. doi:10.1056/NEJMoa1200694

Bray, F., Ferlay, J., Soerjomataram, I., Siegel, R. L., Torre, L. A., and Jemal, A. (2020). Global cancer statistics 2018: GLOBOCAN estimates of incidence and mortality worldwide for 36 cancers in 185 countries. *CA Cancer J. Clin.* 70 (4), 313. doi:10.3322/caac.21492

Chae, C. S., Teran-Cabanillas, E., and Cubillos-Ruiz, J. R. (2017). Dendritic cell rehab: New strategies to unleash therapeutic immunity in ovarian cancer. *Cancer Immunol. Immunother.* 66 (8), 969–977. doi:10.1007/s00262-017-1958-2

Curiel, T. J., Coukos, G., Zou, L., Alvarez, X., Cheng, P., Mottram, P., et al. (2004). Specific recruitment of regulatory T cells in ovarian carcinoma fosters immune privilege and predicts reduced survival. *Nat. Med.* 10 (9), 942–949. doi:10.1038/nm1093

Desai, J., Deva, S., Lee, J. S., Lin, C. C., Yen, C. J., Chao, Y., et al. (2020). Phase IA/IB study of single-agent tislelizumab, an investigational anti-PD-1 antibody, in solid tumors. *J. Immunother. Cancer* 8 (1), e000453. doi:10.1136/jitc-2019-000453

Deshpande, R. P., Sharma, S., and Watabe, K. (2020). The confounders of cancer immunotherapy: Roles of lifestyle, metabolic disorders and sociological factors. *Cancers (Basel)* 12 (10), 2983. doi:10.3390/cancers12102983

Disis, M. L., Taylor, M. H., Kelly, K., Beck, J. T., Gordon, M., Moore, K. M., et al. (2019). Efficacy and safety of Avelumab for patients with recurrent or refractory ovarian cancer: Phase 1b results from the JAVELIN solid tumor trial. *JAMA Oncol.* 5 (3), 393–401. doi:10.1001/jamaoncol.2018.6258

Global (2020). Latest global cancer data: Cancer burden rises to 19.3 million new cases and 10.0 million cancer deaths in 2020. [EB/OL] Available at; https://www.iarc.fr/fr/news.

Gordeeva, O. (2018). Cancer-testis antigens: Unique cancer stem cell biomarkers and targets for cancer therapy. *Semin. Cancer Biol.* 53, 75–89. doi:10.1016/j.semcancer.2018.08.006

Hamanishi, J., Mandai, M., Ikeda, T., Minami, M., Kawaguchi, A., Murayama, T., et al. (2015). Safety and antitumor activity of anti-PD-1 antibody, Nivolumab, in patients with platinum-resistant ovarian cancer. *J. Clin. Oncol.* 33 (34), 4015–4022. doi:10.1200/JCO.2015.62.3397

Hamanishi, J., Takeshima, N., Katsumata, N., Ushijima, K., Kimura, T., Takeuchi, S., et al. (2021). Nivolumab versus gemcitabine or pegylated liposomal doxorubicin for patients with platinum-resistant ovarian cancer: Open-label, randomized trial in Japan (NINJA). *J. Clin. Oncol.* 39 (33), 3671–3681. doi:10.1200/JCO.21.00334

Lim, H. X., Kim, T. S., and Poh, C. L. (2020). Understanding the differentiation, expansion, recruitment and suppressive activities of myeloid-derived suppressor cells in cancers. *Int. J. Mol. Sci.* 21 (10), 3599. doi:10.3390/ijms21103599

Liu, J. F., Gordon, M., Veneris, J., Braiteh, F., Balmanoukian, A., Eder, J. P., et al. (2019). Safety, clinical activity and biomarker assessments of atezolizumab from a Phase

I study in advanced/recurrent ovarian and uterine cancers. *Gynecol. Oncol.* 154 (2), 314–322. doi:10.1016/j.ygyno.2019.05.021

Markham, A. (2021). Dostarlimab: First approval. *Drugs* 81 (10), 1213–1219. doi:10.1007/s40265-021-01539-5

Matulonis, U. A., Shapira-Frommer, R., Santin, A. D., Lisyanskaya, A. S., Pignata, S., Vergote, I., et al. (2019). Antitumor activity and safety of pembrolizumab in patients with advanced recurrent ovarian cancer: Results from the phase II KEYNOTE-100 study. *Ann. Oncol.* 30 (7), 1080–1087. doi:10.1093/annonc/mdz135

Mishra, S., Liao, W., Liu, Y., Yang, M., Ma, C., Wu, H., et al. (2021). TGF-β and Eomes control the homeostasis of CD8+ regulatory T cells. *J. Exp. Med.* 218 (1), e20200030. doi:10.1084/jem.20200030

Moher, D., Liberati, A., Tetzlaff, J., and Altman, D. G.PRISMA Group (2009). Reprint-preferred reporting items for systematic reviews and meta-analyses: The PRISMA statement. *Phys. Ther.* 89 (9), 873–880. doi:10.1093/ptj/89.9.873

Normann, M. C., Türzer, M., Diep, L. M., Oldenburg, J., Gajdzik, B., Solheim, O., et al. (2019). Early experiences with PD-1 inhibitor treatment of platinum resistant epithelial ovarian cancer. *J. Gynecol. Oncol.* 30 (4), e56. doi:10.3802/jgo.2019.30.e56

O'Donnell, J. S., Long, G. V., Scolyer, R. A., Teng, M. W., and Smyth, M. J. (2017). Resistance to PD1/PDL1 checkpoint inhibition. *Cancer Treat. Rev.* 52, 71–81. doi:10.1016/j.ctrv.2016.11.007

Odunsi, K. (2017). Immunotherapy in ovarian cancer. *Ann. Oncol.* 28, viii1–viii7. doi:10.1093/annonc/mdx444

Ovarian (2022). National comprehensive cancer networks. Practice guidelines in oncology: Ovarian cancer. Available at: https://www.nccn.org/patients.Version1.

Pujade-Lauraine, E., Fujiwara, K., Ledermann, J. A., Oza, A. M., Kristeleit, R., Ray-Coquard, I. L., et al. (2021). Avelumab alone or in combination with chemotherapy versus chemotherapy alone in platinum-resistant or platinum-refractory ovarian cancer (JAVELIN ovarian 200): An open-label, three-arm, randomised, phase 3 study. *Lancet Oncol.* 22 (7), 1034–1046. doi:10.1016/S1470-2045(21)00216-3

Puleo, J., and Polyak, K. (2022). A Darwinian perspective on tumor immune evasion. *Biochim. Biophys. Acta Rev. Cancer* 1877 (1), 188671. doi:10.1016/j.bbcan.2021.188671

Schuster, H., Peper, J. K., Bösmüller, H. C., Rohle, K., Backert, L., Bilich, T., et al. (2017). The immunopeptidomic landscape of ovarian carcinomas. *Proc. Natl. Acad. Sci. U. S. A.* 114 (46), E9942–E9951. doi:10.1073/pnas.1707658114

Shimokawa, M., Kogawa, T., Shimada, T., Saito, T., Kumagai, H., Ohki, M., et al. (2018). Overall survival and post-progression survival are potent endpoint in phase III trials of second/third-line chemotherapy for advanced or recurrent epithelial ovarian cancer. *J. Cancer* 9 (5), 872–879. doi:10.7150/jca.17664

Siegel, R. L., Miller, K. D., Fuchs, H. E., and Jemal, A. (2021). Cancer statistics, 2021. *CA Cancer J. Clin.* 71 (4), 359. doi:10.3322/caac.21654

Topalian, S. L., Taube, J. M., and Pardoll, D. M. (2020). Neoadjuvant checkpoint blockade for cancer immunotherapy. *Science* 367 (6477), eaax0182. doi:10.1126/science.aax0182

Varga, A., Piha-Paul, S., Ott, P. A., Mehnert, J. M., Berton-Rigaud, D., Morosky, A., et al. (2019). Pembrolizumab in patients with programmed death ligand 1-positive advanced ovarian cancer: Analysis of KEYNOTE-028. *Gynecol. Oncol.* 152 (2), 243–250. doi:10.1016/j.ygyno.2018.11.017

Zhai, L., Bell, A., Ladomersky, E., Lauing, K. L., Bollu, L., Sosman, J. A., et al. (2020). Immunosuppressive Ido in cancer: Mechanisms of action, animal models, and targeting strategies. *Front. Immunol.* 11, 1185. doi:10.3389/fimmu.2020.01185

Zhu, J., Yan, L., and Wang, Q. (2021). Efficacy of PD-1/PD-L1 inhibitors in ovarian cancer: A single-arm meta-analysis. *J. Ovarian Res.* 14 (1), 112. doi:10.1186/s13048-021-00862-5

Targeted therapy and immunotherapy: Diamonds in the rough in the treatment of epithelial ovarian cancer

Xu Huang[1,2†], Xiao-Yu Li[1,2†], Wu-Lin Shan[1], Yao Chen[3], Qi Zhu[1] and Bai-Rong Xia[2]*

[1]The First Affiliated Hospital of USTC, Division of Life Sciences and Medicine, University of Science and Technology of China, Hefei, Anhui, China, [2]Bengbu Medical College Bengbu, Anhui, China, [3]Department of Obstetrics and Gynecology, The First Affiliated Hospital of USTC, Division of Life Sciences and Medicine, University of Science and Technology of China, Anhui Provincial Cancer Hospital, Hefei, Anhui, China

Currently, for ovarian cancer, which has the highest mortality rate among all gynecological cancers, the standard treatment protocol is initial tumor cytoreductive surgery followed by platinum-based combination chemotherapy. Although the survival rate after standard treatment has improved, the therapeutic effect of traditional chemotherapy is very limited due to problems such as resistance to platinum-based drugs and recurrence. With the advent of the precision medicine era, molecular targeted therapy has gradually entered clinicians' view, and individualized precision therapy has been realized, surpassing the limitations of traditional therapy. The detection of genetic mutations affecting treatment, especially breast cancer susceptibility gene (BRCA) mutations and mutations of other homologous recombination repair defect (HRD) genes, can guide the targeted drug treatment of patients, effectively improve the treatment effect and achieve a better patient prognosis. This article reviews different sites and pathways of targeted therapy, including angiogenesis, cell cycle and DNA repair, and immune and metabolic pathways, and the latest research progress from preclinical and clinical trials related to ovarian cancer therapy.

KEYWORDS

epithelial ovarian cancer, angiogenesis inhibitor, poly (ADP ribose) polymerase inhibitor, immunotherapy, targeted therapy, tumor microenvironment, clinical trials

1 Introduction

Among cancers of the female reproductive system, ovarian cancer (OC) ranks first in terms of recurrence, morbidity and mortality (Lheureux et al., 2019a) and is a serious threat to women's health. According to the survey statistics of the American Cancer Society, there will be 19,880 new cases of OC and 12,810 deaths in the United States in 2022 (Siegel et al., 2022). Approximately 85%–90% of OCs are epithelial in nature (Sisay and Edessa, 2017); however, due to the lack of obvious symptoms in the early stages of epithelial ovarian cancer (EOC) and the lack of effective early screening tools, the EOC of patients is already at an advanced stage (stage III-IV) at the time of diagnosis (Miller et al., 2020). Timely tumor cytoreduction combined with platinum-based chemotherapy combined/not combined with targeted maintenance therapy has become the initial standard of care for OC (Buechel et al., 2019) but tumor recurrence or persistence, with a median progression-free survival (mPFS)

FIGURE 1
Targeted drugs approved by FDA, approval time and corresponding indications.
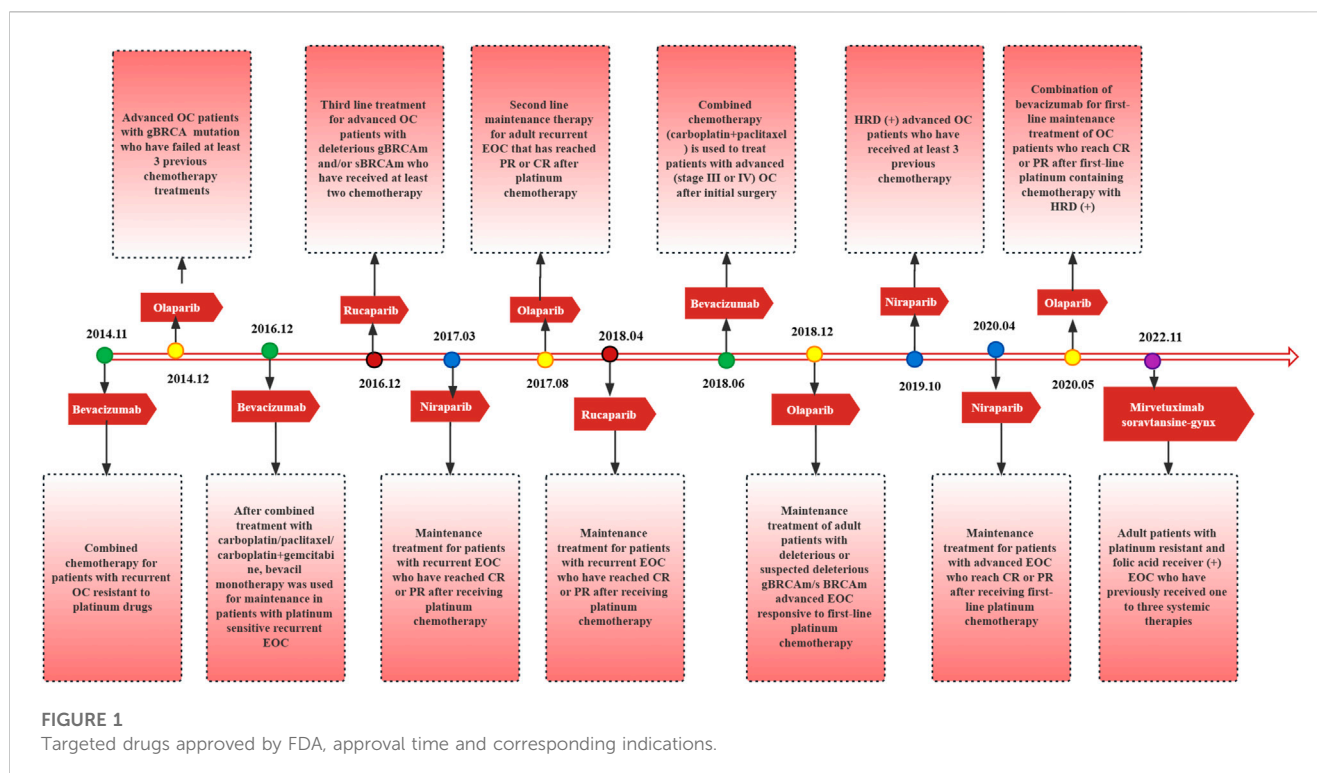
of only 12–18 months (Boussios et al., 2020) and ultimately no treatment, resulting in a 5-year overall survival (OS) rate of only approximately 30% (Lheureux et al., 2019b). Accordingly, a significant need for improved therapeutic approaches more importance has been attached to cancer biological research, which aids the discovery of novel biomarkers, defining more effective molecular targets, and developing new treatment strategies.

Targeted therapies and immunotherapies have emerged as novel treatment strategies for ovarian cancer, which driven the management of ovarian cancer into individualized treatments. A drug targeting angiogenesis, bevacizumab, combined with platinum/taxane-based chemotherapy prolongs progression-free survival (PFS) by 3.5 months in patients with OC and has been recommended by National Comprehensive Cancer Network (NCCN) guidelines as a first-line treatment for OC (Armstrong et al., 2022). In addition, approximately 30% of epithelial ovarian tumors have homologous recombination repair defects (HRDs). EOC tumors with HRDs are resistant to platinum-based chemotherapy, and these tumors show higher sensitivity to poly (ADP ribose) polymerase inhibitor (PARPi) therapy (Miller et al., 2020; Vergote et al., 2022). PARPis have been widely used for first-line maintenance treatment (Lorusso et al., 2020) and second-line and beyond treatment of OC, significantly improving patient (Figure 1) (DiSilvestro and Alvarez Secord, 2018). Currently, the main challenge facing PARPis in clinical application is drug resistance (Li et al., 2020). However, due to the immunosuppressive tumor microenvironment (TME) of OC, monotherapy with immune checkpoint inhibitors (ICIs) targeting PD-1/PD-L1 and CTLA-4 has not achieved therapeutic effects to the satisfaction of investigators when compared to the effects of targeted agents (Kandalaft et al., 2019). Therefore, focusing on the

application of ICIs in combination with chemotherapy and targeted therapy to explore a treatment strategy of one plus one over two is a meaningful research direction for the future (Yang et al., 2020).

In this review, we aimed to discuss the application of targeted lipid metabolism therapies based on omental metastatic OC, as well as immunotherapies other than targeted ICIs (Odunsi, 2017), such as immunization vaccines and oncolytic virus therapy, in the hope of providing possible strategies for the future treatment of EOC (Ventriglia et al., 2017). We also reviewed the results and implications of trials evaluating therapy and immunotherapy in the front-line setting to define the optimal positioning of these agents in the treatment for ovarian cancer and provide a focus on preclinical studies and ongoing clinical trials of combined targeted therapy and immunotherapy as well as perspectives and potential challenges of this combination strategy.

2 Targeting angiogenesis

The recurrence and metastasis of EOC mainly manifest in the formation and invasion of abnormal tumor cells and blood vessels, accompanied by chemotherapy drug resistance (Ferrara et al., 2004). Tumor angiogenesis and metastasis involve the overexpression of hypoxia inducible factor (HIF) induced by the hypoxic microenvironment in which tumor cells live (Muz et al., 2015), which further induces the transcription and translation of vascular endothelial growth factors (VEGF) protein (Semenza, 2010) (Figure 2). Tumor cells overexpress VEGF-A, and the upregulated VEGF-A combines with its receptors on the vascular endothelial cell membrane (VEGFR-1 and VEGFR-2) to form a
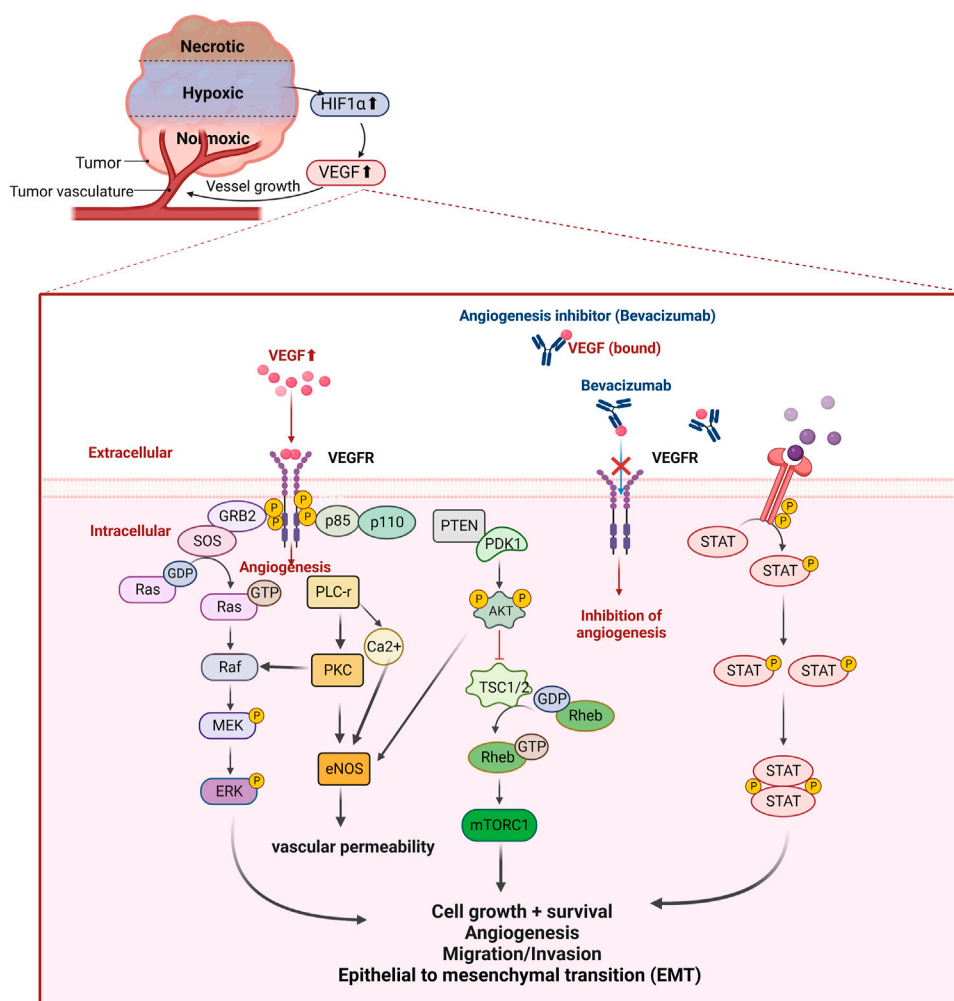
FIGURE 2
Hypoxic microenvironment in ovarian cancer and the principle of action of angiogenesis inhibitors. The hypoxic microenvironment inside the tumor mass induces increased HIF-1α expression and upregulates vascular endothelial growth factor (VEGF), which regulates tumor angiogenesis by binding to its receptor and activates intracellular signaling pathways. Expression to promote EMT-induced angiogenesis mimicry; and activation of JAK-STAT signaling pathway to participate in angiogenesis. Bevacizumab, a recombinant humanized monoclonal antibody targeting VEGF, inhibits tumor neovascularization by specifically binding to VEGF and preventing its binding to VEGFR, blocking the signaling pathway of angiogenesis.

complex, which transmits activation signals to the cascade reaction mediated by mitogen activated protein (MAP) kinase and PI3K/AKT/mTOR, inhibits proapoptotic proteins, leads to cell survival, mediates angiogenesis and lymph angiogenesis, and increases vascular permeability (Aziz et al., 2018; Li et al., 2022c). In preclinical models, VEGF-A signal blockade inhibits angiogenesis and tumor growth, and the new tumor vascular system is particularly sensitive to VEGF-A deprivation (Chen et al., 2019). In this review, we will introduce bevacizumab, which has been approved for use in the treatment of OC, and several potential angiogenesis inhibitors in clinical trials.

2.1 Bevacizumab (Avastin)

The binding of bevacizumab to circulating VEGF-A competitively inhibits VEGF-A binding to its endothelial cell surface receptors, ultimately inhibiting abnormal tumor angiogenesis (Figure 2). The 2022 NCCN guidelines recommended the simultaneous addition of bevacizumab to chemotherapy regimens for first-line treatment of OC, platinum-sensitive relapse, and second-line treatment of platinum-resistant relapse and, if effective, bevacizumab maintenance therapy at the end of chemotherapy (Armstrong et al., 2022). Two classic phase III clinical trials, ICON7 and GOG-0218 (Table 1), provided evidence that the addition of bevacizumab to standard first-line chemotherapy for EOC significantly improves PFS, and patients with poor prognosis, such as those with tumors with a high KELIM score and poor chemotherapy sensitivity, can benefit in terms of OS (Burger et al., 2011; Perren et al., 2011). Furthermore, in GOG-218, the analysis of many tumor biomarkers showed a positive correlation between OS and PFS and the efficacy of bevacizumab in first-line chemotherapy as high microvessel density (above the median) increased; similarly, high expression of tVEGF-a was

TABLE 1 Summary of bevacizumab phase III clinical trial.

Study	Setting	N	Treatment arm	PFS (median, months)	PFS, HR (95% CI)	OS (median, months)	OS, HR (95% CI)	Ref
NCT01239732 **ROSiA**	Stage IIB to IV or Grade 3 Stage I to IIA OC	1,021	Bevacizumab + paclitaxel + carboplatin	25.5 (23.7 to 27.6)	-	-	-	Oza et al. (2017)
NCT00976911 **AURELIA**	Patients with platinum-resistant EOC	361	I: Paclitaxel/topotecan/liposomal doxorubicin	3.4 (2.10 to 3.75)	-	13.3 (11.89 to 16.43)	-	Pujade-Lauraine et al. (2014)
			II: Paclitaxel/topotecan/liposomal doxorubicin + bevacizumab	6.8 (5.62 to 7.79)	0.48 (0.38 to 0.60, $p < 0.001$)	16.6 (13.70 to 18.99)	0.85 (0.66 to 1.08, $p = 0.174$)	
NCT00434642 **OCEANS**	Patients with platinum-sensitive recurrent OC	484	I: Carboplatin + gemcitabine + bevacizumab	12.4 (11.40 to 12.71)	0.484 (0.388 to 0.605, $p < 0.0001$)	33.6 (30.32 to 35.84)	0.952 (0.771 to 1.176, $p = 0.65$)	Aghajanian et al. (2015)
			II: Carboplatin + gemcitabine + placebo	8.4 (8.31 to 9.66)	-	32.9 (29.80 to 37.68)	-	
NCT00951496 **GOG-252**	Stage II-III EOC	1,560	I: Paclitaxel, IV + bevacizumab, IV + carboplatin, IV	24.9 (22.3 to 27.2)	-	75.4 (67.1 to NA)	-	(Walker et al. (2019))
			II: Paclitaxel, IV + bevacizumab, IV + carboplatin, IP	27.4 (24.6 to 28.8)	0.94 (0.81 to 1.09)	74.2 (61.9 to 78.4)	-	
			III: Paclitaxel, IP + bevacizumab, IV + carboplatin, IP	26.2 (23.8 to 28.0)	0.99 (0.86 to 1.15)	67.6 (63.5 to 74.6)	-	
NCT00262847 **GOG-0218**	Newly diagnosed, untreated stage III or IV EOC	1873	I: Placebo + paclitaxel + carboplatin	10.3	-	39.3	-	
			II: Paclitaxel + carboplatin + bevacizumab throughout	14.1	0.717 (0.625 to 0.824, $p < 0.001$)	39.7	0.915 (0.727 to 1.152, $p = 0.45$)	Burger et al. (2011)
			III: Paclitaxel + carboplatin + bevacizumab combination only	11.2	0.908 (0.795 to 1.040, $p = 0.16$)	38.7	1.036 (0.827 to 1.297, $p = 0.76$)	
NCT00483782 **ICON7**	Newly diagnosed ovarian epithelial, fallopian tube, or primary peritoneal cavity cancer	1,528	I: Paclitaxel + carboplatin	22.4	-	28.8	-	Perren et al. (2012)
			II: Paclitaxel + carboplatin + bevacizumab	24.1	0.87 (0.77 to 0.99, $p = 0.04$)	36.6	0.64 (0.48 to 0.85, $p = 0.002$)	

positively associated with prolonged OS (Bais et al., 2017). These findings suggest that in future studies, we could consider microvessel density and tVEGF-a as potential biomarkers to predict the response to first-line treatment with bevacizumab and that specific subgroups of patients with high levels of these biomarkers would be more likely to benefit from first-line treatment including bevacizumab (Bais et al., 2017). Furthermore, in the second-line treatment of patients with platinum-sensitive recurrent OC (PSROC), the OCEANS trial (Table 1) showed that for patients not previously treated with bevacizumab, the mPFS was prolonged by 4 months with the

addition of bevacizumab to the carboplatin and gemcitabine (GC) regimen compared to with the GC regimen alone (12.4 months vs 8.4 months), and the efficacy rate (79% vs 57%) indicated that the bevacizumab combination was more effective than the GC regimen alone (Aghajanian et al., 2012). Another trial (NCT01802749) found that bevacizumab remained effective when reintroduced in second-line therapy, with a 3-month prolongation of the mPFS (11.8 months vs 8.8 months). Combining the findings of these two studies, it can be concluded that patients with platinum-sensitive OC benefit from the use of bevacizumab in combination

with chemotherapy in second-line therapy regardless of whether bevacizumab is used first and that the amplification of resistant clones may not lead to bevacizumab resistance (Pignata et al., 2021). Furthermore, in the GOG-0213 trial, the mPFS (13.8 months vs 10.4 months) and OS (42.2 months vs 37.3 months) were longer with the paclitaxel and carboplatin (PC) regimen plus bevacizumab than with the PC regimen alone; the effectiveness (78% vs 59%) suggests that the advantage of combining bevacizumab (Coleman et al., 2017). Second, in patients with platinum-resistant OC, AURELIA (Table 1) showed that bevacizumab combined with standard monotherapy was also effective in prolonging PFS (3.4 months vs 6.7 months) and the objective response rate ORR (11.8% vs 27.3%, $p < 0.01$) (Pujade-Lauraine et al., 2014). Intriguingly, a subgroup of patients with malignant ascites was distinguished in the AURELIA trial, and the addition of bevacizumab to chemotherapy was also found to improve ascites control (Pujade-Lauraine et al., 2014). In a GOG-218 subgroup analysis, PFS and OS were prolonged in patients with ascites on bevacizumab, although it was not directly reported whether bevacizumab had a direct effect on ascites control (Ferriss et al., 2015). A phase II clinical trial, REZOLVE, demonstrated the potential of intraperitoneal injection of bevacizumab (IP-bev) in delaying malignant ascites formation in chemotherapy-resistant EOC, and we expect more studies to demonstrate that similar palliative therapies can benefit patients with advanced OC with peritoneal metastases (Sjoquist et al., 2021). In Table 1, we summarize a portion of the phase III clinical trials of bevacizumab for OC to date.

2.2 Apatinib (YN968D1)

Apatinib is a new generation oral tyrosine kinase inhibitor that highly selectively targets the VEGFR2 signaling pathway, primarily blocking VEGFR-induced endothelial cell migration and proliferation and reducing tumor microvessel density (Tian et al., 2011). A phase II prospective clinical study evaluated the efficacy and safety of apatinib monotherapy in 28 patients with recurrent platinum-resistant EOC, showing an ORR and disease control rate (DCR) of 41.4% and 68.9%, respectively; a mPFS and OS of 5.1 and 14.5 months, respectively; manageable toxicity; and good patient tolerance (Miao et al., 2018). This trial provided evidence that apatinib monotherapy is effective in patients with relapsed/platinum-resistant OC. In addition, the results from several clinical trials have shown that combination therapy with apatinib is beneficial and well tolerated by patients, although fistulas may occur (Teo et al., 2015). Unlike the single-arm phase II trial AEROC (NCT02867956), APPROVE (NCT04348032) enrolled more patients (152) and added a monotherapy arm with the chemotherapeutic agent pegylated liposomal doxorubicin (PLD) (Lan et al., 2018; Wang et al., 2022). In the comparison of PLD alone and PLD in combination with apatinib, the results showed that the median OS was prolonged by 2.5 months and 8.6 months, respectively, with a favorable safety profile. This study initially showed that combining apatinib with PLD in second-line chemotherapy in patients with platinum-resistant recurrent ovarian cancer (PROC) was more effective than PLD alone (Wang et al., 2014). Wang et al. conducted a small retrospective

study in which they collected and analyzed clinical data from 41 patients who relapsed after receiving apatinib monotherapy or apatinib in combination with chemotherapy, and they found that apatinib delayed progression in OC patients with biochemical relapse (defined as only CA-125 increased by more than twice the normal value, usually 2–6 months earlier than clinical evidence, such as imaging presentation. (Wang et al., 2022). We look forward to further validating this result with a large-scale trial. Furthermore, a study identified profibronectin-1 (FBN1) as a key target of chemoresistance in OC by constructing an OC-like organ model. FBN1 regulates glycolysis and angiogenesis via VEGFR2/STAT2, and its inhibition reduced sensitivity to cisplatin in this model, providing evidence for the combination of an FBN1 inhibitor and apatinib for the treatment of platinum-resistant OC (Wang et al., 2022b). Yang et al. demonstrated that in vivo, PD-L1 binds directly to VEGFR2, induces tumor angiogenesis, and relies on the c-JUN/PD-L1/VEGFR2 signaling axis to participate in the progression, invasion, and metastasis of OC, which provides evidence for the use of the pD-L1 inhibitor durvalumab combined with the VEGFR2 inhibitor anlotinib to improve the OC therapeutic effect (Yang et al., 2021a). Based on previous studies, angiogenesis inhibitor-induced hypoxia induces HRDs by affecting homologous recombination repair (HRR)-related BRCA1, BRCA2, and RAD51, resulting in enhanced effects of PARPis (Figure 2) (Mittica et al., 2018; Ashton and Bristow, 2020). Furthermore, PARP1 inhibition impedes HIF1α accumulation and attenuates HIF1α-mediated anti-angiogenic drug resistance (Martí et al., 2021; An et al., 2021), and the PARP1 inhibitor fluzoparib in combination with anlotinib contributes to treatment efficacy (Wang et al., 2019a). We expect the results of relevant clinical experiments to provide meaningful guidance for the treatment of OC.

2.3 Anlotinib (AL3818)

Anlotinib is a new oral multitarget tyrosine kinase inhibitor. Anlotinib selectively targets VEGFR2/3 and fibroblast growth factor receptor (FGFR) one to four with high affinity to inhibit VEGF/VEGFR signal transduction and platelet-derived growth factor receptor α and β as well as the activity of stem cell factor receptor (c-Kit) and Ret (Sun et al., 2016). Many studies have shown that anlotinib has a good therapeutic effect in patients with platinum-resistant and refractory OC. For example, a retrospective study in 2020 showed the benefits of single-drug treatment with anlotinib; although the number of patients included in this study was small, the DCR was 85.7%, suggesting that anlotinib had good application prospects (Ni et al., 2020). Therefore, large-scale clinical prospective and retrospective studies are needed for further verification. Su et al. found that anlotinib reactivates the immune microenvironment and relies on CD4^{+} T-cell to promote the normalization of tumor blood vessels; therefore, the combination of anlotinib and ICIs can enhance treatment efficacy (Su et al., 2022). A small retrospective study involving 32 patients with advanced EOC who had received at least two existing standard treatments showed that the efficacy of anlotinib combined with a PD-1 blocker in the treatment of advanced EOC was good, with a mPFS of 6.8 months and a

median OS of 18.5 months (Li et al., 2022c). Lan et al. found that the objective effective rate of erlotinib combined with the PDL1 inhibitor TQB2450 was 47.1%, the DCR was 97.1%, and the mPFS was 7.8 months, showing promising antitumor activity and controllable toxicity (Lan et al., 2022). In patients with platinum-resistant or refractory OC, a phase Ib study of the injection of the PD-L1 inhibitor TQB2450 in combination with anlotinib has preliminarily demonstrated an antitumor effect, with a duration of remission (DOR) reaching 97.1% and a DOR of more than 8 months in 61.3% of patients; hypertension and palmar-plantar erythrodysesthesia syndrome were the most common adverse events (AEs), with rates for both reaching 29.4%, and a further phase III experiment (NCT05145218) is recruiting patients (Lan et al., 2022).

2.4 Cediranib (AZD2171)

Cediranib is an oral small-molecule multitarget tyrosine kinase inhibitor that targets VEGFR-1, VEGFR-2, VEGFR-3 and c-kit that has shown antitumor activity against recurrent EOC (Matulonis et al., 2009). Matulonis et al. conducted a phase II study of cediranib monotherapy in patients with recurrent OC and obtained an overall remission rate of 17% and a mPFS of 5.2 months; major adverse effects included grade 3 hypertension (46%), fatigue (24%), diarrhea (13%), and grade 2 hypothyroidism (56%) but no intestinal perforation or fistulas (Ledermann et al., 2021). Compared with previous studies on bevacizumab monotherapy, the advantage is that when PFS is prolonged, the incidence of intestinal perforation or fistula treated with cediranib monotherapy is lower (Cannistra et al., 2007; Burger et al., 2007). It is worth noting that, on the one hand, cediranib targets vascular endothelial growth factor receptor (VEGFR) to induce HRD inhibition related to the hypoxic microenvironment, including the downregulation of HRR protein expression (Lu et al., 2011; Lim et al., 2014); on the other hand, cediranib inhibits platelet-derived growth factor receptor (PDGFR) and activates protein phosphatase 2A (PP2A), which mediates the inhibition of HRDs unrelated to hypoxia (Kaplan et al., 2019). Therefore, a series of clinical experiments were carried out on cediranib in combination with PARPis. ICON6 and ICON9 are phase III clinical trials for patients with PSROC. As of 2016, the mPFS in ICON6 in the chemotherapy plus cediranib and placebo maintenance therapy groups was 11.0 months and 8.7 months, respectively ($p < 0.0001$) (Ledermann et al., 2021). The ICON6 study demonstrated that cediranib maintenance therapy prolongs mPFS more effectively. However, ICON9 research focuses on the difference in the effectiveness of olaparib single-drug maintenance therapy or olaparib in combination with cediranib treatment. At present, patients are being recruited, and we look forward to the publishing of the results (Elyashiv et al., 2021). Interestingly, a preclinical study carried out by Francesca Bizzaro et al. found that for patients with OC xenotransplantation (OC-PDX), olaparib and cediranib played a synergistic role by affecting tumor cells and the TME, respectively. Regardless of the HRR mutation status, cediranib combined with olaparib shows a wider effect of inhibiting tumor vascular growth than the single drug in OC-PDX (Lheureux et al., 2020). A small study

found that when the PARPi drug resistance mechanism is different, the antitumor activity of cediranib and olaparib will also change, just as their efficacy in patients with homologous recombination gene and/or ABCB1 reverse mutations is poor (Zimmer et al., 2019). Another phase I study (NCT02484404) of the combination of olaparib plus cediranib and durvalumab in patients with recurrent platinum-resistant OC found this combination to be tolerable and initially active; thus, the study has moved into a second phase of enrolling more patients with recurrent OC (Zimmer et al., 2019). We expect more practical strategies for the posterior-line treatment of patients with recurrent OC.

3 Targeting the cell cycle and DNA damage repair

3.1 Poly (ADP-ribose) polymerase (PARP)

Poly (ADP-ribose) polymerase (PARP) is a key factor involved in DNA damage repair; on the one hand, PARP is involved in DNA single-strand break (SSB) repair-dependent base excision repair (BER) (Figure 3) (Banerjee et al., 2021); on the other hand, in double-strand break (DSB) repair, PARP contributes to HRR and inhibits error-prone non-homologous and microhomologous-mediated end-joining repair (Mirza et al., 2018). By competitively binding to NAD$^+$, PARPis interfere with BER and inhibit PARP protein activity to prevent or slow down replication divergence, ultimately leading to SSB to DSB progression (Dziadkowiec et al., 2016). In addition, PARPis promote the capture of PARP proteins at the site of DNA damage, leading to a sustained S phase in cells, and the captured PARP-DNA complexes have been shown to be more cytotoxic than unrepaired SSBs (Murai et al., 2012; Gourley et al., 2019). Thus, PARPis enable error-prone repair processes to dominate and exert synthetic lethal effects in cells accompanied by mutations in HRR-associated genes. Many PARPis, such as olaparib, rucaparib, niraparib, pamiparib (BGB-290), and fuzuloparib, play an irreplaceable role in the first-line maintenance treatment and second-line and beyond posttreatment of OC.

3.1.1 Olaparib
3.1.1.1 First-line treatment with olaparib

Olaparib was the first approved PARPi (Figure 1) and has a strong inhibitory effect on PARP enzymes (including PARP-1, PARP-2 and PARP-3) (Figure 3). In SOLO-1 (Table 2), after 2 years of olaparib maintenance therapy in patients with newly diagnosed BRCAm advanced OC, a 5-year follow-up study (through 5 March 2020) showed an mPFS of 56.0 months in the olaparib group compared with 13.8 months in the placebo group. Maintenance therapy with olaparib for 2 years extended PFS to as long as 4.5 years, and the results of this study support the use of olaparib maintenance therapy as the standard of care for this group of patients (Banerjee et al., 2021). The latest OS data from the SOLO-1 study were updated at the European Society for Medical Oncology (ESMO) 2022 meeting, where it was reported that the longest OS data to date had been obtained with olaparib (7-year follow-up showing that 67.0% and 46.5% of patients in the olaparib group and the placebo group survived, respectively); however, no
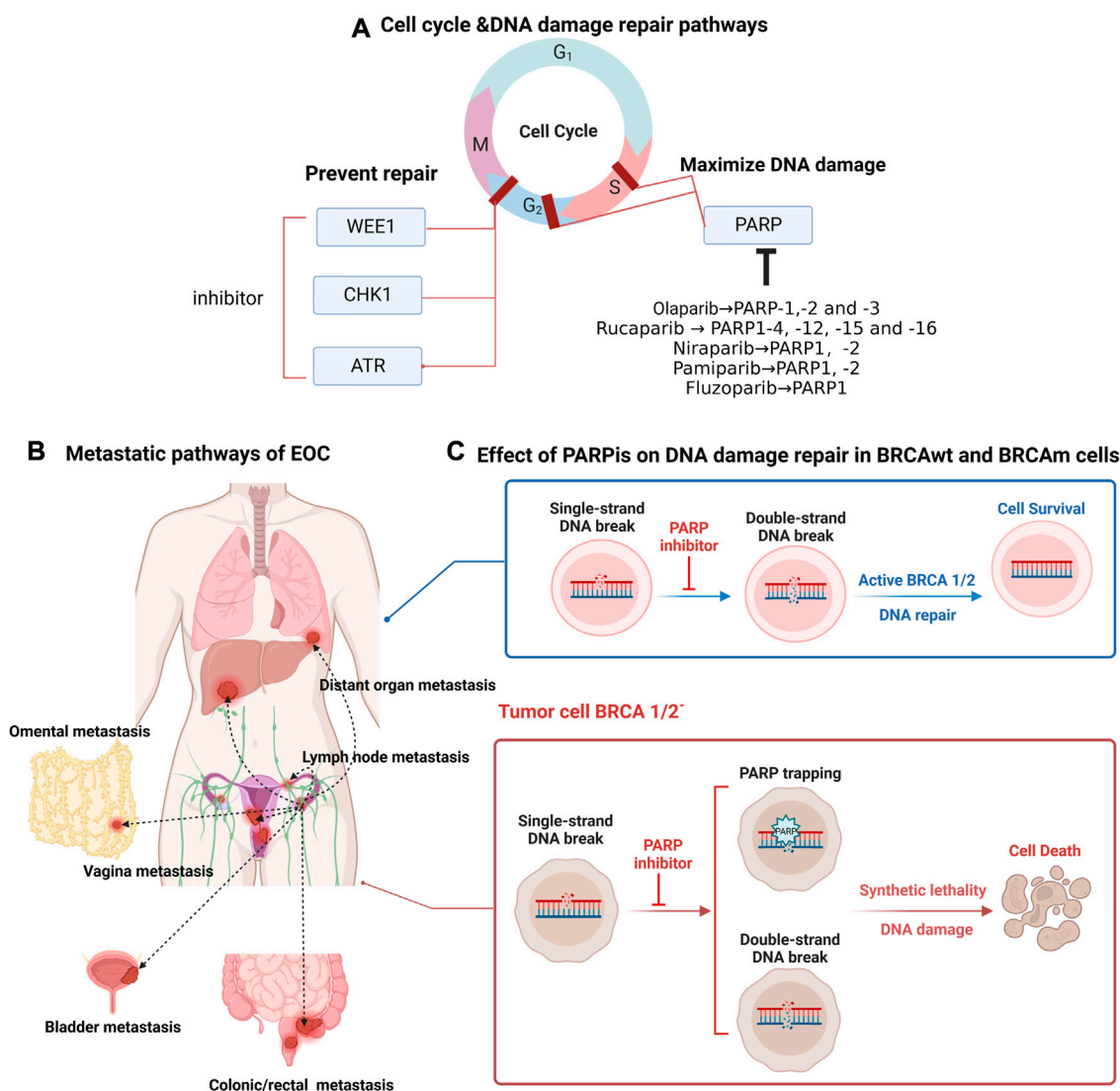
FIGURE 3
Targeting ovarian cancer cell cycle and DNA damage repair pathways, distant metastatic sites in ovarian cancer, principles of action of PARP inhibitors. **(A)** PARP proteins are involved in S-phase and G2-phase repair of the cell cycle. PARPis amplify DNA damage, and the common types of PARPis and their acting PARP proteins are described here; the main loci involved in G2-phase repair include WEE1, CHK1 and ATR, and the design of corresponding inhibitors can help prevent DNA damage repair. **(B)** Common metastatic pathways in epithelial ovarian cancer include: direct invasion of adjacent organs (vagina, bladder, rectum/colon, contralateral ovary); implantation metastases in the omentum and abdominal cavity; lymphatic metastases and hematogenous metastases involving distant organs. **(C)** Poly (ADP-ribose) polymerase (PARP) protein recognizes and repairs DNA single-strand breaks (SSBs), and unrepaired SSBs are converted to double-strand breaks (DSBs) with PARPi, which relies on the homologous recombination repair pathway for cell survival; in the presence of homologous recombination defects, including BRCA1/2 mutations, double-strand breaks cannot be repaired, causing cell death.

new safety events were identified. The median OS endpoint remained unmet, with a high OS of 75.2 months in the placebo group (DiSilvestro et al., 2023). On the basis of the data reported thus far, it is not difficult to speculate that the survival benefit from the administration of 2 years of olaparib maintenance therapy persists for several years after the end of treatment, with long-term survival truly being achieved.

The PAOLA-1 trial, with a median follow-up of 22.9 months, showed a significant PFS benefit in patients with advanced EOC by adding olaparib to bevacizumab maintenance therapy, using first-line platinum-containing agents in combination with bevacizumab,

when compared to placebo maintenance therapy (22.1 months vs 16.6 months, $p < 0.001$) (Ray-Coquard et al., 2019). The study further stratified patients according to HRD status and whether BRCA was mutated and found that bevacizumab combined with olaparib was beneficial regardless of BRCA mutation status as long as the tumor was positive for HRD (Ray-Coquard et al., 2019); in either higher risk (stage III, prior surgery and residual disease or neoadjuvant chemotherapy (NACT); stage IV) or lower risk (stage III, prior surgery, no residual disease) patients, olaparib maintenance regimen can be beneficial (Harter et al., 2022). Interestingly, Callens et al. designed the tBRCA assay based on

TABLE 2 Summary of clinical trials of parmiparib in the treatment of ovarian cancer.

Number	Combination agent	Population	N	Phase	Status	Primary outcome measures/ results
NCT03333915	NR	Chinese patients with advanced OC, fallopian cancer, and primary peritoneal cancer	128	I/II	Active, not recruiting	• Phase I: Number of participants with treatment-related adverse events
						• Phase II: ORR
NCT02361723	NR	PSOC with known or suspected harmful g/s BRCAm or HRD (+)	101	IA/I B	Completed	• ORR: CR + PR
						• Primary PK 1/PK 2/PK 3
NCT03519230	NR	Chinese patients with PSOC	216	III	Active, not recruiting	• PFS
NCT05489926	NR	Patients with EOC who had previously been treated with a PARP inhibitor	15	II	Recruiting	• CBR: CR + PR
NCT03933761	NR	Patients with HGSOC or carcinosarcoma with fusion positive and reverse negative BRCA1/2 m	0	II	Withdrawn	• CBR as assessed by RECIST v1.1 or by Gynecological Cancer Intergroup (GCIG) CA125 criteria
NCT05494580	Surufatinib	PROC patients who have received PARP inhibitor treatment once	38	Ib/II	Not yet recruiting	• MTD (phase Ib)
						• Determination of PR2D (phase Ib)
						• ORR (phase II): CR + PR
NCT04985721	Tislelizumab	Patients with BRCA1/2m or without BRCA1/2m but with other germline or somatic mutations in other HR genes	60	II	Recruiting	• CBR: PR + CR
NCT05044871	**NR**	**Patients with PROC**	**160**	**II**	**Not yet recruiting**	• **ORR: CR + PR**

This study is an open-label, multicenter, umbrella study aimed to evaluate the combined, biomarker-driven, targeted treatment efficiency of Pamiparib, Bevacizumab, Tislelizumab, and Nab-paclitaxel in patients with platinum-resistant recurrent ovarian cancer (PROC). NCT05044871 is the NCT number of this study. NR indicates no combination of drugs. Patients with PROC shows that this study recruit patients with platinum-resistant recurrent ovarian cancer (PROC). ORR: CR + PR is the main clinical evaluation index of this experiment. ORR, Objective response rate; CR, complete response; PR, partial response.

the findings of this study, and they found that the tBRCA assay more reliably identified the population that could benefit in the clinic than germline (gBRCA) assays (Callens et al., 2021). A 2021 study that jointly analyzed data from patients with BRCA mutations in SOLO1 and PAOLA-1 compared newly diagnosed BRCA-mutated OC PFS improvement in patients. Olaparib in combination with bevacizumab for first-line maintenance was the best and more appropriate for patients with BRCA-mutation or HRD-positive OC (Vergote et al., 2021). Updated secondary PFS (PFS2) data at a median follow-up of 35.5 and 36.5 months for PAOLA-1 in 2022 showed that bevacizumab monotherapy in combination with olaparib vs the combination placebo group had a mPFS2 of 36.5 and 32.6 months, respectively, and the effective improvement in PFS2 suggests that the combination regimen provided sustained benefit even after progression with the first treatment (González-Martín et al., 2022).

3.1.1.2 Second-line and beyond treatment with olaparib

In SOLO-2, a study in 2021 updated the median OS prolongation by 12.9 months when reaching a median follow-up time of more than 5 years based on the previously reported significant prolongation of the mPFS in the olaparib group compared to the placebo group (Hutchinson, 2017; Francis et al., 2022), and the olaparib maintenance phase would not have a negative impact on health-related quality of life (HRQOL)

(Friedlander et al., 2018); this study supports the benefit of maintenance treatment with olaparib in patients with PSROC with BRCA1/2 mutations. Based on data provided by SOLO2, Frenel et al. evaluated the time to second progression (TTSP) from RECIST progression to the next progression/death in placebo-treated and olaparib-treated cohorts of patients who received non-platinum and platinum-based chemotherapy, respectively, and they found that when second-line olaparib was maintained for reprogression, patients with recurrent BRCA1/2-mutant PSROC had weaker efficacy when platinum-containing chemotherapy was reapplied than patients who had not previously used PARPis (Frenel et al., 2022). Francis et al. found that dose changes within the first 12 weeks of treatment did not impact survival outcomes, suggesting that in clinical practice, patients who had olaparib reduced or even discontinued due to AE intolerance would not experience an impact on PFS and OS (Domchek et al., 2016). An updated median OS of 32.7 months at a median follow-up of 33.1 months for the phase IIIb OPINION study was published at the 2022 ESMO Annual Meeting; the Kaplan-Meier analysis showed OS rates of 65.8% and 54.9% at 24 and 30 months, respectively, and these data further support the use of olaparib maintenance therapy for the treatment of non-gBRCAm PSROC (Poveda Velasco et al., 2022). The L-MOCA study was the first clinical study to assess the efficacy and tolerability of olaparib maintenance treatment in Asian PSROC patients, and an mPFS

of 16.1 months for all patients as of 25 December 2020, was reported (Gao et al., 2022). Subgroup analysis showed that compared to the corresponding wild-type group mPFS, the BRCA mutation group mPFS (21.2 months vs 11.0 months) and the HRR mutation group mPFS (18.3 months vs 13.3 months) were better. The AE incidence was 99.1%, with the most common AE being anemia (76.4%), and 9.4% of patients discontinued treatment due to treatment-related AEs. This study showed that in Asian PSROC patients, olaparib maintenance therapy had significant efficacy regardless of BRCA status and was well tolerated by patients (Gao et al., 2022). In 2014, the Food and Drug Administration (FDA) approved olaparib in this population based on the results of Study 42 (NCT01078662), in which patients with recurrent gBRCAm OC who had received at least three chemotherapy regimens responded durably to olaparib (Figure 1) (Domchek et al., 2016). In 2020, according to data reported in the SOLO3 trial (NCT02282020), for PSROC patients with gBRCAm and ≥2 prior lines of platinum-based chemotherapy, olaparib monotherapy showed clinically relevant and significant improvements in ORR (primary endpoint) and PFS (secondary endpoint) compared with single-agent non-platinum-based chemotherapy, and the differences were statistically significance (Penson et al., 2020). At the American Society of Gynecologic Oncology (SGO) 2022, a recent analysis of the SOLO3 trial showed that the olaparib group outperformed the non-platinum chemotherapy group in PFS2, with similar OS in both treatment groups and no new safety signals identified; this provides support for olaparib as a platinum-free chemotherapy treatment strategy for patients with PSROC in the third line and beyond (Penson et al., 2022). All the studies provide convincing evidence for the use of olaparib in the second-line and beyond treatment of OC.

3.1.2 Rucaparib
3.1.2.1 First-line treatment with rucaparib

Rucaparib inhibits PARP1-4, −12, −15 and −16, as well as tankyrase 1 and 2 (Figure 3) (Musella et al., 2018). Updated ATHENA-MONO results showed a significant improvement in PFS for all patients studied in the rucaparib group (intention to treat (ITT) patients or all patients) (9.2 months vs 12.1 months); improved mPFS in the HRD-positive patient group (11.3 months vs 28.7 months, $p = 0.0004$); and a treatment benefit at the endpoint of PFS in the HRD-negative subgroup (9.1 months vs 12.1 month, $p = 0.0284$). The incidence of myelodysplastic syndrome (MDS)/acute myeloid leukemia (AML) in the rucaparib group while on treatment was 0.2% (González-Martín et al., 2019). This study supports the significant benefit of rucaparib monotherapy as first-line maintenance for OC, regardless of HRD status, in patients with advanced OC.

3.1.2.2 Second-line and beyond treatment with rucaparib

ARIEL2 (NCT01891344) showed a better outcome for patients with BRCAmut high-grade ovarian cancer (HGOC) who had received at least two chemotherapies, with an mPFS of 7.8 months, an ORR of 45.7%, and a DOR of 9.2 months, than in patients with BRCAwt/LOH-high and BRCAwt/LOH-low HGOC (Swisher et al., 2021b). Based on the phase II study, olaparib and niraparib alone have also been approved by the FDA for the third-line treatment of recurrent OC (Figure 1). In addition, ARIEL2 subgroup analysis showed longer PFS in patients with

loss of heterozygosity (LOH)-high platinum-sensitive HGOC than in patients with LOH-low cancer among BRCAwt patients, suggesting that the assessment of tumor LOH may be a useful approach to identify patients with BRCA wild-type platinum-sensitive OC (Swisher et al., 2021a; Swisher et al., 2017). The ARIEL3 study showed that, in addition to the effect on patients with PSROC, patients who had received at least two platinum-based chemotherapies showed a significantly improved PFS, with a median follow-up time of 28.1 months, compared with the placebo group. The chemotherapy-free interval (CFI), time to start first subsequent treatment (TFST), time to disease progression on subsequent treatment or time to death, and the time to start second follow-up treatment (TSST) were all statistically significantly delayed in the rucaparib maintenance group compared with the intention-to-treat, BRCAm and homologous recombination deficient cohort (PFS2), and the updated safety data are consistent with previous reports (Ledermann et al., 2020; Clamp et al., 2021; Tomao et al., 2020; O'Malley et al., 2022). This suggests that maintenance treatment with rucaparib significantly delays the start of follow-up treatment. The ARIEL4 study showed that PFS was effectively prolonged by a median follow-up time of 25.0 months in the rucaparin group compared to the chemotherapy group; this result supports the use of rucaparib in patients with recurrent BRCA1/2-mutated OC as an alternative to platinum-based chemotherapy (Kristeleit et al., 2022; O'Donnell, 2022).

3.1.3 Niraparib
3.1.3.1 First-line treatment with niraparib

Niraparib is a highly effective and selective small-molecule PARP 1/2 inhibitor (Figure 3) (Jones et al., 2015). PRIMA demonstrated for the first time that niraparib single-agent first-line maintenance therapy was effective in prolonging PFS, with a 2-year OS rate of 84% and a 38% reduction in the risk of recurrence or death, when used after platinum-containing chemotherapy for advanced OC, regardless of BRCA mutation/HRD status (O'Cearbhaill et al., 2022). The PRIME study is the largest randomized controlled phase III clinical study of a PARPi for first-line maintenance therapy in patients with advanced OC in China; data published in the Chinese population complement the PRIMA findings (Li et al., 2022a). At SGO 2022, the updated PRIME study results were encouraging, with niraparib single-agent maintenance prolonging the mPFS to 14 months in patients with "double-negative" (advanced newly diagnosed BRCA and HRD negative) OC, completely rewriting the prognosis for the "double-negative" population (Del Campo et al., 2019). In addition, the PRIME study used a personalized starting dose, which resulted in a much lower incidence of adverse reactions and better patient compliance in the niraparib group than in the PRIMA study (Del Campo et al., 2019). At SGO 2022, the latest data from the OVARIO trial were updated with sequential niraparib combined with bevacizumab maintenance therapy after first-line platinum-containing chemotherapy combined with bevacizumab in patients with newly diagnosed stage IIIB to IV OC, with an mPFS of 19.6 months at 28.7 months, respectively; immature OS data; and an OS event rate of 23.8%. This single-arm study demonstrated that first-line maintenance therapy with niraparib in combination with

bevacizumab results in promising PFS outcomes regardless of the patient's biomarker profile (Hardesty et al., 2022).

3.1.3.2 Second-line and beyond treatment with niraparib

The NOVA study included for the first time a full population of patients with PSROC exploring niraparib maintenance therapy, regardless of gBRCA mutation status, and its primary PFS endpoint was significantly prolonged in the niraparib-treated group compared with the placebo maintenance therapy group (gBRCA mutation population: 21.0 months vs 5.5 months; non-gBRCA mutation population: 9.3 months vs 3.9 months) (Mirza et al., 2016). Patients benefited from niraparib maintenance therapy regardless of whether the response to the last platinum-based treatment was a partial response or a complete response (Mirza et al., 2020). In the latest long-term follow-up data presented at SGO 2021, in the gBRCA mutation population, there was a 34% reduction in the risk of death and a 9.7-month increase in median OS in the niraparib group compared to the placebo group (43.8 months vs 34.1 months). However, in the non-gBRCA mutation population, there was no significant difference in OS between the niraparib and placebo groups (Matulonis et al., 2021). In addition, long-term safety data showed that hematological adverse reactions to niraparib occurred mainly in the first year of dosing and then decreased year by year, supporting that niraparib can be used for long-term maintenance therapy in patients with OC (Mirza et al., 2020). In a retrospective analysis of the NOVA study, it was found that patient weight should be considered when initiating niraparib treatment and that dose reduction (from 300 mg per day to 200 mg per day) in patients in the low weight group significantly reduced complications without compromising efficacy (Berek et al., 2018).

The QUADRA study showed that a 28% ORR was reached in the primary study population (patients with advanced HRD-positive PSROC in treatment lines 4–5), with OS reaching 26 months, 19 months, and 16.6 months in patients with BRCA-mutant HRD-positive, HRD-negative, or unknown HRD status, respectively, and 17.2 months in all patients in treatment lines 4 and above. In addition, in patients with platinum-sensitive OC, the ORR was 39% and 26% in those with BRCA-mutant and HRD-positive tumors, respectively. In patients with platinum-resistant and platinum-refractory OC, the ORR was 27% and 10%, respectively (Moore et al., 2019). The QUADRA study demonstrated that niraparib monotherapy prolonged OS in patients with platinum-resistant or refractory OC treated with third-line chemotherapy and beyond (Moore et al., 2019); this prompted the FDA to expand the indications for receiving niraparib monotherapy to patients with BRCA-mutant HRD + tumors for the first time, offering hope to more patients (Figure 1).

3.1.4 Pamiparib (BGB-290)

Pamiparib is a potential selective oral PARP1/2 inhibitor independently developed in China (Figure 3). Preclinical models have shown that pamiparib has pharmacological properties such as blood–brain barrier penetration and PARP-DNA complex capture (Xiong et al., 2020). Parmiparib is not a substrate of P-glycoprotein (P-gp) or

breakthrough cancer resistance protein (BCRP); thus, it is expected to overcome the PARPi resistance problem caused by their overexpression (Durmus et al., 2015). In a key phase II clinical trial (NCT0333915), pamiparib monotherapy showed sustained antitumor activity and controllable safety in patients with gBRCA-mutated OC who had previously received at least two lines of chemotherapy (Wu et al., 2022). At ESMO 2020, Wu presented results from his phase II data showing that parmiparib showed significant clinical benefit in both PSROC and PROC patients; ORRs were 64.6% and 31.6%, respectively. Notably, Wu's team also concluded that parmiparib is expected to usher in a new era of platinum-free chemotherapy treatment for OC patients (Lickliter et al., 2022). On 7 May 2021, the State Drug Administration (National Medical Products Administration (NMPA)) of China approved the marketing of pamiparib capsules for the treatment of patients with recurrent advanced OC, fallopian tube cancer or primary peritoneal cancer with gBRCA mutations who have been previously treated with second-line or beyond chemotherapy (Figure 1). Given the promising application of pamiparib in OC, in this review, we summarize the findings of all pamiparib clinical trials (https://clinicaltrials.gov) (Table 2).

3.1.5 Fuzuloparib

The FZOCUS-2 study showed a significant improvement in the mPFS in the fuzuloparib group compared to the placebo group in the overall PSROC population. Subgroup analysis showed a direction of benefit consistent with that of the overall population regardless of the presence of gBRCA 1/2 mutations. Based on this study, the first indication for fuzuloparib in the treatment of OC was approved (Li et al., 2022b).

The results of the FZOCUS-3 study showed that in patients with PSROC with gBRCA1/2 mutations previously treated with second-line or beyond chemotherapy, fuzuloparib had an objective remission rate (ORR) of 69.9%, a median time to remission (mDOR) of 10.2 months, and an mPFS of 12.0 months, with safe and controlled treatment and only one AE-induced treatment discontinuation (0.9%) (Li et al., 2021). Based on this study, the second indication for fuzuloparib in the treatment of platinum-sensitive recurrent ovarian, fallopian tube, or primary peritoneal cancer with gBRCAm after prior second-line chemotherapy or higher was approved.

3.2 Targeting folic acid receptor α (FR-α)

Folate receptor α (FRα) is a cell surface transmembrane glycoprotein whose main role is to transport folate to promote cell proliferation and DNA synthesis, and its overexpression is closely associated with an increased metabolic demand for single carbon units in tumor cells. FRα is also involved in cancer cell division and migration, and the inhibition of this receptor provides a degree of direct anticancer activity (Scaranti et al., 2020). Because the percentage of EOC tumors with FRα overexpression is close to 80%, targeting FRα has become a promising treatment for EOC (O'Malley et al., 2020; Köbel et al., 2014).
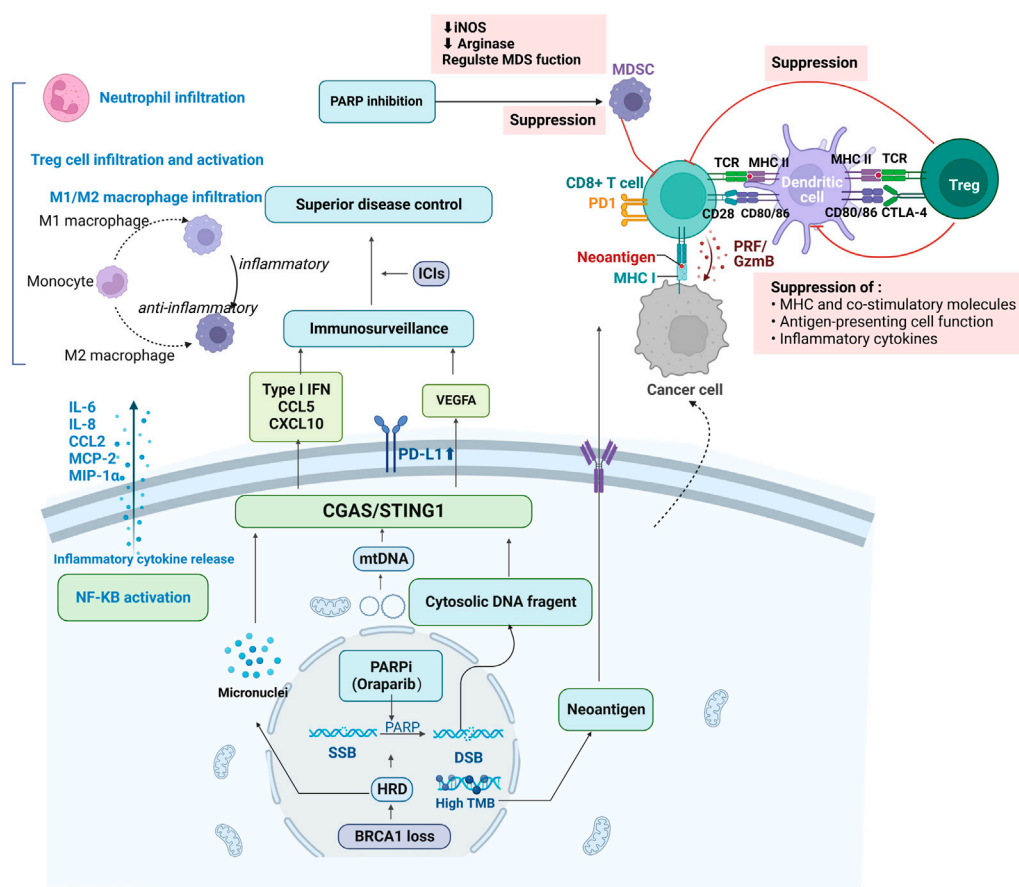
FIGURE 4
Synergy of immune checkpoint inhibitors with PARPi and tumor suppressive immune microenvironment. PARPis induces double-strand breaks in HRD cells, generating cytoplasmic dsDNA fragments, micronuclei and mtDNA, which trigger the activation of the STING pathway by binding to cyclic GMP-AMP synthase (cGAS); on the one hand, it upregulates the secretion of type I interferon, CCL5, CXCL10 and VEGFA, promoting immune escape. On the other hand, low levels of DNA damage stimulate infiltration of suppressive immune cells, such as myeloid-derived suppressor cells (MDSC) or tumor-associated macrophage (TAM), which leads to the release of free radicals and triggers further DNA damage. Antigen-presenting cells, including tumor-associated dendritic cells, are recruited and activated to drive STING-dependent type I IFN signaling. Increased expression of T cell-associated chemokines activates CD4^{+} and CD8^{+} T lymphocytes in tumor and bone marrow-derived cells, increasing infiltration of cytotoxic T-cell in the microenvironment and promoting reprogramming of immune cells to phenotypes with antitumor activity. PARPis also activates PD-L1 transcription, PD-1/PD-L1 blockade and enhances antitumor immunity; activation of the κB pathway and release of various cytokines inhibit epithelial-mesenchymal transition (EMT), thereby increasing immune cell infiltration at tumor sites.

Mirvetuximab soravtansine (IMGN853, MIRV), a first-in-class ADC consisting of a folate receptor alpha-binding antibody, a cleavable linker, and the maytansinoid payload DM4 (a potent microtubulin-targeting agent), causes cycle arrest and apoptosis in targeted cancer cells, and the drug has shown promising activity in women with platinum-based chemoresistant OC (Ponte et al., 2016). At the 2021 ASCO Annual Meeting, partial FORWARD II trial results were reported, and the investigators found strong antitumor activity and tolerability of MIRV in combination with bevacizumab in patients with FRα (+) OC with unknown platinum sensitivity. Based on previously reported data on MIRV/BEV in patients with platinum-resistant OC, this study suggests that MIRV + bevacizumab has the potential to be the combination of choice for patients with FRα-high expressing recurrent OC, regardless of platinum sensitivity

(Lheureux et al., 2019a; Sisay and Edessa, 2017). The SORAYA trial enrolled a total of 106 patients with platinum-resistant OC with high FRα expression who had received up to three prior treatment regimens, at least one of which included bevacizumab. First-line data from SORAYA were presented at the 2022 SGO Annual Meeting, and an ORR of 32.4% and a median DOR of 6.9 months for the overall efficacy population were reported. Eighty-six percent of patients experienced all-grade AEs. Most AEs were of lower grade, with donor keratopathy and blurred vision, occurring in 47% of patients, being labeled as mirvetuximab sorafenib-specific AEs (SGO, 2022; Zamarin et al., 2020). In another phase III study, benefits of MIRV treatment compared to chemotherapy were demonstrated in terms of improvements in the secondary study endpoints of the ORR, CA-125 and patient-reported outcomes, and MIRV demonstrated a more manageable

TABLE 3 Summary of all clinical trials of immune checkpoint inhibitors in the treatment of recurrent ovarian cancer published in Clinical Trials.gov.

Immune checkpoint	Inhibitor	Study	Combination agent	N	Phase	Status	Reaction to platinum
PD-1	Cemiplimab	NCT04590326	±REGN5668 (MUC16xCD28, a costimulatory bispecific) or REGN4018 (MUC16xCD3)	37	I/II	Recruiting	-
		NCT03564340	±REGN4018 (a MUC16xCD3 bispecific antibody)	554	I/II	Recruiting	-
	Pembrolizumab (MK-3475-100/KEYNOTE-100/Keytruda)	NCT03732950	NR	30	II	Recruiting	-
		NCT03734692	Cisplatin + rintatolimod (intraperitoneal)	45	I/II	Recruiting	Sensitive
		NCT02674061	NR	376	II	Completed	-
		NCT04519151	Lenvatinib	24	II	Not yet recruiting	Sensitive
		NCT04713514	± OSE2101	180	II	Recruiting	Sensitive
		NCT05231122	Bevacizumab ± anti-CD40 agonist monoclonal antibody CDX-1140	80	II	Not yet recruiting	Sensitive
		NCT04361370	Olaparib + bevacizumab	44	II	Enrolling by invitation	Sensitive
		NCT05158062	Bevacizumab + platinum-based chemotherapy (PBC)	35	II	Recruiting	Sensitive
			Olaparib as a maintenance therapy				
		NCT05116189	paclitaxel ± bevacizumab/placebo + paclitaxel ± bevacizumab	616	III	Recruiting	Resistant
		NCT02901899	Guadecitabine	45	II	Active, not recruiting	Resistant
		NCT04387227	Carboplatin	22	II	Recruiting	-
		NCT03602586	Epacadostat	14	II	Terminated	-
		NCT04919629	APL-2 (pegcetacoplan)±bevacizumab	40	II	Not yet recruiting	
		NCT02440425	Paclitaxel	42	II	Completed Has Results	Resistant
		NCT02657889	Niraparib	122	I/II	Completed	-
		NCT02537444	Acalabrutinib (ACP-196) ± pembrolizumab	78	II	Completed	-
		NCT03029598	Carboplatin	29	I/II	Completed	Resistant
		NCT02853318	Bevacizumab + cyclophosphamide	40	II	Completed	-
		NCT04781088	Paclitaxel + lenvatinib	38	II	Suspended	Resistant
		NCT03428802	NR	40	II	Recruiting	-
		NCT02608684	Cisplatin + gemcitabine	21	II	Completed	Resistant
		NCT05467670	ALX148 + Doxorubicin (PLD)	31	II	Not yet recruiting	Resistant
		NCT03539328	Pegylated liposomal + doxorubicin/paclitaxel/gemcitabine	138	II	Unknown	Resistant
		NCT03113487	Modified vaccinia virus Ankara vaccine expressing p53	29	II	Active, not recruiting	-
		NCT04575961	Platinum-based chemotherapy (carboplatin + gemcitabine/carboplatin + pegylated liposomal doxorubicin)	33	II	Recruiting	Sensitive

TABLE 3 (*Continued*) Summary of all clinical trials of immune checkpoint inhibitors in the treatment of recurrent ovarian cancer published in Clinical Trials.gov.

Immune checkpoint	Inhibitor	Study	Combination agent	N	Phase	Status	Reaction to platinum
	Nivolumab (Opdivo)	NCT02737787	WT1/ESO-1 vaccine	11	I	Active, not recruiting	-
		NCT02498600	±Ipilimumab	100	II	Active, not recruiting	-
		NCT02873962	Bevacizumab/bevacizumab ± rucaparib	76	II	Recruiting	Sensitive
		NCT03508570	±Ipilimumab	48	I b	Active, not recruiting	Resistant
		NCT05026606	Etigilimab	20	II	Recruiting	Resistant
		NCT03100006	Oregovomab	13	I b/II a	Terminated	-
		NCT04620954	Oregovomab + PLD + carboplatin	31	I/II	Recruiting	Sensitive
		NCT04840589	ZEN003694 ± ipilimumab	36	I/I b	Recruiting	Resistant
		NCT02465060	Targeted therapy directed by genetic testing (The MATCH Screening Trial)	6,452	II	Recruiting	-
PD-L1	Durvalumab (MEDI4736)	NCT03430518	Eribulin	9	I	Completed	-
		NCT04742075	Olaparib + UV1	184	II	Recruiting	-
		NCT03699449	Olaparib/chemotherapy/tremelimumab + chemotherapy/tremelimumab + paclitaxel/olaparib + cediranib	104	II	Recruiting	Resistant
			Olaparib + cediranib (without durvalumab)				
		NCT03267589	MEDI9447 (CD73)/MEDI0562 (OX40)/ MEDI0562 (OX40) + tremelimumab (without durvalumab)	25	II	Completed	-
		NCT04019288	AVB-S6-500	19	I/II	Active, not recruiting	Resistant
		NCT03277482	Tremelimumab + radiotherapy	16	I	Terminated	-
		NCT03026062	Tremelimumab	175	II	Recruiting	Resistant
		NCT02953457	Olaparib	40	II	Active, not recruiting	Resistant/ sensitive
		NCT02431559	Motolimod + PLD	53	I/II	Completed	Resistant
		NCT02484404	Olaparib ± cediranib	384	I/II	Recruiting	-
		NCT03283943	Focal-sensitizing radiotherapy	22	I	Unknown	Resistant
		NCT04739800	Cediranib ± olaparib/cediranib + olaparib (without Durvalumab)	164	II	Recruiting	Resistant
		NCT04015739	Bevacizumab + olaparib	74	II	Active, not recruiting	-
	Atezolizumab (Tecentriq)	NCT03353831	Chemotherapy + bevacizumab/ chemotherapy + Bevacizumab + placebo (without atezolizumab)	550	III	Active, not recruiting	-
		NCT03598270	Platinum-based chemotherapy followed by maintenance niraparib + placebo/ platinum-based chemotherapy followed by maintenance niraparib + atezolizumab	414	III	Active, not recruiting	Sensitive
		NCT03206047	Guadecitabine + CDX-1401 vaccine	75	I/IIb	Active, not recruiting	-
		NCT02839707	PLD + bevacizumab	444	II/III	Active, not recruiting	Resistant

(Continued on following page)

TABLE 3 (*Continued*) Summary of all clinical trials of immune checkpoint inhibitors in the treatment of recurrent ovarian cancer published in Clinical Trials.gov.

Immune checkpoint	Inhibitor	Study	Combination agent	N	Phase	Status	Reaction to platinum
		NCT03430518	Eribulin	9	I	Completed	-
		NCT03363867	Bevacizumab + cobimetinib (ABC)	29	II	Recruiting	Resistant
		NCT02659384	Bevacizumab + placebo/bevacizumab + acetylsalicylic acid/single-agent bevacizumab	122	II	Active, not recruiting	Resistant
		NCT04931342	Bevacizumab (non-matched)	400	II	Recruiting	-
		NCT02891824	Avastin + platinum-based chemotherapy/placebo + avastin + platinum-based chemotherapy		III	Active, not recruiting	Sensitive
	Avelumab (Bavencio)	NCT03312114	SAbR	5	II	Terminated (low accrual)	-
		NCT03704467	Carboplatin + M6620	3	I	Completed	Resistant
		NCT03330405	Talazoparib	226	I b/II	Active, not recruiting	Sensitive
CTLA-4	Ipilimumab (Yervoy)	NCT00060372	Following allogeneic hematopoietic stem cell transplantation	21	I	Completed	-
		NCT00039091	NR	26	I	Terminated	
		NCT01611558	NR	40	II	Completed	Sensitive
		NCT03449108	Autologous tumor infiltrating lymphocytes LN-145-S1	95	II	Recruiting	Resistant
		NCT04840589	Nivolumab + BET bromodomain inhibitor ZEN-3694	36	I	Recruiting	Resistant

safety profile (Moore et al., 2021). In 2022, MIRV was approved by the FDA for application in the treatment of (FR α)-positive, platinum-resistant EOC (Figure 1).

4 Targeting the tumor immune signaling pathway

4.1 Immunosuppressive TME of OC

Important processes of antitumor immunity include adaptive and natural immunity, which rely mainly on the recognition of tumor-associated antigens (TAAs) and tumor-specific antigens (TSAs) by immune cells (Figure 4) (Gajewski et al., 2013). OC tumors are immunogenic, and non-spontaneous antitumor immune responses can be detected in the tumors, peripheral blood and ascites of patients with EOCs (Morand et al., 2021). The histological marker of OC tumor immune recognition is tumor infiltrating lymphocytes (TILs) (Duraiswamy et al., 2021). The presence of CD3+ and CD8+ TILs in the OC TME has been demonstrated, and their recruitment is associated with a good prognosis in patients with EOC (Zhang et al., 2003; Santoiemma et al., 2016). Notably, the response rate of OC to ICIs remains suboptimal, with only 10%–15% of patients treated with single-agent ICIs showing good clinical outcomes (Chambers et al., 2021).

The main reason for this suboptimal response rate is that solid tumors, including OC, have a remodeling effect on the tumor

immune microenvironment (TIM) (Figure 4) (Yang et al., 2022). On the one hand, tumor cells can alter the degree of infiltration as well as the phenotype and function of the TILs present in primary or metastatic tumor tissues directly or through the TME, leading to immune escape (Rådestad et al., 2018). On the other hand, by altering the expression of immune checkpoint-associated proteins, the activity of effector T-cell is suppressed, and the tumor-associated macrophage (TAM) phenotype is induced to convert from an inflammation-inducing M1 type to an anti-inflammatory M2 type. Thus, the efficacy of immunotherapy is closely related to the inflammatory status of the tumor site (An and Yang, 2020). Single-cell transcriptomic analysis of OC ascites and tumors confirmed significant differences in the composition and phenotype of immune cells and immunosuppressive cells in the liquid and solid TME (Zhang et al., 2018; Izar et al., 2020). According to Daniel S. Chen et al., the human TIM is grouped into three main phenotypes: inflammatory tumors, which are hot tumors in which many inflammatory cells and inflammatory factors represented by T-cell infiltrate the tumor parenchyma; immune death tumors, which are cold tumors in which there is a lack of T-cell infiltration in the tumor parenchyma or stroma; and immune rejection immune cells in the stroma, which surround the cancer nest with abundant characteristic immune cells but do not penetrate the tumor parenchyma (Hegde and Chen, 2020). For example, platinum-resistant OC that progresses within 6 months after platinum therapy exhibits a series of "cold tumor" features, namely, low infiltration of CD8 T-cell (Mariya et al., 2014) but increased activation of CD4 T-cell, increased

infiltration of regulatory T-cell (Tregs) (Hao et al., 2018) and increased infiltration of PD-L1 cells (Hamanishi et al., 2015), known to promote peritoneal dissemination (Abiko et al., 2013), in which tumor cells are in an immunosuppressive microenvironment with enhanced proliferation and migration.

4.2 Immune checkpoint inhibitors

Based on the immunosuppressive microenvironment of OC and the background of poor responsiveness to ICIs alone, this review focuses on the combination of ICIs with other therapeutic approaches (Table 3). The combination of ICIs with different sites of action demonstrated some therapeutic efficacy.

In a study that included 100 patients with persistent or recurrent EOC, the efficacy and safety of nivolumab (a human lgG4 anti-PD-1 receptor blocking monoclonal antibody (mAb)) in combination with ipilimumab (a recombinant IgG1 human mAb against CTLA-4) were compared with those of nivolumab monotherapy. The results showed a longer PFS in the nivolumab + ipilimumab group than in the nivolumab group (3.9months vs 2 months). The rate of grade ≥3-related AEs was slightly higher in the nivolumab + ipilimumab group than in the nivolumab group (49%vs 33%). This result suggests that despite slightly higher toxicity, the combination regimen was associated with a higher response rate and longer mPFS than the single-agent regimen, suggesting that a large study should be conducted to better assess the efficacy and safety of the combination regimen (Zamarin et al., 2020). In another study (NCT02335918), it was observed in OC patients that varlilumab, a fully human agonist anti-CD27 mAb in combination with nivolumab, did not show toxicity beyond that of either monotherapy, and prolonged PFS was more pronounced at a ≥5% increase in tumor PD-L1 and intratumoral T-cell infiltration (Sanborn et al., 2022). High VEGF stimulates the expansion of immunosuppressive cells, including Tregs and myeloid-derived suppressor cells (MDSCs), inhibits the migration of immunoreactive T-cell to the TME and promotes their apoptosis, providing a theoretical basis for the combination of angiogenesis inhibitors and ICIs (Figure 4) (Fukumura et al., 2018). In a phase II (NCT02853318) non-randomized clinical trial, the combination of pembrolizumab with bevacizumab and oral cyclophosphamide was well tolerated, showing a clinical benefit and durable treatment response (>12 months) in 95.0% of patients with recurrent OC; this combination may represent a future treatment strategy for recurrent OC (Zsiros et al., 2021) In addition, niraparib further increases immune cell infiltration in the TIM and modulates immune activity by upregulating the activity of interferon genes and interferon pathway stimulators and PD-L1 expression on the tumor cell surface, which may make the combination of niraparib and ICI more toxic (Shen et al., 2019; Wang et al., 2019b). A single-arm phase I and II trial (NCT02657889) subgroup analysis showed that niraparib combined with pembrolizumab showed an ORR benefit regardless of platinum chemosensitivity status, prior bevacizumab treatment or tumor BRCA or HRD biomarker status (Konstantinopoulos et al., 2019). Interestingly, Appleton et al. constructed a three-dimensional spheroid culture model of OC patient origin and demonstrated that either pembrolizumab or

durvalumab synergized with olaparib to reduce the viability of the *in vitro* model (Appleton et al., 2021). Platinum-based chemotherapy is known to induce T-cell proliferation and activation, suggesting that the combination of ICIs may have a synergistic effect (Fucikova et al., 2022). In a study including nine patients with recurrent platinum-resistant OC (NCT03029598), pembrolizumab combined with carboplatin was effective and well tolerated; 23 patients achieved optimal objective remission, with 10.3% in partial remission (PR) and 51.7% with stable disease (SD), in addition to 17.2% with PD (Liao et al., 2021). In OC with BRCA1/2 mutations, the tumor load is increased and TILs are increased; furthermore, PD1/PD-L1 expression is upregulated in response to multiple interferon γ, P53 and BRCA mutations, thus possibly leading to greater sensitivity to PD1/PD-1 inhibitors (Jiang et al., 2021). In patients with PROC, the study by Li et al. suggested that the ORR and mPFS of PLD combined with pembrolizumab treatment were higher than those of the respective monotherapy, but with the inclusion of 23 patients in this study, a larger study is needed for validation (Lee et al., 2020).

5 New therapeutic methods for lipid metabolism-related targets

The characteristic site of OC metastasis is the lipid-rich omentum, and abnormal lipid metabolism plays an important role in tumor progression and metastasis (Ladanyi et al., 2018). Many studies have focused on targeting lipid metabolism-related pathways, suggesting a series of potentially effective new strategies for OC treatment. High-grade plasmacytoid ovarian cancer (HGSOC) metastasizes mainly to fat-rich areas such as the omentum, mesentery and appendicular epidermis over the colon (Figure 3). During metastasis, adipocytes in the microenvironment are recruited by cancer cells and transformed into cancer-associated adipocytes, and adipocytes are able to reprogram OC cell metabolism (Nieman et al., 2011; Mukherjee et al., 2020). When OC cells were cocultured with human omental adipocytes, tumor tissue induced adipocyte lipolysis, releasing more free fatty acids and glycerol and thus providing energy to promote rapid tumor growth while inducing OC cell migration and promoting invasion more significantly than subcutaneous fat (Nieman et al., 2011). In addition, OC cells cocultured with adipocytes have a lipid chaperone protein, FABP4, which regulates lipolysis and is upregulated in the expression of several *in vitro* cell lines of omental metastatic tumors, including OC, and FABP4 may be an important target for the treatment of intra-abdominal metastatic tumors (Nieman et al., 2011). It has been further shown that FABP4 knockdown leads to elevated levels of 5-hydroxymethylcytosine in DNA, downregulates the genetic features associated with OC metastasis, and inhibits tumor cell activity (Mukherjee et al., 2020). The evidence that FABP4 inhibitor monotherapy significantly reduced tumor load in a homozygous *in situ* mouse model and that an FABP4 inhibitor in combination with carboplatin enhanced chemosensitivity both *in vitro* and *in vivo* suggests that FABP4 may be an important target for the treatment of intra-abdominal metastatic tumors, providing an opportunity for specific metabolic targeting of OC metastasis (Mukherjee et al., 2020).

TABLE 4 Application of oncolytic viruses in the treatment of ovarian cancer.

Virus type	Study	Virus	N	Phase	Status	Method of administration	Population
Measles virus	NCT00408590	MV-CEA virus & MV-NIS virus	37	I	Completed	Intraperitoneal	Progressive, recurrent, or refractory ovarian epithelial cancer or primary peritoneal cancer
	NCT02068794	MV-NIS infected mesenchymal stem cells	57	I/II	Recruiting	Intraperitoneal	Recurrent ovarian cancer
	NCT02364713	MV-NIS	66	II	Recruiting	-	Platinum-resistant ovarian, recurrent ovarian carcinoma
Adenovirus	NCT02028117	Enadenotucirev	38	I	Completed	Intraperitoneal	Platinum-resistant epithelial ovarian cancer
	NCT05180851	Recombinant L-IFN adenovirus injection	28	I	Recruiting	Even injection of the drug solution into the tumor edge	Relapsed/refractory solid tumors
	NCT03225989	LOAd703	50	I/II	Recruiting	Intratumoral image-guided injections	Pancreatic cancer, biliary cancer, ovarian cancer and colorectal cancer
	NCT05271318	TILT-123	15	I	Recruiting	-	Platinum-resistant or refractory ovarian cancer
	NCT00964756	Ad5.SSTR/TK.RGD	11	I	Completed	Intravenous	Recurrent ovarian cancer
	NCT00562003	Ad5-Delta 24 RGD	26	I	Completed	Intraperitoneal	Ovarian cancer, primary peritoneal cancer
	NCT00002960	SCH 58500 (rAd/p53)	59	I	Completed	Single intraperitoneal instillation	Primary ovarian, fallopian tube, or peritoneal cancer
	NCT00003880	SCH 58500 (rAd/p53)	132	II/III	Terminated	Intraperitoneal	Newly diagnosed stage III ovarian or stage III primary peritoneal cancer with residual disease following surgery
	NCT02963831	ONCOS-102	67	I/II	Completed	Intraperitoneal infusion	Peritoneal disease for which prior standard chemotherapy has failed and histologically confirmed platinum-resistant or refractory epithelial ovarian cancer or colorectal cancer
Vaccinia virus							
	NCT02017678	JX-594	0	II	Withdrawn	Intravenous	Peritoneal carcinomatosis of ovarian origin in which patients are not eligible for curative treatments
	NCT02759588	GL-ONC1	64	I/II	Active, not recruiting	Intraperitoneal	Recurrent or refractory ovarian cancer
	NCT05281471	GL-ONC1 (Olvi-Vec)	186	III	Recruiting	Intraperitoneal catheter infusions	Platinum-resistant/refractory ovarian cancer
	NCT05051696	H101	60	_	Recruiting	Intratumor injection	Refractory/recurrent gynecological malignancies
	NCT05061537	PF-07263689	10	I	Active, not recruiting	Intravenous	Ovarian cancer for which all available standard-of-care therapies have been exhausted
Reolysin	NCT01199263	Pelareorep	108	II	Completed	Intravenous	Recurrent or persistent ovarian, fallopian tube or primary peritoneal cancer

Kosuke Hiramatsu et al. suggested that lipolysis-stimulated lipoprotein receptor (LSR), which is highly expressed in EOC metastatic lymph nodes and omentum, is regarded as a neoplastic antigen that induces very low density lipoprotein (VLDL) into EOC cells, which in turn promotes lipid uptake in EOC cells and subsequent It is associated with poor prognosis, and

OS was significantly shorter in patients with high expression of human LSR (hLSR) than in those with low expression (61.7 months vs 103.3 months, $p = 0.0322$). The resulting monoclonal antibody (#1–25) designed for hLSR showed significant antitumor effects by targeting the binding of VLDL to hLSR and intracellular storage of lipid metabolites (Hiramatsu et al., 2018). Recently, Lia Tesfay et al. showed that in OC tissues, cell lines and stem cell genetic models, upregulated steroid coenzyme A desaturase (SCD1) increased monounsaturated fatty acid formation to prevent ferroptosis. Blocking SCD1 had a dual antitumor effect, depleting the endogenous membrane antioxidant CoQ10 to induce ferroptosis and enhancing the toxicity of ferroptosis inducers on the one hand and triggering apoptosis by increasing the synthesis of saturated fatty acid-rich ceramides and altering the ratio of saturated to unsaturated fatty acids on the other. The findings of this study suggest that SCD1 inhibitors combined with ferroptosis inducers may be a new strategy for the treatment of OC in the future (Tesfay et al., 2019). Through single-cell sequencing and immunohistochemistry analysis of OC and paraneoplastic tissues, Lin et al. confirmed that Stanniocalcin 1 (STC1) expression was significantly upregulated in OC, especially in peritoneal metastases. STC1 promoted lipid metabolism not only through the *in vitro* pathway by upregulating lipid-related genes such as UCP1, TOM20 and perilipin1 but also through the FOXC2/ITGB6 signaling axis in OC to promote metastasis, lipid metabolism and *in vivo* cisplatin chemoresistance, suggesting that this could be a new treatment for OC patients with cisplatin chemoresistance-targeted pathways (Lin et al., 2022). Notably, metabolic reprogramming in cancer cells relies mainly on the LPA-LPAR-Gαi2 axis to induce a pseudohypoxic response involving the Rac-NOX-ROS-HIF1α pathway, which activates EMT in OC cells, leading to a diminished glycolytic rate and glycolytic capacity. Metabolic reprogramming also induces glucose transporter protein-1 (GLUT1) and glycolytic enzyme hexokinase-2 (HKII) expression, which ultimately leads to metabolic reprogramming, a shift to aerobic glycolysis in OC cells, and tumor progression promotion. Targeted inhibition of HKII by 3-bromopyruvate (3-BP) attenuates the growth of OC xenografts and shows potential for the treatment of OC (Ha et al., 2018). OC cells secrete angiotensin II (ANGII) in a positive feedback manner, triggering the classic receptor (AGTR1) pathway and EGFR transactivation, which is considered to be an important factor in the metastasis of several cancers. Peritoneal metastasis from OC is highly dependent on the formation of multicellular spheroids (MCSs), and the activation of AGTR1 is positively correlated with MCS formation and cell migration and negatively correlated with the prognosis of OC patients; therefore, targeting AGTR1 may be a strategy to eliminate the potential for peritoneal metastasis from EOC (Zhang et al., 2019a).

6 Other potential therapeutic targets

6.1 Immunization vaccines: Autologous dendritic cell immunotherapy

EOC responds poorly to ICIs due to its immunological features, including limited tumor mutational load (TMB) and poor lymphocyte infiltration. The use of immune vaccines and lysoviral therapy is a new strategy to enhance antitumor immunity in OC. A completed phase II clinical study, SOV01 (NCT02107937), found a statistically significant improvement in PFS with the addition of autologous dendritic cell immunotherapy (DCVAC) to first-line standard chemotherapy with carboplatin and paclitaxel (Rob et al., 2022). Interestingly, the clinical benefit of DCVAC was more pronounced in OC patients than in prostate and lung cancer patients, despite an antitumor immune cycle characterized by reduced expression of T-cell-associated genes (Hensler et al., 2022). However, multiple mechanisms, including the restriction of dendritic cell (DC) migration to draining lymph nodes, the immunosuppressive tumor microenvironment (TME) in OC, and metabolic restriction of tumor-associated DC activation, may lead to limited clinical efficacy of DC vaccines (O'Neill and Pearce, 2016). In this regard, several *in vitro* and preclinical studies have provided evidence that modified DC vaccines have shown greater benefit in OC treatment (Cheng et al., 2020).

In 2018, TANYI et al. used a personalized vaccine generated by autologous DCs pulsed with oxidized autologous whole-tumor cells. After the administration of a personalized vaccine generated by autologous DCs pulsed with oxidized autologous whole-tumor cell lysate (OCDC), an increase in IFN-γ-producing T-cell responsive to DC-presented tumor antigens was detected, with a significantly higher 2-year OS in patients who responded to the vaccine than in those who did not (100% vs 25%) and with good tolerability (Tanyi et al., 2018). In addition, Wen Zhang et al. found that the immune responses triggered by DC vaccines prepared with Wilms' tumor protein 1 (WT1) peptides in patients with advanced OC were significantly associated with a decrease in bone marrow-derived suppressor cells ($p = 0.045$) in pretreated peripheral blood, which suggests the potential therapeutic effect of such vaccines (Zhang et al., 2019a). Recently, based on NY-ESO-1 fused with SecPen and ubiquitin, Yunkai Yang and his colleagues prepared a novel DC vaccine (DC-SNU) that induced stronger and specific T-cell immunity in mice (Yang et al., 2021b). In addition, in patients with advanced OC, long-term toxicity was not observed before or after the injection of a Th1 selective IGFBP-2 N-terminus vaccine, and T-cell clones were significantly upregulated ($p = 0.03$) (Cecil et al., 2021).

6.2 Oncolytic virotherapy

Selective infection and direct lysis of tumor cells by an oncolytic virus (OV) leads to the release of viral particles, cytokines and other tumor cell contents, and the release of various substances triggers innate and adaptive proinflammatory immune responses against tumor cells (Cook and Chauhan, 2020). For example, the treatment of cells from patients with OC with an oncolytic adenovirus (Ad5/3-E2F-D24-hTNFa-IRES-hIL2) in isolated cultures reshaped the OC immune microenvironment, activating CD4+ and CD8+ TILs, which in turn enhanced antitumor responsiveness (Santos et al., 2020). OVs have shown efficacy in preclinical models of advanced EOC, and it is significant that the interaction of PD-1 with its ligands PD-L1 and PD-L2 leads to the suppression of T and NK cells without overlapping with OV-mediated activation pathways (van Vloten et al., 2022). In the advanced EOCID8 model, Parapoxvirus ovis (Orf

virus (OrfV)) treatment promoted active recruitment of NK cells in tumor cells and in the ascites TME, stimulated a strong antitumor response, activated NK cells and further induced T-cell recruitment in the OC TME through the CXCR3 chemokine axis, prolonging mouse survival (van Vloten et al., 2022). In a recent study, Lei et al. innovatively used the human IgG family as a scaffold to construct anti-CD47 mAbs piggybacking on tumor soluble herpesvirus (oHSV). This oncolytic herpes simplex virus, which maximizes Fc receptor-mediated antitumor effects and expresses anti-CD47 antibodies to block "do not eat me" signaling, has therapeutic effects (Tian et al., 2022).

Oncolytic herpes simplex virus (HSV) treatment of mice with OC carrying a platinum resistance gene disrupts the extracellular vesicle (EV) pathway associated with cisplatin efflux, not only helping to prevent drug resistance but also promoting DNA damage to activate the immune system and innate immunity and enhance the efficacy against ICIs (Hong et al., 2021). Novel active virus-like nanoparticle (VLP) delivery vehicles are more widely distributed and more long-lasting in OC ground metastatic ascites and have been shown to help improve survival in mice with peritoneal metastases from OC (Wang et al., 2020). In Table 4, we summarize all recent clinical trials using oncolytic viruses in the treatment of OC.

7 Discussion

Ovarian cancer management has changed dramatically with the introduction of targeted therapy and immunotherapy into standard-of-care therapy. For patients in whom initial tumor reduction surgery is feasible, platinum-based standard chemotherapy combined with specific marker-related targeted and immune monotherapy or combination therapy is an important strategy to prevent recurrence. However, neoadjuvant chemotherapy (NACT) followed by interval cytoreductive surgery (CRS) benefits patients if they are suspected to have stage IIIC or IV invasive EOC at the time of initial treatment, tumors are unresectable, optimal resection (R0 and R1) is not achieved, or clinical or imaging assessment indicates a perioperative risk (Cook and Chauhan, 2020; Santos et al., 2020). Genomic analysis revealed that although tumor cell evolutionary mutations were not prevented during NACT treatment, NACT treatment induced transcriptome remodeling through an upregulation of the AP-1 transcriptional network and altered gene copy number in recurrent tumors (Javellana et al., 2022). Previous studies have found that the application of platinum-containing NACT regimens may be more likely to induce cancer cell stemness, leading to platinum resistance and a shortened platinum treatment-free interval (TFIp) (Liu et al., 2020). The use of alternative platinum-based NACT regimens can help avoid platinum resistance without compromising the role of subsequent platinum-based agents in adjuvant therapy. NANT pioneered the exploration of niraparib monotherapy as an alternative to platinum as neoadjuvant therapy in patients with advanced non-R0 resectable BRCAm/HRD-positive OC (Zhou et al., 2022). According to the latest data presented at SGO 2022, CA125 decreased from week 2 of dosing, with a median lower

baseline concentration of 88.5% (26.8%–99.3%) after two cycles (8 weeks in total) of treatment and an ORR of up to 75%. Thrombocytopenia was the predominant TEAE, occurring in parallel with the decline in CA125. The above data provide preliminary evidence that niraparib single-agent neoadjuvant therapy is effective and has a good safety profile (Zhou et al., 2022). Expanding the trial sample size, increasing the number of patients included, and including a control group could make the findings of similar future studies more convincing. In addition, clinicians cannot ignore the issue that OC patients treated with NACT are at extremely high risk of thromboembolic events, especially those with advanced metastatic disease, and increased screening or the use of prophylactic anticoagulation are effective means of preventing associated AEs (Basaran et al., 2021). Notably, the OV21/PETROC study provided RCT data supporting that women undergoing NACT followed by optimal tumor reduction surgery would benefit from chemotherapy with intraperitoneal injections of carboplatin, informing the choice of follow-up treatment after NACT and optimal tumor reduction surgery in the clinic (Provencher et al., 2018). According to the phase III iPocc study reported at SGO 2022, intraperitoneal administration of carboplatin was superior to intravenous administration after initial surgery regardless of residual tumor size, improving PFS in patients with OC (Fujiwara et al., 2022). In addition, several preclinical and clinical studies have focused on improving the TME in OC. Adipose tissue is a key component of the metastatic microenvironment of OC, and preferential metastasis to omental adipose tissue is an important feature of metastatic OC (Motohara et al., 2019). Statins that inhibit a key enzyme of lipid metabolism (HMG-CoA reductase) have been shown to synergistically promote apoptosis with cisplatin in OC (Göbel et al., 2020). Future focus on targeting lipid metabolism-related pathways in OC could be of great value for the treatment of omental metastatic OC.

DNA methyltransferase inhibitors (DNMTis), which are epigenetic modulators, have been shown to induce the cytoplasmic sensing double-stranded RNA (dsRNA) antiviral pathway, upregulate type I IFN (Chiappinelli et al., 2015), activate CD8 T-cell, increase the number of immune cells (Wright et al., 2016; Stone et al., 2017; Vergote et al., 2018), and synergistically downregulate programmed death ligands (PD-L1 and PD-L2) with ICIs to exert antitumor effects. In patients with recurrent chemoresistant OC, hypomethylating agents (HMAs) in combination with ICIs to increase immune signaling and improve the response to immune checkpoint blockade in OC also appear to be a viable therapeutic strategy (Chiappinelli et al., 2022). A phase II clinical trial including 35 patients with platinum-resistant OC (NCT02901899) combined guadecitabine, a second-generation HMA, with pembrolizumab, an inhibitor of PD-1 and found that 34% of patients obtained clinical benefit (Chiappinelli et al., 2015). Song et al. found that ubiquitin UBR5, a protein ligase E3, was overexpressed in human OC cells, regulating the recruitment of immunosuppressive macrophages, i.e., M2 type, to the tumor site, leading to peritoneal colonization and metastasis on the one hand and promoting cell adhesion cancer stem cell (CSC) production by controlling p53 protein levels on the other hand, suggesting that

targeting UBR5 in combination with other therapeutic approaches could benefit OC patients (Song et al., 2020). Indoleamine 2,3-dioxygenase 1 (IDO1) drives tumor immunosuppression in HGSOC by depleting local tryptophan and producing kynurenine inhibition, which is responsible for the downregulation of CD8^{+} tumor infiltrating lymphocytes (TILs) (Munn et al., 2016). The IDO1 inhibitor EPA effectively blocks the Kyn pathway of Trp catabolism in patients with advanced EOC, and Kyn and changes in downstream metabolites were accompanied by an overall increase in net enrichment in IFN and MHC class I antigen processing and gene presentation pathways, which positively correlated with the proportion of activated CD8 T-cell in the TME (Munn et al., 2016; Odunsi et al., 2022). However, IDO1 blockade leads to metabolic adaptation of the ovarian TME and an increase in NAD^{+}, which in turn inhibits T-cell function *via* A2a and A2b purinergic receptors, decreasing T-cell proliferation and function and thereby suppressing antitumor responses; therefore, A2a/A2b purinergic receptor blockade in combination with the IDO1 inhibitor EPA helps to improve antitumor immunity in OC patients (Odunsi et al., 2022). In addition, immunotherapy with intraperitoneal injection of autologous IFN-α, IFN-γ and monocytes was mainly used in OC, and the efficacy was enhanced by the synergistic killing of tumor cells by promoting the development of monocytes toward inflammatory-responsive M1-type macrophages, combined with standard chemotherapy (carboplatin and paclitaxel) (Green et al., 2016). We believe that focusing on the different pathways associated with OC and finding appropriate synergistic strategies are the focuses of future individualized OC treatment.

Targeted therapy and immunotherapy are revolution in ovarian cancer management. Despite the promising treatments that have been developed for cancer immunotherapy, such as immune checkpoint inhibitors, there is still a need to overcome the immunosuppressive tumor microenvironment in order to improve the efficacy of cancer immunotherapy. In the near future, we should be able to dynamically assess tumor evolution and detect reliable biomarkers to identify immunotherapy effect of ovarian cancer. In addition, the appropriate dosing and scheduling of each agent should be determined in order to minimize adverse events while maximizing benefit and outcomes.

Author contributions

XH and X-YL wrote the manuscript and made figures and tables. W-LS, YC, and QZ revised the article. B-RX initiated the study and revised the manuscript. All authors read and approved the final manuscript.

Funding

Acknowledgments

Conflict of interest

The authors declare that the research was conducted in the absence of any commercial or financial relationships that could be construed as a potential conflict of interest.

Publisher's note

References

Abiko, K., Mandai, M., Hamanishi, J., Yoshioka, Y., Matsumura, N., Baba, T., et al. (2013). PD-L1 on tumor cells is induced in ascites and promotes peritoneal dissemination of ovarian cancer through CTL dysfunction. *Clin. Cancer Res.* 19 (6), 1363–1374. doi:10.1158/1078-0432.CCR-12-2199

Aghajanian, C., Blank, S. V., Goff, B. A., Judson, P. L., Teneriello, M. G., Husain, A., et al. (2012). Oceans: A randomized, double-blind, placebo-controlled phase III trial of chemotherapy with or without bevacizumab in patients with platinum-sensitive recurrent epithelial ovarian, primary peritoneal, or fallopian tube cancer. *J. Clin. Oncol.* 30 (17), 2039–2045. doi:10.1200/JCO.2012.42.0505

Aghajanian, C., Goff, B., Nycum, L. R., Wang, Y. V., Husain, A., and Blank, S. V. (2015). Final overall survival and safety analysis of OCEANS, a phase 3 trial of chemotherapy with or without bevacizumab in patients with platinum-sensitive recurrent ovarian cancer. *Gynecol. Oncol.* 139 (1), 10–16. doi:10.1016/j.ygyno.2015.08.004

An, D., Banerjee, S., and Lee, J. M. (2021). Recent advancements of antiangiogenic combination therapies in ovarian cancer. *Cancer Treat. Rev.* 98, 102224. doi:10.1016/j.ctrv.2021.102224

An, Y., and Yang, Q. (2020). MiR-21 modulates the polarization of macrophages and increases the effects of M2 macrophages on promoting the chemoresistance of ovarian cancer. *Life Sci.* 242, 117162. doi:10.1016/j.lfs.2019.117162

Appleton, K. M., Elrod, A. K., Lassahn, K. A., Shuford, S., Holmes, L. M., and DesRochers, T. M. (2021). PD-1/PD-L1 checkpoint inhibitors in combination with olaparib display antitumor activity in ovarian cancer patient-derived three-dimensional spheroid cultures. *Cancer Immunol. Immunother.* 70 (3), 843–856. doi:10.1007/s00262-021-02849-z

Armstrong, D. K., Alvarez, R. D., Backes, F. J., Bakkum-Gamez, J. N., Barroilhet, L., Behbakht, K., et al. (2022). NCCN Guidelines® insights: Ovarian cancer, version 3.2022. *J. Natl. Compr. Canc Netw.* 20 (9), 972–980. doi:10.6004/jnccn.2022.0047

Ashton, J., and Bristow, R. (2020). Bad neighbours: Hypoxia and genomic instability in prostate cancer. *Br. J. Radiol.* 93 (1115), 20200087. doi:10.1259/bjr.20200087

Aziz, A. U. R., Farid, S., Qin, K., Wang, H., and Liu, B. (2018). PIM kinases and their relevance to the PI3K/AKT/mTOR pathway in the regulation of ovarian cancer. *Biomolecules* 8 (1). doi:10.3390/biom8010007

Bais, C., Mueller, B., Brady, M. F., Mannel, R. S., Burger, R. A., Wei, W., et al. (2017). Tumor microvessel density as a potential predictive marker for bevacizumab benefit: GOG-0218 biomarker analyses. *J. Natl. Cancer Inst.* 109 (11), djx066. doi:10.1093/jnci/djx066

Banerjee, S., Moore, K. N., Colombo, N., Scambia, G., Kim, B. G., Oaknin, A., et al. (2021). Maintenance olaparib for patients with newly diagnosed advanced ovarian cancer and a BRCA mutation (SOLO1/GOG 3004): 5-year follow-up of a randomised, double-blind, placebo-controlled, phase 3 trial. *Lancet Oncol.* 22 (12), 1721–1731. doi:10.1016/S1470-2045(21)00531-3

Basaran, D., Boerner, T., Suhner, J., Sassine, D., Liu, Y., Grisham, R. N., et al. (2021). Risk of venous thromboembolism in ovarian cancer patients receiving neoadjuvant chemotherapy. *Gynecol. Oncol.* 163 (1), 36–40. doi:10.1016/j.ygyno.2021.07.030

Berek, J. S., Matulonis, U. A., Peen, U., Mahner, S., Redondo, A., Lesoin, A., et al. (2018). Safety and dose modification for patients receiving niraparib [published correction appears in Ann Oncol. 2019 May 1;30(5):859]. *Ann. Oncol.* 29 (8), 1784–1792. doi:10.1093/annonc/mdy181

Bergamini, A., Ferrero, S., Leone Roberti Maggiore, U., Scala, C., Pella, F., Vellone, V. G., et al. (2016). Folate receptor alpha antagonists in preclinical and early stage clinical development for the treatment of epithelial ovarian cancer. *Expert Opin. Investig. Drugs* 25 (12), 1405–1412. doi:10.1080/13543784.2016.1254616

Bizzaro, F., Fuso Nerini, I., Taylor, M. A., Anastasia, A., Russo, M., Damia, G., et al. (2021). VEGF pathway inhibition potentiates PARP inhibitor efficacy in ovarian cancer independent of BRCA status. *J. Hematol. Oncol.* 14 (1), 186. doi:10.1186/s13045-021-01196-x

Boussios, S., Moschetta, M., Karihtala, P., Samartzis, E. P., Sheriff, M., Pappas-Gogos, G., et al. (2020). Development of new poly(ADP-ribose) polymerase (PARP) inhibitors in ovarian cancer: Quo Vadis? *Ann. Transl. Med.* 8 (24), 1706. doi:10.21037/atm.2020.03.156

Buechel, M., Herzog, T. J., Westin, S. N., Coleman, R. L., Monk, B. J., and Moore, K. N. (2019). Treatment of patients with recurrent epithelial ovarian cancer for whom platinum is still an option. *Ann. Oncol.* 30 (5), 721–732. doi:10.1093/annonc/mdz104

Burger, R. A., Brady, M. F., Bookman, M. A., Fleming, G. F., Monk, B. J., Huang, H., et al. (2011). Incorporation of bevacizumab in the primary treatment of ovarian cancer. *N. Engl. J. Med.* 365 (26), 2473–2483. doi:10.1056/NEJMoa1104390

Burger, R. A., Sill, M. W., Monk, B. J., Greer, B. E., and Sorosky, J. I. (2007). Phase II trial of bevacizumab in persistent or recurrent epithelial ovarian cancer or primary peritoneal cancer: A gynecologic oncology group study. *J. Clin. Oncol.* 25 (33), 5165–5171. doi:10.1200/JCO.2007.11.5345

Callens, C., Vaur, D., Soubeyran, I., Rouleau, E., Just, P. A., Guillerm, E., et al. (2021). Concordance between tumor and germline BRCA status in high-grade ovarian carcinoma patients in the phase III PAOLA-1/ENGOT-ov25 trial. *J. Natl. Cancer Inst.* 113 (7), 917–923. doi:10.1093/jnci/djaa193

Cannistra, S. A., Matulonis, U. A., Penson, R. T., Hambleton, J., Dupont, J., Mackey, H., et al. (2007). Phase II study of bevacizumab in patients with platinum-resistant ovarian cancer or peritoneal serous cancer [published correction appears in J Clin Oncol. 2008 Apr 1;26(10):1773]. *J. Clin. Oncol.* 25 (33), 5180–5186. doi:10.1200/JCO.2007.12.0782

Cecil, D. L., Liao, J. B., Dang, Y., Coveler, A. L., Kask, A., Yang, Y., et al. (2021). Immunization with a plasmid DNA vaccine encoding the N-terminus of insulin-like growth factor binding protein-2 in advanced ovarian cancer leads to high-level type I immune responses. *Clin. Cancer Res.* 27 (23), 6405–6412. doi:10.1158/1078-0432.CCR-21-1579

Chambers, L. M., Michener, C. M., Rose, P. G., Reizes, O., Yao, M., and Vargas, R. (2021). Impact of antibiotic treatment on immunotherapy response in women with recurrent gynecologic cancer. *Gynecol. Oncol.* 161 (1), 211–220. doi:10.1016/j.ygyno.2021.01.015

Chen, L., Cheng, X., Tu, W., Qi, Z., Li, H., Liu, F., et al. (2019). Apatinib inhibits glycolysis by suppressing the VEGFR2/AKT1/SOX5/GLUT4 signaling pathway in ovarian cancer cells. *Cell. Oncol. (Dordr)* 42 (5), 679–690. doi:10.1007/s13402-019-00455-x

Cheng, S., Xu, C., Jin, Y., Li, Y., Zhong, C., Ma, J., et al. (2020). Artificial mini dendritic cells boost T cell-based immunotherapy for ovarian cancer. *Adv. Sci. (Weinh)* 7 (7), 1903301. doi:10.1002/advs.201903301

Chiappinelli, K. B., and Baylin, S. B. (2022). Inhibiting DNA methylation improves antitumor immunity in ovarian cancer. *J. Clin. Invest.* 132 (14), e160186. doi:10.1172/JCI160186

Chiappinelli, K. B., Strissel, P. L., Desrichard, A., Li, H., Henke, C., Akman, B., et al. (2015). Inhibiting DNA methylation causes an interferon response in cancer via dsRNA including endogenous retroviruses [published correction appears in cell. 2016 feb 25; 164(5):1073. Buhu, sadna [corrected to budhu, sadna]; mergoub, taha [corrected to merghoub, taha]] [published correction appears in cell. 2017 apr 6;169(2):361]. *Cell.* 162 (5), 974–986. doi:10.1016/j.cell.2015.07.011

Clamp, A. R., Lorusso, D., Oza, A. M., Aghajanian, C., Oaknin, A., Dean, A., et al. (2021). Rucaparib maintenance treatment for recurrent ovarian carcinoma: The effects of progression-free interval and prior therapies on efficacy and safety in the randomized phase III trial ARIEL3. *Int. J. Gynecol. Cancer* 31 (7), 949–958. doi:10.1136/ijgc-2020-002240

Coleman, R. L., Brady, M. F., Herzog, T. J., Sabbatini, P., Armstrong, D. K., Walker, J. L., et al. (2017). Bevacizumab and paclitaxel-carboplatin chemotherapy and secondary cytoreduction in recurrent, platinum-sensitive ovarian cancer (NRG oncology/gynecologic oncology group study GOG-0213): A multicentre, open-label, randomised, phase 3 trial. *Lancet Oncol.* 18 (6), 779–791. doi:10.1016/S1470-2045(17)30279-6

Cook, M., and Chauhan, A. (2020). Clinical application of oncolytic viruses: A systematic review. *Int. J. Mol. Sci.* 21 (20), 7505. doi:10.3390/ijms21207505

Del Campo, J. M., Matulonis, U. A., Malander, S., Provencher, D., Mahner, S., Follana, P., et al. (2019). Niraparib maintenance therapy in patients with recurrent ovarian cancer after a partial response to the last platinum-based chemotherapy in the ENGOT-OV16/NOVA trial. *J. Clin. Oncol.* 37 (32), 2968–2973. doi:10.1200/JCO.18.02238

DiSilvestro, P., and Alvarez Secord, A. (2018). Maintenance treatment of recurrent ovarian cancer: Is it ready for prime time? *Cancer Treat. Rev.* 69, 53–65. doi:10.1016/j.ctrv.2018.06.001

DiSilvestro, P., Banerjee, S., Colombo, N., Scambia, G., Kim, B. G., Oaknin, A., et al. (2023). Overall survival with maintenance olaparib at a 7-year follow-up in patients with newly diagnosed advanced ovarian cancer and a BRCA mutation: The SOLO1/GOG 3004 trial. *J. Clin. Oncol.* 41 (3), 609–617. doi:10.1200/JCO.22.01549

Domchek, S. M., Aghajanian, C., Shapira-Frommer, R., Schmutzler, R. K., Audeh, M. W., Friedlander, M., et al. (2016). Efficacy and safety of olaparib monotherapy in germline BRCA1/2 mutation carriers with advanced ovarian cancer and three or more lines of prior therapy. *Gynecol. Oncol.* 140 (2), 199–203. doi:10.1016/j.ygyno.2015.12.020

Duraiswamy, J., Turrini, R., Minasyan, A., Barras, D., Crespo, I., Grimm, A. J., et al. (2021). Myeloid antigen-presenting cell niches sustain antitumor T cells and license PD-1 blockade via CD28 costimulation. *Cancer Cell.* 39 (12), 1623–1642.e20. doi:10.1016/j.ccell.2021.10.008

Durmus, S., Sparidans, R. W., van Esch, A., Wagenaar, E., Beijnen, J. H., and Schinkel, A. H. (2015). Breast cancer resistance protein (BCRP/ABCG2) and P-glycoprotein (P-GP/ABCB1) restrict oral availability and brain accumulation of the PARP inhibitor rucaparib (AG-014699). *Pharm. Res.* 32 (1), 37–46. doi:10.1007/s11095-014-1442-z

Dziadkowiec, K. N., Gąsiorowska, E., Nowak-Markwitz, E., and Jankowska, A. (2016). PARP inhibitors: Review of mechanisms of action and BRCA1/2 mutation targeting. *Prz. Menopauzalny* 15 (4), 215–219. doi:10.5114/pm.2016.65667

Elyashiv, O., Ledermann, J., Parmar, G., Farrelly, L., Counsell, N., Feeney, A., et al. (2021). ICON 9-an international phase III randomized study to evaluate the efficacy of maintenance therapy with olaparib and cediranib or olaparib alone in patients with relapsed platinum-sensitive ovarian cancer following a response to platinum-based chemotherapy. *Int. J. Gynecol. Cancer* 31 (1), 134–138. doi:10.1136/ijgc-2020-002073

Ferrara, N., Hillan, K. J., Gerber, H. P., and Novotny, W. (2004). Discovery and development of bevacizumab, an anti-VEGF antibody for treating cancer. *Nat. Rev. Drug Discov.* 3 (5), 391–400. doi:10.1038/nrd1381

Ferriss, J. S., Java, J. J., Bookman, M. A., Fleming, G. F., Monk, B. J., Walker, J. L., et al. (2015). Ascites predicts treatment benefit of bevacizumab in front-line therapy of advanced epithelial ovarian, fallopian tube and peritoneal cancers: An NRG oncology/GOG study. *Gynecol. Oncol.* 139 (1), 17–22. doi:10.1016/j.ygyno.2015.07.103

Francis, K. E., Kim, S. I., Friedlander, M., Gebski, V., Ray-Coquard, I., Clamp, A., et al. (2022). The impact of olaparib dose reduction and treatment interruption on treatment outcome in the SOLO2/ENGOT-ov21 platinum-sensitive recurrent ovarian cancer. *Ann. Oncol.* 33 (6), 593–601. doi:10.1016/j.annonc.2022.02.222

Frenel, J. S., Kim, J. W., Aryal, N., Asher, R., Berton, D., Vidal, L., et al. (2022). Efficacy of subsequent chemotherapy for patients with BRCA1/2-mutated recurrent epithelial ovarian cancer progressing on olaparib versus placebo maintenance: Post-hoc analyses of the SOLO2/ENGOT ov-21 trial. *Ann. Oncol.* 33 (10), 1021–1028. doi:10.1016/j.annonc.2022.06.011

Friedlander, M., Gebski, V., Gibbs, E., Davies, L., Bloomfield, R., Hilpert, F., et al. (2018). Health-related quality of life and patient-centred outcomes with olaparib maintenance after chemotherapy in patients with platinum-sensitive, relapsed ovarian cancer and a BRCA1/2 mutation (SOLO2/ENGOT ov-21): A placebo-controlled, phase 3 randomised trial. *Lancet Oncol.* 19 (8), 1126–1134. doi:10.1016/S1470-2045(18)30343-7

Fucikova, J., Palova-Jelinkova, L., Klapp, V., Holicek, P., Lanickova, T., Kasikova, L., et al. (2022). Immunological control of ovarian carcinoma by chemotherapy and targeted anticancer agents. *Trends Cancer* 8 (5), 426–444. doi:10.1016/j.trecan.2022.01.010

Fujiwara, K., Nagao, S., Yamamoto, K., Tanabe, H., Okamoto, A., Takehara, K., et al. (2022). A randomized phase 3 trial of intraperitoneal versus intravenous carboplatin with dose-dense weekly paclitaxel in patients with ovarian, fallopian tube, or primary peritoneal carcinoma (a GOTIC-001/JGOG-3019/GCIG, iPocc Trial) (LBA 3). *Gynecol. Oncol.* 166, S49–S50. doi:10.1016/s0090-8258(22)01296-3

Fukumura, D., Kloepper, J., Amoozgar, Z., Duda, D. G., and Jain, R. K. (2018). Enhancing cancer immunotherapy using antiangiogenics: Opportunities and challenges. *Nat. Rev. Clin. Oncol.* 15 (5), 325–340. doi:10.1038/nrclinonc.2018.29

Gajewski, T. F., Schreiber, H., and Fu, Y. X. (2013). Innate and adaptive immune cells in the tumor microenvironment. *Nat. Immunol.* 14 (10), 1014–1022. doi:10.1038/ni.2703

Gao, Q., Zhu, J., Zhao, W., Huang, Y., An, R., Zheng, H., et al. (2022). Olaparib maintenance monotherapy in asian patients with platinum-sensitive relapsed ovarian cancer: Phase III trial (L-MOCA). *Clin. Cancer Res.* 28 (11), 2278–2285. doi:10.1158/1078-0432.CCR-21-3023

Göbel, A., Zinna, V. M., Dell'Endice, S., Jaschke, N., Kuhlmann, J. D., Wimberger, P., et al. (2020). Anti-tumor effects of mevalonate pathway inhibition in ovarian cancer. *BMC Cancer* 20 (1), 703. doi:10.1186/s12885-020-07164-x

González-Martín, A., Desauw, C., Heitz, F., Cropet, C., Gargiulo, P., Berger, R., et al. (2022). Maintenance olaparib plus bevacizumab in patients with newly diagnosed advanced high-grade ovarian cancer: Main analysis of second progression-free survival in the phase III PAOLA-1/ENGOT-ov25 trial. *Eur. J. Cancer* 174, 221–231. doi:10.1016/j.ejca.2022.07.022

González-Martín, A., Pothuri, B., Vergote, I., DePont Christensen, R., Graybill, W., Mirza, M. R., et al. (2019). Niraparib in patients with newly diagnosed advanced ovarian cancer. *N. Engl. J. Med.* 381 (25), 2391–2402. doi:10.1056/NEJMoa1910962

Gourley, C., Balmaña, J., Ledermann, J. A., Serra, V., Dent, R., Loibl, S., et al. (2019). Moving from poly (ADP-Ribose) polymerase inhibition to targeting DNA repair and DNA damage response in cancer therapy. *J. Clin. Oncol.* 37 (25), 2257–2269. doi:10.1200/JCO.18.02050

Green, D. S., Nunes, A. T., Annunziata, C. M., and Zoon, K. C. (2016). Monocyte and interferon based therapy for the treatment of ovarian cancer. *Cytokine Growth Factor Rev.* 29, 109–115. doi:10.1016/j.cytogfr.2016.02.006

Ha, J. H., Radhakrishnan, R., Jayaraman, M., Yan, M., Ward, J. D., Fung, K. M., et al. (2018). LPA induces metabolic reprogramming in ovarian cancer via a pseudohypoxic response. *Cancer Res.* 78 (8), 1923–1934. doi:10.1158/0008-5472.CAN-17-1624

Hamanishi, J., Mandai, M., Ikeda, T., Minami, M., Kawaguchi, A., Murayama, T., et al. (2015). Safety and antitumor activity of anti-PD-1 antibody, nivolumab, in patients with platinum-resistant ovarian cancer. *J. Clin. Oncol.* 33 (34), 4015–4022. doi:10.1200/JCO.2015.62.3397

Hao, D., Liu, J., Chen, M., Li, J., Wang, L., Li, X., et al. (2018). Immunogenomic analyses of advanced serous ovarian cancer reveal immune score is a strong prognostic factor and an indicator of chemosensitivity. *Clin. Cancer Res.* 24 (15), 3560–3571. doi:10.1158/1078-0432.CCR-17-3862

Hardesty, M. M., Krivak, T. C., Wright, G. S., Hamilton, E., Fleming, E. L., Belotte, J., et al. (2022). OVARIO phase II trial of combination niraparib plus bevacizumab maintenance therapy in advanced ovarian cancer following first-line platinum-based chemotherapy with bevacizumab. *Gynecol. Oncol.* 166 (2), 219–229. doi:10.1016/j.ygyno.2022.05.020

Harter, P., Mouret-Reynier, M. A., Pignata, S., Cropet, C., Gonzalez-Martin, A., Bogner, G., et al. (2022). Efficacy of maintenance olaparib plus bevacizumab according to clinical risk in patients with newly diagnosed, advanced ovarian cancer in the phase III PAOLA-1/ENGOT-ov25 trial. *Gynecol. Oncol.* 164 (2), 254–264. doi:10.1016/j.ygyno.2021.12.016

Hegde, P. S., and Chen, D. S. (2020). Top 10 challenges in cancer immunotherapy. *Immunity* 52 (1), 17–35. doi:10.1016/j.immuni.2019.12.011

Hensler, M., Rakova, J., Kasikova, L., Lanickova, T., Pasulka, J., Holicek, P., et al. (2022). Peripheral gene signatures reveal distinct cancer patient immunotypes with therapeutic implications for autologous DC-based vaccines. *Oncoimmunology* 11 (1), 2101596. doi:10.1080/2162402X.2022.2101596

Hiramatsu, K., Serada, S., Enomoto, T., Takahashi, Y., Nakagawa, S., Nojima, S., et al. (2018). LSR antibody therapy inhibits ovarian epithelial tumor growth by inhibiting lipid uptake. *Cancer Res.* 78 (2), 516–527. doi:10.1158/0008-5472.CAN-17-0910

Hong, B., Chapa, V., Saini, U., Modgil, P., Cohn, D. E., He, G., et al. (2021). Oncolytic HSV therapy modulates vesicular trafficking inducing cisplatin sensitivity and antitumor immunity. *Clin. Cancer Res.* 27 (2), 542–553. doi:10.1158/1078-0432.CCR-20-2210

Hutchinson, L. (2017). Targeted therapies: SOLO2 confirms olaparib maintenance in ovarian cancer. *Nat. Rev. Clin. Oncol.* 14 (10), 586–587. doi:10.1038/nrclinonc.2017.130

Izar, B., Tirosh, I., Stover, E. H., Wakiro, I., Cuoco, M. S., Alter, I., et al. (2020). A single-cell landscape of high-grade serous ovarian cancer. *Nat. Med.* 26 (8), 1271–1279. doi:10.1038/s41591-020-0926-0

Javellana, M., Eckert, M. A., Heide, J., Zawieracz, K., Weigert, M., Ashley, S., et al. (2022). Neoadjuvant chemotherapy induces genomic and transcriptomic changes in ovarian cancer. *Cancer Res.* 82 (1), 169–176. doi:10.1158/0008-5472.CAN-21-1467

Jiang, M., Jia, K., Wang, L., Li, W., Chen, B., Liu, Y., et al. (2021). Alterations of DNA damage response pathway: Biomarker and therapeutic strategy for cancer immunotherapy. *Acta Pharm. Sin. B* 11 (10), 2983–2994. doi:10.1016/j.apsb.2021.01.003

Jones, P., Wilcoxen, K., Rowley, M., and Toniatti, C. (2015). Niraparib: A poly(ADP-ribose) polymerase (PARP) inhibitor for the treatment of tumors with defective homologous recombination. *J. Med. Chem.* 58 (8), 3302–3314. doi:10.1021/jm5018237

Kandalaft, L. E., Odunsi, K., and Coukos, G. (2019). Immunotherapy in ovarian cancer: Are We there yet? *J. Clin. Oncol.* 37 (27), 2460–2471. doi:10.1200/JCO.19.00508

Kaplan, A. R., Gueble, S. E., Liu, Y., Oeck, S., Kim, H., Yun, Z., et al. (2019). Cediranib suppresses homology-directed DNA repair through down-regulation of BRCA1/2 and RAD51. *Sci. Transl. Med.* 11 (492), eaav4508. doi:10.1126/scitranslmed.aav4508

Köbel, M., Madore, J., Ramus, S. J., Clarke, B. A., Pharoah, P. D. P., Deen, S., et al. (2014). Evidence for a time-dependent association between FOLR1 expression and survival from ovarian carcinoma: Implications for clinical testing. An ovarian tumour tissue analysis consortium study. *Br. J. Cancer* 111 (12), 2297–2307. doi:10.1038/bjc.2014.567

Konstantinopoulos, P. A., Waggoner, S., Vidal, G. A., Mita, M., Moroney, J. W., Holloway, R., et al. (2019). Single-arm phases 1 and 2 trial of niraparib in combination with pembrolizumab in patients with recurrent platinum-resistant ovarian carcinoma. *JAMA Oncol.* 5 (8), 1141–1149. doi:10.1001/jamaoncol.2019.1048

Kristeleit, R., Lisyanskaya, A., Fedenko, A., Dvorkin, M., de Melo, A. C., Shparyk, Y., et al. (2022). Rucaparib versus standard-of-care chemotherapy in patients with relapsed ovarian cancer and a deleterious BRCA1 or BRCA2 mutation (ARIEL4): An international, open-label, randomised, phase 3 trial. *Lancet Oncol.* 23 (4), 465–478. doi:10.1016/S1470-2045(22)00122-X

Ladanyi, A., Mukherjee, A., Kenny, H. A., Johnson, A., Mitra, A. K., Sundaresan, S., et al. (2018). Adipocyte-induced CD36 expression drives ovarian cancer progression and metastasis. *Oncogene* 37 (17), 2285–2301. doi:10.1038/s41388-017-0093-z

Lan, C. Y., Wang, Y., Xiong, Y., Li, J. D., Shen, J. X., Li, Y. F., et al. (2018). Apatinib combined with oral etoposide in patients with platinum-resistant or platinum-refractory ovarian cancer (AEROC): A phase 2, single-arm, prospective study. *Lancet Oncol.* 19 (9), 1239–1246. doi:10.1016/S1470-2045(18)30349-8

Lan, C. Y., Zhao, J., Yang, F., Xiong, Y., Li, R., Huang, Y., et al. (2022). Anlotinib combined with TQB2450 in patients with platinum-resistant or -refractory ovarian cancer: A multi-center, single-arm, phase 1b trial. *Cell. Rep. Med.* 3 (7), 100689. doi:10.1016/j.xcrm.2022.100689

Ledermann, J. A., Embleton-Thirsk, A. C., Perren, T. J., Jayson, G. C., Rustin, G. J. S., Kaye, S. B., et al. (2021). Cediranib in addition to chemotherapy for women with relapsed platinum-sensitive ovarian cancer (ICON6): Overall survival results of a phase III randomised trial. *ESMO Open* 6 (2), 100043. doi:10.1016/j.esmoop.2020.100043

Ledermann, J. A., Oza, A. M., Lorusso, D., Aghajanian, C., Oaknin, A., Dean, A., et al. (2020). Rucaparib for patients with platinum-sensitive, recurrent ovarian carcinoma (ARIEL3): Post-progression outcomes and updated safety results from a randomised, placebo-controlled, phase 3 trial. *Lancet Oncol.* 21 (5), 710–722. doi:10.1016/S1470-2045(20)30061-9

Lee, E. K., Xiong, N., Cheng, S. C., Barry, W. T., Penson, R. T., Konstantinopoulos, P. A., et al. (2020). Combined pembrolizumab and pegylated liposomal doxorubicin in platinum resistant ovarian cancer: A phase 2 clinical trial. *Gynecol. Oncol.* 159 (1), 72–78. doi:10.1016/j.ygyno.2020.07.028

Lheureux, S., Braunstein, M., and Oza, A. M. (2019a). Epithelial ovarian cancer: Evolution of management in the era of precision medicine. *CA Cancer J. Clin.* 69 (4), 280–304. doi:10.3322/caac.21559

Lheureux, S., Gourley, C., Vergote, I., and Oza, A. M. (2019b). Epithelial ovarian cancer. *Lancet* 393 (10177), 1240–1253. doi:10.1016/S0140-6736(18)32552-2

Lheureux, S., Oaknin, A., Garg, S., Bruce, J. P., Madariaga, A., Dhani, N. C., et al. (2020). Evolve: A multicenter open-label single-arm clinical and translational phase II trial of cediranib plus olaparib for ovarian cancer after PARP inhibition progression. *Clin. Cancer Res.* 26 (16), 4206–4215. doi:10.1158/1078-0432.CCR-19-4121

Li, H., Liu, Z. Y., Wu, N., Chen, Y. C., Cheng, Q., and Wang, J. (2020). PARP inhibitor resistance: The underlying mechanisms and clinical implications. *Mol. Cancer* 19 (1), 107. doi:10.1186/s12943-020-01227-0

Li, N., Bu, H., Liu, J., Zhu, J., Zhou, Q., Wang, L., et al. (2021). An open-label, multicenter, single-arm, phase II study of fluzoparib in patients with germline BRCA1/2 mutation and platinum-sensitive recurrent ovarian cancer. *Clin. Cancer Res.* 27 (9), 2452–2458. doi:10.1158/1078-0432.CCR-20-3546

Li, N., Zhu, J., Yin, R., Wang, J., Pan, L., Kong, B., et al. (2022a). Efficacy and safety of niraparib as maintenance treatment in patients with newly diagnosed advanced ovarian cancer using an individualized starting dose (PRIME study): A randomized, double-blind, placebo-controlled, phase 3 trial (LBA 5). *Gynecol. Oncol.* 166, S50–S51. doi:10.1016/s0090-8258(22)01298-7

Li, N., Zhang, Y., Wang, J., Zhu, J., Wang, L., Wu, X., et al. (2022b). Fuzuloparib maintenance therapy in patients with platinum-sensitive, recurrent ovarian carcinoma (FZOCUS-2): A multicenter, randomized, double-blind, placebo-controlled, phase III trial. *J. Clin. Oncol.* 40 (22), 2436–2446. doi:10.1016/s0090-8258(22)01298-7

Li, X. Y., Rao, Y., Sun, B., and Mao, X. M. (2022c). Efficacy and safety of anlotinib combined with PD-1 blockades for patients with previously treated epithelial ovarian cancer: A retrospective study. *Int. J. Gen. Med.* 15, 3977–3989. doi:10.2147/IJGM.S352536

Liao, J. B., Gwin, W. R., Urban, R. R., Hitchcock-Bernhardt, K. M., Coveler, A. L., Higgins, D. M., et al. (2021). Pembrolizumab with low-dose carboplatin for recurrent platinum-resistant ovarian, fallopian tube, and primary peritoneal

cancer: Survival and immune correlates. *J. Immunother. Cancer* 9 (9), e003122. doi:10.1136/jitc-2021-003122

Lickliter, J. D., Voskoboynik, M., Mileshkin, L., Gan, H. K., Kichenadasse, G., Zhang, K., et al. (2022). Phase 1A/1B dose-escalation and -expansion study to evaluate the safety, pharmacokinetics, food effects and antitumor activity of pamiparib in advanced solid tumours [published correction appears in Br J Cancer. 2021 Dec 20;;]. *Br. J. Cancer* 126 (4), 576–585. doi:10.1038/s41416-021-01632-2

Lim, J. J., Yang, K., Taylor-Harding, B., Wiedemeyer, W. R., and Buckanovich, R. J. (2014). VEGFR3 inhibition chemosensitizes ovarian cancer stemlike cells through down-regulation of BRCA1 and BRCA2. *Neoplasia* 16 (4), 343–353.e532. doi:10.1016/j.neo.2014.04.003

Lin, F., Li, X., Wang, X., Sun, H., Wang, Z., and Wang, X. (2022). Stanniocalcin 1 promotes metastasis, lipid metabolism and cisplatin chemoresistance via the FOXC2/ITGB6 signaling axis in ovarian cancer. *J. Exp. Clin. Cancer Res.* 41 (1), 129. doi:10.1186/s13046-022-02315-3

Liu, J., Jiao, X., and Gao, Q. (2020). Neoadjuvant chemotherapy-related platinum resistance in ovarian cancer. *Drug Discov. Today* 25 (7), 1232–1238. doi:10.1016/j.drudis.2020.04.015

Lorusso, D., Ceni, V., Daniele, G., Salutari, V., Pietragalla, A., Muratore, M., et al. (2020). Newly diagnosed ovarian cancer: Which first-line treatment? *Cancer Treat. Rev.* 91, 102111. doi:10.1016/j.ctrv.2020.102111

Lu, Y., Chu, A., Turker, M. S., and Glazer, P. M. (2011). Hypoxia-induced epigenetic regulation and silencing of the BRCA1 promoter. *Mol. Cell. Biol.* 31 (16), 3339–3350. doi:10.1128/MCB.01121-10

Mariya, T., Hirohashi, Y., Torigoe, T., Asano, T., Kuroda, T., Yasuda, K., et al. (2014). Prognostic impact of human leukocyte antigen class I expression and association of platinum resistance with immunologic profiles in epithelial ovarian cancer. *Cancer Immunol. Res.* 2 (12), 1220–1229. doi:10.1158/2326-6066.CIR-14-0101

Martí, J. M., Garcia-Diaz, A., Delgado-Bellido, D., O'Valle, F., Gonzalez-Flores, A., Carlevaris, O., et al. (2021). Selective modulation by PARP-1 of HIF-1α-recruitment to chromatin during hypoxia is required for tumor adaptation to hypoxic conditions. *Redox Biol.* 41, 101885. doi:10.1016/j.redox.2021.101885

Matulonis, U., Herrstedt, J., Oza, A., Mahner, S., Redondo, A., Berton, D., et al. (2021). Long-term safety and secondary efficacy endpoints in the ENGOT-OV16/NOVA phase III trial of niraparib in recurrent ovarian cancer. *Gynecol. Oncol.* 162, S24–S25. doi:10.1016/s0090-8258(21)00693-4

Matulonis, U. A., Berlin, S., Ivy, P., Tyburski, K., Krasner, C., Zarwan, C., et al. (2009). Cediranib, an oral inhibitor of vascular endothelial growth factor receptor kinases, is an active drug in recurrent epithelial ovarian, fallopian tube, and peritoneal cancer. *J. Clin. Oncol.* 27 (33), 5601–5606. doi:10.1200/JCO.2009.23.2777

Miao, M., Deng, G., Luo, S., Zhou, J., Chen, L., Yang, J., et al. (2018). A phase II study of apatinib in patients with recurrent epithelial ovarian cancer. *Gynecol. Oncol.* 148 (2), 286–290. doi:10.1016/j.ygyno.2017.12.013

Miller, R. E., Leary, A., Scott, C. L., Lord, C. J., Bowtell, D., Chang, D. K., et al. (2020). ESMO recommendations on predictive biomarker testing for homologous recombination deficiency and PARP inhibitor benefit in ovarian cancer. *Ann. Oncol.* 31 (12), 1606–1622. doi:10.1016/j.annonc.2020.08.2102

Mirza, M. R., Benigno, B., Dørum, A., Dorum, A., Bessette, P., Barcelo, I. B., et al. (2020). Long-term safety in patients with recurrent ovarian cancer treated with niraparib versus placebo: Results from the phase III ENGOT-OV16/NOVA trial. *Gynecol. Oncol.* 159 (2), 442–448. doi:10.1016/j.ygyno.2020.09.006

Mirza, M. R., Monk, B. J., Herrstedt, J., Oza, A. M., Mahner, S., Redondo, A., et al. (2016). Niraparib maintenance therapy in platinum-sensitive, recurrent ovarian cancer. *N. Engl. J. Med.* 375 (22), 2154–2164. doi:10.1056/NEJMoa1611310

Mirza, M. R., Pignata, S., and Ledermann, J. A. (2018). Latest clinical evidence and further development of PARP inhibitors in ovarian cancer. *Ann. Oncol.* 29 (6), 1366–1376. doi:10.1093/annonc/mdy174

Mittica, G., Ghisoni, E., Giannone, G., Genta, S., Aglietta, M., Sapino, A., et al. (2018). PARP inhibitors in ovarian cancer. *Recent Pat. Anticancer Drug Discov.* 13 (4), 392–410. doi:10.2174/1574892813666180305165256

Moore, K. N., Oza, A. M., Colombo, N., Oaknin, A., Scambia, G., Lorusso, D., et al. (2021). Phase III, randomized trial of mirvetuximab soravtansine versus chemotherapy in patients with platinum-resistant ovarian cancer: Primary analysis of FORWARD I. *Ann. Oncol.* 32 (6), 757–765. doi:10.1016/j.annonc.2021.02.017

Moore, K. N., Secord, A. A., Geller, M. A., Miller, D. S., Cloven, N., Fleming, G. F., et al. (2019). Niraparib monotherapy for late-line treatment of ovarian cancer (QUADRA): A multicentre, open-label, single-arm, phase 2 trial. *Lancet Oncol.* 20 (5), 636–648. doi:10.1016/S1470-2045(19)30029-4

Morand, S., Devanaboyina, M., Staats, H., Stanbery, L., and Nemunaitis, J. (2021). Ovarian cancer immunotherapy and personalized medicine. *Int. J. Mol. Sci.* 22 (12), 6532. doi:10.3390/ijms22126532

Motohara, T., Masuda, K., Morotti, M., Zheng, Y., El-Sahhar, S., Chong, K. Y., et al. (2019). An evolving story of the metastatic voyage of ovarian cancer cells:

Cellular and molecular orchestration of the adipose-rich metastatic microenvironment. *Oncogene* 38 (16), 2885–2898. doi:10.1038/s41388-018-0637-x

Mukherjee, A., Chiang, C. Y., Daifotis, H. A., Nieman, K. M., Fahrmann, J. F., Lastra, R. R., et al. (2020). Adipocyte-induced FABP4 expression in ovarian cancer cells promotes metastasis and mediates carboplatin resistance. *Cancer Res.* 80 (8), 1748–1761. doi:10.1158/0008-5472.CAN-19-1999

Munn, D. H., and Mellor, A. L. (2016). Ido in the tumor microenvironment: Inflammation, counter-regulation, and tolerance. *Trends Immunol.* 37 (3), 193–207. doi:10.1016/j.it.2016.01.002

Murai, J., Huang, S. Y., Das, B. B., Renaud, A., Zhang, Y., Doroshow, J. H., et al. (2012). Trapping of PARP1 and PARP2 by clinical PARP inhibitors. *Cancer Res.* 72 (21), 5588–5599. doi:10.1158/0008-5472.CAN-12-2753

Musella, A., Bardhi, E., Marchetti, C., Vertechy, L., Santangelo, G., Sassu, C., et al. (2018). Rucaparib: An emerging parp inhibitor for treatment of recurrent ovarian cancer. *Cancer Treat. Rev.* 66, 7–14. doi:10.1016/j.ctrv.2018.03.004

Muz, B., de la Puente, P., Azab, F., and Azab, A. K. (2015). The role of hypoxia in cancer progression, angiogenesis, metastasis, and resistance to therapy. *Hypoxia (Auckl)* 3, 83–92. doi:10.2147/HP.S93413

Ni, J., Cheng, X., Chen, J., Guo, W., and Dai, Z. (2020). Anlotinib as exploratory therapy for platinum-resistant ovarian cancer: A retrospective study on efficacy and safety. *Onco Targets Ther.* 13, 9857–9863. doi:10.2147/OTT.S268613

Nieman, K. M., Kenny, H. A., Penicka, C. V., Ladanyi, A., Buell-Gutbrod, R., Zillhardt, M. R., et al. (2011). Adipocytes promote ovarian cancer metastasis and provide energy for rapid tumor growth. *Nat. Med.* 17 (11), 1498–1503. doi:10.1038/nm.2492

O'Cearbhaill, R. E., Pérez-Fidalgo, J. A., Monk, B. J., Tusquets, I., McCormick, C., Fuentes, J., et al. (2022). Efficacy of niraparib by time of surgery and postoperative residual disease status: A post hoc analysis of patients in the PRIMA/ENGOT-OV26/GOG-3012 study. *Gynecol. Oncol.* 166 (1), 36–43. doi:10.1016/j.ygyno.2022.04.012

O'Donnell, D. M. (2022). Rucaparib for BRCA1/2-mutated pretreated ovarian cancer: Reflections from the ARIEL4 trial. *Lancet Oncol.* 23 (4), 440–441. doi:10.1016/S1470-2045(22)00150-4

O'Malley, D. M., Matulonis, U. A., Birrer, M. J., Castro, C. M., Gilbert, L., Vergote, I., et al. (2020). Phase Ib study of mirvetuximab soravtansine, a folate receptor alpha (FRα)-targeting antibody-drug conjugate (ADC), in combination with bevacizumab in patients with platinum-resistant ovarian cancer. *Gynecol. Oncol.* 157 (2), 379–385. doi:10.1016/j.ygyno.2020.01.037

O'Malley, D. M., Oza, A. M., Lorusso, D., Aghajanian, C., Oaknin, A., Dean, A., et al. (2022). Clinical and molecular characteristics of ARIEL3 patients who derived exceptional benefit from rucaparib maintenance treatment for high-grade ovarian carcinoma. *Gynecol. Oncol.* 167 (3), 404–413. doi:10.1016/j.ygyno.2022.08.021

O'Neill, L. A., and Pearce, E. J. (2016). Immunometabolism governs dendritic cell and macrophage function. *J. Exp. Med.* 213 (1), 15–23. doi:10.1084/jem.20151570

Oaknin, A., Moore, K. N., Meyer, T., González, J. L., Devriese, L., Amin, A., et al. (2022). 520MO - safety and efficacy of nivolumab (NIVO) ± ipilimumab (IPI) in patients (pts) with recurrent/metastatic cervical cancer (R/M Cx Ca) in checkmate 358. *Ann. Oncol.* 33 (7), S235–S282. doi:10.1016/annonc/annonc1054

Odunsi, K. (2017). Immunotherapy in ovarian cancer. *Ann. Oncol.* 28 (suppl_8), viii1–viii7. doi:10.1093/annonc/mdx444

Odunsi, K., Qian, F., Lugade, A. A., Yu, H., Geller, M. A., Fling, S. P., et al. (2022). Metabolic adaptation of ovarian tumors in patients treated with an Ido1 inhibitor constrains antitumor immune responses. *Sci. Transl. Med.* 14 (636), eabg8402. doi:10.1126/scitranslmed.abg8402

Oza, A. M., Selle, F., Davidenko, I., Korach, J., Mendiola, C., Pautier, P., et al. (2017). Efficacy and safety of bevacizumab-containing therapy in newly diagnosed ovarian cancer: ROSiA single-arm phase 3B study. *Int. J. Gynecol. Cancer* 27 (1), 50–58. doi:10.1097/IGC.0000000000000836

Penson, R., Valencia, R. V., Colombo, N., Leath, C., Bidzinski, M., Kim, J. W., et al. (2022). Final overall survival results from SOLO3: Phase III trial assessing olaparib monotherapy versus non-platinum chemotherapy in heavily pretreated patients with germline BRCA1-and/or BRCA2-mutated platinum-sensitive relapsed ovarian cancer (026). *Gynecol. Oncol.* 166, S19–S20. doi:10.1016/S0090-8258(22)01244-6

Penson, R. T., Valencia, R. V., Cibula, D., Colombo, N., Leath, C. A., Bidzinski, M., et al. (2020). Olaparib versus nonplatinum chemotherapy in patients with platinum-sensitive relapsed ovarian cancer and a germline BRCA1/2 mutation (SOLO3): A randomized phase III trial. *J. Clin. Oncol.* 38 (11), 1164–1174. doi:10.1200/JCO.19.02745

Perren, T. J., Swart, A. M., Pfisterer, J., Ledermann, J. A., Pujade-Lauraine, E., Kristensen, G., et al. (2011). A phase 3 trial of bevacizumab in ovarian cancer [published correction appears in N Engl J Med. 2012 Jan 19;366(3):284]. *N. Engl. J. Med.* 365 (26), 2484–2496. doi:10.1056/NEJMoa1103799

Pignata, S., Lorusso, D., Joly, F., Gallo, C., Colombo, N., Sessa, C., et al. (2021). Carboplatin-based doublet plus bevacizumab beyond progression versus carboplatin-based doublet alone in patients with platinum-sensitive ovarian cancer: A randomised, phase 3 trial. *Lancet Oncol.* 22 (2), 267–276. doi:10.1016/S1470-2045(20)30637-9

Ponte, J. F., Ab, O., Lanieri, L., Lee, J., Coccia, J., Bartle, L. M., et al. (2016). Mirvetuximab soravtansine (IMGN853), a folate receptor alpha-targeting antibody-drug conjugate, potentiates the activity of standard of care therapeutics in ovarian cancer models. *Neoplasia* 18 (12), 775–784. doi:10.1016/j.neo.2016.11.002

Poveda Velasco, A. M., Lheureux, S., Colombo, N., Cibula, D., Lindemann, K., Weberpals, J., et al. (2022). Maintenance olaparib monotherapy in patients (pts) with platinum-sensitive relapsed ovarian cancer (PSR OC) without a germline BRCA1/BRCA2 mutation (non-gBRCAm): Final overall survival (OS) results from the OPINION trial. Abstract 531P. *Ann. Oncol.* 33 (suppl_7), S235–S282. doi:10.1016/annonc1054

Provencher, D. M., Gallagher, C. J., Parulekar, W. R., Ledermann, J. A., Armstrong, D. K., Brundage, M., et al. (2018). OV21/PETROC: A randomized gynecologic cancer intergroup phase II study of intraperitoneal versus intravenous chemotherapy following neoadjuvant chemotherapy and optimal debulking surgery in epithelial ovarian cancer. *Ann. Oncol.* 29 (2), 431–438. doi:10.1093/annonc/mdx754

Pujade-Lauraine, E., Hilpert, F., Weber, B., Reuss, A., Poveda, A., Kristensen, G., et al. (2014). Bevacizumab combined with chemotherapy for platinum-resistant recurrent ovarian cancer: The AURELIA open-label randomized phase III trial [published correction appears in J Clin Oncol. 2014 Dec 10;32(35):4025]. *J. Clin. Oncol.* 32 (13), 1302–1308. doi:10.1200/JCO.2013.51.4489

Rådestad, E., Klynning, C., Stikvoort, A., Mogensen, O., Nava, S., Magalhaes, I., et al. (2018). Immune profiling and identification of prognostic immune-related risk factors in human ovarian cancer. *Oncoimmunology* 8 (2), e1535730. doi:10.1080/2162402X.2018.1535730

Ray-Coquard, I., Pautier, P., Pignata, S., Perol, D., Gonzalez-Martin, A., Berger, R., et al. (2019). Olaparib plus bevacizumab as first-line maintenance in ovarian cancer. *N. Engl. J. Med.* 381 (25), 2416–2428. doi:10.1056/NEJMoa1911361

Rob, L., Cibula, D., Knapp, P., Mallmann, P., Klat, J., Minar, L., et al. (2022). Safety and efficacy of dendritic cell-based immunotherapy DCVAC/OvCa added to first-line chemotherapy (carboplatin plus paclitaxel) for epithelial ovarian cancer: A phase 2, open-label, multicenter, randomized trial. *J. Immunother. Cancer* 10 (1), e003190. doi:10.1136/jitc-2021-003190

Sanborn, R. E., Pishvaian, M. J., Callahan, M. K., Weise, A., Sikic, B. I., Rahma, O., et al. (2022). Safety, tolerability and efficacy of agonist anti-CD27 antibody (varlilumab) administered in combination with anti-PD-1 (nivolumab) in advanced solid tumors. *J. Immunother. Cancer* 10 (8), e005147. doi:10.1136/jitc-2022-005147

Santoiemma, P. P., Reyes, C., Wang, L. P., McLane, M. W., Feldman, M. D., Tanyi, J. L., et al. (2016). Systematic evaluation of multiple immune markers reveals prognostic factors in ovarian cancer. *Gynecol. Oncol.* 143 (1), 120–127. doi:10.1016/j.ygyno.2016.07.105

Santos, J. M., Heiniö, C., Cervera-Carrascon, V., Quixabeira, D. C. A., Siurala, M., Havunen, R., et al. (2020). Oncolytic adenovirus shapes the ovarian tumor microenvironment for potent tumor-infiltrating lymphocyte tumor reactivity. *J. Immunother. Cancer* 8 (1), e000188. doi:10.1136/jitc-2019-000188

Scaranti, M., Cojocaru, E., Banerjee, S., and Banerji, U. (2020). Exploiting the folate receptor α in oncology. *Nat. Rev. Clin. Oncol.* 17 (6), 349–359. doi:10.1038/s41571-020-0339-5

Semenza, G. L. (2010). Defining the role of hypoxia-inducible factor 1 in cancer biology and therapeutics. *Oncogene* 29 (5), 625–634. doi:10.1038/onc.2009.441

SGO (2022). *Clinically meaningful antitumor activity and an acceptable safety profile were seen with the use of mirvetuximab soravtansine in patients with platinum-resistant ovarian cancer harboring high folate receptor–alpha (FRα) expression, according to the results of the phase 3 SORAYA trial (NCT04296890) presented during the the Society of Gynecologic Oncology (SGO) 2022 Annual Meeting on Women's Cancer.*

Shen, J., Zhao, W., Ju, Z., Wang, L., Peng, Y., Labrie, M., et al. (2019). PARPi triggers the STING-dependent immune response and enhances the therapeutic efficacy of immune checkpoint blockade independent of BRCAness. *Cancer Res.* 79 (2), 311–319. doi:10.1158/0008-5472.CAN-18-1003

Siegel, R. L., Miller, K. D., Fuchs, H. E., and Jemal, A. (2022). Cancer statistics, 2022. *CA Cancer J. Clin.* 72 (1), 7–33. doi:10.3322/caac.21708

Sisay, M., and Edessa, D. (2017). PARP inhibitors as potential therapeutic agents for various cancers: Focus on niraparib and its first global approval for maintenance therapy of gynecologic cancers. *Gynecol. Oncol. Res. Pract.* 4, 18. doi:10.1186/s40661-017-0055-8

Sjoquist, K. M., Espinoza, D., Mileshkin, L., Ananda, S., Shannon, C., Yip, S., et al. (2021). Rezolve (ANZGOG-1101): A phase 2 trial of intraperitoneal bevacizumab to treat symptomatic ascites in patients with chemotherapy-resistant, epithelial ovarian cancer. *Gynecol. Oncol.* 161 (2), 374–381. doi:10.1016/j.ygyno.2021.02.002

Song, M., Yeku, O. O., Rafiq, S., Purdon, T., Dong, X., Zhu, L., et al. (2020). Tumor derived UBR5 promotes ovarian cancer growth and metastasis through inducing immunosuppressive macrophages. *Nat. Commun.* 11 (1), 6298. doi:10.1038/s41467-020-20140-0

Stone, M. L., Chiappinelli, K. B., Li, H., Murphy, L. M., Travers, M. E., Topper, M. J., et al. (2017). Epigenetic therapy activates type I interferon signaling in murine ovarian cancer to reduce immunosuppression and tumor burden. *Proc. Natl. Acad. Sci. U. S. A.* 114 (51), E10981–E10990. doi:10.1073/pnas.1712514114

Su, Y., Luo, B., Lu, Y., Wang, D., Yan, J., Zheng, J., et al. (2022). Anlotinib induces a T cell-inflamed tumor microenvironment by facilitating vessel normalization and enhances the efficacy of PD-1 checkpoint blockade in Neuroblastoma. *Clin. Cancer Res.* 28 (4), 793–809. doi:10.1158/1078-0432.CCR-21-2241

Sun, Y., Niu, W., Du, F., Du, C., Li, S., Wang, J., et al. (2016). Safety, pharmacokinetics, and antitumor properties of anlotinib, an oral multi-target tyrosine kinase inhibitor, in patients with advanced refractory solid tumors. *J. Hematol. Oncol.* 9 (1), 105. doi:10.1186/s13045-016-0332-8

Swisher, E. M., Kristeleit, R. S., Oza, A. M., Tinker, A. V., Ray-Coquard, I., Oaknin, A., et al. (2021a). Characterization of patients with long-term responses to rucaparib treatment in recurrent ovarian cancer. *Gynecol. Oncol.* 163 (3), 490–497. doi:10.1016/j.ygyno.2021.08.030

Swisher, E. M., Kwan, T. T., Oza, A. M., Tinker, A. V., Ray-Coquard, I., Oaknin, A., et al. (2021b). Molecular and clinical determinants of response and resistance to rucaparib for recurrent ovarian cancer treatment in ARIEL2 (Parts 1 and 2). *Nat. Commun.* 12 (1), 2487. doi:10.1038/s41467-021-22582-6

Swisher, E. M., Lin, K. K., Oza, A. M., Scott, C. L., Giordano, H., Sun, J., et al. (2017). Rucaparib in relapsed, platinum-sensitive high-grade ovarian carcinoma (ARIEL2 Part 1): An international, multicentre, open-label, phase 2 trial. *Lancet Oncol.* 18 (1), 75–87. doi:10.1016/S1470-2045(16)30559-9

Tanyi, J. L., Bobisse, S., Ophir, E., Tuyaerts, S., Roberti, A., Genolet, R., et al. (2018). Personalized cancer vaccine effectively mobilizes antitumor T cell immunity in ovarian cancer. *Sci. Transl. Med.* 10 (436), eaao5931. doi:10.1126/scitranslmed.aao5931

Teo, P. Y., Yang, C., Whilding, L. M., Parente-Pereira, A. C., Maher, J., George, A. J. T., et al. (2015). Ovarian cancer immunotherapy using PD-L1 siRNA targeted delivery from folic acid-functionalized polyethylenimine: Strategies to enhance T cell killing. *Adv. Healthc. Mater* 4 (8), 1180–1189. doi:10.1002/adhm.201500089

Tesfay, L., Paul, B. T., Konstorum, A., Deng, Z., Cox, A. O., Lee, J., et al. (2019). Stearoyl-CoA desaturase 1 protects ovarian cancer cells from ferroptotic cell death. *Cancer Res.* 79 (20), 5355–5366. doi:10.1158/0008-5472.CAN-19-0369

Tian, L., Xu, B., Teng, K. Y., Song, M., Zhu, Z., Chen, Y., et al. (2022). Targeting Fc receptor-mediated effects and the "don't eat me" signal with an oncolytic virus expressing an anti-CD47 antibody to treat metastatic ovarian cancer. *Clin. Cancer Res.* 28 (1), 201–214. doi:10.1158/1078-0432.CCR-21-1248

Tian, S., Quan, H., Xie, C., Guo, H., Lu, F., Xu, Y., et al. (2011). YN968D1 is a novel and selective inhibitor of vascular endothelial growth factor receptor-2 tyrosine kinase with potent activity *in vitro* and *in vivo*. *Cancer Sci.* 102 (7), 1374–1380. doi:10.1111/j.1349-7006.2011.01939.x

Tomao, F., Vici, P., and Tomao, S. (2020). Expanding use of rucaparib as maintenance therapy in recurrent ovarian cancer: Updates from the ARIEL3 trial. *Lancet Oncol.* 21 (5), 616–617. doi:10.1016/S1470-2045(20)30079-6

van Vloten, J. P., Matuszewska, K., Minow, M. A. A., Minott, J. A., Santry, L. A., Pereira, M., et al. (2022). Oncolytic Orf virus licenses NK cells via cDC1 to activate innate and adaptive antitumor mechanisms and extends survival in a murine model of late-stage ovarian cancer. *J. Immunother. Cancer* 10 (3), e004335. doi:10.1136/jitc-2021-004335

Ventriglia, J., Paciolla, I., Pisano, C., Cecere, S. C., Di Napoli, M., Tambaro, R., et al. (2017). Immunotherapy in ovarian, endometrial and cervical cancer: State of the art and future perspectives. *Cancer Treat. Rev.* 59, 109–116. doi:10.1016/j.ctrv.2017.07.008

Vergote, I., Coens, C., Nankivell, M., Kristensen, G. B., Parmar, M. K. B., Ehlen, T., et al. (2018). Neoadjuvant chemotherapy versus debulking surgery in advanced tubo-ovarian cancers: Pooled analysis of individual patient data from the EORTC 55971 and CHORUS trials. *Lancet Oncol.* 19 (12), 1680–1687. doi:10.1016/S1470-2045(18)30566-7

Vergote, I., Gonzalez-Martin, A., Ray-Coquard, I., Harter, P., Colombo, N., Pujol, P., et al. (2022). European experts consensus: BRCA/homologous recombination deficiency testing in first-line ovarian cancer. *Ann. Oncol.* 33 (3), 276–287. doi:10.1016/j.annonc.2021.11.013

Vergote, I., Ray-Coquard, I., Anderson, D. M., Cantuaria, G., Colombo, N., Garnier-Tixidre, C., et al. (2021). Population-adjusted indirect treatment comparison of the SOLO1 and PAOLA-1/ENGOT-ov25 trials evaluating maintenance olaparib or bevacizumab or the combination of both in newly diagnosed, advanced BRCA-mutated ovarian cancer. *Eur. J. Cancer* 157, 415–423. doi:10.1016/j.ejca.2021.08.023

Walker, J. L., Brady, M. F., Wenzel, L., Fleming, G. F., Huang, H. Q., DiSilvestro, P. A., et al. (2019). Randomized trial of intravenous versus intraperitoneal chemotherapy plus bevacizumab in advanced ovarian carcinoma: An NRG oncology/gynecologic oncology group study. *J. Clin. Oncol.* 37 (16), 1380–1390. doi:10.1200/JCO.18.01568

Wang, C., Fernández de Ávila, B. E., Mundaca-Uribe, R., Lopez-Ramirez, M. A., Ramirez-Herrera, D. E., Shukla, S., et al. (2020). Active delivery of VLPs promotes anti-tumor activity in a mouse ovarian tumor model. *Small* 16 (20), e1907150. doi:10.1002/smll.201907150

Wang, L., Yang, C., Xie, C., Jiang, J., Gao, M., Fu, L., et al. (2019a). Pharmacologic characterization of fluzoparib, a novel poly(ADP-ribose) polymerase inhibitor undergoing clinical trials. *Cancer Sci.* 110 (3), 1064–1075. doi:10.1111/cas.13947

Wang, T., Tang, J., Yang, H., Yin, R., Zhang, J., Zhou, Q., et al. (2022). Effect of apatinib plus pegylated liposomal doxorubicin vs pegylated liposomal doxorubicin alone on platinum-resistant recurrent ovarian cancer: The APPROVE randomized clinical trial. *JAMA Oncol.* 8 (8), 1169–1176. doi:10.1001/jamaoncol.2022.2253

Wang, Z., Chen, W., Zuo, L., Xu, M., Wu, Y., Huang, J., et al. (2022). The Fibrillin-1/VEGFR2/STAT2 signaling axis promotes chemoresistance via modulating glycolysis and angiogenesis in ovarian cancer organoids and cells. *Cancer Commun. (Lond)* 42 (3), 245–265. doi:10.1002/cac2.12274

Wang, Z., Huang, Y., Long, L., Zhou, L., Huang, Y., Gan, L., et al. (2021). Apatinib treatment efficiently delays biochemical-only recurrent ovarian cancer progression. *J. Ovarian Res.* 14 (1), 91. doi:10.1186/s13048-021-00843-8

Wang, Z., Sun, K., Xiao, Y., Feng, B., Mikule, K., Ma, X., et al. (2019b). Niraparib activates interferon signaling and potentiates anti-PD-1 antibody efficacy in tumor models. *Sci. Rep.* 9 (1), 1853. doi:10.1038/s41598-019-38534-6

Wright, A. A., Bohlke, K., Armstrong, D. K., Bookman, M. A., Cliby, W. A., Coleman, R. L., et al. (2016). Neoadjuvant chemotherapy for newly diagnosed, advanced ovarian cancer: Society of gynecologic oncology and American society of clinical oncology clinical practice guideline. *J. Clin. Oncol.* 34 (28), 3460–3473. doi:10.1200/JCO.2016.68.6907

Wu, X., Zhu, J., Wang, J., Lin, Z., Yin, R., Sun, W., et al. (2022). Pamiparib monotherapy for patients with germline BRCA1/2-mutated ovarian cancer previously treated with at least two lines of chemotherapy: A multicenter, open-label, phase II study. *Clin. Cancer Res.* 28 (4), 653–661. doi:10.1158/1078-0432.CCR-21-1186

Xiong, Y., Guo, Y., Liu, Y., Wang, H., Gong, W., Liu, Y., et al. (2020). Pamiparib is a potent and selective PARP inhibitor with unique potential for the treatment of brain tumor. *Neoplasia* 22 (9), 431–440. doi:10.1016/j.neo.2020.06.009

Yang, C., Xia, B. R., Zhang, Z. C., Zhang, Y. J., Lou, G., and Jin, W. L. (2020). Immunotherapy for ovarian cancer: Adjuvant, combination, and neoadjuvant. *Front. Immunol.* 11, 577869. doi:10.3389/fimmu.2020.577869

Yang, Y., Guo, X., Hu, B., He, P., Jiang, X., Wang, Z., et al. (2021). Generated SecPen_NY-ESO-1_ubiquitin-pulsed dendritic cell cancer vaccine elicits stronger and specific T cell immune responses. *Acta Pharm. Sin. B* 11 (2), 476–487. doi:10.1016/j.apsb.2020.08.004

Yang, Y., Xia, L., Wu, Y., Zhou, H., Chen, X., Li, H., et al. (2021). Programmed death ligand-1 regulates angiogenesis and metastasis by participating in the c-JUN/VEGFR2 signaling axis in ovarian cancer. *Cancer Commun. (Lond)* 41 (6), 511–527. doi:10.1002/cac2.12157

Yang, Y., Zhao, T., Chen, Q., Li, Y., Xiao, Z., Xiang, Y., et al. (2022). Nanomedicine strategies for heating "cold" ovarian cancer (OC): Next evolution in immunotherapy of OC. *Adv. Sci. (Weinh)* 9 (28), e2202797. doi:10.1002/advs.202202797

Zamarin, D., Burger, R. A., Sill, M. W., Powell, D. J., Lankes, H. A., Feldman, M. D., et al. (2020). Randomized phase II trial of nivolumab versus nivolumab and ipilimumab for recurrent or persistent ovarian cancer: An NRG oncology study. *J. Clin. Oncol.* 38 (16), 1814–1823. doi:10.1200/JCO.19.02059

Zhang, A. W., McPherson, A., Milne, K., Kroeger, D. R., Hamilton, P. T., Miranda, A., et al. (2018). Interfaces of malignant and immunologic clonal dynamics in ovarian cancer. *Cell.* 173 (7), 1755–1769. doi:10.1016/j.cell.2018.03.073

Zhang, L., Conejo-Garcia, J. R., Katsaros, D., Gimotty, P. A., Massobrio, M., Regnani, G., et al. (2003). Intratumoral T cells, recurrence, and survival in epithelial ovarian cancer. *N. Engl. J. Med.* 348 (3), 203–213. doi:10.1056/NEJMoa020177

Zhang, Q., Yu, S., Lam, M. M. T., Poon, T. C. W., Sun, L., Jiao, Y., et al. (2019). Angiotensin II promotes ovarian cancer spheroid formation and metastasis by upregulation of lipid desaturation and suppression of endoplasmic reticulum stress. *J. Exp. Clin. Cancer Res.* 38 (1), 116. doi:10.1186/s13046-019-1127-x

Zhang, W., Lu, X., Cui, P., Piao, C., Xiao, M., Liu, X., et al. (2019). Phase I/II clinical trial of a Wilms' tumor 1-targeted dendritic cell vaccination-based immunotherapy in patients with advanced cancer. *Cancer Immunol. Immunother.* 68 (1), 121–130. doi:10.1007/s00262-018-2257-2

Zhou, D., Liu, J., Liu, R., Li, H., Huang, Y., Ma, D., et al. (2022). Effectiveness and safety of niraparib as neoadjuvant therapy in advanced ovarian cancer with homologous recombination deficiency (NANT): Study protocol for a prospective, multicenter, exploratory, phase 2, single-arm study. *Front. Oncol.* 12, 852772. doi:10.3389/fonc.2022.852772

Zimmer, A. S., Nichols, E., Cimino-Mathews, A., Peer, C., Cao, L., Lee, M. J., et al. (2019). A phase I study of the PD-L1 inhibitor, durvalumab, in combination with a PARP inhibitor, olaparib, and a VEGFR1-3 inhibitor, cediranib, in recurrent women's cancers with biomarker analyses. *J. Immunother. Cancer* 7 (1), 197. doi:10.1186/s40425-019-0680-3

Zsiros, E., Lynam, S., Attwood, K. M., Wang, C., Chilakapati, S., Gomez, E. C., et al. (2021). Efficacy and safety of pembrolizumab in combination with bevacizumab and oral metronomic cyclophosphamide in the treatment of recurrent ovarian cancer: A phase 2 nonrandomized clinical trial. *JAMA Oncol.* 7 (1), 78–85. doi:10.1001/jamaoncol.2020.5945

Glossary

BRCA breast cancer susceptibility gene

HRD homologous recombination repair defect

OC ovarian cancer

EOC epithelial ovarian cancer

mPFS median progression-free survival

OS overall survival

PFS progression-free survival

NCCN National Comprehensive Cancer Network

HRR homologous recombination repair

PARPi poly (ADP ribose) polymerase inhibitor

TME tumor microenvironment

ICIs immune checkpoint inhibitors

HIF hypoxia inducible factor

MAP mitogen activated protein

PSROC platinum-sensitive recurrent OC

PROC platinum-resistant recurrent ovarian cancer

GC gemcitabine

PC paclitaxel and carboplatin

DCR disease control rate

ORR objective response rate

PLD pegylated liposomal doxorubicin

FBN1 profibronectin-1

FGFR fibroblast growth factor receptor

DOR duration of remission

AEs adverse events

PP2A protein phosphatase 2A

PDGFR platelet-derived growth factor receptor

SSB single-strand break

DSB double-strand break

BER base excision repair

EMSO European Society for Medical Oncology

TTSP time to second progression

FDA the Food and Drug Administration

SGO Society of Gynecologic Oncology

MDS myelodysplastic syndrome

AML acute myeloid leukemia

HGOC high-grade ovarian cancer

LOH loss of heterozygosity

CFI chemotherapy-free interval

TFST time to start first subsequent treatment

TSST the time to start second follow-up treatment

BRCP breakthrough cancer resistance protein

mDOR median time to remission

FRα Folate receptor α

TAAs tumor-associated antigens

TSAs tumor-specific antigens

TILs tumor infiltrating lymphocytes

TIM tumor immune microenvironment

TAM tumor-associated macrophage

mAb monoclonal antibody

MDSCs myeloid-derived suppressor cells

SD stable disease

LSD lipoprotein receptor

SCs serous carcinomas

SCD steroid coenzyme A desaturase

STC1 Stanniocalcin 1

GLUT1 glucose transporter protein-1

HKII hexokinase-2

MCSs multicellular spheroids

TMB tumor mutational load

DCVAC dendritic cell immunotherapy

DC dendritic cell

OV oncolytic virus

HSV herpes simplex virus

EV extracellular vesicle

VLP virus-like nanoparticle

NACT neoadjuvant chemotherapy

TFIp platinum treatment-free interval

TEAE treatment emergent adverse events

HMAs hypomethylating agents

CSC cancer stem cell

MSI-H MicroSatellite Instability-High

dMMR different Mismatch Repair

CD4+ conventional T cells-related genes signature is a prognostic indicator for ovarian cancer

Tian Hua[1], Deng-xiang Liu[2], Xiao-chong Zhang[2], Shao-teng Li[2], Peng Yan[3], Qun Zhao[4,5]* and Shu-bo Chen[2]*

[1]Department of Gynecology, Affiliated Xingtai People Hospital of Hebei Medical University, Xingtai, China, [2]Department of Oncology, Affiliated Xingtai People Hospital of Hebei Medical University, Xingtai, China, [3]Department of Oncology, The Second Affiliated Hospital Of Xingtai Medical College, Xingtai, China, [4]Department of Oncology, Hebei Medical University, Fourth Hospital, Shijiazhuang, China, [5]Hebei Key Laboratory of Precision Diagnosis and Comprehensive Treatment of Gastric Cancer, Shijiazhuang, China

Introduction: It is believed that ovarian cancer (OC) is the most deadly form of gynecological cancer despite its infrequent occurrence, which makes it one of the most salient public health concerns. Clinical and preclinical studies have revealed that intratumoral CD4+ T cells possess cytotoxic capabilities and were capable of directly killing cancer cells. This study aimed to identify the CD4+ conventional T cells-related genes (CD4TGs) with respect to the prognosis in OC.

Methods: We obtained the transcriptome and clinical data from the Cancer Genome Atlas (TCGA) and Gene Expression Omnibus (GEO) databases. CD4TGs were first identified from single-cell datasets, then univariate Cox regression was used to screen prognosis-related genes, LASSO was conducted to remove genes with coefficient zero, and multivariate Cox regression was used to calculate riskscore and to construct the CD4TGs risk signature. Kaplan-Meier analysis, univariate Cox regression, multivariate Cox regression, time-dependent receiver operating characteristics (ROC), decision curve analysis (DCA), nomogram, and calibration were made to verify and evaluate the risk signature. Gene set enrichment analyses (GSEA) in risk groups were conducted to explore the tightly correlated pathways with the risk group. The role of riskscore has been further explored in the tumor microenvironment (TME), immunotherapy, and chemotherapy. A risk signature with 11 CD4TGs in OC was finally established in the TCGA database and furtherly validated in several GEO cohorts.

Results: High riskscore was significantly associated with a poorer prognosis and proven to be an independent prognostic biomarker by multivariate Cox regression. The 1-, 3-, and 5-year ROC values, DCA curve, nomogram, and calibration results confirmed the excellent prediction power of this model. Compared with the reported risk models, our model showed better performance. The patients were grouped into high-risk and low-risk subgroups according to the riskscore by the median value. The low-risk group patients tended to exhibit a higher immune infiltration, immune-related gene expression and were more sensitive to immunotherapy and chemotherapy.

Discussion: Collectively, our findings of the prognostic value of CD4TGs in prognosis and immune response, provided valuable insights into the molecular mechanisms and clinical management of OC.

Introduction

Among all gynecological malignances, ovarian cancer causes the most deaths, and it is estimated that ovarian cancer accounts for 5% of all cancer deaths in women. In 2023, There will be 19,710 new cases and 13,270 new deaths because of OC in the United States [1]. The reason for death was mainly due to late-stage diagnosis [2]. Given the genetic and non-genetic risk factors of OC, OC was considered a particularly challenging cancer to overcome. Over the past few decades, a higher degree of radicality has been implemented in ovarian cancer surgery [3]. In addition, homologous recombination repair deficiency (HRD) and BRAC1/2 gene mutations testing also optimize PARP inhibitor (PARPi) use aimed to improve the benefit of patients even in the most advanced stages of the disease [4, 5]. Although the treatments have reduced OC-related deaths to a certain extent, patient outcomes remained unfavourable. Therefore, it was necessary to develop new prognostic signatures and molecular biomarkers.

As a result of comprehensive sequencing efforts over the past decade, we have learned about the genomic landscape of common forms of human cancer. Many studies have focused on the promotion or inhibition of cancer genes. High throughput screening, such as RNAi and CRISPR, were used to identify cancer dependency genes and their relationships to genetics, expression, regulatory mechanism, and therapeutic potential [6, 7]. New immunotherapeutics have been developed due to advances in cancer immunology [8, 9]. Cytotoxic T cells were essential effectors of anti-tumor immunity [9]. Zheng et al. demonstrated the tumor infiltrating T cell compendium, dynamics, and regulation in many cancer types by single-cell RNA-seq (scRNA-seq). They compared the phenotype and tissue distribution of CD8+ T cell and CD4+ T cell among blood, normal tissue, tumor tissue. CD8+ T cell has 17 different subclusters, such as ISG+CD8+ T cell and tissue-resident memory T cells (T_{rm}). CD4+ T cell has 24 different subclusters, such as IL26+Th17 and TNFRSF9+Treg. Terminally differentiated effector memory (T_{emra}) and naïve T cells (T_n) were enriched in blood between CD8+ T cell and CD4+ T cell. Most tested cancer types exhibited a notable degree of motility for both CD8+ and CD4+ T_{emra} cells between blood and normal or tumor tissues. The classical CD4+ T cell marker were CD3D, CD3E, CXCR4, IL7R, LTB, TRBC2 [10]. While tumor killing was considered to be CD8+ T cell function, the majority of previous understanding of the functionality of CD4+ T cells came from studies about anti-viral immunity [11, 12]. CD4+ T cells recognized cognate viral antigens in a major histocompatibility complex class II (MHC class II) -restricted manner [13]. Within the cancer context, multiple lines of evidence pointed to an important role for CD4+ T cells in immune responses to cancer immunotherapy [14–19]. For example, Martens et al. indicated that increased CD4+ T cell percentages at 8-14 weeks positively correlated with the expected pharmacodynamic effect [14]. There was also more direct evidence of the therapeutic benefits of CD4+ T cells in neoantigen vaccination, with CD4+ T cell responsed to neoantigen vaccines being more prevalent than CD8+ T cell responses [20, 21]. CD4+ T cells have also played a pivotal role in cancer induced by viruses. The expression of the EBV signaling protein LMP1 in B lymphocytes triggered CD4+ T cell responses against various tumor-associated antigens [22]. Thanks to the rapid development of single-cell sequencing experiments and analytical techniques, some studies found that CD4+ conventional T cells-related lncRNAs signature was associated with hepatocellular carcinoma, breast cancer prognosis, therapy, and tumor microenvironment [23, 24]. However, few studies have focused on the prognosis of CD4+ conventional T cells-related genes in OC.

As a result of bulk sequencing, we averaged the genetic and expression profiles of the different tumor subpopulations [25]. New technologies based on single-cell sequencing have opened new avenues for understanding intra-tumoral heterogeneity and capturing different tumor states with unprecedented resolution and scale [26, 27]. In the present study, based on bulk and single-cell sequencing datasets, we established a prognostic signature based on CD4TGs for OC. Clinical features, overall survival (OS), progress-free survival (PFS), tumor microenvironment, immunotherapy, and chemotherapy were evaluated between high and low riskscore subpopulations.

Materials and methods

Data acquire

We downloaded RNA-seq gene expression data of transcripts per million (TPM) values, clinical information, and masked annotated somatic mutation datasets of OC (tumor type was high-grade serous ovarian cancer) from The Cancer Genome Atlas (TCGA, https://portal.gdc.cancer.gov/). Only primary solid tumor patients were kept in the analysis. Single-cell RNA-seq data (GSE118828, GSE147082) and prognosis validation datasets

(GSE26193, GSE63885, GSE140082) were obtained from GEO databases (https://www.ncbi.nlm.nih.gov/geo/) (28–34). TCGA data tpm value was log2(x+1) transformed and z-scored, GEO matrix was z-scored.

Identifying CD4Tconv-related differential expressed genes OC

The Tumor Immune Single Cell Hub 2 (TISCH2) was a resource of single-cell RNA-seq (scRNA-seq) data from human and mouse tumors, which conducted comprehensive characterization of gene expression in the TME (35). We firstly obtained CD4TGs from TISCH2 with the criteria (|log2FC| > 1 and Adjusted p-value < 0.05). We then intersected the genes in two scRNA-seq GEO datasets, the TCGA dataset, and three external validation GEO datasets. 265 CD4TGs were harvested in the final.

Comprehensive analysis of single-cell datasets and cell cluster annotation

scRNA-seq dataset analysis was performed using the R package Seurat (v4.1.1) (36). UMAP analysis was done through Seurat's built-in function RunUMAP and umap-learn's built-in algorithm, and the Leiden algorithm. Finally, dimplot, featureplot, violin, and dotplot were used for visualization. The metabolic scores of different clusters of cell subtypes were calculated by the R package scMetabolism with the method AUCell in reactome pathway (37). The results of the scMetabolism calculations were integrated and visualised with dotplot pheatmap to demonstrate the metabolism of different clusters of cell subtypes. We also used AddModuleScore function to calculate the risk score in cell subsets level and sample level of the two single-cell GEO datasets.

Construction of CD4+Tconv-related genes riskscore signature

To screen genes associated with OS in OC patients, univariate Cox regression, least absolute shrinkage and selection operator (LASSO) regression, and multivariate Cox regression were executed sequentially to figure out eleven meaningful CD4 +Tconv-related genes. Based on their expression and corresponding multivariate Cox regression coefficients, the riskscore was calculated as follows:

Riskscore = ∑multivariate Cox regression coefficient (gene i) x gene expression value (gene i). The patients were divided into high-risk and low-risk subgroups by median riskscore in TCGA datasets. We also randomly splited the TCGA dataset into train and test datasets at a 1:1 ratio to predict OS by Kaplan-Meier (K-M) survival analysis. The patients were divided into high-risk and low-risk subgroups by best cutoff riskscore value (R package "survminer") to validate OS or PFS by Kaplan-Meier (K-M) survival analysis in validation GEO datasets.

Nomogram and calibration

In the whole TCGA dataset, time-dependent receiver operating characteristic (ROC) curve analysis was conducted to determine the prognostic value of riskscore over time. We also explored the role of the riskscore in different clinical subgroups (age, grade, stage, tumor residual size). The nomogram was constructed using multivariate Cox regression analysis by integrating clinical information and riskscore (R package "regplot"), and calibration curves were used to check the accuracy of the nomogram. The clinical benefits conferred by prognostic evaluation of the nomogram were further compared using decision curve analysis (DCA).

Functional enrichment analysis

Tool GSEA v4.3.2 from the MSigDB database (http://software.broadinstitute.org/gsea/msigdb/) was used to find the highly related GO and HALLMARK pathways between high-risk and low-risk subgroups based on the criterion of selection (FDR q-value < 0.25, Nominal p-value < 0.05 and |NES| >= 1.5) (38, 39).

Tumor microenvironment and immune infiltration level analysis

The "estimate" package was used to determine immune scores, stroma scores, and estimate scores. The abundance of immune cells was estimated using TIMER (40). Immunophenoscore (IPS) derived from The Cancer Group Atlas(TCIA, https://tcia.at/home) was used to predict the response to checkpoint blockade (41, 42). A single-sample gene set enrichment analysis (ssGSEA) was performed to quantify immune cells and immune function (R packages: "GSVA" and "GSEABase"). Immune subtypes information was derived from the previous study (43).

Drug sensitivity analysis

The origin data of chemotherapy response was from Genomics of Drug Sensitivity in Cancer (GDSC version 2) (https://www.cancerrxgene.org/) (44), and we downloaded curated data from https://osf.io/temyk. R package oncoPredict was used to predict the chemotherapy response difference between high-risk and low-risk subgroups (45).

Quantitative real-time PCR

RNA was extracted from ISOE, SKOV3, and A2780 cellines using the Trizol and then reverse-transcripted into cDNA. Primers were designed and obtained from the genewiz company. For real-time PCR, cDNA was used as template, and the PCR reaction was performed using QuantStudio(TM) 7 Flex System. The primer sequences used were listed in Supplementary Table 9.

Statistical analysis

All statistical analyses were performed by R software 4.2.2 or GraphPad 8. p-value < 0.05 was deemed to be statistically significant unless noted otherwise. Ns, *, **, ***, and **** stand for p-value >0.05, p-value <=0.05, pvalue <=0.01, pvalue <=0.001, and pvalue <=0.0001, separately. Survival analysis was carried out using the R packages "survival" and "survminer". We used the Wilcoxon test when comparing two groups and Kruskal-Wallis when comparing more than two groups.

Results

The whole workflow of this study was shown in Figure 1. We firstly obtained two single-cell sequencing (scRNA-seq) datasets from online database, and intersected the significant differential expression genes. Then TCGA bulk-seq data was used to screen prognosis genes by univariate Cox regression. LASSO algorithm was conducted to remove genes with coeffient zero. We furtherly filter gene by stepwise Cox (direction = both), calculated gene coeffients and finally built the risk model. We also made more tumor prognosis-related analyses.

Analysis of OC single-cell sequencing data

Based on the TISCH2 database, we obtained two scRNA-seq datasets, GSE118828 (SMART-seq2 platform) and GSE147082 (Drop-seq platform) and re-analysed using R package Seurat. The markers for each cell type were listed in Supplementary Table 1 and shown in Supplementary Figure S1. It was easy to find the classical marker, CD3D, CD3E, CXCR4, IL7R mainly expressed on CD4Tconv (CD4+ conventional T) subset (Supplementary Figure 1). As shown in Figures 2A, B, 3A, B, we could find that

FIGURE 1
Workflow diagram. The specific workflow graph of data analysis of the study.

CD4Tconv ranked third proportion in two datasets, just behind fibroblasts and malignant cells. In dataset GSE118828, the GSEA analysis of KEGG pathways showed CD4Tconv was significantly enriched in nature killer cell mediated cytotoxicity, T cell receptor signaling pathway, JAK-STAT signaling pathway, complement and coagulation cascades pathways (Supplementary Figures 2A, B). In dataset GSE147082, the GSEA analysis of KEGG pathways showed CD4Tconv was significantly enriched in nature killer cell mediated cytotoxicity, JAK-STAT signaling pathway, T cell receptor signaling pathway, ecm receptor inter pathways (Supplementary Figures 2C, D). These results suggested that CD4Tconv played a vital role in OC immunity-related pathways and was worthy of further study. We also investigated the metabolic status of different clusters of cell types. The result showed that CD4Tconv were enriched in metabolism of RNA, metabolism of amino acids and derivatives, selenoamino acid metabolism, phospholipid metabolism, pi metabolism, inositol phosphate metabolism pathways in dataset GSE118828 (Supplementary Figure 3A). This same metabolism result was also validated in dataset GSE147082 (Supplementary Figure 3B).

Development and validation of prognostic signatures associated with CD4+TGs in OC

After intersecting the genes in two scRNA-seq GEO datasets, the TCGA dataset, and three external validation GEO datasets. 265 CD4TGs were harvested finally. The genes list was in Supplementary Table 2. We first used univariate Cox regression analysis to screen significant genes in OS and found nineteen genes. The list of the genes was in Supplementary Table 3, and the forest plot was shown in Figure 4A. To narrow the list of the genes and get a more robust model, we furtherly conducted the LASSO algorithm according to the optimum lambda value and multivariate Cox regression analyses (Figures 4B, C). eleven genes were selected and generated the riskscore model in the final. The riskscore was calculated as follows: riskscore = (0.678 * CD3D expression) + (-0.897 * KLRB1 expression) + (0.535 * ITK expression) + (0.827 * IL2RB expression) + (-0.261 * CCR7 expression) + (-0.633 * ICOS expression) + (-0.619 * TSC22D1 expression) + (-0.413 * IFNG expression) + (-0.298 * DNAJA1 expression) + (-0.464 * SPON1 expression) + (-0.195 * MYLK expression). We splitted the internal validation TCGA dataset into train and test datasets at a ratio of 1:1. According to the median riskscore, OC patients were divided into high-risk and low-risk subgroups in the TCGA dataset. The results indicated that the high-risk group had a poorer prognosis in the train, test, and whole datasets (Figures 5A–C). In addition, we found the PFS also was significant between high-risk and low-risk subgroups in the TCGA whole dataset (Figure 5D). To avoid the difference of prognosis caused by the difference in clinical data, we compared the clinical features (age, grade, stage, tumor residual size) between high-risk and low-risk subgroups in the TCGA whole dataset and found there was no significant difference (Figure 5E), the statistic comparison result was in Supplementary Table 4. The detailed clinical information was in Supplementary Table 5. Thus proving the difference in prognosis was due to our risk signature instead of the imbalance in clinical data grouping. Additionally, we
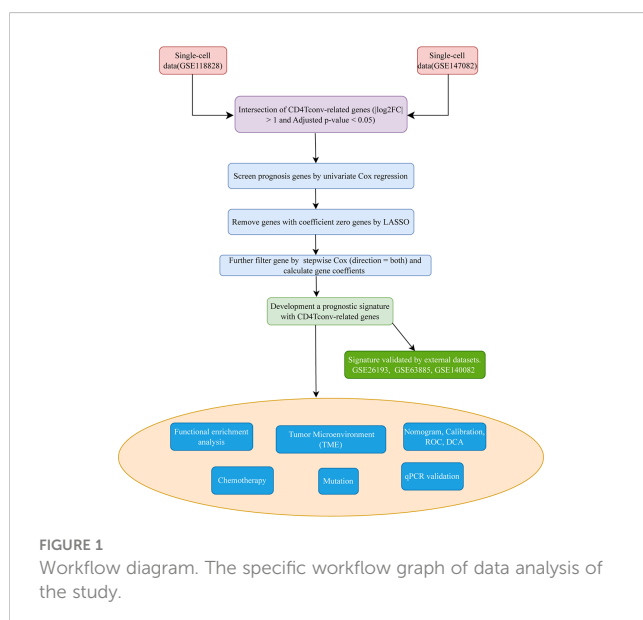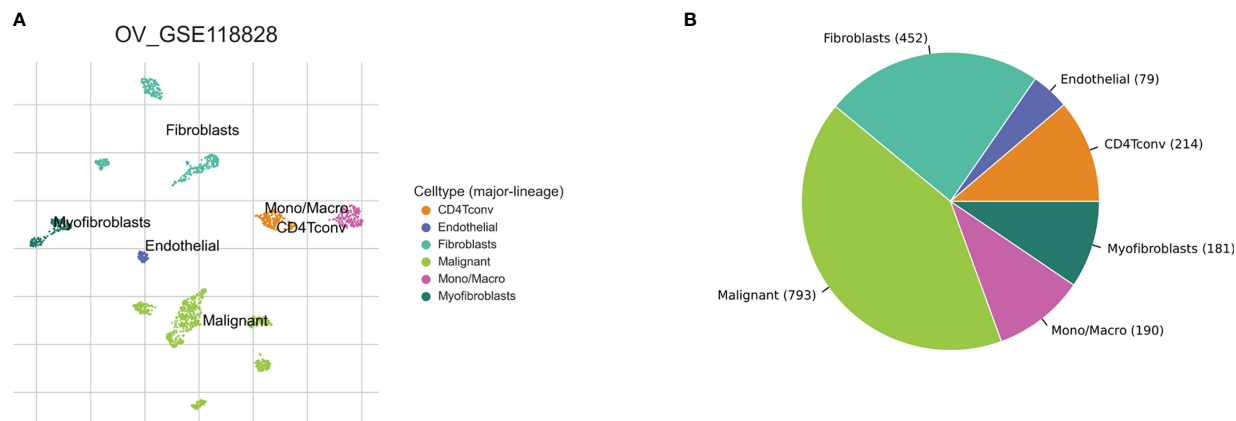
FIGURE 2
Ovary cancer single-cell data analysis based on the GSE118828 dataset. **(A)** The UMAP plots with cells coloured by cell type were displayed. **(B)** The pie plot showed the cell number distribution of each cell type.

evaluated riskscore in different clinical characteristics to further develop the application. Age, stage III, stage IV, and R1 were significant prognostic between high-risk and low-risk subgroups in the TCGA whole dataset (Figure 5F). The above analyses were mostly based on only the TCGA dataset. We sought some external datasets to validate the model to test the accuracy and robustness of the model. It could be seen that the OS were all significant in three independent GEO datasets based on the best cutoff in the riskscore, GSE26193 (p = 0.025), GSE140082 (p < 0.001), GSE63885 (p = 0.047) (Figures 6A–C). We also found that the high-risk group has a poorer PFS, consistent with the TCGA whole dataset (Figure 6D). To test whether A can be an independent prognostic factor, we combined clinical features (age, grade, stage, tumor residual size) and our pre-calculates riskscore into an integrated analysis. The univariate Cox regression analysis result showed the riskscore was significant (p < 0.001), and the hazard ratio was 1.415 (95% confidence interval,

1.228-1.631) (Figure 7A). The multivariate Cox regression analysis result showed the riskscore was an independent significant prognosis factor (p < 0.001), and the hazard ratio was 1.431 (95% confidence interval, 1.240-1.652) (Figure 7B). Time-dependent ROC analysis was performed to evaluate the predictive ability of the risk signature. The area under the curve (AUC) values at 1, 3, and 5 years for predicting OS were 0.716, 0.679, 0.746 in the TCGA train dataset, 0.643, 0.581, 0.526 in the TCGA test dataset, 0.684, 0.629, 0.638 in the TCGA whole dataset respectively (Figure 7C). ROC curves were also compared with other previous established risk models including a panel of three lncRNAs signature (AC136601.1

LINC02273 AC011445.1) (46) (Supplementary Figure 4A), a panel of five lncRNAs signature (GAS5, HCP5, PART1, SNHG11, SNHG5) (47) (Supplementary Figure 4B), a panel of six lncRNAs signature (AC006001.2, LINC02585, AL136162.1, AC005041.3, AL023583.1, LINC02881) (48) (Supplementary Figure 4C), a
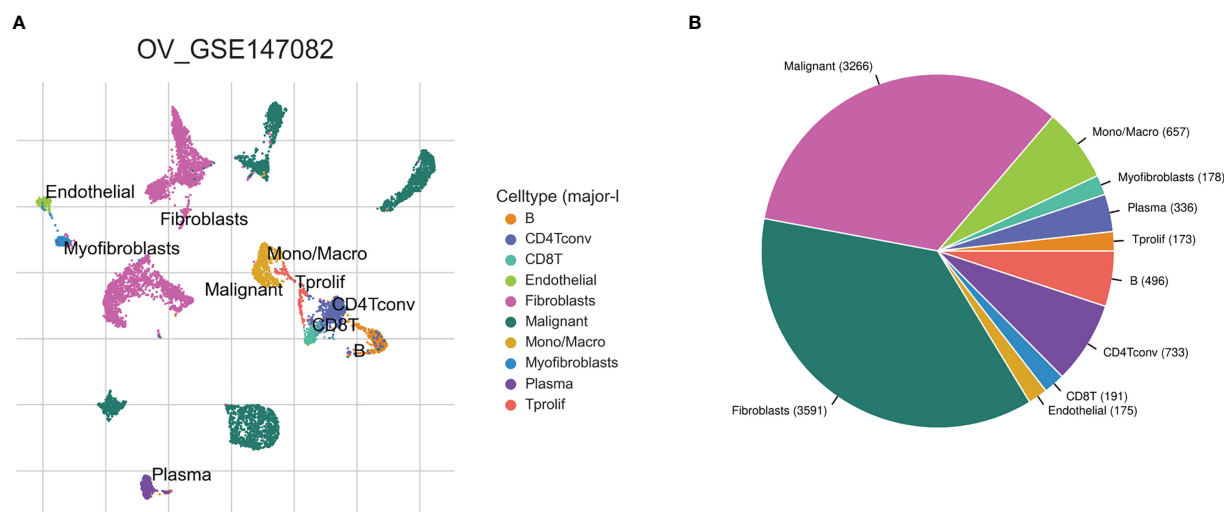

FIGURE 3
Ovary cancer single-cell data analysis based on the GSE147082 dataset. **(A)** The UMAP plots with cells coloured by cell type were displayed. **(B)** The pie plot showed the cell number distribution of each cell type.
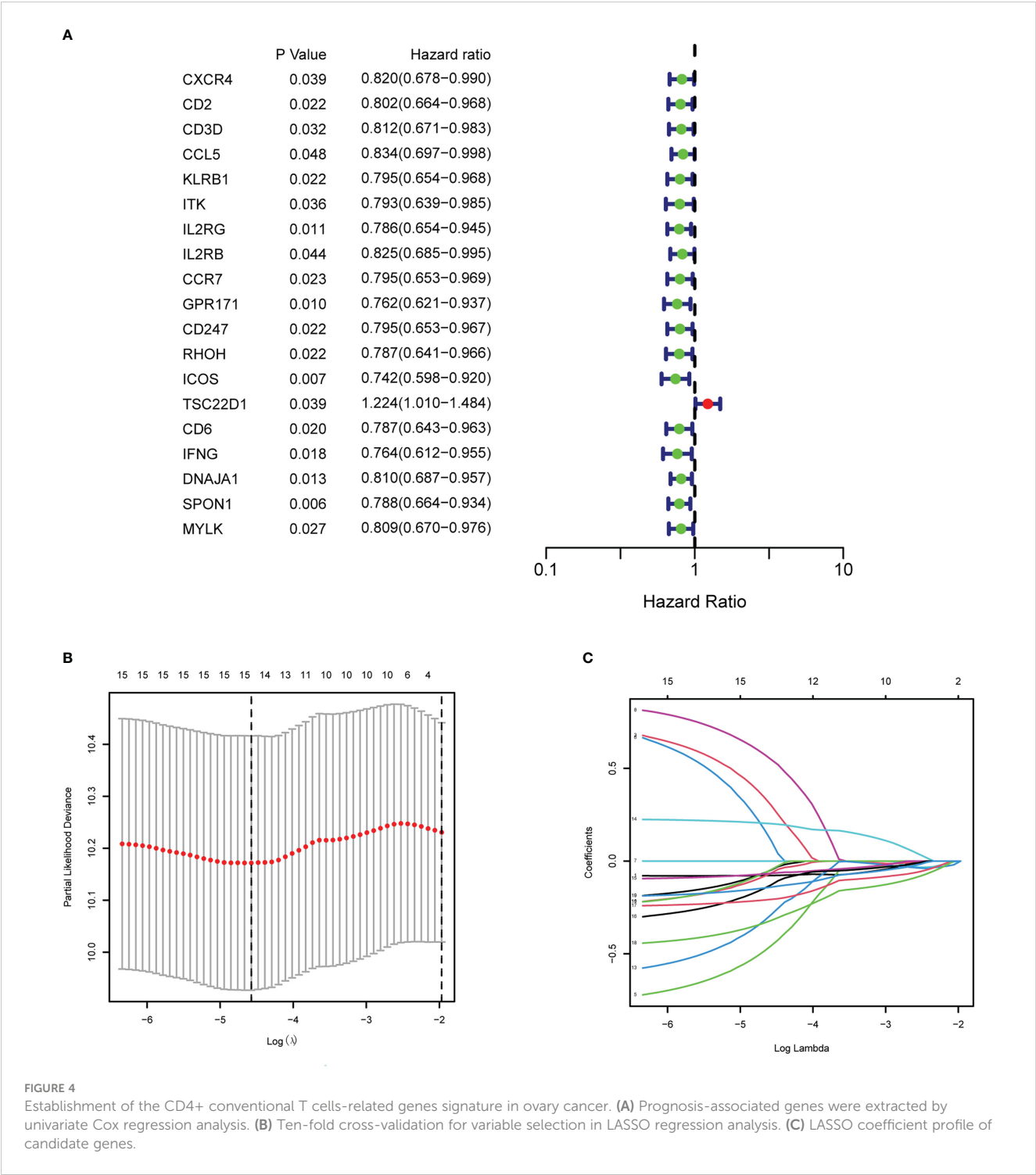
FIGURE 4

Establishment of the CD4+ conventional T cells-related genes signature in ovary cancer. **(A)** Prognosis-associated genes were extracted by univariate Cox regression analysis. **(B)** Ten-fold cross-validation for variable selection in LASSO regression analysis. **(C)** LASSO coefficient profile of candidate genes.

panel of eight mRNAs signature (JAK2, IL2RG, EEF1E1, UBB, EPS8, FOXO1, STAT5A, PAPPA) (49) (Supplementary Figure 4D), a panel of twelve mRNAs signature (CLDN4, EPCAM, MCM3, CXCL13, MIF, FOXO1, UBB, SEC22B, TCEAL4, ECI2, OGN, CFI) (50) (Supplementary Figure 4E). By comparing

the area under the curve (AUC) of ROC in 1 year, 3 years and 5 years. The detailed risk genes expression, riskscore and risk group were in Supplementary Table 6. We found that the predictive performance of our signature exceeded all the above risk models.

Analyzing and estimating nomogram and risk gene expression

To predict the survival risk of OC patients and improve the clinical utility of the risk model, we created a nomogram based on all OC patients with riskscore and four other critical clinical features of OC to calculate an integrated point for each patient in the TCGA cohort. The result demonstrated that the nomogram point could accurately quantify survival rates (Supplementary Figure 5A). The
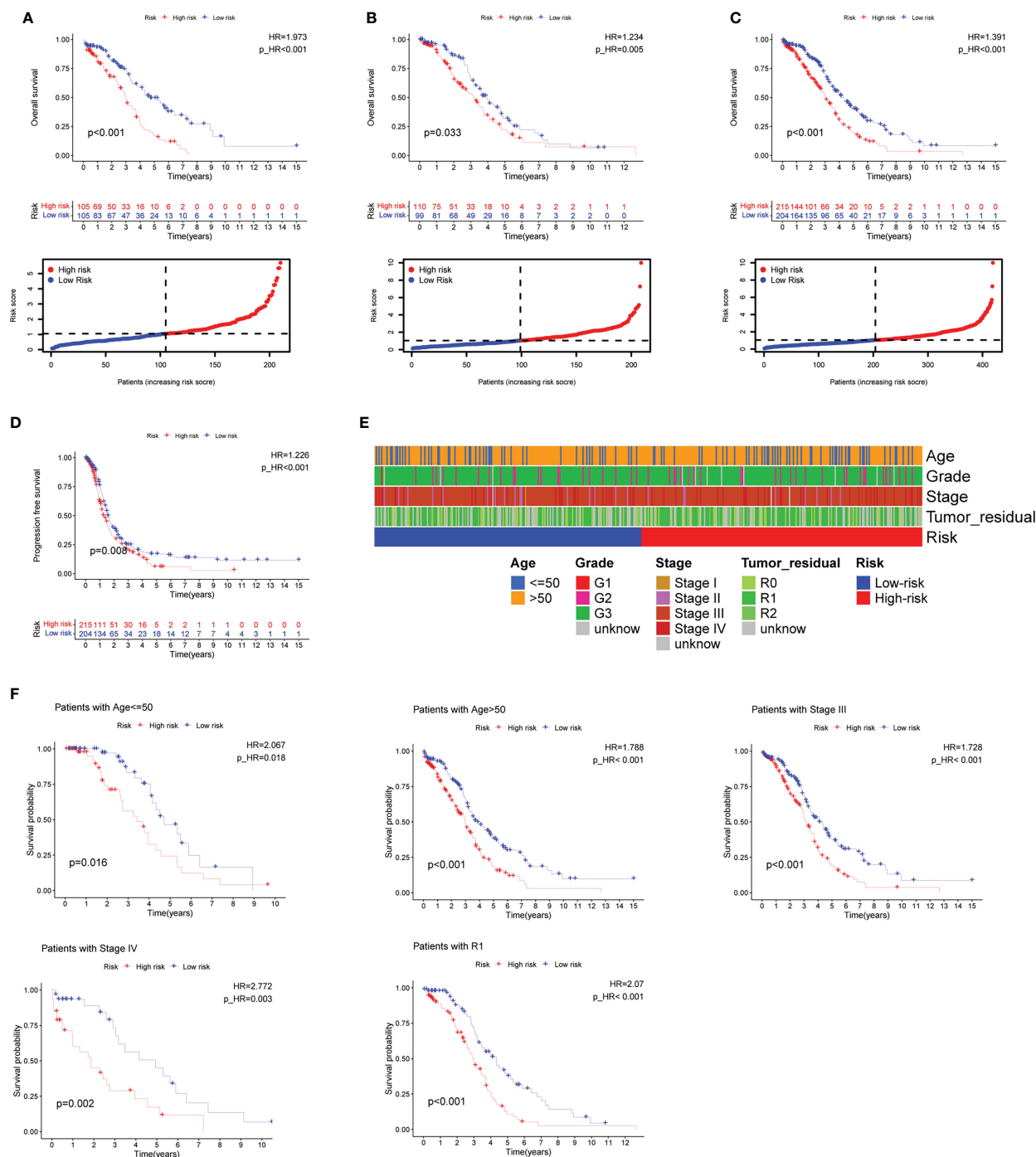
FIGURE 5

Prognosis value of the eleven CD4+ conventional T cells-related genes signature in the training, testing, and whole TCGA datasets. **(A–C)** Overall survival (OS) analysis in the training, testing, and whole TCGA datasets. **(D)** Progress-free survival (PFS) in the whole TCGA dataset. **(E)** Clinical information comparison between the high-risk and low-risk groups. **(F)** The prognostic value was stratified by the age, stage, and tumor residual size between high-risk and low-risk subgroups in the whole TCGA dataset.

calibration curves showed that the actual OS rates at 1-, 3-, and 5-year of patients and those estimated by the nomogram were close (Supplementary Figure 5B). The decision curve analysis (DCA) result suggested that the net rate of return for the OS rates evaluated by the combined risk model performed better than the other clinical characteristics (Supplementary Figure 5C). We explored the expression levels of the genes selected for risk pattern analysis in

two single-cell datasets GSE118828 and GSE147082 by dotplot and violin plots (Supplementary Figures 6A–D). Consistently, most of risk genes (such as CD3D, KLRB1, ITK, CCR7 and ICOS) were up-regulated in CD4Tconv, while other risk genes (such as TSC22D1, SPON1 and MYLK) were down-regulated in CD4Tconv. The risk score calculated by AddModuleScore function was displayed in cell subsets level and sample level, CD4Tconv cells had relatively high
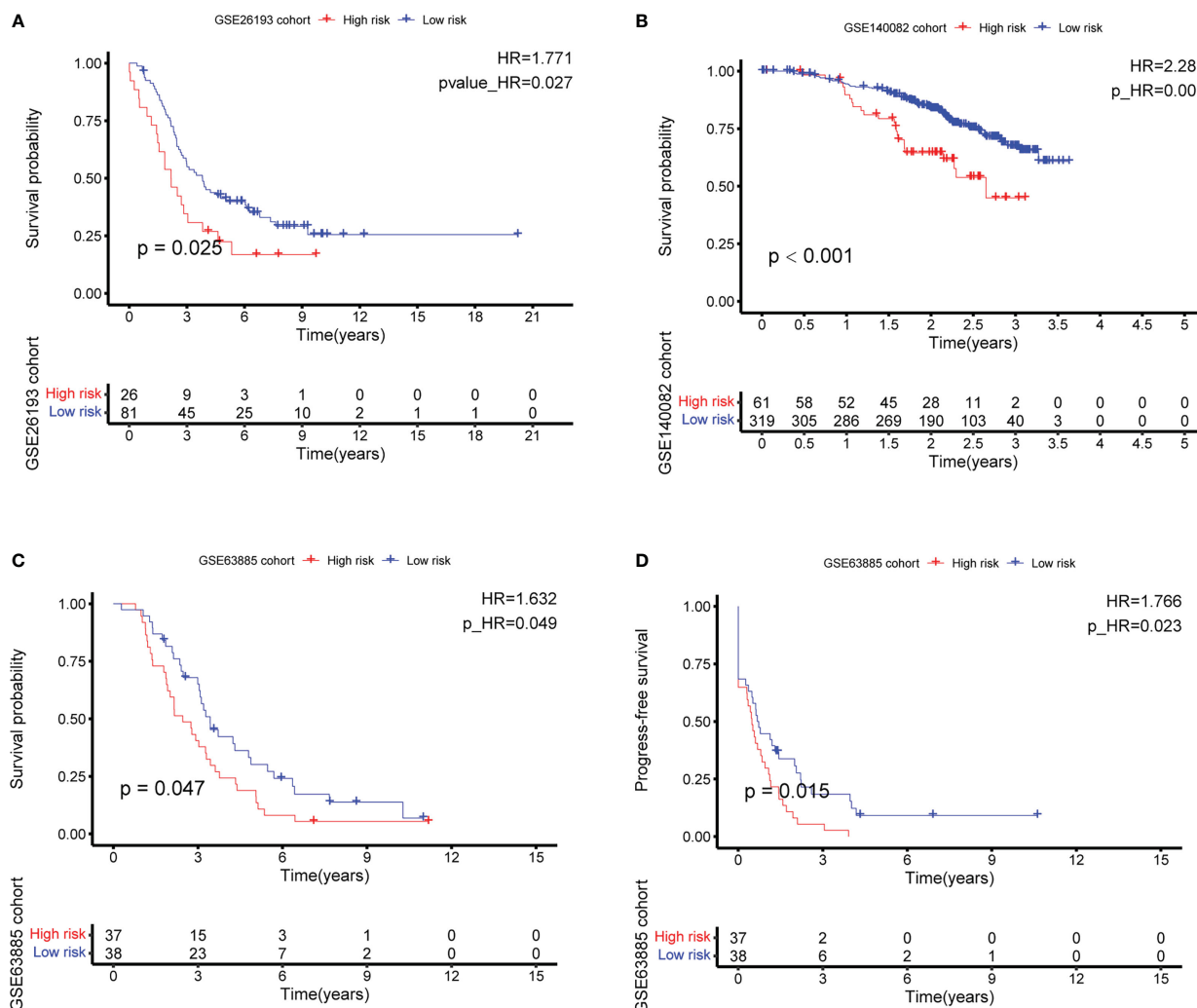
FIGURE 6

External validation of the CD4+ conventional T cells-related genes signature by best cutoff riskscore value. **(A–C)** Overall survival (OS) analysis in GSE26193, GSE140082, and GSE63885. **(D)** Progress-free survival (PFS) analysis in GSE63885.

level of risk scores (Supplementary Figures 6E, F). Besides, the expression of risk genes was also analyzed in TCGA dataset (Supplementary Figure 7A), along with validation cohorts GSE63885 (Supplementary Figure 7B), GSE26193 (Supplementary Figure 7C) and GSE140082 (Supplementary Figure 7D). We also analyzed the risk gene expression in two ovarian cancer celllines (SKOV3, A2780) and one normal ovarian celline (ISOE), the results were in Supplementary Figure 8A.

Functional enrichment analysis of the 11 CD4TGs risk model

To examine differences in biological function between high-risk and low-risk groups based on the riskscore. We first screened the differential genes among high-risk and low-risk groups with the following criteria: |logFC| ≥ 0.5 and a false discovery rate (FDR) < 0.05. The differential gene expression comparison was shown in

Figure 8A. The detailed differential genes information was in Supplementary Table 7. GSEA software was used to search for GO and HALLMARK terms across the whole TCGA dataset in high-risk and low-risk groups with all genes comparison information. The significant enriched GO terms in the low-risk group were GOBP ALPHA BETA T CELL ACTIVATION, GOBP ANTIGEN RECEPTOR MEDIATED SIGNALING PATHWAY, GOBP IMMUNE RESPONSE REGULATING CELL SURFACE RECEPTOR SIGNALING PATHWAY, GOBP IMMUNE RESPONSE REGULATING SIGNALING PATHWAY, GOBP T CELL RECEPTOR SIGNALING PATHWAY, GOCC T CELL RECEPTOR COMPLEX, et al. (Figure 8B). The significant enriched HALLMARK terms in the low-risk group were HALLMARK ALLOGRAFT REJECTION, HALLMARK IL2 STAT5 SIGNALING, HALLMARK IL6 JAK STAT3 SIGNALING, HALLMARK INTERFERON ALPHA RESPONSE, HALLMARK INTERFERON GAMMA RESPONSE, HALLMARK PROTEIN SECRETION, et al. (Figure 8C).
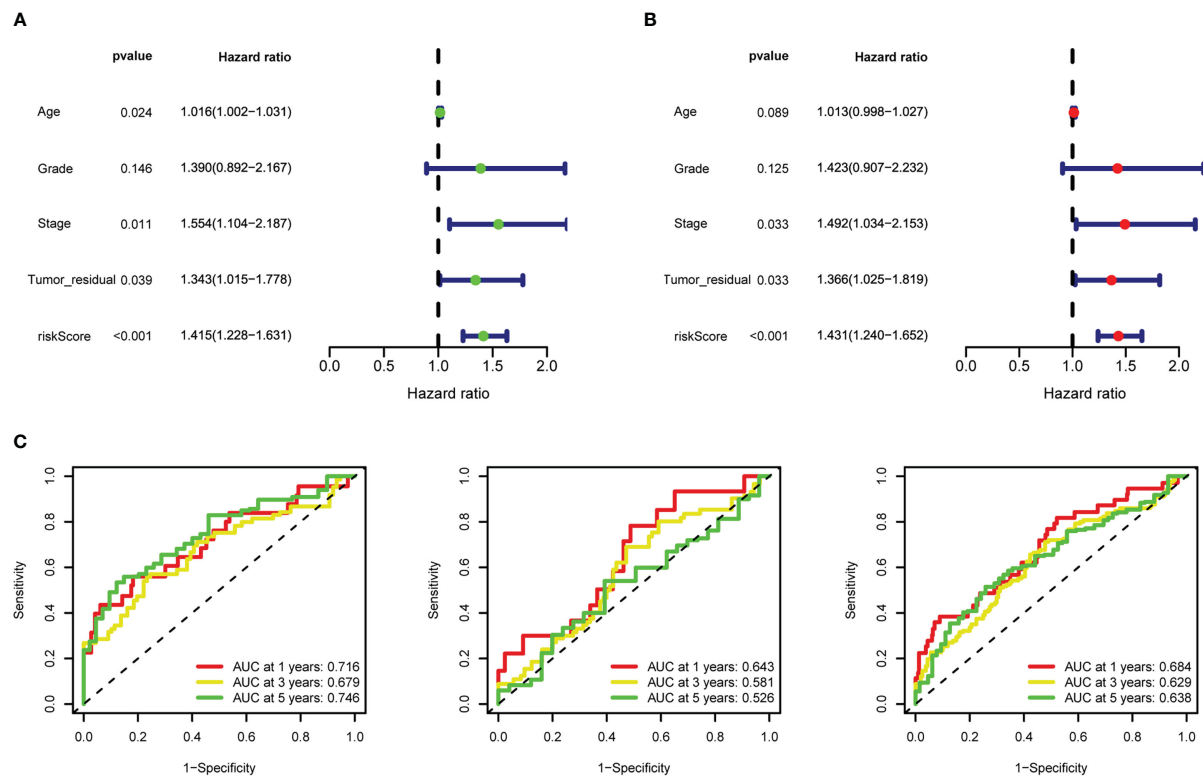
FIGURE 7
Riskscore as an independent prognostic factor. **(A)** Univariate Cox regression analysis of riskscore, age, stage, grade, tumor residual size. **(B)** Multivariate Cox regression analysis of riskscore, age, stage, grade, tumor residual size. **(C)** 1-, 3-, and 5-year time-dependent receiver operating characteristic (ROC) curves of the training, testing, and whole datasets, respectively.

The relationship between riskscore and tumor microenvironment

It was essential to exploit the role of TME in ovarian cancer progression and metastasis to discover novel therapeutics for this deadly disease due to the successful drugs targeting TME. Figure 9A showed the correlation between immune infiltration level and riskscore based on the TIMER, CIBERSORT, CIBERSORT_ABS, QUANTISEQ, MCPCOUNTER, XCELL, and EPIC algorithms. It was easy to find that most immune cell infiltration levels were negatively correlated with riskscore (Figure 9B, Supplementary Table 8). Such as Macrophage M1, T cell CD4+ memory resting, and T cell follicular helper by algorithm CIBERSORT–ABS, T cell regulatory (Tregs) by algorithm QUANTISEQ (Figure 9B). We assessed immune scores and estimate scores in OC based on the estimate algorithm, and we found that low-risk groups tended to have higher scores (Figure 9C). Additionally, we used the ssGSEA to examine the distribution of immune cell infiltration and the enrichment of immune-related functional pathways in high-risk and low-risk subgroups, it was obvious that the majority of immune cell infiltration levels were significantly higher in the low-risk group and immune-related functional pathways were significantly enriched in the low-risk group (Figures 9D, E). We also found almost all immune checkpoints exhibited higher expression in the low-risk group, such as CD274, CD28, and LAG3 (Figure 9F). Human leukocyte antigen

(HLA) genes were essential in antigen presentation. Our results also implied that most HLA genes had high expression levels in the low-risk group (Figure 9G). Thorsson et al. dentified six immune subtypes in 33 diverse cancer types, which was a resource for exploring immunogenicity in cancer. There was a significant immune subtypes composition difference between high-risk and low-risk groups (Figure 9H), indicating the different TME among the two risk groups. The above results proved that the riskscore was closely related to TME and time in OC patients. Therefore, we further explored the role of riskscore in immunotherapy through the TCIA database. The results indicated that the patients in the low-risk group were more sensitive to immunotherapy (Figures 9I–K).

Mutation and chemotherapeutic drug responses

We assessed the top fifteen mutated genes in both risk groups. The oncoplot presented that most genes had different mutation frequency in the low-risk than high-risk group, such as genes APOB, FLG2 had higher mutation frequency in the low-risk (Supplementary Figures 9A, B). We also evaluated chemotherapeutic drug responses in patients of two groups. The results showed that chemotherapeutic drugs had lower half-maximal inhibitory concentration (IC50) in the low-risk group, such as ML323, Pictilisib, and Ruxolitinib (Supplementary Figures 9C).

FIGURE 8

Gene set enrichment analyses (GSEA) of the Risk Groups. **(A)** Differential gene expression levels between high-risk and low-risk groups. **(B)** Highly enriched GO terms in the low-risk group. **(C)** Highly enriched Hallmark pathways in the low-risk group (all p < 0.05; FDR <0.25; |NES| > 1.5). ns, p > 0.05; *p <= 0.05; **p <= 0.01; ***p <= 0.001; ****p <= 0.0001.

FIGURE 9

Investigation of tumor microenvironment in the high-risk and low-risk subgroups. **(A)** Correlation bubble plot of the abundance of the immune cells infiltration levels with riskscore. **(B)** A negative association between immune infiltration and risk score. **(C)** Comparison of immune-related scores between the low- and high-risk groups. **(D, E)** Enrichment analysis of immune cell infiltration and immune-related pathways. **(F)** The difference in the checkpoint expression between the risk groups. **(G)** The difference in the checkpoint expression between the risk groups. **(G)** The difference in the expression of human leukocyte antigen (HLA) genes between the risk groups. **(H)** Immune subtype difference between the risk groups. **(I)** Immunophenoscore (IPS) for immunotherapy. **(I)** CTLA4− PD1+. **(J)** CTLA4+ PD1−. **(K)** CTLA4+ PD1+.

Discussion

In the world, OC is the leading cause of mortality among gynecologic malignancies with a high mortality on incidence ratio, accounting for the greatest proportion of gynecologic cancers. Although after primary treatment with surgery resection and chemotherapy, most patients achieved a complete response, 65-80% succumbed to recurrence with chemotherapeutic resistance in the first five years. In the past two decades, growing evidence suggested that immunotherapies have been widely used in the clinical treatment of various tumors. Despite treatments in cancer vaccines (such as BVX-0918), immune modulators (such as checkpoint inhibitors and cytokines), targeted antibodies (such as monoclonal antibodies), adoptive cell therapy (such as chimeric antigen receptor (CAR)- and TCR-engineered T cells) have been rapidly developing, immunotherapy response rates among ovarian cancer patients remained modest. Therefore, there was still a need to explore other biomarkers that may facilitate the not responded patients. The combination of therapeutic immunotherapy and chemotherapeutic therapy may improve treatment efficiency significantly.

Cytotoxic T cells were essential effectors of anti-tumor immunity. CD4+ T cell refered to a population of T lymphocytes which exhibited T cell receptors (TCRs) that specifically recognized

peptide antigens presented in association with Class II major histocompatibility complex (MHC II) molecules. CD4+ T cell were remarkably versatile and possessed multifunctional characteristics. These cells made up the secondary component of adaptive T cell-mediated immunity. In response to signals that varied based on the situation, CD4+ T cells had the ability to differentiate into multiple distinct functional subtypes. In response to signals that vary based on the situation, CD4+ T cells have the ability to differentiate into multiple distinct functional subtypes (51, 52). Much of the previous studies have put the focus of research on CD8 T cell instead of CD4 T cell function in cancer (53–55). Most insights into CD4+ T cells have focused on anti-viral immunity and autoimmunity, such as human cytomegalovirus (56, 57), epstein-barr virus (58), and autoimmune encephalomyelitis (59). In recent years, multiple studies have demonstrated that CD4+ T cells are critical to the response to cancer immunotherapy. Kwek et al. revealed pre-existing levels of PD-1+CD4+ T cells instead of CD8 + T cells in the circulation associated with improved overall survival in prostate cancer patients treated with ipilimumab (15). Cohen first discovered that B cell maturation antigen-specific chimeric antigen receptor (CAR) T cells reponse were positively associated with higher premanufacturing CD4/CD8 T cell ratio in multiple myeloma (18). The neoantigen vaccination derived from RNA-seq and whole-exome sequencing datasets that were currently of interest to major pharmaceutical companies, the neoantigens recognized by CD4 T cell and MHC class II-restricted manner played a vital role in the recovery of cancer patients (60, 61).

Currently, there have been many predictive signatures developed to predict patient prognosis outcomes for a better understanding of precision genomic medicine. Such as immune-related genes risk signature in glioblastomas (62), cuproptosis-related genes risk signature in hepatocellular carcinoma (63), ferroptosis-related genes signature in hepatocellular carcinoma (64). However, there were a handful of known studies with CD4 T cells related signatures, such as CD4+ conventional T cells-related lncRNA signature in breast cancer and hepatocellular carcinoma prognosis (23, 24). Recent applications of scRNA-seq in dissecting TME have allowed a detailed understanding of the biology of tumor-infiltrating immune cells properties of heterogeneity and potential roles in both tumor progression and response to immune checkpoint inhibitors and other immunotherapies. In the present study, we constructed a novel risk signature to predict prognosis and survival for OC based on the CD4+ conventional T cells-related genes based on scRNA-seq and TCGA bulk-seq datasets. Internal validation was conducted firstly by splitting the TCGA bulk-seq datasets into train and test at a ratio of 1:1. We then validated the risk signature OS and PFS in another three GEO datasets. This result proved that our risk signature was robust. The risk signature was an independent prognostic factor through multivariate Cox regression analysis. Nomogram was used to improve the clinical unity of riskscore. Calibration curve, DCA, and ROC were performed to test the accuracy of the risk signature. Furthermore, we compared our model with some models reported in the past and found our model was better in 1 year,found our model was better in 1 year, 3 years and 5 years. We also found that there were significant differences in the expression of many immune checkpoint genes

expression, some of which promoted immunity and some inhibited immunity. Among them, the survival condition of patients in the high-risk group was even worse, which may be due to the formation of an immunosuppressive microenvironment in this group of patients.We also expanded the risk signature to immunotherapy by thoroughly analysing the TME status difference between high-risk and low-risk groups. Chemotherapeutic drugs were also examined among high-risk and low-risk groups.

However, this study had certain limitations. Firstly, the present findings require further prospective validation by multicenter study cohorts. Secondly, further study of the functions and molecular mechanisms of these 11 CD4TGs in combination with more *in vitro* and *in vivo* experiments were required in OC. Nonetheless, we provided clues to identify CD4TGs that could be used as potential prognostic biomarkers and therapeutic targets with a good clinical prediction value.

Conclusion

Overall, we identified 11 CD4TGs involved in a risk model as a biomarker in OC based on scRNA-seq datasets, TGCA bulk-seq datasets and GEO probe datasets. Significant differences in survival rate and TME status were observed between the high-risk and low-risk groups, thus implying useful information for predicting clinical outcomes and may become a therapeutic target for patients with OC. As the nature of cancer immunotherapy was increasingly revealed, our study may provide new ideas on the role of CD4TGs in treating OC.

Data availability statement

The datasets presented in this study can be found in online repositories. The names of the repository/repositories and accession number(s) can be found within the article/Supplementary Material.

Author contributions

TH, D-XL, X-CZ, S-TL, and PY performed data collection and analysis. The study design and manuscript edition was done by TH, QZ, and S-BC, with all authors contributing to previous versions of the manuscript. All authors contributed to the article and approved the submitted version.

Funding

Acknowledgments

Conflict of interest

The authors declare that the research was conducted in the absence of any commercial or financial relationships that could be construed as a potential conflict of interest.

Publisher's note

All claims expressed in this article are solely those of the authors and do not necessarily represent those of their affiliated organizations, or those of the publisher, the editors and the reviewers. Any product that may be evaluated in this article, or claim that may be made by its manufacturer, is not guaranteed or endorsed by the publisher.

Supplementary material

The Supplementary Material for this article can be found online at: https://www.frontiersin.org/articles/10.3389/fimmu.2023.1151109/full#supplementary-material

SUPPLEMENTARY FIGURE 1
The expression of classical markers across different subsets in two single-cell RNA-seq datasets. **(A)** The expression of some classical markers on dotplot, **(B)** umap, **(C)** violin plots across different cell subsets in dataset GSE118828. **(D)** The expression of some classical markers on dotplot, **(E)** umap, **(F)** violin plots across different cell subsets in dataset GSE147082.

SUPPLEMENTARY FIGURE 2
Functionally enriched KEGG pathways. **(A)** The heatmap showed functionally enriched up-regulated KEGG pathways identified based on differential genes in each cell type in dataset GSE118828. **(B)** The heatmap showed functionally enriched down-regulated KEGG pathways identified based on differential genes in each cell type in dataset GSE118828. **(C)** The heatmap showed functionally enriched up-regulated KEGG pathways identified based on differential genes in each cell type in dataset GSE147082. **(D)** The heatmap showed functionally enriched down-regulated KEGG pathways identified based on differential genes in each cell type in dataset GSE147082.

SUPPLEMENTARY FIGURE 3
The single-cell metabolic features of cell subsets. **(A)** The metabolic status of different clusters of cell types in dataset GSE118828. **(B)**. The single-cell metabolic features of cell subsets in dataset GSE147082.

SUPPLEMENTARY FIGURE 4
The ROC of other previous established risk models at 1 year, 3 years and 5 years. **(A)** 3 lncRNA risk model. **(B)** 5 lncRNA risk model. **(C)** 6 lncRNA risk model. **(D)** 8 mRNA risk model. **(E)** 12 mRNA risk model.

SUPPLEMENTARY FIGURE 5
Analyzing and Estimating Nomogram. **(A)** Nomogram that integrated the riskscore, age, grade, stage, and tumor residual size predicted the probability of the 1-, 3-, and 5-year OS. **(B)** Calibration curves analysis for 1-, 3-, and 5-year OS. **(C)** decision curve analysis (DCA) of the nomogram in TCGA whole dataset for evaluating the clinical usefulness in 1-year OS.

SUPPLEMENTARY FIGURE 6
The expression levels of the genes selected for risk pattern analysis in single-cell dataset. **(A)** In single-cell dataset GSE118828 by dotplot. **(B)** In single-cell dataset GSE118828 by violin plot. **(C)** In single-cell dataset GSE147082 by dotplot. **(D)** In single-cell dataset GSE147082 by violin plot. **(E)** The risk score calculated by AddModuleScore function was displayed in cell subsets level in datasets GSE118828 and GSE147082. **(F)** The risk score calculated by AddModuleScore function was displayed in sample level in datasets GSE118828 and GSE147082.

SUPPLEMENTARY FIGURE 7
The risk genes expression in bulk-seq datasets. **(A)** In dataset TCGA by violin plot. **(B)** In dataset GSE63885 by violin plot. **(C)** In dataset GSE26193 by violin plot. **(D)** In dataset GSE147082 by violin plot.

SUPPLEMENTARY FIGURE 8
The risk gene expression in two ovarian cancer celllines (SKOV3, A2780) and one normal ovarian celline (ISOE). **(A)** The 11 risk genes expression, and were normalized to gene expression in celline ISOE.

SUPPLEMENTARY FIGURE 9
Mutation and Chemotherapeutic Drug Responses. **(A, B)** Top fifteen mutated genes frequency in both risk groups. **(C)** Chemotherapeutic drug half-maximal inhibitory concentration (IC50) in patients of two groups.

SUPPLEMENTARY TABLE 1
Cell markers of cell subsets.

SUPPLEMENTARY TABLE 2
The list of CD4+ conventional T cells-related genes.

SUPPLEMENTARY TABLE 3
The genes list after performing univariate Cox regression analysis.

SUPPLEMENTARY TABLE 4
Clinical features comparison between high-risk and low-risk subgroups.

SUPPLEMENTARY TABLE 5
The concrete clinical information for TCGA whole dataset patients.

SUPPLEMENTARY TABLE 6
The detailed risk genes expression, riskscore and risk group in all models.

SUPPLEMENTARY TABLE 7
Differential genes information between high-risk and low-risk subgroups.

SUPPLEMENTARY TABLE 8
Profile of significantly different infiltrated immune cells between high-risk and low-risk subgroups by different algorithms.

SUPPLEMENTARY TABLE 9
11 risk genes primer sequences.

References

1. Siegel RL, Miller KD, Wagle NS, Jemal A. Cancer statistics, 2023. *CA Cancer J Clin* (2023) 73(1):17–48. doi: 10.3322/caac.21763

2. Torre LA, Trabert B, DeSantis CE, Miller KD, Samimi G, Runowicz CD, et al. Ovarian cancer statistics, 2018. *CA Cancer J Clin* (2018) 68(4):284–96. doi: 10.3322/caac.21456

3. Fotopoulou C, Planchamp F, Aytulu T, Chiva L, Cina A, Ergönül Ö, et al. European Society of gynaecological oncology guidelines for the peri-operative management of advanced ovarian cancer patients undergoing debulking surgery. *Int J Gynecol Cancer* (2021) 31(9):1199–206. doi: 10.1136/ijgc-2021-002951

4. Kim A, Ueda Y, Naka T, Enomoto T. Therapeutic strategies in epithelial ovarian cancer. *J Exp Clin Cancer Res* (2012) 31(1):14. doi: 10.1186/1756-9966-31-14

5. Miller RE, Leary A, Scott CL, Serra V, Lord CJ, Bowtell D, et al. ESMO recommendations on predictive biomarker testing for homologous recombination deficiency and PARP inhibitor benefit in ovarian cancer. *Ann Oncol* (2020) 31 (12):1606–22. doi: 10.1016/j.annonc.2020.08.2102

6. McDonald ER3rd, de Weck A, Schlabach MR, Billy E, Mavrakis KJ, Hoffman GR, et al. Project DRIVE: A compendium of cancer dependencies and synthetic lethal

relationships uncovered by Large-scale, deep RNAi screening. *Cell* (2017) 170(3):577–92.e10. doi: 10.1016/j.cell.2017.07.005

7. Wang SW, Gao C, Zheng YM, Yi Y, Lu JC, Huang XY, et al. Current applications and future perspective of CRISPR/Cas9 gene editing in cancer. *Mol Cancer* (2022) 21 (1):57. doi: 10.1186/s12943-022-01518-8

8. Miller JF, Sadelain M. The journey from discoveries in fundamental immunology to cancer immunotherapy. *Cancer Cell* (2015) 27(4):439–49. doi: 10.1016/j.ccell.2015.03.007

9. Binnewies M, Roberts EW, Kersten K, Chan V, Fearon DF, Merad M, et al. Understanding the tumor immune microenvironment (TIME) for effective therapy. *Nat Med* (2018) 24(5):541–50. doi: 10.1038/s41591-018-0014-x

10. Zheng L, Qin S, Si W, Wang A, Xing B, Gao R, et al. Pan-cancer single-cell landscape of tumor-infiltrating T cells. *Science* (2021) 374(6574):abe6474. doi: 10.1126/science.abe6474

11. Brown DM, Román E, Swain SL. CD4 T cell responses to influenza infection. *Semin Immunol* (2004) 16(3):171–7. doi: 10.1016/j.smim.2004.02.004

12. Lissina A, Chakrabarti LA, Takiguchi M, Appay V. TCR clonotypes: molecular determinants of T-cell efficacy against HIV. *Curr Opin Virol* (2016) 16:77–85. doi: 10.1016/j.coviro.2016.01.017

13. Haabeth OA, Tveita AA, Fauskanger M, Schjesvold F, Lorvik KB, Hofgaard PO, et al. How do CD4(+) T cells detect and eliminate tumor cells that either lack or express MHC class II molecules? *Front Immunol* (2014) 5:174. doi: 10.3389/fimmu.2014.00174

14. Martens A, Wistuba-Hamprecht K, Yuan J, Postow MA, Wong P, Capone M, et al. Increases in absolute lymphocytes and circulating CD4+ and CD8+ T cells are associated with positive clinical outcome of melanoma patients treated with ipilimumab. *Clin Cancer Res* (2016) 22(19):4848–58. doi: 10.1158/1078-0432.CCR-16-0249

15. Kwek SS, Lewis J, Zhang L, Weinberg V, Greaney SK, Harzstark AL, et al. Preexisting levels of CD4 T cells expressing PD-1 are related to overall survival in prostate cancer patients treated with ipilimumab. *Cancer Immunol Res* (2015) 3 (9):1008–16. doi: 10.1158/2326-6066.CIR-14-0227

16. Johnson DB, Estrada MV, Salgado R, Sanchez V, Doxie DB, Opalenik SR, et al. Melanoma-specific MHC-II expression represents a tumour-autonomous phenotype and predicts response to anti-PD-1/PD-L1 therapy. *Nat Commun* (2016) 7:10582. doi: 10.1038/ncomms10582

17. Rodig SJ, Gusenleitner D, Jackson DG, Gjini E, Giobbie-Hurder A, Jin C, et al. MHC proteins confer differential sensitivity to CTLA-4 and PD-1 blockade in untreated metastatic melanoma. *Sci Transl Med* (2018) 10(450):1–13. doi: 10.1126/scitranslmed.aar3342

18. Cohen AD, Garfall AL, Stadtmauer EA, Melenhorst JJ, Lacey SF, Lancaster E, et al. B cell maturation antigen-specific CAR T cells are clinically active in multiple myeloma. *J Clin Invest* (2019) 129(6):2210–21. doi: 10.1172/JCI126397

19. Alspach E, Lussier DM, Miceli AP, Kizhvatov I, DuPage M, Luoma AM, et al. MHC-II neoantigens shape tumour immunity and response to immunotherapy. *Nature* (2019) 574(7780):696–701. doi: 10.1038/s41586-019-1671-8

20. Ott PA, Hu Z, Keskin DB, Shukla SA, Sun J, Bozym DJ, et al. An immunogenic personal neoantigen vaccine for patients with melanoma. *Nature* (2017) 547 (7662):217–21. doi: 10.1038/nature22991

21. Sahin U, Derhovanessian E, Miller M, Kloke BP, Simon P, Löwer M, et al. Personalized RNA mutanome vaccines mobilize poly-specific therapeutic immunity against cancer. *Nature* (2017) 547(7662):222–6. doi: 10.1038/nature23003

22. Choi IK, Wang Z, Ke Q, Hong M, Paul DW Jr., Fernandes SM, et al. Mechanism of EBV inducing anti-tumour immunity and its therapeutic use. *Nature* (2021) 590 (7844):157–62. doi: 10.1038/s41586-020-03075-w

23. Ning S, Wu J, Pan Y, Qiao K, Li L, Huang Q. Identification of CD4(+) conventional T cells-related lncRNA signature to improve the prediction of prognosis and immunotherapy response in breast cancer. *Front Immunol* (2022) 13:880769. doi: 10.3389/fimmu.2022.880769

24. Zhu L, Zhang X-P, Xu S, Hu M-G, Zhao Z-M, Zhao G-D, et al. Identification of a CD4+ conventional T cells-related lncRNAs signature associated with hepatocellular carcinoma prognosis, therapy, and tumor microenvironment. *Front Immunol* (2023) 13. doi: 10.3389/fimmu.2022.1111246

25. Kuksin M, Morel D, Aglave M, Danlos FX, Marabelle A, Zinovyev A, et al. Applications of single-cell and bulk RNA sequencing in onco-immunology. *Eur J Cancer.* (2021) 149:193–210. doi: 10.1016/j.ejca.2021.03.005

26. Lei Y, Tang R, Xu J, Wang W, Zhang B, Liu J, et al. Applications of single-cell sequencing in cancer research: Progress and perspectives. *J Hematol Oncol* (2021) 14 (1):91. doi: 10.1186/s13045-021-01105-2

27. Papalexi E, Satija R. Single-cell RNA sequencing to explore immune cell heterogeneity. *Nat Rev Immunol* (2018) 18(1):35–45. doi: 10.1038/nri.2017.76

28. Barrett T, Wilhite SE, Ledoux P, Evangelista C, Kim IF, Tomashevsky M, et al. NCBI GEO: archive for functional genomics data sets–update. *Nucleic Acids Res* (2013) 41(Database issue):D991–5. doi: 10.1093/nar/gks1193

29. Shih AJ, Menzin A, Whyte J, Lovecchio J, Liew A, Khalili H, et al. Identification of grade and origin specific cell populations in serous epithelial ovarian cancer by single cell RNA-seq. *PloS One* (2018) 13(11):e0206785. doi: 10.1371/journal.pone.0206785

30. Olalekan S, Xie B, Back R, Eckart H, Basu A. Characterizing the tumor microenvironment of metastatic ovarian cancer by single-cell transcriptomics. *Cell Rep* (2021) 35(8):109165. doi: 10.1016/j.celrep.2021.109165

31. Mateescu B, Batista L, Cardon M, Gruosso T, de Feraudy Y, Mariani O, et al. miR-141 and miR-200a act on ovarian tumorigenesis by controlling oxidative stress response. *Nat Med* (2011) 17(12):1627–35. doi: 10.1038/nm.2512

32. Vathipadiekal V, Wang V, Wei W, Waldron L, Drapkin R, Gillette M, et al. Creation of a human secretome: A novel composite library of human secreted proteins: Validation using ovarian cancer gene expression data and a virtual secretome array. *Clin Cancer Res* (2015) 21(21):4960–9. doi: 10.1158/1078-0432.CCR-14-3173

33. Lisowska KM, Olbryt M, Dudaladava V, Pamuła-Piłat J, Kujawa K, Grzybowska E, et al. Gene expression analysis in ovarian cancer - faults and hints from DNA microarray study. *Front Oncol* (2014) 4:6. doi: 10.3389/fonc.2014.00006

34. Kommoss S, Winterhoff B, Oberg AL, Konecny GE, Wang C, Riska SM, et al. Bevacizumab may differentially improve ovarian cancer outcome in patients with proliferative and mesenchymal molecular subtypes. *Clin Cancer Res* (2017) 23 (14):3794–801. doi: 10.1158/1078-0432.CCR-16-2196

35. Han Y, Wang Y, Dong X, Sun D, Liu Z, Yue J, et al. TISCH2: expanded datasets and new tools for single-cell transcriptome analyses of the tumor microenvironment. *Nucleic Acids Res* (2023) 51(D1):D1425–d31. doi: 10.1093/nar/gkac959

36. Hao Y, Hao S, Andersen-Nissen E, Mauck WM3rd, Zheng S, Butler A, et al. Integrated analysis of multimodal single-cell data. *Cell* (2021) 184(13):3573–87.e29. doi: 10.1016/j.cell.2021.04.048

37. Wu Y, Yang S, Ma J, Chen Z, Song G, Rao D, et al. Spatiotemporal immune landscape of colorectal cancer liver metastasis at single-cell level. *Cancer Discov* (2022) 12(1):134–53. doi: 10.1158/2159-8290.CD-21-0316

38. Mootha VK, Lindgren CM, Eriksson KF, Subramanian A, Sihag S, Lehar J, et al. PGC-1alpha-responsive genes involved in oxidative phosphorylation are coordinately downregulated in human diabetes. *Nat Genet* (2003) 34(3):267–73. doi: 10.1038/ng1180

39. Subramanian A, Tamayo P, Mootha VK, Mukherjee S, Ebert BL, Gillette MA, et al. Gene set enrichment analysis: a knowledge-based approach for interpreting genome-wide expression profiles. *Proc Natl Acad Sci USA* (2005) 102(43):15545–50. doi: 10.1073/pnas.0506580102

40. Li T, Fu J, Zeng Z, Cohen D, Li J, Chen Q, et al. TIMER2.0 for analysis of tumor-infiltrating immune cells. *Nucleic Acids Res* (2020) 48(W1):W509–14. doi: 10.1093/nar/gkaa407

41. Van Allen EM, Miao D, Schilling B, Shukla SA, Blank C, Zimmer L, et al. Genomic correlates of response to CTLA-4 blockade in metastatic melanoma. *Science* (2015) 350(6257):207–11. doi: 10.1126/science.aad0095

42. Hugo W, Zaretsky JM, Sun L, Song C, Moreno BH, Hu-Lieskovan S, et al. Genomic and transcriptomic features of response to anti-PD-1 therapy in metastatic melanoma. *Cell* (2016) 165(1):35–44. doi: 10.1016/j.cell.2016.02.065

43. Huang TX, Fu L. The immune landscape of esophageal cancer. *Cancer Commun (Lond).* (2019) 39(1):79. doi: 10.1186/s40880-019-0427-z

44. Geeleher P, Cox N, Huang RS. pRRophetic: an r package for prediction of clinical chemotherapeutic response from tumor gene expression levels. *PloS One* (2014) 9(9):e107468. doi: 10.1371/journal.pone.0107468

45. Maeser D, Gruener RF, Huang RS. oncoPredict: an r package for predicting in vivo or cancer patient drug response and biomarkers from cell line screening data. *Brief Bioinform* (2021) 22(6):1–7. doi: 10.1093/bib/bbab260

46. Zhang J, Yan H, Fu Y. Effects of autophagy-related genes on the prognosis and immune microenvironment of ovarian cancer. *BioMed Res Int* (2022) 2022:6609195. doi: 10.1155/2022/6609195

47. Zhao Q, Fan C. A novel risk score system for assessment of ovarian cancer based on co-expression network analysis and expression level of five lncRNAs. *BMC Med Genet* (2019) 20(1):103. doi: 10.1186/s12881-019-0832-9

48. Zhang Z, Xu Z, Yan Y. Role of a pyroptosis-related lncRNA signature in risk stratification and immunotherapy of ovarian cancer. *Front Med (Lausanne)* (2021) 8:793515. doi: 10.3389/fmed.2021.793515

49. Liu L, Zhao J, Du X, Zhao Y, Zou C, Zhou H, et al. Construction and validation of a novel aging-related gene signature and prognostic nomogram for predicting the overall survival in ovarian cancer. *Cancer Med* (2021) 10(24):9097–114. doi: 10.1002/cam4.4404

50. Bai W-p, Sheng W. Identification of hypoxia-related prognostic signature for ovarian cancer based on cox regression model. *Eur J Gynaecological Oncol* (2022) 43 (2):247–56. doi: 10.3389/fimmu.2022.982026

51. Tay RE, Richardson EK, Toh HC. Revisiting the role of CD4(+) T cells in cancer immunotherapy-new insights into old paradigms. *Cancer Gene Ther* (2021) 28(1-2):5–17. doi: 10.1038/s41417-020-0183-x

52. Borst J, Ahrends T, Bąbała N, Melief CJM, Kastenmüller W. CD4(+) T cell help in cancer immunology and immunotherapy. *Nat Rev Immunol* (2018) 18(10):635–47. doi: 10.1038/s41577-018-0044-0

53. Echchakir H, Vergnon I, Dorothée G, Grunenwald D, Chouaib S, Mami-Chouaib F. Evidence for *in situ* expansion of diverse antitumor-specific cytotoxic T lymphocyte clones in a human large cell carcinoma of the lung. *Int Immunol* (2000) 12 (4):537–46. doi: 10.1093/intimm/12.4.537

54. Hashimoto M, Kamphorst AO, Im SJ, Kissick HT, Pillai RN, Ramalingam SS, et al. CD8 T cell exhaustion in chronic infection and cancer: Opportunities for interventions. *Annu Rev Med* (2018) 69:301–18. doi: 10.1146/annurev-med-012017-043208

55. Durgeau A, Virk Y, Corgnac S, Mami-Chouaib F. Recent advances in targeting CD8 T-cell immunity for more effective cancer immunotherapy. *Front Immunol* (2018) 9:14. doi: 10.3389/fimmu.2018.00014

56. Zaunders JJ, Dyer WB, Wang B, Munier ML, Miranda-Saksena M, Newton R, et al. Identification of circulating antigen-specific CD4+ T lymphocytes with a CCR5+, cytotoxic phenotype in an HIV-1 long-term nonprogressor and in CMV infection. *Blood* (2004) 103(6):2238–47. doi: 10.1182/blood-2003-08-2765

57. Appay V, Zaunders JJ, Papagno L, Sutton J, Jaramillo A, Waters A, et al. Characterization of CD4(+) CTLs *ex vivo*. *J Immunol* (2002) 168(11):5954–8. doi: 10.4049/jimmunol.168.11.5954

58. Paludan C, Schmid D, Landthaler M, Vockerodt M, Kube D, Tuschl T, et al. Endogenous MHC class II processing of a viral nuclear antigen after autophagy. *Science* (2005) 307(5709):593–6. doi: 10.1126/science.1104904

59. Raveney BJ, Oki S, Hohjoh H, Nakamura M, Sato W, Murata M, et al. Eomesodermin-expressing T-helper cells are essential for chronic neuroinflammation. *Nat Commun* (2015) 6:8437. doi: 10.1038/ncomms9437

60. Veatch JR, Lee SM, Shasha C, Singhi N, Szeto JL, Moshiri AS, et al. Neoantigen-specific CD4(+) T cells in human melanoma have diverse differentiation states and correlate with CD8(+) T cell, macrophage, and b cell function. *Cancer Cell* (2022) 40 (4):393–409.e9. doi: 10.1016/j.ccell.2022.03.006

61. Brightman SE, Naradikian MS, Miller AM, Schoenberger SP. Harnessing neoantigen specific CD4 T cells for cancer immunotherapy. *J Leukoc Biol* (2020) 107 (4):625–33. doi: 10.1002/JLB.5RI0220-603RR

62. Huang S, Song Z, Zhang T, He X, Huang K, Zhang Q, et al. Identification of immune cell infiltration and immune-related genes in the tumor microenvironment of glioblastomas. *Front Immunol* (2020) 11:585034. doi: 10.3389/fimmu.2020.585034

63. Liu X, Sun B, Yao Y, Lai L, Wang X, Xiong J, et al. Identification of copper metabolism and cuproptosis-related subtypes for predicting prognosis tumor microenvironment and drug candidates in hepatocellular carcinoma. *Front Immunol* (2022) 13:996308. doi: 10.3389/fimmu.2022.996308

64. Liang JY, Wang DS, Lin HC, Chen XX, Yang H, Zheng Y, et al. A novel ferroptosis-related gene signature for overall survival prediction in patients with hepatocellular carcinoma. *Int J Biol Sci* (2020) 16(13):2430–41. doi: 10.7150/ijbs.45050

Check for updates

Machine learning-based integration develops an immune-related risk model for predicting prognosis of high-grade serous ovarian cancer and providing therapeutic strategies

Qihui Wu[1,2†], Ruotong Tian[3†], Xiaoyun He[2,4], Jiaxin Liu[5], Chunlin Ou[2,6*], Yimin Li[7,8*] and Xiaodan Fu[2,6*]

[1]Department of Gynecology, Xiangya Hospital, Central South University, Changsha, China, [2]National Clinical Research Center for Geriatric Disorders, Xiangya Hospital, Changsha, China, [3]Department of Pharmacology, School of Basic Medical Sciences, Shanghai Medical College, Fudan University, Shanghai, China, [4]Departments of Ultrasound Imaging, Xiangya Hospital, Central South University, Changsha, Hunan, China, [5]Department of Pathology, School of Basic Medical Sciences, Central South University, Changsha, China, [6]Department of Pathology, Xiangya Hospital, Central South University, Changsha, China, [7]Department of Pathology, Fudan University Shanghai Cancer Center, Shanghai, China, [8]Department of Oncology, Shanghai Medical College, Fudan University, Shanghai, China

Background: High-grade serous ovarian cancer (HGSOC) is a highly lethal gynecological cancer that requires accurate prognostic models and personalized treatment strategies. The tumor microenvironment (TME) is crucial for disease progression and treatment. Machine learning-based integration is a powerful tool for identifying predictive biomarkers and developing prognostic models. Hence, an immune-related risk model developed using machine learning-based integration could improve prognostic prediction and guide personalized treatment for HGSOC.

Methods: During the bioinformatic study in HGSOC, we performed (i) consensus clustering to identify immune subtypes based on signatures of immune and stromal cells, (ii) differentially expressed genes and univariate Cox regression analysis to derive TME- and prognosis-related genes, (iii) machine learning-based procedures constructed by ten independent machine learning algorithms to screen and construct a TME-related risk score (TMErisk), and (iv) evaluation of the effect of TMErisk on the deconstruction of TME, indication of genomic instability, and guidance of immunotherapy and chemotherapy.

Results: We identified two different immune microenvironment phenotypes and a robust and clinically practicable prognostic scoring system. TMErisk demonstrated superior performance over most clinical features and other published signatures in predicting HGSOC prognosis across cohorts. The low TMErisk group with a notably favorable prognosis was characterized by BRCA1 mutation, activation of immunity, and a better immune response. Conversely, the

high TMErisk group was significantly associated with C-X-C motif chemokine ligands deletion and carcinogenic activation pathways. Additionally, low TMErisk group patients were more responsive to eleven candidate agents.

Conclusion: Our study developed a novel immune-related risk model that predicts the prognosis of ovarian cancer patients using machine learning-based integration. Additionally, the study not only depicts the diversity of cell components in the TME of HGSOC but also guides the development of potential therapeutic techniques for addressing tumor immunosuppression and enhancing the response to cancer therapy.

KEYWORDS

tumor microenvironment, ovarian cancer, machine learning, prognosis, treatment

Introduction

Although targeted drugs for ovarian cancer (OC), consisting of PARP inhibitors and Bevacizumab, limitedly prolong the survival of patients with advanced disease, OC continues to be the leading cause of cancer death in women [1]. Among multiple histological types of epithelial OC, high-grade serous ovarian cancer (HGSOC) is the most common type, accounting for 60–80% of all cases and being responsible for approximately 80% of all OC deaths [2, 3]. For more precise clinical management of patients, the researchers devote themselves to investigating the subtypes of OC, including The Cancer Genome Atlas (TCGA) project, generally suggesting that, in addition to molecular subtypes of tumor cells with different mutations or abnormal activation states, heterogeneity in proportion and anatomical location of non-tumor cells also leads to different phenotypes [4–6]. Indeed, molecular or immunological subtyping gives unique insights for basic research, but the robustness of these subtypes across studies and their clinical implications remain controversial [7].

Inarguably, cancer immunotherapies, including immune checkpoint blockade (ICB), have significantly improved the treatment of advanced solid tumors and benefited overall survival of patients when compared to conventional therapy [8, 9]. However, in patients with advanced ovarian cancer, the benefit of ICBs is limited [10, 11]. The mortality rate continues to be a growing concern. Despite repeated associations between HGSOC survival and T cell infiltration, especially for tumor-infiltrating CD8+ T lymphocytes (TILs), human HGSOC remains poorly responsive to immunotherapy [12, 13]. One possible explanation for this failure is that T cells are unable to penetrate the extracellular matrix [14, 15].

It is now well recognized that the TME, the soil in which tumors live and thrive, influences prognosis and therapy effectiveness. With advances in single-cell sequencing, depicting the cellular diversity in the TME at high resolution provides a characterization of the cellular composition in three tumor immune phenotypes (infiltrated, excluded, and desert) in HGSOC [16] and highlight the contributions of tumor-associated stromal components

in supporting tumor growth and hindering the efficacy of immunotherapy [4, 17, 18].

While previous studies have explored the potential of constructing gene signatures based on TME or immune-related genes as predictive indicators for tumor prognosis and immunotherapy [19, 20]. The published studies have limited predictive performance when assessed in different independent cohorts. In this study, mining data from several HGSOC bulk RNA-seq datasets, we aim to uncover the TME subtypes in HGSOC with consistency across multiple datasets and develop a robust and clinically practicable prognostic scoring system. Considering the contributions of both immune and stromal components, we start with identifying the inherent TME subtypes from a meta-cohort of HGSOC and TME-related genes. To address the robustness of the scoring system, we have implemented 108 combination frames constructed by 10 machine learning algorithms to achieve the best prognostic scoring performance that was assessed in multiple independent cohorts. The scoring system was termed the TMErisk score, which was able to indicate genomic instability, recognize the tumor immune microenvironment and cancer-related dysfunctions, and guide the identification of effective treatments for individual HGSOC patients.

Materials and methods

Data collection and processing

This study included seven public cohorts of HGSOC tumors, including two RNA-Seq datasets from the International Cancer Genome Consortium (ICGC; OV-AU) portal and The Cancer Genome Atlas (TCGA; TCGA-OV), as well as five microarray datasets from the Gene Expression Omnibus (GEO: GSE13876, GSE140082, GSE30161, GSE32062, and GSE9891) (Table S1). Besides the transcript data, the corresponding clinical data was also taken into account. A total of 1386 HGSOC tumor samples were included in this study, which excluded patients whose overall survival

data was insufficient. From the Genotype-Tissue Expression Database (GTEx, https://gtexportal.org/home/), the expression information of normal ovarian samples was downloaded. The IMvigor210 cohort, an immune checkpoint blockade treatment cohort, was obtained from http://research-pub.gene.com/IMvigor210CoreBiolo. These cohorts' initial raw data were pre-processed and normalized in accordance with our previous studies (19, 21). As for RNA-Seq datasets, raw counts were converted into values for the number of transcripts per million bases (TPM). The batch effects among various cohorts were eliminated using the "ComBat" algorithm of the "SVA" package. Somatic mutations and copy number variations (CNAs) of HGSOC were downloaded from TCGA. The mutation landscape of TCGA-OV was examined and represented using the "maftools" and "ComplexHeatmap" packages. Fisher's exact test was used to identify the top 20 mutation genes and differentially mutated genes. A GISTIC 2.0 analysis was conducted to investigate the CNV associated with HGSOC by GenePattern (https://www.genepattern.org/).

Human tissue specimens

In this study, a total of 25 patients with high-grade serous ovarian cancer (HGSOC) who had undergone curative resection at Xiangya Hospital, Central South University, were recruited. All patients provided informed consent, and the study was approved by the Xiangya Hospital Ethics Committee.

RNA extraction and real-time quantitative PCR

Total RNA was extracted from human tissue specimens using FFPE RNA Extraction Kits (AmoyDx, Xiamen, China), in accordance with the manufacturer's instructions. The purity and quantity of RNA were evaluated using the NanoDrop 1000 Spectrophotometer (Thermo Fisher, USA), with OD260/OD280 ratios of 1.8-2.0 and OD260/230 ratios of 2.0-2.2. Reverse transcription was carried out using HiScript II Reverse Transcriptase (Vazyme, Nanjing, China) from 1 μg of total RNA, to obtain first-strand cDNA. Quantitative real-time PCR (qRT-PCR) was conducted in triplicate on an ABI Prism 700 thermal cycler (Applied Biosystems, Foster City, CA, USA), as previously described (22). GAPDH was used as the reference gene for RNA quantification. The following primer sequences were used: SNRPE (forward primer: ATGTCAGGACTAGGAGCCACTGTG; reverse primer: AGCATGATCCGACCCAGTTGTTTTC), CD274 (forward primer: GACCACCACCACCAATTCCAAGAG; reverse primer: TGAATGTCAGTGCTACACCAAGGC), CD8A (forward primer: GCGAGACAGTGGAGCTGAAGTG; reverse primer: ACGAAGTGGCTGAAGTACATGATGG), and GAPDH (forward primer: AACGGATTTGGTCGTATTGG; reverse primer: TTGATTTTGGAGGGATCTCG).

Estimation of TME cell infiltration

The relative abundance of immune and stromal cells infiltrated in the TME of HGSOC was quantified using the "XCELL" package in accordance with the gene expression profiles. In this study, the abundance of CD8+ T cells and the ESTIMATE score were calculated using the ssGSEA, EPIC, TIMER, QUANTISEQ, MCPCOUNTER, XCELL, CIBERSORT, CIBERSORT-ABS, and ESTIMATE algorithms (23–29).

Identification of ovarian cancer TME-related genes

Consensus clustering was carried out using the "ConsensusClusterPlus" package to identify TME-related subtypes for additional investigation in accordance with the infiltration of immune and stromal cells (30). Using the limma package (31), the differentially expressed genes (DEGs) between various immune subtypes were screened with an adjusted $P < 0.05$. TME-related genes of HGSOC were defined as genes that are co-upregulated or co-downregulated in not fewer than six cohorts.

Construction of the TMErisk score

We used the same procedures as in the previous study to screen out the most valuable TMErisk score (32, 33). First, ovarian cancer TME-related genes in each cohort were subjected to univariate Cox regression analysis. Genes with a stable prognostic value were then further filtered out, with the filter criteria being an adjusted $P < 0.1$ and the same hazard ratio direction for at least five cohorts. Second, a machine learning-based integrative method was developed using ten distinct machine learning algorithms, including Lasso, Ridge, stepwise Cox, CoxBoost, random survival forest (RSF), elastic network (Enet), partial least squares regression for Cox (plsRcox), supervised principal components (SuperPC), generalized boosted regression modeling (GBM), and survival support vector machine (survival-SVM). Then, to fit the most useful prediction models in the TCGA-OV cohort, 108 algorithm combinations from 10 machine learning algorithms were applied to the TME- and prognostic-related genes. Each of these prediction models was further tested in validation cohorts, and the C-index was calculated for each cohort. Finally, the TMErisk signature was built using the CoxBoost and SuperPC algorithms, which had the highest average C-index in the validation cohorts.

Pathway enrichment analysis

The R package "clusterProfiler" was used to conduct analyses of the Gene Ontology (GO), Kyoto Encyclopedia of Genes and Genomes (KEGG), and gene set enrichment analysis (GSEA) (34). With the "GSVA" package, single-sample GSEA (ssGSEA) was also carried out (35).

Prediction of response to immunotherapy or chemotherapy

Different tumor immune evasion mechanisms were modeled using the Tumor Immune Dysfunction and Exclusion (TIDE) algorithm (36). Immunophenoscore (IPS) and Subclass mapping were used to predict anti-PD-1 and anti-CTLA-4 immunotherapy responses between low- and high-TMErisk groups (37). Based on the genomics of drug sensitivity in cancer, the ridge regression model implemented in the "pRRophetic" package was chosen to predict the chemotherapy response of each sample (38). To find potential therapeutic agents, Spearman correlation analysis and differential analysis between various TMErisk groups were conducted.

Statistical analysis

All data processing was carried out using R 4.0.5 software. To compare continuous variables, the Wilcoxon and Kruskal-Wallis tests were used, and the chi-square (χ2) test was used to test categorical data. Correlation coefficients were calculated using Spearman's correlation test. To examine any associated independent predictors of prognosis in HGSOC, the log-rank test, univariate, and multivariable Cox regression models were used. Statistical significance was defined as a two-sided P value < 0.05.

Results

Consensus clustering for TME-infiltrating cells

The TME of HGSOC requires consideration of more than just immune cells due to its significant stromal characteristics. To identify potential tumor-immune-stroma phenotypes of HGSOC, we performed consensus cluster analyses in seven independent cohorts (GSE13876, GSE140082, GSE30161, GSE32062, GSE9891, ICGC, and TCGA-OV) and an integrated meta-cohort based on 48 signatures of non-tumor components in TME, including lymphocytes, myeloid, and stromal cells (Figure 1A, Figure S1). As shown in Figures S1A, B, two clusters could achieve the best clustering efficacy in the meta-cohort, and similar clustering results were obtained in all seven independent cohorts (Figures S1C–I). The result of clustering demonstrated that the distribution of cell signatures was biased between the two clusters. Thus, we defined the cluster with higher infiltration of immune and stromal cells as cluster-H and named the cluster with lower ones as cluster-L (Figure 1A). Principal component analysis (PCA) suggested a significant difference between the two clusters (Figure 1B). Survival analyses indicated that cluster-H was correlated with a notably favorable prognosis in GSE13876 (log-rank test, P = 0.003), GSE32062 (log-rank test, P = 0.011), and the meta-cohort (log-rank
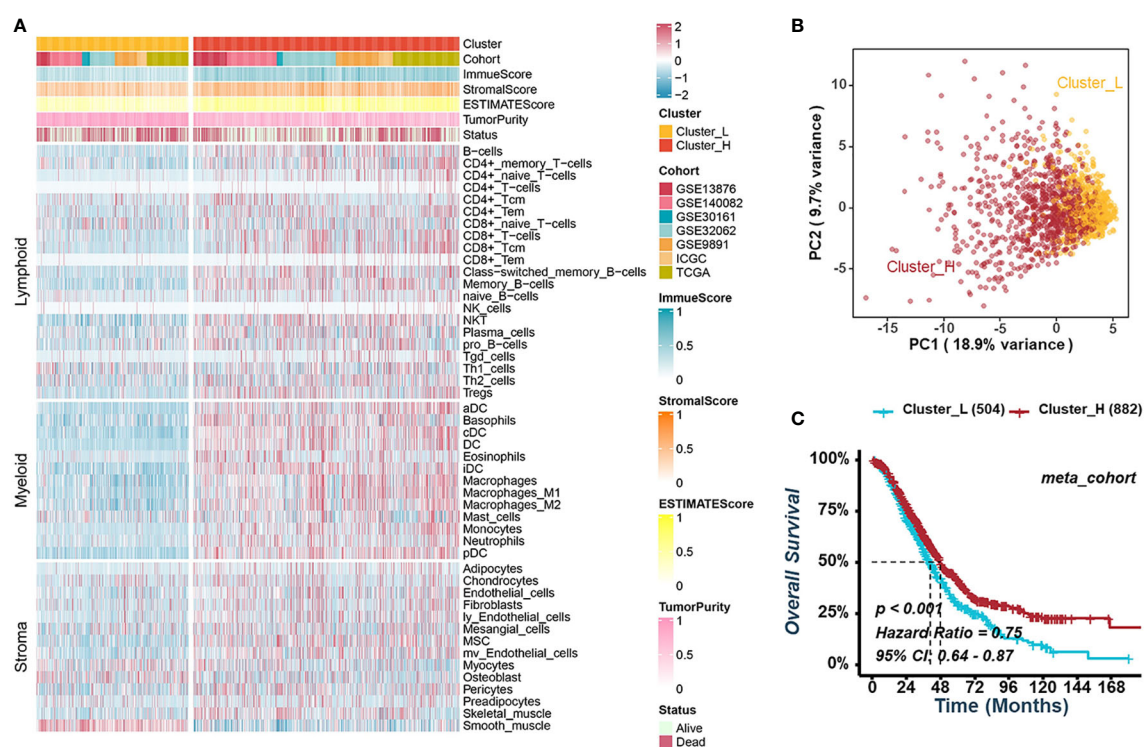

FIGURE 1
Consensus clustering for TME-infiltrating cells in HGSOC. (A) Heatmap illustrating the infiltration of immune and stromal cells between clusters-L and cluster-H in the meta-cohort. (B) Principal component analysis suggesting two distinct clusters in the meta-cohort. (C) Kaplan-Meier analysis estimating the overall survival between cluster-L and cluster-H.

test, $P < 0.001$), while there was no significant correlation in the other cohorts (Figures 1C, S2).

Construction of the TME-related risk score in HGSOC

To mine for TME-related genes specific to HGSOC, we screened out the differentially expressed genes (DEGs) between Cluster-H and Cluster-L with an adjusted $P < 0.05$ in all cohorts. The gene that was upregulated or downregulated in no less than six cohorts was defined as TME-related genes of HGSOC for further integrated analysis. In Cluster-H, there were 390 upregulated genes and 1260 downregulated genes, respectively (Figures S3A, B). Gene Ontology (GO) and Kyoto Encyclopedia of Genes and Genomes (KEGG) pathway enrichment analyses indicated that the upregulated genes in Cluster-H were mainly enriched in immune-related signatures, indicating the reliable results we obtained before (Figures S3C–F). Subsequently, univariate Cox regression analysis was performed on TME-related genes, and 76 genes had stable

prognostic value in different cohorts (Figure S4A). These 76 genes associated with prognosis were included in the procedures based on different combinations of machine learning algorithms to develop a TME-related risk score (TMErisk). As in the previous study by Zaoqu Liu et al. (32), we integrated 10 machine learning algorithms, including CoxBoost, stepwise Cox, Ridge, RSF, GBM, survival-SVM, Lasso, Enet, plsRcox, and SuperPC, to acquire the TMErisk with high accuracy and stability performance in different cohorts. In the TCGA-OV cohort, 108 kinds of prediction models were fitted, and the average C-index of each model in the other seven validation cohorts was further calculated (Figure S4B). Among these prediction models, a combination of CoxBoost and SuperPC algorithms had the highest average C-index in validation cohorts, and the 16 most valuable TME-related genes (APC, CD38, CXCL13, GTF2F2, ING4, PEX3, RAB10, SMNDC1, SNRPE, SOCS5, SOX6, TM2D1, TSPAN13, TWSG1, ZNF780A, and ZNF780B) were identified by the CoxBoost algorithm (Figure 2A, S4B). CD38 and CXCL13 were negatively correlated with the TMErisk score, while the others were positively correlated with the TMErisk score (Figure 2A). Also, we compared the expression of 16 TME-related
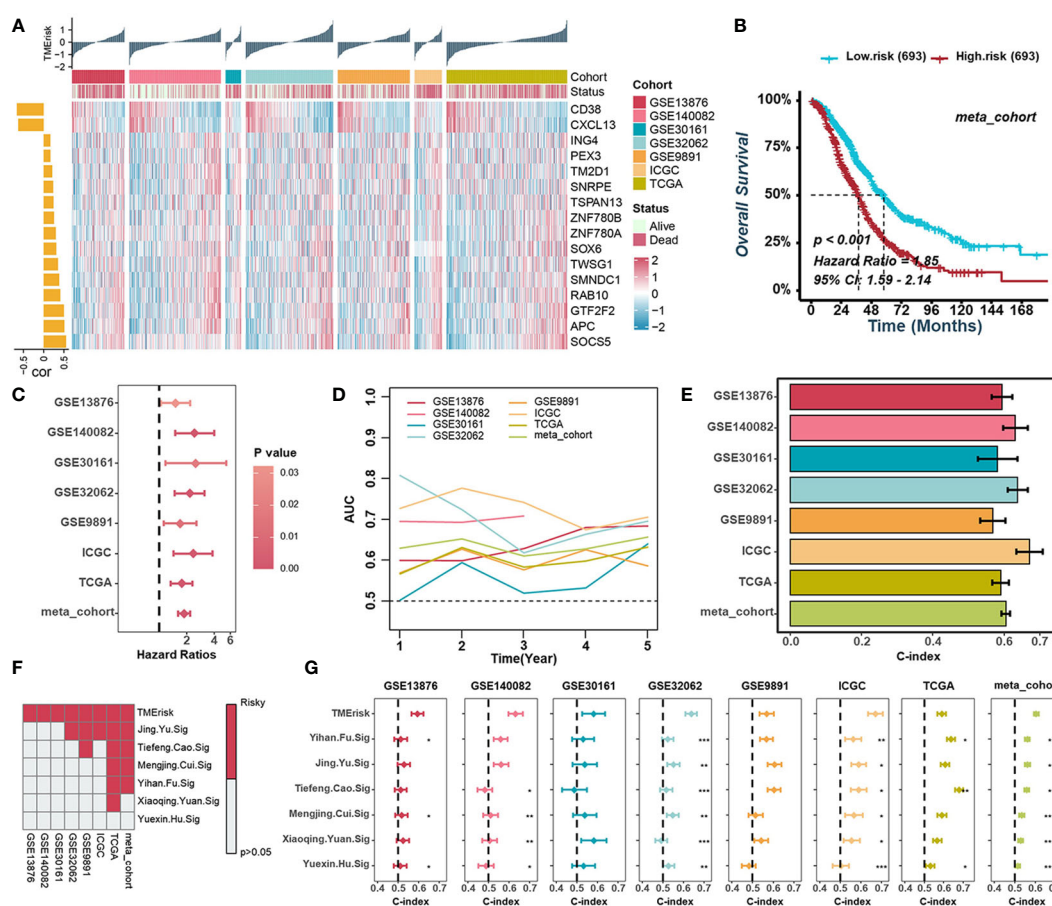
FIGURE 2
Construction of the TMErisk score in HGSOC. **(A)** Heatmap illustrating the expression of 16 TME-related genes and the TMErisk score in low- and high-TMErisk groups. The bar chart on the left illustrates the relationships between TME-related genes and TMErisk score. **(B)** Kaplan-Meier analysis estimating the overall survival between low- and high-TMErisk groups in meta-cohort. **(C)** Univariate Cox regression analyses revealing the correlation between TMErisk score and HGSOC survival. **(D)** Time-dependent AUC value of the TMErisk score in different cohorts. **(E)** C-index of the TMErisk score in different cohorts. **(F)** Univariate Cox regression analysis of the TMErisk score and other published signatures across diverse cohorts. **(G)** C-index of the TMErisk score and other published signatures across diverse cohorts. *$P < 0.05$; **$P < 0.01$; ***$P < 0.001$; ****$P < 0.0001$.

genes between HGSOC (TCGA-C) and normal ovarian tissue (GTEx-N) and noticed that CD38, CXCL13, RAB10, SNRPE, SOX6, TSPAN13, and TWSG were upregulated in HGSOC, while APC, GTF2F2, SOCS5, TM2D1, ZNF780A, and ZNF780B were downregulated in HGSOC (Figure S5A).

Prognostic value of the TMErisk score in HGSOC

It should be considered that TME in HGSOC patients is not only determined by the type of cells infiltrated but also by the molecular characteristics of the tumor and the individual conditions of the patients. Therefore, we examined the scores in different types of patient groups. There was no difference in TMErisk scores between age, grade, or stage subgroups. TMErisk score did, nevertheless, correlate with immune and molecular subtypes (Figure S6A). Specifically, the TMErisk scored highest in the proliferative molecular subtype and lowest in the immunoreactive and IFN-dominant subtypes (Figure S6A). Meanwhile, the cluster-L group had a higher TMErisk score (Figure S6A). According to the median TMErisk score in each cohort, HGSOC patients were divided into high- or low- TMErisk groups. Kaplan–Meier survival analyses exhibited that the patients in the high TMErisk score group had poorer overall survival in all cohorts, and unfavorable progression-free survival in six cohorts (Figures 2B, S7A, B). Univariate and multivariate Cox regression analyses were applied to test the significance of the impact of TMErisk in terms of the overall survival of HGSOC patients. The TMErisk score was an independent prognostic biomarker for evaluating patient survival in various cohorts (Figures 2C, S8A). Meanwhile, the time-dependent area under the curve (AUC) suggests that the TMErisk score is a prognostic biomarker for predicting survival of HGSOC patients in the TCGA and GEO datasets (Figure 2D). All these results suggested that the TMErisk score had stable as well as robust performance in diverse independent cohorts. The C-index of the TMErisk score and other clinical variables in HGSOC patients were calculated, and the TMErisk score presented significantly greater accuracy than other variables (Figures 2E, S8B). To further evaluate the predictive performance of the TMErisk score in HGSOC patients, we compared our TMErisk signature with other published signatures (Table S2). Due to the differences in platforms, the gene expression (mRNA level) signatures that can be detected in the seven cohorts mentioned above were taken into account. A univariate Cox regression analysis and the C-index of each signature were performed. Generally, the predictive performance of the TMErisk signature was much better than that of other signatures (Figures 2F, G).

Genomic status of different TMErisk groups

Somatic mutations caused by genome instability result in an abundance of neoantigens, which were thought to influence TME and contribute to effective immunotherapy. To characterize the genomic states of different TMErisk groups in the TCGA-OV database, the somatic mutation frequency was first analyzed. We identified a negative correlation between the TMErisk score and somatic mutation count, suggesting the low-TMErisk group had more somatic mutations, including synonymous and non-synonymous mutations (Figure 3A). The top 20 genes with the highest mutation rates in the two TMErisk groups were then identified, but there was no significant difference in mutation rates between groups (Figure S9A). Moreover, using Fisher's exact test, distinct mutant genes were identified between the low- and high-TMErisk groups at a $P < 0.05$ significance level (Figure S9B). In the low-TMErisk group, the genes with the highest mutation rates were SETDB1, BRCA1, LRP4, XIRP1, and TOMM70A (Figure S9B). Preliminary evidence suggests that BRCA1/2 mutated tumors tend to contain more neoantigens and greater lymphocyte infiltration compared to non-BRCA1/2 tumors (39, 40). Here, we investigated the association between TMErisk score and BRCA1 mutation and discovered that BRCA1 mutation samples had lower TMErisk scores (Figure 3B). Different tumor types show a variety of copy number variations (CNVs), of which serous HGSOC has a wide and diverse alterations (5, 41). To further understand the relationship between genomic variation and TMErisk score, we analyzed and screened the CNVs in the different TMErisk groups of each group. For example, in the high TMErisk group, the genes on chromosomes 1, 2, and 13 tended to have amplified copy number, whereas on chromosomes 4 and 9, genes were likely to be deletions (Figure 3C). CXC chemokines and receptors are momentous for attracting immune cells from the circulatory system to inflammation or tumor sites (42). According to a recent study, a copy number deletion of chromosome arm 4q was found in an immune-cold type of HGSOC, which tended to be associated with immunosuppression (40). In detail, genes in chromosomal bands 4q13.3 (including CXCL1–3, CXCL5–6, and CXCL8) and 4q21.1 (including CXCL9/10/11, and CXCL13) were widely deleted in the high TMErisk group compared to the low TMErisk group (Figure 3D).

The TMErisk score was associated with immune-related pathways

To describe the biological characteristics of tumors under the TMErisk classification system, GSEA was performed with annotations of the GO and KEGG gene sets. The top 10 enriched pathways according to the normalized enriched score (NES) for each TMErisk group were displayed. ECM receptor interaction, Tgf-ß signaling, Wnt, focal adhesion, and mesenchymal cell proliferation signaling were enriched in the high TMErisk group. While gene sets associated with chemokines, chemokine receptors, antigen processing and presentation, and immunological response were enriched in the low TMErisk group (Figures 4A, B, S10A). When comparing the high- and low-TMErisk groups, GSVA enrichment analysis was also conducted. The low TMErisk group was markedly enriched in immune response-related pathways, and the high TMErisk group was enriched in pathways associated with carcinogenic activation pathways (Figure 4C). Moreover, the TMErisk score was adversely linked with the vast majority of
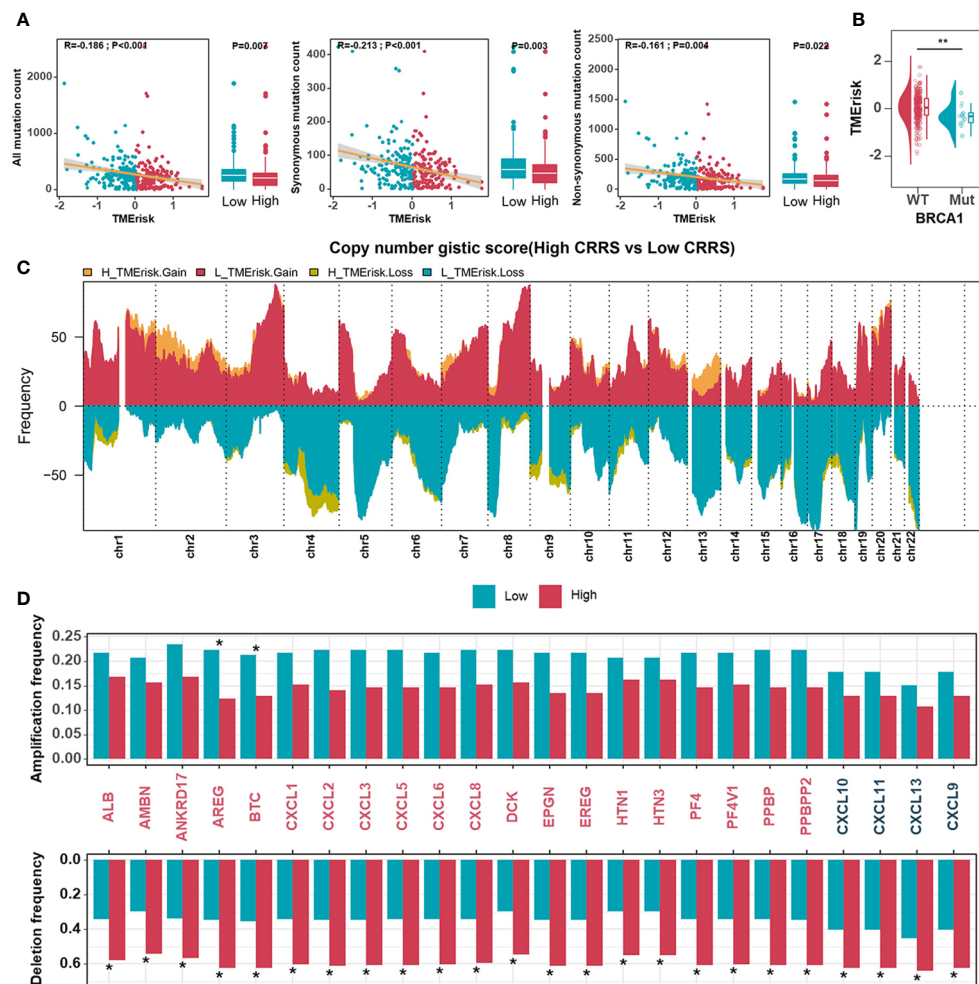
FIGURE 3

Genomic states of different TMErisk groups in HGSOC. **(A)** Boxplots comparing all mutation counts (left), synonymous mutation counts (middle), and non-synonymous mutation counts (right) between low- and high-TMErisk groups, and the correlation between mutation count and the TMErisk score in TCGA-OV cohort. **(B)** Distribution of TMErisk scores in the BRCA1 mutant and wild-type groups. **(C)** Gains and losses in copy numbers in groups with low and high TMErisk. **(D)** Copy number variations at chromosomal bands 4q13.3 and 4q21.1 between low- and high-TMErisk groups. *P < 0.05; **P < 0.01.

immune-related signature scores (Figure 4D). We concluded, based on these findings, that the TMErisk scoring system effectively discriminated between distinct HGSOC tumor microenvironments.

Immune landscapes of different TMErisk groups

To depict the specific characteristics of TMErisk in the immune landscape of HGSOC samples, the differences in the chemokines, interleukins, and interferons between the low- and high-TMErisk groups were first compared. It has been previously shown that the CXCL9/CXCL10-CXCR3 axis is able to dictate the chemoattraction of gamma-delta T-cells, activated Th1 cells, natural killer cells, macrophages, and dendritic cells towards tumors (43, 44). The majority of chemokines/interleukins were expressed at higher levels in the low-TMErisk group compared to the high-TMErisk group, especially CXCL9/10/11 and CXCL13 located on chromosome band

4q21.1 (Figure 5A). Further investigation focusing on the immune components in TME between the two groups revealed that the low-TMErisk group had many signatures representing lymphoid and myeloid cells but few signatures representing stromal cells (Figure 5B). To ensure that the results were not biased by the analytical algorithm, the relationship between the TMErisk score and CD8+ T cells was further verified by multiple algorithms (Figure S11A). In the Cancer Digital Slide Archive (CDSA) database (45), we confirmed that there was more infiltration of immune cells in the tumor nests of low-TMErisk groups but less infiltration of immune cells in the tumor tissue of high-TMErisk groups (Figure 5C). Next, we explored associations between the TMErisk score and immune-related functions (46). The low-TMErisk group was enriched in immune activation signatures (Figure 5D). Meanwhile, the TMErisk score was negatively correlated with the critical steps of cancer–immunity cycle, including the release of cancer cell antigens (Step 1), priming and activation (Step 3), trafficking of immune cells to tumors (Step 4),

infiltration of immune cells into tumors (Step 5), and killing of cancer cells (Step 7) (Figure S11B). In line with the characteristics of infiltrated immune cell and immune signatures, many immune checkpoint genes and HLA family genes were generally upregulated in low TMErisk groups indicating a tumor immune microenvironment with more neoantigens and potential effective immunotherapy (Figure 5E).

Besides, we further evaluated the correlation between 16 immune-related genes and immune cells, immune checkpoint genes, as well as HLA family genes. CD38 and CXCL13 showed mostly positive correlations with lymphoid and myeloid cells, immune checkpoints, and HLA genes, while others, especially SNRPE, exhibited the opposite results (Figures S12A, B). To investigate the roles of CD38, CXCL13, and SNRPE in the TME of HGSOC, we detected relationships between the three genes with the CD8 T effector signature (CD8A, GZMA, GZMB, IFNG, CXCL9, CXCL10, PRF1, and TBX21) and immune checkpoint signature (CD274, PDCD1LG2, CTLA4, PDCD1, LAG3, and HAVCR2) in eight cohorts. The results showed that CD8 T effector signatures and immune checkpoint signatures correlated positively with CD38 and CXCL13 but negatively with SNRPE

(Figures S12C–E). Prior research has demonstrated that CD38 is expressed in activated T, B, and natural killer (NK) cells (47). Meanwhile, CXCL13 is typically expressed in secondary lymphoid organs by follicular dendritic cells, macrophages, and fibroblasts, and the presence of CXCL13-positive T cells has been associated with increased sensitivity to anti-PD-L1 therapy (48, 49). In this study, we sought to confirm the relationship between SNRPE and the CD8 T effector signature and immune checkpoint signature in ovarian cancer tissues. Our qRT-PCR analysis revealed a negative correlation between SNRPE expression and the expression of CD274 and CD8A in ovarian cancer tissues (Figure S12F).

Predictive value of the TMErisk score in immunotherapy and chemotherapy

The TMErisk score was constructed by 16 TME-related genes and associated with infiltration of immune cells, the immune checkpoint signature, and immune-related pathways. Therefore, we assumed that there were differences in immunotherapy effects for HGSOC patients with different TMErisk scores. Firstly, we
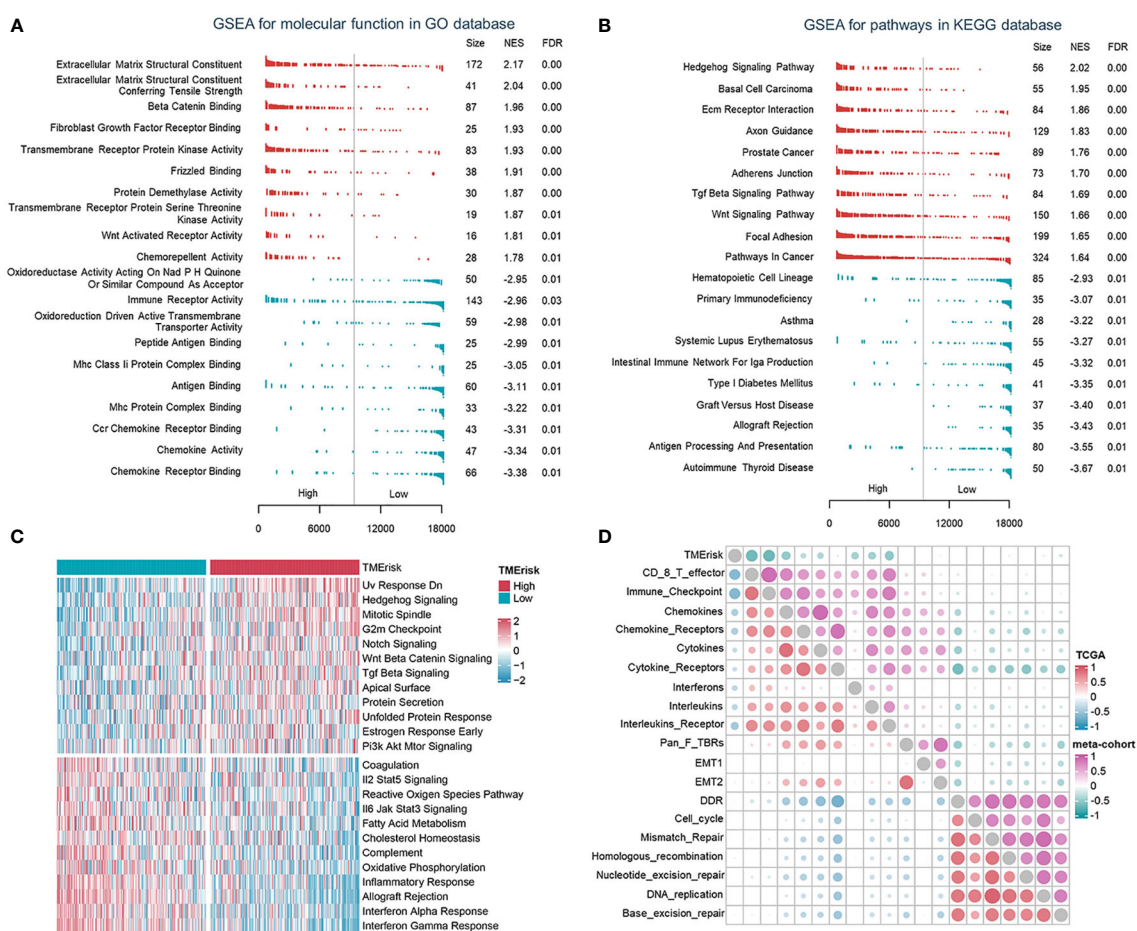

FIGURE 4

The TMErisk score was associated with immune-related pathways in HGSOC. **(A, B)** Analysis of GO molecular function **(A)** and KEGG pathway gene sets **(B)** in the low- and high-TMErisk groups. **(C)** Analysis of hallmark gene sets in the low- and high-TMErisk groups. **(D)** The correlations between TMErisk score and immune-related signatures.

applied the TIDE algorithm to assess the potential clinical efficacy of immunotherapy for TCGA-OV samples. We found that the TMErisk score was negatively correlated with dysfunction (r = -0.304, $P < 0.001$) and positively correlated with TIDE scores and exclusion (TIDE: r = 0.156, $P = 0.003$; exclusion: r = 0.546, $P < 0.001$) (Figure 6A). The IPS was a superior predictor to identify determinants of immunogenicity and characterize the tumor immune landscape. Higher IPS scores usually represented better outcomes with ICB treatment (50, 51). The results showed that the low TMErisk group had higher IPS, PD1-blocker, CTLA-blocker, and CTLA4-PD1-blocker scores (Figure 6B). In addition, we applied a subclass mapping approach to assess the treatment response of immunotherapy specifically targeting CTLA-4 and PD-1 in TCGA and ICGC samples. We discovered that patients with low TMErisk exhibited promising responses to anti-PD-1 therapy, while patients with high TMErisk showed no responses to anti-PD-1 therapy (Figure 6C). In the IMvigor210 cohort, we investigated whether TMErisk could predict patient response to the ICB therapy in an independent immunotherapy cohort. As expected, the patients with a higher TMErisk score were less likely to benefit from immune checkpoint therapy and had a worse prognosis than those with a lower TMErisk score (Figures 6D, E).

To study further the treatment methods for the various TMErisk groups, the pRRophetic software was used to predict the medication response of each sample. We investigated correlations between the TMErisk score and the IC_{50} of drug candidates in the GDSC database. Using Spearman correlation analysis, we discovered that the IC_{50} of eleven candidates was positively correlated with the TMErisk score, while the IC_{50} of eleven other drugs was negatively correlated (Figure 6F). The predicted IC_{50} of these medicines differed significantly across the two TMErisk groups (Figures 6G, S13A). Paclitaxel was considered the first-line drug for HGSOC treatment among these drugs, and patients in the low-TMErisk group may be more sensitive to Paclitaxel (Figure S13A).

Discussion

HGSOC tumors are comprised of multiple populations of various tumor, immune, and stromal cells that are inherently

FIGURE 5

Immune landscape of different TMErisk groups in HGSOC. **(A)** Expression of chemokines, interferons, interleukins, and other cytokines in low- and high-TMErisk groups in TCGA-OV cohort. **(B)** Heatmap showing the infiltration of immune and stromal cells between low- and high-TMErisk groups in TCGA-OV cohort. **(C)** CDSA images of representative HE-stained samples of HGSOC from TCGA in low- and high-TMErisk groups. **(D, E)** Differences in immune-related functions **(D)**, immune checkpoints and HLA gene expression **(E)** between low- and high-TMErisk groups. $^{ns}P > 0.05$; $*P < 0.05$; $**P < 0.01$; $***P < 0.001$

heterogeneous and could develop different phenotypes. Pathbreaking research by Tothill et al. (4) identified six subtypes of HGSOC through optimal clustering of array data. Significantly, patients from the high stromal response subtype (C1) had the poorest survival. C2 and C4 subtypes with more abundant CD3+ cells and lower expression of stromal genes had better survival than C1. They also identified a high-grade serous subtype with a mesenchymal expression pattern, characterized by highly expressed N-cadherin and P-cadherin and low expression of differentiation markers, with relatively reduced OS compared with C2 and C4 subtypes. Similarly, TCGA project delineated four HGSOC transcriptional subtypes, including proliferative, mesenchymal, differentiated, and immunoreactive subtypes, generally suggesting that, in addition to molecular subtypes of tumor cells, heterogeneity in proportion and anatomical location of non-tumor cells also leads to different phenotypes (5). For example, high expression of HOX genes and markers suggestive of increased stromal components characterized the mesenchymal subtype. T-cell chemokine ligands and receptors characterize the immunoreactive subtype. However, some research casts doubt on

these models due to independent validation efforts that failed to identify subtypes or only two or three reproducible subtypes (6, 52). A large proportion of models exhibited lower accuracy in other new datasets than in the validation sets used in their own papers. And the robustness across studies and clinical relevance of these subtypes require improvement to be of value (7). Significant effort is needed to translate these subtypes into clinical practice.

Heterogeneity and diversity of cell composition pose a major challenge to determining the immune landscape and effective immunotherapy in HGSOC. Given the previously reported prognostic significance of intertumoral T cells within HGSOC (12, 53), CD8+ TILs are undoubtedly a key factor in certain histotypes of HGSOC and need to be studied additionally for immunotherapy (13). The immunoreactive subtype from TCGA is so named because these tumors display prominent T cell infiltration (5). Additionally, stromal cells are a significant population of cells that also influence immunological state and subtyping. Cancer-associated fibroblasts (mCAF) in matrix expressing vimentin, SMA, COL3A, COL10, and MMP11 were predominant in HGSOC tumors and were capable of inducing EMT
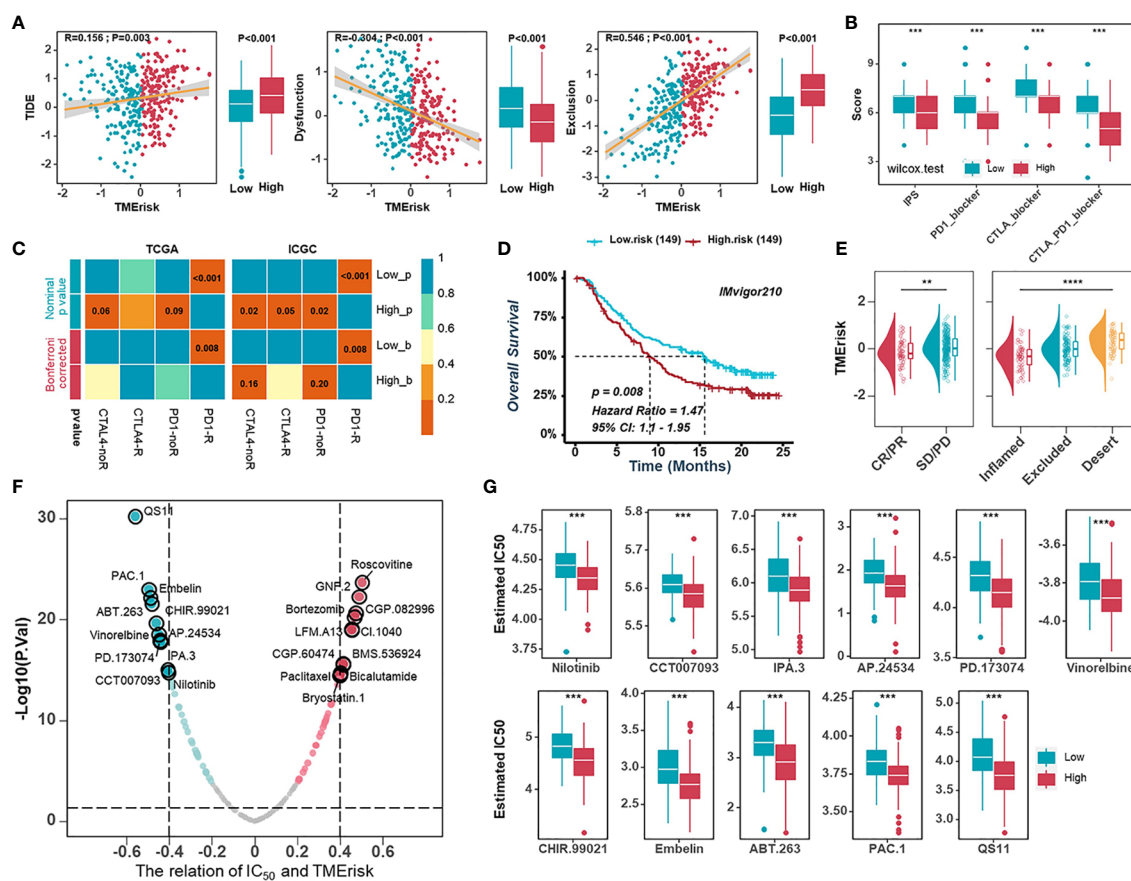
FIGURE 6
Predictive value of the TMErisk score in immunotherapy and chemotherapy. (A) The correlations between the TMErisk score with TIDE score (left), dysfunction score (middle), and exclusion score (right). (B) The correlation between the TMErisk score and IPS predictor. (C) Submap analyses predicting the probability of immunotherapy responses (anti-PD-1 and anti-CTLA-4) in low- and high-TMErisk groups, in TCGA-OV and ICGC cohort, respectively. (D) Kaplan-Meier analysis estimating the overall survival of low- and high-TMErisk groups in IMvigor210 cohort. (E) The distribution of TMErisk scores across groups with different immune response status (left) and immune phenotypes (right). (F) The relation between the IC$_{50}$ of candidate drugs and TMErisk scores. (G) Boxplots showing the estimated higher IC$_{50}$ values of drugs in the low-TMErisk group. **$P < 0.01$; ***$P < 0.001$; ****$P < 0.0001$.

characteristics in HGSOC cells (18). Meanwhile, an elevated stromal response and its relevant gene expression signature are significant prognostic indicators within HGSOC (4). Therefore, it is desirable to consider the immune cells as well as stromal cells in a coordinated way for elucidating the TME of HGSOC.

Out of regard for consistent results across independent cohorts and clinical feasibility, we extensively collect multiple HGSOC datasets. The consensus cluster analyses were performed in seven independent cohorts and an integrated meta-cohort to identify tumor-immune-stroma phenotypes. Explicitly, two clusters could achieve the best clustering efficacy in the meta-cohort, and consistent clustering results were obtained in all independent cohorts. When establishing the TMErisk scoring system, we integrated ten independent machine learning algorithms to acquire the TMErisk with stable performance and high accuracy in different cohorts. 108 combinations of prediction models were fitted out in the TCGA-OV cohort, and the average C-index of each model in the other seven validation cohorts was further calculated. To confirm the robust and stable performance of the TMErisk in multiple independent cohorts, we compared our TMErisk signature with other published signatures. Univariate Cox regression analysis and the C-index of each signature revealed that the predictive performance of the TMErisk signature was much better than that of other signatures.

The close association of somatically mutated genes with specific tumor subtypes or immunological phenotypes led to the discovery of molecules or antibodies specific to these cancer targets (54). To identify possible targets influencing TME and contributing to the efficacy of immunotherapy for patients with different TMErisk scores, we examined the frequency of somatic mutations and copy number variations. Preliminary studies suggested HGSOC patients with BRCA1 mutations demonstrated higher CD8+ TILs, and neoantigen load might explain higher CD8+ TILs (39, 40), which is consistent with patients with low TMErisk scores exhibiting more neoantigens and an increased number of tumor-infiltrating lymphocytes. It has been suggested that copy number variations may contribute more than somatic mutations to the process of tumorigenesis (55). T-cell chemokine ligands CXCL11 and CXCL10, and their receptor CXCR3, characterized the immunoreactive subtype of TCGA, which is consistent with that in the low-TMErisk group in our study. CNV analysis reminded us of the mechanism underlying the abnormal expression of chemokines and relevant receptors and revealed that the 4q21.1 region (including CXCL9/10/11 and CXCL13) was widely deleted in the high TMErisk group compared to the low TMErisk group, probably explaining the prominent T cell infiltration in the low TMErisk group.

To develop a patient-specific treatment based on the phenotyping of HGSOC tumors, we evaluated the effectiveness of the TMErisk score in guiding immunotherapy and chemotherapy. Using TIDE, IPS and subclass mapping to measure the immune response, HGSOC patients with a high TMErisk score were not only less likely to respond to ICB treatment but also more susceptible to immunological escape. In addition, a patient with a low TMErisk score and a positive response to ICBs were observed in anti-PD-1 immunotherapy cohorts. Moreover, we recognize some medications with considerably distinct IC_{50} estimates between two TMErisk groups. Among them, Paclitaxel was regarded as the first-line treatment for HGSOC, and individuals with a low TMErisk were more likely to be sensitive to the medicine.

The current study has several limitations that warrant discussion. Firstly, the results were derived from an online database, and all samples were retrospective, necessitating larger clinical trials, particularly prospective trials, to validate the findings. Secondly, we screened many genes that are associated with the immune microenvironment of ovarian cancer, and further *in vitro* and *in vivo* experiments are necessary to confirm the function of these genes. Furthermore, owing to the lack of immunotherapy information for ovarian cancer, the study only confirmed the association between TMErisk and immunotherapy response through website predictions and the analysis of the IMvigor210 cohort. Therefore, a new ovarian cancer cohort is required for further investigation.

In conclusion, our study not only depicts the diversity of cell components in the TME of HGSOC, but also highlights the contributions of the cross-talk within those components in shaping the biology of the TME, which eventually influences the patients' response to immunotherapies. To address the robustness across studies and clinical relevance of subtyping when designing a prognostic scoring system for HGSOC patients, we have performed a machine learning-based procedure to guide the identification of the TMErisk score, achieving high accuracy and stability performance in different independent cohorts. Significantly, the predictive performance of the TMErisk signature was much better than other published signatures. Finally, our findings assist to identify potential targets and provide novel therapeutic strategies for addressing tumor immunosuppression and enhancing the response to cancer therapy.

Data availability statement

The datasets presented in this study can be found in online repositories. The names of the repository/repositories and accession number(s) can be found within the article/Supplementary Materials.

Author contributions

YL and XF conceived the work and analyzed the data. RT and QW prepared the figures and drafted the manuscript. JL, CO, XH and XF edited and revised the manuscript. All authors contributed to the article and approved the submitted version.

Funding

Acknowledgments

Conflict of interest

The authors declare that the research was conducted in the absence of any commercial or financial relationships that could be construed as a potential conflict of interest.

Publisher's note

All claims expressed in this article are solely those of the authors and do not necessarily represent those of their affiliated organizations, or those of the publisher, the editors and the reviewers. Any product that may be evaluated in this article, or claim that may be made by its manufacturer, is not guaranteed or endorsed by the publisher.

Supplementary material

The Supplementary Material for this article can be found online at: https://www.frontiersin.org/articles/10.3389/fimmu.2023.1164408/full#supplementary-material

References

1. Siegel RL, Miller KD, Fuchs HE, Jemal A. Cancer statistics, 2022. *CA Cancer J Clin* (2022) 72(1):7–33. doi: 10.3322/caac.21708

2. Vaughan S, Coward JI, Bast RCJr., Berchuck A, Berek JS, Brenton JD, et al. Rethinking ovarian cancer: Recommendations for improving outcomes. *Nat Rev Cancer* (2011) 11(10):719–25. doi: 10.1038/nrc3144

3. Seidman JD, Horkayne-Szakaly I, Haiba M, Boice CR, Kurman RJ, Ronnett BM. The histologic type and stage distribution of ovarian carcinomas of surface epithelial origin. *Int J Gynecol Pathol* (2004) 23(1):41–4. doi: 10.1097/01.pgp.0000101080.35393.16

4. Tothill RW, Tinker AV, George J, Brown R, Fox SB, Lade S, et al. Novel molecular subtypes of serous and endometrioid ovarian cancer linked to clinical outcome. *Clin Cancer Res* (2008) 14(16):5198–208. doi: 10.1158/1078-0432.CCR-08-0196

5. Cancer Genome Atlas Research N. Integrated genomic analyses of ovarian carcinoma. *Nature* (2011) 474(7353):609–15. doi: 10.1038/nature10166

6. Chen GM, Kannan L, Geistlinger L, Kofia V, Safikhani Z, Gendoo DMA, et al. Consensus on molecular subtypes of high-grade serous ovarian carcinoma. *Clin Cancer Res* (2018) 24(20):5037–47. doi: 10.1158/1078-0432.CCR-18-0784

7. Waldron L, Haibe-Kains B, Culhane AC, Riester M, Ding J, Wang XV, et al. Comparative meta-analysis of prognostic gene signatures for late-stage ovarian cancer. *J Natl Cancer Inst* (2014) 106(5). doi: 10.1093/jnci/dju049

8. Brahmer J, Reckamp KL, Baas P, Crino L, Eberhardt WE, Poddubskaya E, et al. Nivolumab versus docetaxel in advanced squamous-cell non-Small-Cell lung cancer. *N Engl J Med* (2015) 373(2):123–35. doi: 10.1056/NEJMoa1504627

9. Wolchok JD, Chiarion-Sileni V, Gonzalez R, Rutkowski P, Grob JJ, Cowey CL, et al. Overall survival with combined nivolumab and ipilimumab in advanced melanoma. *N Engl J Med* (2017) 377(14):1345–56. doi: 10.1056/NEJMoa1709684

10. Matulonis UA, Shapira-Frommer R, Santin AD, Lisyanskaya AS, Pignata S, Vergote I, et al. Antitumor activity and safety of pembrolizumab in patients with advanced recurrent ovarian cancer: Results from the phase ii keynote-100 study. *Ann Oncol* (2019) 30(7):1080–7. doi: 10.1093/annonc/mdz135

11. Hamanishi J, Mandai M, Konishi I. Immune checkpoint inhibition in ovarian cancer. *Int Immunol* (2016) 28(7):339–48. doi: 10.1093/intimm/dxw020

12. Zhang L, Conejo-Garcia JR, Katsaros D, Gimotty PA, Massobrio M, Regnani G, et al. Intratumoral T cells, recurrence, and survival in epithelial ovarian cancer. *N Engl J Med* (2003) 348(3):203–13. doi: 10.1056/NEJMoa020177

13. Ovarian Tumor Tissue Analysis C, Goode EL, Block MS, Kalli KR, Vierkant RA, Chen W, et al. Dose-response association of Cd8+ tumor-infiltrating lymphocytes and survival time in high-grade serous ovarian cancer. *JAMA Oncol* (2017) 3(12):e173290. doi: 10.1001/jamaoncol.2017.3290

14. Tanaka Y, Kobayashi H, Suzuki M, Hirashima Y, Kanayama N, Terao T. Genetic downregulation of pregnancy-associated plasma protein-a (Papp-a) by bikunin reduces igf-I-Dependent akt and Erk1/2 activation and subsequently reduces ovarian cancer cell growth, invasion and metastasis. *Int J Cancer* (2004) 109(3):336–47. doi: 10.1002/ijc.11700

15. Boldt HB, Conover CA. Overexpression of pregnancy-associated plasma protein-a in ovarian cancer cells promotes tumor growth in vivo. *Endocrinology* (2011) 152(4):1470–8. doi: 10.1210/en.2010-1095

16. Hornburg M, Desbois M, Lu S, Guan Y, Lo AA, Kaufman S, et al. Single-cell dissection of cellular components and interactions shaping the tumor immune phenotypes in ovarian cancer. *Cancer Cell* (2021) 39(7):928–44 e6. doi: 10.1016/j.ccell.2021.04.004

17. Olbrecht S, Busschaert P, Qian J, Vanderstichele A, Loverix L, Van Gorp T, et al. High-grade serous tubo-ovarian cancer refined with single-cell rna sequencing: Specific cell subtypes influence survival and determine molecular subtype classification. *Genome Med* (2021) 13(1):111. doi: 10.1186/s13073-021-00922-x

18. Xu J, Fang Y, Chen K, Li S, Tang S, Ren Y, et al. Single-cell rna sequencing reveals the tissue architecture in human high-grade serous ovarian cancer. *Clin Cancer Res* (2022) 28(16):3590–602. doi: 10.1158/1078-0432.CCR-22-0296

19. Li Y, Tian R, Liu J, Li J, Tan H, Wu Q, et al. Deciphering the immune landscape dominated by cancer-associated fibroblasts to investigate their potential in indicating prognosis and guiding therapeutic regimens in high grade serous ovarian carcinoma. *Front Immunol* (2022) 13:940801. doi: 10.3389/fimmu.2022.940801

20. Liu J, Wang Y, Yuan S, Wei J, Bai J. Construction of an immune cell infiltration score to evaluate the prognosis and therapeutic efficacy of ovarian cancer patients. *Front Immunol* (2021) 12:751594. doi: 10.3389/fimmu.2021.751594

21. Li Y, Gan Y, Liu J, Li J, Zhou Z, Tian R, et al. Downregulation of Meis1 mediated by Elfn1-As1/Ezh2/Dnmt3a axis promotes tumorigenesis and oxaliplatin resistance in colorectal cancer. *Signal Transduct Target Ther* (2022) 7(1):87. doi: 10.1038/s41392-022-00902-6

22. Li Y, Liu J, Xiao Q, Tian R, Zhou Z, Gan Y, et al. En2 as an oncogene promotes tumor progression *Via* regulating Ccl20 in colorectal cancer. *Cell Death Dis* (2020) 11(7):604. doi: 10.1038/s41419-020-02804-3

23. Charoentong P, Finotello F, Angelova M, Mayer C, Efremova M, Rieder D, et al. Pan-cancer immunogenomic analyses reveal genotype-immunophenotype relationships and predictors of response to checkpoint blockade. *Cell Rep* (2017) 18(1):248–62. doi: 10.1016/j.celrep.2016.12.019

24. Zeng D, Ye Z, Shen R, Yu G, Wu J, Xiong Y, et al. Iobr: Multi-omics immuno-oncology biological research to decode tumor microenvironment and signatures. *Front Immunol* (2021) 12:687975. doi: 10.3389/fimmu.2021.687975

25. Newman AM, Liu CL, Green MR, Gentles AJ, Feng W, Xu Y, et al. Robust enumeration of cell subsets from tissue expression profiles. *Nat Methods* (2015) 12(5):453–7. doi: 10.1038/nmeth.3337

26. Racle J, Gfeller D. Epic: A tool to estimate the proportions of different cell types from bulk gene expression data. *Methods Mol Biol* (2020) 2120:233–48. doi: 10.1007/978-1-0716-0327-7_17

27. Finotello F, Mayer C, Plattner C, Laschober G, Rieder D, Hackl H, et al. Molecular and pharmacological modulators of the tumor immune contexture revealed by deconvolution of rna-seq data. *Genome Med* (2019) 11(1):34. doi: 10.1186/s13073-019-0638-6

28. Aran D, Hu Z, Butte AJ. Xcell: Digitally portraying the tissue cellular heterogeneity landscape. *Genome Biol* (2017) 18(1):220. doi: 10.1186/s13059-017-1349-1

29. Becht E, Giraldo NA, Lacroix L, Buttard B, Elarouci N, Petitprez F, et al. Estimating the population abundance of tissue-infiltrating immune and stromal cell populations using gene expression. *Genome Biol* (2016) 17(1):218. doi: 10.1186/s13059-016-1070-5

30. Wilkerson MD, Hayes DN. Consensusclusterplus: A class discovery tool with confidence assessments and item tracking. *Bioinformatics* (2010) 26(12):1572–3. doi: 10.1093/bioinformatics/btq170

31. Yu Z, Lan J, Li W, Jin L, Qi F, Yu C, et al. Circular rna Hsa_Circ_0002360 promotes proliferation and invasion and inhibits oxidative stress in gastric cancer by sponging mir-629-3p and regulating the Pdlim4 expression. *Oxid Med Cell Longev* (2022) 2022:2775433. doi: 10.1155/2022/2775433

32. Liu Z, Liu L, Weng S, Guo C, Dang Q, Xu H, et al. Machine learning-based integration develops an immune-derived lncrna signature for improving outcomes in colorectal cancer. *Nat Commun* (2022) 13(1):816. doi: 10.1038/s41467-022-28421-6

33. Liu Z, Guo C, Dang Q, Wang L, Liu L, Weng S, et al. Integrative analysis from multi-center studies identifies a consensus machine learning-derived lncrna signature for stage Ii/Iii colorectal cancer. *EBioMedicine* (2022) 75:103750. doi: 10.1016/j.ebiom.2021.103750

34. Wu T, Hu E, Xu S, Chen M, Guo P, Dai Z, et al. Clusterprofiler 4.0: A universal enrichment tool for interpreting omics data. *Innovation (Camb)* (2021) 2(3):100141. doi: 10.1016/j.xinn.2021.100141

35. Hanzelmann S, Castelo R, Guinney J. Gsva: Gene set variation analysis for microarray and rna-seq data. *BMC Bioinf* (2013) 14:7. doi: 10.1186/1471-2105-14-7

36. Jiang P, Gu S, Pan D, Fu J, Sahu A, Hu X, et al. Signatures of T cell dysfunction and exclusion predict cancer immunotherapy response. *Nat Med* (2018) 24(10):1550–8. doi: 10.1038/s41591-018-0136-1

37. Hoshida Y, Brunet JP, Tamayo P, Golub TR, Mesirov JP. Subclass mapping: Identifying common subtypes in independent disease data sets. *PloS One* (2007) 2(11): e1195. doi: 10.1371/journal.pone.0001195

38. Lu X, Jiang L, Zhang L, Zhu Y, Hu W, Wang J, et al. Immune signature-based subtypes of cervical squamous cell carcinoma tightly associated with human papillomavirus type 16 expression, molecular features, and clinical outcome. *Neoplasia* (2019) 21(6):591–601. doi: 10.1016/j.neo.2019.04.003

39. Launonen IM, Lyytikainen N, Casado J, Anttila EA, Szabo A, Haltia UM, et al. Single-cell tumor-immune microenvironment of Brca1/2 mutated high-grade serous ovarian cancer. *Nat Commun* (2022) 13(1):835. doi: 10.1038/s41467-022-28389-3

40. Sun J, Yan C, Xu D, Zhang Z, Li K, Li X, et al. Immuno-genomic characterisation of high-grade serous ovarian cancer reveals immune evasion mechanisms and identifies an immunological subtype with a favourable prognosis and improved therapeutic efficacy. *Br J Cancer* (2022) 126(11):1570–80. doi: 10.1038/s41416-021-01692-4

41. Graf RP, Eskander R, Brueggeman L, Stupack DG. Association of copy number variation signature and survival in patients with serous ovarian cancer. *JAMA Netw Open* (2021) 4(6):e2114162. doi: 10.1001/jamanetworkopen.2021.14162

42. Huang X, Hao J, Tan YQ, Zhu T, Pandey V, Lobie PE. Cxc chemokine signaling in progression of epithelial ovarian cancer: Theranostic perspectives. *Int J Mol Sci* (2022) 23(5). doi: 10.3390/ijms23052642

43. Rainczuk A, Rao J, Gathercole J, Stephens AN. The emerging role of cxc chemokines in epithelial ovarian cancer. *Reproduction* (2012) 144(3):303–17. doi: 10.1530/REP-12-0153

44. Strieter RM, Burdick MD, Mestas J, Gomperts B, Keane MP, Belperio JA. Cancer cxc chemokine networks and tumour angiogenesis. *Eur J Cancer* (2006) 42(6):768–78. doi: 10.1016/j.ejca.2006.01.006

45. Gutman DA, Cobb J, Somanna D, Park Y, Wang F, Kurc T, et al. Cancer digital slide archive: An informatics resource to support integrated in silico analysis of tcga pathology data. *J Am Med Inform Assoc* (2013) 20(6):1091–8. doi: 10.1136/amiajnl-2012-001469

46. Zheng S, Liang JY, Tang Y, Xie J, Zou Y, Yang A, et al. Dissecting the role of cancer-associated fibroblast-derived biglycan as a potential therapeutic target in immunotherapy resistance: A tumor bulk and single-cell transcriptomic study. *Clin Transl Med* (2023) 13(2):e1189. doi: 10.1002/ctm2.1189

47. Frasca L, Fedele G, Deaglio S, Capuano C, Palazzo R, Vaisitti T, et al. Cd38 orchestrates migration, survival, and Th1 immune response of human mature dendritic cells. *Blood* (2006) 107(6):2392–9. doi: 10.1182/blood-2005-07-2913

48. Beider K, Voevoda-Dimenshtein V, Zoabi A, Rosenberg E, Magen H, Ostrovsky O, et al. Cxcl13 chemokine is a novel player in multiple myeloma osteolytic microenvironment, M2 macrophage polarization, and tumor progression. *J Hematol Oncol* (2022) 15(1):144. doi: 10.1186/s13045-022-01366-5

49. Zou Y, Ye F, Kong Y, Hu X, Deng X, Xie J, et al. The single-cell landscape of intratumoral heterogeneity and the immunosuppressive microenvironment in liver and brain metastases of breast cancer. *Adv Sci (Weinh)* (2023) 10(5):e2203699. doi: 10.1002/advs.202203699

50. Huang X, Zhao L, Jin Y, Wang Z, Li T, Xu H, et al. Up-regulated misp is associated with poor prognosis and immune infiltration in pancreatic ductal adenocarcinoma. *Front Oncol* (2022) 12:827051. doi: 10.3389/fonc.2022.827051

51. Yang Z, Yan G, Zheng L, Gu W, Liu F, Chen W, et al. Ykt6, as a potential predictor of prognosis and immunotherapy response for oral squamous cell carcinoma, is related to cell invasion, metastasis, and Cd8+ T cell infiltration. *Oncoimmunology* (2021) 10(1):1938890. doi: 10.1080/2162402X.2021.1938890

52. Way GP, Rudd J, Wang C, Hamidi H, Fridley BL, Konecny GE, et al. Comprehensive cross-population analysis of high-grade serous ovarian cancer supports no more than three subtypes. *G3 (Bethesda)* (2016) 6(12):4097–103. doi: 10.1534/g3.116.033514

53. Verhaak RG, Tamayo P, Yang JY, Hubbard D, Zhang H, Creighton CJ, et al. Prognostically relevant gene signatures of high-grade serous ovarian carcinoma. *J Clin Invest* (2013) 123(1):517–25. doi: 10.1172/JCI65833

54. Hahn WC, Bader JS, Braun TP, Califano A, Clemons PA, Druker BJ, et al. An expanded universe of cancer targets. *Cell* (2021) 184(5):1142–55. doi: 10.1016/j.cell.2021.02.020

55. Alexandrov LB, Nik-Zainal S, Wedge DC, Aparicio SA, Behjati S, Biankin AV, et al. Signatures of mutational processes in human cancer. *Nature* (2013) 500 (7463):415–21. doi: 10.1038/nature12477

Check for updates

Comparative analysis between high-grade serous ovarian cancer and healthy ovarian tissues using single-cell RNA sequencing

Xiao Zhang[1†], Shihao Hong[1†], Chengying Yu[2], Xiaozhong Shen[3], Fangying Sun[1] and Jianhua Yang[1*]

[1]Department of Obstetrics and Gynecology, Sir Run Run Shaw Hospital, School of Medicine, Zhejiang University, Key Laboratory of Reproductive Dysfunction Management of Zhejiang Province, Hangzhou, China, [2]Department of Obstetrics and Gynecology, Longyou People's Hospital, Quzhou, China, [3]Medical School, Nantong University, Nantong, China

Introduction: High-grade serous ovarian cancer (HGSOC) is the most common histological subtype of ovarian cancer, and is associated with high mortality rates.

Methods: In this study, we analyzed specific cell subpopulations and compared different gene functions between healthy ovarian and ovarian cancer cells using single-cell RNA sequencing (ScRNA-seq). We delved deeper into the differences between healthy ovarian and ovarian cancer cells at different levels, and performed specific analysis on endothelial cells.

Results: We obtained scRNA-seq data of 6867 and 17056 cells from healthy ovarian samples and ovarian cancer samples, respectively. The transcriptional profiles of the groups differed at various stages of ovarian cell development. A detailed comparison of the cell cycle, and cell communication of different groups, revealed significant differences between healthy ovarian and ovarian cancer cells. We also found that apoptosis-related genes, URI1, PAK2, PARP1, CLU and TIMP3, were highly expressed, while immune-related genes, UBB, RPL11, CAV1, NUPR1 and Hsp90ab1, were lowly expressed in ovarian cancer cells. The results of the ScRNA-seq were verified using qPCR.

Discussion: Our findings revealed differences in function, gene expression and cell interaction patterns between ovarian cancer and healthy ovarian cell populations. These findings provide key insights on further research into the treatment of ovarian cancer.

Introduction

Ovarian cancer is one of the most common gynecologic malignancies in the world, with dismal prognosis (1). High-grade serous ovarian cancer (HGSOC) is the most aggressive type of ovarian cancer (2). High-grade ovarian serous cancer is associated with poor survival rates compared with early-stage and high-grade cancers, with the 5-year survival rate being only 27% (3). Advanced high-grade serous ovarian cancers tend to invade adjacent organs, metastasizing to the peritoneum and lymph nodes (4). So far, studies of high-grade serous ovarian cancer and the discovery of long-term effective treatment strategies for this disease are limited. Therefore, there is need for in depth research into the regulation mechanisms of genes associated with progression of high-grade ovarian cancer. Data from high throughput sequencing technologies indicate that many human genes are transcribed into RNAs, but only a small part of RNAs is finally translated into proteins (5, 6). Genome information flows through various molecular layers, including epigenome, transcriptome, proteome, and metabolome, to produce characteristic traits (7). As a result, we have gained a deeper understanding of the molecular complexity of ovarian cancer, especially the complexity of the genome. RNA-seq is a technique used to analyze RNA expression in whole tissues. However, this approach does not highlight contributions from different cell types (8). Single-cell RNA sequencing (scRNA-Seq) technologies provide essential opportunities to study cellular heterogeneity on the gene level (9).

Single-cell sequencing technology involves separation of groups of cells within tissues and body fluid into single cells, and analyzing their genetic materials using high-throughput sequencing techniques to reveal cellular heterogeneity among different tissues and cell types (10, 11). Each single cell found within high-grade serous ovarian cancer has unique microenvironment, transcriptomic and epigenomic characteristics (12). Although cells contain the same genes, differences in mechanisms of transcriptional modulation drives stochastic gene expression. RNA sequencing (RNA-seq) is a bulk sequencing technique that analyzes the molecular complexity of tumor environment based on the average expression level of different cells, and cannot reveal the internal differences between different cell subsets (13). Single-cell sequencing differs from conventional tissue sequencing because it involves genome or transcriptome sequencing of nucleic acid (DNA or RNA) in a single cell, which is useful for identifying new markers, rare subpopulations and evolutionary patterns (14). ScRNA-seq can be used to determine the effect of gene expression on genetic structure diversity (15), individual cell level and interaction with host immune system in tumors (16). The analysis of single cell transcriptome RNA in a single tumor sample is especially important for understanding the cells in the cancer microenvironment. ScRNA-seq has become an indispensable part of the scientific research process. It can dissect tumor tissues into various cell types or cell shapes, and characterize tumor tissues (17). Clinically, it provides new insights into pharmacological mechanisms and provides new targets for tumor treatment.

In this study, we aimed to identify the potential key genes and pathways associated with HGSOC progression using single-cell transcriptome-specific analysis. We first determined the specific proportions of cell populations and special subpopulation of endothelial cells utilizing the data in the GEO public database. Next, we systematically analyzed signaling pathways involved in cellular function in HGSOC. Meanwhile, we characterized different cell interaction patterns in HGSOC and normal ovarian tissues through Cellchat analysis. We further identified differentially expressed genes *via* Gene ontology (GO) analyses, then we verified the reliability of the ten most differential expression of mRNAs by quantitative real-time PCR (qPCR) in clinical samples of HGSOC and in normal tissues. This research could help to understand tumor heterogeneity at the transcriptome level and the mechanisms of ovarian cancer metastasis and refractory to treatment may have major implications for therapeutic development and patient survival.

Materials and methods

Data sources and collection of human samples

We collected tumor and normal samples from ovarian cancer patients at Zhejiang University Sir Run Run Shaw Hospital, all detailed information of patients are listed in Supplementary Table 1. We downloaded two datasets, GSE147082 (18), and GSE118127 (19), which consisted of scRNA-seq data from Gene Expression Omnibus (GEO; https://www.ncbi.nlm.nih.gov/geo/) database.

Data integration and analysis

The basic analysis steps of single-cell transcriptome were based on the R package Seurat (https://satijalab.org/seurat/, v.3.2.0) (20, 21). We read in the relevant single cell transcriptome matrix through the Read10X function, and set the following quality control standards: $1000<nFeature\_RNA<6000$, percent.mt<10. We normalized the data by LogNormalize method to eliminate the influence of library size (scale.factor = 10000), and identified 2000 hypervariable genes in each sample by "vst" method. We removed batch effects and integrated data using the standard procedures of Seurat v3 (22). We identified the anchors of the data through FindIntegrationAnchors, and integrated the datasets through the IntegrateData function. Then we scaled the data through ScaleData and performd principal component dimensionality reduction on the data through RunPCA (npcs=30). After that, We constructed k-NN graph through FindNeighbors (k.param = 20, reduction = "pca", dims = 1:30) and performed t-Distributed Stochastic Neighbor Embedding (t-SNE) visualization dimensionality reduction on the data (dims = 1:30). Choosing the resolution as 0.25, we clustered cells by the FindClusters function. Through the FindAllMarkers function, we identified specifically expressed genes in each cell population to assist us in cell type definition (logfc.threshold = 0.1, test.use = "wilcox"), and displayed the top5 highly expressed genes through DoHeatmap. We annotated the cells through the annotation information in literature and known markers. GO enrichment analysis of the differentially expressed genes was implemented using the clusterProfiler (3.12.0) package in R, and

analyzed through the enrichGO function (p valueCutoff =0.05, pAdjustMethod = "BH",qvalueCutoff = 0.2) (23). Cellchat analysis was mainly based on the R package CellChat (version 1.1.3) (24). We used the normal and tumor samples as input sets to construct objects through the CreateCellChat function, and imported the Secreted Signaling database of human ligand receptors in CellChat for analysis. Then, we identified significantly expressed genes by identifyOverExpressedGenes (thresh.fc = 0, thresh. p= 0.05) and identifyOverExpressedInteractions to identify significant interactions.

Real-time quantitative PCR (qRT-PCR)

Total RNA from tumor samples and normal samples were extracted using RNA Quick Purification Kit (ES Science, Shanghai, China). Complementary DNA (cDNA) synthesis was then carried out using 1 μg of total RNA using the cDNA Reverse Transcription kit (Vazyme, Nanjing, China). QRT-PCR was performed using TB Green™ Premix Ex Taq™ II (RR420A; Takara, China) on a Bio-Rad CFX-96 Real-time PCR system (Bio-Rad, USA), QRT-PCR was run at the following condition: 95℃, 3min; (95℃, 15s; 60℃, 30s;72℃, 30s)×40 cycles, according to the manufacturer's instructions. All PCR primers for genes are listed in Supplementary Table 2 and were synthesized by Tsingke Biological Technology (Tsingke, Beijing, China). Relative abundance of mRNA expression was calculated using the $2^{-\Delta\Delta Ct}$ method, and normalized to GAPDH mRNA expression levels.

Results

Single-cell transcriptional profiling of ovarian samples and cell-type identification

After integrating the data from healthy ovarian and ovarian cancer samples, the cells clustered into 11 groups, including 6867 tumor cells and 17056 healthy cells (Figure 1A, Supplementary Figure 1). Dot plots were used to display the marker genes of different clusters, and the characteristics of these genes were used to annotate the cell types (Figure 1B). Then, we used the CopyKAT (v1.0.8) to identify the benign and malignant cells in the tumor dataset, in which there were 1492 aneuploid cells (tumor cells) and 4983 cells were defined as diploid cells (normal cells) (Figure 1C, Supplementary Figure 2). In addition, by calculating the proportions of various cell types, in the ovarian cancer samples, we found a significant decrease in the ratio of Stroma cell–1 and a significant increase in the ratio of Granulosa−1 and fibroblasts (Figures 1D, E).

Differential gene and cell cycle analysis revealed significant functional changes

We carried out differential gene expression analysis between ovarian cancer and healthy ovarian tissues for each cell population, and found that C1orf60, TRABD2A, CAND2 and other genes were

significantly up-regulated genes in multiple clusters (Figure 2A). Enrichment analysis of up-regulated and down-regulated genes in ovarian cancer, revealed that up-regulated genes were closely related to apoptosis signaling, inflammatory response, and methylation, while down-regulated genes were closely related to immune system and cell homeostasis (Figures 2B, C). Finally, we calculated the proportion of cells in different stages of the cell cycle for each population of ovarian cancer and healthy ovarian cells, and found significant differences among different cell populations. For example, a high proportion of cells in the G2M phase were Granulosa−2 cells (Figure 2D).

Cellchat analysis of ovarian cancer and healthy ovarian tissues revealed different cell interaction patterns

We found significant differences in the communication patterns of different cell groups between healthy ovarian and ovarian cancer tissues using CellChat (Figure 3A). Several ovarian cancer cell types generated more signals than healthy ovarian cells, with the cancer cells generating significant levels of PARs and VEGF signals. We found that PARs signaling in ovarian cancer was predominantly generated by Immune-2 and received by various other cell populations (Figure 3B). Moreover, VEGF signals were mainly produced by EC-1 and Granulosa cells in ovarian cancer tissues, and EC-2 received the signal, suggesting that the production of EC-2 was closely related to the secretion of VEGF by these two groups of cells (Figure 3C).

Ovarian cancers induced important changes in endothelial cells

To further explore the difference in endothelial cells between healthy ovarian and ovarian cancer tissues, we performed differential analysis based on two populations of cells, EC-1 and EC-2. A comparison of endothelial cells between healthy ovarian and ovarian cancer tissues revealed that genes such as RACK1, S100A6, and C1orf186 were significantly upregulated, while GMB2L1, TM4SF1, and EIF1 were significantly downregulated in the ovarian cancer samples (Figure 4A). GO enrichment analysis on differentially expressed genes showed that the genes were enriched in important pathways related to endothelial cell differentiation, migration, and differentiation (Figure 4B). The expression of these genes differed significantly in healthy ovarian and ovarian cancer EC-1 cells, and ovarian cancer-specific EC-2 cells. For example, genes such as VEGFA and EZR were significantly expressed in EC-1-Cancer cells, but genes such as PDE4D and AFDN were not expressed (Figure 4C).

The expression of apoptosis- and immune-related genes was altered in ovarian cancer tissues

Based on the results of GO analysis, we further explored the genes related to apoptosis and immunity. We found that apoptosis-related
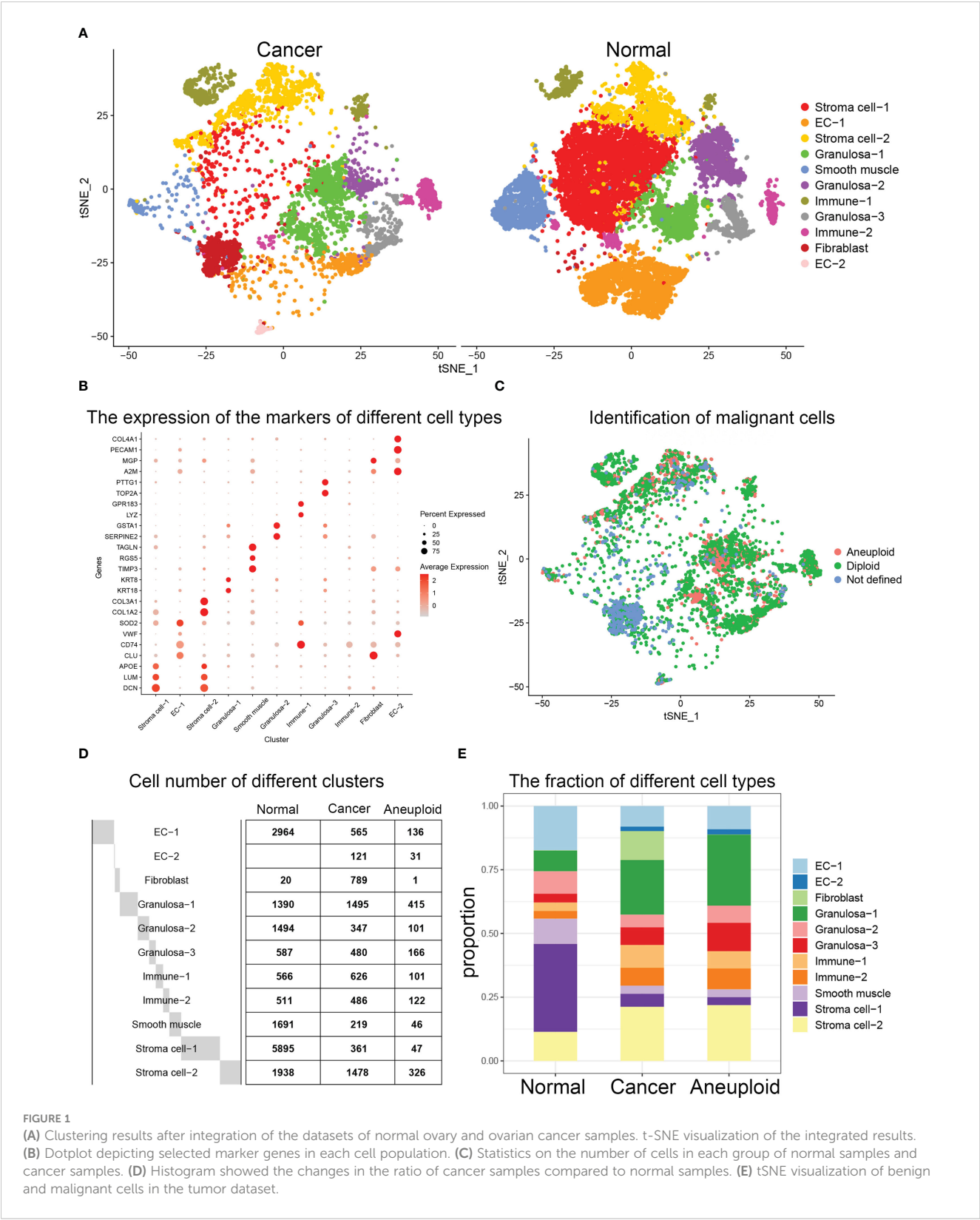
FIGURE 1
(A) Clustering results after integration of the datasets of normal ovary and ovarian cancer samples. t-SNE visualization of the integrated results.
(B) Dotplot depicting selected marker genes in each cell population. **(C)** Statistics on the number of cells in each group of normal samples and cancer samples. **(D)** Histogram showed the changes in the ratio of cancer samples compared to normal samples. **(E)** tSNE visualization of benign and malignant cells in the tumor dataset.

genes URI1, PAK2, PARP1, CLU, and TIMP3 were significantly upregulated in multiple cell populations of cancer cells (Figure 5A). However, the immune-related genes UBB, RPL11, CAV1, NUPR1, and Hsp90ab1 were downregulated in multiple cell populations

(Figure 5B). RT-qPCR analysis revealed that URI1, PAK2, PARP1, CLU, and TIMP3 were significantly upregulated, while UBB, RPL11, CAV1, NUPR1, and Hsp90ab1 were significantly downregulated in the ovarian cancer samples (Figure 5C).
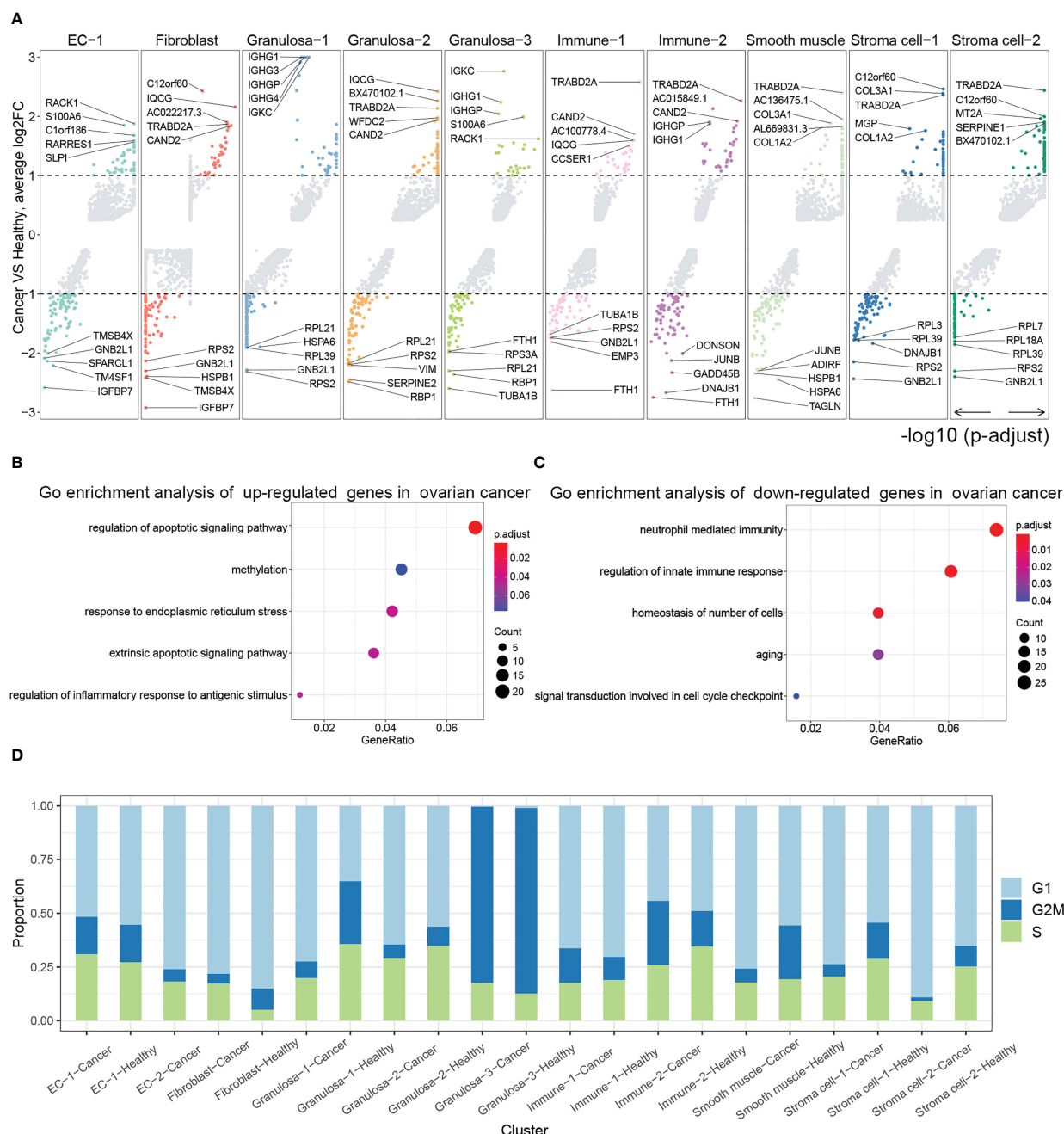
FIGURE 2

(A) Differential analysis between ovarian cancer samples and normal samples. Analysis of the differential genes of each group in ovarian cancer samples compared with normal samples and display of the most significantly up-regulated and down-regulated genes through volcano plots (adjust p value <0.05 and |logFC| ≥1 were set as the cut-off criteria). Go enrichment analysis of **(B)** up-regulated genes and **(C)** down- regulated genes in cancer ovary. **(D)** Histogram showing the proportion of cell cycles for each cell population in normal ovary and ovarian cancer.

Discussion

The application of ScRNA-seq technology in ovarian cancer research is expected to significantly expand our understanding of the disease. ScRNA-seq in ovarian cancer has led to the identification of different cell types, characterization of tumor heterogeneity, identification of more promising immunotherapeutic targets, and enhancement of our understanding of therapy-induced resistance (25–27). The technology can also be used to identify ovarian cancer

stem cells that are important in studying changes in immune pathway-related genes during immunotherapy, to study differences in expression between immunotherapy and immune response, and to provide new insights for the study of tumor exosomes (28, 29). High-grade serous ovarian carcinoma (HGSOC) is the most common histological subtype of ovarian cancer, yet ScRNA-seq has not been extensively used to understand the genetic complexity in high-grade ovarian cancers. ScRNA-seq was used to examine gene expression patterns from
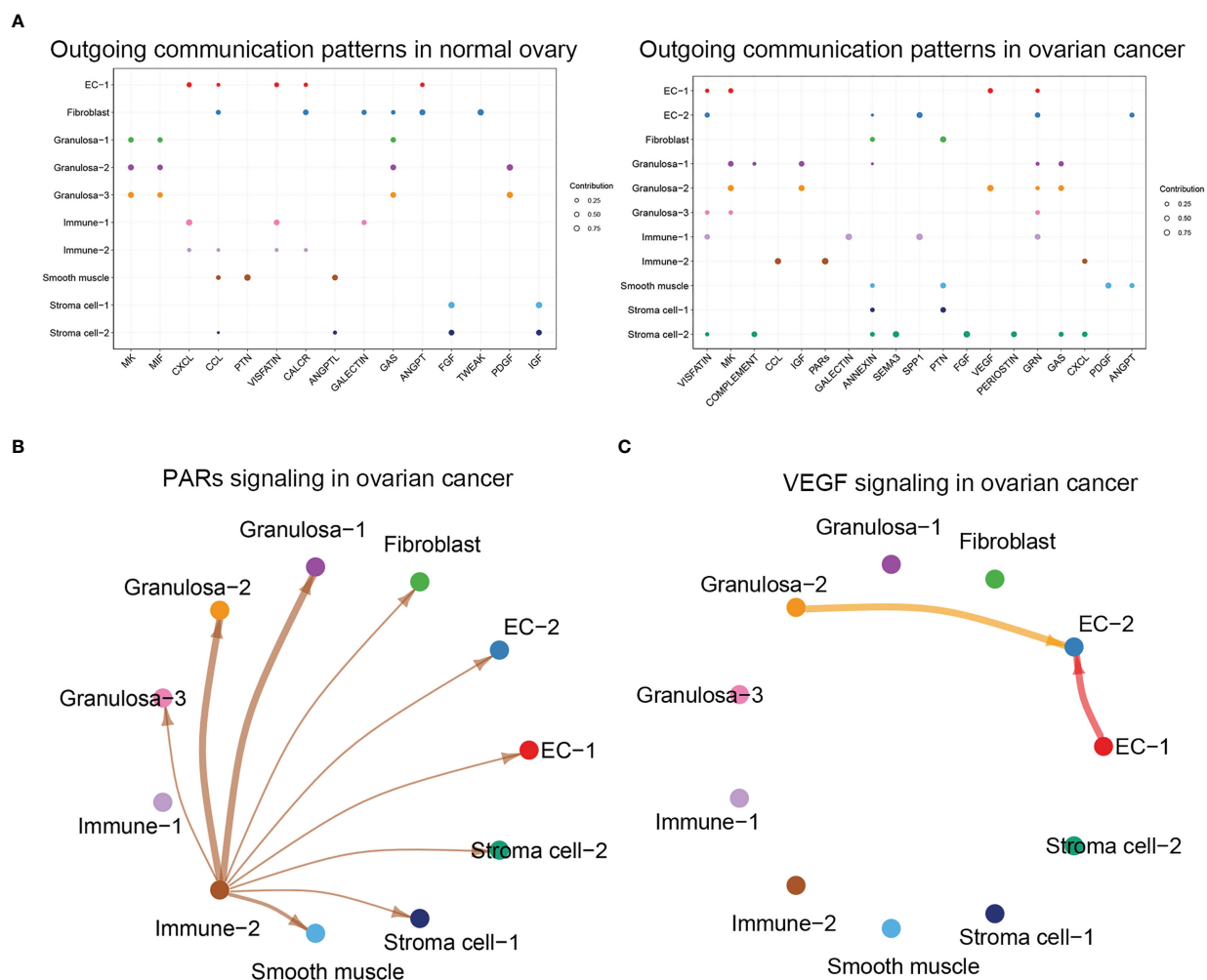
FIGURE 3
(A) Analysis of cellular communication in each cell population in normal ovary and ovarian cancer, dotplot showed the outgoing communication patterns in normal ovary and ovarian cancer. (B) Visualization result of PARs signaling in ovarian cancer. (C) Visualization result of VEGF signaling in ovarian cancer.

single cells of high-grade serous ovarian cancer obtained from a patient. From that study, epithelial and stromal cells were identified as the major subsets based on the RNA expression patterns of 66 evaluable single tumor cells. Findings from the study provided a first glimpse at the application of single-cell gene expression analysis in ovarian cancer to solve the etiology of the disease (30). In another study, single-cell RNA technology revealed the presence of heterogeneity in primary tumor cells among different patients, and differences in the expression profiles between metastatic lesions and primary lesions in different patients (31). Analysis of ascites samples from patients with high-grade ovarian cancer using single cell sequencing identified the JAK/STAT pathway as a therapeutic target in women (32).

Through bioinformatic analysis, we identified several genes associated with ovarian cancer and the signaling pathways associated with the genes. The DNA methylation status has been proven to be a prognostic biomarker for High-grade serous ovarian cancer (33). Our study also demonstrated that up-regulated genes in High-grade serous

ovarian cancer were closely associated with methylation levels and were implicated in the inflammatory response. VEGFA is a member of the VEGF family of cytokines that mediates ovarian cancer progression. VEGF is a significant therapeutic target for ovarian cancer since it is highly expressed in the tumor tissues. VEGF inhibitors could have significant therapeutic value in treating ovarian cancer (34). In our research, VEGF signals were significantly enriched in ovarian cancer and VEGFA was significantly expressed in EC-1-Cancer cells. VEGF stimulates endothelial cell proliferation through VEGF receptor 2, which is found on endothelial cells (35).We also found that Ovarian cancers induced important changes in endothelial cells.

QPCR analysis verified the high expression of some genes in human high-grade serous ovarian carcinoma. URI1 may be a 'non-oncogene' that supports the oncogenic phenotype of cancer cells that depend on a molecular chaperone system to survive (36). Ovarian cancer cells overexpress or amplify certain R2TP/PFDL subunits, such as URI1, which have been linked to tumour progression (37). Ovarian cancer progression is also mediated by
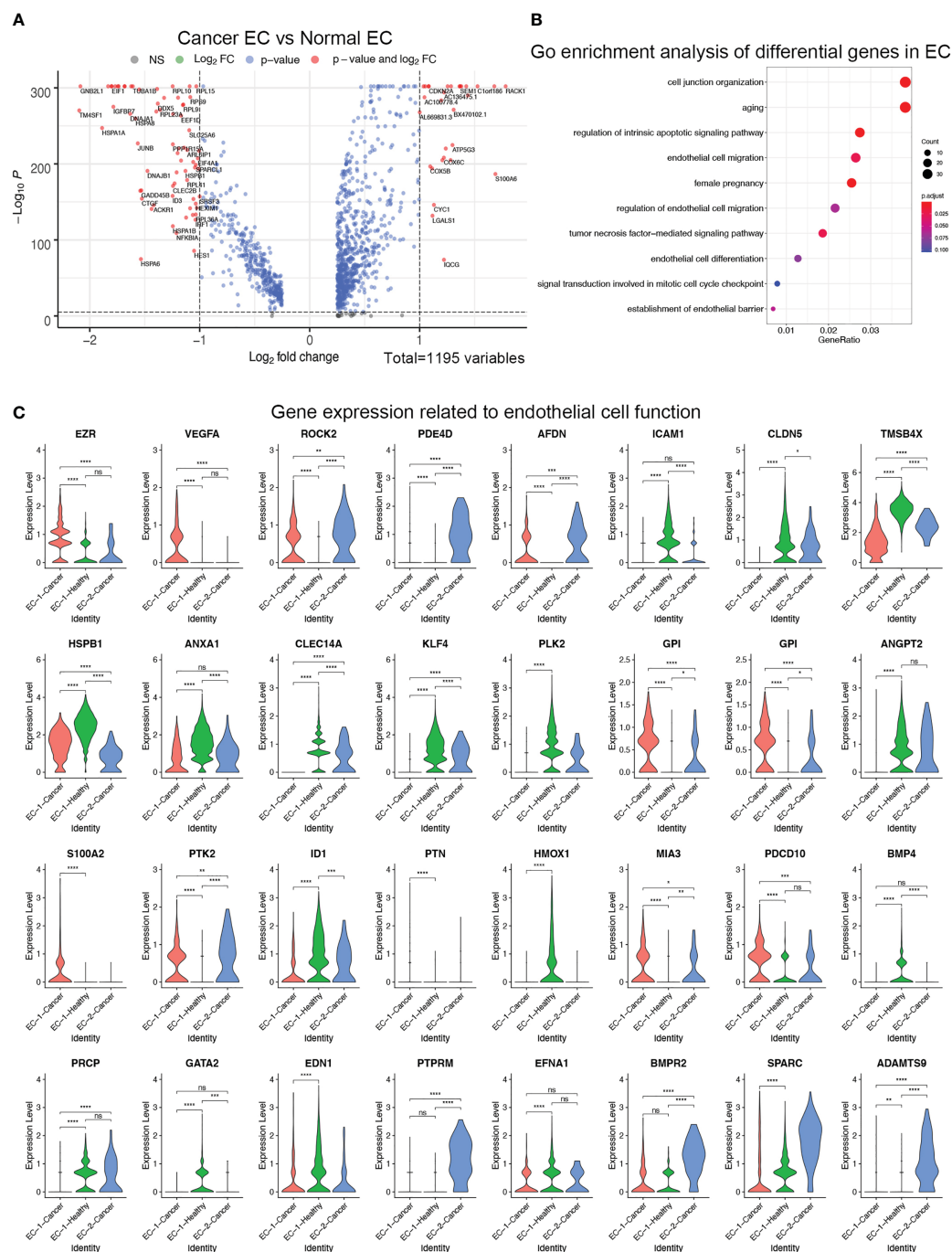
FIGURE 4
(A) Differential analysis of endothelial cells from normal ovary and ovarian cancer. Volcano plot revealed upregulated and downregulated genes in endothelial cells from ovarian cancer versus normal ovary. **(B)** GO enrichment analysis of differential genes between normal endothelial cells and ovarian cancer endothelial cells. **(C)** Violin plots showed the expression of genes related to endothelial cell function in normal endothelial cells and ovarian cancer endothelial cells. ****$p > 0.0001$; ***$p > 0.001$; **$p > 0.01$; *$p > 0.05$; ns, not significant ($P<0.05$).

PAK2. The knockdown of PAK2 in ovarian cancer cell lines reduced migration and invasion but had no effect on proliferation or apoptosis, suggesting a possible role for PAK2 in ovarian cancer development (38). The PARP1 inhibitor, rucaparib, has recently been approved by the FDA for the treatment of ovarian cancer (39). Based on findings from this study, PARP1 expression may also contribute to carcinogenesis, in addition to its enzymatic activity

(40). Additionally, our findings show the distribution of this gene in ovarian cancer cells, which could be useful for the treatment of ovarian cancer. It is interesting to note that CLU serum levels are elevated in ovarian cancer (41), and that CLU is expressed in malignant tissues of all ovarian cancer patients (42). In our study, we found that CLU was differentially expressed among different cell populations in normal and cancer samples. There is evidence that
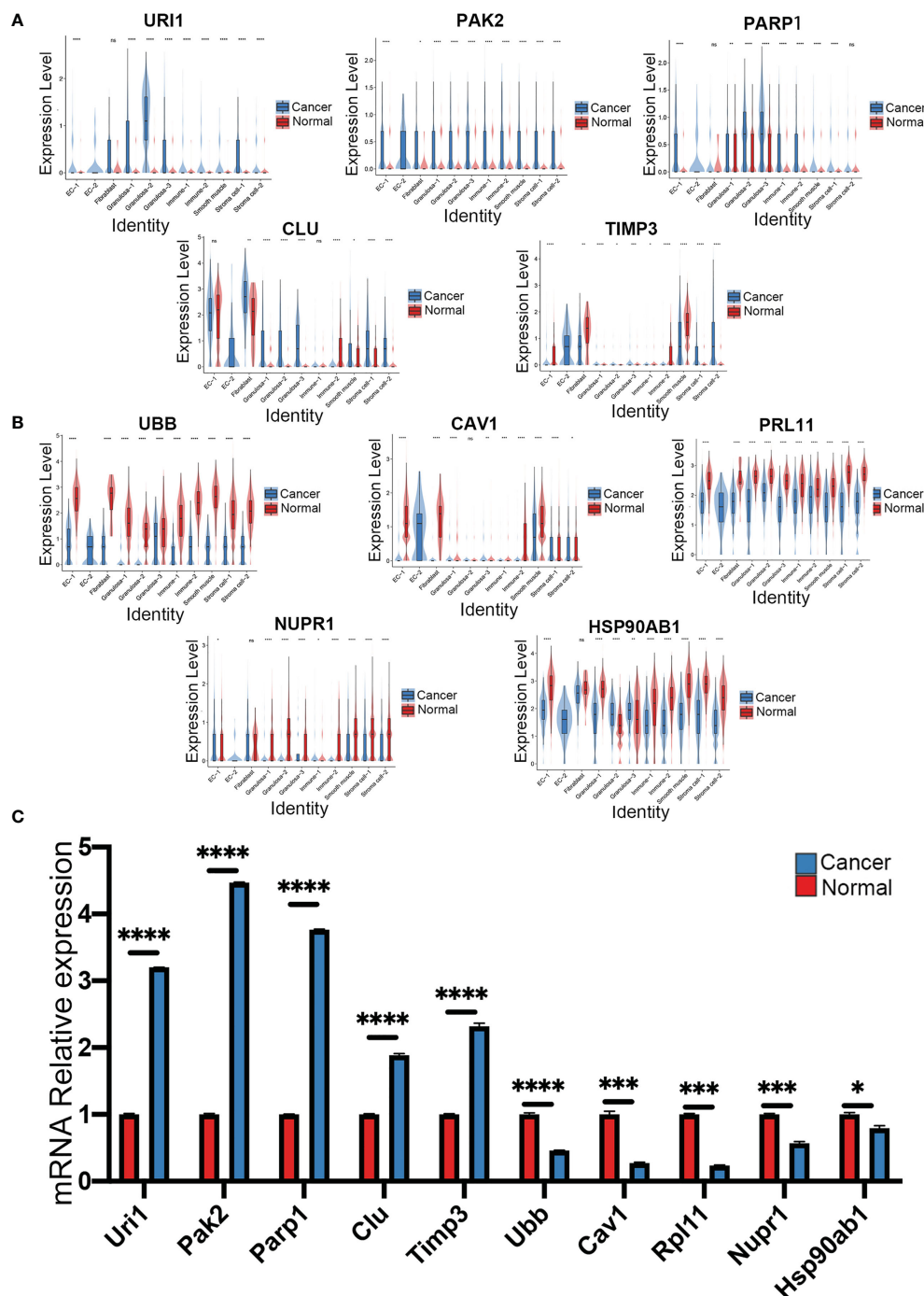
FIGURE 5
Analysis of apoptosis and immune related pathway genes normal ovary and ovarian cancer, violin plots showed **(A)** apoptosis-related genes and **(B)** immune-related genes in each cluster of the datasets. **(C)** The mRNA expression of ten genes in normal ovary and ovarian cancer was measured by qRT-PCR (****p < 0.0001; ***p < 0.001; **p < 0.01; *p < 0.05, Error bars are ± SEM). ns, not significant (P<0.05).

TIMP3 participates in tumor invasion as well as preferential methylation in ovarian cancer (43), while a similar study showed that TIMP3 mRNA expression was higher in ovarian cancer patients than healthy individuals (44). Findings from the two studies are consistent with our experimental results.

In our study, we found that some genes were down-regulated in cancer tissues compared with normal tissue, suggesting that these genes may play a role in suppressing ovarian cancer development.

The expression of UBB is significantly suppressed in certain cancers, including endometrial carcinoma and ovarian cancer (45). This was consistent with our data. UBB is likely to play different roles in different cancer cell types, however, no studies have analyzed the role of UBB. Although RPL11 has not been reported as a cancer suppressor gene in ovarian cancer studies, it is involved in the development of gastric cancer, colorectal cancer, fibroblasts, lymphoma, and esophageal squamous carcinoma.

Furthermore, deletion of RPL11 inhibited colon cancer cell death by preventing p53 activation (46, 47). CAV1 plays an oncogenic role in solid tumors, and its expression correlates negatively with tumor invasion. Additionally, CAV1 can be found in the nucleus of ovarian cancer cells (48), suggesting that CAV1 may also inhibit in ovarian cancer. NUPR1 gene plays a variety of roles in benign and malignant tumors. NUPR1 may affect ovarian cancer proliferation and invasion by signaling through the AKT pathway (49). The purpose of our study was to explore the expression of NUPR1 in each cell population in ovarian cancer.

In summary, our ScRNA-Seq data revealed the main cell types and growth processes in the human healthy ovarian tissues. In addition, we showed differences in function, gene expression and cell interaction patterns between ovarian cancer and healthy ovarian tissues for each cell population. These single-cell transcriptome datasets could shed light on major drivers of tumor development and progression. Increased understanding of ovarian cancer at the single-cell level will lead to the development of novel therapies. However, further studies on the functions of the differentially expressed genes in ovarian cancer are required.

Data availability statement

The original contributions presented in the study are included in the article/Supplementary Material. Further inquiries can be directed to the corresponding author.

Ethics statement

The research protocol was reviewed and approved by the Research Ethics Committee of Sir Run Run Shaw Hospital, School of Medicine, Zhejiang University. The patients/participants provided their written informed consent to participate in this study.

Author contributions

XZ was mainly responsible for the writing of the manuscript and carried out statistical analyses. SH and CY participated in the designing the study and analysis of data. XS and FS participated in the experiments. JY critically revised the final manuscript and was responsible for the submitted manuscript.

All authors contributed to the article and approved the submitted version.

Conflict of interest

The authors declare that the research was conducted in the absence of any commercial or financial relationships that could be construed as a potential conflict of interest.

Publisher's note

All claims expressed in this article are solely those of the authors and do not necessarily represent those of their affiliated organizations, or those of the publisher, the editors and the reviewers. Any product that may be evaluated in this article, or claim that may be made by its manufacturer, is not guaranteed or endorsed by the publisher.

Supplementary material

The Supplementary Material for this article can be found online at: https://www.frontiersin.org/articles/10.3389/fonc.2023.1148628/full#supplementary-material

References

1. Jiang Y, Lyu T, Che X, Jia N, Li Q, Feng W. Overexpression of Smyd3 in ovarian cancer is associated with ovarian cancer proliferation and apoptosis Via methylating H3k4 and H4k20. J Cancer (2019) 10(17):4072–84. doi: 10.7150/jca.29861

2. Bowtell DD, Bohm S, Ahmed AA, Aspuria PJ, Bast RC Jr., Beral V, et al. Rethinking ovarian cancer ii: Reducing mortality from high-grade serous ovarian cancer. Nat Rev Cancer (2015) 15(11):668–79. doi: 10.1038/nrc4019

3. DeSantis C, Ma J, Bryan L, Jemal A. Breast cancer statistics, 2013. CA Cancer J Clin (2014) 64(1):52–62. doi: 10.3322/caac.21203

4. Yiwei T, Hua H, Hui G, Mao M, Xiang L. Hotair interacting with Mapk1 regulates ovarian cancer Skov3 cell proliferation, migration, and invasion. Med Sci Monit (2015) 21:1856–63. doi: 10.12659/MSM.893528

5. Samuels DC, Han L, Li J, Quanghu S, Clark TA, Shyr Y, et al. Finding the lost treasures in exome sequencing data. Trends Genet (2013) 29(10):593–9. doi: 10.1016/j.tig.2013.07.006

6. Ye F, Samuels DC, Clark T, Guo Y. High-throughput sequencing in mitochondrial DNA research. *Mitochondrion* (2014) 17:157–63. doi: 10.1016/j.mito.2014.05.004

7. Cesar ASM, Regitano LCA, Reecy JM, Poleti MD, Oliveira PSN, de Oliveira GB, et al. Identification of putative regulatory regions and transcription factors associated with intramuscular fat content traits. *BMC Genomics* (2018) 19(1):499. doi: 10.1186/s12864-018-4871-y

8. Malek JA, Mery E, Mahmoud YA, Al-Azwani EK, Roger L, Huang R, et al. Copy number variation analysis of matched ovarian primary tumors and peritoneal metastasis. *PloS One* (2011) 6(12):e28561. doi: 10.1371/journal.pone.0028561

9. Stanley N, Stelzer IA, Tsai AS, Fallahzadeh R, Ganio E, Becker M, et al. Vopo leverages cellular heterogeneity for predictive modeling of single-cell data. *Nat Commun* (2020) 11(1):3738. doi: 10.1038/s41467-020-17569-8

10. Trapnell C. Defining cell types and states with single-cell genomics. *Genome Res* (2015) 25(10):1491–8. doi: 10.1101/gr.190595.115

11. Wagner A, Regev A, Yosef N. Revealing the vectors of cellular identity with single-cell genomics. *Nat Biotechnol* (2016) 34(11):1145–60. doi: 10.1038/nbt.3711

12. Jeong S, Park S, Jo YS, Choi MJ, Lee G, Lee SG, et al. Long non-coding rna-based functional prediction reveals novel targets in notch-upregulated ovarian cancer. *Cancers (Basel)* (2022) 14(6):1557. doi: 10.3390/cancers14061557

13. Li WV, Li JJ. An accurate and robust imputation method scimpute for single-cell rna-seq data. *Nat Commun* (2018) 9(1):997. doi: 10.1038/s41467-018-03405-7

14. Ye F, Huang W, Guo G. Studying hematopoiesis using single-cell technologies. *J Hematol Oncol* (2017) 10(1):27. doi: 10.1186/s13045-017-0401-7

15. Liu W, Wu A, Pellegrini M, Wang X. Integrative analysis of human protein, function and disease networks. *Sci Rep* (2015) 5:14344. doi: 10.1038/srep14344

16. Zhao W, Yu J, Jiang F, Wang W, Kang L, Cui F. Coordination between terminal variation of the viral genome and insect micrornas regulates rice stripe virus replication in insect vectors. *PloS Pathog* (2021) 17(3):e1009424. doi: 10.1371/journal.ppat.1009424

17. Nguyen H, Tran D, Tran B, Pehlivan B, Nguyen T. A comprehensive survey of regulatory network inference methods using single cell rna sequencing data. *Brief Bioinform* (2021) 22(3):bbaa190. doi: 10.1093/bib/bbaa190

18. Olalekan S, Xie B, Back R, Eckart H, Basu A. Characterizing the tumor microenvironment of metastatic ovarian cancer by single-cell transcriptomics. *Cell Rep* (2021) 35(8):109165. doi: 10.1016/j.celrep.2021.109165

19. Fan X, Bialecka M, Moustakas I, Lam E, Torrens-Juaneda V, Borggreven NV, et al. Single-cell reconstruction of follicular remodeling in the human adult ovary. *Nat Commun* (2019) 10(1):3164. doi: 10.1038/s41467-019-11036-9

20. Argelaguet R, Arnol D, Bredikhin D, Deloro Y, Velten B, Marioni JC, et al. Mofa +: A statistical framework for comprehensive integration of multi-modal single-cell data. *Genome Biol* (2020) 21(1):111. doi: 10.1186/s13059-020-02015-1

21. Stuart T, Butler A, Hoffman P, Hafemeister C, Papalexi E, Mauck WM3rd, et al. Comprehensive integration of single-cell data. *Cell* (2019) 177(7):1888–902 e21. doi: 10.1016/j.cell.2019.05.031

22. Chothani S, Adami E, Ouyang JF, Viswanathan S, Hubner N, Cook SA, et al. Deltate: Detection of translationally regulated genes by integrative analysis of ribo-seq and rna-seq data. *Curr Protoc Mol Biol* (2019) 129(1):e108. doi: 10.1002/cpmb.108

23. Yu G, Wang LG, Han Y, He QY. Clusterprofiler: An r package for comparing biological themes among gene clusters. *OMICS* (2012) 16(5):284–7. doi: 10.1089/omi.2011.0118

24. Jin S, Guerrero-Juarez CF, Zhang L, Chang I, Ramos R, Kuan CH, et al. Inference and analysis of cell-cell communication using cellchat. *Nat Commun* (2021) 12(1):1088. doi: 10.1038/s41467-021-21246-9

25. Donati G. The niche in single-cell technologies. *Immunol Cell Biol* (2016) 94 (3):250–5. doi: 10.1038/icb.2015.107

26. Parsons DW, Jones S, Zhang X, Lin JC, Leary RJ, Angenendt P, et al. An integrated genomic analysis of human glioblastoma multiforme. *Science* (2008) 321 (5897):1807–12. doi: 10.1126/science.1164382

27. Eppert K, Takenaka K, Lechman ER, Waldron L, Nilsson B, van Galen P, et al. Stem cell gene expression programs influence clinical outcome in human leukemia. *Nat Med* (2011) 17(9):1086–93. doi: 10.1038/nm.2415

28. Shah MM, Landen CN. Ovarian cancer stem cells: Are they real and why are they important? *Gynecol Oncol* (2014) 132(2):483–9. doi: 10.1016/j.ygyno.2013.12.001

29. Fidler IJ. The pathogenesis of cancer metastasis: The 'Seed and soil' hypothesis revisited. *Nat Rev Cancer* (2003) 3(6):453–8. doi: 10.1038/nrc1098

30. Winterhoff BJ, Maile M, Mitra AK, Sebe A, Bazzaro M, Geller MA, et al. Single cell sequencing reveals heterogeneity within ovarian cancer epithelium and cancer associated stromal cells. *Gynecol Oncol* (2017) 144(3):598–606. doi: 10.1016/j.ygyno.2017.01.015

31. Shih AJ, Menzin A, Whyte J, Lovecchio J, Liew A, Khalili H, et al. Identification of grade and origin specific cell populations in serous epithelial ovarian cancer by single cell rna-seq. *PloS One* (2018) 13(11):e0206785. doi: 10.1371/journal.pone.0206785

32. Izar B, Tirosh I, Stover EH, Wakiro I, Cuoco MS, Alter I, et al. A single-cell landscape of high-grade serous ovarian cancer. *Nat Med* (2020) 26(8):1271–9. doi: 10.1038/s41591-020-0926-0

33. Mase S, Shinjo K, Totani H, Katsushima K, Arakawa A, Takahashi S, et al. Znf671 DNA methylation as a molecular predictor for the early recurrence of serous ovarian cancer. *Cancer Sci* (2019) 110(3):1105–16. doi: 10.1111/cas.13936

34. Amini A, Masoumi Moghaddam S, Morris DL, Pourgholami MH. Utility of vascular endothelial growth factor inhibitors in the treatment of ovarian cancer: From concept to application. *J Oncol* (2012) 2012:540791. doi: 10.1155/2012/540791

35. Pang C, Gao Z, Yin J, Zhang J, Jia W, Ye J. Macrophage infiltration into adipose tissue may promote angiogenesis for adipose tissue remodeling in obesity. *Am J Physiol Endocrinol Metab* (2008) 295(2):E313–22. doi: 10.1152/ajpendo.90296.2008

36. Theurillat JP, Metzler SC, Henzi N, Djouder N, Helbling M, Zimmermann AK, et al. Uri Is an oncogene amplified in ovarian cancer cells and is required for their survival. *Cancer Cell* (2011) 19(3):317–32. doi: 10.1016/j.ccr.2011.01.019

37. Fan JL, Zhang J, Dong LW, Fu WJ, Du J, Shi HG, et al. Uri Regulates tumorigenicity and chemotherapeutic resistance of multiple myeloma by modulating il-6 transcription. *Cell Death Dis* (2014) 5(3):e1126. doi: 10.1038/cddis.2014.93

38. Livak KJ, Schmittgen TD. Analysis of relative gene expression data using real-time quantitative pcr and the 2(-delta delta C(T)) method. *Methods* (2001) 25(4):402–8. doi: 10.1006/meth.2001.1262

39. Park TH, Kim CW, Choi JS, Park YJ, Chong Y, Park MJ, et al. Parp1 inhibition as a novel therapeutic target for keloid disease. *Adv Wound Care (New Rochelle)* (2019) 8(5):186–94. doi: 10.1089/wound.2018.0910

40. Zhang Y, Huang J, Huang Y, Zhang S, Wu W, Long H, et al. Tanshinone&Nbsp; I and simvastatin inhibit melanoma tumour cell growth by regulating poly (Adp ribose) Polymerase&Nbsp;1 expression. *Mol Med Rep* (2021) 23(1):40. doi: 10.3892/mmr.2020.11678

41. Rizzi F, Bettuzzi S. The clusterin paradigm in prostate and breast carcinogenesis. *Endocr Relat Cancer* (2010) 17(1):R1–17. doi: 10.1677/ERC-09-0140

42. Chen Y, Lim BK, Peh SC, Abdul-Rahman PS, Hashim OH. Profiling of serum and tissue high abundance acute-phase proteins of patients with epithelial and germ line ovarian carcinoma. *Proteome Sci* (2008) 6:20. doi: 10.1186/1477-5956-6-20

43. Kaja S, Hilgenberg JD, Collins JL, Shah AA, Wawro D, Zimmerman S, et al. Detection of novel biomarkers for ovarian cancer with an optical nanotechnology detection system enabling label-free diagnostics. *J BioMed Opt* (2012) 17(8):081412–1. doi: 10.1117/1.JBO.17.8.081412

44. Hu X, Li D, Zhang W, Zhou J, Tang B, Li L. Matrix metalloproteinase-9 expression correlates with prognosis and involved in ovarian cancer cell invasion. *Arch Gynecol Obstet* (2012) 286(6):1537–43. doi: 10.1007/s00404-012-2456-6

45. Haakonsen DL, Rape M. Ubiquitin levels: The next target against gynecological cancers? *J Clin Invest* (2017) 127(12):4228–30. doi: 10.1172/JCI98262

46. Deng X, Li S, Kong F, Ruan H, Xu X, Zhang X, et al. Long noncoding rna pihl regulates P53 protein stability through Grwd1/Rpl11/Mdm2 axis in colorectal cancer. *Theranostics* (2020) 10(1):265–80. doi: 10.7150/thno.36045

47. Uchi R, Kogo R, Kawahara K, Sudo T, Yokobori T, Eguchi H, et al. Pict1 regulates Tp53 *Via* Rpl11 and is involved in gastric cancer progression. *Br J Cancer* (2013) 109(8):2199–206. doi: 10.1038/bjc.2013.561

48. Sanna E, Miotti S, Mazzi M, De Santis G, Canevari S, Tomassetti A. Binding of nuclear caveolin-1 to promoter elements of growth-associated genes in ovarian carcinoma cells. *Exp Cell Res* (2007) 313(7):1307–17. doi: 10.1016/j.yexcr.2007.02.005

49. Yu J, Zhu H, Li R, Jiang Q, Luan W, Shi J, et al. Oncogenic role of Nupr1 in ovarian cancer. *Onco Targets Ther* (2020) 13:12289–300. doi: 10.2147/OTT.S262224

Combined treatment of disulfiram with PARP inhibitors suppresses ovarian cancer

Bin Tang[1†], Min Wu[2†], Lin Zhang[2†], Shuyi Jian[2], Shiyi Lv[2], Tongyuan Lin[1], Shuangshuang Zhu[2], Layang Liu[2], Yixue Wang[2], Zhengfang Yi[2*] and Feiyun Jiang[1*]

[1]Department of Gynecology, East China Normal University Wuhu Affiliated Hospital (The Second People's Hospital of Wuhu City), Wuhu, China, [2]Shanghai Key Laboratory of Regulatory Biology, Institute of Biomedical Sciences and School of Life Sciences, East China Normal University, Shanghai, China

Introduction: Due to the difficulty of early diagnosis, nearly 70% of ovarian cancer patients are first diagnosed at an advanced stage. Thus, improving current treatment strategies is of great significance for ovarian cancer patients. Fast-developing poly (ADP-ribose) polymerases inhibitors (PARPis) have been beneficial in the treatment of ovarian cancer at different stages of the disease, but PARPis have serious side effects and can result in drug resistance. Using PARPis in combination with other drug therapies could improve the efficacy of PRAPis.In this study, we identified Disulfiram as a potential therapeutic candidate through drug screening and tested its use in combination with PARPis.

Methods: Cytotoxicity tests and colony formation experiments showed that the combination of Disulfiram and PARPis decreased the viability of ovarian cancer cells

Results: The combination of PARPis with Disulfiram also significantly increased the expression of DNA damage index gH2AX and induced more PARP cleavage. In addition, Disulfiram inhibited the expression of genes associated with the DNA damage repair pathway, indicating that Disulfiram functions through the DNA repair pathway.

Discussion: Based on these findings, we propose that Disulfiram reinforces PARPis activity in ovarian cancer cells by improving drug sensitivity. The combined use of Disulfiram and PARPis provides a novel treatment strategy for patients with ovarian cancer.

KEYWORDS

poly (ADP-ribose) polymerase inhibitors, ovarian cancer, drug combination, disulfiram, DNA damage repair

Introduction

Ovarian cancer is one of the deadliest gynecological malignancies in the world (1). 90% of ovarian cancers are of an epithelial cell type and comprise multiple histologic types, with various specific molecular changes, clinical behaviours, and treatment outcomes. The remaining 10% are non-epithelial ovarian cancers, which include mainly germ cell tumours, sex cord-stromal tumours, and some extremely rare tumours such as small cell carcinomas (2). In the United States, it is estimated that there were 21,410 new cases and 13,770 deaths in 2021, ranking the fifth highest among female malignancies (3). Approximately 20–30% of epithelial ovarian cancers occur in females with an inherited predisposition; most of these hereditary ovarian cancers are due to germline mutations in BRCA1 and BRCA2 genes. The identification of BRCA1 and BRCA2 pathogenic variants is recommended as an effort of primary prevention for epithelial ovarian cancer (4). Due to the complexity of histological subtypes, biology and clinical features of ovarian cancer, establishing a successful early screening strategy for ovarian cancer is still a major challenge, nearly 70% of ovarian cancer patients are diagnosed at advanced statges, and the 5-year survival rate is only approximately 25%. There are several therapeutic options, such as poly (ADP-ribose) polymerases inhibitors (PARPis), that have been shown to improve ovarian cancer patient survival.

PARPis are the first anti-cancer drugs that successfully applied the synthetic lethal concept. PAPRis have been used to effectively treat Homologous Recombination Deficiency (HRD) tumors (3). Currently, some PARPis, such as Olaparib, Rucaparib, and Niraparib, have been approved for the clinical and maintenance treatment of ovarian cancer (5). They also have been shown to play a very important role in the maintenance treatment of ovarian cancer (6). Based on the 7-year follow-up results of the phase III SOLO1/GOG-3004 trial (NCT01844986) presented at ESMO 2022, Olaparib (Lynparza) maintenance therapy resulted in a long-term overall survival benefit compard to placebo in newly diagnosed advanced ovarian cancer patients with BRCA mutations (7). However, PAPRis treatment is asosociated with serious side effects and drug resistance. To overcome these challenges, PARPis treatment in combination with other targeted drugs, such as Topotecan and Gemcitabine, has been explored (8, 9), but the results are still not satisfactory, and some even produced more serious adverse effects. In a recent phase III trial of Veliparib with platinum therapy, treatment was stopped before determination of disease progression due to high toxicity (10).

Disulfiram has been approved by the FDA and has been widely used in alcoholism treatment for more than 60 years, with low toxicity and controllable side effects (11). Several *in vitro* studies showed that Disulfiram induced apoptosis in cancer cell lines such as breast and ovarian cancer (12). Clinical studies have shown that the main metabolite of Disulfiram, Diethyldithiocarbamate (DDTC), as an adjuvant immunotherapy improves survival of breast cancer patients (13). It was also found that DDTC-copper complex targets NPL4 (the aptamer of separase p97) interferes with the ubiquitinated protease degradation system, inducing cancer cell death. As tumor tissues contain a higher level of copper metabolites than normal tissues, Disulfiram does not cause obvious toxicity for normal cells and has the potential of targeting cancer cells (14).

In this work, we used a drug screen and identified Disulfiram as a potential candidate to be combined with PARPis to treat ovarian cancer. We found that Disulfiram in combination with PARPis synergistically inhibited ovarian cancer progression, indicating a novel combinatorial treatment strategy for patients with ovarian cancer.

Materials and methods

Cell lines, cell culture, and drugs

Ovarian cancer cells SKOV3, ES-2, OVCA420, and HeyA8 were purchased from the American Type Cell Culture (ATCC). SKOV3 cells were cultured in RPMI-1640 medium containing 10% fetal bovine serum (FBS) and 1% penicillin/streptomycin. ES-2, OVCA420, and HeyA8 cells were cultured in DMEM/High Glucose medium containing 10% FBS and 1% penicillin/streptomycin. These cell lines were cultured at 37°C with 5% CO_2 and 95% humidity. Olaparib (OP) was purchased from MedChemExpress and 100 mM DMSO stock solution was prepared. Disulfiram (DSF) was purchased from Target Molecule, Niraparib (NP) was provided by Zai Lab Co., Ltd., (Shanghai) and a 25 mM stock solution in DMSO was prepared for each drug.

Cell viability assay and combination index

We seeded SKOV3 and ES-2 cells on 96-well plates at a density of 5×10^3 cells per well. Cells were treated for 72 h with DMSO, olaparib only (50 µM per well), screening compounds (10 µM per well), and the combination (50 µM Olaparib/10 µM compound per well)., and cell viability was measured using the sulforhodamine B (SRB) assay to determine the relative cell proliferation (15). The SRB test results were analyzed using GraphPad Prism 8 software to calculate the half-inhibition rate of cell proliferation (IC_{50}) of the compounds (16), and the results are expressed as the means of triplicate measurements.

According to the IC_{50} value of each drug in the cell lines, the final concentration gradient was set as 0.5 IC_{50}, 0.75 IC_{50}, 1.0 IC_{50}, and 1.25 IC_{50}. The CI and fraction affected (FA) values were calculated using Calcusyn software, which was based on the Chou-Talalay theorem (17). FA refers to the fraction of cell viability affected. Survivability plots and CI value scatter plots were made in GraphPad Prism 8.

Colony formation rates

SKOV3 and ES-2 cells were seeded in 6-well cell culture plates in triplicate at a concentration of 5×10^3 cells per well in 2 mL medium supplemented with 10% FBS and incubated overnight. The

media was removed and fresh media containing drugs was added, and the same volume of DMSO was added as a control. The cells were incubated at 37 °C for one week until the colonies were visible to the naked eye. The cells were then fixed with 4% paraformaldehyde for 25 to 30 min, washed with PBS, and stained with 2% crystal violet solution for 15 to 20 min. Finally, the cells were washed with water and air-dried. The number of cell colonies in the wells was counted and the clone formation rate was calculate as: clone formation rate (%)/clone formation rate (control) (%) (18).

Flow cytometry

SKOV3 cells were seeded in medium containing PARP inhibitors and Disulfiram, and the same volume of DMSO was added as a control. After 48 h of treatment, the supernatants and digested cell suspension were collected. Whole cells in the binding buffer suspension were stained with 1 μL RNA enzyme (Sigma, USA), 2 μL annexin V–FITC (BD, USA), and 2 μL propidium iodide (PI) (Sigma, USA) for 15 min at room temperature in the dark. Unstained cells and single-stained cells were prepared as controls. These samples were detected using flow cytometry, and the stained cells were analyzed using a FACS Calibur (BD). Data were analyzed with FlowJo software (v10).

Western blot analysis

SKOV3 and ES-2 cells were seeded in 10 cm dishes. Cells were collected after 48 h of drug treatment. Proteins were extracted using RIPA lysis buffer (Sigma) and protein concentrations were determined using the BCA assay. SDS-PAGE (Shanghai Sangon Biological Engineering and Technological Service Company, China) was done according to instruction on the Cell Signaling Technology webstie (19). The following antibodies were used: rabbit anti-PARP antibody (9532s), rabbit anti-γH2AX antibody (9718s), and rabbit anti-GAPDH (ab9485, Abcam). Membranes were scanned using an Odyssey Infrared Imaging System (LI-COR Biosciences), and data were quantified using the Image Studio Lite software.

Immunofluorescence

Glass coverslips were placed into 24-well plates and 8×10^3 cells were seeded per well. The cells were treated with Disulfiram and Olaparib at different concentrations and incubated 37°C with 5% CO_2 and 95% humidity for 48 h. Fixed cells were permeabilized with 0.2% Triton (Sangon, China) in 1×PBS for 30 min. Cells were incubated in 1% BSA (Sangon) in 0.2% Triton/PBS for 30 min. Cells were then incubated with primary rabbit anti-γH2AX antibody (1:400) at 4°C overnight. Cells were then washed with 0.2% triton/PBS three times for 3 min per wash and incubated with a secondary anti-rabbit 800 antibody for 1 h in the dark. Cell nuclei were counterstained with DAPI (D9542, Sigma) for 5 min, and washed with 0.2% triton/PBS three times for 5 min per wash. Images were taken using an Olympus inverted fluorescence microscope.

Quantitative real-time PCR

SKOV3, ES-2, HeyA8, and OVCA420 cells were treated for 8 h with 15 μM Disulfiram, and total RNA was isolated using the TRIzol reagent (Invitrogen). RNA was extracted and reverse transcribed into cDNA with the Prime Script RT Reagent Kit (Takara). The cDNA was then used as the template for the RT-qPCR reaction that was performed using SYBR-Green (Takara) on QuantStudio®3 Real-Time PCR System (Applied Biosystems). GAPDH was used as an internal control. The reaction parameters were as follows: 5 min at 25°C, 30 min at 42°C, 5 min at 85°C, and then held at 16°C. The PCR profile was 95°C for 2 min, followed by 40 cycles of 95°C for 10s and 60°C for 30s. Data were analyzed using GraphPad Prism (version 8; GraphPad Software), and relative gene expression was calculated using the 2-ΔΔCT method.

Xenograft tumor growth

The ES-2 xenograft tumor models were developed by injecting 1×10^7 cells into female nude mice (6–8 weeks old). The mice were grouped randomly when the volume of the tumor nodules reached 100 mm^3 and were then treated with the indicated compounds or vehicle *via* intraperitoneal injection for 18 days. Body weight and tumor dimension were measured. Tumor volume was calculated using the following equation: tumor volume = length × width (2) × 0.52. After the study, the mice were euthanized, and tumors and major organs were collected.

Immunohistochemistry

Tissue ections were cut from formalin-fixed paraffin-embedded xenografts. For IHC staining, samples were stained using the VECTASTAIN ABC kit (Vector). Anti–Ki67 (1:250; Catalogue #ab15580, Abcam) was used as the primary antibody. Hematoxylin and eosin (HE) staining was performed following standard protocols.

Statistical analysis

The results are expressed as the mean ± SD. All experiments were performed at least three times, except for the animal experiments. Statistical significance of the difference between two groups was determined by Student's t-test. Two-way ANOVA was used to analyze animal data. The statistical analyses were performed using GraphPad Prism 7.0. The significant differences in the means were determined at the level of *$P < 0.05$, **$P < 0.01$, ***$P < 0.001$ and ****$P < 0.0001$.

Results

Drug screening in combination with PARPis

To identify drugs that might enhance the effect of PARPis, we screened 170 drug molecules retrieved from the FDA/CFDA compound library using SKOV3 and ES-2 cells. The experiments were performed with the screening compounds alone and the combination with Olaparib. DMSO and Olaparib alone were used as controls. Cell viability of the cells treated with the screening compounds vs the drug combination with Olaparib was plotted (Figures 1A, B). In both cases, each dot represents one compound. Dots located below the orange dashed line (slope of 1) indicates that the cell viability ratio of +Olaparib to -Olaparib is below one in the presence of these compounds; the dots located above the dashed line indicated that the cell viability ratio of +Olaparib to -Olaparib is above one. Ninety compounds decreased SKOV3 cell viability, and 151 compounds decreased ES-2 cell viability, indicating that the combinatorial effects of Olaparib were greater in the ES-2 cells (Figure 1B). The average survival rate ratios following combined treatment with PARPis vs the compound alone were 0.55 (37.61 vs 68.22%) and 0.22 (4.58 vs 21.28%) for the SKOV3 and ES-2 cells, respectively. Disulfiram (red dot) had the biggest effect on decreasing ES-2 cell viability among the 170 compounds

(Figure 1B). The chemical structure of Disulfiram is shown in Figure 1C.

Disulfiram in comibation with PARPis inhibited ovarian cell growth

To further confirm the effect of Disulfiram in combination with PARPis, we examined the effect of Disulfiram with PARPis (Olaparib or Niraparib) on cell viability in two additional cell lines, OVCA420 and HEYA8. We first determined the IC_{50} values of Olaparib and Niraparib and in combination with Disulfiram, resepectively. The IC_{50} of Olaparib was higher compared to the IC_{50} of Niraparib, which was relatively low (Table S1), consistent with the literature [20]. Interestingly, Disulfiram showed relatively low IC_{50} values with in all four cell lines.

We used the CI (combination index) to evaluate whether the effect Disulfiram was additional or synergistic [17]. Based on the different IC_{50} values of Olaparib, Niraparib, and Disulfiram (Figure S1), we set the concentration of Olaparib or Niraparib with Disulfiram at 50, 75, 100, or 125% of its IC_{50}. Figure 2 shows cell growth at the different concentrations of Olaparib or Niraparib in combination with Disulfram. The green trace of each figure represents the cell growth in the presence of Olaparib (left
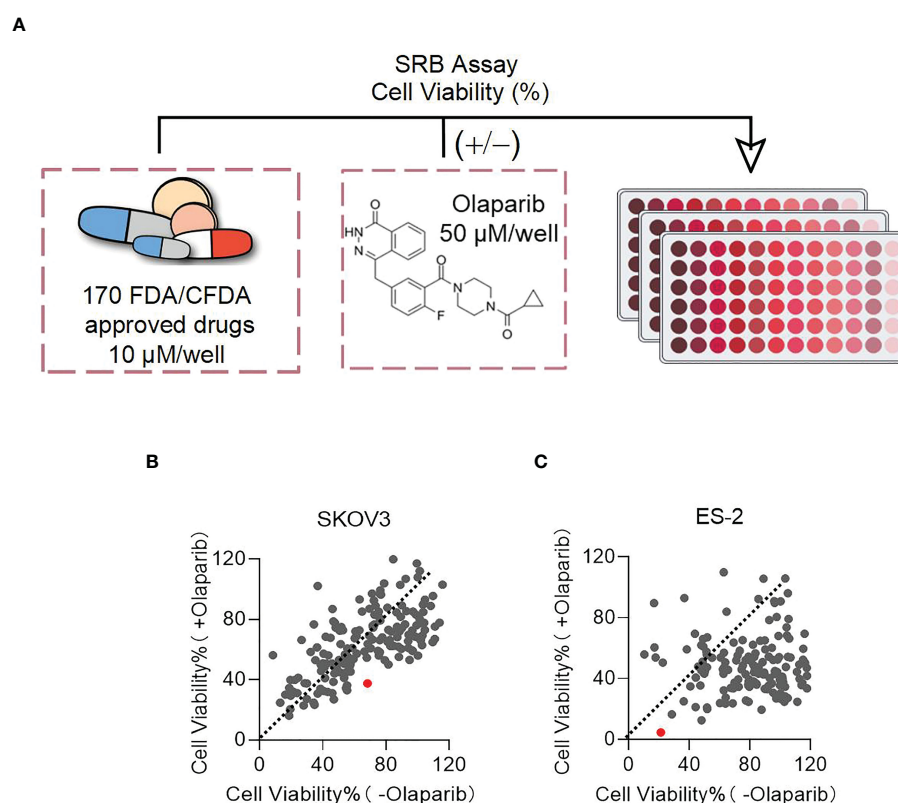
FIGURE 1
Disulfiram is identified as a target drug to test in combination with PARPis. **(A)** Scheme of the sulforhodamine B (SRB) screening. Plots of cell viability of Disulfiram with Olaparib vs without Olaparib in SKOV3 **(B)** and ES-2 cells **(C)**. The dashed line in each figure represents a slope of 1. Each dot represents a compound: red dots represent Disulfiram. Cell viability was determined as described in the Methods section.

column) or Niraparib (right column) alone from 0 IC$_{50}$ to 1.25 IC$_{50}$; the purple trace of each figure represents the cell growth in the presence of Disulfiram alone from 0 to 60 µM; and the red trace of each figure represents the cell growth in the presence of Disulfram/Olaparib (left column) and Disulfram/Niraparib (right column) at different concentrations. In all figures, red traces decreased more compared to the corresponding green and purple traces with increasing drug concentrations, indicating that cell growth was more inhibited by the combination of Disulfiram compared to the PARPis alone. The mean CI values of Disulfiram combined with

Olaparib or Niraparib in the SKOV3, ES-2, HeyA8, and OVCA420 cells are denoted at the bottom of each figure. The CI values were all below one, indicating that Disulfiram works synergistically with Olaparib or Niraparib to inhibit ovarian cancer cell growth, especially in SKOV3 cells. Moreover, combinational matrix (DSF +OP and DSF+NP) showed effect of Disulfiram in combination with and Olaparib or Niraparib on ovarian cancer cell growth. (Figures S2A–D).

We further examined the effect of Disulfiram in combination with PARPis on colony formation. Compared with Disulfiram or
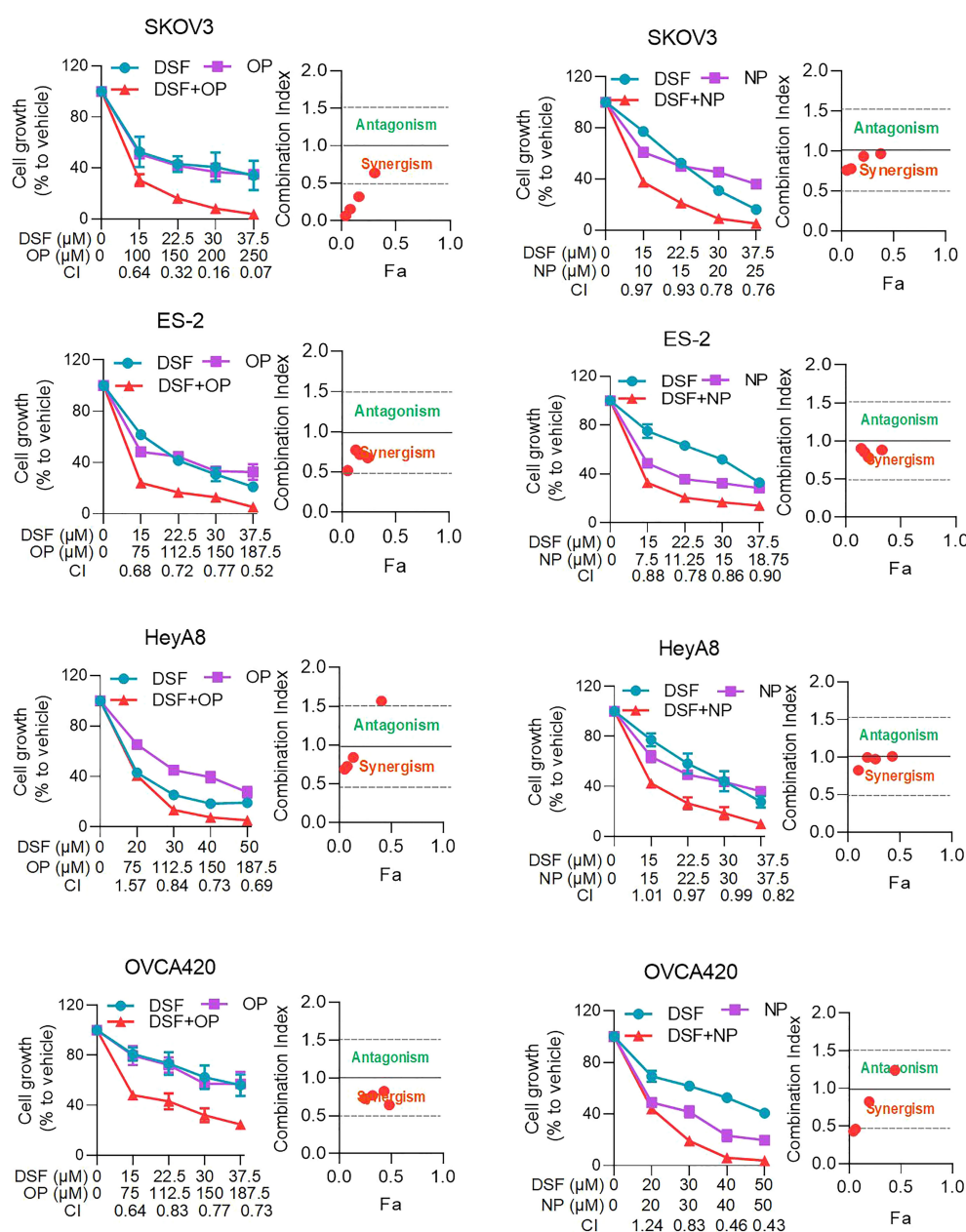
FIGURE 2
Effect of Disulfiram in combination with and Olaparib and Niraparib on ovarian cancer cell growth. The right column shows the plots of proliferation after treatment with Niraparib and Disulfiram in SKOV3, ES-2, HeyA8, and OVCA420 cell lines. The left column shows the plots of proliferation after treatment with Olaparib and Disulfiram in the SKOV3, ES-2, HeyA8, and OVCA420 cell lines, respectively. The plot of the CI *vs* inhibition rate (Fraction affected, Fa) of each case are shown next to the columns. Dot falls on red "Synergism"indicate a CI below one, and green "Antagonism"indicated a CI above one. Data are represented as mean ± SD (n=4 per group).

PARPis alone, the rate of colony formation in the combination group was significantly reduced (Figure 3). The average colony formation rate for the combination of Olaparib (5 µM) and Disulfiram (0.194 µM) in SKOV3 cells was reduced to 6.04%, and dropped to 8.33% with Olaparib (4 µM) and Disulfiram (0.194 µM) in ES-2 cells (Figures 3A–D). These results are consistent with the findings of cell growth inhibition (Figure 2).

Disulfiram in combination with PARPis increased SKOV3 cell apoptosis

To understand the synergist effect of Disulfiram and PARPis, we measured cell apoptosis of SKOV3 cells after treatment with Disulfiram and Olaparib alone and in combination. After 48 h of drug treatment the total apoptosis rate of Disulfiram (30 µM) with
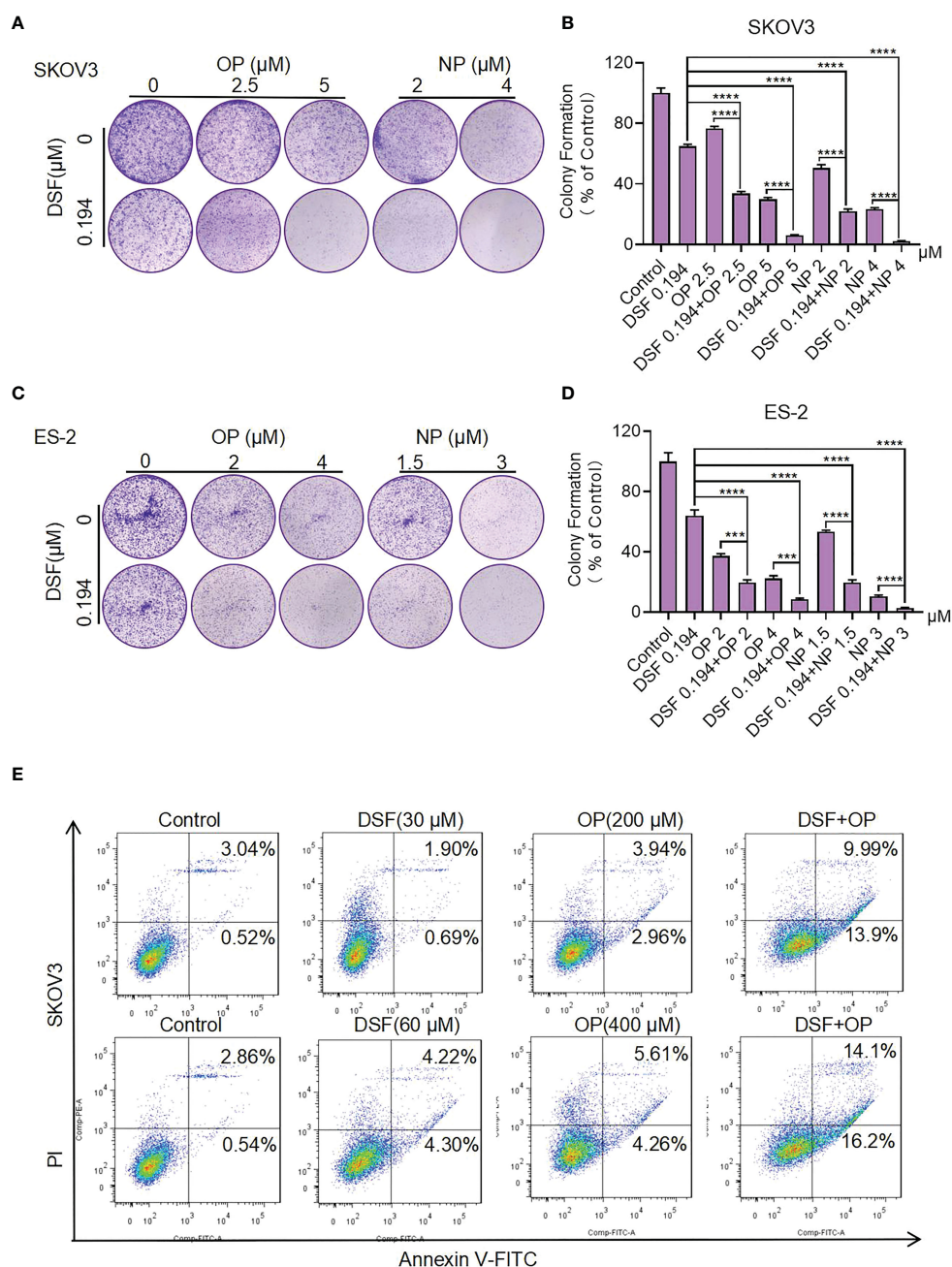
FIGURE 3

The effect of Disulfiram in combination with PARP inhibitors on colony proliferation and apoptosis of ovarian cancer cells. Clonal Proliferation assay of SKOV3 **(A, B)** and ES-2 cells **(C, D)** treated with the indicated concentrations of Olaparib or Niraparib alone or combined with Disulfiram. Representative images of SKOV3 and ES-2 cell colonies are shown. Apoptosis of SKOV3 cells after treatment with Disulfiram and Olaparib alone and in combination for 48 h at different concentrations **(E)**. Experiments were repeated three times and represented as mean $\pm$ SD. Unpaired t-test: ***$P<0.001$,****$P<0.0001$.

Olaparib (200 μM) was 23.89%, which was approximately 4-fold higher than the apoptosis rate of Olaparib (6.90%) and approximately 10-fold higher than Disulfiram (2.59%) alone. When the concnetration of Disulfiram and Olaparib was doubled, the total apoptosis rate of Disulfiram with Olaparib was 30.3%, approximately 3-fold higher than the apopotosis rate of Olaparib (9.87%) and approximately 3.5-fold higher than Disulfiram (8.52%) alone (Figure 3E) and analyzed apopotosis rate (Figure S3B). In OVCA420, the proportion of apoptotic cells after drug addition was also detected (Figure S3A). Compared with the single drug group, the combination drug induced the generation of apoptotic cells (Figure S3C). These results indicate that the combination of Disulfiram with Olaparib increases apoptosis of SKOV3 and OVCA420 cells, which is consistent with the findings for cell growth.

Disulfiram combined with PARPis increased double-stranded DNA damage.

As shown in Figure 3, the combination of Disulfiram with PARPis increased cell apoptosis. Therefore, we next measured the level of cleaved PARP, which is considered a markers of apoptosis (21), in SKOV3 and ES-2 cells in the presence of Disulfiram and PARPis. We also measured the level of γH2AX (phosphorylation of H2AX, which is one of the most conserved histone H2AX variants), a widely recognized marker of DNA double-strand cleavage (22). Figures 4A, B show that Dislfiram in compbination with PARPis increased H2AX protein expression and PARP cleavage compared to PARPis or Disulfiram alone, indicating that the combined treatment increased DNA double-strand cleavage in SKOV3 and ES-2 cells. Apparently, the densitometry analysis showed that the formation of H2AX increased after drug addition or combined drug group in SKOV3 (Figure 4C) and ES-2 (Figure 4D)

Immunofluorescence assays showed that the percentage of the cells with H2AX foci >10 was 91.72% in the combination group, which was much higher than the Disulfiram (21.67%) or Olaparib (79.05%) alone groups (Figures 4E–G). These results confirmed that Disulfiram in combination with Olaparib enhances DNA double-strand damage (Figure 3). It is worth noting that the level of DNA damage induced by Disulfiram alone was not significantly different from the Control group (18.46%).

Disulfiram downregulated genes involved in the homologous recombination repair pathway

HRD cells are more sensitive to PARP inhibitors due to the synthetic lethalilty and because the HRR pathway is not limited to the most common BRCA1/2 mutations. Deletions or mutations in other genes can be directly or indirectly involved in the HRR pathway, which could affect cancer cells sensitivity to PARP inhibitors. We used real-time PCR to determine the transcripton levels of *BRCA1*, *BRCA2*, *RAD51*, *RAD52*, *ATR*, *ATM*, *PALB2*. Figure 5 shows the expression level of these genes in SKOV3, ES-2,

HeyA8, and OVCA420 cells that were treated with 15 μM Disulfiram for 8 h. Compared to the control, Disulfiram significantly inhibited the expression of all-tested genes in the four cell lines, except for *RAD51* in HeyA8 and OZVCA420 cells. These results suggest that the effect of Disulfiram alone on ovarian cancer cells might involve the HRR pathway. However, we did not observe much difference in gene expression in response to the combination of Disulfiram with PARPis *vs* Disulfiram alone (data not shown).

Disulfiram in combination with Niraparib suppresses growth of ovarian cancer *in vivo*

Based on the cellular level data, we established an ovarian cancer xenograft model *in vivo* by subcutaneously injecting ES-2 cells into nude mice. Figure 6 shows that Disulfiram combined with Niraparib suppressed ES-2-derived xenograft tumor growth *in vivo*. Female nude mice bearing ES-2-derived tumors were randomized into four treatment groups: DMSO, Disulfiram, Niraparib, and Niraparib+Disulfiram. Figures 6A, B show the change in tumor volume after DMSO (blue trace), Disulfiram (green trace), Niraparib (red trace), and Niraparib+Disulfiram (purple trace) treatment for 18 days. Compared to the DMSO control, both Disulfiram and Niraparib inhibited tumor growth approximately 2-fold after 18 days of the injection, the combination of Disulfiram and Niraparib dramatically inhibited tumor growth compared to the other groups. The change in tumor weight exhibited a similar trend (Figure 6C), but the body weight of the mice after the injection of different compounds was very similar across the groups, indicating that Disulfiram, Niraparib, and Niraparib +Disulfiram have negligible toxicity (Figure 6D). We did not observe any abnormal behavior or side effects in any of the groups during treatment. This result was confirmed by HE staining of the heart, kidney, lung, liver, and spleen (Figure 6E). In immunohistochemistry experiment (23), compared to the control, the proliferation marker Ki67 was dramatically decreased in the Disulfiram+Niraparib group, which confirmed the anticancer effect shown *in vivo* (Figure 6F). These *in vivo* data demonstrate that Disulfiram in combination with Niraparib is an effective anti-cancer treatment strategy with minimal to no toxicity.

Discussion

The proteome closely mirrors the dynamic state of cells, tissues and organisms, proteomics has great potential to deliver clinically relevant biomarkers for ovarian cancer diagnosis. Technologies of proteomics, such as mass spectrometry and protein array analysis, have advanced the dissection of the underlying molecular signaling events and the proteomic characterization of ovarian cancer. Moreover, proteomics analysis of ovarian cancer can uncover new therapeutic choices, which can reduce the emergence of drug resistance (24). Despite rapid developments in cancer diagnosis and precision medicine, ovarian cancer is still recognized as one of

most difficult cancers to diagnose early in women, with a high recurrence rate and the highest degree of death (25). PARPis have been successful in prolonging progression-free survival, but tumor recurrence is still inevitable. Some PARPis, such as Olaparib and Niraparib, have already been approved in different settings to treat relapsed epithelial ovarian cancer (26). Combinations of PARP inhibitors with drugs that inhibit homologous recombination may sensitize cancers with a primary or secondary homologous

recombination proficiency to PARP inhibitors and potentially expand their use beyond HR-deficient cancers. PARPis in combination with other therapies, such as cytotoxic agents, immunotherapy, and antiangiogenic agents, have shown promising outocmes, and some cases have already been moved to clinical trials. Moreover, PARP inhibitors may be combined separately with PI3K, AKT, mTOR, WEE1, MEK, and CDK4/6 inhibitors (27–29). Studies on the combination of Cediranib (an
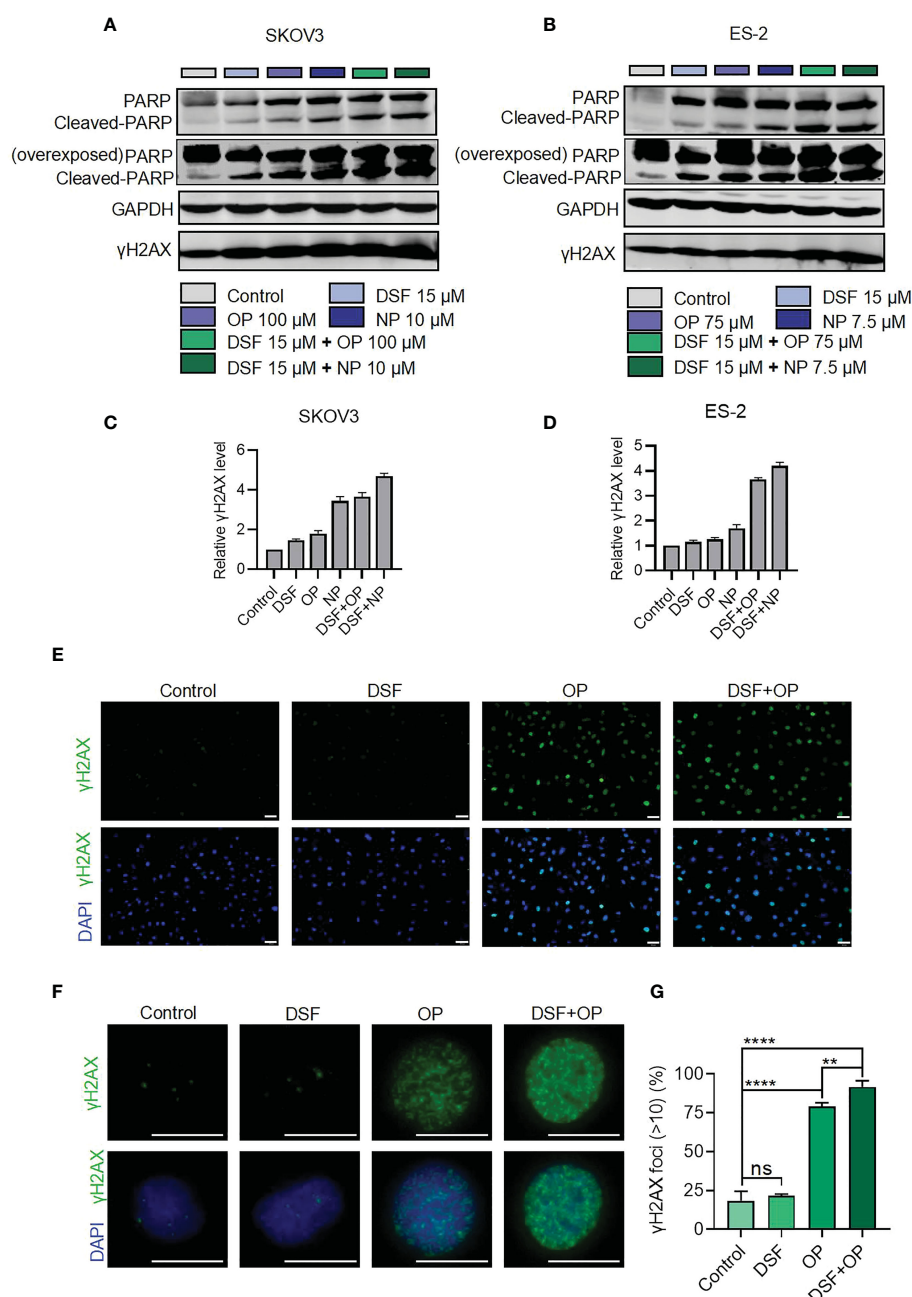
FIGURE 4
Protein expression of PARP and γH2AX in the presence of Disulfiram and Olaparib and Niraparib. Expression of PARP and γH2AX detected using western blot analysis after treatment with disulfiram and PARP inhibitors alone or in combination in SKOV3 (A) and ES-2 cells (B). Densitometry analysis of γH2AX levels normalized to GAPDH in SKOV3 (C) and ES-2 (D). Immunofluorescence staining for H2AX in cells treated with Disulfiram (3.75 μM) and Olaparib (25 μM) (E and F). Scale bars are 50 μm (E), and 20 μm (F). Quantification of γH2AX expression (G). The γH2AX foci >10 in all cells in each case were calculated. The experiment was repeated three times. Error bars represent mean ± SD. Unpaired t-test, ns indicates no significant difference, **$P<0.01$, ****$P<0.0001$.

oral tyrosine kinase inhibitor of vascular endothelial growth factor receptor) with Olaparib have been reported (30). Such combination strategies will open more avenues to optimize the efficacy of PARPis and eventually benefit ovarian cancer patients. We found that the combination of Disulfiram with PARPis has great potential for the development of PARPis combination therapies and expands therapeutic strategies for ovarian cancer.

Disulfiram is an FDA-approved abstinence drug that has advantages of controllable toxicity and side effects and low cost (31). In recent years, many studies have shown that Disulfiram also inhibits cancer progression (32). Here we showed that the anti-cancer activity of Olaparib was greatly enhanced by Disulfiram. We further determined the CI, using the theorm developed by Chou and Talalay, to evaluate the effect of the drug combination. The CI value of each combination case was determined using CompuSyn and Calcusyn software to quantify the synergistic effect of the combined drugs (17). The mean CI values of Disulfiram combined with Olaparib were all below one, which defines synergism. Similar values were found for Disulfiram and Niraparib. Very different CI-*vs*-effect traces were observed for the combinations of Disulfiram/Olaparib and Disulfiram/Niraparib. The combination of Disulfiram/Olaparib showed increasing CI values with increasing effect levels, while the CI values of the combination of Disulfiram/Niraparib were slightly varied with

increasing effect levels. This difference in CI values between Niraparib and Olaparib may be attributed to their chemical and physical properties. PARP inhibitors function by trapping PARP1 and PARP2 at DNA lesions, thus abolishing PARylation-mediated DNA damage repair. PARP–DNA complexes have the ability to interfere with DNA replication, and PARP trapping is important for the cytotoxicity of PARP inhibitors. This explains the different magnitude of cytotoxicity exerted by different PARP inhibitors (32, 33).

The combination of Disulfiram and PARPis also increased SKOV3 cell apoptosis. Moreover, a dramatic increase in γH2AX expression level and PARP cleavage in the presence of Disulfiram and PARPis suggest that they work synergistically to cause DNA damage. The combination of Disulfiram with Niraparib suppressed ES-2-derived xenograft tumors *in vivo*, further supporting their synergetic effects. Disulfiram also downregulated the expression of some homologous recombination repair-related genes, such as *BRCA1*, *BRCA2*, *RAD51*, *RAD52*, *ATR*, *ATM*, and *PALB2* in SKOV3, ES-2, OVCA420, and HeyA8 cells (34). Since Disulfiram alone caused no obvious DNA damage (35), these results support that Disulfiram might induce its toxitcity through PARPis in their combnation. In fact, previous work proposed that the anti-cancer activity of Disulfiram was mediated through PARP cleavage, although other mechanisms were proposed as well (36, 37).
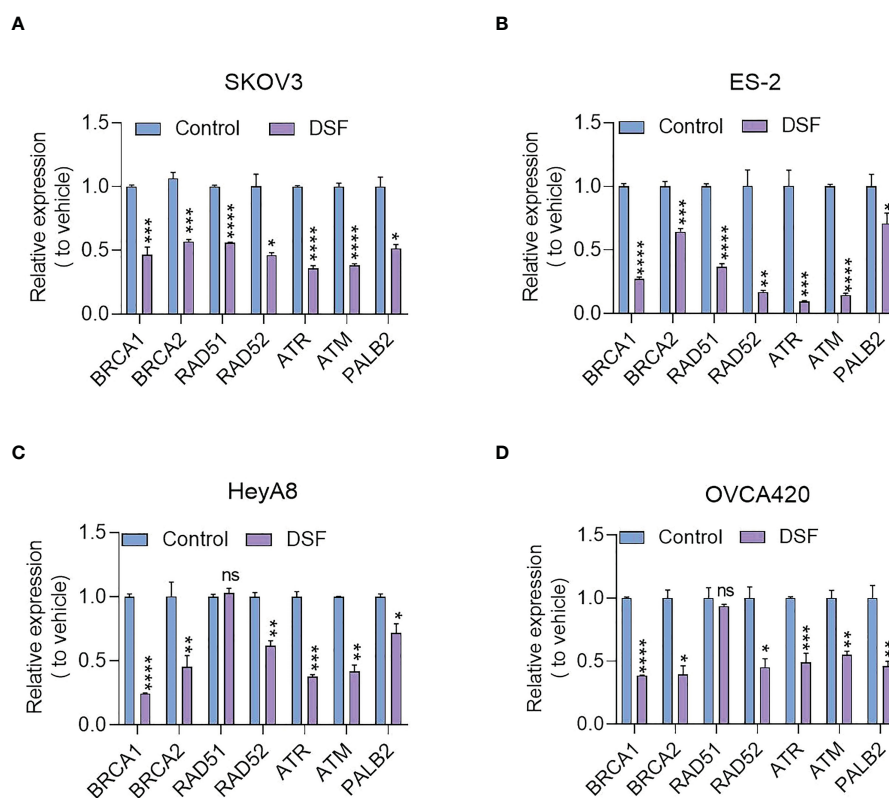
FIGURE 5
Effect of Disulfiram on expression of HRR-related genes in SKOV3 (A), ES-2 (B) HeyA8 (C), and OVCA420 cells (D). The fold-change of inhibition after Disulfiram treatment was plotted in comparison to the control (blue). Each gene is denoted in the Figure. Experiments were repeated three times and represented as mean $\pm$ SD. Unpaired t-test, ns, no significant difference; *$P<0.05$, **$P<0.01$, ***$P<0.001$, ****$P<0.0001$.
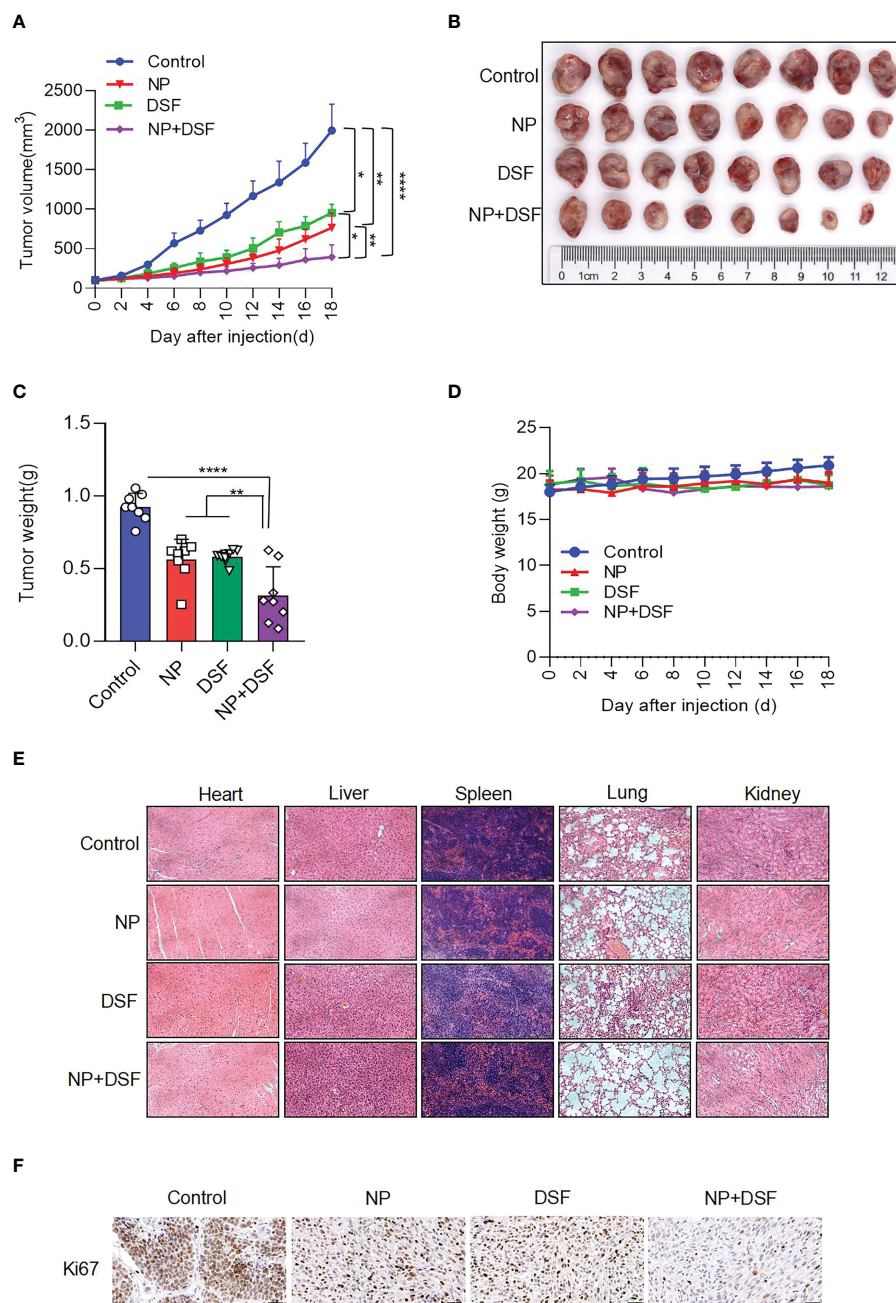
FIGURE 6

Disulfiram combined with Niraparib suppresses ES-2-derived xenograft tumors *in vivo*. Female nude mice bearing ES-2-derived tumors were randomized into four treatment groups: DMSO, Disulfiram (DSF, 50 mg/kg, daily by i.p.), Niraparib (NP, 50 mg/kg, daily by i.p.), and NP+DSF. After 18 days of treatment **(A)** tumor volumes were measured every 2 days. **(B, C)**. The tumors were photographed and weighed. **(D)** Body weight change was measured **(E)**. HE staining of the heart, liver, lung, kidney, and spleen from the four groups. **(F)** IHC staining of Ki67. Scale bars, 50 μm. *$P<0.05$; **$P<0.01$; ****$P<0.0001$.

Because Disulfiram synergistically enhanced the activity of PARPis and affected the genes and proteins associated with DNA damage, we propose that Disulfiram reinforces the activity of PARPis. This reinforcement could be realized by Disulfiram and PARPis individually or through their interaction. It was recently reported that small-molecule p97-complex inhibitors, including a metabolite of Disulfiram, prolonged PARP1 trapping (preventing DNA repair leading to cell death) and enhanced PARP inhibitor-induced cytotoxicity in homologous recombination-defective tumor cells

and patient-derived tumor organoids (38, 39). The work proposed that p97 ATPase plays a key role in the processing of trapped PARP1 and the response of tumor cells to PARP inhibitors. Therefore, Disulfiram might increase cell sensitivity to PARPis in a PARP1-dependent manner. Disulfiram likely enhances PARP inhibitor-induced cytotoxicity by inhibiting the normal function of p97 and thereby prolonging PARP1 trapping, which requires further experimentation (39). The variability of the ability of different PARP inhibitors to capture PARP1 (some PARP

inhibitors, such as Veliparib, attenuate the interaction between PARP1 and DNA) may explain the difference in the effects of Disulfiram in combination with different PAPR inhibitors (40). The combination of PARPis with other drugs has been suggested to improve anti-cancer efficacy in the clinic for ovarian cancer patients (41). We demonstrated that the combination of Disulfiram and PARP inhibitors expands therapeutic strategies for ovarian cancer patients.

Data availability statement

The original contributions presented in the study are included in the article/Supplementary Material. Further inquiries can be directed to the corresponding authors.

Ethics statement

All animals were obtained from the Animal Center of East China Normal University. Their care was in accordance with the guidelines of Animal Investigation Committee of the Institute of Biomedical Sciences, East China Normal University.

Author contributions

BT, MW and LZ contributed equally to this work. BT, LZ, SJ, SL, TL, SZ, LL and YW designed the experiments. BT, LZ, SJ, SL, TL, SZ, LL and YW performed the experiments. BT, LZ, SJ, SL and TL performed the data analysis. BT, LZ, SJ and SL wrote the

manuscript. All authors contributed to the article and approved the submitted version.

Conflict of interest

The authors declare that the research was conducted in the absence of any commercial or financial relationships that could be construed as a potential conflict of interest.

Publisher's note

All claims expressed in this article are solely those of the authors and do not necessarily represent those of their affiliated organizations, or those of the publisher, the editors and the reviewers. Any product that may be evaluated in this article, or claim that may be made by its manufacturer, is not guaranteed or endorsed by the publisher.

Supplementary material

The Supplementary Material for this article can be found online at: https://www.frontiersin.org/articles/10.3389/fonc.2023.1154073/full#supplementary-material

References

1. Vargas AN. Natural history of ovarian cancer. *Ecancermedicalscience* (2014) 8:465. doi: 10.3332/ecancer.2014.465

2. Cheung A, Shah S, Parker J, Soor P, Limbu A, Sheriff M, et al. Non-epithelial ovarian cancers: how much do we really know? *Int J Environ Res Public Health* (2022) 19(3):1-4. doi: 10.3390/ijerph19031106

3. Siegel RL, Miller KD, Fuchs HE, Jemal A. Cancer statistics, 2021. *CA: Cancer J Clin* (2021) 71(1):7–33. doi: 10.3322/caac.21654

4. Shah S, Cheung A, Kutka M, Sheriff M, Boussios S. Epithelial ovarian cancer: providing evidence of predisposition genes. *Int J Environ Res Public Health* (2022) 19 (13):1-5. doi: 10.3390/ijerph19138113

5. Curtin NJ, Szabo C. Poly(ADP-ribose) polymerase inhibition: past, present and future. *Nat Rev Drug Discovery* (2020) 19(10):711–36. doi: 10.1038/s41573-020-0076-6

6. Cass I, Roberts JNT, Benoit PR, Jensen NV. Multidisciplinary considerations in the maintenance treatment of poly(ADP-ribose) polymerase inhibitors for homologous recombination-proficient, advanced-stage epithelial ovarian cancer. *CA: Cancer J Clin* (2023) 73(1):8–16. doi: 10.3322/caac.21764

7. DiSilvestro P, Banerjee S, Colombo N, Scambia G, Kim BG, Oaknin A, et al. Overall survival with maintenance olaparib at a 7-year follow-up in patients with newly diagnosed advanced ovarian cancer and a BRCA mutation: the SOLO1/GOG 3004 trial. *J Clin Oncol* (2023) 41(3):609–17. doi: 10.1200/JCO.22.01549

8. Kummar S, Chen A, Ji J, Zhang Y, Reid JM, Ames M, et al. Phase I study of PARP inhibitor ABT-888 in combination with topotecan in adults with refractory solid tumors and lymphomas. *Cancer Res* (2011) 71(17):5626–34. doi: 10.1158/0008-5472.CAN-11-1227

9. Bendell J, O'Reilly EM, Middleton MR, Chau I, Hochster H, Fielding A, et al. Phase I study of olaparib plus gemcitabine in patients with advanced solid tumours and comparison with gemcitabine alone in patients with locally advanced/metastatic pancreatic cancer. *Ann Oncol* (2015) 26(4):804–11. doi: 10.1093/annonc/mdu581

10. Diéras V, Han HS, Kaufman B, Wildiers H, Friedlander M, Ayoub JP, et al. Veliparib with carboplatin and paclitaxel in BRCA-mutated advanced breast cancer (BROCADE3): a randomised, double-blind, placebo-controlled, phase 3 trial. *Lancet Oncol* (2020) 21(10):1269–82. doi: 10.1016/S1470-2045(20)30447-2

11. Johansson B. A review of the pharmacokinetics and pharmacodynamics of disulfiram and its metabolites. *Acta Psychiatr Scand Suppl* (1992) 369:15–26. doi: 10.1111/j.1600-0447.1992.tb03310.x

12. Lu C, Li X, Ren Y, Zhang X. Disulfiram: a novel repurposed drug for cancer therapy. *Cancer Chemother Pharmacol* (2021) 87(2):159–72. doi: 10.1007/s00280-020-04216-8

13. Dufour P, Lang JM, Giron C, Duclos B, Haehnel P, Jaeck D, et al. Sodium dithiocarb as adjuvant immunotherapy for high risk breast cancer: a randomized study. *Biotherapy* (1993) 6(1):9–12. doi: 10.1007/BF01877380

14. Greco WR, Bravo G, Parsons JC. The search for synergy: a critical review from a response surface perspective. *Pharmacol Rev* (1995) 47(2):331–85.

15. He XL, Xing Y, Gu XZ, Xiao JX, Wang YY, Yi Z, et al. The synthesis and antitumor activity of lithocholic acid and its derivatives. *Steroids* (2017) 125:54–60. doi: 10.1016/j.steroids.2017.06.009

16. Chen H, Bian A, Yang LF, Yin X, Wang J, Ti C, et al. Targeting STAT3 by a small molecule suppresses pancreatic cancer progression. *Oncogene* (2021) 40(8):1440–57. doi: 10.1038/s41388-020-01626-z

17. Chou TC. Theoretical basis, experimental design, and computerized simulation of synergism and antagonism in drug combination studies. *Pharmacol Rev* (2006) 58 (3):621–81. doi: 10.1124/pr.58.3.10

18. Cong X, He Y, Wu H, Wang D, Liu Y, Shao T, et al. Regression of castration-resistant prostate cancer by a novel compound HG122. *Front Oncol* (2021) 11:650919. doi: 10.3389/fonc.2021.650919

19. Yan B, Ai Y, Zhang Z, Wang X. Assessing POR and CYB5R1 oxidoreductase-mediated oxidative rupture of PUFA in liposomes. *STAR Protoc* (2021) 2(1):100360. doi: 10.1016/j.xpro.2021.100360

20. Cortez AJ, Tudrej P, Kujawa KA, Lisowska KM. Advances in ovarian cancer therapy. *Cancer chemotherapy Pharmacol* (2018) 81(1):17–38. doi: 10.1007/s00280-017-3501-8

21. Bonner WM, Redon CE, Dickey JS, Nakamura AJ, Sedelnikova OA, Solier S, et al. GammaH2AX and cancer. *Nat Rev Cancer* (2008) 8(12):957–67. doi: 10.1038/nrc2523

22. Kinner A, Wu W, Staudt C, Iliakis G. Gamma-H2AX in recognition and signaling of DNA double-strand breaks in the context of chromatin. *Nucleic Acids Res* (2008) 36(17):5678–94. doi: 10.1093/nar/gkn550

23. Xing Y, Guo W, Wu M, Xie J, Huang D, Hu P, et al. An orally available small molecule BCL6 inhibitor effectively suppresses diffuse large b cell lymphoma cells growth *in vitro* and *in vivo. Cancer Lett* (2022) 529:100–11. doi: 10.1016/j.canlet.2021.12.035

24. Ghose A, Gullapalli SVN, Chohan N, Bolina A, Moschetta M, Rassy E, et al. Applications of proteomics in ovarian cancer: dawn of a new era. *Proteomes* (2022) 10 (2):2-6. doi: 10.3390/proteomes10020016

25. Torre LA, Trabert B, DeSantis CE, Miller KD, Samimi G, Runowicz CD, et al. Ovarian cancer statistics, 2018. *CA: Cancer J Clin* (2018) 68(4):284–96. doi: 10.3322/caac.21456

26. Konecny GE, Kristeleit RS. PARP inhibitors for BRCA1/2-mutated and sporadic ovarian cancer: current practice and future directions. *Br J Cancer* (2016) 115 (10):1157–73. doi: 10.1038/bjc.2016.311

27. Alvarez Secord A, O'Malley DM, Sood AK, Westin SN, Liu JF. Rationale for combination PARP inhibitor and antiangiogenic treatment in advanced epithelial ovarian cancer: a review. *Gynecologic Oncol* (2021) 162(2):482–95. doi: 10.1016/j.ygyno.2021.05.018

28. Haynes B, Murai J, Lee JM. Restored replication fork stabilization, a mechanism of PARP inhibitor resistance, can be overcome by cell cycle checkpoint inhibition. *Cancer Treat Rev* (2018) 71:1–7. doi: 10.1016/j.ctrv.2018.09.003

29. Revythis A, Limbu A, Mikropoulos C, Ghose A, Sanchez E, Sheriff M, et al. Recent insights into PARP and immuno-checkpoint inhibitors in epithelial ovarian cancer. *Int J Environ Res Public Health* (2022) 19(14):1-14 doi: 10.3390/ijerph19148577

30. Mansouri A, McGregor N, Dunn R, Dobbie S, Holmes J, Collins L, et al. Randomised phase II trial of olaparib, chemotherapy or olaparib and cediranib in patients with platinum-resistant ovarian cancer (OCTOVA): a study protocol. *BMJ Open* (2021) 11(1):e041463. doi: 10.1136/bmjopen-2020-041463

31. Meier S, Cantilena S, Niklison Chirou MV, Anderson J, Hargrave D, Salomoni P, et al. Alcohol-abuse drug disulfiram targets pediatric glioma *via* MLL degradation. *Cell Death Dis* (2021) 12(8):785. doi: 10.1038/s41419-021-04078-9

32. Viola-Rhenals M, Patel KR, Jaimes-Santamaria L, Wu G, Liu J, Dou QP. Recent advances in antabuse (Disulfiram): the importance of its metal-binding ability to its anticancer activity. *Curr medicinal Chem* (2018) 25(4):506–24. doi: 10.2174/0929867324666171023161121

33. Boussios S, Rassy E, Moschetta M, Ghose A, Adeleke S, Sanchez E, et al. BRCA mutations in ovarian and prostate cancer: bench to bedside. *Cancers* (2022) 14(16):2-16. doi: 10.3390/cancers14163888

34. Marzio A, Puccini J, Kwon Y, Maverakis NK, Arbini A, Sung P, et al. The f-box domain-dependent activity of EMI1 regulates PARPi sensitivity in triple-negative breast cancers. *Mol Cell* (2019) 73(2):224–237.e226. doi: 10.1016/j.molcel.2018.11.003

35. Li Z, Xie X, Tan G, Xie F, Liu N, Li W, et al. Disulfiram synergizes with SRC inhibitors to suppress the growth of pancreatic ductal adenocarcinoma cells *in vitro* and *in vivo. Biol Pharm Bull* (2021) 44(9):1323–31. doi: 10.1248/bpb.b21-00353

36. Ekinci E, Rohondia S, Khan R, Dou QP. Repurposing disulfiram as an anti-cancer agent: updated review on literature and patents. *Recent patents anti-cancer Drug Discovery* (2019) 14(2):113–32. doi: 10.2174/1574892814666190514104035

37. Oltersdorf T, Elmore SW, Shoemaker AR, Armstrong RC, Augeri DJ, Belli BA, et al. An inhibitor of bcl-2 family proteins induces regression of solid tumours. *Nature* (2005) 435(7042):677–81. doi: 10.1038/nature03579

38. Götz MJ, Stingele J. Releasing the trap: how the segregase p97 extracts PARP1 from chromatin. *Mol Cell* (2022) 82(5):889–90. doi: 10.1016/j.molcel.2022.02.012

39. Krastev DB, Li S, Sun Y, Wicks AJ, Hoslett G, Weekes D, et al. The ubiquitin-dependent ATPase p97 removes cytotoxic trapped PARP1 from chromatin. *Nat Cell Biol* (2022) 24(1):62–73. doi: 10.1038/s41556-021-00807-6

40. Zandarashvili L, Langelier MF, Velagapudi UK, Hancock MA, Steffen JD, Billur R, et al. Structural basis for allosteric PARP-1 retention on DNA breaks. *Sci (New York NY)* (2020) 368(6486):2-16 doi: 10.1126/science.aax6367

41. Mittica G, Ghisoni E, Giannone G, Genta S, Aglietta M, Sapino A, et al. PARP inhibitors in ovarian cancer. *Recent patents anti-cancer Drug Discovery* (2018) 13 (4):392–410. doi: 10.2174/1574892813666180305165256

Olaparib and advanced ovarian cancer: Summary of the past and looking into the future

Brigida Anna Maiorano[1,2], Mauro Francesco Pio Maiorano[3]* and Evaristo Maiello[1]

[1]Oncology Unit, Foundation Casa Sollievo della Sofferenza IRCCS, San Giovanni Rotondo, Italy,
[2]Department of Translational Medicine and Surgery, Catholic University of the Sacred Heart, Rome, Italy,
[3]Division of Obstetrics and Gynecology, Biomedical and Human Oncological Science, University of Bari "Aldo Moro", Bari, Italy

Ovarian cancer (OC) is women's eighth most common cancer, bearing the highest mortality rates of all female reproductive system malignancies. Poly (ADP-ribose) polymerase inhibitors (PARPis) have reshaped the treatment scenario of metastatic OC as a maintenance post platinum-based chemotherapy. Olaparib is the first PARPi developed for this disease. Results from Study 42, Study 19, SOLO2, OPINION, SOLO1, and PAOLA-1 clinical trials, led to the FDA and EMA approval of olaparib for the maintenance treatment of women with high-grade epithelial ovarian, fallopian tube, or primary peritoneal cancer without platinum progression: in the platinum-sensitive recurrent OC; in the newly diagnosed setting in case Breast Cancer (BRCA) mutations and, in combination with bevacizumab, in case of BRCA mutation or deficiency of homologous recombination genes. In this review, we synthetized olaparib's pharmacokinetic and pharmacodynamic properties and its use in special populations. We summarized the efficacy and safety of the studies leading to the current approvals and discussed the future developments of this agent.

KEYWORDS

olaparib (Lynparza™), PARP, ovarian cancer, BRCA, target therapy

1 Introduction

With an incidence of 8.1 cases/100,000 inhabitants/year, ovarian cancer (OC) is the eighth most common cancer among women worldwide. It accounts for more deaths than any other malignancy of the female reproductive system, bearing a mortality rate of 5.4 deaths/ 100,000 inhabitants/year. Most OC cases are diagnosed as metastatic (57%), with a 5-year survival rate of only 30.8% (Siegel et al., 2022; Cancer stat facts: ovarian cancer, 2023). Platinum-based chemotherapy (CHT) represents the first choice in the metastatic setting of OC. However, despite initial benefits, over 2 out of 3 patients will relapse within the first 2 years (McGuire et al., 1996; Neijt et al., 2000; Piccart et al., 2000; Ozols et al., 2003; Armstrong et al., 2006; Kehoe et al., 2015; Walker et al., 2019). Poly-(ADP-ribose)-polymerase (PARP) inhibitors (PARPis) are a class of antitumor agents whose mechanism of action relies on the exploitation of the defective DNA repair pathways in Breast Cancer (BRCA) mutant and Homologous Recombination (HR) repair genes deficient (HRD) cells, a group of crucial genes for double-stranded breaks (DSBs) and interstrand crosslinks (ICLs) repairing pathways, a process notably known as "synthetic lethality" (Farmer et al., 2005; Lord and Ashworth, 2012). Of note, half of all OCs are associated with HRD, and 22% of cases bear a germline or somatic mutation of BRCA1 and BRCA2, thus indicating the use of PARPis as a possible target therapy for OC (The Cancer Genome Atlas Research Network,

TABLE 1 Pharmacokinetics and pharmacodynamics of olaparib.

	Dose (mg)	Cmax (ng/mL)	Tmax (h)	T1/2 (h)	IC50 (nM)	Metabolism	Cytocrome metabolism
Olaparib	300/12 h	7,700	1.5	11.9	PARP1: 5, PARP2: 1, PARP3: 4, PARP5a: 1500	Liver (42% recovered in feces), kidney (44% recovered in urine)	CYP 3A4/5 with 3 metabolites: M12 (ring opened hydroxy-cyclopropyl), M15 (mono-oxygenated), M18 (dehydrogenated piperazine)
	400/12 h	9,300	2				

CYP3A4/5, cytochrome P 3A4/5; PARP1/2/3, Poly (ADP-ribose) polymerase 1/2/3.

2011). Olaparib (LYNPARZA®, AstraZeneca Pharmaceuticals LP), a potent inhibitor of human PARP-1, PARP-2, and PARP-3, is historically the first PARPi developed and approved for the clinical use of metastatic OC. Currently, olaparib is approved in USA and EU for the maintenance treatment of women with high-grade (HG) epithelial ovarian, fallopian tube, or primary peritoneal cancer, if BRCA1/2-mutated (germline or somatic) in the first line, or platinum-sensitive relapsed OC (PS-ROC), after any response (complete or partial) to platinum-based CHT. In combination with bevacizumab, olaparib is approved in case of HRD after any response to platinum-based CHT (FDA approved Olaparib, 2019; EMA Olaparib product information, 2023).

In our review, we aimed to summarize the pharmacological properties, therapeutic efficacy, and tolerability of olaparib, examining its role and use in treating advanced OC.

2 Pharmacodynamic properties of olaparib

In vitro, olaparib inhibits PARP-1, -2, and -3 with IC50 5, 1, and 4 nM, respectively. It also has weak activity against PARP-5a (tankyrase 1 [TNKS1]) with IC50 1,500 nM (Committee for Medicinal Products for Human, 2014; US Food and Drug Administration FDA, 2014; McCormick et al., 2018; Zhou et al., 2019) (Table 1).

Similarly to other PARPis, olaparib acts through the mechanism of "synthetic lethality," as it inhibits PARP enzymes, causing the accumulation of DNA damage. In the case of HRD, this inhibition leads to apoptosis. Moreover, olaparib causes cytotoxic and pro-apoptotic PARP-DNA trapping. In pre-clinical models, these effects seemed additive or synergistic with the cytotoxicity exerted on DNA by chemotherapeutic agents, with even more contribution to DNA fragmentation and cell apoptosis than olaparib alone (McCormick et al., 2018). Among resistance mechanisms, BRCA reversion mutations that restore the HR function are the main findings in olaparib-resistant cells. Moreover, the occurrence of somatic mutations which restore the open reading frame of HRR genes, defects in non-homologous end-joining, increased drug efflux [e.g., with mutations of P-glycoprotein (P-gp)], or loss of 53BP1, have been found (Noordermeer and van Attikum, 2019).

3 Pharmacokinetic properties of olaparib

At the daily dosage of 600 mg tablets divided into two administrations (BID), olaparib's mean maximum plasma concentration (Cmax) is 7,700 ng/mL, reached in a median time

(Tmax) of 1.5 h, and the half-life is 14.9 h. Olaparib is available as capsules or tablets. The two formulations are not equivalent: as evidenced by different studies, the 300 mg tablets had a 13% higher mean relative exposure at the steady state than the 400 mg capsules. In the case of 400 mg BID, Cmax is around 9,300 ng/mL, and Tmax is around 2 h (Dean et al., 2012; Yamamoto et al., 2012; Mateo et al., 2016; Yonemori et al., 2016; Plummer et al., 2018; Yuan et al., 2019) (Table 1). Cytochromes P450 (CYP)3A4 and -5 mainly metabolize olaparib, forming three principal metabolites: M12 (ring opened hydroxy-cyclopropyl) M15 (mono-oxygenated), and M18 (dehydrogenated piperazine), with the potency to inhibit the growth of BRCA1-mutant cells and PARP-1 30-fold, 30-fold and 4-fold lower than olaparib, respectively (Committee for Medicinal Products for Human, 2014). The use of potent inhibitors of CYP3A, such as clarithromycin, erythromycin, diltiazem, itraconazole, ketoconazole, ritonavir, verapamil, goldenseal, and grapefruit, increases the Cmax of olaparib of 42% [90% confidence interval (CI), 33%–52%] and the median area under the curve (AUC) of 170% (90% CI, 144%–197%). Thus, co-administration is not recommended unless the dose of olaparib is reduced to 100 mg or 150 mg BID if a potent or moderate inhibitor is used, respectively. Olaparib also weakly inhibits CYP3A4 *in vitro* and CYP3A *in vivo*, thus possibly increasing the exposure to CYP3A substrates, which could be important for drugs with a narrow therapeutic window, such as simvastatin, cisapride, ciclosporin, ergotamine alkaloids, fentanyl, pimozide, sirolimus, tacrolimus e quetiapine. Furthermore, it has been demonstrated that the use of potent inducers of CYP3A, such as apalutamide, carbamazepine, enzalutamide, fosphenytoin, lumacaftor, lumacaftor-ivacaftor, mitotane, phenobarbital, phenytoin, primidone, rifampin (rifampicin) and St. John's wort might substantially decrease olaparib efficacy, reducing its median Cmax of 71% (90% CI, 76%–67%) and the median AUC of 87% (90% CI, 89%–84%); thus the co-administration should be avoided. The efficacy of hormonal contraceptives might be reduced, as olaparib slightly induces CYP1A2 and 2B6 *in vitro*. The liver metabolizes olaparib: after the drug administration, 44% is recovered in urine (of which 15% is unaltered, M15 representing the main metabolite) and 42% in feces (6% unaltered, M12 and M15 being among the most abundant metabolites) (Table 1) (Ang et al., 2010; Dean et al., 2012; Yamamoto et al., 2012; Committee for Medicinal Products for Human, 2014; Mateo et al., 2016; Yonemori et al., 2016; Plummer et al., 2018; Rolfo et al., 2019; Yuan et al., 2019).

4 Olaparib in special populations

4.1 Renal and liver impairment

In patients with renal impairment, olaparib pharmacokinetic properties are altered, significantly increasing AUC and Cmax.

TABLE 2 Summary of studies employing Olaparib as maintenance in advanced OC.

Study name (NCT)—year	Phase	Target population (number of pts)	Olaparib dosage	Comparative arm	Primary EP	Results
Maintenance in advanced gBRCAm OC after 3 or more lines of chemotherapy						
Study 42 (NCT01078662) - 2010 Domchek et al., (2016); Matulonis et al., (2016)	II	gBRCAm tumors (n = 298) 3 or more prior lines of CHT (n = 137) PS (n = 39) PRes (n = 81) PRef (n = 14)	400 mg BID	—	ORR mDoR	Overall
						ORR 34% (95% CI, 26%–42%)
						2 CRs (2%)
						44 PRs (32%)
						mDoR 7.9 months (95% CI, 5.6–9.6 months)
						mPFS 6.7 months (95% CI, 5.5–7.6 months)
						PS
						ORR 46% (95% CI, 30%–63%) mDoR 8.2 months (95% CI, 5.6–13.5 months)
						PFS 9.4 months (95% CI, 6.7–11.4 months)
						PRes
						ORR 30% (95% CI, 20%–41%) mDoR 8.0 months (95% CI, 4.8–14.8 months)
						PRef
						ORR 14% (95% CI, 2%–43%) mDoR 6.4 months (95% CI, 5.4–7.4 months)
						PFS 5.5 months (95% CI, 4.2–6.7 months)
Maintenance in PS-ROC						
Study 19 (NCT00753545) - 2012 Ledermann et al., (2012)	II	PS-ROC (n = 265)	400 mg BID	PBO	PFS	Overall
		O group (n = 136)				PFS 8.4 months vs. 4.8 months (HR 0.35; 95% CI, 0.25–0.49; p < 0.001)
		PBO group (n = 129)				OS 29.8 months v. 27.8 months (HR 0.88; p = 0.44)
		g/sBRCAm (screened n = 254)				BRCAm
		O (n = 74, 56%)				PFS 11.2 months vs. 4.3 months (HR 0.18; 95% CI, 0.10–0.31; p < 0.0001)
		PBO (n = 62, 50%)				OS 34.9 months vs. 31.9 months (HR 0.73; p = 0.19)
SOLO2/ENGOT-Ov21 (NCT01874353)— 2013 Pujade-Lauraine et al., (2017); Poveda et al., (2021)	III	PS-ROC g/sBRCAm (n = 294)	300 mg BID	PBO	PFS	PFS 19.1 mos vs. 5.5 months (HR 0.30; 95% CI, 0.22–0.41; p < 0.0001)
		O group (n = 195)				
		PBO (n = 99)				
OPINION (NCT03402841) - 2018 Poveda et al., (2022)	IIIb	PS-ROC gBRCAwt (n = 279)	300 mg BID	-	PFS	Overall PFS 9.1 mos tBRCAm PFS 16.4 months

TABLE 2 (*Continued*) Summary of studies employing Olaparib as maintenance in advanced OC.

Study name (NCT)—year	Phase	Target population (*number of pts*)	Olaparib dosage	Comparative arm	Primary EP	Results
		Biomarker status tBRCAm (*n* = 27)				HRD + including BRCAm PFS 11.1 mos
		tBRCAwt (*n* = 232)				HRD + excluding BRCAm PFS 9.7 months
		HRD+ (*n* = 94)				HRD- PFS 7.3 months
First-line maintenance in newly diagnosed OC						
SOLO1/GOG 3004 (NCT01844986) - 2013 Moore et al., (2018)	III	First-line advanced g/sBRCAm OC after CR or PR to CHT (*n* = 391)	300 mg BID	PBO	PFS	PFS 56 months vs. 13.8 months (HR 0.30; 95% CI, 0.23–0.41; *p* < 0.001)
		O group (*n* = 260)				PFS2 NR vs. 41.9 months (HR 0.50; 95% CI, 0.35–0.72; *p* < 0.001) mOS NR vs. 75.2 months (HR 0.55; 95% CI, 0.40–0.76; *p* = 0.0004)
		PBO group (*n* = 131)				
PAOLA-1/ENGOT-ov25 (NCT02477644) - 2015 Ray-Coquard et al. (2019)	III	First-line advanced OC after CR or PR to CHT (*n* = 806)	300 mg BID plus bevacizumab 15 mg/kg q3w for 15 months	PBO + B	PFS	Overall HR for PFS 0.60 (95% CI, 0.49–0.74)
		O + B (*n* = 537)				HiR group
		PBO + B (*n* = 269)				Overall
		HiR group (74%)				PFS 20.3 months vs. 14.7 months (HR 0.60; 95% CI, 0.49–0.74)
						BRCAm
		LoR group (26%)				PFS US vs. 19.4 months (HR 0.37; 95% CI, 0.23–0.59)
						HRD+ (including BRCAm)
						PFS US vs. 16.0 months (HR 0.39; 95% CI, 0.28–0.54)
						HRD-PFS 15.6 vs. 13.8 months (HR 0.93; 95% CI, 0.68–1.30)
						LoR group
						Overall
						PFS US vs. 22.9 months (HR 0.46; 95% CI, 0.30–0.72)
						BRCAm
						PFS 29.2 months vs. 22.9 months (HR0.11; 95% CI, 0.03–0.31)
						HRD+
						PFS NR vs. 22.1 mos (HR 0.15; 95% CI, 0.07–0.30)

B, bevacizumab; BID, twice a day; BRCA, breast cancer gene; BRCAm, mutated BRCA; BRCAwt, BRCA, wild-type; CHT, chemotherapy; CI, confidence interval; CR, complete response; EP, endpoint; g/s/tBRCAm, germline/somatic/tumor-associated BRCA mutation; HiR, higher risk [subgroup]; HR, hazard ratio; HRD, homologous recombination deficiency [genes]; LoR, lower risk [subgroup]; mos, months; NR, not reached; O, olaparib [arm]; OC, ovarian cancer; OS, overall survival; PBO, placebo [arm]; PFS, progression-free survival; PR, partial response; PRes, platinum resistant; PRef, platinum refractory; PS, platinum sensitive; PS-ROC, platinum sensitive - recurrent ovarian cancer; q3w, once every 3 weeks; US, unstable; vs., *versus*.

Therefore, a higher exposure might eventually increase toxicity. In clinical studies, no relevant increase in exposure to olaparib was found in case of mild renal impairment. In the NCT01894256 phase I trial, patients received olaparib if they had normal renal function or mild to moderate renal impairment. In patients with moderate reduction of renal function, exposure to olaparib could increase

up to 44%; therefore, dose adjustments (e.g., 200 mg twice daily) should be used. In case of severe renal dysfunction, without specific evidence, it is not safe to recommend olaparib (Rolfo et al., 2019).

On the contrary, hepatic dysfunction did not alter olaparib pharmacokinetics, therefore not requiring dose adjustments, except in patients with severe liver impairment, for which no dedicated studies exist; hence, olaparib should not be recommended (Rolfo et al., 2020).

4.2 Older patients

Although most OCs develop after age 65, only around 1 out of 3 patients is aged ≥65 in the major clinical trials of olaparib. In an ancillary analysis of ≥65 patients included in olaparib trials, no differences in adverse events (AEs), even those of severe grade, were detected between the older and the younger patients. The discontinuation rate of the two groups stood around 44.7%–64.7% of patients but was not significantly different between the age subgroups (Dockery et al., 2017). We recently performed a meta-analysis, showing no differences in efficacy between older and younger patients, both with single agents and in combination with bevacizumab. Moreover, no increased risk of hematologic toxicity emerged in ≥65 women (Maiorano et al., 2022a). However, only SOLO1, SOLO2, and PAOLA-1 trials published data explicitly focusing on older patients (Moore et al., 2018; Ray-Coquard et al., 2019; Trillsch et al., 2020). Therefore, even if the evidence did not limit the use of full-dose olaparib in the old population, considering the high median age at diagnosis of mOC and the aging population in the next years, trials explicitly focusing on the elder age subgroups should be designed.

5 Therapeutic efficacy of olaparib

5.1 Advanced BRCA mutant OC after 3 or more lines of chemotherapy

In December 2014, the FDA approved olaparib for treating women with deleterious or suspected deleterious gBRCAm advanced OC who have been previously treated with three or more lines of chemotherapy, based on the results of the phase II trial Study 42 (NCT01078662). The study treated 298 germline BRCA mutant (gBRCAm) cancers, of whom 193 (65%) had OC, with olaparib. They had received at least three lines of CHT, with 39 patients defined as platinum-sensitive (PS), 81 platinum-resistant (PRes), and 14 platinum-refractory (PRef) if the time from completion of last platinum CHT to study start was >6 months, <6 months or <2 months and progressive disease (PD) was the best response to last platinum, respectively. There was no prespecified primary endpoint, but the overall response rate (ORR) and median duration of response (mDoR) were collected first. The overall ORR was 34%. The PS subgroup reached the highest ORR (46%) while in the PRes group, ORR was 30%. The lowest ORR was reached by the PRef subgroup (14%). mPFS was 6.7 months, ranging from 5.5 to 9.4 months in the PRes and the PS groups, respectively (Domchek et al., 2016; Matulonis et al., 2016) (Table 2).

5.2 Maintenance treatment of recurrent ovarian cancer after complete or partial response to platinum-based chemotherapy

Olaparib is currently indicated for the maintenance treatment of adult patients with recurrent OC in complete or partial response to platinum-based CHT after FDA approval in August 2017 based on Study 19, SOLO2, and OPINION trials (Ledermann et al., 2012; Pujade-Lauraine et al., 2017; LaFargue et al., 2019; Poveda et al., 2021; Poveda et al., 2022).

Study 19 (NCT00753545) was a randomized, phase II study to evaluate maintenance therapy with olaparib in patients with PS-ROC after receiving two or more platinum-based regimens. A pre-planned retrospective analysis of the BRCAm population was later performed and included (Ledermann et al., 2014). The primary endpoint was PFS—by overall population and by BRCA status. 265 patients were enrolled to receive olaparib (n = 136) or placebo (PBO—n = 129). A significantly longer PFS was observed with olaparib than PBO: mPFS in the overall population was 8.4 *versus* 4.8 months. In the BRCAm population, the benefit of olaparib over PBO was even more remarkable, with mPFS of 11.2 *versus* 4.3 months, if compared with BRCA wild type (BRCAwt) population, reaching an mPFS of 7.4 *versus* 5.5 months. No significant differences in terms of overall survival (OS) emerged. Of note, although the authors did not pre-plan the analysis, efficacy data seemed consistent with the hypothesis that olaparib is effective irrespectively of germline or somatic mutation of BRCA (Domchek et al., 2016; Matulonis et al., 2016).

In the randomized, double-blind, phase III study SOLO2/ENGOT-Ov21 (NCT01874353), evaluating olaparib maintenance in PS-ROC with somatic or germline BRCAm, 294 patients were randomized to olaparib (n = 195) or PBO (n = 99). The study met its primary endpoint, as PFS was significantly longer in the olaparib subgroup: indeed, mPFS was 19.1 *versus* 5.5 months. The OS data, although immature, showed no detrimental survival for patients receiving olaparib (Pujade-Lauraine et al., 2017; Poveda et al., 2021).

279 patients with gBRCAwt, PS-ROC were enrolled in the phase IIIb OPINION trial (NCT03402841) to receive olaparib. At screening, 264 (94.6%) patients presented gBRCAwt. Retrospective analyses of somatic BRCA mutations also resulted in 37 (13.3%) patients bearing a BRCA mutation, 27 of which had a sBRCAm (9.7%) and 6 (2.2%) with a gBRCAm. Furthermore, among the 232 (83.2%) non-tBRCAm patients - namely, patients not bearing deleterious or suspected deleterious sBRCAm, 94 resulted in HRD (33.7%). 165 (59.1%), 84 (30.1%). PFS was the primary endpoint, while mPFS according to biomarker status (e.g., HRD and tBRCAm), and the number of prior lines of treatment, were secondary endpoints. The overall mPFS was 9.2 months. In the tBRCAm subgroup, mPFS was 16.4 months mPFS was 11.1 months in the HRD group including BRCAm, 9.7 months in the HRD excluding BRCAm, and 7.3 months in the HR proficient (HRP) subgroup. Although the study lacked a PBO comparator group that could quantify the magnitude of olaparib benefit in terms of PFS, it demonstrated the activity of maintenance olaparib in the context of PS-ROC, regardless of HRD or BRCA status (Poveda et al., 2022).

5.3 First-line maintenance treatment of either BRCAm or HRD-positive advanced ovarian cancer

Olaparib is also indicated, in combination with bevacizumab, for the maintenance treatment of women with advanced OC after CR or PR to first-line platinum-based CHT, bearing HRD and/or BRCA mutation (Arora et al., 2021). FDA approved in December 2018, based on the pivotal results of the randomized, phase III clinical trial SOLO1/GOG 3004, employing olaparib (n = 260) *versus* PBO (n = 131). The primary endpoint was PFS, while the second-interval PFS (PFS2) and OS were secondary endpoints. 5-year PFS rate was 60% in the olaparib and 27% in the PBO group, mPFS was 56 months in the olaparib *versus* 13.8 months in the PBO group. PFS2 rate was 75% in the olaparib and 60% in the PBO group, and mPFS2 was NR in the olaparib and 41.9 months in the PBO group. The OS analysis was recently updated after a 7-year follow-up, showing that 67.0% of patients in the olaparib group were still alive compared with 46.5% in the PBO group. (Moore et al., 2018; DiSilvestro et al., 2023).

Furthermore, in the phase III PAOLA-1/ENGOT-ov25 trial (NCT02477644), 806 patients with advanced newly diagnosed advanced OC, with CR or PR to platinum-based CHT, were randomized to receive olaparib plus bevacizumab (n = 537) or PBO plus bevacizumab (n = 269). In this analysis, patients were divided into a higher-risk subgroup (HiR—74%) in case of surgery performed on a FIGO stage III disease with residual disease or neoadjuvant chemotherapy administered or FIGO stage IV disease, and a lower-risk subgroup (LoR—26%), with radical surgery performed on a FIGO stage III disease. BRCA status was assessed only on tumor samples; thus, germline BRCA status was unknown. After a median follow-up of 22.9 months, PFS favored the olaparib plus bevacizumab group in both risk subgroups, thus confirming the benefit of olaparib as in SOLO1, and showing, in addition, the efficacy of the combination with bevacizumab. In fact, based on the PAOLA-1 results, the combination was approved by FDA in May 2020. In the HiR subgroup, mPFS was 20.3 *versus* 14.7 months. In the LoR subgroup, HR for PFS was 0.46 in the olaparib plus bevacizumab group. At the same time, the mPFS was inestimable in the olaparib plus bevacizumab group *versus* 22.9 months in the PBO group. Among the HiR BRCAm patients, mPFS was inestimable for the olaparib plus bevacizumab group *versus* 19.4 months in the PBO group, while in the lower-risk mBRCA patients, mPFS was 29.2 *versus* 22.9 months. In HRD patients mPFS was not estimable *versus* 16.0 months in the HiR subgroup, while in the LoR subgroup, mPFS was NR vs 22.1 months. Considering the HiR HRP patients, mPFS was 15.6 *versus* 13.8 months. No benefit in terms of PFS among LoR HRP patients derived from olaparib plus bevacizumab. PAOLA-1 was more representative of advanced OC patients than SOLO1, as patients' selection was not based on BRCA status. The PFS benefit observed with olaparib plus bevacizumab in patients with tBRCAm tumors in the PAOLA-1 appears consistent with the SOLO-1 results, supporting the efficacy of olaparib in BRCAm tumors regardless of somatic or germline mutation origin (Ray-Coquard et al., 2019; González-Martín et al., 2022; Harter et al., 2022).

6 Tolerability of olaparib

Hematological toxicities are common class effects of PARPis, representing the most common cause of dose modification, interruption, and discontinuation. They tend to occur early after treatment start and to recover after a few months. Anemia, usually the most common among haematologic AEs, might be related to PARP2 inhibition that affects the differentiation of erythroid progenitors, reducing erythrocytes' life expectancy in mice, even if erythropoietin plasma concentrations are increased, thus suggesting that supplementation might not be the best therapeutic option to manage anemia in these patients. On the contrary, transfusions are generally recommended for symptomatic anemia and hemoglobin values less than 7 g/dL. A baseline blood count should be obtained before starting olaparib and monitored monthly, at least during the first year of treatment. Olaparib should not be restarted if hematologic toxicity results > G1 (e.g., haemoglobin<10 g/dL, neutrophils <1,500/mm^3, platelets <75,000/mm^3) from previous therapy (Committee for Medicinal Products for Human, 2014; US Food and Drug Administration FDA, 2014; EMA Olaparib product information, 2023). A bone marrow analysis is recommended if severe hematologic toxicity lasts over 4 months. As the fundamental mechanism of PARP inhibition is interfering with DNA repair pathways, another severe class effect, although rare, is the onset of secondary malignancies, namely, myelodysplastic syndrome (MDS) and acute myeloid leukemia (AML), with an incidence of 0.5%–1.4%, usually after long-term treatment. The true incidence of SPMs after PARPis is difficult to estimate, as almost all patients also received other DNA-damaging drugs, such as platinum-based CHT (LaFargue et al., 2019). The risk of developing new second primary malignancies (SPMs), reported in 0.7%–2% of patients in the SOLO2, OPINION, SOLO1, and PAOLA-1—especially breast, thyroid, and rectal cancers, was not found to be increased in the olaparib group in a recent meta-analysis of 23 randomized clinical trials, thus suggesting no additional close monitoring of patients treated with PARPis. Among 8,857 patients included in the analysis, 51 SPMs were reported in the PARPis (0.9%) and 24 in the PBO group (0.7%). PARPis exposure was not associated with an increased risk of developing SPM *versus* PBO (p = 0.62) after up to 78 months of follow-up (Pujade-Lauraine et al., 2017; Moore et al., 2018; Ray-Coquard et al., 2019; Morice et al., 2021; Poveda et al., 2021; Poveda et al., 2022).

Gastrointestinal toxicities are also very commonly associated with PARPis, and patients should be aware of the high incidence of nausea to prevent its occurrence prophylactically. To lessen symptoms, daily prokinetic and antihistamine drugs can be administered. Persistent nausea or vomiting can be managed using various antiemetic drugs, such as metoclopramide, prochlorperazine, phenothiazine, dexamethasone, olanzapine, haloperidol, or lorazepam. The neurokinin-1 receptor antagonist, aprepitant, should be avoided with olaparib since it strongly inhibits CYP3A4, thus affecting olaparib plasma concentrations. Fatigue and asthenia also seem to be a class effect and can be managed using non-pharmacological approaches, such as exercise, massage therapy, and cognitive and behavioral therapy. The use of psychostimulants such as methylphenidate and ginseng is currently being investigated. Of note, it is confirmed by several

animal studies that olaparib is embryo-toxic and teratogenic and, thus, should be avoided during pregnancy. In addition, fertile women should avoid pregnancy during treatment and at least 6 months after olaparib stops and thus be counseled about birth control. Breastfeeding is also contraindicated during treatment and until 2–4 weeks after the last dose of olaparib (LaFargue et al., 2019). Analyzing the tolerability of olaparib as maintenance therapy in advanced OC, we found a median duration of treatment ranging from 5.6 to 22.6 months, while if considering the PBO arms, from 5.6 to 19.8 months. Almost every patient experienced any grade AEs, ranging from 95.6% to 99% of patients receiving olaparib and from 90.6% to 96% of patients in the PBO arms. Focusing on the olaparib arms, nausea was the most commonly reported all-grade AEs, ranging from 60% to 75.9%, followed by fatigue/asthenia (48.5%–64%), vomiting (22%–44%), diarrhea (14.3%–35%) while, among the haematologic toxicity, anemia was by far the most commonly reported, ranging from 16.9% to 43.6%. However, if considering only ≥ G3 AEs, reported by 29%–57% of patients treated with olaparib *versus* 19%–51% of patients receiving PBO, hematological toxicities were the most frequent, with ≥G3 anemia as the most common by far, ranging from 5.1% to 22%. Neutropenia ranged from 0% to 9%, and thrombocytopenia from 1% to 2.2%. ≥G3 fatigue ranged from 3.2% to 7.3%, and abdominal pain from 0% to 8%, while nausea, vomiting, and diarrhea were experienced only by less than 5% of patients. Anaemia was the most frequent AE that led to treatment discontinuation, which occurred in 2.2%–25% of patients receiving olaparib *versus* 0.7%–6% of the PBO group. AEs were managed with dose interruptions (27.9%–60% *versus* 8.6%–26%) or reductions (22%–41% *versus* 3%–7%) rather than discontinuation.

Considering the safety data from olaparib studies, we found that, in Study 42, the median treatment duration was 168 days 43% of dose interruptions were reported, 22% of dose reductions and 5% of patients discontinued treatment. 98% of patients experienced AEs of any grade, while 55% experienced ≥ G3 AEs. The most common any-grade AEs were nausea (60%), fatigue (55%), vomiting (44%), anemia (34%), abdominal pain (29%), and diarrhea (30%), while the most common ≥ G3 AEs were anemia (20%), abdominal pain (8%), fatigue (7%) and dyspnea (4%) (Domchek et al., 2016; Matulonis et al., 2016). In Study 19, the median treatment duration was 206.5 days with olaparib and 141 days with PBO. 95.6% and 90.6% of patients developed any-grade AEs in the olaparib and PBO groups, respectively. Among patients in the olaparib group, the most common AEs were nausea (68.4%), fatigue (48.5%), vomiting (31.6%), diarrhea (22.8%), abdominal pain (17.6%), anemia (16.9%). ≥G3 AEs occurred in 35.3% of patients treated with olaparib *versus* 20.3% of patients receiving PBO, most commonly fatigue (6.6%), anemia (5.1%), nausea/vomiting/diarrhea (each 2.2%), and abdominal pain (1.5%). In the olaparib group, 27.9% and 22.8% of patients experienced dose interruption or reductions (vs 8.6% and 4.7% of the PBO group). Three patients in the olaparib group permanently discontinued treatment *versus* one treatment interruption with PBO. No deaths were recorded (Ledermann et al., 2012). In the SOLO2/ENGOT-Ov21 trial, the median treatment duration was 19.4 months with olaparib and 5.6 months with PBO. 98.5% of patients in the olaparib group and 94.9% in the PBO group experienced any grades AEs, with

36.9% and 18.2% experiencing ≥ G3 AEs, respectively. The most common all-grade toxicities were nausea (75.9% vs 33.3%), fatigue/asthenia (65.6% vs 39.4%), anemia (43.6% vs 8.1%), vomiting (37.4% vs 19.2%), and diarrhea (32.8% vs 20.2%). However, anemia was the most common ≥ G3 AE (19.5% vs 2.0%), while the incidences of ≥G3 neutropenia (5.1% vs 4.0%) and thrombocytopenia (both 1.0%) were not significantly increased in the olaparib subgroup. SOLO2 had a higher incidence of anemia than Study 19, which could be explained by more prolonged exposure to olaparib for patients in this study. Of note, one patient (0.5%) of the olaparib group experienced AML, resulting in death. The long-term incidence of AML, MDS, and chronic myelomonocytic leukemia (CMML) was 2.1% with olaparib and 4.0% with PBO. 45.1% and 18.2% of patients in the olaparib and PBO groups required dose interruptions, while 25.1% and 3.0% required dose reductions due to AEs, respectively. 10.8% of patients in the olaparib and 2.0% in the PBO group discontinued treatment because of toxicity, mainly anemia (3.1%) and neutropenia (1.0%) (Pujade-Lauraine et al., 2017; Poveda et al., 2021).

All grades and ≥G3 AEs were reported in 95.7% and 29.0% of patients in the OPINION trial, respectively. Nausea (48.4%), fatigue/asthenia (44.1%), anemia (39.1%), and diarrhea (14.3%) were the most common AEs of all grades, while anemia (13.6%) and fatigue/asthenia (3.2%) were the most common ≥ G3 AEs. Dose interruption, dose reduction, and treatment discontinuation were applied to 47.0%, 22.6%, and 7.5% of patients. The median treatment duration was 9.4 months. Anaemia (1.8%), decreased platelet count, depression, fatigue/asthenia, and thrombocytopenia (0.7% each) were the most common AEs leading to treatment discontinuation. MDS and SPMs (mainly rectal and breast cancer) were reported in 0.7% of patients each (Poveda et al., 2022). 98% of olaparib and 92% of PBO patients of the SOLO1 trial experienced AEs of any grade, among which ≥ G3 AEs were reported in 40% and 19% of patients. Nausea (78% and 38%), fatigue/asthenia (64% and 42%), vomiting (40% and 15%), anemia (40% and 10%), and diarrhea (35%) were the most common all-grade AEs. The most frequent ≥ G3 AE was anemia, which occurred in 22% of olaparib and 2% of PBO patients. Dose interruptions occurred in 52% of olaparib vs 17% of PBO patients, while dose reductions occurred in 29% vs 3%. Discontinuations were less frequent with olaparib (12%) than with PBO (3%). One (1%) fatal AML occurred over 30 days after olaparib discontinuation. Of note, 2% of olaparib patients developed SPMs (breast, oral cavity, and thyroid), and 2% of PBO patients developed SPMs (breast cancer) (Moore et al., 2018). Finally, in the PAOLA-1 trial, the median duration of treatment was 16.6 months for olaparib plus bevacizumab and 13.4 months for PBO in the HiR group, while for the LoR group, 22.6 vs19.8 months 99% and 96% of patients experienced AEs, with olaparib plus bevacizumab and PBO plus bevacizumab, respectively. 57% of patients experienced severe AEs with olaparib plus bevacizumab vs 51% in the PBO/bevacizumab arm, showing no significant safety differences among all subgroups. Fatigue or asthenia (53% vs 22%), nausea (53% vs 22%), hypertension (46% vs 60%), and anemia (41% vs 10%) were the most frequent all-grade AEs. Hypertension (19% vs 30%) and anemia (17% vs 1%) were the most frequently reported ≥ G3 AEs. Dose interruptions occurred in 53% vs 26% of HiR

FIGURE 1
Most frequent all-grades adverse events during olaparib therapy.

FIGURE 2
Most frequent ≥G3 adverse events during olaparib therapy.
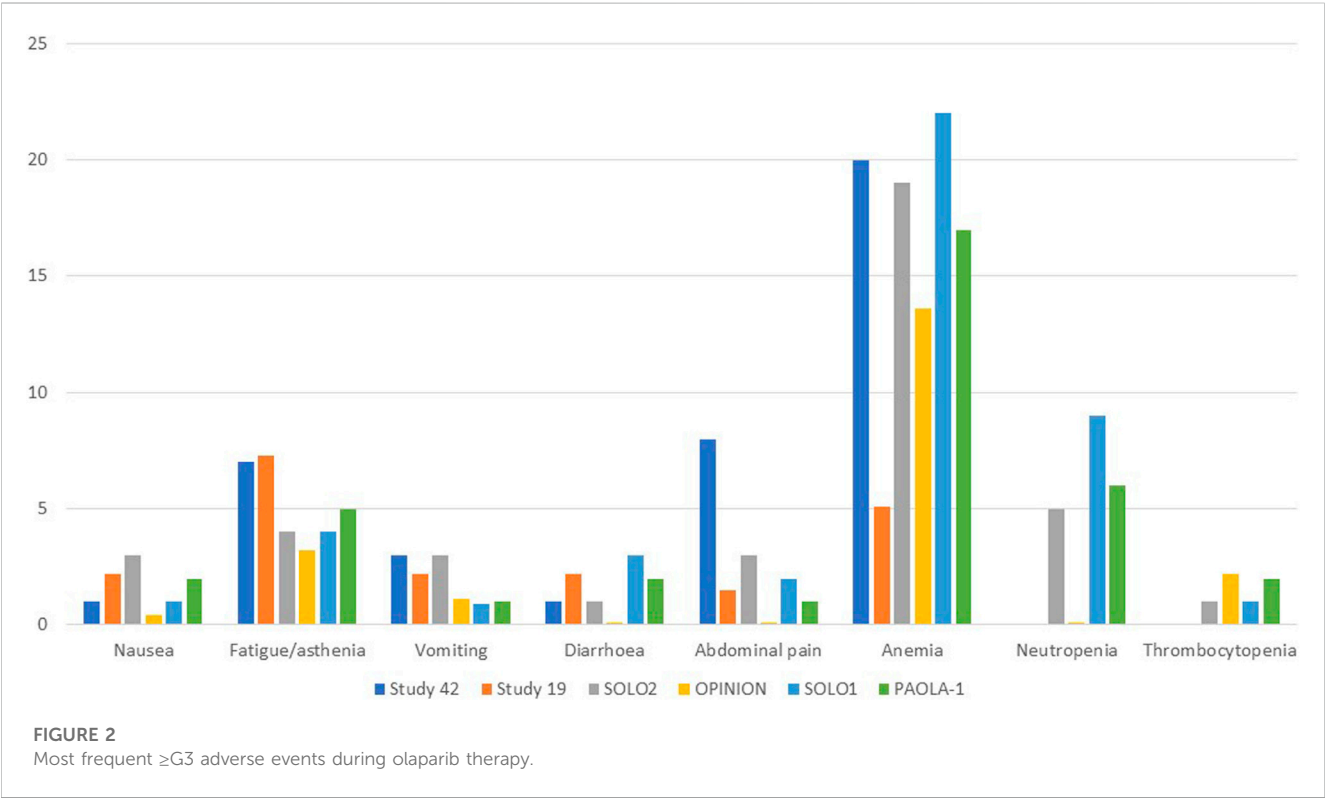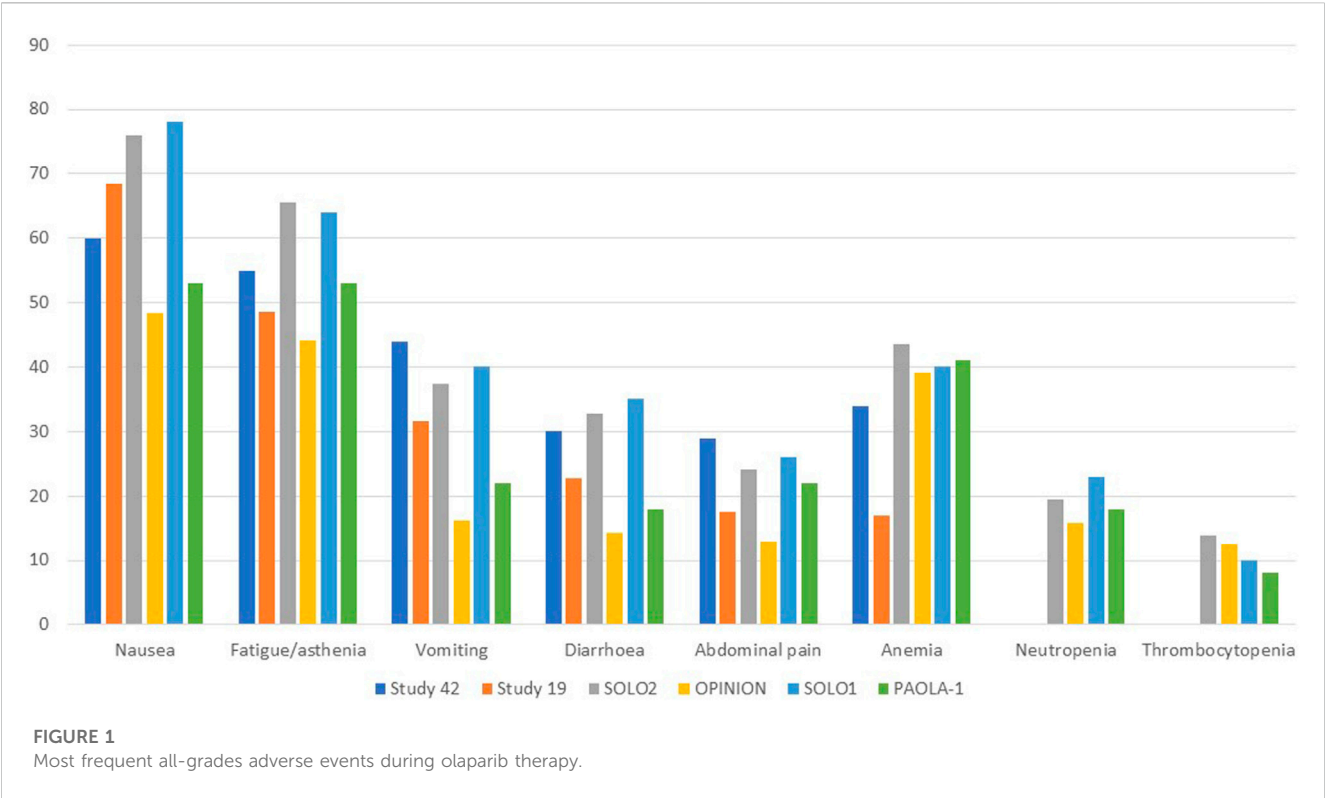
patients and 60% vs 21% of LoR patients, while discontinuation in 19% vs 6% in the HiR and 25% vs 5% in the LoR subgroups. One patient (0.3%) receiving olaparib/bevacizumab and 2 (1%) receiving PBO/bevacizumab experienced fatal AEs. A total of 6 patients (1%) in the olaparib/bevacizumab and 1 (<1%) in the PBO/bevacizumab group developed AML or MDS, while 7 patients

TABLE 3 Adverse events of Olaparib in clinical trials according to CTCAE.

AEs	Study 42		Study 19		SOLO2		OPINION		SOLO1		PAOLA-1	
	All grades (%)	≥G3 (%)	All grades (%)	≥G3 (%)	All grades (%)	≥G3 (%)	All grades (%)	≥G3 (%)	All grades (%)	≥G3 (%)	All grades (%)	≥G3 (%)
Nausea	60	1	68.4	2.2	75.9	3	48.4	0.4	78	1	53	2
Fatigue	55	7	48.5	6.6	65.6	4	44.1	3.2	64	4	53	5
Vomiting	44	3	31.6	2.2	37.4	3	16.1	1.1	40	<1	22	1
Diarrhoea	30	1	22.8	2.2	32.8	1	14.3	14.3	35	3	18	2
Abdominal pain	29	8	17.6	1.5	23	3	12.9	12.9	25	2	19	1
Anemia	34	20	16.9	5.1	43.6	19	39.1	13.6	40	22	41	17
Neutropenia	NA	NA	NA	NA	19	5	15.8	1.8	11	9	18	6
TCP	NA	NA	NA	NA	14	1	12.5	2.2	11	1	8	2

AE(s), adverse event(s); G3, grade 3; NA, not available; TCP, thrombocytopenia.

TABLE 4 Results of studies employing olaparib and ICIs.

Study name (NCT)	Phase	Target population (number of patients)	Combination	Results
NCT02484404 Lampert et al., (2020)	II	ROC (n = 35: 30 PR-ROC +5 PS-ROC)	Olaparib plus durvalumab (anti-PD-L1)	ORR 14% mPFS 3.0 months
		BRCAwt (n = 27) gBRCAmut (n = 6)		
		sBRCAmut (n = 2)		
MEDIOLA Banerjee et al., (2022)	II	PS-ROC gBRCAmut (n = 32)	Olaparib plus durvalumab	ORR 71.9% mPFS 11.1 mos
				mOS NR
		PS-ROC BRCAwt	Olaparib plus durvalumab	ORR 31.3% mPFS 5.5 months
				mOS 23.3 months
		PS-ROC BRCAwt	Olaparib plus bevacizumab plus durvalumab	ORR 77.4% mPFS 14.7 months
				mOS 31.9 months
NCT02571725 Adams et al. (2017)	Ib/II	gBRCAmut ROC (n = 3)	Olaparib plus tremelimumab (anti-CTLA4)	ORR 100%

BRCA, breast cancer associated gene; BRCAwt, BRCA, wild-type; CTLA4, cytotoxic T.lymphocyte-associated protein 4; gBRCAmut, germline mutated BRCA; mos, months; NR, not reached; ORR, overall response rate; PD-L1, programmed death-ligand 1; PFS, progression free survival; PR/PS-ROC, platinum-resistant/platinum-sensitive recurrent ovarian cancer; ROC, recurrent ovarian cancer; sBRCAmut, somatic mutated BRCA.

(1%) and 3 (<1%) developed SPMs (Ray-Coquard et al., 2019). Figures 1, 2 resume the most frequent all-grades and ≥G3 AEs during olaparib treatment. Table 3 enlists the main AEs grouped according to CTCAE (Common Terminology Criteria for Adverse Events) grading.

7 Future perspectives and conclusions

PARPis have transformed the therapeutic landscape of advanced OC in the last decade, and olaparib was a pioneer drug in this field. We provided an overview of the clinical and pre-clinical characteristics of olaparib, synthesizing the results of trials that led to its approval in different settings and analyzing its safety profile. Olaparib resulted in effective maintenance therapy in the recurrent and newly diagnosed advanced OC setting in all patients' subgroups, regardless of BRCA status, with a generally good safety profile and quality of life. Some queries, however, remain unanswered and are currently being investigated by new ongoing trials, mainly the combination with different agents, and the use of olaparib in the platinum-resistant setting.

Combination studies are trying to meet the need for new therapeutic approaches, increasing the potential for new or augmented adverse events. An exciting strategy, currently under investigation, is to combine PARPis with immune checkpoint inhibitors (ICIs), with a strong rationale behind this combination. In fact, PARPis upregulate Programmed death-ligand 1 (PD-L1) expression; they interact with the tumor microenvironment, being able to switch it towards an immune-responsive state and increase tumor-infiltrating lymphocytes. Moreover, through DNA damage, PARPis stimulate neo-antigen production, therefore augmenting the tumor mutational burden. PARPis also switch on the STING pathway that, on its hand, reinforces interferon-γ dependent immune cells (Maiorano et al., 2022b). The combination of olaparib and the anti-PD-L1 durvalumab was tested in two ongoing phase II trials, reporting strong response rates. In the context of PS-ROC BRCAm OC, the MEDIOLA study reported an ORR of 71.9%, mOS NR, and mPFS of 11.1 months (Drew et al., 2019). Subsequently, the study randomized 63 BRCAwt patients to durvalumab plus olaparib with or without bevacizumab. The doublet cohort reached an ORR of 31.3%, and the triplet cohort of 77.4% (Drew et al., 2020). A final mOS analysis presented at ESMO2022 showed an mOS of 23.3 months vs 31.9 months in the doublet and triplet cohorts, respectively (Banerjee et al., 2022). The same combination was administered in the NCT02484404 phase II trial, with an ORR of 14% and an mPFS of 3.0 months (Lampert et al., 2020). The NCT02571725 phase Ib/II trial investigated the combination of olaparib with the anti-Cytotoxic T-lymphocyte-associated protein 4 (CTLA4) tremelimumab. Only 3 patients were treated, all of them achieving a PR (Adams et al., 2017) (Table 4).

The rationale behind the combination of PARPis and anti-angiogenic drugs stands on two main mechanisms: PARP inhibition decreases angiogenesis; hypoxia and Vascular endothelial growth factor receptor 3 (VEGFR3) inhibition also induce the downregulation of HR proteins (Bindra et al., 2005; Tentori et al., 2007; Lim et al., 2014). PAOLA-1 already showed the efficacy and safety of the combination of olaparib and bevacizumab (Ray-Coquard et al., 2019). A phase II trial combining cediranib with olaparib versus olaparib alone in PS-ROC showed a significantly better mPFS in the combination group (17.7 vs 9.0 months) (Liu et al., 2014). NRG-GY004, a phase III randomized clinical trial, compared the efficacy of olaparib, with or without cediranib, versus platinum-based CHT in PS-ROC. However, in this study, olaparib/cediranib did not improve PFS versus chemotherapy regardless of BRCA status, but increased AEs (Liu et al., 2022).

OC with a "BRCAness" phenotype exhibits a higher sensitivity to both platinum and PARPis, than OC without a "BRCAness" phenotype. Hence, platinum sensitivity might represent a potential biomarker for olaparib sensitivity. In fact, the clinical benefit rate of olaparib fell from 69.2% in platinum-sensitive to 45.8% in platinum-resistant and 23.1% in platinum-refractory BRCA1/2-mutated OC (Fong et al., 2010). In BRCA1/2 wild-type OC, half of the platinum-sensitive patients responded to olaparib versus only 4% of the platinum-resistant women. However, a response to platinum does not always guarantee a response to olaparib. Indeed, differently from PARPis, platinum sensitivity results from

defective nucleotide excision repair (NER) (Ceccaldi et al., 2015). The platinum-induced DNA cross-links are highly deleterious and more cytotoxic than the SSBs caused by PARPis. In addition, the partial restoration of HR is insufficient to repair the cross-links caused by platinum salts. Therefore, such OCs retain platinum sensitivity but exhibit PARPis resistance (Lord and Ashworth, 2013). It has also been evidenced that an increased platinum-to-platinum interval during olaparib treatment is associated with a response to subsequent platinum treatment [(Ang et al., 2013), (Norquist et al., 2011). As for the platinum-resistant recurrent OC (PR-ROC) setting, patients relapsing within 12 months of platinum-based CHT usually have a poorer response to subsequent treatments (Markman et al., 2004). Several trials involving PR-ROC patients have not yet resulted in improved responses or benefits in terms of survival, thus justifying further experimental work and clinical trials with novel agents. The phase II BAROCCO trial (NCT03314740) compared weekly paclitaxel with the olaparib-cediranib combination in PR-ROC, not significantly impacting PFS) (Colombo et al., 2022). Clinical activity of the olaparib-cediranib combination was shown by the phase IIb CONCERTO trial, with 60 BRCAwt PR-ROC reaching an ORR of 15.3%, an mPFS of 5.1 months, and a mOS of 13.2 months (Lee et al., 2022). The same combination is also being investigated in the phase II OCTOVA trial (NCT03117933) (Mansouri et al., 2021). The GEICO1601-ROLANDO phase II trial (NCT03161132) will assess the efficacy of olaparib with pegylated liposomal doxorubicin (PLD) in PR-ROC, regardless of BRCA status, while the randomized phase II CLIO/BGOG-ov10 trial compared olaparib monotherapy vs physicians' CHT of choice (PLD, Topotecan, Paclitaxel or Gemcitabine) in 100 PR-ROC patients. Olaparib monotherapy showed higher efficacy than CHT in the PR-ROC setting, with an ORR of 17.9% vs 6.1% for olaparib versus CHT. Even in heavily pretreated PR-ROC, ORR was 22.9% for olaparib versus 0% for CHT. mPFS in PR-ROC was not significantly improved (Perez-Fidalgo et al., 2019; Vanderstichele et al., 2022).

PARP1 has currently been identified as a more significant driver of synthetic lethality than PARP2 (Murai et al., 2012). Therefore, a new generation of highly-selective PARP1-inhibitors is under development. AZD5305 is a first-in-class PARP1-inhibitor and trapper (Johannes et al., 2021; Illuzzi et al., 2022; Zheng et al., 2023). Preliminary results of the phase I/IIa PETRA study (NCT04644068) in patients with BRCA1/2, PALB2, RAD51C/D mutations have been recently presented. Around half of 61 patients with OC (n = 19) had PR or SD to AZD5305. The drug's safety profile is of particular interest, as no discontinuations occurred. The most common AEs were nausea (34%), anemia (21.3%), neutropenia, and TCP (18%). 14.8% of patients experienced ≥ G3 AEs (Yap et al., 2022). This is in line with mouse models, in which the PARP1 selectivity was associated with a more manageable safety profile than common PARPis (Johannes et al., 2021; Illuzzi et al., 2022; Zheng et al., 2023).

In summary, olaparib displays clinical activity and is therefore approved as maintenance treatment of OC starting

from the first line, as monotherapy in BRCA mutant, and combined with bevacizumab in HRD patients, and in the PS-ROC independent from BRCA status, with a good balance between efficacy and safety. Further studies are required to expand this drug's therapeutic application and better select patients most likely to benefit from olaparib.

Author contributions

Conception of the work: BAM; acquisition, analysis, interpretation of data, drafting of the work: BAM, MFPM; revising of the work: EM All the authors provide approval for publication of the content of the manuscript.

Conflict of interest

The authors declare that the research was conducted in the absence of any commercial or financial relationships that could be construed as a potential conflict of interest.

Publisher's note

All claims expressed in this article are solely those of the authors and do not necessarily represent those of their affiliated organizations, or those of the publisher, the editors and the reviewers. Any product that may be evaluated in this article, or claim that may be made by its manufacturer, is not guaranteed or endorsed by the publisher.

References

Adams, S. F., Rixe, O., Lee, J. H., McCance, D. J., Westgate, S., Eberhardt, S. C., et al. (2017). Phase I study combining olaparib and tremelimumab for the treatment of women with BRCA-deficient recurrent ovarian cancer. *JCO* 35, e17052. doi:10.1200/JCO.2017.35.15_suppl.e17052

Ang, J. E., Clarkson-Jones, J. A., Swaisland, H., Brunetto, A. T., Lal, R., Farnsworth, A. P., et al. (2010). 405 A mass balance study to investigate the metabolism, excretion and pharmacokinetics of [14C]-olaparib (AZD2281) in patients with advanced solid tumours refractory to standard treatments. *Eur. J. Cancer Suppl.* 8, 128–129. doi:10.1016/S1359-6349(10)72112-1

Ang, J. E., Gourley, C., Powell, C. B., High, H., Shapira-Frommer, R., Castonguay, V., et al. (2013). Efficacy of chemotherapy in *BRCA1/2* mutation carrier ovarian cancer in the setting of PARP inhibitor resistance: A multi-institutional study. *Clin. Cancer Res.* 19, 5485–5493. doi:10.1158/1078-0432.CCR-13-1262

Armstrong, D. K., Bundy, B., Wenzel, L., Huang, H. Q., Baergen, R., Lele, S., et al. (2006). Intraperitoneal cisplatin and paclitaxel in ovarian cancer. *N. Engl. J. Med.* 354, 34–43. doi:10.1056/NEJMoa052985

Arora, S., Balasubramaniam, S., Zhang, H., Berman, T., Narayan, P., Suzman, D., et al. (2021). FDA approval summary: Olaparib monotherapy or in combination with bevacizumab for the maintenance treatment of patients with advanced ovarian cancer. *Oncol.* 26, e164–e172. doi:10.1002/onco.13551

Banerjee, S., Imbimbo, M., Roxburgh, P., Kim, J., Kim, M. H., Plummer, R., et al. (2022). 529MO - phase II study of olaparib plus durvalumab with or without bevacizumab (MEDIOLA): Final analysis of overall survival in patients with non-germline BRCA-mutated platinum-sensitive relapsed ovarian cancer. *Ann. Oncol.* 33, S788–S789. doi:10.1016/j.annonc.2022.07.657

Bindra, R. S., Gibson, S. L., Meng, A., Westermark, U., Jasin, M., Pierce, A. J., et al. (2005). Hypoxia-induced down-regulation of BRCA1 expression by E2Fs. *Cancer Res.* 65, 11597–11604. doi:10.1158/0008-5472.CAN-05-2119

Cancer stat facts: ovarian cancer *Cancer stat facts: Ovarian cancer*. available at https://seer.cancer.gov/statfacts/html/ovary.html (accessed on 02 07, 2023).

Ceccaldi, R., O'Connor, K. W., Mouw, K. W., Li, A. Y., Matulonis, U. A., D'Andrea, A. D., et al. (2015). A unique subset of epithelial ovarian cancers with platinum sensitivity and PARP inhibitor resistance. *Cancer Res.* 75, 628–634. doi:10.1158/0008-5472.CAN-14-2593

Colombo, N., Tomao, F., Benedetti Panici, P., Nicoletto, M. O., Tognon, G., Bologna, A., et al. (2022). Randomized phase II trial of weekly paclitaxel vs. cediranib-olaparib (continuous or intermittent schedule) in platinum-resistant high-grade epithelial ovarian cancer. *Gynecol. Oncol.* 164, 505–513. doi:10.1016/j.ygyno.2022.01.015

Committee for Medicinal Products for Human (2014). *Committee for medicinal products for human use (CHMP) European medicines agency (EMA). Public assessment report olaparib.* available at https://www.ema.europa.eu/en/documents/assessment-report/lynparza-epar-public-assessment-report_en.pdf (accessed on 02 07, 2023).

Dean, E., Middleton, M. R., Pwint, T., Swaisland, H., Carmichael, J., Goodege-Kunwar, P., et al. (2012). Phase I study to assess the safety and tolerability of olaparib in combination with bevacizumab in patients with advanced solid tumours. *Br. J. Cancer* 106, 468–474. doi:10.1038/bjc.2011.555

DiSilvestro, P., Banerjee, S., Colombo, N., Scambia, G., Kim, B. G., Oaknin, A., et al. (2023). Overall survival with maintenance olaparib at a 7-year follow-up in patients with newly diagnosed advanced ovarian cancer and a BRCA mutation: The SOLO1/GOG 3004 trial. *J. Clin. Oncol.* 41, 609–617. doi:10.1200/JCO.22.01549

Dockery, L. E., Tew, W. P., Ding, K., and Moore, K. N. (2017). Tolerance and toxicity of the PARP inhibitor olaparib in older women with epithelial ovarian cancer. *Gynecol. Oncol.* 147, 509–513. doi:10.1016/j.ygyno.2017.10.007

Domchek, S. M., Aghajanian, C., Shapira-Frommer, R., Schmutzler, R. K., Audeh, M. W., Friedlander, M., et al. (2016). Efficacy and safety of olaparib monotherapy in germline BRCA1/2 mutation carriers with advanced ovarian cancer and three or more lines of prior therapy. *Gynecol. Oncol.* 140, 199–203. doi:10.1016/j.ygyno.2015.12.020

Drew, Y., Kaufman, B., Banerjee, S., Lortholary, A., Hong, S. H., Park, Y. H., et al. (2019). Phase II study of olaparib + durvalumab (MEDIOLA): Updated results in germline BRCA-mutated platinum-sensitive relapsed (PSR) ovarian cancer (OC). *Ann. Oncol.* 30, v485–v486. doi:10.1093/annonc/mdz253.016

Drew, Y., Penson, R. T., O'Malley, D. M., Kim, J-W., Zimmermann, S., Roxburgh, P., et al. (2020). 814MO Phase II study of olaparib (O) plus durvalumab (D) and bevacizumab (B) (MEDIOLA): Initial results in patients (pts) with non-germline BRCA-mutated (non-gBRCAm) platinum sensitive relapsed (PSR) ovarian cancer (OC). *Ann. Oncol.* 31, S615–S616. doi:10.1016/j.annonc.2020.08.953

EMA Olaparib product information *EMA Olaparib product information.* available at https://www.ema.europa.eu/en/documents/product-information/lynparza-epar-product-information_en.pdf (accessed on 02 07, 2023).

Farmer, H., McCabe, N., Lord, C. J., Tutt, A. N. J., Johnson, D. A., Richardson, T. B., et al. (2005). Targeting the DNA repair defect in BRCA mutant cells as a therapeutic strategy. *Nature* 434, 917–921. doi:10.1038/nature03445

FDA approved Olaparib *FDA approved Olaparib.* available at https://www.fda.gov/drugs/fda-approved-olaparib-lynparza-astrazeneca-pharmaceuticals-lp-maintenance-treatment-adult-patients#:~:text=On%20December%2019%2C%202018%2C%20the,ovarian%2C%20fallopian%20tube%20or%20primary (accessed on 02 07, 2023).

Fong, P. C., Yap, T. A., Boss, D. S., Carden, C. P., Mergui-Roelvink, M., Gourley, C., et al. (2010). Poly(ADP)-Ribose polymerase inhibition: Frequent durable responses in *BRCA* carrier ovarian cancer correlating with platinum-free interval. *JCO* 28, 2512–2519. doi:10.1200/JCO.2009.26.9589

González-Martín, A., Desauw, C., Heitz, F., Cropet, C., Gargiulo, P., Berger, R., et al. (2022). Maintenance olaparib plus bevacizumab in patients with newly diagnosed advanced high-grade ovarian cancer: Main analysis of second progression-free survival in the phase III PAOLA-1/ENGOT-ov25 trial. *Eur. J. Cancer* 174, 221–231. doi:10.1016/j.ejca.2022.07.022

Harter, P., Mouret-Reynier, M. A., Pignata, S., Cropet, C., González-Martín, A., Bogner, G., et al. (2022). Efficacy of maintenance olaparib plus bevacizumab according to clinical risk in patients with newly diagnosed, advanced ovarian cancer in the phase III PAOLA-1/ENGOT-ov25 trial. *Gynecol. Oncol.* 164, 254–264. doi:10.1016/j.ygyno.2021.12.016

Illuzzi, G., Staniszewska, A. D., Gill, S. J., Pike, A., McWilliams, L., Critchlow, S. E., et al. (2022). Preclinical characterization of AZD5305, A next-generation, highly selective PARP1 inhibitor and trapper. *Clin. Cancer Res.* 28 (21), 4724–4736. doi:10.1158/1078-0432.CCR-22-0301

Johannes, J. W., Balazs, A., Barratt, D., Bista, M., Chuba, M. D., Cosulich, S., et al. (2021). Discovery of 5-{4-[(7-Ethyl-6-oxo-5,6-dihydro-1,5-naphthyridin-3-yl)methyl]piperazin-1-yl}-*N*-methylpyridine-2-carboxamide (AZD5305): A PARP1-DNA trapper with high selectivity for PARP1 over PARP2 and other PARPs. *J. Med. Chem.* 64 (19), 14498–14512. doi:10.1021/acs.jmedchem.1c01012

Kehoe, S., Hook, J., Nankivell, M., Jayson, G. C., Kitchener, H., Lopes, T., et al. (2015). Primary chemotherapy versus primary surgery for newly diagnosed advanced ovarian cancer (CHORUS): An open-label, randomised, controlled, non-inferiority trial. *Lancet* 386, 249–257. doi:10.1016/S0140-6736(14)62223-6

LaFargue, C. J., Dal Molin, G. Z., Sood, A. K., and Coleman, R. L. (2019). Exploring and comparing adverse events between PARP inhibitors. *Lancet Oncol.* 20, e15–e28. doi:10.1016/S1470-2045(18)30786-1

Lampert, E. J., Zimmer, A., Padget, M., Cimino-Mathews, A., Nair, J. R., Liu, Y., et al. (2020). Combination of PARP inhibitor olaparib, and PD-L1 inhibitor durvalumab, in recurrent ovarian cancer: A proof-of-concept phase II study. *Clin. Cancer Res.* 26, 4268–4279. doi:10.1158/1078-0432.CCR-20-0056

Ledermann, J., Harter, P., Gourley, C., Friedlander, M., Vergote, I., Rustin, G., et al. (2012). Olaparib maintenance therapy in platinum-sensitive relapsed ovarian cancer. *N. Engl. J. Med.* 366, 1382–1392. doi:10.1056/NEJMoa1105535

Ledermann, J., Harter, P., Gourley, C., Friedlander, M., Vergote, I., Rustin, G., et al. (2014). Olaparib maintenance therapy in patients with platinum-sensitive relapsed serous ovarian cancer: A preplanned retrospective analysis of outcomes by BRCA status in a randomised phase 2 trial. *Lancet Oncol.* 15, 852–861. doi:10.1016/S1470-2045(14)70228-1

Lee, J. M., Moore, R. G., Ghamande, S., Park, M. S., Diaz, J. P., Chapman, J., et al. (2022). Cediranib in combination with olaparib in patients without a germline BRCA1/2 mutation and with recurrent platinum-resistant ovarian cancer: Phase IIb CONCERTO trial. *Clin. Cancer Res.* 28, 4186–4193. doi:10.1158/1078-0432.CCR-21-1733

Lim, J. J., Yang, K., Taylor-Harding, B., Wiedemeyer, W. R., and Buckanovich, R. J. (2014). VEGFR3 inhibition chemosensitizes ovarian cancer stemlike cells through down-regulation of BRCA1 and BRCA2. *Neoplasia* 16, 343–353. e1-2. doi:10.1016/j.neo.2014.04.003

Liu, J. F., Barry, W. T., Birrer, M., Lee, J-M., Buckanovich, R. J., Fleming, G. F., et al. (2014). Combination cediranib and olaparib versus olaparib alone for women with recurrent platinum-sensitive ovarian cancer: A randomised phase 2 study. *Lancet Oncol.* 15, 1207–1214. doi:10.1016/S1470-2045(14)70391-2

Liu, J. F., Brady, M. F., Matulonis, U. A., Miller, A., Kohn, E. C., Swisher, E. M., et al. (2022). Olaparib with or without cediranib versus platinum-based chemotherapy in recurrent platinum-sensitive ovarian cancer (NRG-GY004): A randomized, open-label, phase III trial. *JCO* 40, 2138–2147. doi:10.1200/JCO.21.02011

Lord, C. J., and Ashworth, A. (2013). Mechanisms of resistance to therapies targeting BRCA-mutant cancers. *Nat. Med.* 19, 1381–1388. doi:10.1038/nm.3369

Lord, C. J., and Ashworth, A. (2012). The DNA damage response and cancer therapy. *Nature* 481, 287–294. doi:10.1038/nature10760

Maiorano, B. A., Lorusso, D., Maiorano, M. F. P., Ciardiello, D., Parrella, P., Petracca, A., et al. (2022). The interplay between PARP inhibitors and immunotherapy in ovarian cancer: The rationale behind a new combination therapy. *IJMS* 23, 3871. doi:10.3390/ijms23073871

Maiorano, B. A., Maiorano, M. F. P., Lorusso, D., Di Maio, M., and Maiello, E. (2022). Efficacy and safety of PARP inhibitors in elderly patients with advanced ovarian cancer: A systematic review and meta-analysis. *Int. J. Gynecol. Cancer* 32, 1410–1418. doi:10.1136/ijgc-2022-003614

Mansouri, A., McGregor, N., Dunn, R., Dobbie, S., Holmes, J., Collins, L., et al. (2021). Randomised phase II trial of olaparib, chemotherapy or olaparib and cediranib in patients with platinum-resistant ovarian cancer (OCTOVA): A study protocol. *BMJ Open* 11, e041463. doi:10.1136/bmjopen-2020-041463

Markman, M., Markman, J., Webster, K., Zanotti, K., Kulp, B., Peterson, G., et al. (2004). Duration of response to second-line, platinum-based chemotherapy for ovarian cancer: Implications for patient management and clinical trial design. *J. Clin. Oncol.* 22, 3120–3125. doi:10.1200/JCO.2004.05.195

Mateo, J., Moreno, V., Gupta, A., Kaye, S. B., Dean, E., Middleton, M. R., et al. (2016). An adaptive study to determine the optimal dose of the tablet formulation of the PARP inhibitor olaparib. *Targ. Oncol.* 11, 401–415. doi:10.1007/s11523-016-0435-8

Matulonis, U. A., Penson, R. T., Domchek, S. M., Kaufman, B., Shapira-Frommer, R., Audeh, M. W., et al. (2016). Olaparib monotherapy in patients with advanced relapsed ovarian cancer and a germline BRCA1/2 mutation: A multistudy analysis of response rates and safety. *Ann. Oncol.* 27, 1013–1019. doi:10.1093/annonc/mdw133

McCormick, A., Swaisland, H., Reddy, V. P., Learoyd, M., and Scarfe, G. (2018). *In vitro* evaluation of the inhibition and induction potential of olaparib, a potent poly(ADP-ribose) polymerase inhibitor, on cytochrome P450. *Xenobiotica* 48, 555–564. doi:10.1080/00498254.2017.1346332

McGuire, W. P., Hoskins, W. J., Brady, M. F., Kucera, P. R., Partridge, E. E., Look, K. Y., et al. (1996). Cyclophosphamide and cisplatin compared with paclitaxel and cisplatin in patients with stage III and stage IV ovarian cancer. *N. Engl. J. Med.* 334, 1–6. doi:10.1056/NEJM199601043340101

Moore, K., Colombo, N., Scambia, G., Kim, B-G., Oaknin, A., Friedlander, M., et al. (2018). Maintenance olaparib in patients with newly diagnosed advanced ovarian cancer. *N. Engl. J. Med.* 379, 2495–2505. doi:10.1056/NEJMoa1810858

Morice, P-M., Ray-Coquard, I., Moore, K. N., Diéras, V., and Alexandre, J. (2021). PARP inhibitors and newly second primary malignancies in cancer patients: A systematic review and safety meta-analysis of placebo randomized controlled trials. *Ann. Oncol.* 32, 1048–1050. doi:10.1016/j.annonc.2021.04.023

Murai, J., Huang, S. Y., Das, B. B., Renaud, A., Zhang, Y., Doroshow, J. H., et al. (2012). Trapping of PARP1 and PARP2 by clinical PARP inhibitors. *Cancer Res.* 72 (21), 5588–5599. doi:10.1158/0008-5472.CAN-12-2753

Neijt, J. P., Engelholm, S. A., Tuxen, M. K., Sørensen, P. G., Hansen, M., Sessa, C., et al. (2000). Exploratory phase III study of paclitaxel and cisplatin versus paclitaxel and carboplatin in advanced ovarian cancer. *JCO* 18, 3084–3092. doi:10.1200/JCO.2000.18.17.3084

Noordermeer, S. M., and van Attikum, H. (2019). PARP inhibitor resistance: A tug-of-war in BRCA-mutated cells. *Trends Cell Biol.* 10, 820–834. doi:10.1016/j.tcb.2019.07.008

Norquist, B., Wurz, K. A., Pennil, C. C., Garcia, R., Gross, J., Sakai, W., et al. (2011). Secondary somatic mutations restoring *BRCA1/2* predict chemotherapy resistance in hereditary ovarian carcinomas. *JCO* 29, 3008–3015. doi:10.1200/JCO.2010.34.2980

Ozols, R. F., Bundy, B. N., Greer, B. E., Fowler, J. M., Clarke-Pearson, D., Burger, R. A., et al. (2003). Phase III trial of carboplatin and paclitaxel compared with cisplatin and paclitaxel in patients with optimally resected stage III ovarian cancer: A gynecologic oncology group study. *JCO* 21, 3194–3200. doi:10.1200/JCO.2003.02.153

Perez-Fidalgo, J. A., Iglesias, M., Bohn, U., Calvo, E., Garcia, Y., Guerra, E., et al. (2019). GEICO1601-ROLANDO: A multicentric single arm phase II clinical trial to evaluate the combination of olaparib and pegylated liposomal doxorubicin for platinum-resistant ovarian cancer. *Future Sci. OA* 5, FSO370. doi:10.4155/fsoa-2018-0107

Piccart, M. J., Bertelsen, K., James, K., Cassidy, J., Mangioni, C., Simonsen, E., et al. (2000). Randomized intergroup trial of cisplatin-paclitaxel versus cisplatin-cyclophosphamide in women with advanced epithelial ovarian cancer: Three-year results. *J. Natl. Cancer Inst.* 92, 699–708. doi:10.1093/jnci/92.9.699

Plummer, R., Verheul, H. M., De Vos, F. Y. F. L., Leunen, K., Molife, L. R., Rolfo, C.\, et al. (2018). Pharmacokinetic effects and safety of olaparib administered with endocrine therapy: A phase I study in patients with advanced solid tumours. *Adv. Ther.* 35, 1945–1964. doi:10.1007/s12325-018-0804-z

Poveda, A., Floquet, A., Ledermann, J. A., Asher, R., Penson, R. T., Oza, A. M., et al. (2021). Olaparib tablets as maintenance therapy in patients with platinum-sensitive relapsed ovarian cancer and a BRCA1/2 mutation (SOLO2/ENGOT-Ov21): A final analysis of a double-blind, randomised, placebo-controlled, phase 3 trial. *Lancet Oncol.* 22, 620–631. doi:10.1016/S1470-2045(21)00073-5

Poveda, A., Lheureux, S., Colombo, N., Cibula, D., Lindemann, K., Weberpals, J., et al. (2022). Olaparib maintenance monotherapy in platinum-sensitive relapsed ovarian cancer patients without a germline BRCA1/BRCA2 mutation: OPINION primary analysis. *Gynecol. Oncol.* 164, 498–504. doi:10.1016/j.ygyno.2021.12.025

Pujade-Lauraine, E., Ledermann, J. A., Selle, F., Gebski, V., Penson, R. T., Oza, A. M., et al. (2017). Olaparib tablets as maintenance therapy in patients with platinum-sensitive, relapsed ovarian cancer and a BRCA1/2 mutation (SOLO2/ENGOT-Ov21): A double-blind, randomised, placebo-controlled, phase 3 trial. *Lancet Oncol.* 18, 1274–1284. doi:10.1016/S1470-2045(17)30469-2

Ray-Coquard, I., Pautier, P., Pignata, S., Pérol, D., González-Martín, A., Berger, R., et al. (2019). Olaparib plus bevacizumab as first-line maintenance in ovarian cancer. *N. Engl. J. Med.* 381, 2416–2428. doi:10.1056/NEJMoa1911361

Rolfo, C., de Vos-Geelen, J., Isambert, N., Molife, L. R., Schellens, J. H. M., De Grève, J., et al. (2019). Pharmacokinetics and safety of olaparib in patients with advanced solid tumours and renal impairment. *Clin. Pharmacokinet.* 58, 1165–1174. doi:10.1007/s40262-019-00754-4

Rolfo, C., Isambert, N., Italiano, A., Molife, L. R., Schellens, J. H. M., Blay, J., et al. (2020). Pharmacokinetics and safety of olaparib in patients with advanced solid tumours and mild or moderate hepatic impairment. *Br. J. Clin. Pharmacol.* 86, 1807–1818. doi:10.1111/bcp.14283

Siegel, R. L., Miller, K. D., Fuchs, H. E., and Jemal, A., Cancer statistics, 2022. *CA A Cancer J. Clin.* 72(2022) 7–33. doi:10.3322/caac.21708

Tentori, L., Lacal, P. M., Muzi, A., Dorio, A. S., Leonetti, C., Scarsella, M., et al. (2007). Poly(ADP-ribose) polymerase (PARP) inhibition or PARP-1 gene deletion reduces angiogenesis. *Eur. J. Cancer* 43, 2124–2133. doi:10.1016/j.ejca.2007.07.010

The Cancer Genome Atlas Research Network (2011). Integrated genomic analyses of ovarian carcinoma. *Nature* 474, 609–615. doi:10.1038/nature10166

Trillsch, F., Mahner, S., Ataseven, B., Asher, R., Dubot, C., Clamp, A. R., et al. (2020). Efficacy and safety of olaparib according to age in BRCA-1/2 mutated patients with recurrent platinum-sensitive ovarian cancer: Analysis of the phase III SOLO2 (AGO-OVAR 2.23/ENGOT-Ov21) study. *JCO* 38, 6068. doi:10.1200/JCO.2020.38.15_suppl.6068

US Food and Drug Administration (FDA) (2014). *Center for drug evalu-ation and research-clinical pharmacology and biopharmaceutics review(s), Olaparib.* available at https://www.accessdata.fda.gov/drugsatfda_docs/nda/2014/206162Orig1s000ClinPharmR.pdf (accessed on 02 07, 2023).

Vanderstichele, A., Loverix, L., Busschaert, P., Van Nieuwenhuysen, E., Han, S. N., Concin, N., et al. (2022). Randomized CLIO/BGOG-ov10 trial of olaparib monotherapy versus physician's choice chemotherapy in relapsed ovarian cancer. *Gynecol. Oncol.* 165, 14–22. doi:10.1016/j.ygyno.2022.01.034

Walker, J. L., Brady, M. F., Wenzel, L., Fleming, G. F., Huang, H. Q., DiSilvestro, P. A., et al. (2019). Randomized trial of intravenous versus intraperitoneal chemotherapy plus bevacizumab in advanced ovarian carcinoma: An NRG oncology/gynecologic oncology group study. *JCO* 37, 1380–1390. doi:10.1200/JCO.18.01568

Yamamoto, N., Nokihara, H., Yamada, Y., Goto, Y., Tanioka, M., Shibata, T., et al. (2012). A Phase I, dose-finding and pharmacokinetic study of olaparib (AZD2281) in

Japanese patients with advanced solid tumors. *Cancer Sci.* 103, 504–509. doi:10.1111/j. 1349-7006.2011.02179.x

Yap, T., Im, S., Schram, A., Sharp, A., Balmana, J., Baird, R. D., et al. Petra: First in class, first in human trial of the next generation PARP1-selective inhibitor AZD5305 in patients (pts) with BRCA1/2, PALB2 or RAD51C/D mutations. Presented at American Association for Cancer Research Annual Meeting 2022, available at https://bit.ly/3jsOmgo, accessed on 03/14/2023

Yonemori, K., Tamura, K., Kodaira, M., Fujikawa, K., Sagawa, T., Esaki, T., et al. (2016). Safety and tolerability of the olaparib tablet formulation in Japanese patients with advanced solid tumours. *Cancer Chemother. Pharmacol.* 78, 525–531. doi:10.1007/s00280-016-3106-7

Yuan, P., Shentu, J., Xu, J., Burke, W., Hsu, K., Learoyd, M., et al. (2019). Pharmacokinetics and safety of olaparib tablets as monotherapy and in combination with paclitaxel: Results of a phase I study in Chinese patients with advanced solid tumours. *Cancer Chemother. Pharmacol.* 83, 963–974. doi:10.1007/s00280-019-03799-1

Zheng, J., Li, Z., and Min, W. (2023). Current status and future promise of next-generation poly (ADP-Ribose) polymerase 1-selective inhibitor AZD5305. *Front. Pharmacol.* 13, 979873. doi:10.3389/fphar.2022.979873

Zhou, D., Li, J., Bui, K., Learoyd, M., Berges, A., Milenkova, T., et al. (2019). Bridging olaparib capsule and tablet formulations using population pharmacokinetic meta-analysis in oncology patients. *Clin. Pharmacokinet.* 58, 615–625. doi:10.1007/s40262-018-0714-x

Frontiers in
Pharmacology

Explores the interactions between chemicals and living beings

The most cited journal in its field, which advances access to pharmacological discoveries to prevent and treat human disease.

Discover the latest Research Topics

See more →

Frontiers

Avenue du Tribunal-Fédéral 34
1005 Lausanne, Switzerland
frontiersin.org

Contact us

+41 (0)21 510 17 00
frontiersin.org/about/contact

frontiers

Frontiers in
Pharmacology

frontiers | Research Topics